MILANDIP KARAK

A STEREOSELECTIVE VINYLOGOUS ALDOL REACTION OF TETRONAMIDES AND THE SYNTHESIS OF RUBROLIDES AND BETA-SUBSTITUTED BUTENOLIDES

Tese apresentada à Universidade Federal de Viçosa, como parte das exigências do Programa de Pós-Graduação em Agroquímica, para obtenção do título de *Doctor Scientiae.*

VIÇOSA

MINAS GERAIS - BRASIL

2017

MILANDIP KARAK

A STEREOSELECTIVE VINYLOGOUS ALDOL REACTION OF TETRONAMIDES AND THE SYNTHESIS OF RUBROLIDES AND BETA-SUBSTITUTED BUTENOLIDES

Tese apresentada à Universidade Federal de Viçosa, como parte das exigências do Programa de Pós-Graduação em Agroquímica, para obtenção do título de *Doctor Scientiae*.

APROVADA: 27 de janeiro de 2017.
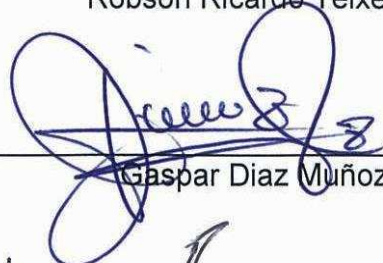
_____
Elson Santiago de Alvarenga

_____
Robson Ricardo Teixeira

_____
Jason Guy Taylor

_____
Gaspar Diaz Muñoz

_____
Luiz Cláudio de Almeida Barbosa
(Orientador)

Organic synthesis is all about simplicity. It may lead to a sophisticated outcome, but it has to be simple to carry out in order to have practical applications.

— Professor Huw M. L. Davies (Emory University)

To

My Parents

Who wanted to see me as a Doctor, but I failed

ACKNOWLEDGEMENT

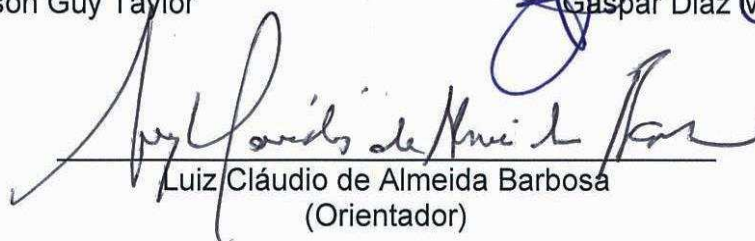People say 'it takes a village to raise a child'. Likewise, it takes a department to raise a graduate student. If so, then every single person in that department deserves thanks. First of all, I must thank my advisor, Professor Luiz Cláudio Barbosa, for the fantastic opportunity to work in his laboratory at UFV and UFMG. Luiz has been an excellent mentor and advisor for me. I thank Luiz for his expertise, advice, friendship, and most importantly for his support. He has always been open to my ideas and given me the freedom to test my ideas in the lab.

I thank our collaborators Dr. Gráinne Hargaden (Dublin Institute of Technology – Ireland), Dr. Ariel Sarotti (Universidad Nacional de Rosario – Argentina), Dr. Felipe Martins (Universidade Federal de Goiás– Brazil), and Professor John Boukouvalas (Université Laval – Canada), for their indispensable inputs during my entire research work. I am lucky enough to have John as a mentor who taught me how to work independently and think critically and helped me to build confidence. Latter, he turned out to be one of my great supporters over the past years.

I also thank my committee members: Dr. Elson Santiago de Alvarenga (UFV), Dr. Róbson Ricardo Teixeira (UFV), Dr. Jason Guy Taylor (UFOP), Dr. Gaspar Diaz Muñoz (UFMG), Dr. Célia Regina Álvares Maltha (UFV), Dr. Sergio Antonio Fernandes (UFV), and Dr. Adão Aparecido Sabino (UFMG), for their advices and corrections of my thesis.

It has been a real pleasure, privilege, and honor to work with the present and past members of the Barbosa lab whom I thank for making it a truly marvelous place to work and learn, and for being great colleagues and fantastic friends. They have been invaluable for discussing chemistry, proof readings, and keeping me sane over the past years.

I would also like to thank all the chemistry department staff for keeping things running smoothly and appreciate everything that they have done for me.

It would not have been nearly as easy to make it this far in my academic training without some excellent instructors over the years. I would like to thank my all teachers, supervisors, mentors and seniors for everything that they have done for me.

Finally, the contributions of my friends and family have been magnificent. Without all of you, I would have never made it to this point. Thank you so very, very much.

ABOUT THE AUTHOR

Milandip was born and raised in a small rural village named Tilaboni, located in eastern part of India under the state of West Bengal. He received his B.Sc. in Chemistry with Honours from Vidyasagar University (India) in 2009. He has obtained a M.Sc. in Chemistry from Rashtrasant Tukadoji Maharaj Nagpur University (India) in 2011. Shortly after completion of his Master's degree, he joined Chemgen Pharma International (India) as a Research Chemist in October 2011 and spent more than a year there. In 2013, he moved to Universidade Federal de Viçosa (Brazil) and joined the laboratory of Professor Luiz Cláudio Barbosa as a Ph.D. student. His doctoral research was focused on the chemistry of butenolides which included the discovery of a stereoselective vinylogous aldol reaction of tetronamides and the total synthesis of bioactive marine natural products, rubrolides.

TABLE OF CONTENTS

LIST OF ABBREVIATIONS

Ac	acetyl group
AED	antiepileptic drug
Ar	aryl group
atm	atmosphere
BINOL	1,1′-binaphthalene-2,2′-diol
br	broad
Bn	benzyl
CBS	Corey-Bakshi-Shibata
COSY	correlation spectroscopy
CSD	Cambridge structural database
$δ$	chemical shift
d	doublet
DBU	1,8-diazabicyclo[5.4.0]undec-7-ene
dd	doublet of doublet
DFT	density functional theory
DIPEA	N,N-diisopropylethylamine
dr	diastereomeric ratio
EDG	electron donating group
ee	enantiomeric excess
equiv	equivalent
eq	equation
ESI	electrospray ionization
EWG	electron withdrawing group
FPF	flupyradifurone
FWHM	full width at half maximum
GC	gas chromatography
GIAO	gauge-independent atomic orbital
HMBC	heteronuclear multiple bond correlation
HRMS	high resolution mass spectroscopy
Hz	hertz
IR	infrared
J	coupling constant
M	molar
m	milli, multiplet (in NMR)
m/z	mass to charge ratio

μM	micromolar
MHz	megahertz
MP	melting point
NBS	N-bromosuccinimide
NMP	N-Methyl-2-pyrrolidone
NMR	nuclear magnetic resonance
NSAID	nonsteroidal anti-inflammatory drug
PCM	polarizable continuum model
pKa	acidity constant
ppm	part(s) per million
q	quartet
RMSD	root-mean-square deviation
σ	Hammett parameter
s	singlet
t	triplet
TBAB	tetra -butylammonium bromide
TBDMSOTf	*t*-butyldimethylsilyl trifluoromethanesulfonate
Temp	temperature
TLC	thin layer chromatography
VAR	vinylogous aldol reaction
VMAR	vinylogous Mukaiyama aldol reaction
v/v	volume to volume
XRD	X-ray diffraction or X-ray powder diffraction

LIST OF FIGURES

LIST OF SCHEMES

LIST OF TABLES

ABSTRACT

KARAK, Milandip, D.Sc., Universidade Federal de Viçosa, January, 2017. **A stereoselective vinylogous aldol reaction of tetronamides and the synthesis of rubrolides and beta-substituted butenolides**. Advisor: Luiz Cláudio de Almeida Barbosa.

Butenolides are α,β-unsaturated lactone and are found in many natural and unnatural products with diverse biological properties. Owing to the prevalence of the substituted butenolides, much effort has been directed towards developing efficient methodologies for their synthesis and transformations. Among them, stereoselective access of the γ-substituted butenolide derivatives by utilizing the concept of vinylogy, which usually involves the carbon–carbon formation with an appropriate electrophile at the γ-position of butenolides, has triggered increasing interest. This thesis presents an efficient, simple, scalable and direct stereoselective vinylogous aldol reaction (VAR) of β-aminosubstituted butenolides (tetronamides) with aldehydes. In addition, this thesis also describes the total syntheses of butenolide core bearing marine natural metabolites, rubrolides by using a highly regioselective late-stage bromination from appropriate intermediates, and apprises a facile reductive dehalogenation of α-halo-β-substituted butenolides. An introduction to the general background, including versatile synthetic strategies, total syntheses, and biological properties of substituted butenolides is documented in Chapter 1. It is followed by an illustration of selected methods for construction of the butenolide core. Also discussed are the various methods for preparation of some selected natural products which either possess a butenolide core or synthesized from butenolide building blocks. Finally, some synthetic butenolide derivatives are described which are recently marketed as either medicines or agrochemicals. The results of the stereoselective VAR of tetronamides are compiled in Chapter 2. The described procedure, is simple and scalable, works well with both aromatic and aliphatic aldehydes, and affords mainly the corresponding *syn*-aldol adducts. In many cases, the latter are obtained essentially free of their *anti*-isomers in high yields. A detailed computational study was also carried out to establish the reaction mechanism. The experimental and computational studies suggest that the observed diastereoselectivity arises through *anti–syn* isomer interconversion, enabled by an iterative retro-aldol/aldol reaction. In Chapter 3, the crystal structures of several tetronamide aldol products with two stereocenters are described. Those compounds revealed conformational and supramolecular trends with the substitution pattern of a side aromatic/ heteroaromatic ring. The major contribution of this study concerns the control over the molecular conformation of tetronamide aldolates bearing several rotatable bonds and the high conformational freedom through the substitution pattern of a single ring. The first total syntheses of the marine natural products rubrolides I and O and some of their unnatural congeners are reported in Chapter 4. A versatile late-stage

bromination strategy allowed functionalization of the aromatic rings in a highly regioselective fashion, enabling rapid access to the target rubrolides from common precursors. Next, the regioselective chlorination was also applied to the preparation of biologically important synthetic analogous of rubrolides from easily accessible precursors. In Chapter 5, a binary palladium catalyzed reductive dehalogenation of α-halo-β-substituted butenolides is documented. The synthetic procedure allowed rapid access to the β-substituted butenolides under mild conditions with high yields and excellent regioselectivity. In addition, a protecting group free step-economical synthesis of rubrolides E, F and 3"-bromorubrolide F has been reported by employing this protocol.

RESUMO

KARAK, Milandip, D.Sc., Universidade Federal de Viçosa, janeiro de 2017. **Reação viníloga-aldol estereosseletiva de tetronamidas e síntese de rubrolídeos e butenolídeos beta-substituídos**. Orientador: Luiz Cláudio de Almeida Barbosa.

Os butenolídeos, que apresentam em sua estrutura o núcleo lactona α,β-insaturada, são encontrados em produtos naturais e não naturais com diversas propriedades biológicas. Devido à prevalência dos butenolídeos substituídos, muitos esforços têm sido direcionados para explorar metodologias eficientes para suas sínteses e transformações. Entre elas, o acesso estereosseletivo dos derivados de butenolídeos γ-substituídos utilizando o conceito de vinilogia, o qual envolve a formação de ligação carbono-carbono com um eletrófilo apropriado na posição γ do butenolídeo, tem provocado um interesse crescente. Portanto, esta tese apresenta uma reação aldólica viníloga estereosseleva (VAR) eficiente, simples, escalável e diretamente estereosseletiva de butenolídeos β-amino-substituídos (tetronamidas) com aldeídos. Esta tese também descreve as sínteses totais de butenolídeos contendo metabólitos naturais marinhos rubrolídeos pela bromação altamente regiosseletiva de fase tardia a partir de intermediários apropriados. Além disso, a tese inclui uma desalogenação redutiva de butenolídeos α-halo-β-substituídos sob condições suaves com rendimentos elevados e regiosseletivos. Uma introdução ao contexto geral, incluindo estratégias sintéticas versáteis, sínteses totais e propriedades biológicas dos butenolídeos substituídos estão documentadas na seção: Capítulo 1. Sendo seguida por uma ilustração dos métodos selecionados para a construção do núcleo de butenolídeos. São também discutidos os vários métodos para a preparação de alguns produtos naturais selecionados que possuem o núcleo de butenolídeo ou sintetizados a partir de butenolídeos que atuam como "building blocks". Finalmente, foram descritos alguns butenolídeos sintéticos que são comercializados como medicamentos ou agroquimicos recentemente. Os resultados da VAR estereosseletiva de tetronamidas estão apresentatos no Capítulo 2. O procedimento descrito, simples e escalável, funciona bem com aldeídos aromáticos e alifáticos, proporcionando principalmente os adutos correspondentes de *syn*-aldol. Em muitos casos, estes últimos são obtidos isentos dos seus isômeros *anti* com rendimentos elevados. Foi também realizado um estudo computacional detalhado. Os estudos experimentais e computacionais sugerem que a diastereosseletividade observada surge através da interconversão do isômero *anti-syn*, através da reação reversível retro-aldólica. No Capítulo 3, as estruturas cristalinas de alguns produtos aldólicos de tetronamida com dois estereocentros foram descritos. Os compostos relacionados revelaram tendências conformacionais e supramoleculares com padrões de substituição do anel aromático/heteroaromático. Tais tendências foram racionalizadas com base nos perfis

energéticos dos principais confôrmeros. A principal contribuição deste estudo refere-se ao controle sobre a conformação molecular de tetronamidas que apresentam várias ligações que permitem giros, além da elevada liberdade conformacional através do padrão de substituição de um único anel. As primeiras sínteses totais de produtos naturais marinhos, os rubrolídeos I e O e alguns de seus derivados não naturais são relatadas no Capítulo 4. Uma versátil estratégia de bromação na última etapa permitiu a funcionalização dos anéis aromáticos de maneira altamente regiosseletiva, permitindo o acesso rápido aos alvos, rubrolídeos, a partir de precursores comuns. Posteriormente, a cloração regiosselectiva foi também aplicada à preparação de análogos sintéticos biologicamente importantes a partir de precursores facilmente acessíveis. No Capítulo 5, foi relatado a desalogenação redutiva catalisada por paládio binário de butenolídeos α-halo-β-substituídos. O procedimento sintético permitiu o acesso rápido aos butenolídeos β substituídos sob condições suaves, com rendimentos elevados e excelente regiosseletividade. Além disso, uma nova proposta para a síntese dos rubrolídeos E, F e composto com a estrutura correspondente à descrita para 3"-bromorubrolídeo F de ocorrência natural utilizando este mesmo protocolo.

CHAPTER 1

Advances in the Chemistry of Butenolides: A Concise Overview

1. Introduction

Butenolides occupy a central position between butyrolactone and furan structures, both in terms of synthetic chemistry and biosynthesis [1]. Butenolides, commonly referred as 2(5*H*)-furanone, a five-membered γ-lactone with an unsaturated α,β-carbon atoms (Figure 1.1), are heterocyclic ubiquitous moieties precursor of many complex natural products and its unnatural congeners. They often display an immense range of biological activities which are important for the development of physiological and therapeutic agents [2-7].

Structures and nomenclature of butenolides

- γ-Butenolide
- Crotonolactone
- Furan-2(5*H*)-one

- α-Butenolide
- Isocrotonolactone
- Furan-2(3*H*)-one

α−Angelica lactone   β-Angelica lactone
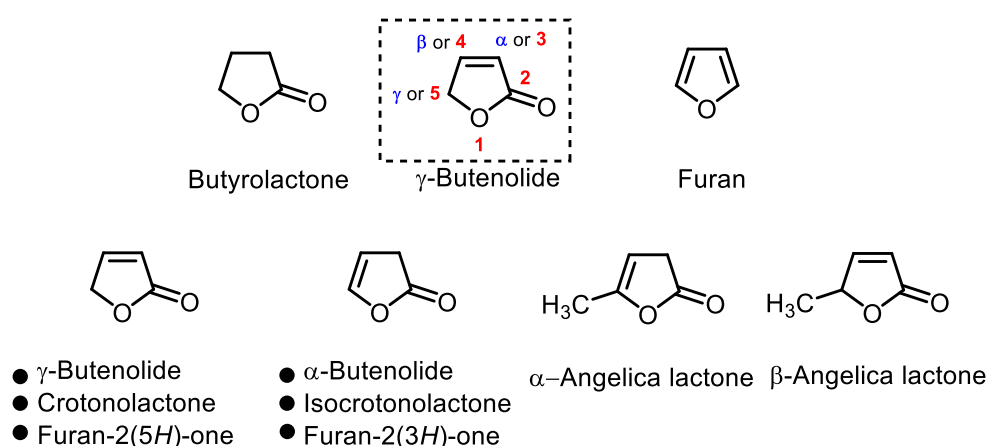
Some classical butenolide diterpene and sesterterpenoid natural products

Labdadienolide A   4-Epiphyllanthine   Jolkinolide E   Dysidiolide
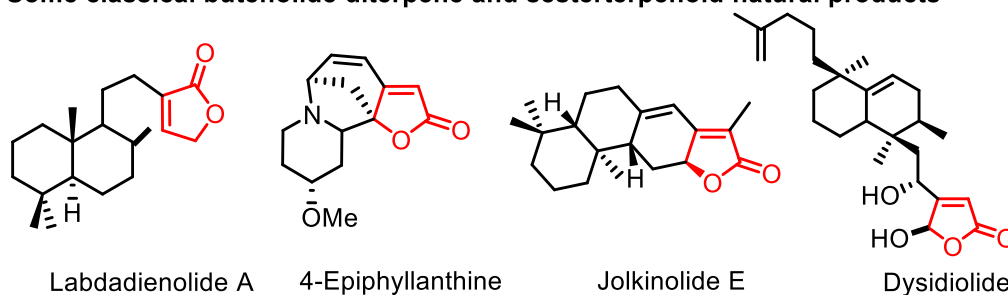
Figure 1.1 Nomenclature of butenolides and examples of some unique butenolide natural products

In the past, for many years, butenolides have been called crotonolactones [8]. However, a given "crotonolactone" is an $\Delta^{\alpha,\beta}$ isomer and usually indicated by specifying the position of the double bond by numbers or Greek letters. The term "isocrotonolactone" was used for the $\Delta^{\beta,\gamma}$ isomer [8]. The lactones derived from levulinic acid are known as α-angelica lactone, the $\Delta^{\beta,\gamma}$ isomer, and β-angelica lactone, the $\Delta^{\alpha,\beta}$ isomer [8].

Moreover, mucohalic acids, such as mucochloric acid and mucobromic acid are inexpensive, commercially available starting materials consisting of multiple functionalities:

one double bond between C-2 and C-3 with *Z*-configuration (open-chain form), two halogen atoms attached to the sp^2 carbons, and two carbonyl groups possessing different reactivity at C-1 and C-4 (open-chain form) [9]. Mucohalic acids can exist either in the open-chain form, or as a butenolide structure, although the latter one being the favored form under normal conditions. Mucohalic acids are generally synthesized from furfural (Scheme 1.1) [10-14]. Furfural itself obtained from xylose containing biomass by heating with sulfuric acid (Scheme 1.1) [15]. The reduced derivatives of mucohalic acids [16], i.e. 3,4-dihalofuran-2(5*H*)-ones (Scheme 1.1) also form an important and diverse group of natural products in their own right, and they display a wide range of biological activities [17-22].
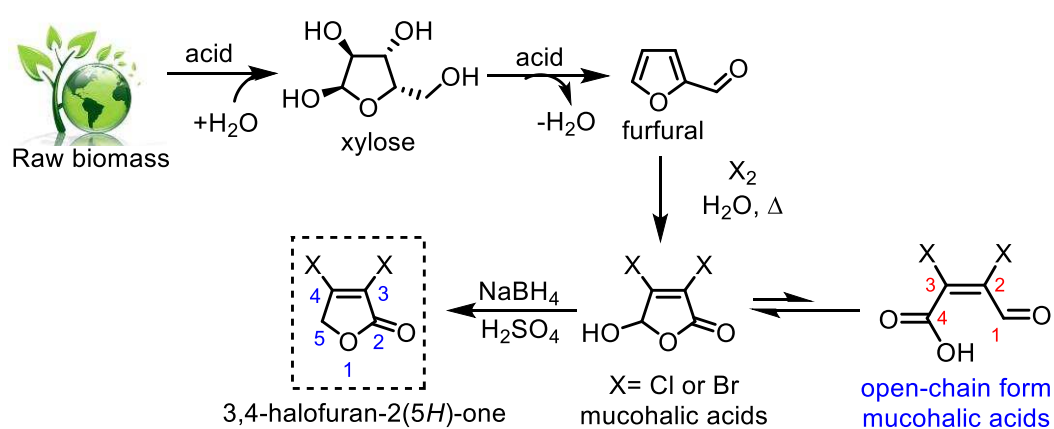
Scheme 1.1 Preparation of 3,4-dihalofuran-2(5*H*)-ones from biomass

A concise overview for the synthesis of substituted butenolides using transition-metal based catalysts or organocatalysts and their application in the total synthesis of natural products with emphasis on representative examples from the recent literature are discussed briefly in this chapter. In addition, some synthetic butenolides are also described which are recently marketed either as medicines or agrochemicals.

2. Versatile Synthetic Approaches to the Substituted Butenolides

Taking into account the interesting biological properties and synthetic potential associated with the butenolide structure, much attention has been paid towards the development of synthetic strategies for assembling such challenging scaffolds for a long time. Among them, organocatalyzed and transition-metal catalyzed syntheses has emerged as rapid and efficient methods to prepare structurally diverse substituted butenolides.

2.1. Synthesis through the Ring-closing Reactions

For instance, 4-Methyl-5-alkyl-2(5*H*)-furanones had been prepared by first-generation Grubbs' catalyzed ring-closing metathesis of the suitable methallyl acrylates [23]. Despite the electron deficiency of the conjugated double bond and of the gem-disubstitution of the allylic alkene moiety in the starting acrylates, the first-generation Grubbs' catalyst proved to be an effective promoter for the ring closure, affording the butenolides in good yields (Scheme 1.2).
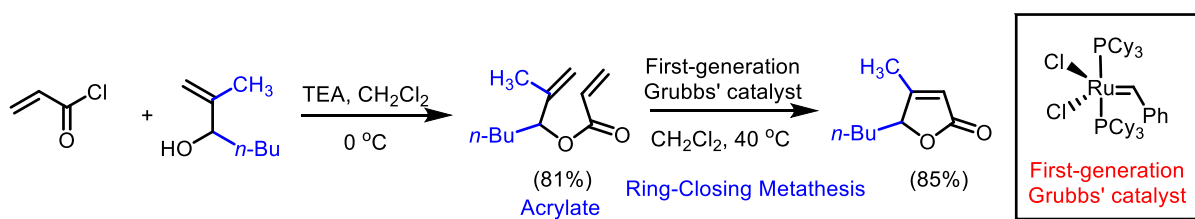
Scheme 1.2 Synthesis of 4,5-Disubstituted γ-Lactones *via* Ring-Closing Metathesis [23]

Another study described a convenient method for the preparation of the γ-methylene 2(5*H*)-furanones from 3,4-allenoic acids through Pd-catalyzed cyclization (Scheme 1.3) [24].
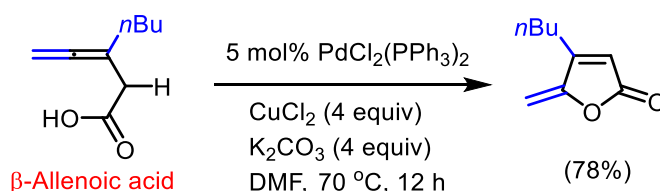
Scheme 1.3 Preparation of γ-methylene 2(5*H*)-furanones from 3,4-allenoic acids [24]

The synthesis of butenolides from butenoic acids using catalytic amounts of diphenyl diselenide and stoichiometric amount of hypervalent iodine[bis(trifluoroacetoxy)iodo]-benzene as an oxidant has been developed [25]. A similar recent study demonstrated that a chiral electrophilic selenium catalysts efficiently converts β,γ-unsaturated carboxylic acids into enantioenriched γ-butenolides *via* oxidative cyclization (Scheme 1.4) [26].
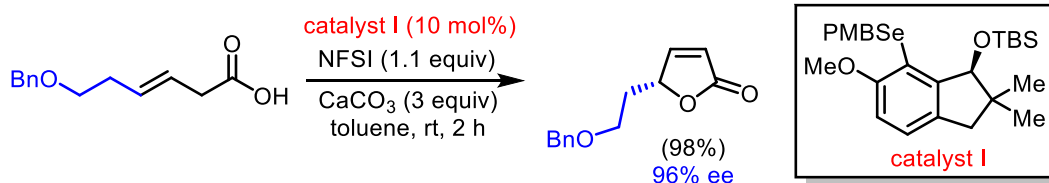
Scheme 1.4 Preparation of γ-butenolides *via* catalytic addition−elimination reaction [26]

In 2009, Buchwald et. al. described an efficient preparation of quaternary γ-aryl butenolides with a Pd-catalyzed cross coupling method [27]. The reaction has broad substrates scope and selectivity with respect to the different aryl halides. A versatile new approach to a wide variety of 3-iodobutenolides has been achieved from the electrophilic iodocyclization of various semiprotected 1-ethoxy-1-alkyne diols [28]. The reactions proceeded under mild conditions and tolerate considerable functionality (Scheme 1.5).
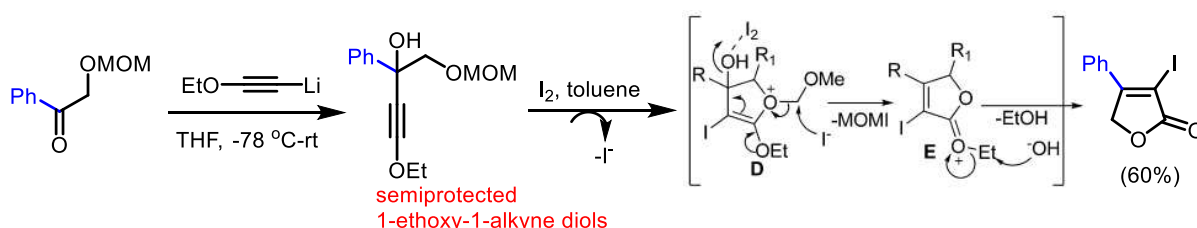
Scheme 1.5 Synthesis of butenolides *via* electrophilic iodocyclization of ethoxyalkyne diols [28]

In another approach, chiral amino-thiocarbamate catalyzed asymmetric bromolactonization of tri-substituted olefinic acids afforded moderate enantiomeric excess of the γ-substituted butenolides (Scheme 1.6) [29].
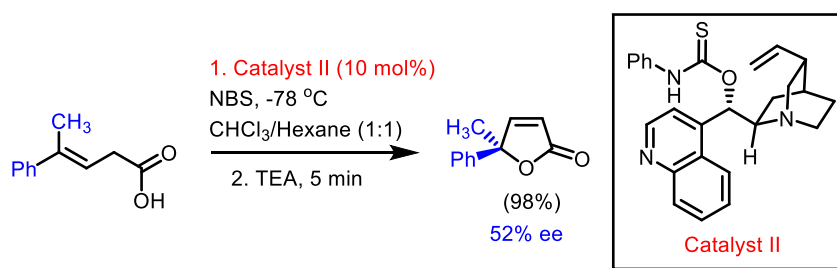
Scheme 1.6 Synthesis of chiral γ-substituted butenolides using chiral amino-thiocarbamate [29]

Very recently, an Au−Pd bimetallic catalytic system, based on their redox properties, has been developed to prepare a variety of substituted butenolides in a simple way using allenoates and aryl/heteroaryl iodides as starting materials (Scheme 1.7) [30].
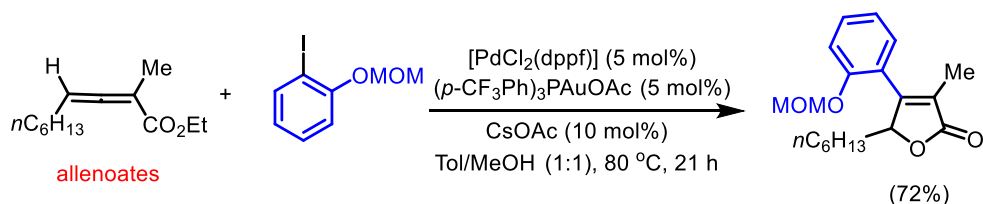
Scheme 1.7 Preparation of substituted butenolides catalyzed by Au−Pd Bimetallic Catalysis [30]

Several major approaches for the synthesis of butenolides have been reported, such as gold(I)-catalyzed tandem cyclization/oxidative cleavage of carbon-carbon triple bond [31], rhodium-catalyzed addition/lactonization reaction of organoboron derivatives to alkyl 4-hydroxy-2-alkynoates [32], lithium-bromine exchange and subsequent derivatization with carbon or heteroatom electrophiles [33], boron-catalyzed aldol reaction of pyruvic acids with aldehydes [34], Cu(II)-catalyzed acylation of acyloins with a thiol ester present in Wittig reagents *via* a push-pull mechanism [35], AgOTf-catalyzed intramolecular cyclization of phenoxyethynyl diols [36] and Cu-mediated carbomagnesiation of 2,3-allenols with Grignard reagents with carbon dioxide [37] as the prominent synthetic steps.

2.2.   Synthesis from the Butenolide Motifs

Cross-coupling Reactions

As a privileged fragment, β-substituted butenolide is a ubiquitous subunit in many butenolide-containing natural products with remarkable biological activities. Synthetically, to generate β-substituted butenolide is more challenging than γ-substituted butenolide [38]. The ever-increasing importance of transition metal catalyzed cross-coupling reactions has driven synthetic chemists to apply this chemistry to these intriguing structures and explore the untapped chemical resource. Among them, the Suzuki–Miyaura coupling reactions are the most widely known method for β–substituted carbon-carbon bond formation.

During the last decade, much effort has been employed in the optimization of Suzuki–Miyaura coupling reaction of butenolides due to its potential applications in natural products syntheses. A facile synthesis of β-substituted butenolides using Suzuki–Miyaura cross-coupling reactions with appropriate derivatives from commercially available tetronic acid and boronic acids has been developed (Scheme 1.8) [39, 40]. Although palladium is the most common catalyst for Suzuki–Miyaura coupling of butenolides, other catalysts were also investigated. For example, Ni(0)/PCy$_3$ [41] and RhCl(PPh$_3$)$_3$/dppf [42] catalyzed Suzuki–Miyaura coupling of the 4-(*p*-toluenesulfonyloxy)-2(5*H*)-furanone with arylboronic acids has been reported in recent years.
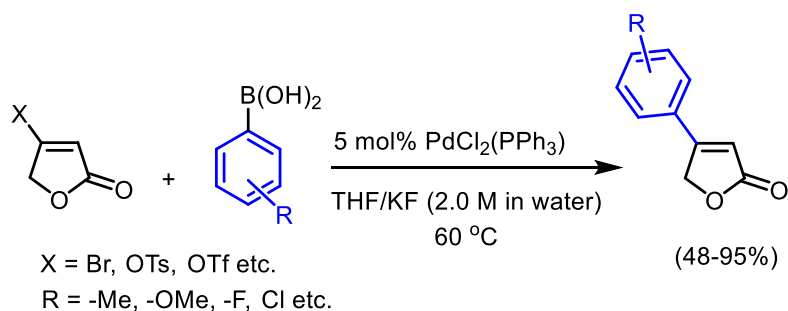
Scheme 1.8 Preparation of β-substituted butenolides *via* Suzuki–Miyaura coupling reaction [39, 40]

Moreover, α,β-dihalo butenolides are also highly attractive and useful building blocks in synthesis. Thus, a number of methods have been developed for the synthesis of α-halo-β-substituted butenolides. Although Suzuki–Miyaura coupling is the most explored reaction in this area [43-46], other cross-coupling reactions, such as Stille coupling [43, 47], Sonogashira coupling [48] has also been explored. The first Stille coupling of α,β-dibromo butenolides was reported by Rossi et al. by using palladium catalyst (Scheme 1.9) [43].
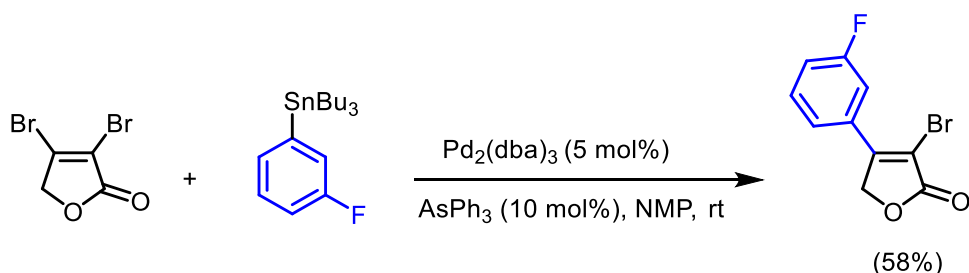
Scheme 1.9 Preparation of 3-halo-4-substituted-2(5*H*)-furanones *via* Stille coupling reaction [43]

Synthesis of α-halo-β-substituted butenolides have also been reported by a Pd/Cu-catalyzed Sonogashira reaction involving treatment of terminal alkynes with α,β-dihalo butenolides (Scheme 1.10) [48]. Latter, Boukouvalas et al. reported the use of Sonogashira coupling of β-bromotetronic acid in the synthesis of the natural product cleviolide [49].
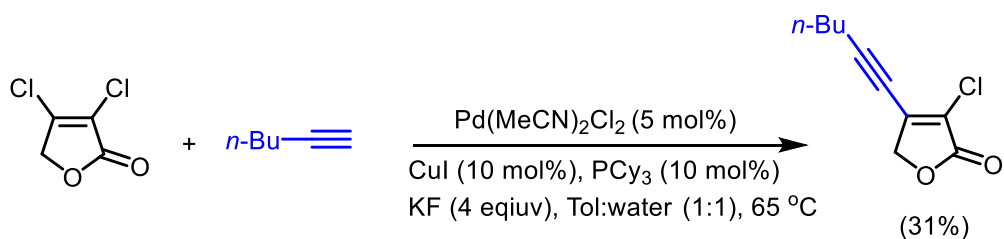
Scheme 1.10 Preparation of α-halo-β-(1-alkynyl) butenolides *via* Sonogashira coupling reaction [48]

In addition, it is important to note that a few relevant simple 4-(1-alkynyl)-2(5*H*)-furanones have also been prepared *via* different coupling reactions, notably by palladium-catalyzed cross-coupling reaction of β-tetronic acid bromide with tributylstannylacetylenes [50, 51], 1-alkynylzinc chlorides [52], and potassium alkynyltrifluoroborates [53].

Synthesis of Tetronamides

Tetronamides, commonly referred as 4-amino-2(5*H*)-furanones, are an important class of β-heterosubstituted butenolides that has attracted growing attention from synthetic and medicinal chemists alike [54, 55]. Synthesis of tetronamides are commonly based on the nucleophilicity of the enamine function [56], including *N*-bromosuccinimide promoted cyclization of enaminoesters [57]. In addition, preparation of enantio-enriched tetronamides have been reported *via* diastereoselective alkylation of lithium enolates of vinylogous urethanes [58], as well as *via* enantioselective alkyne additions to aldehydes using (*S*)-BINOL for the chiral induction followed by conjugate addition of an amine; the latter method afforded β-amino butenolides with 84−90% *ee* (Scheme 1.11) [59].
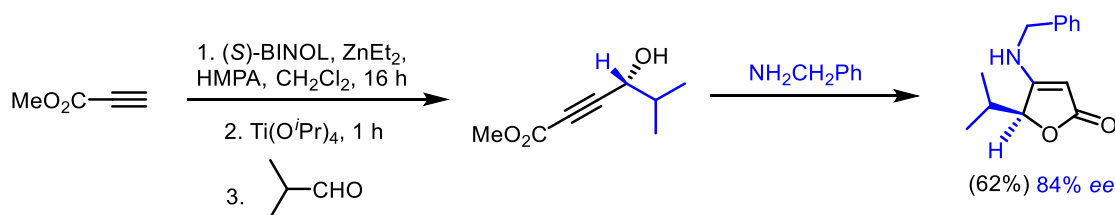
Scheme 1.11 Preparation of enantioselective tetronamides by using (*S*)-BINOL as a catalyst [59]

A particular class of synthetically useful α-halotetronamides is also synthesized by the direct halogenation of a preformed enaminone [59-61] or by employing the aza-Michael addition/elimination reaction of mucohalic acids (Scheme 1.12) [62, 63].
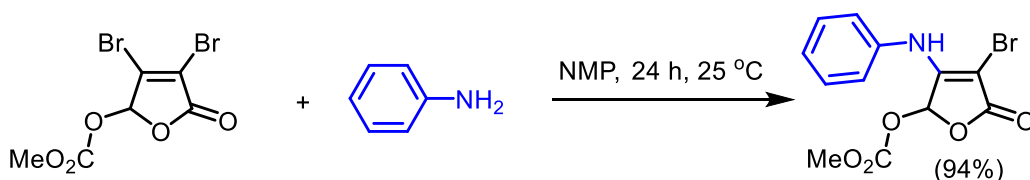
Scheme 1.12 Preparation of α-halo tetronamides *via* aza-Michael addition/elimination reaction [62]

Recently, a report revealed that the synthesis enantioenriched tetronamides could be achieved from *O*-(α-bromoacyl) cyanohydrins *via* Blaise intramolecular cyclizations [64].

Vinylogous Aldol Reactions

The vinylogous aldol reaction (VAR), carried our either directly from butenolides or, *via* conversion to the corresponding 2-silyloxyfurans (Mukaiyama variant; VMAR), represents one of the most widely explored avenues for installing a γ−carbon substituent [65-68]. Much effort has been devoted in recent years in controlling the relative and absolute stereochemistry of the newly formed stereogenic centers [69-78], [79-82]. To date, several heterosubstituted butenolides, including tetronates, have been utilized as substrates in VA reactions. The first catalytic asymmetric aldol reaction reported in 2003, between the reaction of trimethylsiloxyfuran with achiral aldehydes in the presence of BINOL/Ti(O^{i}Pr)$_4$ complex [83]. Subsequently, several asymmetric VMA and VA reactions developed for 2-silyloxyfurans and γ-butenolides using different organocatalysts [84]. For example, an asymmetric, bifunctional alkaloid thiourea organocatalyzed (Catalyst III) VMA reaction of 2-(trimethylsilyloxy)furan [85] and unactivated γ-butenolides [80] with aldehydes was developed with high enantioselectivities and anti-selectivities (Scheme 1.13).
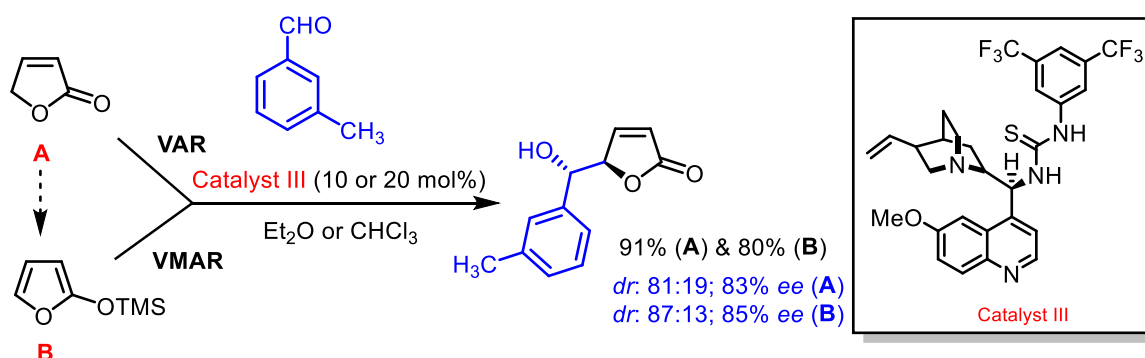
Scheme 1.13 Enantioselective vinylogous aldol reaction of butenolides [80, 85]

Lately, several new approaches for the stereo-selective VMAR and VAR of 2-silyloxyfurans and γ-butenolides catalyzed by simple base, e.g. trimethylamine [75], BF$_3$·OEt$_2$ [86], Bi(OTf)$_3$.4H$_2$O [87] and by organocatalysts, e.g. axially chiral guanidine base [88], tryptophan derived bifunctional organocatalyst [89], bifunctional aminothiourea and aminosquaramide organocatalysts [90], chiral ammonium amide (generated *in situ* from chiral ammonium aryloxide and BSA) [91] has been developed.

Vinylogous Mannich Reactions

Stereoselective vinylogous Mannich reactions are of significant utility in organic synthesis. A vinyl insertion Mannich reaction generates a new C−C bond and leads to the formation of δ-amino α,β-unsaturated carbonyl compounds. In 1999, Martin and Lopez

reported a method (Ti-catalyzed) for addition of siloxyfurans to 2-aminophenolderived imines; reactions proceeded in 40–92% *de* and up to 54% *ee* [92]. Terada and co-workers have outlined an enantioselective (up to 97% *ee*) protocol for Brønsted acid catalyzed Friedel–Crafts reactions of *N*-Boc aldimines with 2-methoxyfuran. Enantiomerically enriched furan-2-yl-amines may be oxidized to afford alkylamine-substituted γ-butenolides by a two-step sequence that generates the carbinol stereogenic center with moderate diastereoselectivity (70% *de*) [93]. Subsequently, a high diastereo- and enantioselective protocol for catalytic asymmetric vinylogous Mannich reaction has been reported *via* Ag-catalyst and a chiral phosphine ligand (Scheme 1.14) [94].
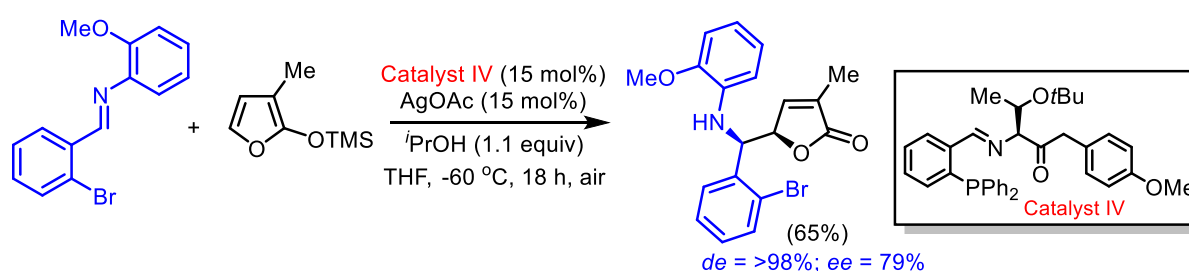
Scheme 1.14 Ag-catalyzed asymmetric vinylogous Mannich reactions with siloxyfurans [94]

Generally, the utilization of 2-silyloxyfuran as the nucleophile for vinylogous Mannich reaction catalyzed by transition metal catalysts [95-97] and chiral phosphoric acids [93] has been well reported. However, the direct asymmetric vinylogous Mannich reaction of butenolide derivatives has drawn enough attention recently. Shibasaki's group reported the first direct asymmetric Mannich-type reactions of γ-butenolides catalyzed by a chiral lanthanumpyridine bisoxazolinecomplex [98]. More recently, the same group developed another direct catalytic asymmetric vinylogous Mannich-type reaction of ketimines. Activation of the *N*-thiophosphinoyl group by a soft Lewis acid was the key to achieve the enantioselective addition of the dienolate generated *in situ* to unreactive ketimine substrates
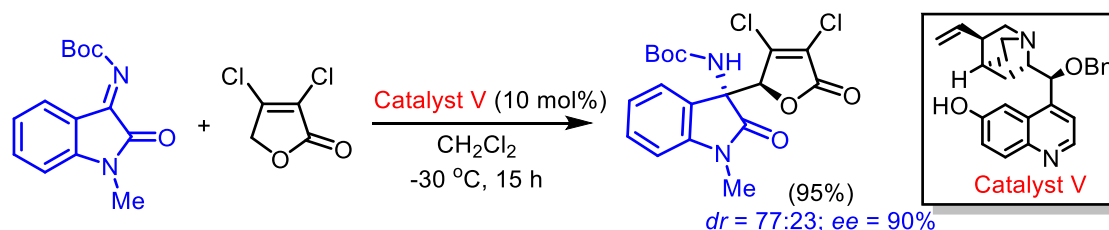
Scheme 1.15 Direct asymmetric vinylogous Mannich reaction of γ-butenolides [101]

[99]. Another relevant example of direct asymmetric vinylogous Mannich reaction of γ-butenolide with various ketimines by using a new cinchona alkaloid amide catalyst and Lewis

acid Zn(OTf)$_2$ has been reported [100]. Recently, the first direct asymmetric vinylogous Mannich reaction of α,β-dihalo butenolides with isatin-derived ketimines was developed by a bifunctional quinidine-derived catalyst (Catalyst V) with broad substrates scope and high enantioselectivity (Scheme 1.15) [101].

In addition, a series of γ-butenolides was obtained in good yields and enantioselectivities *via* a direct vinylogous Mannich reaction of aldimines with α,β-dihalo butenolides catalyzed by quinine [102]. Interestingly, a direct asymmetric vinylogous Mannich-type reaction of aldimines with non-activated α-angelica lactone has been successfully developed by using a new *N,N*-dioxide ligand and Sc(OTf)$_3$ catalyst [103].

Vinylogous Michael Addition

The Michael addition is one of the most powerful C-C bond forming transformations, and the diversity in donors and acceptors that can be combined is remarkable [104]. The first organocatalytic asymmetric Mukaiyama–Michael reaction of 2-silyloxyfurans was reported by MacMillan [Scheme 1.16 (eq. 1)] [105]. Latter, Trost and co-workers disclosed the first direct use of butenolides in Michael reactions with nitroalkenes under zinc catalyst [Scheme 1.16
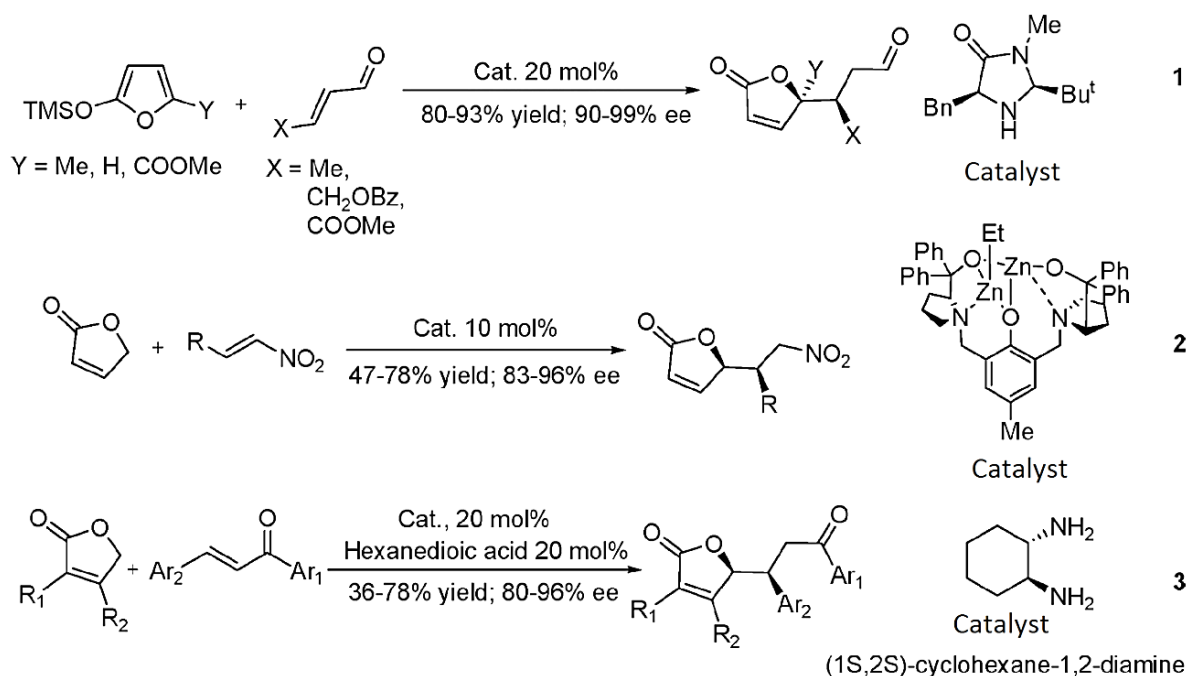
Scheme 1.16 Asymmetric Michael addition reaction for the synthesis of chiral γ- butenolides

(eq. 2)] [104], which avoided the preformation of 2-silyloxyfurans from γ-butenolides. However, in 2010, the first direct organocatalytic asymmetric vinylogous Michael addition

reaction of γ-butenolides to chalcones catalyzed by vicinal primarydiamine salts in good yields, diastereo- and enatioselectivities [Scheme 1.16 (eq. 3)] has been reported [106]. More recently, Terada et al. (1990) demonstrated a high *syn*-diastereo- and enantioselective direct vinylogous Michael addition of α-thio substituted furanones with conjugate nitroalkenes using an axially chiral guanidine base catalyst [107].
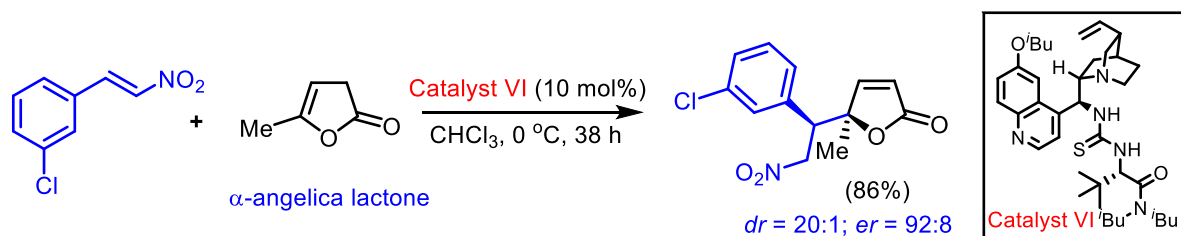
Scheme 1.17 Catalytic asymmetric direct vinylogous Michael reaction of butenolides [108]

Importantly, another direct vinylogous Michael reaction of α-angelica lactone and other deconjugated butenolides with nitroalkenes has been developed with quinine-derived thiourea based bifunctional organocatalyst (Catalyst VI). This approach allowed the synthesis of densely functionalized γ-butenolides with contiguous quaternary and tertiary stereocenters in high yields with excellent diastereo- and enantioselectivity (Scheme 1.17) [108].

3. Butenolides: Perspectives in Total Synthesis

A large number of butenolides are widespread in nature – found in sponges, fungus, lichens, and molds, as well as in higher plants, to name a few. Many of them exhibit a wide array of biological properties such as antibiotic, antitumor, anticoagulant, antiepileptic, antifungal, insecticidal, and anti-inflammatory activities. In certain butenolide natural products, the five-membered butenolide core constitutes the main structural feature of the molecule, while in others, butenolide is fused to more complex structural motifs such as alkaloids, macrolides, terpenoids, etc. The synthetic work on this class of natural products has resulted in numerous efficient methodologies towards functionalized butenolides, as well to several total syntheses, some of which are classical examples of synthetic ingenuity.

3.1. Synthesis of the Natural Products from Butenolide Building Blocks

Jiadifenolide is a sesquiterpenoid natural product, bearing butyrolactone core unit, with neurotrophic activity, found in *Illicium jiadifengpi* [109]. Its biological activity and congested polycyclic structure have made it a popular target for total synthesis. The first synthesis of jiadifenolide was reported by Paterson group in 23 steps with 2.3% overall yield, showing a pivotal SmI$_2$-mediated reductive cyclization reaction to establish the tricyclic core [110]. However, in 2015, a protecting-group-free total synthesis of (−)-jiadifenolide was accomplished in 15 steps with an overall yield of 7.9% from (+)-pulegone [111]. The key steps include a SmI$_2$/H$_2$O-mediated stereoselective reductive cyclization, an unprecedented formal [4+1] annulative tetrahydrofuran-forming reaction and programmed redox manipulations. Probably the most important synthesis of (−)-jiadifenolide has been reported
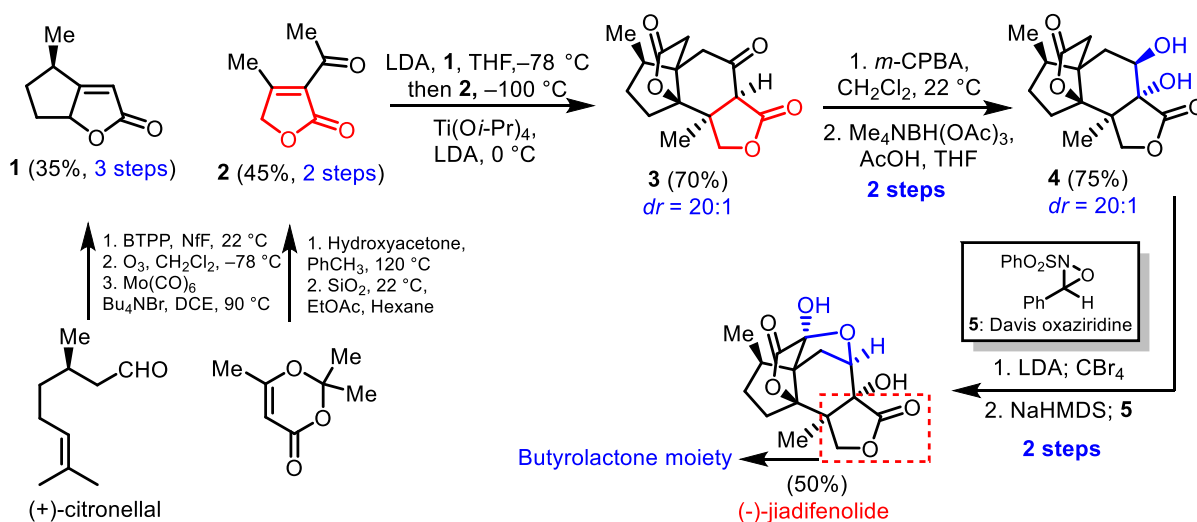
Scheme 1.18 Shenvi's total synthesis of (−)-jiadifenolide from butenolide building blocks **1** and **2** [112]

By Shenvi's research group where they obtained a gram-scale quantity of (−)-jiadifenolide just in eight steps [112]. The reported synthetic route relies on a stereoselective coupling of two simple butenolides to build the entire skeleton of (−)-jiadifenolide just in one step (Scheme 1.18). Most recently, a new strategy to access the (−)-jiadifenolide has been reported [113]. For the construction of the tricyclic core of the (−)-jiadifenolide structure, an unusual intramolecular diastereoselective Nozaki−Hiyama−Kishi reaction involving a ketone as electrophilic coupling partner was developed.

3.2.   Synthesis of the Butenolide Core Bearing Natural Products

Among the several possible natural compounds bearing the butenolide core is **dysidiolide**, a sesterterpenoid isolated in 1996 from the Caribbean sponge *Dysidea etheria de Laubenfels*, exhibits antitumor activity at the micromolar level, and most importantly, it is the first natural product discovered so far to inhibit protein phosphatase cdc25A (IC$_{50}$ = 9.4 µM) [114]. Dysidiolide possesses a unique molecular architecture with a hydrophobic bicyclo[4.4.0]decane structural subunit having an unprecedent side chain in the top half and a hydrophilic hydroxybutenolide in the bottom. Interestingly, the hydrophobic and hydrophilic side chains are in close proximity. Owing to its unique properties, the synthesis of dysidiolide attracted the attention of many research groups worldwide. However, the first total synthesis of the dysidiolide was reported by Corey's research group [115]. Corey used the
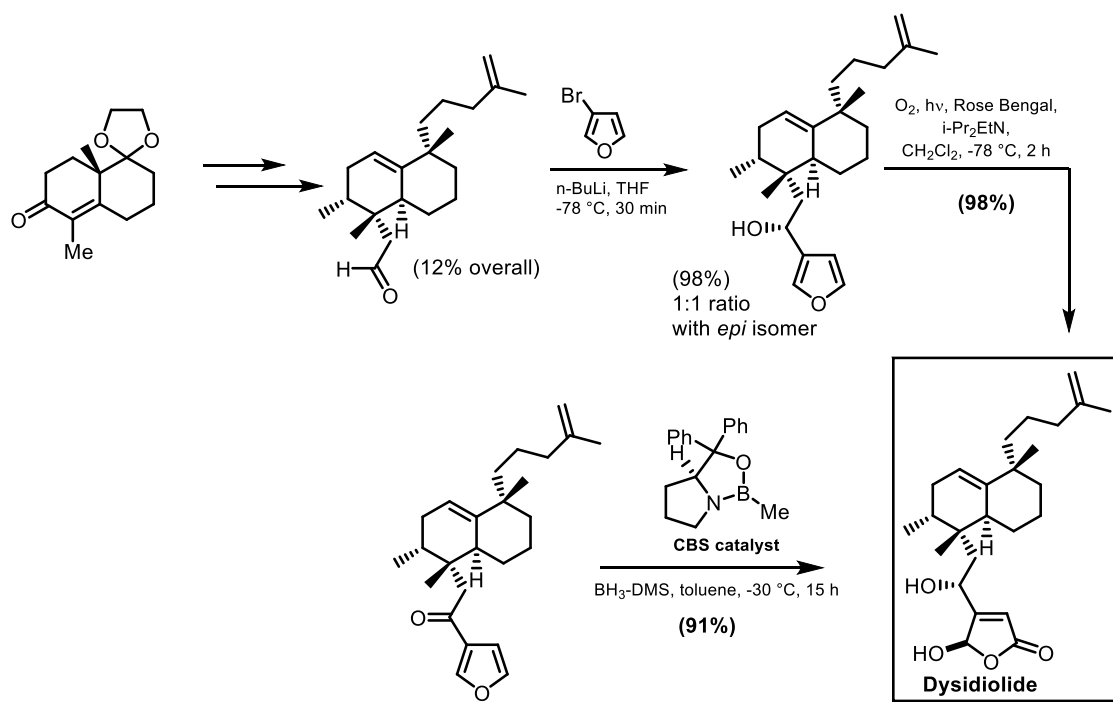
Scheme 1.19 Corey's total synthesis of dysidiolide [115]

enantiomerically pure Wieland–Miescher ketone as a decalin template and a cationic rearrangement as the key step to produce the fully substituted bicyclic core of the natural product (Scheme 1.19). Then, a enantioselective Corey-Bakshi-Shibata (CBS) reduction by using a borane-dimethylsulfide complex provided enantiopure dysidiolide. In 1998, Boukouvalas research group [116] used Diels–Alder cycloadditions to construct the core bicyclic ring system of dysidiolide. Importantly, in the same year Danishefsky's group reported a racemic dysidiolide synthesis [117]. In Danishefsky's approach to the core bicyclic ring system of dysidiolide was installed *via* diastereoselective Diels–Alder reaction of a transient dioxolenium dienophile and chiral vinylcyclohexene. The triene was prepared from α-quaternary ketone (±) in racemic form (Scheme 1.20).
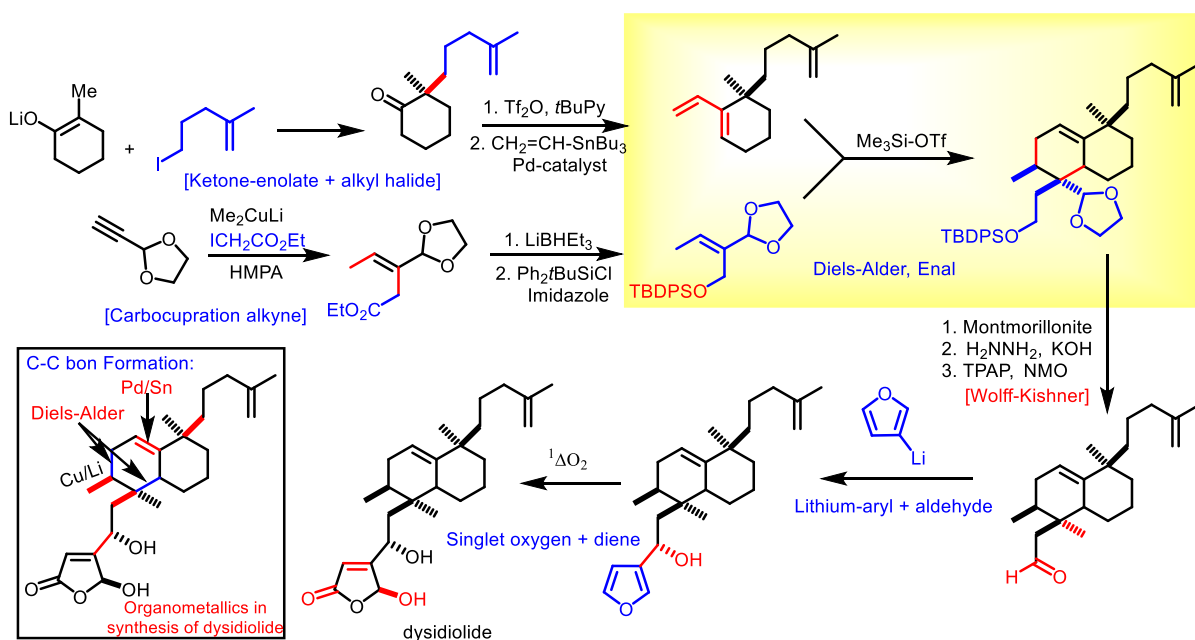
Scheme 1.20 Danishefsky's total synthesis of dysidiolide [117]

Subsequently, several syntheses employed Diels-Alder reactions (either inter- or intra-molecular) as key transformations in the overall synthetic pathways [118-123]. Moreover, some alternative synthesis of dysidiolide also has been reported by several research groups. Among of them, a quite different approach has been demonstrated by Piers et al. [124]. The key steps include Ozonolytic cleavage, Mitsunobu reaction, Eschenmoser-Claisen rearrangement, and Magnus-Roy protocol. The racemic dysidiolide was also achieved with a high level of intramolecular stereoinduction *via* regioselective photooxidation-fragmentation of an incorporated furan moiety [125]. Another study reported the synthesis of dysidiolide from an acyclic precursor by using alkylations of a nitrile with different electrophiles and an efficient enyne metathesis [126]. More recently, Yoshimitsu's research group developed a stereoconvergent approach to enantiomerically pure quaternary

carbocycles through the sequence of asymmetric side chain construction followed by remote stereoinduction and repotred a formal synthesis of dysidiolide by using this strategy [127].

Rubriflordilactones **A** and **B**, two novel highly unsaturated rearranged bis-nortriterpenoid natural products have been isolated from the leaves and stems of Chinese herbal plants *Schisandra rubriflora* [128]. Due to the promising levels of anti-HIV activity, the synthesis of rubriflordilactones has attracted global attention. However, the first synthesis of
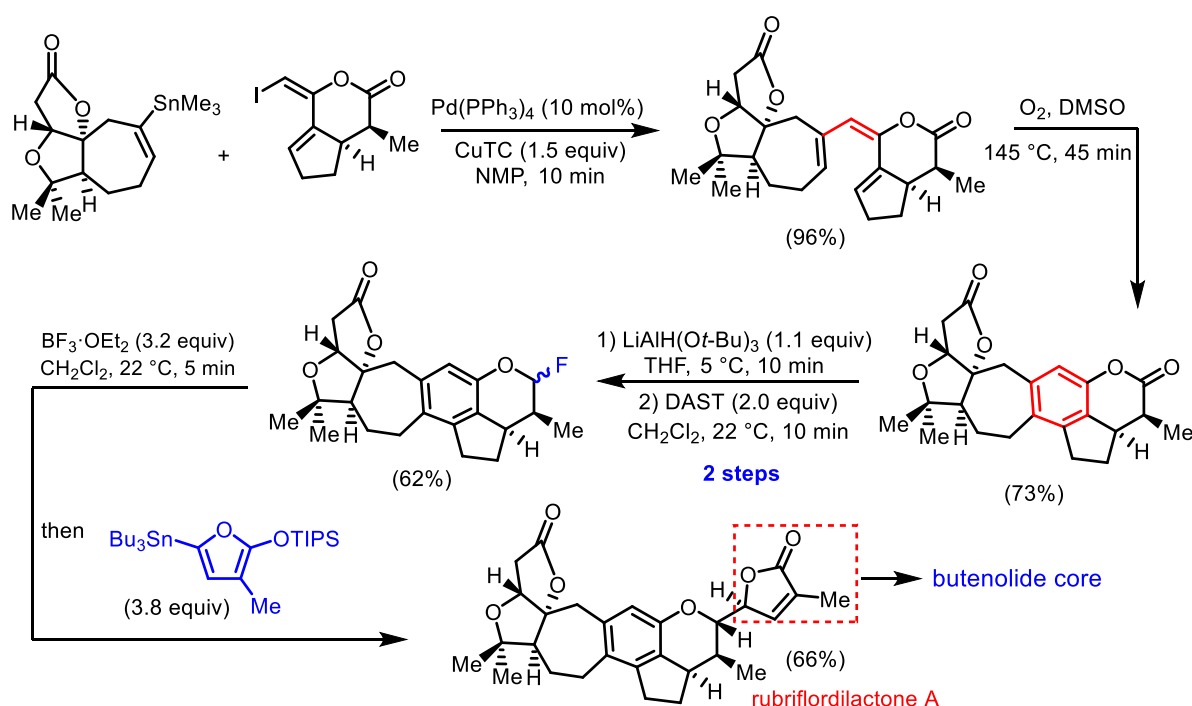
Scheme 1.21 Li's total synthesis of rubriflordilactone A [129]

enantiopure rubriflordilactone A has been reported by Li et al. in 2014, by using a one-pot 6π-electrocyclization/oxidative aromatization as the key step. Next, a vinylogous Mukaiyama aldol reaction installed the butenolide side chain at the final stage (Scheme 1.21) [129]. More recently, Anderson's research group reported a new enantioselective syntheses of rubriflordilactone A in a highly convergent manner which use palladium- or cobalt-catalyzed ring cyclizations as the key step [130]. In 2016, taking the advantage of 6π-electrocyclization–aromatization strategy, Li research group also reported the first synthesis of rubriflordilactone B, a heptacyclic Schisandraceae bis-nortriterpenoid featuring a tetrasubstituted arene moiety (Scheme 1.22) [131]. During the synthesis, it was observed, the Sonogashira–hydrosilylation–electrocyclization–aromatization sequence could be streamlined as a general approach towards the synthesis of pentasubstituted arenes bearing silyl groups as versatile handles.
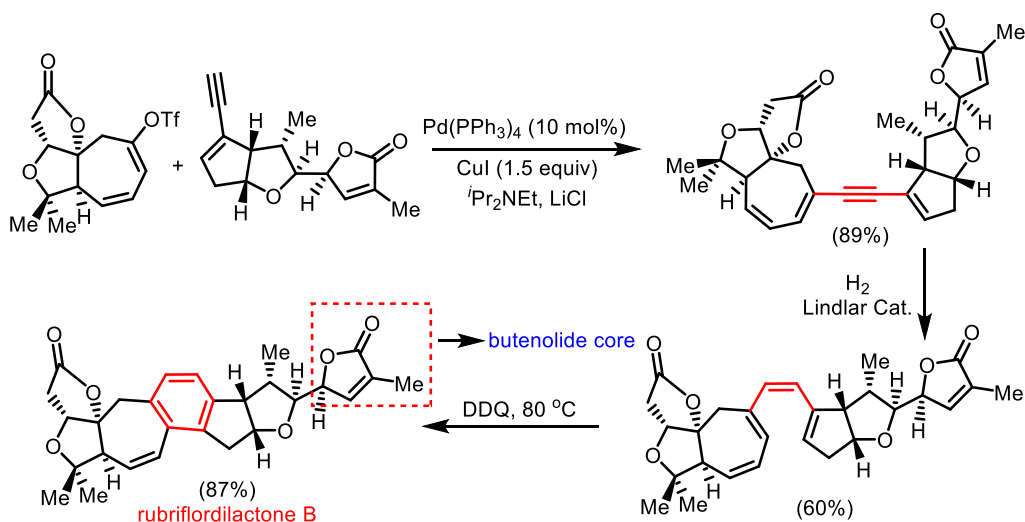
Scheme 1.22 Li's total synthesis of rubriflordilactone B [131]

Cadiolides comprise a group of noncytotoxic, densely functionalized butenolides isolated in 1998 and 2012 from Indonesian and Korean ascidians, respectively [132-134]. The first synthesis of cadiolide B was reported in 2005 by the Boukouvalas group [135]. Since then, a formal synthesis of cadiolide A, B and C has been reported, notably by Frank and co-workers [136, 137]. More recently, a new step-economical synthesis of cadiolide A, B and D has been reported by Boukouvalas group (Scheme 1.23) [138].
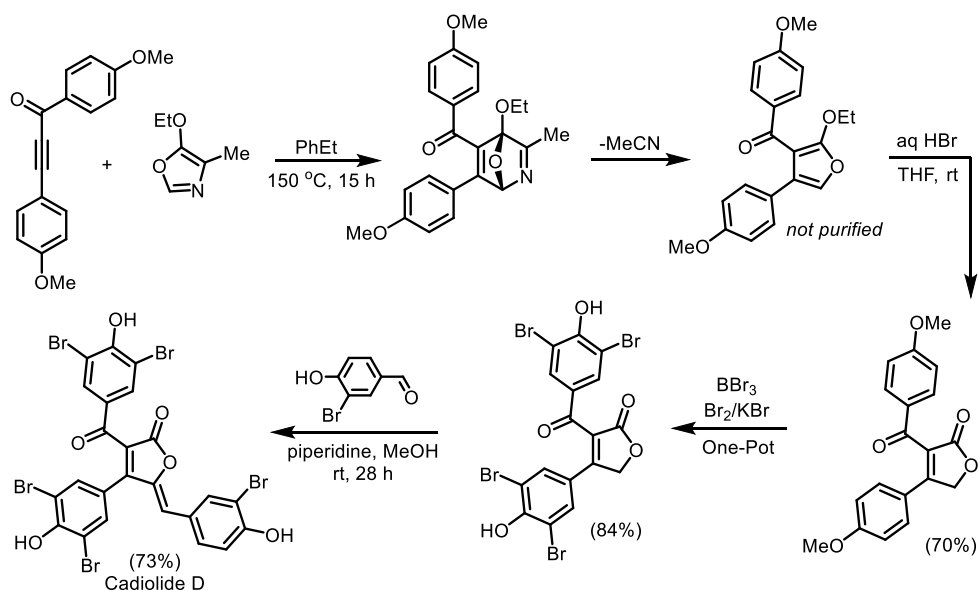
Scheme 1.23 Boukouvalas total synthesis of cadiolide D [138]

The key steps of Boukouvalas cadiolide synthesis includes a one-pot assembly of a key β-aryl-α-benzoylbutenolide building block by regiocontrolled "click−unclick" oxazole−ynone Diels−Alder cycloaddition/cycloreversion and ensuing 2-alkoxyfuran hydrolysis.

4. Butenolides: Synthesis for Biology, Medicine, and Agrochemicals

Small organic molecules have proven to be invaluable tools for investigating biological systems. To discover and to use more effectively new chemical tools to understand biology, strategies are needed that allow us to systematically explore 'biological-activity space'. Such strategies involve analysing both protein binding of, and phenotypic responses to, small organic molecules. The use of small organic molecules, such as butenolides can complement gene-based methods of perturbing protein function and in some cases, can offer advantages over such methods [139].
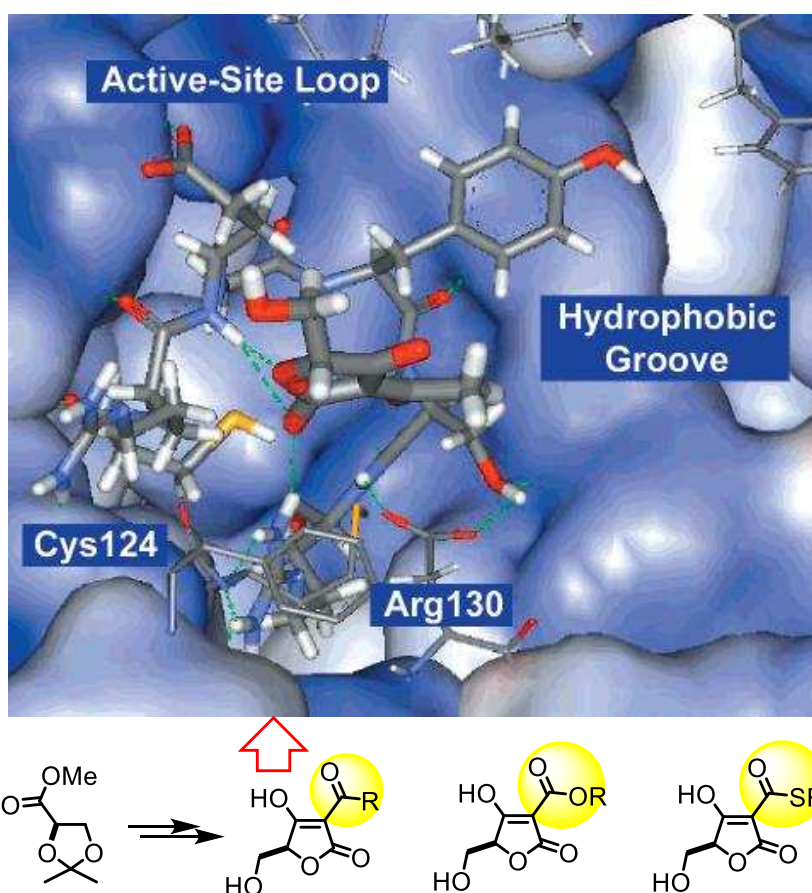
Figure 1.2 3-Acetyl-5-hydroxymethyltetronic acid anion bound to protein phosphatases VHR [140]

In practice, there are two types of chemical libraries that can be synthesized today: 'focused libraries' and 'diversity-oriented libraries'[139]. Focused libraries are designed around a specific piece of a small molecule, known as a scaffold, and are used to target a specific class of proteins. The goal of focused library synthesis is to create analogues of the same core structure to optimize binding to a target or class of targets. If the compounds created are too diverse, they may lose their propensity to interact with the designated target protein. In Figure 1.2, Sodeoka et al. [140] created a collection of acyltetronic acids that act

as phosphate mimetics and so are likely to inhibit phosphatases. Their synthesis resulted in a library of compounds that are identical except for the portion highlighted in yellow. In contrast, diversity-oriented libraries are not targeted to any specific protein class and are often used in broad screens in which the target proteins are not known. Because the goal of diversity-oriented synthesis is to create a maximally diverse collection of compounds, the synthetic planning algorithms required are distinct from those used to create single compounds or focused libraries [139]. So, if we wish to create an 'ideal' chemical library for chemical genetics — one that contains a small-molecule ligand or binding partner for each protein — structures that bind to each protein need to be identified.

Of course, no existing chemical library contains compounds that bind selectively to every protein. Furthermore, there are many proteins for which no small-molecule ligand has yet been identified. Identifying new compounds with differing selectivities, that could bind to novel proteins, typically involves some type of screening experiment in which a library of compounds is assessed for the property of interest.

4.1. From Butenolides to Medicine

Butenolides have long served as an important source of drugs. For example, **Rofecoxib** (Figure 1.3), a nonsteroidal anti-inflammatory drug (NSAID) was identified as a selective COX-2 inhibitor after several functional group modifications of the butenolide core bearing 4-methylsulfonylphenyl series [141, 142]. Selective COX-2 inhibitors are a type of NSAID that directly targets cyclooxygenase-2, an enzyme responsible for inflammation and pain. The drug was marketed by *Merck & Co.* to treat osteoarthritis, acute pain conditions, and dysmenorrhea. It was approved by the U.S. Food and Drug Administration (FDA) on May 20, 1999, and was marketed under the brand names **Vioxx**, **Ceoxx**, and **Ceeoxx**. On September 30, 2004, *Merck* withdrew rofecoxib from the market because of concerns about increased risk of heart attack and stroke associated with long-term, high-dosage use.

More recently, in 2007, **Firocoxib**, another butenolide NSAID of the COX-2 inhibitor, approved as a veterinary medicine, in particular for use in dogs and horses [144, 145]. Firocoxib was the first COX-2 inhibitor approved by the FDA for horses [146]. The drug is marketed by *Merial Ltd.* under the brand names **Equioxx** and **Previcox** for the treatment of pain, and inflammation in animals. Importantly, the drug is not intended or approved for use in human medicine. The synthetic procedure of firocoxib is outlined in Scheme 1.24 [147].
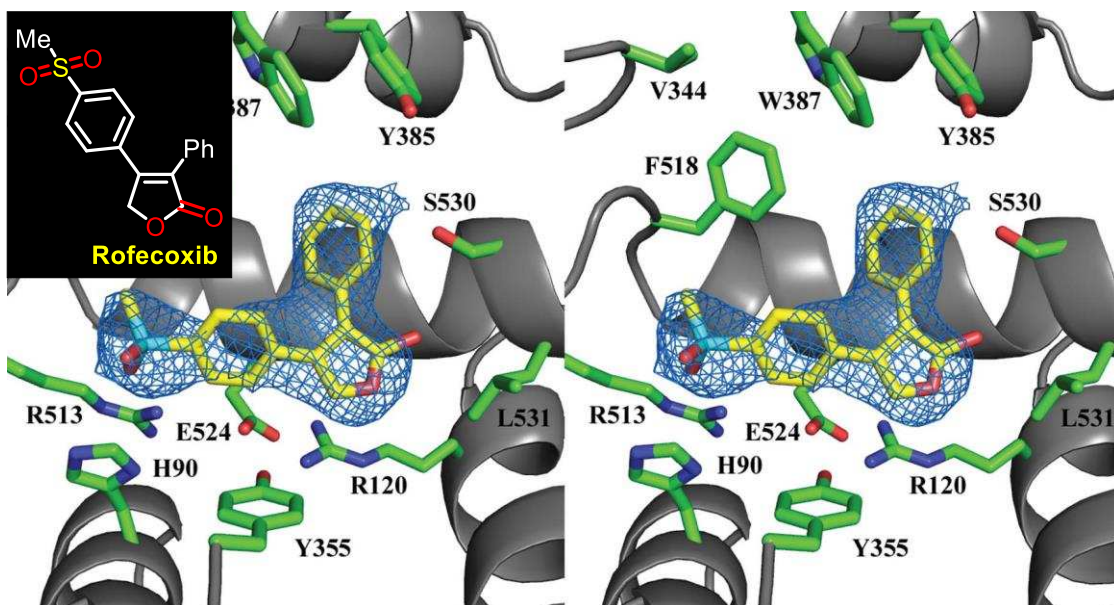
Figure 1.3 Vioxx bound within the cyclooxygenase channel of human COX-2. Stereoview of Vioxx bound within the cyclooxygenase channel of monomer *A* of the huCOX-2–Vioxx crystal structure. $F_o - F_c$ simulated-annealing OMIT electron density (blue) contoured at 3σ is shown with the final refined model of Vioxx (yellow). Residues lining the cyclooxygenase channel are labeled accordingly. C atoms of residues lining the channel are colored green, while N, O and S atoms are colored blue, red and cyan respectively [143].
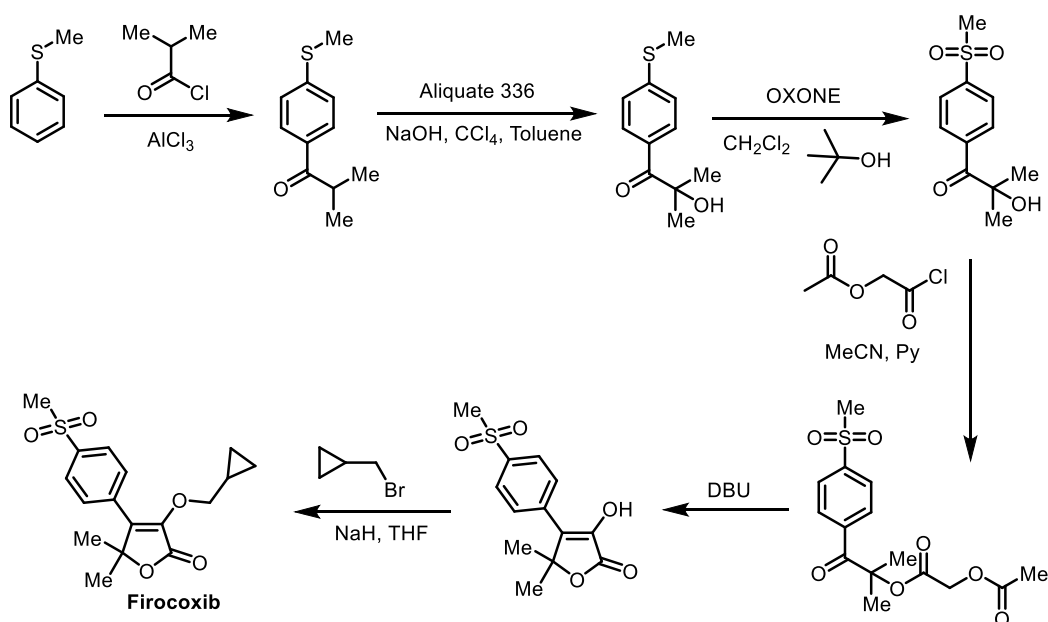
Scheme 1.24 Synthesis of COX-2 inhibitor veterinary medicine firocoxib [147]

Furthermore, it is important to note that apart from the above mentioned NSAID, several steroidal (Figure 1.4; **1**) [148-151] and non-steroidal synthetic drugs [152, 153] with butenolide core structure are either marketed or currently under investigation. Among them,

benfurodil hemisuccinate (Figure 1.4; **2**), a synthetic drug, was previously used for the chronic treatment of congestive heart failure [152]. The tetronate *syn*-aldol product losigamone [153, 154] (Figure 1.4; **3**) is a synthetic antiepileptic drug (AED) that has been investigated as an add-on therapy for the partial seizures.
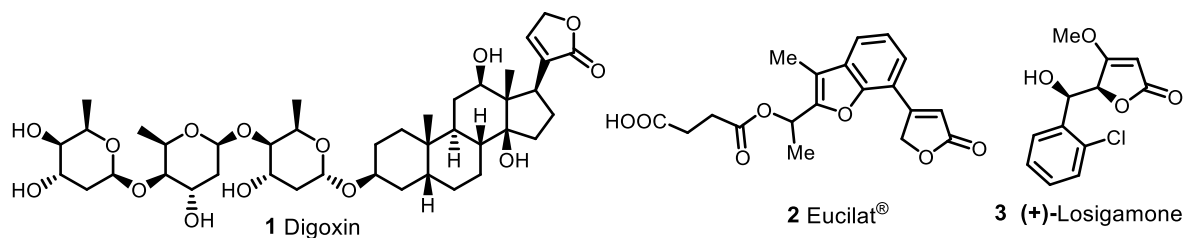
Figure 1.4 Structures of butenolide core bearing drugs Digoxin, Eucilat® and Losigamone

When orally administered, losigamone is well absorbed through the gastrointestinal tract and reaches a peak plasma concentration within two to three hours of administration. Its plasma elimination half-life is approximately four to seven hours [155]. In two double-blind, placebo controlled, add-on studies, losigamone has shown possible effects in patients with partial epilepsy [156, 157]. It is important to note that, the results from both *in vitro* and *in vivo* experiments confirm that excitatory amino acid-mediated processes are involved in the mode of action of (+)-losigamone, whereas (–)-losigamone does not possess such properties.

4.2.   Butenolides in Modern Agrochemical Research

"Agrochemicals, including insecticides, herbicides, and fungicides, play an important role in modern agriculture by increasing both crop quality and yield while reducing labor costs in major crops such as rice, corn, fruits, and vegetables. To meet the increasing demand for food supply due to a growing population as well as increasingly stringent regulatory requirements for protecting the environment and ensuring food safety, new agrochemicals that are more efficacious, and possess novel modes of action and better safety profiles are continuously sought. Typically, a novel agrochemical is invented initially by the discovery of a bioactive lead compound through chemical synthesis followed by modification of the chemical structure and optimization of the biological activity; selection of the commercial candidate may involve consideration of cost, efficacy, selectivity, and safety factors."

— [Chem. Rev. **2014**, 114, 7079]

Usually, new agrochemicals may be obtained by following up an initial bioactive lead compound. The methods for discovering agrochemical lead compounds may be classified as Random Synthesis and Screening, Modification of Natural Compounds, "Me Too Chemistry"

(molecules with similar structures to existing products), Combinatorial Chemistry, and Rational Design. Statistical data of agrochemical discovery methods show that Random Synthesis and Screening and "Me Too Chemistry" have been the two most successful approaches for new product discovery. Recently, new approaches, e.g. Chemical Genetics, Fragment based or Molecule-based Design, Target-oriented Synthesis, and Diversity-oriented Synthesis, for lead discovery have been proposed in the agrochemical field [158].

Very recently, inspired by the stemofoline, a nAChR agonist isolated from the *Stemona japonica,* lactone "head group" as a topological pharmacophore pattern and molecular modelling investigations by using structural features of relevant nAChR agonists, a new bioactive scaffold was identified by *Bayer* (Figure 1.5) [159]. A nicotinic agonist is a drug that mimics the action of acetylcholine (ACh) at nicotinic acetylcholine receptors (nAChRs).The nAChR is named for its affinity for nicotine. Examples include nicotine, acetylcholine, choline, epibatidine, lobeline, varenicline, and cytisine. The nAChR has been an insecticide molecular target site of growing importance for many years, which plays an important role in the mediation of fast excitatory synaptic transmission in the insect central nervous system (CNS.
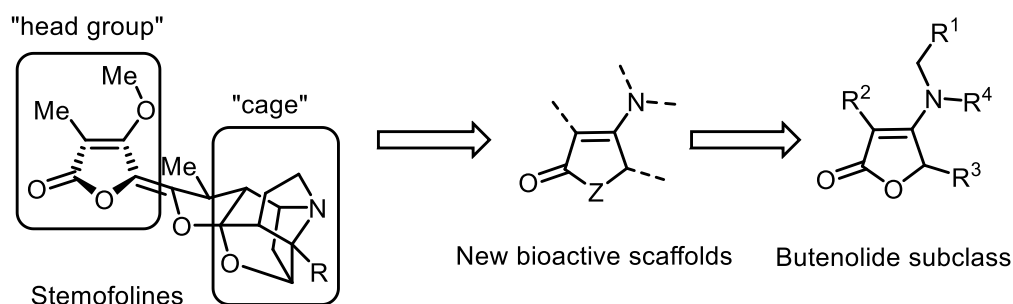
Figure 1.5 Lactone "head group" of stemofoline alkaloids (R = *n*-Bu, —CH=CHEt) and structural features of relevant nAChR agonists as sources for the identification of the new bioactive scaffold containing in the butenolide subclass [159, 160].

The selection of the 2,2-difluoroethyl chemical moiety resulted in the discovery of the highly potent butenolide insecticide flupyradifurone (Sivanto™). The synthetic procedure for the preparation of flupyradifurone (FPF) is outlined in Figure 1.6 [159]. The butenolide insecticide FPF acts selectively on the insect CNS as a partial agonist of postsynaptic nAChRs and binds to the ACh binding site. Based on a structural model of CYP6CM1vQ from *B. tabaci*, molecular docking studies with FPF was reported (Figure 1.6) [160]. Cluster analysis of FPF binding poses revealed 23 clusters of interaction poses within the CYP6CM1vQ cavity model (Figure 1.6). In summary, the 23 docking poses of FPF appear quite similar with respect to the overall orientation within the active site [160].
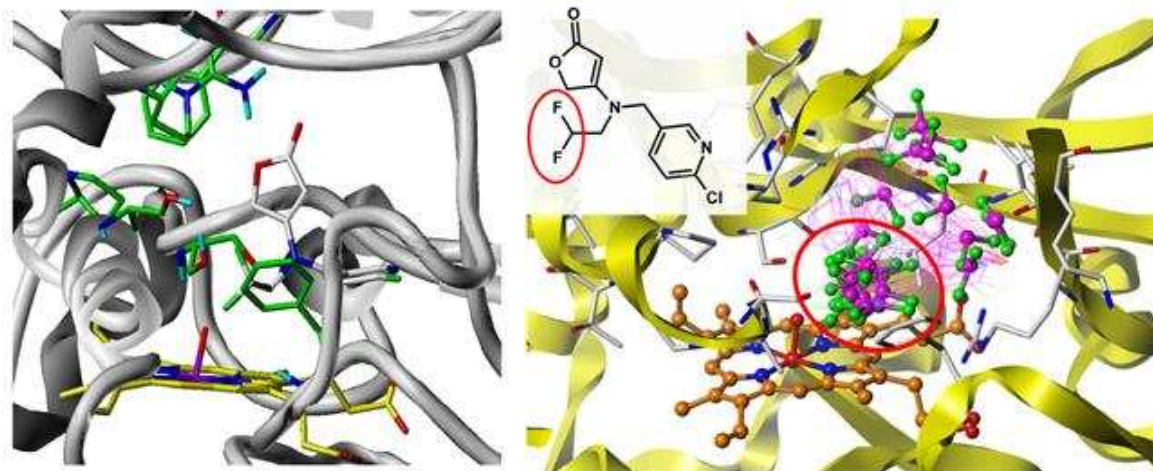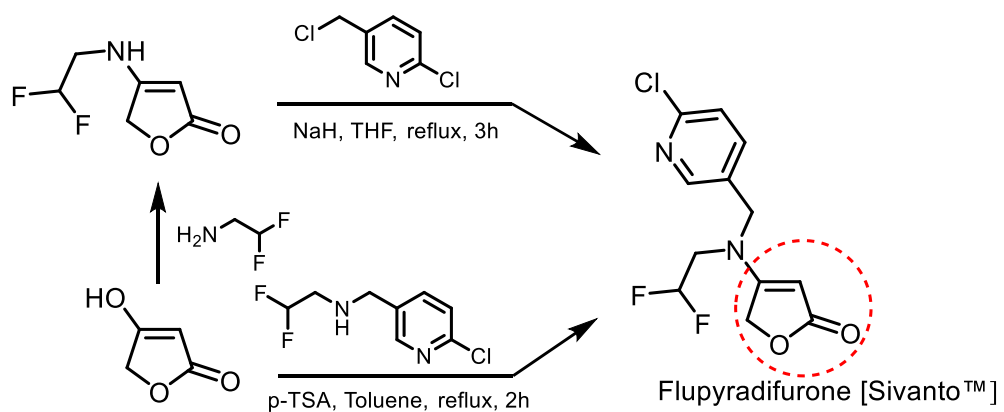
Figure 1.6 Commercial synthesis of FPF; Molecular docking studies of FPF within the CYP6CM1vQ cavity model and Cluster analysis of FPF binding poses [159, 160].

5. Objectives and Outline of Thesis

Taking into account the interesting biological and synthetic potential associated with the tetronamides and other butenolides, there are two clear objectives in this thesis:

[1] Development of synthetic methodologies for the stereoselective synthesis of γ-substituted tetronamides and the investigation of their possible biological activities.

[2] Total synthesis of biologically active rubrolides and their synthetic analogous as an effort to discover new medicines and agrochemicals.

Tetronamide aldol products logically belong to the central position of two unique molecules; losigamone, an experimental antiepileptic drug and sivanto, a newly developed insecticide (Scheme 1.25). On other hand, the synthetic methodologies to access stereoselective tetronamide aldol products are few and far between. Thus, the first part of the project aimed to develop a robust synthetic strategy to access highly stereoselective tetronamide aldol products by using a direct VA reaction as illustrated in Scheme 1.25.
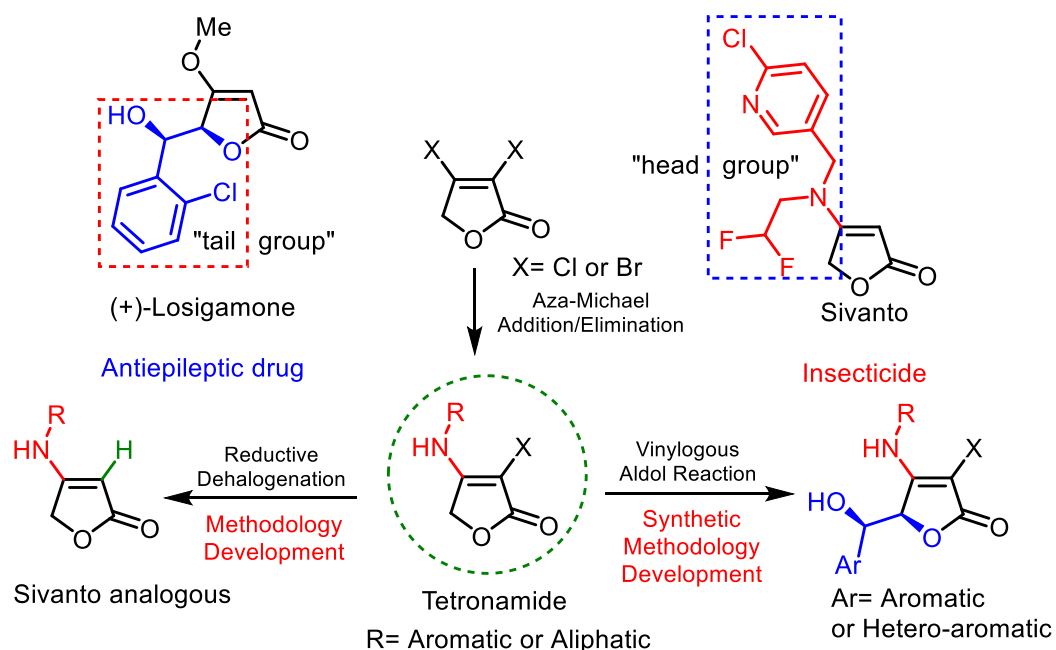
Scheme 1.25 Proposed synthetic stratagies to the synthesis of potential tetronamide derivatives

The final part of the project directed to the total synthesis of biologically active marine natural products, rubrolides and their synthetic analogous as an effort in the search for new drugs and agrochemicals (Scheme 1.26).
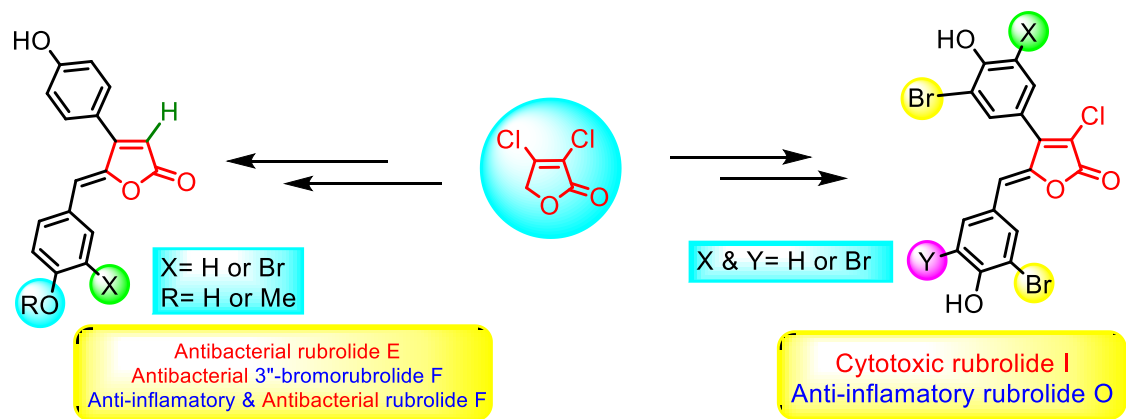
Scheme 1.26 Proposed total synthesis of biologically active marine natural products, rubrolides

The figure contains the following labels:

Left structure:
HO
H
O
RO
X
X= H or Br
R= H or Me

Antibacterial rubrolide E
Antibacterial 3"-bromorubrolide F
Anti-inflamatory & Antibacterial rubrolide F

Center:
Cl   Cl
O

Right structure:
HO
X
Br
Cl
O
Y
Br
HO
X & Y= H or Br

Cytotoxic rubrolide I
Anti-inflamatory rubrolide O

6. References and Notes

[1] KNIGHT, D. W. Synthetic approaches to butenolides. Contemp. Org. Synth., v. 1, p. 287-315, **1994**.

[2] HAKIMELAHI, G. H.; MEI, N.-W.; MOOSAVI-MOVAHEDI, A. A.; DAVARI, H.; HAKIMELAHI, S.; KING, K.-Y.; HWU, J. R.; WEN, Y.-S. Synthesis and Biological Evaluation of Purine-Containing Butenolides. J. Med. Chem., v. 44, p. 1749-1757, **2001**.

[3] HAKIMELAHI, G. H.; MOOSAVI-MOVAHEDI, A. A.; SAMBAIAH, T.; ZHU, J.-L.; ETHIRAJ, K. S.; PASDAR, M.; HAKIMELAHI, S. Reactions of purines-containing butenolides with l-cysteine or N-acetyl-l-cysteine as model biological nucleophiles: a potent mechanism-based inhibitor of ribonucleotide reductase caused apoptosis in breast carcinoma MCF7 cells. Eur. J. Med. Chem., v. 37, p. 207-217, **2002**.

[4] FLEMATTI, G. R. A Compound from Smoke That Promotes Seed Germination. Science, v. 305, p. 977-977, **2004**.

[5] LIGHT, M. E.; DAWS, M. I.; VAN STADEN, J. Smoke-derived butenolide: Towards understanding its biological effects. S. Afr. J. Bot., v. 75, p. 1-7, **2009**.

[6] WEI, M.-X.; FENG, L.; LI, X.-Q.; ZHOU, X.-Z.; SHAO, Z.-H. Synthesis of new chiral 2,5-disubstituted 1,3,4-thiadiazoles possessing γ-butenolide moiety and preliminary evaluation of in vitro anticancer activity. Eur. J. Med. Chem., v. 44, p. 3340-3344, **2009**.

[7] LIGHT, M. E.; BURGER, B. V.; STAERK, D.; KOHOUT, L.; VAN STADEN, J. Butenolides from Plant-Derived Smoke: Natural Plant-Growth Regulators with Antagonistic Actions on Seed Germination. J. Nat. Prod., v. 73, p. 267-269, **2010**.

[8] RAO, Y. S. Chemistry of Butenolides. Chem. Rev., v. 64, p. 353-388, **1964**.

[9] ZHANG, J.; SARMA, K.; CURRAN, T. Recent Progress in the Chemistry of Mucohalic Acids: Versatile Building Blocks in Organic Synthesis. Synlett, v. 24, p. 550-569, **2013**.

[10] SIMONIS, H. Ber. Dtsch. Chem. Ges., v. 32, p. 2085, **1899**.

[11] SIMONIS, H. Ber. Dtsch. Chem. Ges., v. 34, p. 509, **1901**.

[12] MOWRY, D. T. Mucochloric Acid. I. Reactions of the Pseudo Acid Group. J. Am.Chem. Soc., v. 72, p. 2535-2537, **1950**.

[13] HACHIHAMA, Y.; SHONO, T.; IKEDA, S. Chlorination of Furfural in Concentrated Hydrochloric Acid. J. Org. Chem., v. 29, p. 1371-1373, **1964**.

[14] ZHANG, J.; ZHANG, Y. Reinvestigation of Mucohalic Acids: Recent Development and Application in Drug Discovery. Chinese J. Org. Chem., v. 33, p. 409, **2013**.

[15] WANG, J.; LIU, X.; HU, B.; LU, G.; WANG, Y. Efficient catalytic conversion of lignocellulosic biomass into renewable liquid biofuels via furan derivatives. RSC Adv., v. 4, p. 31101, **2014**.

[16] ROSSI, R.; BELLINA, F. An Efficient and Inexpensive Multigram Synthesis of 3,4-Dibromo- and 3,4-Dichlorofuran-2(5H)-one. Synthesis, v. 2007, p. 1887-1889, **2007**.

[17] MAJO, V. J.; PRABHAKARAN, J.; SIMPSON, N. R.; VAN HEERTUM, R. L.; MANN, J. J.; DILEEP KUMAR, J. S. A general method for the synthesis of aryl [11C]methylsulfones: Potential PET probes for imaging cyclooxygenase-2 expression. Bioorg. Med. Chem. Lett., v. 15, p. 4268-4271, **2005**.

[18] GUERRERO, M. D.; AQUINO, M.; BRUNO, I.; TERENCIO, M. C.; PAYA, M.; RICCIO, R.; GOMEZ-PALOMA, L. Synthesis and Pharmacological Evaluation of a Selected Library of New Potential Anti-inflammatory Agents Bearing the γ-Hydroxybutenolide Scaffold: a New Class of Inhibitors of Prostanoid Production through the Selective Modulation of Microsomal Prostaglandin E Synthase-1 Expression. J. Med. Chem., v. 50, p. 2176-2184, **2007**.

[19] BARBOSA, L. C. A.; MALTHA, C. R. A.; LAGE, M. R.; BARCELOS, R. C.; DONÀ, A.; CARNEIRO, J. W. M.; FORLANI, G. Synthesis of Rubrolide Analogues as New Inhibitors of the Photosynthetic Electron Transport Chain. J. Agric. Food Chem., v. 60, p. 10555-10563, **2012**.

[20] VAREJAO, J. O. S.; BARBOSA, L. C. A.; MALTHA, C. R. A.; LAGE, M. R.; LANZNASTER, M.; CARNEIRO, J. W. M.; FORLANI, G. Voltammetric and Theoretical Study of the Redox Properties of Rubrolide Analogues. Electrochim. Acta, v. 120, p. 334-343, **2014**.

[21] PEREIRA, U. A.; BARBOSA, L. C. A.; MALTHA, C. R. A.; DEMUNER, A. J.; MASOOD, M. A.; PIMENTA, A. L. Inhibition of Enterococcus faecalis biofilm formation by highly active lactones and lactams analogues of rubrolides. Eur. J. Med. Chem., v. 82, p. 127-138, **2014**.

[22] PEREIRA, U. A.; BARBOSA, L. C. A.; DEMUNER, A. J.; SILVA, A. A.; BERTAZZINI, M.; FORLANI, G. Rubrolides as Model for the Development of New Lactones and Their Aza Analogs as Potential Photosynthesis Inhibitors. Chem. Biodivers., v. 12, p. 987-1006, **2015**.

[23] BASSETTI, M.; D'ANNIBALE, A.; FANFONI, A.; MINISSI, F. Synthesis of α,β-Unsaturated 4,5-Disubstituted γ-Lactones via Ring-Closing Metathesis Catalyzed by the First-Generation Grubbs' Catalyst. Org. Lett., v. 7, p. 1805-1808, **2005**.

[24] MA, S.; YU, F. A palladium catalyzed efficient synthesis of γ-methylene-α,β-unsaturated γ-lactones via cyclization of 3,4-alkadienoic acids. Tetrahedron, v. 61, p. 9896-9901, **2005**.

[25] BROWNE, D. M.; NIYOMURA, O.; WIRTH, T. Catalytic Use of Selenium Electrophiles in Cyclizations. Org. Lett., v. 9, p. 3169-3171, **2007**.

[26] KAWAMATA, Y.; HASHIMOTO, T.; MARUOKA, K. A Chiral Electrophilic Selenium Catalyst for Highly Enantioselective Oxidative Cyclization. J. Am.Chem. Soc., v. 138, p. 5206-5209, **2016**.

[27] HYDE, A. M.; BUCHWALD, S. L. Synthesis of 5,5-Disubstituted Butenolides Based on a Pd-Catalyzed γ-Arylation Strategy. Org. Lett., v. 11, p. 2663-2666, **2009**.

[28] REDDY, M. S.; THIRUPATHI, N.; HARI BABU, M.; PURI, S. Synthesis of Substituted 3-Iodocoumarins and 3-Iodobutenolides via Electrophilic Iodocyclization of Ethoxyalkyne Diols. J. Org. Chem., v. 78, p. 5878-5888, **2013**.

[29] TAN, C. K.; ER, J. C.; YEUNG, Y.-Y. Synthesis of chiral butenolides using amino-thiocarbamate-catalyzed asymmetric bromolactonization. Tetrahedron Lett., v. 55, p. 1243-1246, **2014**.

[30] GARCÍA-DOMÍNGUEZ, P.; NEVADO, C. Au–Pd Bimetallic Catalysis: The Importance of Anionic Ligands in Catalyst Speciation. J. Am.Chem. Soc., v. 138, p. 3266-3269, **2016**.

[31] LIU, Y.; SONG, F.; GUO, S. Cleavage of a Carbon−Carbon Triple Bond via Gold-Catalyzed Cascade Cyclization/Oxidative Cleavage Reactions of (Z)-Enynols with Molecular Oxygen. J. Am.Chem. Soc., v. 128, p. 11332-11333, **2006**.

[32] ALFONSI, M.; ARCADI, A.; CHIARINI, M.; MARINELLI, F. Sequential Rhodium-Catalyzed Stereo- and Regioselective Addition of Organoboron Derivatives to the Alkyl 4-Hydroxy-2-Alkynoates/Lactonizaction Reaction. J. Org. Chem., v. 72, p. 9510-9517, **2007**.

[33] BOUKOUVALAS, J.; LOACH, R. P. General, Regiodefined Access to α-Substituted Butenolides through Metal−Halogen Exchange of 3-Bromo-2-silyloxyfurans. Efficient Synthesis of an Anti-inflammatory Gorgonian Lipid. J. Org. Chem., v. 73, p. 8109-8112, **2008**.

[34] LEE, D.; NEWMAN, S. G.; TAYLOR, M. S. Boron-Catalyzed Direct Aldol Reactions of Pyruvic Acids. Org. Lett., v. 11, p. 5486-5489, **2009**.

[35] MATSUO, K.; SHINDO, M. Cu(II)-Catalyzed Acylation by Thiol Esters Under Neutral Conditions: Tandem Acylation-Wittig Reaction Leading to a One-Pot Synthesis of Butenolides. Org. Lett., v. 12, p. 5346-5349, **2010**.

[36] EGI, M.; OTA, Y.; NISHIMURA, Y.; SHIMIZU, K.; AZECHI, K.; AKAI, S. Efficient Intramolecular Cyclizations of Phenoxyethynyl Diols into Multisubstituted α,β-Unsaturated Lactones. Org. Lett., v. 15, p. 4150-4153, **2013**.

[37] SMITHA, D.; KUMAR, M. M. K.; RAMANA, H.; RAO, D. V. Rubrolide R: a new furanone metabolite from the ascidian Synoicum of the Indian Ocean. Nat. Prod. Res., v. 28, p. 12-17, **2013**.

[38] BELLINA, F.; ROSSI, R. Mucochloric and Mucobromic Acids: Inexpensive, Highly Functionalised Starting Materials for the Selective Synthesis of Variously Substituted 2(5H)-Furanone Derivatives, Sulfur- or Nitrogen-Containing Heterocycles and Stereodefined Acyclic Unsaturated Dihalogenated Compounds. Curr. Org. Chem., v. 8, p. 1089-1103, **2004**.

[39] BOUKOUVALAS, J.; LACHANCE, N.; OUELLET, M.; TRUDEAU, M. Facile access to 4-aryl-2(5H)-furanones by Suzuki cross coupling: Efficient synthesis of rubrolides C and E. Tetrahedron Lett., v. 39, p. 7665-7668, **1998**.

[40] WU, J.; ZHU, Q.; WANG, L.; FATHI, R.; YANG, Z. Palladium-Catalyzed Cross-Coupling Reactions of 4-Tosyl-2(5H)-furanone with Boronic Acids: A Facile and Efficient Route to Generate 4-Substituted 2(5H)-Furanones. J. Org. Chem., v. 68, p. 670-673, **2003**.

[41] TANG, Z.-Y.; HU, Q.-S. Room Temperature Nickel(0)-Catalyzed Suzuki-Miyaura Cross-Couplings of Activated Alkenyl Tosylates: Efficient Synthesis of 4-Substituted Coumarins and 4-Substituted 2(5H)- Furanones. Adv. Synth. Catal., v. 346, p. 1635-1637, **2004**.

[42] WU, J.; ZHANG, L.; GAO, K. RhCl(PPh3)3/DPPF: A Useful and Efficient Catalyst for Cross-Coupling Reactions of Activated Alkenyl Tosylates with Arylboronic Acids. Eur. J. Org. Chem., v. 2006, p. 5260-5263, **2006**.

[43] ROSSI, R.; BELLINA, F.; RAUGEI, E. Selective Synthesis of Unsymmetrical 3,4-Disubstituted and 4-Substituted 2(5H)-Furanones. Synlett, v. 2000, p. 1749-1752, **2000**.

[44] BELLINA, F.; ANSELMI, C.; VIEL, S.; MANNINA, L.; ROSSI, R. Selective synthesis of (Z)-4-aryl-5-[1-(aryl)methylidene]-3-bromo-2(5H)-furanones. Tetrahedron, v. 57, p. 9997-10007, **2001**.

[45] ZHANG, J.; BLAZECKA, P. G.; BELMONT, D.; DAVIDSON, J. G. Reinvestigation of Mucohalic Acids, Versatile and Useful Building Blocks for Highly Functionalized α,β-Unsaturated γ-Butyrolactones. Org. Lett., v. 4, p. 4559-4561, **2002**.

[46] BISWAS, K.; GHOLAP, R.; SRINIVAS, P.; KANYAL, S.; SARMA, K. D. [small beta]-Substituted [gamma]-butyrolactams from mucochloric acid: synthesis of (+/-)-baclofen and other [gamma]-aminobutyric acids and useful building blocks. RSC Adv., v. 4, p. 2538-2545, **2014**.

[47] BELLINA, F.; ANSELMI, C.; MARTINA, F.; ROSSI, R. Mucochloric Acid: A Useful Synthon for the Selective Synthesis of 4-Aryl-3-chloro-2(5H)-furanones, (Z)-4-Aryl-5-[1-(aryl)methylidene]-3-chloro-2(5H)-furanones and 3,4-Diaryl-2(5H)-furanones. Eur. J. Org. Chem., v. 2003, p. 2290-2302, **2003**.

[48] BELLINA, F.; FALCHI, E.; ROSSI, R. Regioselective synthesis of cytotoxic 4-(1-alkynyl)-substituted 2-(5H)-furanones. Tetrahedron, v. 59, p. 9091-9100, **2003**.

[49] BOUKOUVALAS, J.; CÔTÉ, S.; NDZI, B. Facile access to 4-(1-alkynyl)-2(5H)-furanones by Sonogashira coupling of terminal acetylenes with β-tetronic acid bromide: efficient synthesis of cleviolide. Tetrahedron Lett., v. 48, p. 105-107, **2007**.

[50] HOFFMANN, H. M. R.; GERLACH, K.; LATTMANN, E. New Bicyclic Conjugates of Three- and Five-Membered Heterocycles with 5-Alkoxyfuran-2(5H)-ones (4-Alkoxy-Δ2-butenolides). Synthesis, v. 1996, p. 164-170, **1996**.

[51] ROSSI, R.; BELLINA, F.; BIAGETTI, M. A Concise and Efficient Novel Synthesis of Cleviolide. Synth. Commun., v. 29, p. 3415-3420, **2007**.

[52] ROSSI, R.; BELLINA, F.; BIAGETTI, M.; MANNINA, L. Selective palladium-mediated synthesis of racemic 4,5-disubstituted 5H-furan-2-ones from 3-ynoic acids and organic halides. Tetrahedron Lett., v. 39, p. 7599-7602, **1998**.

[53] KABALKA, G. W.; DONG, G.; VENKATAIAH, B. Syntheses of 4-(1-alkynyl)-2(5H)-furanones and coumarins via the palladium catalyzed cross-coupling reactions of potassium alkynyltrifluoroborates. Tetrahedron Lett., v. 45, p. 5139-5141, **2004**.

[54] SCHLESSINGER, R. H.; LI, Y.-J. Total Synthesis of (−)-Virginiamycin M2Using Second-Generation Vinylogous Urethane Chemistry. J. Am.Chem. Soc., v. 118, p. 3301-3302, **1996**.

[55] LI, Y.-J.; HO, G.-M.; CHEN, P.-Z. Asymmetric [2,3]-Wittig rearrangement of the dienolates of chiral secondary alcohol-substituted β-pyrrolidinyl-γ-allyloxyl-α,β-unsaturated esters: total synthesis of (+)-eldanolide. Tetrahedron: Asymmetry, v. 20, p. 1854-1863, **2009**.

[56] HERTZBERG, R.; MOBERG, C. One-Step Preparation of O-(α-Bromoacyl) Cyanohydrins by Minor Enantiomer Recycling: Synthesis of 4-Amino-2(5H)-furanones. J. Org. Chem., v. 78, p. 9174-9180, **2013**.

[57] DECHOUX, L.; EAR, A.; TOUM, V.; THORIMBERT, S. Decarboxylative Knoevenagel-Type Reactions on Tetronamides: Synthesis of 5-Ylidene-4-Amino-2(5H)-Furanones. Synlett, v. 25, p. 1713-1716, **2014**.

[58] SCHLESSINGER, R. H.; IWANOWICZ, E. J.; SPRINGER, J. P. Highly diastereoselective alkylation reactions of vinylogous urethanes derived from simple tetronic acids. Tetrahedron Lett., v. 29, p. 1489-1492, **1988**.

[59] ZHOU, L.-H.; YU, X.-Q.; PU, L. Reactivity of γ-Hydroxy-α,β-acetylenic Esters with Amines: Facile Synthesis of the Optically Active 4-Amino-2(5H)-furanones. J. Org. Chem., v. 74, p. 2013-2017, **2009**.

[60] CAMPOS, P. J.; ARRANZ, J.; RODRÍGUEZ, M. A. α-Iodination of enaminones with bis(pyridine)iodonium(I) tetrafluoroborate. Tetrahedron Lett., v. 38, p. 8397-8400, **1997**.

[61] KIM, J. M.; NA, J. E.; KIM, J. N. α-Iodination of enaminones using the modified Johnson's procedure: the use of I2 and Et3N. Tetrahedron Lett., v. 44, p. 6317-6318, **2003**.

[62] BLAZECKA, P. G.; BELMONT, D.; CURRAN, T.; PFLUM, D.; ZHANG, J. Further Utilization of Mucohalic Acids: Palladium-Free, Regioselective Etherification and Amination of α,β-Dihalo γ-Methoxycarbonyloxy and γ-Acetoxy Butenolides. Org. Lett., v. 5, p. 5015-5017, **2003**.

[63] CUNHA, S.; OLIVEIRA, C. C.; SABINO, J. R. Synthesis of 3-bromotetronamides via amination of 3,4-dibromofuran-2(5H)-one. J. Braz. Chem. Soc., v. 22, p. 598-603, **2011**.

[64] HERTZBERG, R.; MOBERG, C. One-Step Preparation ofO-(α-Bromoacyl) Cyanohydrins by Minor Enantiomer Recycling: Synthesis of 4-Amino-2(5H)-furanones. J. Org. Chem., v. 78, p. 9174-9180, **2013**.

[65] CASIRAGHI, G.; ZANARDI, F.; APPENDINO, G.; RASSU, G. The Vinylogous Aldol Reaction: A Valuable, Yet Understated Carbon−Carbon Bond-Forming Maneuver. Chem. Rev., v. 100, p. 1929-1972, **2000**.

[66] CASIRAGHI, G.; BATTISTINI, L.; CURTI, C.; RASSU, G.; ZANARDI, F. The Vinylogous Aldol and Related Addition Reactions: Ten Years of Progress†. Chem. Rev., v. 111, p. 3076-3154, **2011**.

[67] PANSARE, S. V.; PAUL, E. K. The Organocatalytic Vinylogous Aldol Reaction: Recent Advances. Chem. – Eur. J., v. 17, p. 8770-8779, **2011**.

[68] BISAI, V. Organocatalytic Asymmetric Vinylogous Aldol Reactions. Synthesis, v. 44, p. 1453-1463, **2012**.

[69] BROWN, D. W.; CAMPBELL, M. M.; TAYLOR, A. P.; ZHANG, X.-A. Regio- and diastereoselectivity in aldol reactions of cyclopent-2-enone, 2-(5H)furanone and their derived trimethylsilyloxydienes. Tetrahedron Lett., v. 28, p. 985-988, **1987**.

[70] JEFFORD, C. W.; JAGGI, D.; BOUKOUVALAS, J. Diastereoselectivity in the directed aldol condensation of 2-trimethylsiloxyfuran with aldehydes. A stereodivergent route to threo and erythro δ-hydroxy-γ-lactones. Tetrahedron Lett., v. 28, p. 4037-4040, **1987**.

[71] JEFFORD, C. W.; JAGGI, D.; BERNARDINELLI, G.; BOUKOUVALAS, J. The synthesis of (±)-cavernosine. Tetrahedron Lett., v. 28, p. 4041-4044, **1987**.

[72] BOUKOUVALAS, J.; MALTAIS, F. An efficient total synthesis of neopatulin. Tetrahedron Lett., v. 35, p. 5769-5770, **1994**.

[73] LÓPEZ, C. S.; ÁLVAREZ, R.; VAZ, B.; FAZA, O. N.; DE LERA, Á. R. Simple Diastereoselectivity of the BF3·OEt2-Catalyzed Vinylogous Mukaiyama Aldol Reaction of 2-(Trimethylsiloxy)furans with Aldehydes. J. Org. Chem., v. 70, p. 3654-3659, **2005**.

[74] BOUKOUVALAS, J.; BELTRÁN, P. P.; LACHANCE, N.; CÔTÉ, S.; MALTAIS, F.; POULIOT, M. A New, Highly Stereoselective Synthesis of β-Unsubstituted (Z)-γ-Alkylidenebutenolides Using Bromine as a Removable Stereocontrol Element. Synlett, p. 0219-0222, **2007**.

[75] DAS SARMA, K.; ZHANG, J.; CURRAN, T. T. Novel Synthons from Mucochloric Acid: The First Use of α,β-Dichloro-γ-butenolides and γ-Butyrolactams for Direct Vinylogous Aldol Addition. J. Org. Chem., v. 72, p. 3311-3318, **2007**.

[76] LIU, G.-Y.; GUO, B.-Q.; CHEN, W.-N.; CHENG, C.; ZHANG, Q.-L.; DAI, M.-B.; SUN, J.-R.; SUN, P.-H.; CHEN, W.-M. Synthesis, Molecular Docking, and Biofilm Formation Inhibitory Activity of 5-Substituted 3,4-Dihalo-5H-furan-2-one Derivatives on Pseudomonas aeruginosa. Chem. Biol. Drug. Des., v. 79, p. 628-638, **2012**.

[77] DAVID, J. G.; BAI, W.-J.; WEAVER, M. G.; PETTUS, T. R. R. A General Diastereoselective Catalytic Vinylogous Aldol Reaction Among Tetramic Acid-Derived Pyrroles. Org. Lett., v. 16, p. 4384-4387, **2014**.

[78] KABESHOV, M. A.; KYSILKA, O.; RULÍŠEK, L.; SULEIMANOV, Y. V.; BELLA, M.; MALKOV, A. V.; KOČOVSKÝ, P. Cross-Aldol Reaction of Isatin with Acetone Catalyzed by Leucinol: A Mechanistic Investigation. Chem. – Eur. J., v. 21, p. 12203-12203, **2015**.

[79] FRINGS, M.; ATODIRESEI, I.; WANG, Y.; RUNSINK, J.; RAABE, G.; BOLM, C. C1-Symmetric Aminosulfoximines in Copper-Catalyzed Asymmetric Vinylogous Mukaiyama Aldol Reactions. Chem. – Eur. J., v. 16, p. 4577-4587, **2010**.

[80] YANG, Y.; ZHENG, K.; ZHAO, J.; SHI, J.; LIN, L.; LIU, X.; FENG, X. Asymmetric Direct Vinylogous Aldol Reaction of Unactivated γ-Butenolide to Aldehydes. J. Org. Chem., v. 75, p. 5382-5384, **2010**.

[81] UBE, H.; SHIMADA, N.; TERADA, M. Asymmetric Direct Vinylogous Aldol Reaction of Furanone Derivatives Catalyzed by an Axially Chiral Guanidine Base. Angew. Chem. Int. Ed., v. 49, p. 1858-1861, **2010**.

[82] LUO, J.; WANG, H.; HAN, X.; XU, L.-W.; KWIATKOWSKI, J.; HUANG, K.-W.; LU, Y. The Direct Asymmetric Vinylogous Aldol Reaction of Furanones with α-Ketoesters: Access to Chiral γ-Butenolides and Glycerol Derivatives. Angew. Chem., Int. Ed., v. 50, p. 1861-1864, **2011**.

[83] SZLOSEK, M.; FIGADÈRE, B. Highly Enantioselective Aldol Reaction with 2-Trimethylsilyloxyfuran: The First Catalytic Asymmetric Autoinductive Aldol Reaction. Angew. Chem. Int. Ed., v. 112, p. 1869-1871, **2000**.

[84] SINGH, R. P.; FOXMAN, B. M.; DENG, L. Asymmetric Vinylogous Aldol Reaction of Silyloxy Furans with a Chiral Organic Salt. J. Am.Chem. Soc., v. 132, p. 9558-9560, **2010**.

[85] ZHU, N.; MA, B.-C.; ZHANG, Y.; WANG, W. Organocatalyzed Highly Enantioselective and anti-Selective Construction of γ-Butenolides through Vinylogous Mukaiyama Aldol Reaction. Adv. Synth. Catal., v. 352, p. 1291-1295, **2010**.

[86] LÓPEZ, C. S.; ÁLVAREZ, R.; VAZ, B.; FAZA, O. N.; DE LERA, Á. R. Simple Diastereoselectivity of the BF3·OEt2-Catalyzed Vinylogous Mukaiyama Aldol Reaction of 2-(Trimethylsiloxy)furans with Aldehydes. J. Org. Chem., v. 70, p. 3654-3659, **2005**.

[87] OLLEVIER, T.; BOUCHARD, J.-E.; DESYROY, V. Diastereoselective Mukaiyama Aldol Reaction of 2-(Trimethylsilyloxy)furan Catalyzed by Bismuth Triflate. J. Org. Chem., v. 73, p. 331-334, **2008**.

[88] UBE, H.; SHIMADA, N.; TERADA, M. Asymmetric Direct Vinylogous Aldol Reaction of Furanone Derivatives Catalyzed by an Axially Chiral Guanidine Base. Angew. Chem. Int. Ed., v. 49, p. 1858-1861, **2010**.

[89] LUO, J.; WANG, H.; HAN, X.; XU, L.-W.; KWIATKOWSKI, J.; HUANG, K.-W.; LU, Y. The Direct Asymmetric Vinylogous Aldol Reaction of Furanones with α-Ketoesters: Access to Chiral γ-Butenolides and Glycerol Derivatives. Angew. Chem. Int. Ed., v. 50, p. 1861-1864, **2011**.

[90] PANSARE, S. V.; PAUL, E. K. Organocatalytic asymmetric direct vinylogous aldol reactions of γ-crotonolactone with aromatic aldehydes. Chem. Commun., v. 47, p. 1027-1029, **2011**.

[91] CLARAZ, A.; OUDEYER, S.; LEVACHER, V. Chiral Quaternary Ammonium Aryloxide/N,O-Bis(trimethyl- silyl)acetamide Combination as Efficient Organocatalytic System for the Direct Vinylogous Aldol Reaction of (5H)-Furan-2-one Derivatives. Adv. Synth. Catal., v. 355, p. 841-846, **2013**.

[92] MARTIN, S. F.; LOPEZ, O. D. Vinylogous Mannich reactions. Catalytic, asymmetric additions of triisopropylsilyloxyfurans to aldimines. Tetrahedron Lett., v. 40, p. 8949-8953, **1999**.

[93] URAGUCHI, D.; SORIMACHI, K.; TERADA, M. Organocatalytic Asymmetric Aza-Friedel−Crafts Alkylation of Furan. J. Am.Chem. Soc., v. 126, p. 11804-11805, **2004**.

[94] CARSWELL, E. L.; SNAPPER, M. L.; HOVEYDA, A. H. A Highly Efficient and Practical Method for Catalytic Asymmetric Vinylogous Mannich (AVM) Reactions. Angew. Chem. Int. Ed., v. 45, p. 7230-7233, **2006**.

[95] WIELAND, L. C.; VIEIRA, E. M.; SNAPPER, M. L.; HOVEYDA, A. H. Ag-Catalyzed Diastereo- and Enantioselective Vinylogous Mannich Reactions of α-Ketoimine Esters. Development of a Method and Investigation of its Mechanism. J. Am.Chem. Soc., v. 131, p. 570-576, **2009**.

[96] YUAN, Z.-L.; JIANG, J.-J.; SHI, M. The application of chiral phosphine-Schiff base type ligands in silver(I)-catalyzed asymmetric vinylogous Mannich reaction of aldimines with trimethylsiloxyfuran. Tetrahedron, v. 65, p. 6001-6007, **2009**.

[97] SHI, Y.-H.; WANG, Z.; SHI, Y.; DENG, W.-P. Facile and highly diastereoselective synthesis of 3-aminooxindoles via AgOAc-catalyzed vinylogous Mannich reaction. Tetrahedron, v. 68, p. 3649-3653, **2012**.

[98] YAMAGUCHI, A.; MATSUNAGA, S.; SHIBASAKI, M. Direct Catalytic Asymmetric Mannich-Type Reactions of γ-Butenolides: Effectiveness of Brønsted Acid in Chiral Metal Catalysis. Org. Lett., v. 10, p. 2319-2322, **2008**.

[99] YIN, L.; TAKADA, H.; KUMAGAI, N.; SHIBASAKI, M. Direct Catalytic Asymmetric Vinylogous Mannich-Type Reaction of γ-Butenolides with Ketimines. Angew. Chem. Int. Ed., v. 52, p. 7310-7313, **2013**.

[100] NAKAMURA, S.; YAMAJI, R.; HAYASHI, M. Direct Enantioselective Vinylogous Mannich Reaction of Ketimines with γ-Butenolide by Using Cinchona Alkaloid Amide/Zinc(II) Catalysts. Chem. – Eur. J., v. 21, p. 9615-9618, **2015**.

[101] GUO, Y.; ZHANG, Y.; QI, L.; TIAN, F.; WANG, L. Organocatalytic direct asymmetric vinylogous Mannich reaction of γ-butenolides with isatin-derived ketimines. RSC Adv., v. 4, p. 27286, **2014**.

[102] GUO, Y.-L.; BAI, J.-F.; PENG, L.; WANG, L.-L.; JIA, L.-N.; LUO, X.-Y.; TIAN, F.; XU, X.-Y.; WANG, L.-X. Direct Asymmetric Vinylogous Mannich Reaction of 3,4-Dihalofuran-2(5H)-one with Aldimine Catalyzed by Quinine. J. Org. Chem., v. 77, p. 8338-8343, **2012**.

[103] ZHOU, L.; LIN, L.; JI, J.; XIE, M.; LIU, X.; FENG, X. Catalytic Asymmetric Vinylogous Mannich-type (AVM) Reaction of Nonactivated α-Angelica Lactone. Org. Lett., v. 13, p. 3056-3059, **2011**.

[104] TROST, B. M.; HITCE, J. Direct Asymmetric Michael Addition to Nitroalkenes: Vinylogous Nucleophilicity under Dinuclear Zinc Catalysis. J. Am.Chem. Soc., v. 131, p. 4572-4573, **2009**.

[105] BROWN, S. P.; GOODWIN, N. C.; MACMILLAN, D. W. C. The First Enantioselective Organocatalytic Mukaiyama−Michael Reaction: A Direct Method for the Synthesis of Enantioenriched γ-Butenolide Architecture. J. Am.Chem. Soc., v. 125, p. 1192-1194, **2003**.

[106] WANG, J.; QI, C.; GE, Z.; CHENG, T.; LI, R. Efficient direct asymmetric vinylogous Michael addition reactions of γ-butenolides to chalcones catalyzed by vicinal primary-diamine salts. Chem. Commun., v. 46, p. 2124, **2010**.

[107] TERADA, M.; ANDO, K. Enantioselective Direct Vinylogous Michael Addition of Functionalized Furanones to Nitroalkenes Catalyzed by an Axially Chiral Guanidine Base. Org. Lett., v. 13, p. 2026-2029, **2011**.

[108] MANNA, M. S.; KUMAR, V.; MUKHERJEE, S. Catalytic enantioselective construction of quaternary stereocenters by direct vinylogous Michael addition of deconjugated butenolides to nitroolefins. Chem. Commun., v. 48, p. 5193-5195, **2012**.

[109] KUBO, M.; OKADA, C.; HUANG, J.-M.; HARADA, K.; HIOKI, H.; FUKUYAMA, Y. Novel Pentacyclicseco-Prezizaane-Type Sesquiterpenoids with Neurotrophic Properties fromIllicium jiadifengpi. Org. Lett., v. 11, p. 5190-5193, **2009**.

[110] PATERSON, I.; XUAN, M.; DALBY, S. M. Total Synthesis of Jiadifenolide. Angew. Chem. Int. Ed., v. 53, p. 7286-7289, **2014**.

[111] SHEN, Y.; LI, L.; PAN, Z.; WANG, Y.; LI, J.; WANG, K.; WANG, X.; ZHANG, Y.; HU, T.; ZHANG, Y. Protecting-Group-Free Total Synthesis of (−)-Jiadifenolide: Development of a [4 + 1] Annulation toward Multisubstituted Tetrahydrofurans. Org. Lett., v. 17, p. 5480-5483, **2015**.

[112] LU, H.-H.; MARTINEZ, M. D.; SHENVI, R. A. An eight-step gram-scale synthesis of (−)-jiadifenolide. Nat. Chem., v. 7, p. 604-607, **2015**.

[113] GOMES, J.; DAEPPEN, C.; LIFFERT, R.; ROESSLEIN, J.; KAUFMANN, E.; HEIKINHEIMO, A.; NEUBURGER, M.; GADEMANN, K. Formal Total Synthesis of (−)-Jiadifenolide and Synthetic Studies toward seco-Prezizaane-Type Sesquiterpenes. J. Org. Chem., v. 81, p. 11017–11034, **2016**.

[114] GUNASEKERA, S. P.; MCCARTHY, P. J.; KELLY-BORGES, M.; LOBKOVSKY, E.; CLARDY, J. Dysidiolide: A Novel Protein Phosphatase Inhibitor from the Caribbean Sponge Dysidea etheria de Laubenfels. J. Am.Chem. Soc., v. 118, p. 8759-8760, **1996**.

[115] COREY, E. J.; ROBERTS, B. E. Total Synthesis of Dysidiolide. J. Am.Chem. Soc., v. 119, p. 12425-12431, **1997**.

[116] BOUKOUVALAS, J.; CHENG, Y.-X.; ROBICHAUD, J. Total Synthesis of (+)-Dysidiolide. J. Org. Chem., v. 63, p. 228-229, **1998**.

[117] MAGNUSON, S. R.; SEPP-LORENZINO, L.; ROSEN, N.; DANISHEFSKY, S. J. A Concise Total Synthesis of Dysidiolide through Application of a Dioxolenium-Mediated Diels−Alder Reaction. J. Am.Chem. Soc., v. 120, p. 1615-1616, **1998**.

[118] PACZKOWSKI, R.; MAICHLE-MÖSSMER, C.; MAIER, M. E. A Formal Total Synthesis of Dysidiolide. Org. Lett., v. 2, p. 3967-3969, **2000**.

[119] MIYAOKA, H.; KAJIWARA, Y.; YAMADA, Y. Synthesis of marine sesterterpenoid dysidiolide. Tetrahedron Lett., v. 41, p. 911-914, **2000**.

[120] TAKAHASHI, M.; DODO, K.; HASHIMOTO, Y.; SHIRAI, R. Concise asymmetric synthesis of dysidiolide. Tetrahedron Lett., v. 41, p. 2111-2114, **2000**.

[121] MIYAOKA, H.; KAJIWARA, Y.; HARA, Y.; YAMADA, Y. Total Synthesis of Natural Dysidiolide. J. Org. Chem., v. 66, p. 1429-1435, **2001**.

[122] JUNG, M. E.; NISHIMURA, N. Enantioselective Formal Total Synthesis of (−)-Dysidiolide. Org. Lett., v. 3, p. 2113-2115, **2001**.

[123] LIU, Y.; LINIGER, M.; MCFADDEN, R. M.; ROIZEN, J. L.; MALETTE, J.; REEVES, C. M.; BEHENNA, D. C.; SETO, M.; KIM, J.; MOHR, J. T.; VIRGIL, S. C.; STOLTZ, B. M. Formal total syntheses of classic natural product target molecules via palladium-catalyzed enantioselective alkylation. Beilstein J. Org. Chem., v. 10, p. 2501-2512, **2014**.

[124] PIERS, E.; CAILLÉ, S.; CHEN, G. A Formal Total Synthesis of the Sesterterpenoid (±)-Dysidiolide and Approaches to the Syntheses of (±)-6-Epi-, (±)-15-Epi-, and (±)-6,15-Bisepidysidiolide. Org. Lett., v. 2, p. 2483-2486, **2000**.

[125] DEMEKE, D.; FORSYTH, C. J. Total synthesis of (±)-dysidiolide. Tetrahedron, v. 58, p. 6531-6544, **2002**.

[126] KALIAPPAN, K. P.; GOWRISANKAR, P. An expedient enyne metathesis approach to dysidiolide. Tetrahedron Lett., v. 45, p. 8207-8209, **2004**.

[127] MOUSTAFA, G. A. I.; KAMADA, Y.; TANAKA, T.; YOSHIMITSU, T. Stereoconvergent route to chiral cyclohexenone building blocks: formal synthesis of (−)-dysidiolide. Org. Biomol. Chem., v. 10, p. 8609, **2012**.

[128] XIAO, W.-L.; YANG, L.-M.; GONG, N.-B.; WU, L.; WANG, R.-R.; PU, J.-X.; LI, X.-L.; HUANG, S.-X.; ZHENG, Y.-T.; LI, R.-T.; LU, Y.; ZHENG, Q.-T.; SUN, H.-D. Rubriflordilactones A and B, Two Novel Bisnortriterpenoids fromSchisandrarubrifloraand Their Biological Activities. Org. Lett., v. 8, p. 991-994, **2006**.

[129] LI, J.; YANG, P.; YAO, M.; DENG, J.; LI, A. Total Synthesis of Rubriflordilactone A. J. Am.Chem. Soc., v. 136, p. 16477-16480, **2014**.

[130] GOH, S. S.; CHAUBET, G.; GOCKEL, B.; CORDONNIER, M.-C. A.; BAARS, H.; PHILLIPS, A. W.; ANDERSON, E. A. Total Synthesis of (+)-Rubriflordilactone A. Angew. Chem. Int. Ed., v. 54, p. 12618-12621, **2015**.

[131] YANG, P.; YAO, M.; LI, J.; LI, Y.; LI, A. Total Synthesis of Rubriflordilactone B. Angew. Chem. Int. Ed., v. 55, p. 6964-6968, **2016**.

[132] SMITH, C. J.; HETTICH, R. L.; JOMPA, J.; TAHIR, A.; BUCHANAN, M. V.; IRELAND, C. M. Cadiolides A and B, New Metabolites from an Ascidian of the GenusBotryllus. J. Org. Chem., v. 63, p. 4147-4150, **1998**.

[133] WANG, W.; KIM, H.; NAM, S.-J.; RHO, B. J.; KANG, H. Antibacterial Butenolides from the Korean Tunicate Pseudodistoma antinboja. J. Nat. Prod., v. 75, p. 2049-2054, **2012**.

[134] WON, T. H.; JEON, J.-E.; KIM, S.-H.; LEE, S.-H.; RHO, B. J.; OH, D.-C.; OH, K.-B.; SHIN, J. Brominated Aromatic Furanones and Related Esters from the AscidianSynoicumsp. J. Nat. Prod., v. 75, p. 2055-2061, **2012**.

[135] BOUKOUVALAS, J.; POULIOT, M. Short and Efficient Synthesis of Cadiolide B. Synlett, v. p. 343-345, **2005**.

[136] PEIXOTO, P. A.; BOULANGÉ, A.; LELEU, S.; FRANCK, X. Versatile Synthesis of Acylfuranones by Reaction of Acylketenes with α-Hydroxy Ketones: Application to the One-Step Multicomponent Synthesis of Cadiolide B and Its Analogues. Eur. J. Org. Chem., v. 2013, p. 3316-3327, **2013**.

[137] BOULANGÉ, A.; PARRAGA, J.; GALÁN, A.; CABEDO, N.; LELEU, S.; SANZ, M. J.; CORTES, D.; FRANCK, X. Synthesis and antibacterial activities of cadiolides A, B and C and analogues. Bioorg. Med. Chem., v. 23, p. 3618-3628, **2015**.

[138] BOUKOUVALAS, J.; THIBAULT, C. Step-Economical Synthesis of the Marine Ascidian Antibiotics Cadiolide A, B, and D. J. Org. Chem., v. 80, p. 681-684, **2015**.

[139] STOCKWELL, B. R. Exploring biology with small organic molecules. Nature, v. 432, p. 846-854, **2004**.

[140] SODEOKA, M.; SAMPE, R.; KOJIMA, S.; BABA, Y.; USUI, T.; UEDA, K.; OSADA, H. Synthesis of a Tetronic Acid Library Focused on Inhibitors of Tyrosine and Dual-Specificity Protein Phosphatases and Its Evaluation Regarding VHR and Cdc25B Inhibition. J. Med. Chem., v. 44, p. 3216-3222, **2001**.

[141] PRASIT, P.; WANG, Z.; BRIDEAU, C.; CHAN, C. C.; CHARLESON, S.; CROMLISH, W.; ETHIER, D.; EVANS, J. F.; FORD-HUTCHINSON, A. W.; GAUTHIER, J. Y.; GORDON, R.; GUAY, J.; GRESSER, M.; KARGMAN, S.; KENNEDY, B.; LEBLANC, Y.; LÉGER, S.; MANCINI, J.; O'NEILL, G. P.; OUELLET, M.; PERCIVAL, M. D.; PERRIER, H.; RIENDEAU, D.; RODGER, I.; TAGARI, P.; THÉRIEN, M.; VICKERS, P.; WONG, E.; XU, L. J.; YOUNG, R. N.; ZAMBONI, R.; BOYCE, S.; RUPNIAK, N.; FORREST, M.; VISCO, D.; PATRICK, D. The discovery of rofecoxib, [MK 966, VIOXX®], an orally active cyclooxygenase-2 inhibitor. Bioorg. Med. Chem. Lett., v. 9, p. 1773-1778, **1999**.

[142] CHAN, C.-C.; BOYCE, S.; BRIDEAU, C.; CHARLESON, S.; CROMLISH, W.; ETHIER, D.; EVANS, J.; FORD-HUTCHINSON, A. W.; FORREST, M. J.; GAUTHIER, J. Y.; GORDON, R.; GRESSER, M.; GUAY, J.; KARGMAN, S.; KENNEDY, B.; LEBLANC, Y.; LEGER, S.; MANCINI, J.; O'NEILL, G. P.; OUELLET, M.; PATRICK, D.; PERCIVAL, M. D.; PERRIER, H.; PRASIT, P.; RODGER, I.; TAGARI, P.; THERIEN, M.; VICKERS, P.; VISCO, D.; WANG, Z.; WEBB, J.; WONG, E.; XU, L.-J.; YOUNG, R. N.; ZAMBONI, R.; RIENDEAU, D. Rofecoxib [Vioxx, MK-0966]: A Potent and Orally Active Cyclooxygenase-2 Inhibitor. Pharmacological and Biochemical Profiles. J. Pharm. Exp. Ther., v. 290, p. 551-560, **1999**.

[143] ORLANDO, B. J.; MALKOWSKI, M. G. Crystal structure of rofecoxib bound to human cyclooxygenase-2. Acta Cryst. F : Structural Biology Communications, v. 72, p. 772-776, **2016**.

[144] HANSON, P. D.; BROOKS, K. C.; CASE, J.; CONZEMIUS, M.; GORDON, W.; SCHUESSLER, J.; SHELLEY, B. Efficacy and safety of firocoxib in the management of canine osteoarthritis under field conditions. Vet. Ther., v. 7, p. 127, **2006**.

[145] DRAG, M.; KUNKLE, B. N.; ROMANO, D.; HANSON, P. D. Efficacy of firocoxib in preventing urate-induced synovitis, pain, and inflammation in dogs. Vet. Ther., v. 8, p. 41, **2007**.

[146] KVATERNICK, V.; POLLMEIER, M.; FISCHER, J.; HANSON, P. D. Pharmacokinetics and metabolism of orally administered firocoxib, a novel second generation coxib, in horses. J. Vet. Pharmacol. Ther., v. 30, p. 208-217, **2007**.

[147] 戴振亚; 赵云德; 王子昱; 徐沛; 董晓阳, Synthesis of firocoxib, CN104803956A, **2015**.

[148] KUROWSKI, V.; IVEN, H.; DJONLAGIC, H. Treatment of a patient with severe digitoxin intoxication by Fab fragments of anti-digitalis antibodies. Intensive Care Med., v. 18, p. 439-442, **1992**.

[149] HOLLMAN, A. Digoxin comes from Digitalis lanata. BMJ, v. 312, p. 912-912, **1996**.

[150] BELZ, G. G.; BREITHAUPT-GRÖGLER, K.; OSOWSKI, U. Treatment of congestive heart failure - current status of use of digitoxin. Eur. J. Clin. Invest., v. 31, p. 10-17, **2008**.

[151] VAMOS, M.; ERATH, J. W.; HOHNLOSER, S. H. Digoxin-associated mortality: a systematic review and meta-analysis of the literature. Eur. Heart J., v. 36, p. 1831-1838, **2015**.

[152] SCHMITT, J.; SUGNET, M.; SALLE, J.; COMOY, P.; CALLET, G.; LEMEUR, J. Chim. Ther., v. 5-6, p. 305, **1966**.

[153] XIAO, Y.; LUO, M.; WANG, J.; LUO, H.; WANG, J. Losigamone add-on therapy for partial epilepsy. Cochrane Database Syst. Rev. , v. 12, CD009324, **2015**.

[154] LIU, G.; WU, Y.; XU, H.; LIU, H. A Green Route for the Synthesis of Antiepileptic Drug Losigamone and Its Analogues. Chinese J. Org. Chem., v. 33, p. 1527-1531, **2013**.

[155] ŁUSZCZKI, J. J. Third-generation antiepileptic drugs: mechanisms of action, pharmacokinetics and interactions. Pharmacol. Rep., v. 61, p. 197-216, **2009**.

[156] BAUER, J.; DIENEL, A.; ELGER, C. E. Losigamone add-on therapy in partial epilepsy: a placebo-controlled study. Acta Neurol. Scand., v. 103, p. 226-230, **2001**.

[157] BAULAC, M.; KLEMENT, S. Efficacy and safety of Losigamone in partial seizures: a randomized double-blind study. Epilepsy Res., v. 55, p. 177-189, **2003**.

[158] GUAN, A.; LIU, C.; YANG, X.; DEKEYSER, M. Application of the Intermediate Derivatization Approach in Agrochemical Discovery. Chem. Rev., v. 114, p. 7079-7107, **2014**.

[159] NAUEN, R.; JESCHKE, P.; VELTEN, R.; BECK, M. E.; EBBINGHAUS-KINTSCHER, U.; THIELERT, W.; WÖLFEL, K.; HAAS, M.; KUNZ, K.; RAUPACH, G. Flupyradifurone: a brief profile of a new butenolide insecticide. Pest Manag. Sci., v. 71, p. 850-862, **2015**.

[160] JESCHKE, P.; NAUEN, R.; GUTBROD, O.; BECK, M. E.; MATTHIESEN, S.; HAAS, M.; VELTEN, R. Flupyradifurone (Sivanto™) and its novel butenolide pharmacophore: Structural considerations☆. Pest. Biochem. Physiol., v. 121, p. 31-38, **2015**.

CHAPTER 2

Vinylogous Aldol Reaction of Tetronamides with Aldehydes: Controlling Diastereoselectivity *via* Retro-aldol/Aldol Equilibration

1. Introduction

Tetronamides are an important class of β-aminosubstituted butenolides that have attracted growing attention from synthetic and medicinal chemists alike [1-10], [11-14]. Although not nearly as common as their tetronate counterparts [15, 16], several tetronamides have been shown to display significant biological activities, as represented by the antitumor antibiotic basidalin **1**, [17, 18] the newly marketed systemic insecticide flupyradifurone (Sivanto®, **2**) [19, 20], some potent antimitotic aza-lignans, e.g. compound **3** [21], and broad-acting antibacterials [22] (**4-5**, Figure 2.1).
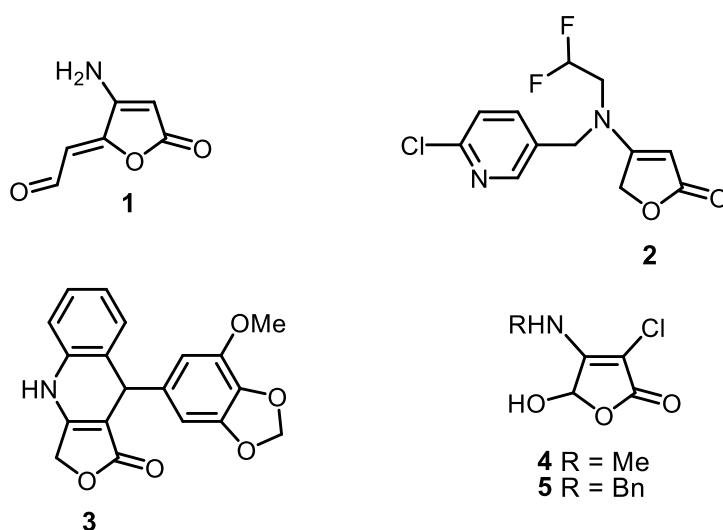
Figure 2.1 Examples of natural and non-natural bioactive tetronamides **1-5**

Moreover, the tetronate *syn*-aldol adduct (+)-losigamone [23-27] **6** (Figure 2.2) is a newer AED that has been investigated as an add-on therapy for partial epilepsy patients. Inspired by the structure of losigamone, a library of new analogues in which the alkoxy group is replaced by an aromatic amine (cf. tetronamides **A**) has been sought to prepare [28-30]. Thus, the scope of a direct VA reaction of related α-halotetronamides with a practical method enabling stereoselective access to *syn*-aldolates from functionalized tetronamides and diverse aldehydes were investigated. The vinylogous aldol reaction (VAR), carried out either directly from butenolides or, *via* conversion to the corresponding 2-silyloxyfurans (Mukaiyama variant; VMAR), represents one of the most widely explored avenues for installing a γ-carbon substituent (Scheme 2.1) [31-34].
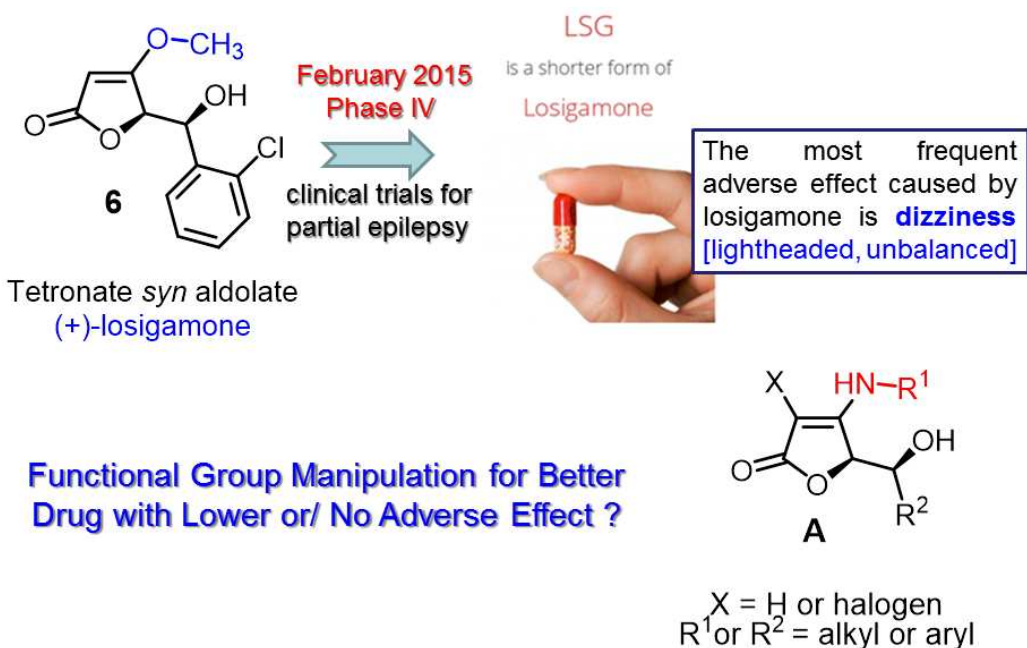
Figure 2.2 Antiepileptic tetronate *syn*-aldolate losigamone **6** and analogues **A**

Much effort has been devoted in recent years to controlling the relative and absolute configuration of the newly formed stereogenic centers [35-44], [45-48]. Although several hetero substituted butenolides [39-42, 47, 48], including tetronates, have been utilized as substrates in VA reactions, surprisingly little is known concerning the serviceability of tetronamides [49-56]. The few pertinent examples invariably employ *N,N*-disubstituted
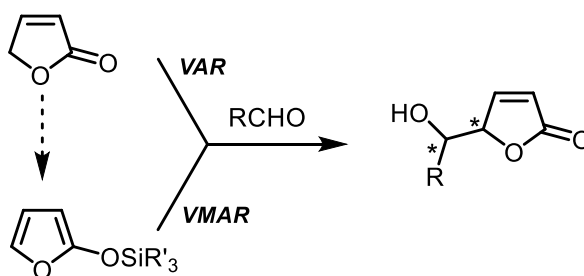
Scheme 2.1 General VA pathways to substituted butenolides

tetronamides in conjuction with a strong base (*t*-BuLi, **–**78 °C), leading mainly to *anti*-aldol products (Scheme 2.2) [57-60]. To date, only two *N*-monosubstituted tetronamide-derived aldolates have been described in the literature; both were obtained as mixtures of diastereoisomers (dr ≈ 1:1 to 2:1) using a decarboxylative Knoevenagel-type reaction of γ-carboxymethyl tetronamides with aldehydes [61].
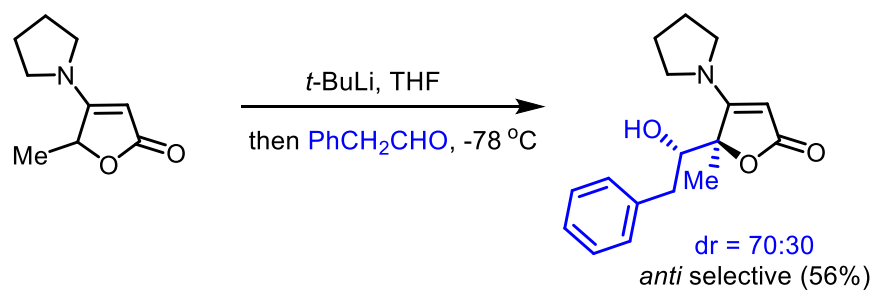
Scheme 2.2 *Anti*-selective VA reaction of *N,N*-disubstituted tetronamide [57]

Reported in this Chapter, the hitherto unexplored VAR of unactivated *N*-monosubstituted tetronamides along with the development of a simple, mild and scalable method enabling stereoselective access to *syn*-aldolate adducts.

2. Results and Discussion

2.1. Preparation of α-Halotetronamides

The starting tetronamides of the present work were prepared by utilizing a procedure reported by Cunha and co-workers [62]. Thus, treatment of commercially available α,β-dihalobutenolides **7a**-**b** with appropriate amines in the presence of NaHCO$_3$ at room temperature readily accomplished an aza-Michael addition/elimination [63, 64] to deliver the desired α-halotetronamides **8a**-**e** in moderate to high yields (Scheme 2.3).
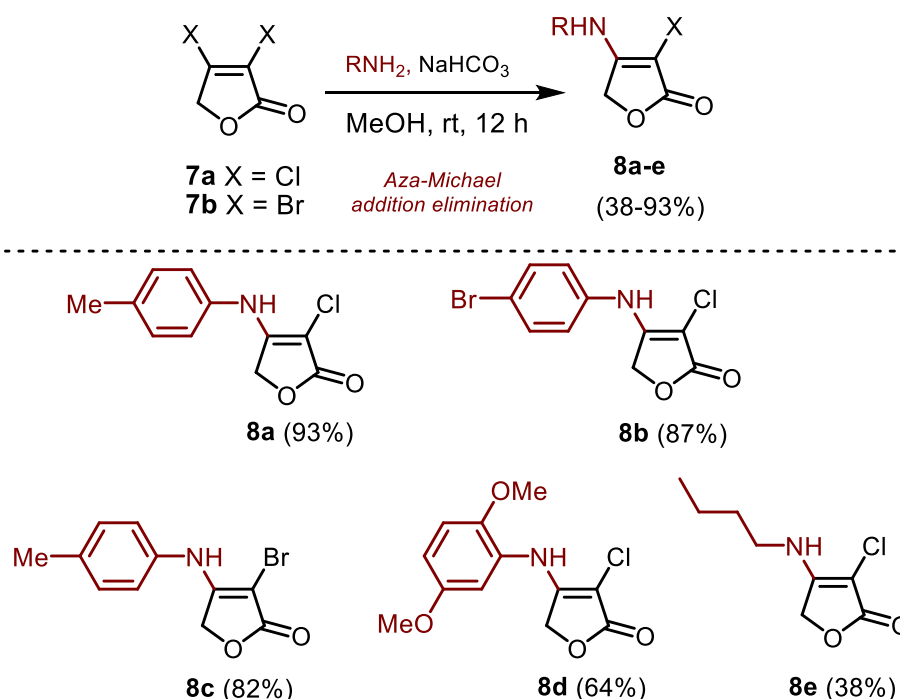
Scheme 2.3 Preparation α-halotetronamides **8a-e** from α,β-dihalofuran-2(*5H*)-ones [62]

2.2. Optimization of the VAR of Tetronamide

To assess the feasibility of the VAR, unprotected tetronamide **8a** and benzaldehyde were subjected to a range of base/solvent combinations, as outlined in Table 2.1. Adaptation of the conditions of Zhang [41] (cf. Et$_3$N/MeOH, rt), which had worked well for the VAR of α,β-dichlorobutenolide with benzaldehydes, were only modestly effective in providing the desired adducts **9** (14% yield, entry 1, Table 2.1). Replacing triethylamine with DBU or DIPEA did not improve matters either (entries 2-3). A slight improvement in the yield of **9** was observed when switching to mineral bases such as NaHCO$_3$ and Na$_2$CO$_3$ (entries 4-5).

Table 2.1 Optimization of the VA reaction of tetronamide **8a** with benzaldehyde
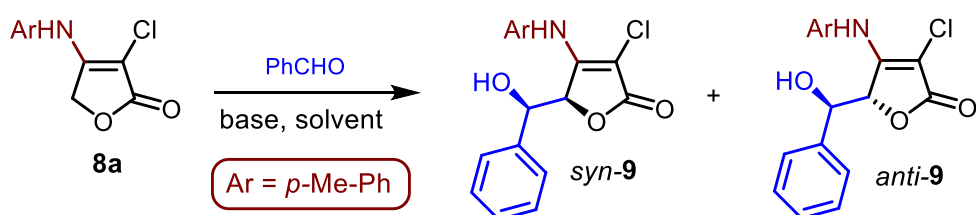
Entry	Base	Solvent	Time[a] (h)	Yield[b] (%)	dr[c] (*syn:anti*)
1	Et$_3$N	MeOH	4	14	ND[d]
2	DBU	MeOH	12	11	ND[d]
3	DIPEA	MeOH	24	trace	ND[d]
4	NaHCO$_3$	MeOH	24	23	ND[d]
5	Na$_2$CO$_3$	MeOH	24	21	50:50
6	NaOH	MeOH	3	83	68:32
7	NaOH	CH$_2$Cl$_2$	12	36	60:40
8	NaOH	Toluene	16	48	44:56
9	NaOH	THF	8	23	ND[d]
10	KOH	MeOH	3	65	63:37
11	*t*-BuOK	MeOH	4	78	50:50
12	NaOH	MeOH/H$_2$O[e]	3	91	>99:1
13	LiOH	MeOH/H$_2$O[e]	2	90	>99:1

[a] All reactions were run at room temperature and were quenched when **8a** was completely consumed according to TLC. [b] Yield of isolated product by column chromatography. [c] Determined by ^{1}H NMR analysis; all products are racemic. [d] ND = not determined. [e] Using a 2:1 MeOH/H$_2$O ratio (v/v).

Pleasingly, the use of the stronger base NaOH led to a substantial increase in yield (83%) along with low selectivity in favour of the *syn*-adduct (68:32, entry 6). Next, the diastereoselectivity issue was addressed by assessing the effect of different solvents and mineral bases (entries 7-11). It is immediately seen from the results, that replacing MeOH by a less polar solvent, such as dichloromethane, toluene or THF, has a detrimental effect to product yield and/or diastereoselectivity (entry 6 vs entries 7-9). Accordingly, we decided to explore the effect of more polar solvents, such as the binary system methanol:water (2:1 v/v). Surprisingly, the use of NaOH or LiOH in this solvent delivered *syn*-**9** as the sole detectable isomer in excellent yield (entries 12-13).

Whilst water has been successfully employed as solvent/additive in aldol reactions [65, 66], most of the reported cases involve either pyrrole-mediated [67] or Mukaiyama variants [68, 69]. A notable example pertains to the use of brine/MeOH in uncatalyzed VMA reactions of 2-silyoxyfurans and pyrroles with benzaldehydes, leading mainly to the corresponding *syn* and *anti* aldol-adducts, respectively [70]. It was suggested that water may serve as an H-bond donor to activate the aldehyde acceptor and control the arrangement of the reactants in the transition state [70]. Conceivably, the present VAR may also be speeded

TS

Synclinal Model
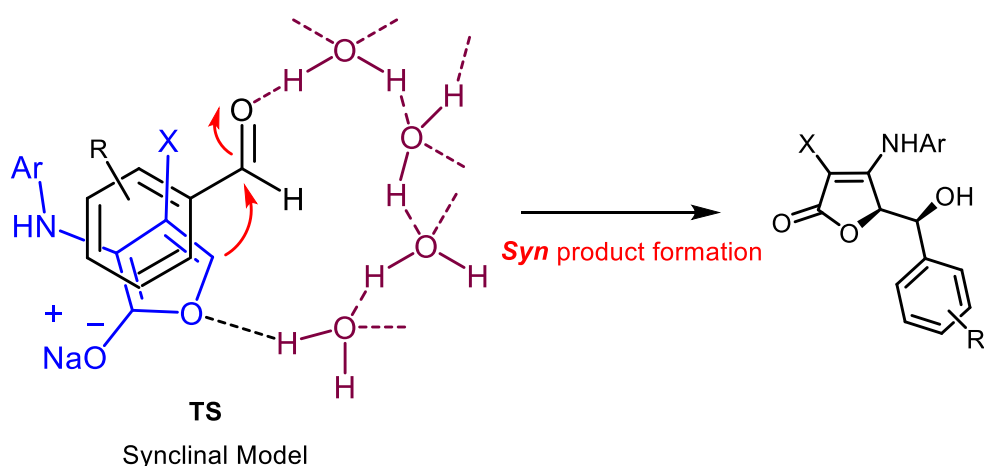
Figure 2.11 Proposed Transition State (TS) for the role of water in VAR of tetronamides [70]

by intermolecular H-bonding (Figure 2.11), although, as will be discussed later, the diastero-selectivity is likely to arise by thermodynamic process involving *syn*/*anti*-isomer equilibration.

2.3. Substrate Scope in the VAR of Tetronamides with Aldehydes

Having established a simple and efficient method enabling stereoselective access to *syn*-**9**, the next task was to investigate the substrate scope. Thus, tetronamides **8a-d** were screened with several aldehydes using NaOH in methanol:water (2:1 v/v) at room temperature (Table 2.2). The results show that product yields are generally moderate to excellent (51-91%), and in most cases, the *syn:anti* ratio is at least 90:10. All the prepared tetronamides tested behaved similarly in terms of yield and diastereoselectivity. However, the nature of the aldehyde did impact selectivity in some cases. Benzaldehydes bearing electron-donating substituents performed remarkably well, leading uniquely to *syn*-adducts (**10**, **11**, **17**, **19**, **20** and **24**), as did benzaldehyde itself (**9** and **22**). High *syn*-selectivities (>90:10) were also observed with *p*-nitrobenzaldahyde and 2-chloro-4-fluorobenzaldahyde (cf. **14**, **21** and **28**). The lowest selectivities, but still in favour of the *syn*-isomer, were observed with *meta*-nitrobenzaldehyde (cf. **15** and **23**) [71], 2-napthalenecarbaldehyde (**18**),

Table 2.2 Substrate scope in the VAR of tetronamides with aldehydes [a,b]

RCHO (1.2 equiv)
NaOH (1.0 equiv)

MeOH:H₂O (2:1)
rt, 3-12 h

ArHN X

8a-c

ArHN X + ArHN X

syn/anti-**9-28**

9 (>99:1)
3 h, 91%
[1 g, 5h, 81%]

10 (>99:1)
4 h, 74%
[1.9 g, 6h, 70%]

11 (>99:1)
5 h, 64%

12 (78:22)
4 h, 68%
[X-ray]

13 (83:17)
6 h, 72%

14 (91:9)
3 h, 78%

15 (56:44)
8 h, 54%

16 (80:20)
4 h, 62%

17 (>99:1)
4 h, 77%
[2.3 g, 6h, 71%]

18 (64:36)
7 h, 67%

19 (>99:1)
6 h, 68%

20 (>99:1)
6 h, 75%

21 (93:7)
3 h, 81%

22 (>99:1)
3 h, 86%

23 (53:47)
8 h, 51%

24 (>99:1)
4 h, 71%

25 (>99:1)
6 h, 79%

26 (>99:1)
8 h, 76%

27 (66:33)
6 h, 61%

28 (97:3)
5 h, 70%
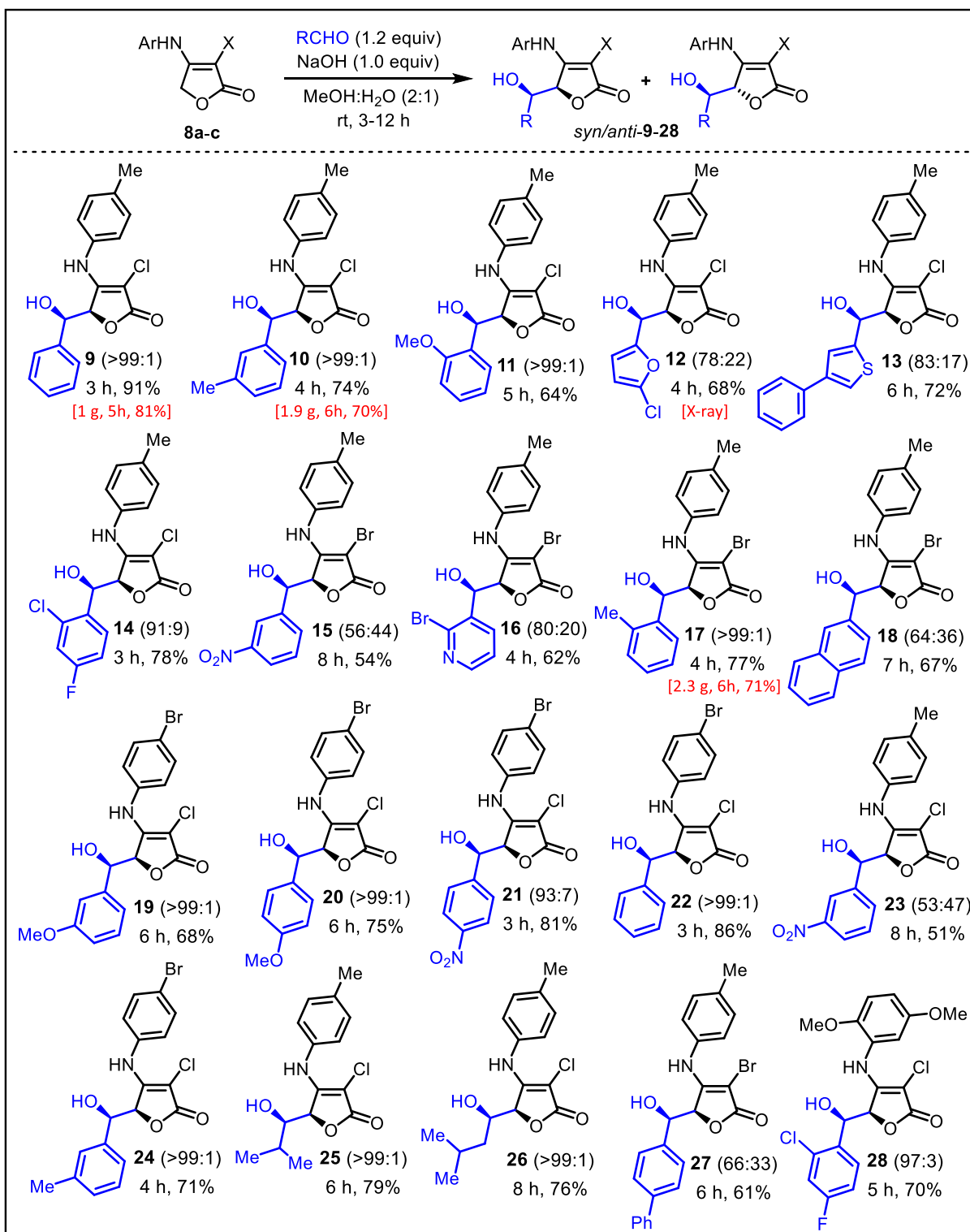
[a] For the sake of clarity only the *syn* (major) isomer is shown along with the *syn:anti* ratio (in brackets) [b] Very similar yields and *syn:anti* ratios were obtained (cf. compounds **9**, **12**, **15**, **17**, and **26**) by replacing NaOH by LiOH.

4-phenyl- carbaldehyde (**27**), and some heteroaromatic aldehydes (**12**, **13** and **16**). Importantly, excellent results were obtained with the two aliphatic aldehydes tried, providing solely the *syn*-adducts in high yield (**25** and **26**). As indicated in Table 2.2, we have also demonstrated the preparative value of this method by the gram-scale synthesis of *syn*-adducts **9**, **10** and **17**. Indeed, the scale-up did not affect diastereoselectivity, and yields were fairly close to those obtained from the 1 mmol scale experiments (e.g. 71 vs 77% for **17**).

In general, these reactions were fairly clean. Also, no by-products arising from dehydration of the aldol adducts could be observed within 3-12 h. However, it was found that the yield of the desired adducts was time dependent. Careful monitoring by TLC revealed that *syn*/*anti* ratios improved in favour of the *syn* isomer. At this point, a more detailed study of the VAR reaction of **8a** with benzaldahyde was performed using the optimized conditions, where the aldol adducts *syn*-**9**/*anti*-**9** were isolated at different time intervals (Figure 2.3).
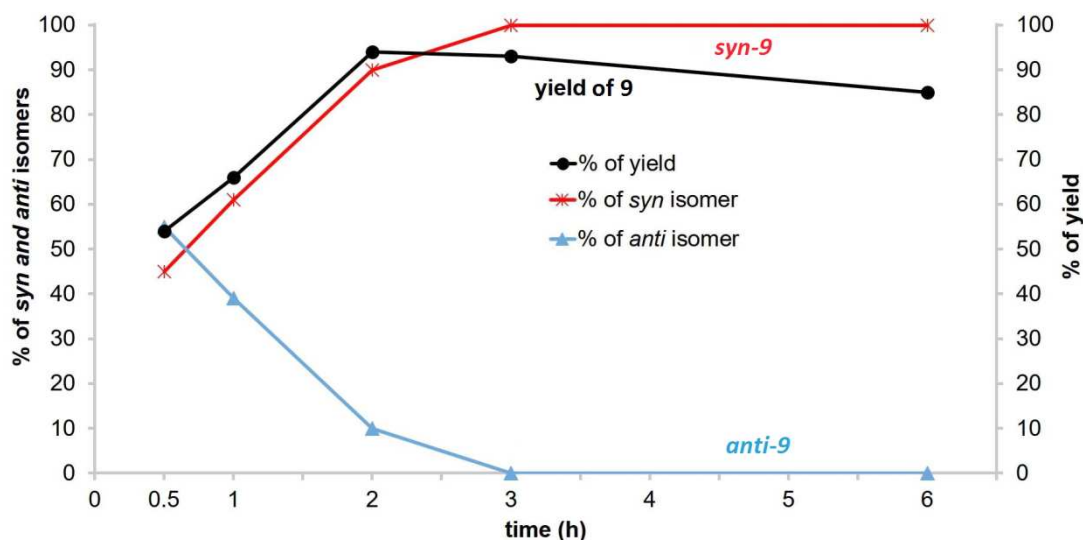
Figure 2.3 Yield and *syn*/*anti* composition (%) of aldol product **9** versus time for the VAR of tetronamide **8a** with benzaldehyde

Thus, compound **9** was obtained in 54% yield after 0.5 h with a *syn:anti* ratio of 45:55. When the reaction time increased to 2 hours, the yield reached a maximum (94%) while the *syn:anti* ratio had improved to 90:10. Further increase in the reaction time to 3 hours led to virtually complete control of diastereoselectivity (*syn:anti* >99:1) but a slightly lower yield (91%). After 6 hours the product yield decreased to 82% although the selectivity was still excellent. From the preparative standpoint, these findings show that quenching the VAR at

the right time, in this case 3 hours, is critical to ensure an optimal balance between diastereoselectivity and the product yields.

2.4. Mechanistic Considerations and Evidence

The variation of diastereoselectivity over time can best be explained by a dynamic resolution process, whereby diastereomeric equilibration ultimately affords the most stable isomer. From this point of view, two pathways were considered by which *anti-syn* interconversion may occur. The first involves an iterative retro-aldol/aldol reaction (**path A,** Scheme 2.4). Alternatively, the butenolide stereogenic center may epimerize *via* intervention of furanolate **F2** (**path B,** Scheme 2.4). Given the high thermodynamic acidity of butenolides (pK_a ca. 12-15) [72], direct abstraction of the C5-H is possible, especially under basic conditions. Indeed, furanolate formation has been invoked to explain the racemization of a formal VAR-adduct, namely γ-hydroxymethylbutenolide [73]. Moreover, a γ-benzyltetronate was shown to epimerize in the presence of Hünig's base, but not pyridine [74]. Whilst some
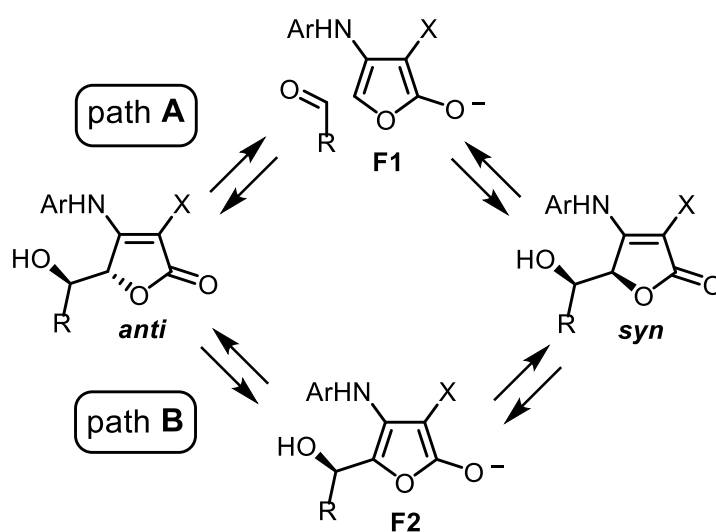
Scheme 2.4 Plausible pathways for isomer interconversion

classical retro-aldol/aldol reactions have been previously investigated, notably in the context of catalytic kinetic resolution [75, 76] and total synthesis [77], there have been no such studies on vinylogous variants involving butenolides.

With this in mind, the feasibility of **path A** was tested by conducting "transfer-aldol" experiments, as shown in Scheme 2.5. Thus, a 1:1 mixture of *anti-***10** and *anti-***22** were subjected to the optimized procedure and the reaction was quenched after 3 hours. Flash

column chromatography afforded three mixtures, each consisting of only two compounds: (i) tetronamides **8a** and **8b** (1:1), (ii) *syn*-**9** and *syn*-**22** (1:2), and (iii) a 3:1 ratio of *syn*-**10** and
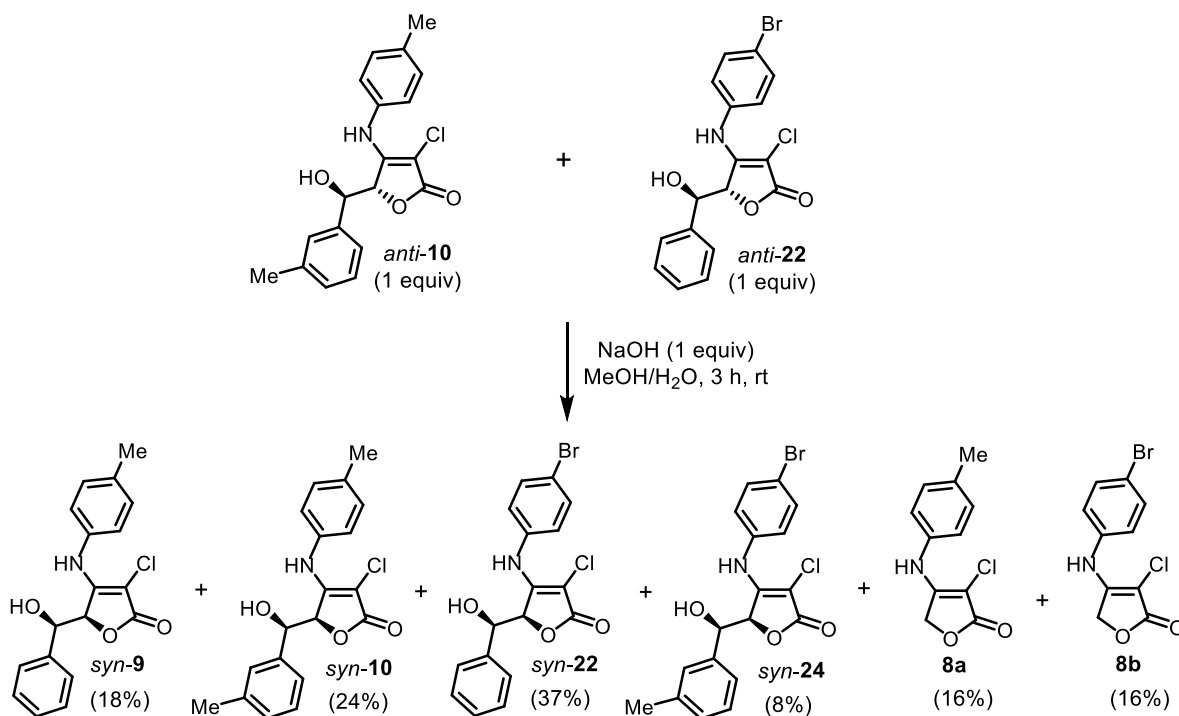
Scheme 2.5 Base-catalysed transfer-aldol reaction of *anti*-**10** and *anti*-**22**

syn-**24**. ^{1}H NMR analysis of these mixtures, and comparison with those of authentic compound samples permitted both the identity and yield of each product to be determined. The crude reaction mixture also revealed signals for the expected aldehydes, but no signals corresponding to the starting *anti* compounds (Figure A2.21; p. 185). These findings demonstrate that the reto-aldol/aldol sequence (**path A**) is indeed involved and capable of accomplishing complete *anti*-to-*syn* conversion.

To explore the possibility of direct C5-H (**path B**), the following experiment was performed. Pure *anti*-**9** was dissolved in CD$_3$OD/D$_2$O and a ^{1}H NMR spectrum was taken immediately and after one hour. Both spectra showed that only the NH and OH protons underwent deuterium exchange (Figure A2.22; p. 186). The doublets at 4.85 ppm (H-6, *J* = 5.5 Hz) and 5.60 ppm (H-5, *J* = 5.5 Hz) were used as diagnostic signals to monitor the isomerization process. To this solution, NaOH was added and the ^{1}H NMR spectrum was taken after 10 minutes. In this spectrum (Figure A2.23; p. 186) the signals corresponding to H-5 and H-6 for the *anti*-**9** isomer had disappeared and new signals at 4.88 ppm (H-6, broad singlet for *syn*-**9**) and 5.40 ppm (H-5, broad singlet for *syn*-**9**) were observed. The 1:1 integral ratio of the new signals clearly indicates that no deuterium exchange took place at C5. In

addition, new signals corresponding to tetronamide **8a** and benzaldehyde could be seen. Therefore, *anti*-**9** is converted into the *syn*-**9** isomer *via* a retro-aldol process and not *via* C5-H abstraction. Only after 30 minutes the C5-H signal of *syn*-**9** disappeared, revealing that complete deuterium exchange had taken place (Figure A2.24; p. 187). Whether this occurs by direct abstraction of the C5-H in *syn*-**9** (cf. **Path B**, Scheme 2.4) or indirectly *via* deuteration of furanolate **F2** (**Path A**) is an open question. It is fairly clear though, that C5-deuteration is substantially slower than the iterative retro-aldol/aldol reaction.

Taken together, the experiments just described leave little doubt that (i) a retro-aldol/aldol sequence is involved, and (ii) that the latter readily accomplishes conversion of the *anti* to the presumably more stable *syn*-isomer. To verify that this is indeed the case, the stability of the *syn* and *anti* isomers was computed for the simplified model compound **29** using the increasingly popular meta hybrid exchange-correlation functional M06-2X developed by Truhlar and co-workers, coupled with the high 6-311+G** basis set. This functional has been shown to perform well in main-group thermochemistry, and to describe non-covalent interactions [78]. The enthalpies and Gibbs free energies differences (ΔH and ΔG, respectively) between *syn/anti* aldol adducts were computed to provide computational
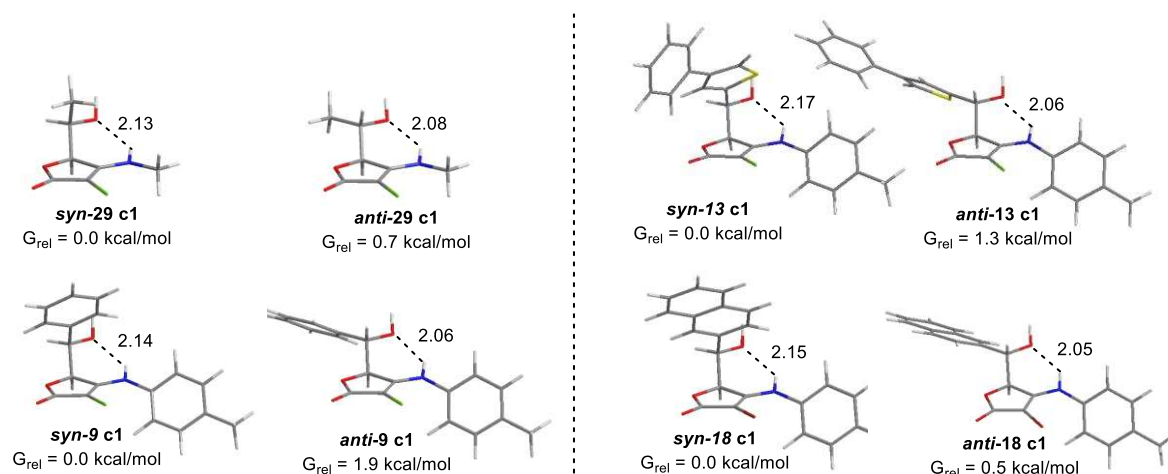
Figure 2.4 M06-2X/6-311+G** optimized geometries (global minima) found for *syn* and *anti* aldol adducts **29** (model compounds) **9, 13** and **18**, with selected distances in Å

support to the proposed thermodynamic equilibration. As shown in Figure 2.4, the *syn*-**29** aldol was found to be more stable than its *anti*-**29** isomer (ΔH = 0.5 kcal/mol; ΔG = 0.7 kcal/mol), as expected. Interestingly, when similar calculations were carried out for compound **9**, the preference towards the *syn* aldol was increased (ΔH = 1.5 kcal/mol; ΔG = 1.9 kcal/mol). Under equilibration conditions at room temperature, such energy differences predict a *syn/anti* ratio of 93/7 and 96/4 (based on formation enthalpies and Gibbs free

energies, respectively), which are in good agreement with the experimental findings. Similar calculations were carried out for the aldol products **13** and **18** (*syn* and *anti* isomers). The ratios computed from the *ΔG* values (90:10 and 70:30, respectively) are close to those found experimentally (83:17 and 64:36).

2.5. Computational and NMR Studies on the Relative Configuration of Aldol Adducts

All the discussion up to this point was made considering that the relative configuration of the major and minor isomers were assigned based on the ^{1}H-NMR data. Here, a representative example of the ^{1}H-NMR of both isomers of compound **9** was taken (Figure 2.5) for the detailed discussion on this assignment.
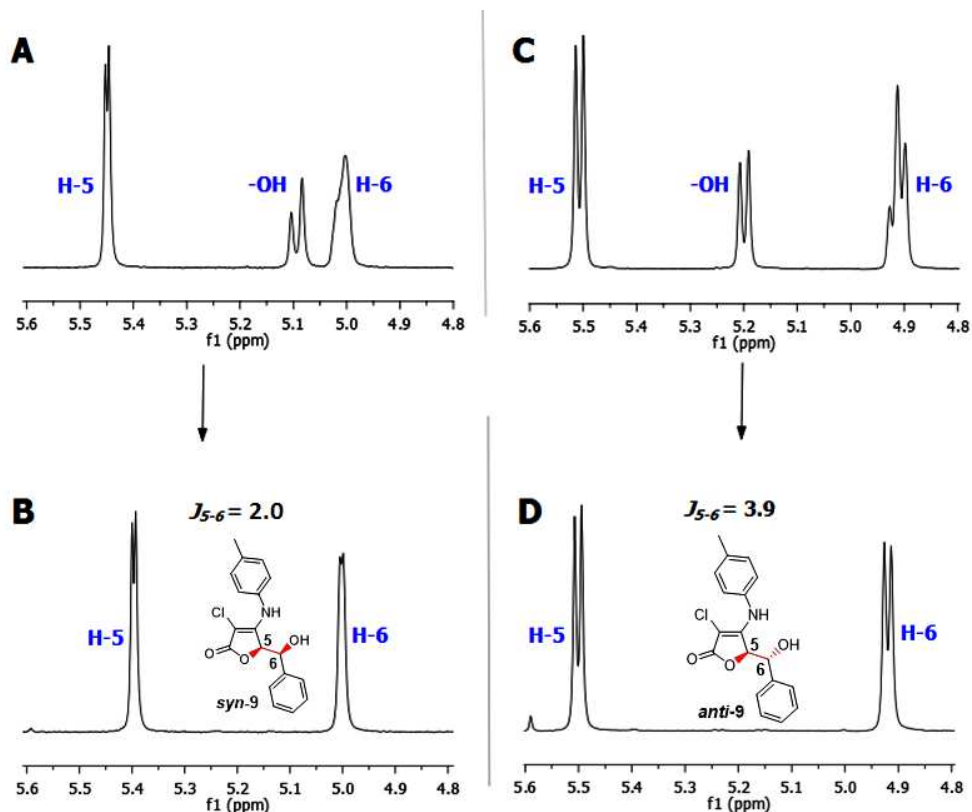
Figure 2.5 Expansion of the ^{1}H-NMR (300 MHz, acetone-d$_6$) spectra of *syn*-**9** (**2.5A**) and *anti*-**9** (**2.5C**) isomers. The corresponding D$_2$O exchange spectra are shown in **2.5B** (*syn*-**9**) and **2.5D** (*anti*-**9**).

The major difference in the spectra of both isomers is the value of ^3J between H-5 and H-6. In the spectra run in acetone-d$_6$ the signal for H-5 is a doublet with J_{5-6} = 2.0 Hz for the major isomer (Figure 2.5A) and a doublet with J_{5-6} = 3.9 Hz for the minor isomer (Figure 2.5C). The signals for H-6 around $δ$ = 4.9-5.1 is a multiplet due to a further coupling between H-6 and OH (Figure 2.5A, 2.5C). So, doing a D$_2$O exchange a clear doublet is observed in both cases (Figure 2.5B and 2.5D), confirming the coupling reported for H-5. Since no one

has prepared these types of aldol-tetronamides before, a reliable way was necessary to secure a correct assignment of the stereochemistry of the synthesized compounds. To accomplish this, a DFT study using Gaussian 09 was performed [79]. Since the coupling constant J_{5-6} strongly depends on the conformational preference of the aldols, an extensive conformational search of a simplified system (compounds syn-**29** and anti-**29**, Figure 2.6) at the B3LYP/6-31G* level of theory was primarily performed.

In both cases, a clear preference towards the conformer characterized by an intramolecular N-H---OH hydrogen bond was found. In such conformation, a *gauche* relationship between H-5 and H-6 was found for the *syn* isomer (ϕ 62.4°), and an *anti* relationship between both hydrogen atoms in the case of the *anti* isomer (ϕ 173.7°), indicating that the lower J_{5-6} value should be expected for the former.
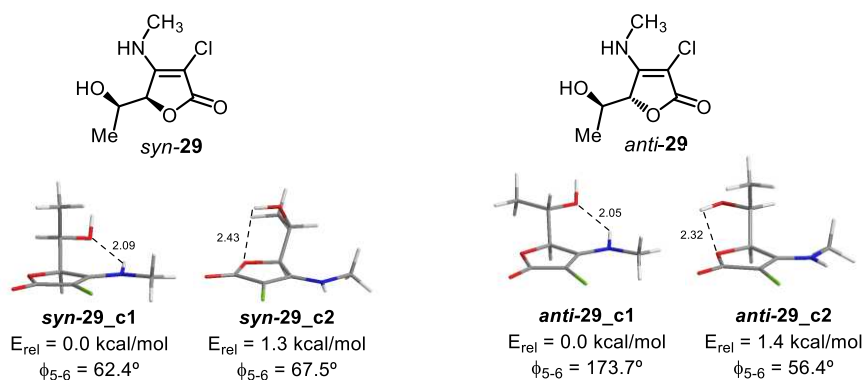
Figure 2.6 B3LYP/6-31G* optimized geometries (global minima) of all significantly populated conformers of s*yn*-**29** and *anti*-**29**, with selected distances in angstrom (Å).

This was further confirmed after Boltzmann-averaged *J*-coupling calculations of all significantly populated conformers at the B3LYP/6-31G**//B3LYP/6-31G* level (Table 2.3): the computed J_{5-6} was 4.1 Hz (*syn*-**29**) and 7.4 Hz (*anti*-**29**).

Table 2.3 B3LYP/6-31G**//B3LYP/6-31G* total nuclear spin-spin coupling J_{5-6}

Conformer	J_{5-6}
syn-**29**_c1	4.5 Hz
syn-**29**_c2	0.9 Hz
Boltzmann averaged	**4.1 Hz**
anti-**29**_c1	7.8 Hz
anti-**29**_c2	3.3 Hz
Boltzmann averaged	**7.4 Hz**

To validate the assignment, a full conformational search over three selected aldol pairs synthesized in this work was performed: compounds **9**, **12**, and **13** (Figures 2.7-2.9).

syn-9_c1
E_{rel} = 0.00 kcal/mol
ϕ_{5-6} = 60.7º
Contribution = 58%

syn-9_c2
E_{rel} = 0.48 kcal/mol
ϕ_{5-6} = 64.7º
Contribution = 26%

anti-9_c1
E_{rel} = 0.00 kcal/mol
ϕ_{5-6} = 177.8º
Contribution = 85%

anti-9_c2
E_{rel} = 1.17 kcal/mol
ϕ_{5-6} = 173.1º
Contribution = 12%

syn-9_c3
E_{rel} = 1.02 kcal/mol
ϕ_{5-6} = 77.2º
Contribution = 11%

syn-9_c4
E_{rel} = 1.34 kcal/mol
ϕ_{5-6} = 76.8º
Contribution = 6%

anti-9_c3
E_{rel} = 2.03 kcal/mol
ϕ_{5-6} = 55.6º
Contribution = 3%
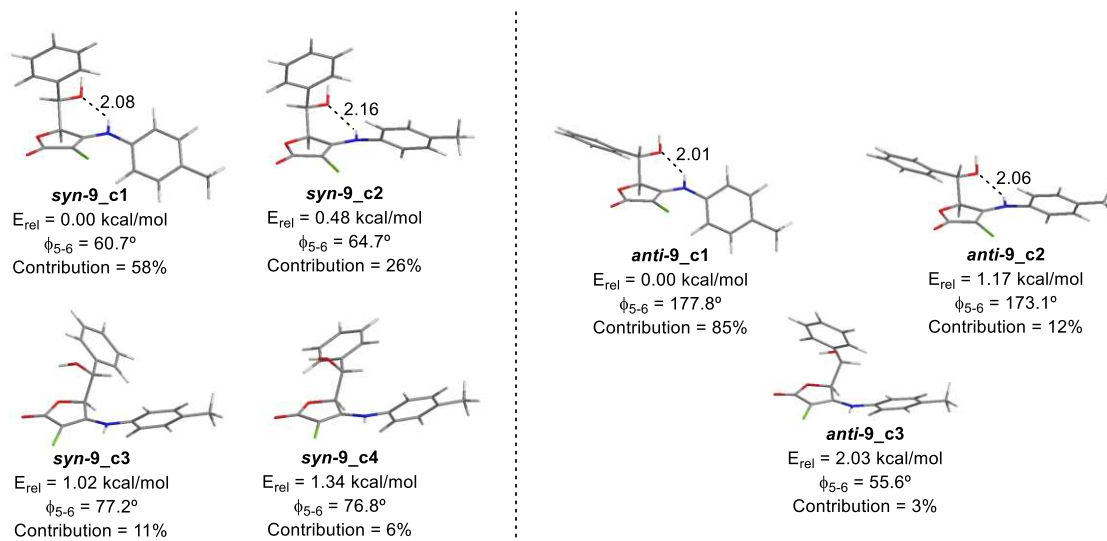
Figure 2.7 B3LYP/6-31G* optimized geometries (global minima) found for compound **9**, with selected distances in angstrom (Å).

syn-12_c1
E_{rel} = 0.00 kcal/mol
ϕ_{5-6} = 64.6º
Contribution = 39%

syn-12_c2
E_{rel} = 0.03 kcal/mol
ϕ_{5-6} = 68.0º
Contribution = 37%

syn-12_c3
E_{rel} = 0.64 kcal/mol
ϕ_{5-6} = 64.8º
Contribution = 13%

syn-12_c4
E_{rel} = 0.75 kcal/mol
ϕ_{5-6} = 61.2º
Contribution = 11%

anti-12_c1
E_{rel} = 0.00 kcal/mol
ϕ_{5-6} = 179.1º
Contribution = 53%

anti-12_c2
E_{rel} = 0.63 kcal/mol
ϕ_{5-6} = 175.7º
Contribution = 19%

anti-12_c3
E_{rel} = 1.01 kcal/mol
ϕ_{5-6} = 54.6º
Contribution = 10%

anti-12_c4
E_{rel} = 1.03 kcal/mol
ϕ_{5-6} = 173.8º
Contribution = 10%

anti-12_c5
E_{rel} = 1.09 kcal/mol
ϕ_{5-6} = 54.0º
Contribution = 9%

Figure 2.8 B3LYP/6-31G* optimized geometries (global minima) found for compound **12**, with selected distances in angstrom (Å).
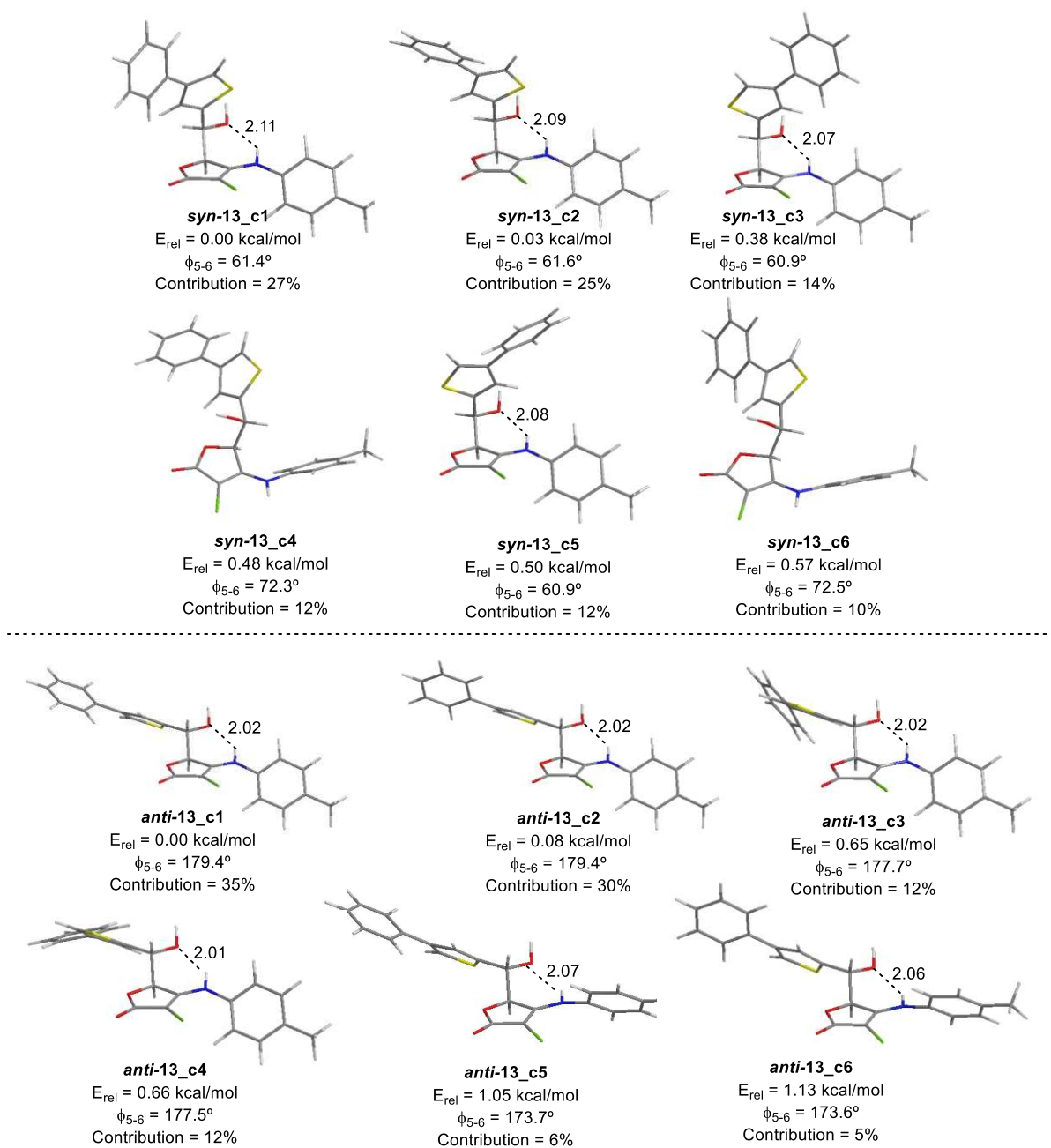
Figure 2.9 B3LYP/6-31G* optimized geometries (global minima) found for compound **13**, with selected distances in angstrom (Å).

Interestingly, despite the degree of conformational freedom was higher than that of the simplified model, in all cases the rotational preference towards the conformers showing intramolecular N-H---OH hydrogen bond was found. This result suggested that the major isolated adducts, showing smaller J_{5-6} coupling values, should display a *syn* stereochemistry. In an additional supporting of the findings, GIAO ^{13}C-NMR calculations was also performed, which represent a valuable and indisputable tool in modern structural elucidation [80, 81]. The magnetic shielding tensors of all significantly populated conformers were computed at

the mPW1PW91/6-31+G**//B3LYP/6-31G* level of theory in solution (PCM, CHCl$_3$), using the multi-standard approach to extract the chemical shifts [82, 83].

Next, the Goodman's CP3 parameter was computed to address the question of assigning two sets of experimental data to two plausible candidates [84]. In all cases, positive CP3 values were computed for the "matched" cases (major-*syn*/minor-*anti*, Table 2.4), while negative CP3 values were found for the "mismatched" cases (major-*anti*/minor-*syn*, Table 2.5). It is important to note that positive values indicate good agreement (assignment likely to be correct), whereas negative values are likely to be incorrect [84].

Table 2.4 CP3 values computed for the matched pairs

Pair	CP3 (based on ^{13}C data)
major- *syn*-**9**/ minor- *anti*-**9**	0.54
major- *syn*-**12**/ minor- *anti*-**12**	0.35
major- *syn*-**13**/ minor- *anti*-**13**	0.37

Table 2.5 CP3 values computed for the mismatched pairs

Pair	CP3 (based on ^{13}C data)
major- *anti*-**9**/ minor- *syn*-**9**	-0.58
major- *anti*-**12** / minor- *syn*-**12**	-0.55
major- *anti*-**13**/ minor- *syn*-**13**	-1.47

Finally, the *in silico* stereochemical assignment performed was further unambiguously validated by X-ray diffraction analysis on single crystals of both diastereomers of compound **12** (Figure 2.10). As seen from Figure 2.10, the major aldol adduct of compound **12** is the *syn* isomer, while the minor is the *anti,* as predicted by the computational studies.

Syn-**12**   *Anti*-**12**
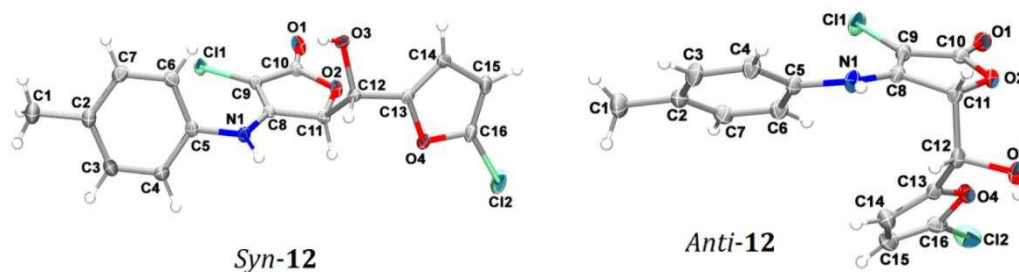
Figure 2.10 X-ray structures for both diastereomers of compound **12**

In the particular case of aldol product **12**, it is also clear that in the solid crystalline form no intramolecular N-H---OH hydrogen bond is observed, as predicted by calculations in the gas phase and in solution.

3. Conclusion

The foregoing inaugural study of the vinylogous aldol reaction of *N*-monosubstituted tetronamides has enabled the development of a viable new method for constructing medicinally relevant *syn*-aldol adducts. Of great practicality, this method simply employs NaOH in aq. MeOH at ambient temperature, thereby allowing easy access to *syn*-aldols from aromatic as well as aliphatic aldehydes. Importantly, most of the VA reactions tried afforded single diastereoisomers (*syn*/*anti* > 99:1) in good to excellent yields. Several lines of evidence suggest that the observed selectivity arises from *anti*-to-*syn* isomer interconversion *via* an iterative retro-aldol/aldol reaction sequence. Studies on the molecular properties (both experimental and theoretical) of novel tetronamide aldol products are discussed in Chapter 3.

4. Materials and Methods

4.1. General Experimental

All reactions were performed using analytical grade solvents without further purifications, unless otherwise stated. The ^{1}H and ^{13}C NMR spectra were recorded on a Varian Mercury 300 instrument (300 MHz and 75 MHz, respectively), using deuterated chloroform, acetone or DMSO as a solvent and tetramethylsilane (TMS) as internal standard (δ = 0). The experiments were performed at controlled probe temperature of 25 °C, using a number of scans (nt) of 16, a number of points in the FID of 43686 (np); 90° pulse width; spectral width of 4800.8 Hz; acquisition time (at) of 4.550 s; delay time (D1) of 1.00 s. Chemical shifts of ^{1}H and ^{13}C NMR spectra are reported in ppm. All coupling constants (J values) were expressed in Hertz (Hz). Multiplicities are reported as follows: singlet (s), doublet (d), doublet of doublets (dd), triplet (t), multiplet (m) and broad (br). Infrared spectra were recorded on a Varian 660-IR, equipped with GladiATR scanning from 4000 to 500 cm^{-1}. Melting points are uncorrected and were obtained from MQAPF-301 melting point apparatus (Microquimica, Brazil). High resolution mass spectra were recorded on a Bruker MicroTof (resolution = 10,000 FWHM) under electrospray ionization (ESI) and are given to four decimal places. XRD was recorded on Bruker D8 focus X-ray Diffraction spectrometer. Analytical thin layer chromatography analysis was conducted on aluminum packed precoated silica gel plates. Column chromatography was performed over silica gel (230-400 mesh).

4.2. General Procedure for the Preparation of Compounds 8a-e

To a 100 mL round bottomed flask, were added **7a** (2 g, 13.08 mmol), MeOH (20 mL for a 13.08 mmol scale reaction), NaHCO$_3$ (550 mg, 6.54 mmol) and *p*-toluidine (1.4 g, 13.08 mmol). The reaction mixture was stirred at room temperature for 12 h. After the consumption of the starting butenolide **7a**, the reaction mixture was quenched by addition of aqueous HCl solution (1M, 10 mL). The methanol was then removed under reduced pressure and the aqueous mixture was extracted with ethyl acetate (3×30 mL). The combined organic layers were dried over anhydrous Na$_2$SO$_4$, filtrated and the solvent evaporated. The crude residue was purified by silica gel column chromatography, eluted with hexane/ethyl acetate (70:30 v/v) to afford compound **8a** as white solid in 93% yield (2.7 g, 12.16 mmol). Compound **8b-e** was synthesized using a method similar to that of compound **8a.**

3-chloro-4-(*p*-tolylamino)furan-2(5*H*)-one (8a)
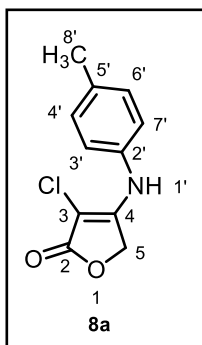
MP: 213.8-215.1 °C. R_f = 0.4 (hexane: ethyl acetate, 1:1, v/v). **FTIR:** $\bar{v}_{max}$ 3234, 3068, 1741, 1629, 1052, 982, 899, 741, 531 cm^{-1}. **^{1}H NMR** (300 MHz, Acetone-d$_6$:DMSO-d$_6$; 9:1) δ 9.06 (s, 1H, -NH), 7.19 (apparent singlet, 4H, H-3′, H-4′, H-6′ and H-7′), 4.99 (s, 2H, H-5), 2.31 (s, 3H, H-8′). **^{13}C NMR** (75 MHz, Acetone-d$_6$:DMSO-d$_6$; 9:1) δ: 168.76 (C-2), 158.51 (C-4), 135.95 (C-2′), 134.85 (C-5′), 129.78 (2C, C-4′ and C-6′), 122.48(2C, C-3′ and C-7′), 87.21 (C-3), 66.07 (C-5), 20.01 (C-8′). **HRMS (ESI) [M-H]$^-$** calculated for C$_{11}$H$_9$ClNO$_2$, 222.0322; found, 222.0326

4-[(4-bromophenyl)amino]-3-chlorofuran-2(5*H*)-one (8b)
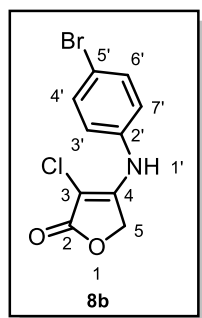
Compound **8b** was isolated as white solid in 87% yield (3.3 g, 11.38 mmol); purified by column chromatography, eluent hexane/ethyl acetate (68:32 v/v). **MP:**

221.3-222.6 °C. R_f = 0.4 (hexane: ethyl acetate, 1:1, v/v). **FTIR v_{max}** 3235, 3061, 1749, 1632, 1054, 977, 891, 739, 515 cm^{-1}. **^{1}H NMR** (300 MHz, Acetone-d$_6$) δ: 8.80 (s, 1H, -NH), 7.56 (d, *J*= 8.9 Hz, 2H, H-4′ and H-6′), 7.27 (d, *J*= 8.9 Hz, 2H, H-3′ and H-7′), 5.12 (s, 2H, H-5) . **^{13}C NMR** (75 MHz, Acetone-d$_6$) δ: 168.38 (C-2), 157.65 (C-4), 137.90 (C-2′), 132.31 (2C, C-4′ and C-6′), 123.69 (C-3′), 123.58 (C-7′), 117.36 (C-5′), 89.13 (C-3), 66.15 (C-5). **HRMS (ESI) [M-H]$^-$** calculated for C$_{10}$H$_6$BrClNO$_2$, 285.9270; found, 285.9273

3-bromo-4-(*p*-tolylamino)furan-2(5*H*)-one (8c)
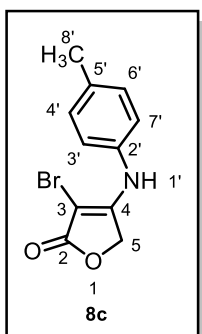
Compound **8c** was isolated as orange solid in 82% yield (1.8 g, 6.78 mmol); purified by column chromatography, eluent hexane/ethyl acetate (70:30 v/v). **MP:**

225.2-226.8 °C. R_f = 0.4 (hexane: ethyl acetate, 1:1, v/v). **FTIR:** $\bar{v}_{max}$ 3230, 3074, 1729, 1628, 1050, 985, 896, 740, 520 cm^{-1}. **^{1}H NMR** (300 MHz, DMSO-d$_6$) δ: 9.45 (s, 1H, -NH), 7.15 (apparent singlet, 4H, H-3′, H-4′, H-6′ and H-7′), 4.99 (s, 2H, H-5), 2.27 (s, 3H, H-8′). **^{13}C NMR** (75 MHz, DMSO-d$_6$) δ: 170.09 (C-2), 162.19 (C-4), 135.91 (C-2′), 135.05 (C-5′), 130.09 (2C, C-4′ and C-6′), 123.21 (2C, C-3′ and C-7′), 73.82 (C-3), 67.66 (C-5), 20.87 (C-8′). **HRMS (ESI) [M-H]$^-$** calculated for C$_{11}$H$_9$BrNO$_2$, 265.9817; found, 265.9832

3-chloro-4-((2,5-dimethoxyphenyl)amino)furan-2(5*H*)-one (8d)

Compound **8d** was isolated as a off-white solid in 64% yield (1.3 g); purified by column chromatography, eluent hexane/ethyl acetate (80:20 v/v). **¹H NMR** (300 MHz, Acetone-d₆) *δ* 8.04 (s, 1H, -NH), 7.04 (d, *J* = 8.9 Hz, 1H, H-6′), 6.83 (d, *J* = 2.9 Hz, 1H, H-3'), 6.79 (dd, *J* = 8.9 and 2.9 Hz, 1H, H-5'), 4.99 (singlet, 2H, H-5), 3.86 (s, 3H, H-8′) and 3.78 (s, 3H, H-9′). **¹³C NMR** (75 MHz, Acetone-d₆) *δ* 168.40 (C-2), 158.42 (C-4'), 153.82 (C-4), 146.20 (C-7') 127.26 (C-2'), 112.62 (C-6'), 110.90 (C-5'), 109.66 (C-3'), 88.26 (C-3), 66.14 (C-5), 55.82 (C-8') and 55.13 (C-9'). **HRMS (ESI)** calculated for **[M-H]⁻**, 268.0377; found, 268.0423.
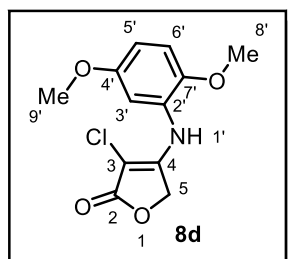
4-(butylamino)-3-chlorofuran-2(5*H*)-one (8e)

Compound **8e** was isolated as a yellow oil in 38% yield (423 mg); purified by column chromatography, eluent hexane/ethyl acetate (85:15 v/v). **¹H NMR** (400 MHz, CDCl₃) *δ* 5.44 (br s, 1H, -NH), 4.75 (s, 2H, H-5), 3.26 (br s, 2H, H-2'), 1.61 (quintet, *J* = 7.3 Hz, 2H, H-3'), 1.39 (sextet, *J* = 7.3 Hz, 2H, H-4'), and 0.95 (t, *J* = 7.3 Hz, 3H, H-5'). **¹³C NMR** (100 MHz, CDCl₃) *δ* 170.53 (C-2), 160.50 (C-4), 85.36 (C-3), 65.53 (C-5), 47.87 (C-2'), 32.37 (C-3'), 19.71 (C-4') and 13.60 (C-5'). **HRMS (ESI)** calculated for $C_8H_{13}ClNO_2$ **[M+H]⁺**, 190.0635; found, 190.0583
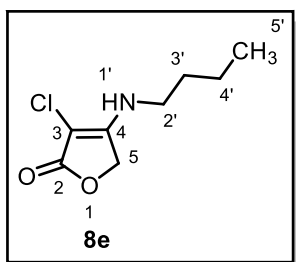
4.3.   Typical Procedure for the VAR of Tetronamides (9–28)

To a 25 mL one neck round bottomed flask were added tetronamide **8a** (200 mg, 0.89 mmol), a mixture of MeOH and H_2O (4 and 2 mL, v/v), followed by NaOH (36 mg, 0.89 mmol). After stirring the reaction mixture for 5 min at room temperature, benzaldehyde (114 mg, 1.07 mmol) was added slowly. The reaction mixture was stirred at room temperature until TLC analysis revealed total consumption of **8a**. The reaction was then quenched by addition of an aqueous solution of HCl (1M, 10 mL). The methanol was removed under reduced pressure and the aqueous mixture was extracted with ethyl acetate (3×15 mL). The combined organic layers were dried over anhydrous Na_2SO_4, filtrated and the solvent evaporated. The crude residue was purified by silica gel column chromatography eluting with hexane/ethyl acetate (80:20 v/v) to afford pure *syn*-**9** as white solid in 91% yield (267 mg, 0.81 mmol). Compounds **10-28** were synthesized using a method similar to that described for compound *syn*-**9**.

3-chloro-5-[hydroxy(phenyl)methyl]-4-(*p*-tolylamino)furan-2(5*H*)-one (*syn*-9)

MP: 192.3-194.6 °C. R_f = 0.35 (hexane: ethyl acetate, 80:20, v/v). **FTIR:** $\bar{v}_{max}$ 3386, 3282, 3228, 3070, 3037, 3002, 2971, 1754, 1635, 1197, 1029, 647 cm^{-1}. **^{1}H NMR** (300 MHz, Acetone-d$_6$) *δ*: 8.54 (s, 1H, -NH), 7.40-7.25 (m, 5H, H-8 to H-12), 7.25 (d, *J* = 8.7 Hz, 2H, H-4′ and H-6′), 7.21 (d, *J* = 8.7 Hz, 2H, H-3′ and H-7′), 5.45 (d, *J* = 2.0 Hz, 1H, H-5), 5.09 (d, *J* = 6.0 Hz, 1H, -OH), 5.00 (m, 1H, H-6), 2.35 (s, 3H, H-8′). **^{1}H NMR** (300 MHz, D$_2$O Exchange) *δ*: 7.23-7.39 (m, 5H, H-8 to H-12), 7.21 (d, *J* = 8.6 Hz, 2H, H-4′ and H-6′), 7.16 (d, *J* = 8.6 Hz, 2H, H-3′ and H-7′), 5.40 (d, *J* = 2.0 Hz, 1H, H-5), 5.00 (d, *J* = 2.0 Hz, 1H, H-6), 2.32 (s, 1H, H-

syn-9
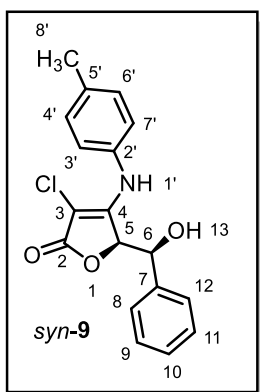
8′). **^{1}H NMR** (300 MHz, CDCl$_3$: DMSO-d$_6$; 9:1) *δ*: 7.83(s, 1H, -NH), 7.32-7.18 (m, 5H, H-8 to H-12), 7.07 (d, *J* = 8.3 Hz, 2H, H-4′ and H-6′), 6.89 (d, *J*= 8.3 Hz, 2H, H-3′ and H-7′), 5.15 (d, *J* = 3.6 Hz, 1H, H-5), 5.03 (d, *J* = 3.6 Hz, 1H, H-6), 2.27 (s, 3H, H-8′). **^{13}C NMR** (75 MHz, CDCl$_3$: DMSO-d$_6$; 9:1) *δ*: 169.74 (C-2), 156.24 (C-4), 138.85 (C-7), 135.28 (C-2′), 134.24 (C-5′), 129.10 (2C, C-4′ and C-6′), 127.89 (2C, C-8 and C-12), 127.78 (C-10), 126.40 (2C, C-8 and C-12), 123.96 (2C, C-3′ and C-7′), 88.62 (C-3), 79.40 (C-5), 71.26 (C-6), 20.80 (C-8′). **HRMS (ESI) [M-H]$^-$** calculated for C$_{18}$H$_{15}$ClNO$_3$, 328.0740; found, 328.0732

3-chloro-5-[hydroxy(m-tolyl)methyl]-4-(*p*-tolylamino)furan-2(5*H*)-one (*syn*-10)

The crude residue was purified by column chromatography on silica gel eluted with

syn-10

hexane/ethyl acetate (75:25 v/v) to afford pure *syn*-**10** as white solid in 74% yield (227 mg, 0.66 mmol). **MP**: 170.3-172.8 °C. **FTIR:** $\bar{v}_{max}$ 3409, 3284, 3257, 3062, 3031, 2967, 2939, 2919, 1751, 1633, 1608, 1511, 1390, 1195, 1008, 707 cm^{-1}. **^{1}H NMR** (300 MHz, CDCl$_3$:DMSO-d$_6$; 3:1) *δ*: 8.43 (s, 1H, -NH), 7.16-6.97 (m, 6H, H-8 to H-10, H-12, H-4′, H-6′), 6.94 (d, *J* = 7.8 Hz, 2H, H-3′ and H-7′), 5.12 (br, 1H, H-5), 4.95 (br, 1H, H-6), 2.28 (s, 3H, H-14), 2.24 (s, 3H, H-8′). **^{13}C NMR** (75 MHz, CDCl$_3$:DMSO-d$_6$; 3:1) *δ*: 169.85 (C-2), 156.43 (C-4), 139.21 (C-7), 137.44 (C-11), 135.34 (C-2′), 134.51 (C-5′), 129.23 (2C, C-4′ and C-6′), 128.60 (C-12), 127.93 (C-9), 127.21 (C-10), 124.13 (2C, C-3′ and C-7′), 123.70 (C-8), 88.70 (C-3), 79.71 (C-5), 71.41 (C-6), 21.46 (C-14), 20.97 (C-8′). **HRMS (ESI) [M-H]$^-$** calculated for C$_{19}$H$_{17}$ClNO$_3$, 342.0897; found, 342.0891
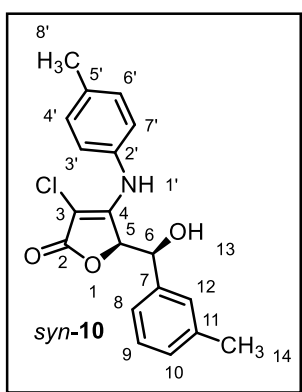
3-chloro-5-[hydroxy(2-methoxyphenyl)methyl]-4-(*p*-tolylamino)furan-2(5*H*)-one (*syn*-11)

The crude residue was purified by column chromatography on silica gel eluted with hexane/ethyl acetate (74:26 v/v) to afford pure *syn*-**11** as white solid in 64% yield (206 mg, 0.57 mmol). **MP:** 202.4-204.0 °C. **FTIR:** $\bar{v}_{max}$ 3424, 3286, 3178, 3070, 3004, 2989, 2960, 2933, 2834, 1741, 1627, 1608, 1492, 1390, 1240, 1078, 1022, 740 cm^{-1}. **^{1}H NMR** (300 MHz, CDCl$_3$:DMSO-d$_6$; 3:1) *δ*: 8.46 (s, 1H, -NH), 7.43 (d, *J*= 6.6 Hz, 1H, H-8), 7.21-7.01 (m, 5H, H-9, H-3′, H-4′, H-6′ and H-7′), 6.85 (t, *J* = 7.4 Hz, 1H, H-10), 6.72 (d, *J* = 8.1 Hz, 1H, H-11), 5.33 (d, *J* = 1.3 Hz, 1H, H-5), 5.04 (br, 1H, H-6), 3.60 (s, 3H, H-14), 2.30 (s, 3H, H-8′). **^{13}C NMR** (75 MHz, CDCl$_3$:DMSO-d$_6$; 3:1) *δ*: 169.76 (C-2), 157.95 (C-12), 155.43 (C-4), 135.52 (C-2′), 135.18 (C-5′), 129.54 (2C, C-4′ and C-6′), 128.54 (C-10), 128.25 (C-7), 128.02 (C-8), 123.99 (2C, C-3′ and C-7′), 120.42 (C-9), 109.86 (C-11), 89.91 (C-3), 79.07 (C-5), 65.05 (C-6), 55.03 (C-14), 20.99 (C-8′). **HRMS (ESI) [M-H]**$^-$ calculated for C$_{19}$H$_{17}$ClNO$_4$, 358.0846; found, 358.0853
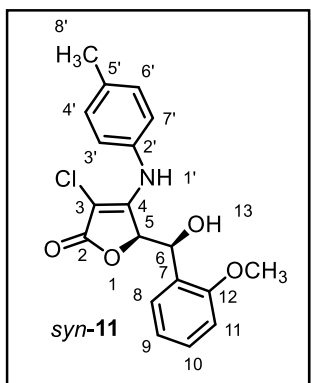
3-chloro-5-[(5-chlorofuran-2-yl)(hydroxyl)methyl]-4-(*p*-tolylamino)furan-2(5*H*)-one (*syn*/*anti*-12)

The crude residue was purified by silica gel column chromatography eluting with hexane/ethyl acetate (79:21 v/v) to afford the *syn*-**12** as white solid in 53% yield (168 mg, 0.47 mmol) and eluting with hexane/ethyl acetate (79.5:20.5 v/v) to afford *anti*-**12** as light yellow solid in 15% yield (48 mg, 0.13 mmol).
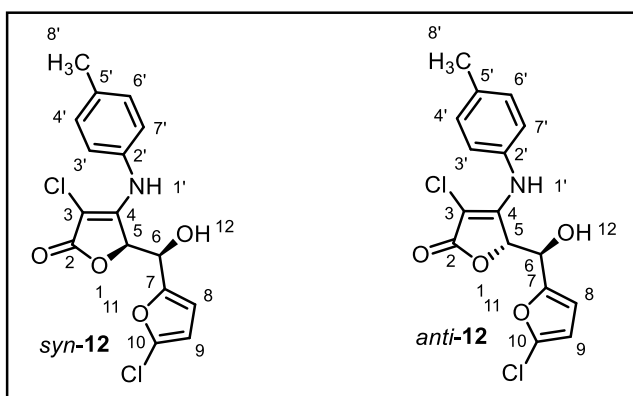
Data for *syn*-12: **MP:** 184.7-186.4 °C. **FTIR:** $\bar{v}_{max}$ 3239, 3208, 3124, 3033, 3006, 1722, 1621, 1598, 1517, 1351, 1280, 1197, 1031, 1006, 792 cm^{-1}. **^{1}H NMR** (300 MHz, Acetone-d$_6$) *δ*: 8.56 (s, 1H, -NH), 7.21 (apparent singlet, 4H, H-3′, H-4′, H-6′and H-7′), 6.47 (d, *J* = 3.3 Hz, 1H, H-9), 6.30 (d, *J* = 3.3 Hz, 1H, H-8), 5.57 (d, *J* = 1.8 Hz, 1H, H-5), 5.29 (br, 1H, -OH), 4.94 (br, 1H, H-6), 2.33 (s, 3H, H-8′). **^{13}C NMR** (75 MHz, Acetone-d$_6$) *δ*: 168.27 (C-2), 156.11 (C-4), 153.38 (C-7), 135.28 (C-2′), 134.90 (C-10), 129.45 (2C, C-4′ and C-6′), 123.77 (2C, C-3′ and C-7′), 123.73 (C-5′), 110.15 (C-8), 107.27 (C-9), 89.62 (C-3), 77.84 (C-5), 65.61 (C-6), 20.01 (C-8′). **HRMS (ESI) [M-H]**$^-$ calculated for C$_{16}$H$_{12}$Cl$_2$NO$_4$, 352.0143; found, 352.0135

Data for *anti*-12: MP: 131.5-133.4 °C. **FTIR:** $\bar{v}_{max}$ 3305, 3257, 3145, 3060, 3031, 2966, 1718, 1621, 1602, 1535, 1511, 1348, 1186, 1029, 1008, 786 cm^{-1}. **^{1}H NMR** (300 MHz, Acetone-d$_6$) *δ*: 8.52 (s, 1H, -NH), 7.21 (d, *J* = 8.4 Hz, 2H, H-4′ and H-6′), 7.15 (d, *J* = 8.4 Hz, 2H, H-3′ and H-7′), 6.44 (d, *J* = 3.3 Hz, 1H, H-9), 6.27 (d, *J* = 3.3 Hz, 1H, H-8), 5.48 (d, *J* = 4.7 Hz, 2H, -OH and H-5), 4.90 (d, *J* = 4.7 Hz, 1H, H-6), 2.33 (s, 3H, H-8′). **^{13}C NMR** (75 MHz, Acetone-d$_6$) *δ*: 168.12 (C-2), 156.24 (C-4), 152.15 (C-7), 135.28 (C-2′), 135.20 (C-10), 129.37 (2C, C-4′ and C-6′), 123.86 (2C, C-3′ and C-7′), 123.82 (C-5′), 110.93 (C-8), 107.25 (C-9), 89.22 (C-3), 78.18 (C-5), 67.87 (C-6), 20.04 (C-8′). **HRMS (ESI) [M-H]$^-$** calculated for C$_{16}$H$_{12}$Cl$_2$NO$_4$, 352.0143; found, 352.0157

3-chloro-5-[hydroxy(5-phenylthiophen-2-yl)methyl]-4-(*p*-tolylamino)furan-2(5*H*)-one (*syn/anti*-13)

The crude residue was purified by silica gel column chromatography eluting with hexane/ethyl acetate (78:22 v/v) to afford the *syn*-13 as white solid in 60% yield (221 mg, 0.54 mmol) and eluting with hexane/ethyl acetate (79:21 v/v) to afford *anti*-13 as light grey solid in 12% yield (44 mg, 0.11 mmol).
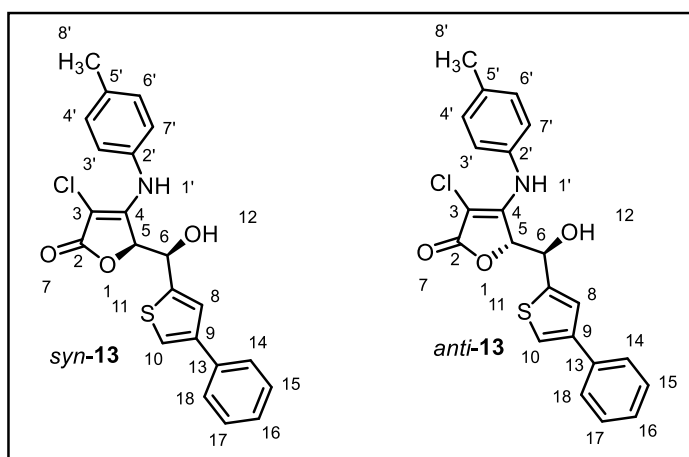
Data for *syn*-13: MP: 196.7-198.2 °C. **FTIR:** $\bar{v}_{max}$ 3253, 3214, 3029, 1729, 1621, 1600, 1511, 1496, 1187, 1112, 1014, 736 cm^{-1}. **^{1}H NMR** (300 MHz, CDCl$_3$: DMSO-d$_6$; 9:1) *δ*: 7.88 (s,1H, -NH), 7.44 (d, *J* = 7.4 Hz, 2H, H-8 and H-10), 7.33-7.14 (m, 5H, H-14 to H-18), 7.04 (d, *J* = 8.1 Hz, 2H, H-4′ and H-6′), 6.92 (d, *J* = 8.1 Hz, 2H, H-3′ and H-7′), 6.20 (d, *J* = 5.1 Hz, 1H, -OH), 5.32 (d, *J* = 3.7 Hz, 1H, H-5), 5.18 (d, *J*= 3.7 Hz, 1H, H-6), 2.25 (s, 3H, H-8′). **^{13}C NMR** (75 MHz, CDCl$_3$: DMSO-d$_6$; 9:1) *δ*: 169.60 (C-2), 155.56 (C-4), 142.22 (C-7), 141.77 (C-9), 135.72 (C-13), 135.49 (C-2′), 133.89 (C-5′), 129.14 (2C, C-4′ and C-6′), 128.72 (2C, C-15 and C-17), 127.11 (C-16), 126.16 (2C, C-14 and C-18), 124.44 (C-10), 124.36 (2C, C-3′ and C-7′), 119.93 (C-8), 88.99 (C-3), 78.01 (C-5), 69.18 (C-6), 20.91 (C-8′). **HRMS (ESI) [M-H]$^-$** calculated for C$_{22}$H$_{17}$ClNO$_3$S, 410.0618; found, 410.0605

Data for *anti*-13: MP: 158.4-160.2 °C. **FTIR:** $\bar{v}_{max}$ 3261, 3058, 3033, 1731, 1627, 1606, 1513, 1411, 1265, 1193, 1020, 740 cm^{-1}. **^{1}H NMR** (300 MHz, CDCl$_3$:DMSO -d$_6$; 9:1) *δ*: 7.77 (s, 1H,-NH), 7.51 (d, *J* =7.7 Hz, 2H, H-8 and H-10), 7.41-7.23 (m, 5H, H-14 to H-18), 7.12 (d, *J* = 7.7 Hz, 2H, H-4′ and H-6′), 6.98 (d, *J* = 7.7 Hz, 2H, H-3′ and H-7′), 5.66 (br, 1H, -OH),

5.15 (d, J= 6.2 Hz, 1H, H-5), 5.08 (br, 1H, H-6), 2.32 (s, 3H, H-8'). ^{13}**C NMR** (75 MHz, CDCl$_3$: DMSO-d$_6$; 9:1) δ: 169.48 (C-2), 156.36 (C-4), 143.16 (C-7), 141.95 (C-9), 135.80 (C-13), 135.45 (C-2'), 134.04 (C-5'), 129.43 (2C, C-4' and C-6'), 128.81 (2C, C-15 and C-17), 127.26 (C-16), 126.23 (2C, C-14 and C-18), 125.08 (C-10), 123.90 (2C, C-3' and C-7'), 120.50 (C-8), 89.73 (C-3), 79.22 (C-5), 70.69 (C-6), 20.95 (C-8'). **HRMS (ESI) [M-H]$^-$** calculated for C$_{22}$H$_{17}$ClNO$_3$S, 410.0618; found, 410.0585

3-chloro-5-[(2-chloro-4-fluorophenyl)(hydroxy)-methyl]-4-(tolylamino)furan-2,5H-one (*syn/anti*-14)

The crude residue was purified by column chromatography on silica gel eluted with hexane/ethyl acetate (76:24 v/v) to afford mixture of *syn/anti*-**14**, in a *91:09* ratio as a white

syn/anti-**14**
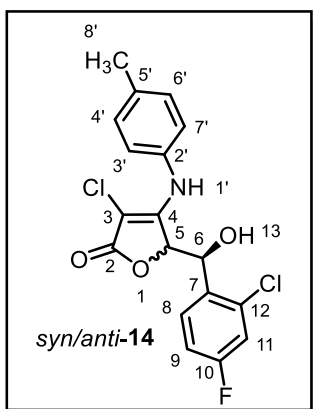
solid in 78% yield (267 mg, 0.70 mmol). **MP:** 223.5-226.1 °C. The spectroscopic data are for the mixture compound, and in case of NMR, the assinments were made as much as possible. **FTIR:** $\bar{v}_{max}$ 3396, 3241, 3108, 3083, 3041, 2962, 2923, 1751, 1629, 1581, 1488, 1392, 1220, 1197, 1025, 1008, 792, 659 cm^{-1}. ^{1}**H NMR** (300 MHz, Acetone-d$_6$:DMSO-d$_6$; 9:1) δ: 8.93 (s, 0.91H, -NH), 8.64 (s, 0.09H, -NH), 7.72 (dd, J = 6.4, 9.6 Hz, 1H, H-9), 7.29 (d, J = 8.5 Hz, 2H, H-4' and H-6'), 7.24 (d, J = 8.5 Hz, 2H, H-3' and H-7'), 7.20-6.98 (m, 2H, H-8 and H-11), 6.08 (d, J = 4.7Hz, 0.09H, -OH), 5.65 (d, J = 5.8 Hz, 0.91H, -OH), 5.49 (d, J = 4.2 Hz, 0.09H, H-5), 5.43 (br, 0.91H, H-5), 5.16 (d, J = 2.1 Hz, 0.91H, H-6), 5.00 (br, 0.09H, , H-6), 2.34 (s, 0.91H, H-8') and 2.30 (s, 0.09H, H-8'). ^{13}**C NMR** (75 MHz, Acetone-d$_6$: DMSO-d$_6$; 9:1) δ: 168.45 (0.91C, C-10), 168.28 (0.09C, C-10), 163.41 (0.91C, C-2), 163.55 (0.09C, C-2), 157.64 (0.91C, C-4), 157.51 (0.09C, C-4), 135.91 (0.91C, C-2'), 135.78 (0.09C, C-2'), 135.39 (0.91C, C-12), 135.39 (0.09C, C-12), 134.79 (0.91C, C-7), 134.30 (0.09C, C-7), 131.59 (0.91C, C-5'), 131.42 (0.09C, C-5'), 131.47 (0.91C, C-8), 131.28 (0.09C, C-8), 129.73 (0.91C, C-4' and C-6') and 129.02 (0.09C, C-4' and C-6'), 124.58 (0.91C, C-7' and C-3'), 123.15 (0.09C, C-7' and C-3'), 115.75 (0.91C, C-11), 115.41 (0.09C, C-11), 113.75 (0.91C, C-9), 114.03 (0.09C, C-9), 89.97 (0.91C, C-3), 89.93 (0.09C, C-3), 78.11 (0.91C, C-5), 79.14 (0.09C, C-5), 66.33 (0.91C, C-6), 66.24 (0.09C, C-6), 20.11 (0.91C, C-8') and 20.05 (0.09H, C-8'). **HRMS (ESI) [M-H]$^-$** calculated for C$_{18}$H$_{13}$Cl$_2$FNO$_3$, 380.0257; found, 380.0239

3-bromo-5-[hydroxy(3-nitrophenyl)methyl]-4-(*p*-tolylamino]furan-2(5*H*)-one (*syn/anti*-15)

The crude residue was purified by column chromatography on silica gel eluted with hexane/ethyl acetate (76:24 v/v) to afford mixture of *syn/anti*-**15**, in a *56:44* ratio as a yellow solid in 54% yield (169 mg, 0.40 mmol). **MP:** 103.2-105.9 °C. The spectroscopic data are for the mixture compound, and in case of NMR, the assinments were made as much as possible. **FTIR:** $\bar{v}_{max}$ 3212, 3058, 3029, 3004, 1727, 1621, 1600, 1523, 1346, 1191, 1046, 997, 727 cm^{-1}. **^{1}H NMR** (300 MHz, Acetone-d$_6$) δ: 8.62 and 8.53 (s, -NH), 8.27-8.11 (m, 2H, H-10 and H-12), 7.82 (d, *J* = 7.8 Hz, 0.56H, H-8) 7.76 (d, *J* = 7.8 Hz, 0.44H, H-8), 7.65 (t, *J* = 5.9 Hz, 0.56H, H-9), 7.60 (t, *J* = 5.9 Hz, 0.44H, H-9), 7.32-7.16 (m, 4H, H-3′, H-4′, H-6′ and H-7′), 5.70 (d, *J* = 3.5 Hz, 0.44H, H-5), 5.59 (d, *J* = 1.9 Hz, 0.56H, H-5), 5.49 (br, -OH), 5.12 (br, 0.56H, H-6) and 5.08 (d, *J* = 3.5 Hz, 0.44H, H-6), 2.36 and 2.34 (s, 3H, H-8′).**^{13}C NMR** (75 MHz, Acetone-d$_6$) δ: 168.60, 168.04 (C-2), 159.26, 159.11 (C-4), 148.17, 147.81 (C-11), 143.05, 140.62 (C-7), 135.71, 135.47 (C-2′), 135.07, 134.46 (C-8), 133.54, 132.67 (C-9), 129.76, 129.57 (C-4′ and C-6′), 129.40, 129.11 (C-5′), 124.43, 124.40, 123.77, 123.74 (C-3′ and C-7′), 122.80, 122.43 (C-12), 121.98, 121.12 (C-10), 80.75, 80.70 (C-5), 76.75, 76.68 (C-3), 71.93, 69.61 (C-6), 20.06, 20.02 (C-8′). **HRMS (ESI) [M-H]** calculated for $C_{18}H_{14}BrN_2O_5$, 417.0086; found, 417.0075

5-[(2-bromopyridin-3-yl)(hydroxy)methyl]-3-bromo-4-(*p*-tolylamino) furan-2(5*H*)-one (*syn/anti*-16)

The crude residue was purified by column chromatography on silica gel eluted with hexane/ethyl acetate (60:40 v/v) to afford mixture of *syn/anti*-**16**, in a *80:20* ratio as a white solid in 62% yield (210 mg, 0.46 mmol). **MP:** 204.8-207.1 °C. The spectroscopic data are for the mixture compound, and in case of NMR, the assinments were made as much as possible. **FTIR:** $\bar{v}_{max}$ 3442, 3330, 3131, 3060, 3023, 2942, 1733, 1621, 1604, 1575, 1560, 1400, 1191, 1022, 993, 734, 576 cm^{-1}. **^{1}H NMR** (300 MHz, Acetone-d$_6$:DMSO-d$_6$; 9:1) δ: 8.94 (s, 0.8H, -NH) and 8.69 (s, 0.2H, -NH), 8.26 (dd, *J* = 2.0, 4.7 Hz, 0.8H, H-10), 8.23 (d, *J* = 2.0, 0.2H, H-10), 7.99 (dd, *J* = 1.9, 7.7 Hz, 1H, H-8), 7.44 (dd, *J* = 4.7, 7.7 Hz, 1H, H-9), 7.35 (d, *J* = 8.3 Hz, 0.8H, H-4′ and H-6′), 7.12 (d, *J* = 8.4 Hz, 0.2H, H-4′ and H-6′), 7.27 (d, *J* = 8.3 Hz, 0.8H, H-3′ and H-7′), 7.05 (d, *J* = 8.4 Hz, 0.2H, H-3′ and H-7′), 6.29 (d, *J* = 4.8 Hz, 0.2H, -OH), 5.87 (d, *J* = 5.7 Hz, 0.8H, -OH), 5.57 (d, *J* = 3.6 Hz, 0.2H, H-5), 5.51 (br,
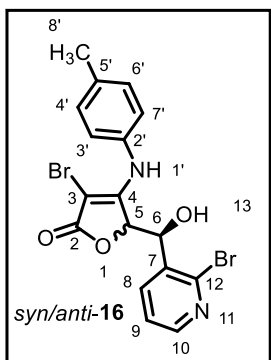
0.8H, H-5), 5.35 (br, 0.2H, H-6), 5.02 (d, J = 1.3 Hz, 0.8H, H-6), 2.34 (s, 0.8H, H-8′) and 2.30 (s, 0.2H, H-8′). **^{13}C NMR** (75 MHz, Acetone-d$_6$: DMSO-d$_6$; 9:1) δ: 168.76 (C-2), 160.75 (0.8C, C-4), 158.68 (0.2C, C-4), 149.34 (0.8C, C-10), 149.53 (0.2C, C-10), 142.03 (0.2C, C-7), 140.12 (0.8C, C-7), 139.14 (0.8C, C-12), 138.86 (0.2C, C-12), 137.71 (0.8C, C-8), 137.67 (0.2C, C-8), 136.02 (0.2C, C-2′), 135.92 (0.8C, C-2′), 135.75 (0.8C, C-5′), 134.43 (0.2C, C-5′), 130.00 (0.8C, C-4′ and C-6′), 129.09 (0.2C, C-4′ and C-6′), 125.26 (0.8C, C-3′ and C-7′), 123.56 (0.2C, C-3′ and C-7′), 123.14 (0.8C, C-9), 123.08 (0.2C, C-9), 80.17 (0.2C, C-5), 78.73 (0.8C, C-5), 77.39 (0.8C, C-3), 76.87 (0.2C,C-3), 71.63 (0.2C, C-6), 68.02 (0.8C, C-6), 20.18 (0.8C, C-2) and 20.14 (0.2C, C-2). **HRMS (ESI) [M-H]$^-$** calculated for $C_{17}H_{13}Br_2N_2O_3$, 450.9293; found, 450.9252

3-bromo-5-[hydroxy(o-tolyl)methyl]-4-(*p*-tolylamino)furan-2(5*H*)-one (*syn*-17)

The crude residue was purified by column chromatography on silica gel eluted with hexane/ethyl acetate (79:21 v/v) to afford pure *syn*-17 as a white solid in 77% yield (223 mg, 0.57 mmol). **MP:** 174.6-175.8 °C. **FTIR:** $\bar{v}_{max}$ 3406, 3280, 3251, 3063, 3032 2968, 2938, 2923, 1749, 1632, 1609, 1510, 1392, 1197, 1009, 708 cm^{-1}. **^{1}H NMR** (300 MHz, DMSO-d$_6$) δ: 9.40 (s, 1H, -NH), 7.46 (d, J = 6.9 Hz, 1H, H-11), 7.21 (apparent singlet, 4H, H-3′, H-4′, H-6′ and H-7′), 7.18-7.07 (m, 2H, H-9 and H-10), 5.57 (d, J = 6.7 Hz, 1H, H-8), 5.60 (d, J = 3.8 Hz, 1H, -OH), 5.35 (br, 1H, H-5), 4.85 (br, 1H, H-6), 2.30 (s, 1H, H-8′), 1.89 (s, 1H, H-14). **^{13}C NMR** (75 MHz, DMSO-d$_6$) δ: 169.98 (C-2), 161.44 (C-4), 139.57 (C-2′), 135.95 (C-7), 135.40 (C-12), 134.29 (C-5′), 130.12 (C-11), 129.98 (2C, C-4′ and C-6′), 128.24 (C-10), 127.52 (C-8), 125.79 (C-9), 124.07 (2C, C-3′ and C-7′), 80.14 (C-5), 76.26 (C-3), 66.30 (C-6), 20.98 (C-14), 18.84 (C-8′). **HRMS (ESI) [M-H]$^-$** calculated for $C_{19}H_{17}BrNO_3$, 386.0392; found, 386.0390

3-bromo-5-[hydroxy(naphthalen-2-yl)methyl)-4-(*p*-tolyl amino]furan-2(5*H*)-one (*syn*-18/ *anti*-18)

The crude residue was purified by silica gel column chromatography eluting with hexane/ethyl acetate (76:24 v/v) to afford the *syn*-18 as white solid in 43% yield (136 mg, 0.32 mmol) and eluting with hexane/ethyl acetate (75.5:24.5 v/v) to afford *anti*-18 as white solid in 24% yield (76 mg, 0.18 mmol).

Data for *syn*-18: **Mp**: 170.7-173.0 °C. **FTIR:** $\bar{v}_{max}$ 3235, 3216, 3120, 3037, 2913, 2852, 1720, 1619, 1594, 1525, 1510, 1319, 1191, 1106, 1006, 806, 738 cm^{-1}. **^{1}H NMR** (300 MHz, Acetone-d$_6$:DMSO-d$_6$; 9:1) δ: 8.94 (s, 1H, -NH), 7.92-7.78 (m, 4H, H-8, H-9, H-12 and H-13),

7.55-7.44 (m, 3H, H-10, H-11 and H-14), 7.26 (apparent singlet, 4H, H-3′, H-4′, H-6′ and H-7′), 5.57 (d, *J* = 5.7 Hz, 1H, -OH), 5.53 (d, *J* = 1.6 Hz, 1H, H-5), 5.14 (br, 1H, H-6), 2.36 (s, 1H, H-8′). **^{13}C NMR** (75 MHz, Acetone-d$_6$:DMSO-d$_6$; 9:1) *δ*: 169.13 (C-2), 159.83 (C-4), [138.73, 135.49, 135.21, 133.14, 133.01, 129.40 (2C), 127.89, 127.60, 127.49, 126.04, 125.78, 125.19, 124.68, 124.44 (2C)] (C-7 to C-16 and C-2′ to C-7′), 81.51 (C-5), 76.33 (C-3), 70.50 (C-6), 20.14 (C-8′). **HRMS (ESI) [M-H]$^-$** calculated for C$_{22}$H$_{17}$BrNO$_3$, 422.0392; found, 422.0331

syn-18   *anti*-18
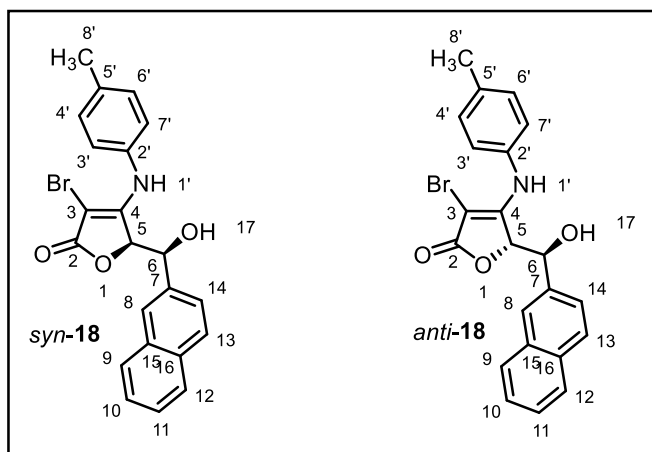
Data for *anti*-18: MP: 155.5-157.9 °C. **FTIR:** $\bar{v}_{max}$ 3378, 3224, 3052, 3025, 1710, 1693, 1618, 1591, 1531, 1292, 1187, 1016, 995, 748 cm^{-1}. **^{1}H NMR** (300 MHz, Acetone-d$_6$) *δ*: 8.46 (s, 1H, -NH), 7.92-7.78 (m, 4H, H-8, H-9, H-12 and H-13), 7.62-7.44 (m, 3H, H-10, H-11 and H-14), 7.24 (apparent singlet, 4H, H-3′, H-4′, H-6′ and H-7′), 5.67 (d, *J* = 3.8 Hz, 1H, H-5), 5.31 (br, 1H, -OH), 5.08 (d, *J* = 3.8 Hz, 1H, H-6), 2.34 (s, 1H, H-8′).**^{13}C NMR** (75 MHz, Acetone-d$_6$) *δ*: 168.19 (C-2), 159.56 (C-4), [136.06, 135.46, 135.27, 133.33, 132.95, 129.59 (2C), 127.95, 127.57, 127.34, 126.47, 125.95 (2C), 125.19, 123.87 (2C)] (C-7 to C-16 and C-2′ to C-7′), 81.17 (C-5), 77.23 (C-3), 73.28 (C-6), 20.04 (C-8′). **HRMS (ESI) [M-H]$^-$** calculated for C$_{22}$H$_{17}$BrNO$_3$, 422.0392; found, 422.0389

4-[(4-bromophenyl)amino)-3-chloro-5-(hydroxyl (3-methoxy phenyl)methyl]furan2,5*H*-one (*syn*-19)

The crude residue was purified by column chromatography on silica gel eluted with hexane/ethyl acetate (76:24 v/v) to afford pure *syn*-19 as a white solid in 68% yield (200 mg, 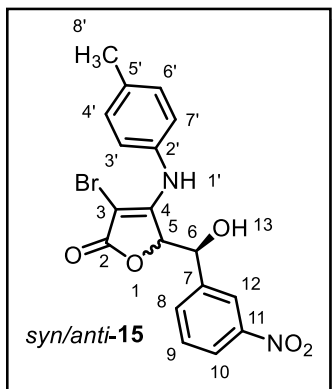0.47 mmol). **MP:** 170.3-172.8 °C. **FTIR:** $\bar{v}_{max}$ 3347, 3193, 3083, 3018, 2996, 2950, 2929, 1752, 1656, 1635, 1587, 1486, 1029, 703 cm^{-1}. **^{1}H NMR** (300 MHz, CDCl$_3$: DMSO-d$_6$; 3:2) *δ*: 9.09 (s, 1H, -NH), 7.38 (d, *J* = 8.6 Hz, 2H, H-4′ and H-6′), 7.15 (t, *J* = 8.0 Hz, 1H, H-9), 6.97 (d, *J* = 8.6 Hz, 2H, H-3′and H-7′), 6.89 (d, *J* = 7.6 Hz, 2H, H-8 and H-12), 6.73 (dd, *J* = 1.7, 8.6 Hz, 1H, H-10), 5.14 (d, *J* = 1.6 Hz, 1H, H-5), 4.95 (br, 1H, H-6), 3.69 (s, 3H, H-14). **^{13}C NMR** (75 MHz, CDCl$_3$: DMSO-d$_6$; 3:2) *δ*: 169.62 (C-2), 159.39 (C-11), 155.77 (C-4), 141.97 (C-7), 136.88 (C-2′), 131.50 (2C, C-4′ and C-6′), 129.11 (C-9), 125.26 (2C, C-3′ and C-7′), 118.70 (C-8), 117.68 (C-5′), 113.01 (C-

syn-19
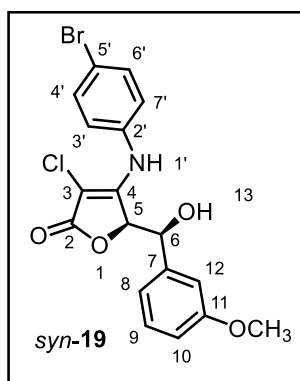
10), 112.37 (C-12), 90.08 (C-3), 80.62 (C-5), 70.94 (C-6), 55.16 (C-14). **HRMS (ESI) [M-H]**⁻ calculated for $C_{18}H_{14}BrClNO_4$, 421.9795; found, 421.9789

4-[(4-bromophenyl)amino]-3-chloro-5-[hydroxy(4-methoxyphenyl) methyl]furan-2,5*H*-one (*syn*-20)

The crude residue was purified by column chromatography on silica gel eluted with hexane/ethyl acetate (77:23 v/v) to afford pure *syn*-**20** as a white solid in 75% yield (221 mg, 0.52 mmol). **MP**: 170.3-172.8 °C. **FTIR:** $\bar{v}_{max}$ 3212, 3174, 3031, 3010, 2989, 2929, 2886, 1714, 1614, 1581, 1511, 1251, 1191, 1170, 1022, 744 cm⁻¹. **¹H NMR** (300 MHz, Acetone-d₆) *δ*: 8.88 (s, 1H, -NH), 7.56 (d, *J* = 8.7, 2H, H-4′ and H-6′), 7.34 (d, *J* = 8.7 Hz, 2H, H-8 and H-12), 7.20 (d, *J* = 8.7 Hz, 2H, H-9 and H-11), 6.89 (d, *J* = 8.7 Hz, 2H, H-3′ and H-7′), 5.35 (d, *J* = 2.3 Hz, 2H, H-5), 5.29 (d, *J* = 4.9 Hz, 1H, -OH), 5.06 (br, 1H, H-6), 3.78 (s, 3H, H-14). **¹³C NMR** (75 MHz, Acetone-d₆) *δ*: 168.50 (C-2), 159.33 (C-10), 155.78 (C-4), 137.44 (C-2′), 132.22 (C-7), 131.62 (2C, C-4′ and C-6′), 127.74 (2C, C-8 and C-12), 125.26 (2C, C-3′ and C-7′),

117.26 (C-5′), 113.28 (2C, C-9 and C-11), 90.69 (C-3), 80.39 (C-5), 70.81 (C-6), 54.63 (C-14). **HRMS (ESI) [M-H]**⁻ calculated for $C_{18}H_{14}BrClNO_4$, 421.9795; found, 421.9804

4-[4-bromophenyl)amino)-3-chloro-5-(hydroxyl (4-nitrophenyl)methyl]furan2,5*H*-one (*syn/anti*-21)

The crude residue was purified by column chromatography on silica gel eluted with hexane/ethyl acetate (79:21 v/v) to afford mixture of *syn/anti*-**21**, in a *93:07* ratio as a yellow solid in 81% yield (247 mg, 0.56 mmol). **MP:** 127.2-129.3 °C. The spectroscopic data are for the mixture compound, and in case of NMR, the assinments were made as much as possible. **FTIR:** $\bar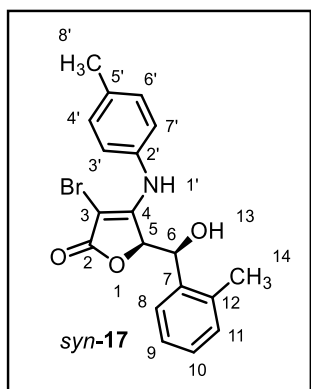{v}_{max}$ 3241, 3187, 3145, 3052, 2969, 2805, 1718, 1619, 1585, 1515, 1486, 1344, 1191, 1031, 1010, 821, 703 cm⁻¹. **¹H NMR** (300 MHz, Acetone-d₆) *δ*: 8.85 (s, 0.93H, -NH) and 8.70 (s, 0.07H, -NH), 8.22 (d, *J* = 8.8 Hz, 0.93H, H-9 and H-11), 8.17 (d, *J* = 8.6 Hz, 0.07H, H-9 and H-11), 7.71 (d, *J* = 8.8

Hz, 0.93H, H-8 and H-12),7.7 (d, *J* = 8.6 Hz, 0.07H, H-8 and H-12), 7.58 (d, *J* = 8.56 Hz, 0.93H, H-4′ and H-6′),7.53 (d, *J* = 8.8 Hz, 0.07H, H-4′ and H-6′), 7.25 (d, *J* = 8.6 Hz, 0.93H, H-3′ and H-7′),7.19 (d, *J* = 8.8 Hz, 0.07H, H-3′ and H-7′), 5.62 (d, *J* = 5.3 Hz, 0.93H, -OH), 5.57 (d, *J* = 1.8 Hz, 0.93H, H-5) and 5.32 (d, *J* = 1.8 Hz, 0.93H, H-6). **¹³C NMR** (75 MHz, Acetone-d₆) *δ*: 168.32 (C-2), 155.42 (C-4), 147.82 (C-10), 147.56 (C-7), 137.16 (C-2′), 131.82 (2C, C-4′ and C-6′), 127.59 (2C, C-8 and C-12), 125.34 (2C, C-3′ and C-7′), 123.09

(2C, C-9 and C-11), 117.74 (C-5'), 91.02 (C-3), 79.92 (C-5), 70.32 (C-6). **HRMS (ESI) [M-H]⁻** calculated for $C_{17}H_{11}BrClN_2O_5$, 436.9540; found, 436.9519

4-[(4-bromophenyl)amino]-3-chloro-5-(hydroxyl (phenyl)methyl]furan-2(5H)-one (*syn*-22)

The crude residue was purified by column chromatography on silica gel eluted with hexane/ethyl acetate (77:23 v/v) to afford pure *syn*-**22** as a white solid in 86% yield (235 mg, 0.60 mmol). **MP**: 225.3-227.7 °C. **FTIR:** $\bar{v}_{max}$ 3390, 3222, 3101, 3064, 2967, 2923, 2902, 1754, 1635, 1581, 1477, 1378, 1195, 1016, 829, 696 cm⁻¹. **¹H NMR** (300 MHz,CDCl₃:DMSO-d₆; 3:2) δ: 9.21 (s, 1H, -NH), 7.39 (d, *J* = 8.5 Hz, 2H, H-4' and H-6'), 7.35-7.14 (m, 5H, H-8 to H-12), 7.00 (d, *J* = 8.5 Hz, 2H, H-3' and H-7'), 5.16 (br, 1H, H-5), 4.97 (br, 1H, H-6). **¹³C NMR** (75 MHz, CDCl₃: DMSO-d₆; 3:2) δ: 169.52 (C-2), 155.86 (C-4), 140.60 (C-7), 137.01 (C-2'), 131.52 (2C, C-4' and C-6'), 128.08 (2C, C-9 and C-11), 127.70 (C-10), 126.60 (2C, C-8 and C-12), 125.25 (C-3' and C-7'), 117.59 (C-5'), 90.04 (C-3), 80.76 (C-5), 70.89 (C-6).
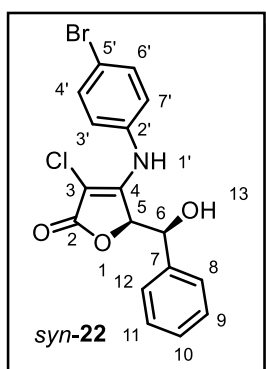
HRMS (ESI) [M-H]⁻ calculated for $C_{17}H_{12}BrClNO_3$, 391.9689; found, 391.9676

3-chloro-5-[(hydroxy(3-nitrophenyl)methyl]-4-(*p*-tolylamino)furan-2(5H)-one (*syn/anti*-23)

The crude residue was purified by column chromatography on silica gel eluted with hexane/ethyl acetate (77:23 v/v) to afford mixture of *syn/anti*-**23**, in a *53:47* ratio as a yellow solid in 51% yield (171 mg, 0.46 mmol). **MP:** 224.5-226.8 °C. The spectroscopic data are for the mixture compound, and in case of NMR, the assinments were made as much as possible. **FTIR:** $\bar{v}_{max}$ 3261, 3060, 3029, 3006, 1724, 1627, 1604, 1523, 1348, 1020, 811, 680 cm⁻¹. **¹H NMR** (300 MHz, Acetone-d₆) δ: 8.68 and 8.59 (s, -NH), 8.31-8.11 (m, H-12 and H-8), 7.82 (t, *J*= 8.8, H-9) 7.71-7.56 (m, H-10), 7.30-7.10 (m, 4H, H-3' to H-7'), 5.65 (d, *J* = 3.8 Hz, 0.47H, H-5 and -OH), 5.55 (d, *J* = 3.1 Hz, 0.53H, H-5 and -OH), 5.22 (br, 0.53H, H-6), 5.15 (d, *J* = 3.8 Hz, 0.47H, H-6), 2.33 and 2.35 (s, H-8'). **¹³C NMR** (75 MHz, Acetone-d₆) δ: 168.35, 167.78 (C-2), 156.24, 156.24(C-4), 148.17, 147.86 (C-11), 142.95, 140.77 (C-7), 135.42, 135.38 (C-2'), 135.24, 135.20 (C-8), 133.59, 132.75 (C-9), 129.63, 129.45 (2C, C-4' and C-6'), 129.41, 129.18 (C-5'), 124.00, 123.44 (2C, C-3' and C-7'), 122.86, 122.48 (C-12), 121.99, 121.16 (C-10), 90.16, 89.52 (C-3), 79.72, 79.60 (C-5), 72.32, 69.95 (C-6), 20.06 and 20.01 (C-8'). **HRMS (ESI) [M-H]⁻** calculated for $C_{18}H_{14}ClN_2O_5$, 373.0591; found, 373.0598
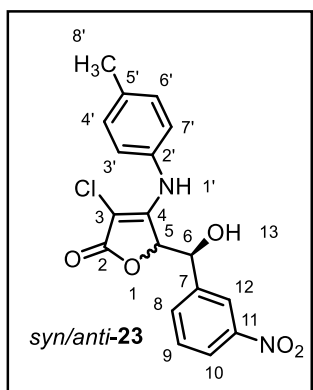
*"During the purification of crude compound **23** by column chromatography on silica gel, two new compounds were also isolated, namely, **23a** and **23b**. Products structure were proposed by ^{1}H and ^{13}C NMR data and HRMS analysis. The stereochemistry of proposed compounds were not assigned."*

3-chloro-5-[hydroxy(3-nitrophenyl)methyl]-5-[hydroxyl(3-nitrophenyl)methyl]-4-(*p*-tolylamino) furan 2(5*H*)-one (23a)

Compound **23a** was eluted with hexane/ethyl acetate (64:36 v/v) as a yellow solid in 9% yield (42 mg, 0.08 mmol). **^{1}H NMR** (300 MHz, Acetone-d$_6$) δ: 8.52 (br, 2H, H-12 and H-21), 8.25-8.16 (m, 2H, H-10 and H-19), 8.10 (br, 1H, H-8), 8.08 (br, 1H, H-17), 7.64 (br dd, *J* =8.00Hz, 2H, H-9 and H-18), 7.10 (d, *J* = 8.00 Hz, 2C, H-3′ and H-7′), 6.82 (d, *J* = 8.30 Hz, 2C, H-4′ and H-6′), 6.09 (br, 2H, -OH), 5.84 (s, 2H, H-6 and H-15), 2.28 (s, 3H, H-8′).**^{13}C NMR** (75 MHz, Acetone-d$_6$) δ: 167.66 (C-2), 154.62 (C-4), 147.86(C-11), 147.86 (C-20), 140.94 (2C, C-7 and C-16), 135.69 (C-2′), 134.32 (2C, C-8 and C-17), 133.75 (C-5′), 129.28 (2C, C-9 and C-18), 128.73 (2C, C- C-4′ and C-6′), 124.83 (2C, C-3′ and C-7′), 123.13 (2C, C-12 and C-21), 122.74 (2C, C-10 and C-19), 89.88 (C-5), 87.51 (C-3), 73.93 (2C, C-6 and C-15) and 20.01 (C-8′). **HRMS (ESI) [M-H]**$^{-}$ calculated for C$_{25}$H$_{19}$ClN$_3$O$_8$, 524.0861; found, 524.0820
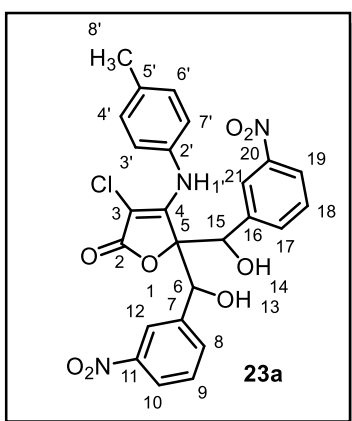
3-chloro-5-hydroxy(3-nitrophenyl)methyl)-5-(hydroxyl(3-nitrophenyl)methyl)-4-(*p*-tolylamino) furan-2(5*H*)-one (23b)
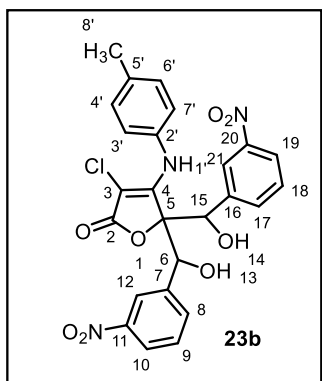
Compound **23b** was eluted with hexane/ethyl acetate (60:40 v/v) as a yellow solid in 7% yield (33 mg, 0.06 mmol). **^{1}H NMR** (300 MHz, Acetone-d$_6$) δ: 8.72 (s, 1H, -NH), 8.52 (br, 2H, H-12 and H-21), 8.25-8.12(m, 2H, H-10 and H-19), 8.06 (d, *J* = 7.80 Hz, 1H, H-8), 7.91 (d, *J* = 7.70Hz, 1H, H-17), 7.64 (dd, *J* =8.10, 8.10 Hz, 2H, H-9 and H-18), 7.13 (d, *J* = 8.1 Hz, 2C, H-3′ and H-7′), 6.93 (d, *J* = 8.30 Hz, 2H, H-4′ and H-6′), 6.56 (br, 1H, -OH), 6.02 (s, 1H, H-6), 5.94 (s, 1H, H-15), 5.82 (br, 1H, -OH) and 2.30 (s, 3H, H-8′). **^{13}C NMR** (75 MHz, Acetone-d$_6$) δ: 166.88 (C-2), 155.10 (C-4), 147.83 (C-11), 147.74 (C-20), 141.46 (C-7), 141.34 (C-16), 135.77 (C-2′), 134.20 (C-8), 133.96 (C-17), 133.79 (C-5′), 129.20 (C-9), 128.99 (C-18), 128.70 (2C, C- C-4′ and C-6′), 125.03 (2C, C-3′ and C-7′), 123.05 (C-12), 122.88 (C-21),122.60 (C-19), 121.79 (C-10), 88.51 (C-5) 86.21 (C-3),72.44

(C-6), 71.61 (C-15) and 20.03 (C-8′). **HRMS (ESI) [M-H]⁻** calculated for $C_{25}H_{19}ClN_3O_8$, 524.0861; found, 524.0815

4-[(4-bromophenyl)amino]-3-chloro-5-[hydroxy(m-tolyl)methyl]furan-2(5H)-one (*syn*-24)

The crude residue was purified by column chromatography on silica gel eluted with hexane/ethyl acetate (70:30 v/v) to afford pure *s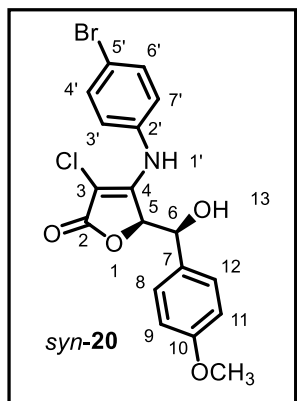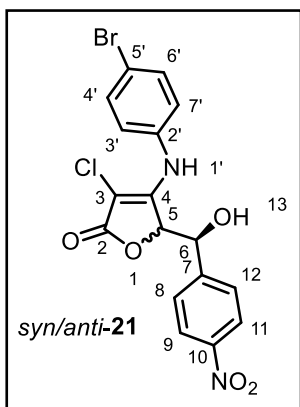yn*-**24** as white solid in 71% yield (201 mg, 0.49 mmol). **MP**: 197.5-198.8 °C. **FTIR**: $\bar{v}_{max}$ 3416, 3292, 3266, 3054, 3030, 2961, 2943, 2920, 1756, 1626, 1613, 1516, 1394, 1195, 1013, 706 cm⁻¹. **¹H NMR** (300 MHz, DMSO-d₆) *δ*: 9.63 (s, 1H, -NH), 7.57 (d, *J* = 8.6 Hz, 2H, H-4′ and H-6′), 7.29-7.01 (m, 6H, H-8 to H-10, H-12, H-3′, H-7′), 5.76 (br, 1H, -OH), 5.36 (apparent singlet, 1H, H-5), 4.87 (br, 1H, H-6), 2.29 (s, 3H, H-14). **¹³C NMR** (75 MHz, DMSO-d₆) *δ*: 169.42 (C-2), 156.68 (C-4), 141.62 (C-7), 137.59 (C-11), 137.39 (C-2′), 131.96 (2C, C-4′ and C-6′), 128.34 (C-10), 128.31 (C-9), 127.15 (C-12), 125.57 (2C, C-3′ and C-7′), 123.73 (C-8), 117.28 (C-5′), 89.64 (C-3), 81.31 (C-5), 70.35 (C-6) and 21.59 (C-14). **HRMS (ESI) [M-H]⁻** calculated for $C_{18}H_{14}BrClNO_3$, 405.9846; found, 405.9841
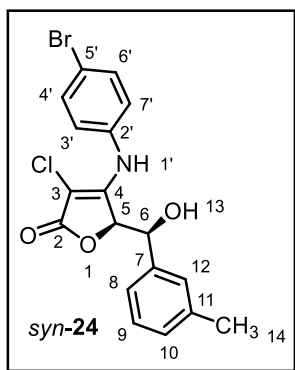
3-chloro-5-(1-hydroxy-2-methylpropyl)-4-(p-tolylamino)furan-2(5H)-one (*syn*-25)

The crude residue of compound **25** was purified by column chromatography on silica gel eluted with hexane/ethyl acetate (70:30 v/v) to afford pure *syn*-**25** as a white solid in 79% yield (209 mg, 0.71 mmol). **MP:** 203.2-204.5 °C. **FTIR**: $\bar{v}_{max}$ 3381, 3284, 3225, 3071, 3031, 2976, 1748, 1632, 1191, 1024, 644 cm⁻¹. **¹H NMR** (300 MHz, DMSO-d₆) *δ*: 9.30 (s, 1H, -NH), 7.14 (d, *J* = 8.2 Hz, 2H, H-4′ and H-6′), 7.06 (d, *J*= 8.2 Hz, 2H, H-3′ and H-7′), 5.35 (apparent singlet, 1H, H-5), 4.87 (d, *J* = 7.7 Hz, 1H, -OH), 3.19 (t, *J* = 8.1 Hz, 1H, H-6), 2.27 (s, 3H, H-8′), 1.79-1.67 (m, 1H, H-7) and 0.88-0.78 (m, 6H, H-8 and H-9). **¹³C NMR** (75 MHz, DMSO-d₆) *δ*: 169.78 (C-2), 158.80 (C-4), 135.71 (C-2′), 134.57 (C-5′), 129.52 (2C, C-4′ and C-6′), 123.94 (2C, C-3′ and C-7′), 87.74 (C-3), 78.21 (C-5), 73.58 (C-6), 31.60 (C-7), 20.92 (C-8′), 20.18 (C-8) and 19.34 (C-9). **HRMS (ESI) [M-H]⁻** calculated for $C_{15}H_{17}ClNO_3$, 294.0897; found, 294.0893
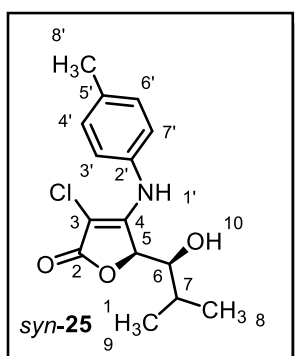
3-chloro-5-[1-hydroxy-3-methylbutyl]-4-(*p*-tolylamino)furan-2(5*H*)-one (*syn*-26)

The crude residue of compound **26** was purified by column chromatography on silica gel eluted with hexane/ethyl acetate (70:30 v/v) to afford pure *syn*-**26** as a white solid in 76% yield (210 mg, 0.68 mmol). **MP:** 206.7-208.1 ºC. **FTIR:** $\bar{v}_{max}$ 3383, 3289, 3232, 3079, 3023, 2972, 1746, 1627, 1196, 1021, 635 cm^{-1}. **^{1}H NMR** (300 MHz, DMSO-d$_6$) *δ*: 9.32 (s, 1H, -NH), 7.15 (d, *J* = 7.8 Hz, 2H, H-4′ and H-6′), 7.07 (d, *J*= 7.8 Hz, 2H, H-3′ and H-7′), 5.11 (apparent singlet, 1H, H-5), 4.80 (d, *J* = 7.1 Hz, 1H, -OH), 3.69 (apparent singlet, 1H, H-6), 2.27 (s, 3H, H-8′), 1.74-1.55 (m, 1H, H-8), 1.54-1.43 (m, 1H, H-7a) 1.32-1.14 (m, 1H, H-7b) and 0.86-0.65 (m, 6H, H-9 and H-10). **^{13}C NMR** (75 MHz, DMSO-d$_6$) *δ*: 169.66 (C-2), 158.29 (C-4), 135.64 (C-2′), 134.66 (C-5′), 129.49 (2C, C-4′ and C-6′), 124.06 (2C, C-3′ and C-7′), 87.56 (C-3), 80.29 (C-5), 66.10 (C-6), 43.04 (C-7), 24.22 (C-8), 23.37 (C-9), 22.20 (C-10) and 20.85 (C-8′). **HRMS (ESI) [M-H]$^-$** calculated for C$_{16}$H$_{19}$ClNO$_3$, 308.1053; found, 308.1049
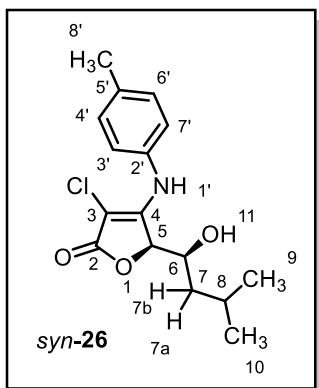
5-[(1,1'-biphenyl)-4-yl(hydroxy)methyl]-3-bromo-4-(*p*-tolylamino)furan-2(5*H*)-one (*syn*-27/ *anti*-27)

The crude residue was purified by silica gel column chromatography eluting with hexane/ethyl acetate (76:24 v/v) to afford the *syn*-**27** as white solid in 40% yield and eluting with hexane/ethyl acetate (75.5:24.5 v/v) to afford *anti*-**27** as white solid in 21% yield.

Data for *syn*-27: **MP:** 189.0-190.9 °C. **FTIR:** $\bar{v}_{max}$ 3241, 3054, 3029, 2969, 1722, 1619, 1592, 1517, 1315, 1191, 1006, 744, 696 cm^{-1}. **^{1}H NMR** (300 MHz, Acetone-d$_6$:DMSO-d$_6$; 9:1) *δ* 9.29 (s, 1H, -NH), 7.72-7.58 (m, 4H, H-15, H-16, H-18 and H-19), 7.53-7.40 (m, 4H, H-8, H-9, H-11 and H-12), 7.35 (t, *J* =7.3 Hz, 1H, H-17), 7.25 (brd singlet, 4H, H-3′, H-4′, H-6′ and H-7′), 5.72 (d, *J* = 6.1, 1H, -OH), 5.44 (d, *J* = 1.6 Hz, 1H, H-5), 5.01 (d, *J* = 1.6 Hz, 1H, H-6), 2.35 (s, 3H, H-8′). **^{13}C NMR** (75 MHz, Acetone-d$_6$:DMSO-d$_6$; 9:1) *δ* 169.59(C-2), 159.99 (C-4), [140.94, 140.67, 139.84, 135.60, 134.96, 129.37 (2C), 128.96 (2C), 127.37, 127.12 (2C), 126.87 (2C), 126.46 (2C), 124.49 (2C)] (C-7 to C-19 and C-2′ to
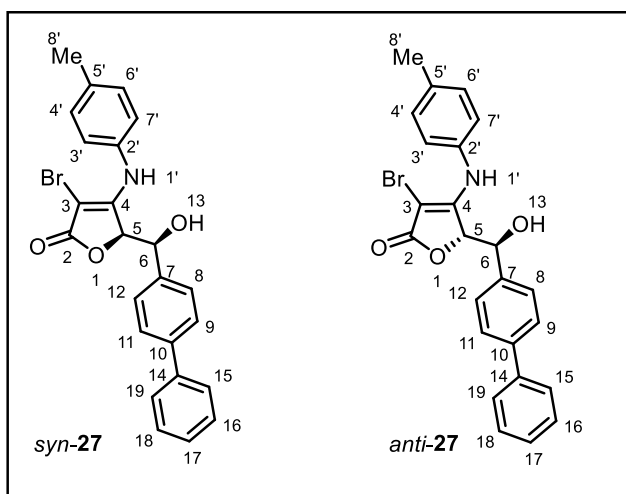
C-7'), 81.97 (C-5), 75.96 (C-3), 69.95 (C-6), 20.33 (C-8'). **HRMS (ESI)** calculated for **[M-H]⁻**, 448.0548; found, 448.0542

Data for *anti*-27: **MP**: 163.7-165.6 °C. **FTIR:** $\bar{\nu}_{max}$ 3297, 3075, 3050, 3025, 2969, 2908, 1720, 1619, 1594, 1515, 1184, 1039, 1010, 987, 767, 730 cm⁻¹. **¹H NMR** (300 MHz, Acetone-d₆:DMSO-d₆; 9:1) *δ* 8.80 (s, 1H, -NH), 7.70-7.56 (m, 4H, H-15, H-16, H-18 and H-19), 7.53-7.40 (m, 4H, H-8, H-9, H-11 and H-12), 7.35 (t, *J* = 7.3 Hz, 1H, H-17), 7.23 (brd singlet, 4H, H-3', H-4', H-6' and H-7'), 5.63 (brd, 1H, -OH), 5.56 (d, *J* = 4.0 Hz, 1H, H-5), 4.94 (d, *J* = 4.0 Hz, 1H, H-6), 2.34 (s, 3H, H-8'). **¹³C NMR** (75 MHz, Acetone-d₆:DMSO-d₆; 9:1) *δ* 168.67 (C-2), 159.52 (C-4), [140.51, 140.37, 137.93, 135.47, 135.05, 129.49 (2C), 128.83 (2C), 128.07 (2C), 127.31, 126.76 (2C), 126.11 (2C), 123.95 (2C)] (C-7 to C-19 and C-2' to C-7'), 81.24 (C-5), 76.74 (C-3), 72.94 (C-6), 20.11 (C-8'). **HRMS (ESI)** calculated for **[M-H]⁻**, 448.0548; found, 448.0531

3-chloro-5-((2-chloro-4-fluorophenyl)(hydroxy)methyl)-4-((2,5-dimethoxyphenyl)amino)furan-2(5*H*)-one (*syn/anti*-28)

The crude residue was purified by column chromatography on silica gel eluted with hexane/ethyl acetate (79:21 v/v) to afford mixture of *syn/anti*-**28**, in a *97:03* ratio as a white solid in 70% yield. **MP:** 211.7-212.2 °C. The spectroscopic data are for the mixture
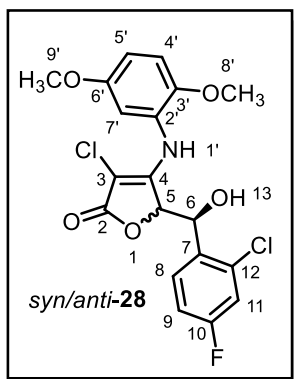
compound, and in case of NMR, the assinments were made as much as possible. **FTIR:** $\bar{\nu}_{max}$ 3488, 3201, 3143, 3037, 3006, 2967, 2939, 2832, 1733, 1631, 1614, 1560, 1508, 1486, 1248, 1213, 1049, 1018, 665 cm⁻¹. **¹H NMR** (300 MHz, Acetone-d₆) *δ*: 8.62 (s, 1H, -NH), 7.71 (dd, *J* = 6.4, 9.6 Hz, 1H, H-9), 7.20-7.10 (m, 2H, H-8 and H-11), 7.07 (d, *J* = 9.0 Hz, 1H, H-4'), 7.02 (d, *J* = 3.0 Hz, 1H, H-7'), 6.87 (dd, *J* = 3.0, 9.0 Hz, 1H, H-5'), 5.69 (brd, 0.97H, -OH), 5.25 (d, *J* = 1.8 Hz, 0.97H, H-5), 5.10 (brd, 0.97H, H-6), 3.85 (s, 0.97H, H-8') and 3.80 (s, 0.03H, H-8'), 3.78 (s, 0.97H, H-9') and 3.75 (s,

0.03H, H-9'). **¹³C NMR** (75 MHz, Acetone-d₆) *δ*: 168.45 (C-10), 163.38 (C-2), 160.10 (C-4), 158.74 (C-6'), 153.84 (C-3'), 147.93 (C-12), 134.83 (C-2'), 131.37 (C-7), 127.34 (C-8), 115.76 (C-11), 114.05 (C-9), 113.77 (C-4'), 113.15 (C-5'), 112.27 (C-7'), 89.70 (C-3), 78.66 (C-5), 66.49 (C-6), 55.84 (C-9'), 55.28 (C-8'). **HRMS (ESI) [M-H]⁻** calculated for C₁₉H₁₅Cl₂FNO₅, 426.0311; found, 426.0341

4.4. Typical Procedure for the Synthesis of *Anti-* 9, 10 and 22

To a dry 25 mL one neck round bottomed flask were added tetronamide **8a** (200 mg, 0.89 mmol), anhydrous MeOH (5 mL), followed by *t*-BuOK (99 mg, 0.89 mmol). After stirring the reaction mixture for 5 min at room temperature, benzaldehyde (114 mg, 1.07 mmol) was added slowly. The reaction mixture was stirred at room temperature under nitrogen atmosphere until TLC analysis revealed total consumption of **8a**. The reaction was then quenched by addition of an aqueous solution of HCl (1M, 10 mL). The methanol was removed under reduced pressure and the aqueous mixture was extracted with ethyl acetate (3×15 mL). The combined organic layers were dried over anhydrous Na_2SO_4, filtrated and the solvent evaporated. The crude residue was purified by silica gel column chromatography eluting with hexane/ethyl acetate (80:20 v/v) to afford the *syn*-**9** (117 mg, 0.36 mmol) as white solid in 40% yield and eluting with hexane/ethyl acetate (79.5:20.5 v/v) to afford *anti*-**9** as light yellow solid in 39% yield (114 mg, 0.35 mmol). Compound *anti*-**10** and *anti*-**22** were synthesized using a method similar to that described for compound *anti*-**9.**

3-chloro-5-[hydroxy(phenyl)methyl]-4-(*p*-tolylamino)furan-2(5*H*)-one (*anti*-9)

MP: 190.1-191.2 °C. R_f = 0.33 (hexane: ethyl acetate, 3:2, v/v). **FTIR:** $\bar{v}_{max}$ 3309, 3278, 3191, 3081, 3068, 3029, 1743, 1631, 1583, 1195, 1008, 734 cm^{-1}. **^{1}H NMR** (300 MHz, Acetone-d$_6$) *δ*: 8.44 (s, 1H, -NH), 7.43-7.26 (m, 5H, H-8 to H-12), 7.24 (d, *J* = 8.5 Hz, 2H, H-4′ and H-6′), 7.18 (d, *J* = 8.5 Hz, 2H, H-3′ and H-7′), 5.51 (d, *J* = 4.3 Hz, 1H, H-5), 5.20 (d, *J* = 4.8 Hz, 1H, -OH), 4.91 (m, 1H, H-6), 2.34 (s, 3H, H-8′). **^{1}H NMR** (300 MHz, D$_2$O Exchange) *δ*: 7.24-7.40 (m, 5H, H-8 to H-12), 7.20 (d, *J* = 8.4 Hz, 2H, H-4′ and H-6′), 7.12 (d, *J* = 8.4 Hz, 2H, H-3′ and H-7′), 5.50 (d, *J* = 3.9 Hz, 1H, H-5), 4.92 (d, *J* = 3.9, 1H, H-6), 2.31 (s, 3H, H-8′). **^{1}H NMR** (300 MHz; CDCl$_3$:DMSO-d$_6$; 9:1) *δ*: 8.04 (s, 1H, -NH), 7.31-7.10 (m, 5H, H-8 to H-12), 7.05-6.94 (m, 2H, H-4′ and H-6′), 6.91-6.81 (m, 2H, H-3′ and H-7′), 4.97 (dd, *J* = 6.0, 4.3 Hz, 1H, H-5), 4.70 (dd, *J* = 6.0, 4.3 Hz, 1H, H-6), 2.22 (s, 3H, H-8′). **^{13}C NMR** (75 MHz, CDCl$_3$: DMSO-d$_6$ 9:1) *δ*: 169.62 (C-2), 156.80 (C-4), 139.21 (C-7), 135.34 (C-2′), 134.11 (C-5′), 129.18 (2C, C-4′ and C-6′), 128.48 (C-10), 128.26 (2C, C-8 and C-12), 127.16 (2C, C-8 and C-12), 123.76 (2C, C-3′ and C-7′), 88.86 (C-3), 79.36 (C-5), 74.49 (C-6), 20.89 (C-8′). **HRMS (ESI) [M-H]$^-$** calculated for $C_{18}H_{15}ClNO_3$, 328.0740; found, 328.0678
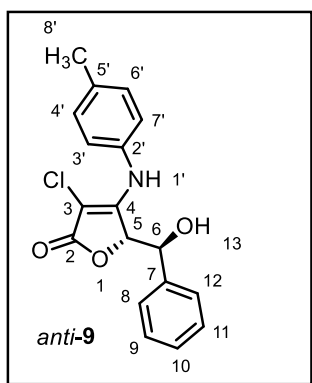
3-chloro-5-[hydroxy(m-tolyl)methyl]-4-(p-tolylamino)furan-2(5H)-one (anti-10)
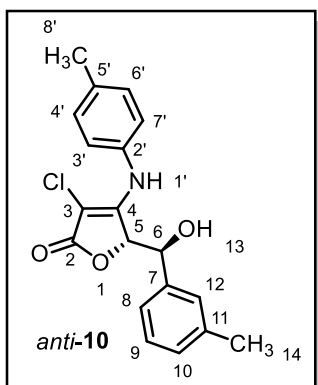
anti-10

The crude residue was purified by silica gel column chromatography eluting with hexane/ethyl acetate (81:19 v/v) to afford the syn-10 as white solid and eluting with hexane/ethyl acetate (80:20 v/v) to afford anti-10 as pale yellow solid in 33% yield (101 mg, 0.30 mmol). Data for anti-10: **MP**: 158.4-159.2 °C. **FTIR:** $\bar{v}_{max}$ 3413, 3287, 3261, 3059, 3027, 2966, 2942, 2923, 1749, 1632, 1610, 1513, 1392, 1197, 1013, 704 cm^{-1}. **^{1}H NMR** (300 MHz, DMSO-d$_6$) δ: 9.49 (s, 1H, -NH), 7.39-6.80 (m, 8H, H-8 to H-10, H-12, H-3′, H-4′, H-6′ and H-7′), 5.93 (d, J= 3.3 Hz, 1H, -OH), 5.49 (d, J= 4.1 Hz, 1H, H-5), 4.80 (br, 1H, H-6), 2.28 (s, 3H, H-14), 2.23 (s, 3H, H-8′). **^{13}C NMR** (75 MHz, DMSO-d$_6$) δ: 169.07 (C-2), 156.63 (C-4), 138.31 (C-7), 136.85 (C-11), 135.50 (C-2′), 134.72 (C-5′), 129.72 (2C, C-4′ and C-6′), 128.90 (C-12), 128.38 (C-9), 127.90 (C-10), 124.81 (C-8), 123.57 (2C, C-3′ and C-7′), 88.49 (C-3), 80.57 (C-5), 72.89 (C-6), 21.47 (C-14), 20.93 (C-8′). **HRMS (ESI) [M-H]$^-$** calculated for C$_{19}$H$_{17}$ClNO$_3$, 342.0897; found, 342.0899

4-[(4-bromophenyl)amino]-3-chloro-5-(hydroxyl (phenyl)methyl] furan-2(5H)-one (anti-22)

The crude residue was purified by silica gel column chromatography eluting with hexane/ethyl acetate (81:19 v/v) to afford the syn-22 as white solid and eluting with
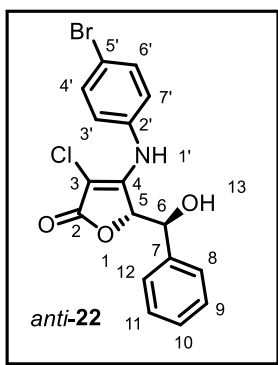
anti-22

hexane/ethyl acetate (80:20 v/v) to afford anti-22 as white solid in 41% yield (156 mg, 0.39 mmol). Data for anti-22: **MP:** 208.7-210.1 °C. **FTIR:** $\bar{v}_{max}$ 3394, 3226, 3105, 3062, 2973, 2921, 2898, 1751, 1634, 1583, 1471, 1381, 1198, 1011, 824, 689 cm^{-1}. **^{1}H NMR** (300 MHz, DMSO-d$_6$) δ: 9.63 (s, 1H, -NH), 7.54 (d, J = 8.4 Hz, 2H, H-4′ and H-6′), 7.32-7.16 (m, 5H, H-8 to H-12), 7.05 (d, J = 8.4 Hz, 2H, H-3′ and H-7′), 6.03 (br, 1H, -OH), 5.53 (d, J= 3.2, 1H, H-5), 4.85 (br, 1H, H-6). **^{13}C NMR** (75 MHz, DMSO-d$_6$) δ: 168.83 (C-2), 156.08 (C-4), 138.33 (C-7), 137.53 (C-2′), 132.10 (2C, C-4′ and C-6′), 128.37 (C-10), 128.06 (2C, C-9 and C-11), 127.64 (2C, C-8 and C-12), 125.25 (2C, C-3′ and C-7′), 117.40 (C-5′), 89.97 (C-3), 80.71 (C-5), 72.93 (C-6). **HRMS (ESI) [M-H]$^-$** calculated for C$_{17}$H$_{12}$BrClNO$_3$, 391.9689; found, 391.9684

4.5.   Procedure for the Retro-Aldol Reaction

To a solution of aldol compound *anti*-**10** (87 mg, 0.25 mmol) and *anti*-**22** (100 mg, 0.25 mmol) in MeOH/H$_2$O (2:1 mL, v/v), NaOH (10 mg, 0.25 mmol) was added with continuous stirring at room temperature. The reaction mixture was then stirred at room temperature for 3 h and quenched by addition of aqueous HCl solution (1M, 5 mL). The methanol was then removed under reduced pressure and the aqueous mixture was extracted with ethyl acetate (3×10 mL). The combined organic layers were dried over anhydrous Na$_2$SO$_4$, filtrated and the solvent evaporated. The crude residue was subjected to silica gel column chromatography, eluting with hexane/ethyl acetate (82:18 v/v) and isolated three different fractions as a mixture of tetronamides **8a/8b** (21 mg), *syn*-**9/22** (52 mg), and *syn*-**10/24** (28 mg), respectively.

Mixture of 3-chloro-4-(*p*-tolylamino)furan-2(5*H*)-one (8a) and 4-[(4-bromophenyl)amino]-3-chlorofuran-2(5*H*)-one (8b)

The crude mixture was purified by column chromatography on silica gel eluted with
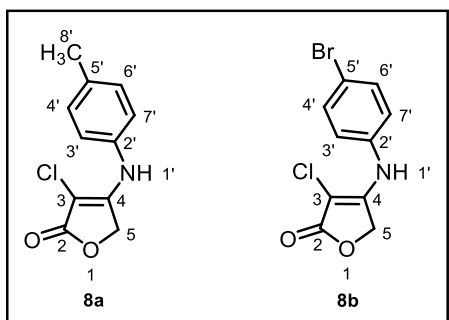
hexane/ethyl acetate (82:18 v/v) to afford mixture of **8a/8b**, in a *47:53* ratio as a brown solid. **^{1}H NMR** (300 MHz, DMSO-d$_6$) *δ*: 9.69 (s, -NH, **8b**), 9.55 (s, - NH, **8a**), 7.52 (d, *J* = 8.6 Hz, H-4'/6', **8b**), 7.18 (d, *J*= 8.6 Hz, H-3'/7', **8b**), 7.15-7.08 (m, H-3' to 7', **8a**), 5.10 (s, H-5, **8b**), 5.02 (s, H-5, **8a**) and 2.26 (s, H-8', **8a**). **HRMS (ESI) [M-H]$^-$** calculated for C$_{11}$H$_9$ClNO$_2$ and C$_{10}$H$_6$BrClNO$_2$

222.0322 and 285.9270 respectively; found, 222.0323 and 285.9269

Mixture of 3-chloro-5-[hydroxy(phenyl)methyl]-4-(*p*-tolylamino)furan-2(5*H*)-one (*syn*-9) and 4-[(4-bromophenyl)amino)-3-chloro-5-(hydroxyl (phenyl)methyl] furan-2(5*H*)-one (*syn*-22)
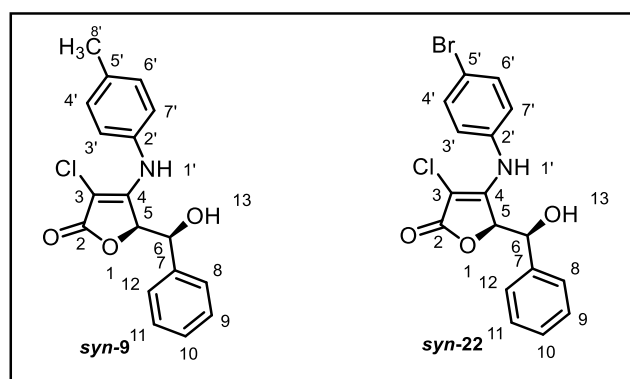
The crude mixture was purified by column chromatography on silica gel eluted with hexane/ethyl acetate (80:20 v/v) to afford mixture of *syn*-**9**/*syn*-**22**, in a *33:67* ratio as a white solid. **^{1}H NMR** (300 MHz, DMSO-d$_6$) *δ*: 9.65 (s, -NH, *syn*-**22**), 9.49 (s, -NH, *syn*-**9**), 7.57 (d, *J* = 8.5 Hz, H-4'/6', *syn*-**22**), 7.41-7.10 (m, H-3'/7', H-8 to 12, *syn*-**22** and H-3' to 7', H-8 to 12, *syn*-**9**), 5.81 (br, -OH, *syn*-**22**), 5.76 (d, *J* =

5.7 Hz, -OH, *syn*-**9**), 5.39 (apparent singlet, H-5, *syn*-**22**/*syn*-**9**), 4.91 (apparent singlet, H-6, *syn*-**22**), 4.85 (d, *J* = 2.1 Hz, H-5, *syn*-**9**), 2.35 (s, H-8', *syn*-**9**). **HRMS (ESI) [M-H]⁻** calculated for $C_{18}H_{15}ClNO_3$ and $C_{17}H_{12}BrClNO_3$ 328.0740 and 391.9689 respectively; found, 328.0732, and 391.9681

Mixture of 3-chloro-5-[hydroxy(m-tolyl)methyl]-4-(*p*-tolylamino)furan-2(5*H*)-one (*syn*-10) and 4-[(4-bromophenyl)amino]-3-chloro-5-[hydroxy(*m*-tolyl)methyl]furan-2(5*H*)-one (*syn*-24)

The crude mixture was purified by column chromatography on silica gel eluted with hexane/ethyl acetate (79:21 v/v) to afford mixture of *syn*-**10**/*syn*-**24**, in a *76:24* ratio as a white solid. **¹H NMR** (300 MHz, DMSO-d₆) *δ*: 9.64 (s, -NH, *syn*-**24**), 9.48 (s, -NH, *syn*-**10**), 7.57 (d, *J* = 8.6 Hz, H-4'/6', *syn*-**24**), 7.23-7.02 (m, H-3'/7', H-8 to 12, *syn*-**24** and H-3' to 7', H-8 to 12, *syn*-**10**), 5.76 (d, *J* = 5.1 Hz, -OH, *syn*-**24**), 5.71 (d, *J* = 5.8 Hz, -OH, *syn*-**10**), 5.35 (apparent singlet, H-5, *syn*-**10**/*syn*-**24**),
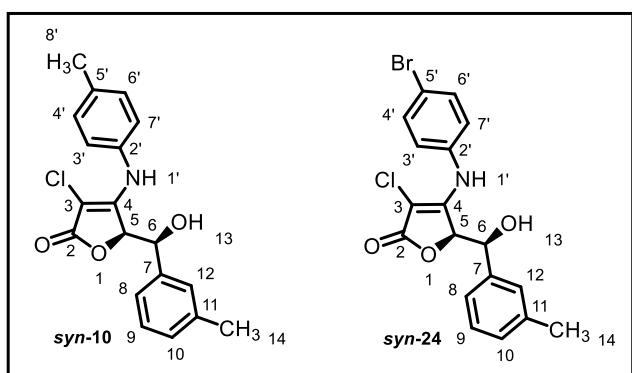
4.87 (d, *J* =2.0 Hz, H-6, *syn*-**24**), 4.82 (d, *J* = 1.9 Hz, H-5, *syn*-**10**), 2.30 (s, H-14, *syn*-**10**/*syn*-**24**) and 2.29 (s, H-8', *syn*-**10**). **HRMS (ESI) [M-H]⁻** calculated for $C_{19}H_{17}ClNO_3$ and $C_{18}H_{14}BrClNO_3$ 342.0897 and 405.9846 respectively; found, 342.0894, and 405.9842

4.6. Experimental Procedure for the 'D' Incorporation *vs*. Isomerization

A solution of *anti*-**9** (25 mg, 0.08 mmol) in $CD_3OD:D_2O$ (0.7 mL, 4:1 v/v) was transferred to a NMR tube and the ¹H NMR spectrum was obtained. Then anhydrous NaOH (3 mg, 0.08 mmol) was added to the solution and the NMR was obtained after 10, 20, 40 and 180 minutes. The spectra obtained are presented in the annex (Figure A2.22-A2.26; p. 188).

4.7. Computational Methods

All molecular mechanics calculations were performed using Hyperchem with the MM+ force field [85], and the quantum mechanical calculations were performed using Gaussian 09 [79]. Conformational searches were run to locate the minimum energy conformers of all the structures. Initially, the conformational search was done in the gas phase using the MM+ force field, with the number of steps large enough to find all low-energy conformers at least 10 times. All conformers within 5 kcal/mol of the lowest energy conformer were subjected to further reoptimization at the HF/3-21G level of theory. With the most stable conformers in

hand (up to 5 kcal/mol of the lowest energy conformer) were then further optimized at the B3LYP/6-31G* level of theory. Frequency calculations were used to confirm the nature of the stationary points and to evaluate the thermochemical properties, that were calculated at 1 atm and 298.15 K. Energies in solution were computed on the structures optimized in the gas phase at the B3LYP/6-31G* level of theory with the Polarizable Continuum Model (PCM) as implemented in Gaussian 09 using chloroform as the solvent [86].

The next step was the shielding constants single point calculation using the GIAO (gauge including atomic orbitals) method, [87-90] with the mPW1PW91 functional [91] (one of the most reliable DFT functionals for NMR calculations) [80] and the 6-31+G** basis set, with the PCM model using chloroform as the solvent. The NMR shielding constants were subjected to Boltzmann averaging over all conformers according to:

$$\sigma^x = \frac{\sum_i \sigma^x_i \exp(-E_i/RT)}{\sum_i \exp(-E_i/RT)}$$

Where σ^x is the Boltzmann-averaged shielding constant for nucleus x, σ^x_i is the shielding constant for nucleus x in conformer i, R is the molar gas constant (8.3145 J K^{-1} mol^{-1}), T is the temperature (298 K), and E_i is the B3LYP/6-31G* energy in solution of conformer i (relative to the lowest energy conformer). Once the shielding constants were computed, the chemical shifts were calculated according to:[82, 83]

$$\delta^x_{calc} = \sigma_{ref} - \sigma^x + \delta_{ref}$$

where σ_{ref} is the NMR isotropic magnetic shielding values for the reference compound, and δ_{ref} is the experimental chemical shift of the reference compound in deuterated chloroform. In this study the multi-standard approach (MSTD) to calculate the NMR chemical shifts was used. Therefore, methanol (δ_{ref} = 50.41 ppm for ^{13}C) and benzene (δ_{ref} =128.37 ppm for ^{13}C) were used as reference standards for sp^3 and sp-sp^2 hybridized carbon atoms, or for the protons attached to them, respectively. Sarotti and Pellegrinet have recently found that this simple modification allowed much better accuracy and lower dependence on the theory level employed, both for ^{13}C and ^{1}H NMR shift calculation procedure. The CP3 parameters were computed as described by Goodman [84]. The J values were computed at the B3LYP/6-31G**//B3LYP/6-31G* level of theory using the nmr=spinspin keyword as implemented in Gaussian 09. The M062X/6-311+G** calculations were carried out from the most stable conformations found at the B3LYP/6-31G* level (up to 2 kcal/mol from the global minima) and reoptimized at the M062X/6-311+G** level. Frequency calculations were used to confirm the nature of the stationary points and to evaluate the thermochemical properties, that were calculated at 1 atm and 298.15 K.

5. References and Notes

[1] WANG, J.; JIANG, X.; CHEN, M.; GE, Z.; HU, Y.; HU, H. TFA-catalyzed ring transformation of 4-hydroxycyclobutenone: A simple and general route for preparation of 3-substituted 4-aminofuran-2(5H)-ones. J. Chem. Soc., Perkin Trans. 1, p. 66-71, **2001**.

[2] BASLER, B.; SCHUSTER, O.; BACH, T. Conformationally Constrained β-Amino Acid Derivatives by Intramolecular [2 + 2]-Photocycloaddition of a Tetronic Acid Amide and Subsequent Lactone Ring Opening. J. Org. Chem., v. 70, p. 9798-9808, **2005**.

[3] SYDORENKO, N.; HSUNG, R. P.; VERA, E. L. Torquoselective 6π-Electron Electrocyclic Ring Closure of 1-Azatrienes Containing Acyclic Chirality at theC-Terminus. Org. Lett., v. 8, p. 2611-2614, **2006**.

[4] POLI, G.; MADEC, D.; MINGOIA, F.; PRESTAT, G. N-Substituted Tetronamides as Ambident Nucleophilic Building Blocks for the Synthesis of New 4-Aza-2,3-didehydropodophyllotoxins. Synlett, p. 1475-1478, **2008**.

[5] ZHOU, L.-H.; YU, X.-Q.; PU, L. Reactivity of γ-Hydroxy-α,β-acetylenic Esters with Amines: Facile Synthesis of the Optically Active 4-Amino-2(5H)-furanones. J. Org. Chem., v. 74, p. 2013-2017, **2009**.

[6] JIANG, B.; FENG, B.-M.; WANG, S.-L.; TU, S.-J.; LI, G. Domino Constructions of Pentacyclic Indeno[2,1-c]quinolines and Pyrano[4,3-b]oxepines by [4+1]/[3+2+1]/[5+1] and [4+3] Multiple Cyclizations. Chem. – Eur. J., v. 18, p. 9823-9826, **2012**.

[7] HERTZBERG, R.; MOBERG, C. One-Step Preparation ofO-(α-Bromoacyl) Cyanohydrins by Minor Enantiomer Recycling: Synthesis of 4-Amino-2(5H)-furanones. J. Org. Chem., v. 78, p. 9174-9180, **2013**.

[8] GHAHREMANZADEH, R.; RASHID, Z.; ZARNANI, A.-H.; NAEIMI, H. Manganese ferrite nanoparticle catalyzed tandem and green synthesis of spirooxindoles. RSC Adv., v. 4, p. 43661-43670, **2014**.

[9] AILLERIE, A.; TALANCÉ, V. L. D.; MONCOMBLE, A.; BOUSQUET, T.; PÉLINSKI, L. Enantioselective Organocatalytic Partial Transfer Hydrogenation of Lactone-Fused Quinolines. Org. Lett., v. 16, p. 2982-2985, **2014**.

[10] YANG, Z.; HAO, W.-J.; XU, H.-W.; WANG, S.-L.; JIANG, B.; LI, G.; TU, S.-J. Base-Promoted Transannulation of Heterocyclic Enamines and 2,3-Epoxypropan-1-ones: Regio- and Stereoselective Synthesis of Fused Pyridines and Pyrroles. J. Org. Chem., v. 80, p. 2781-2789, **2015**.

[11] TANOURY, G. J.; CHEN, M.; DONG, Y.; FORSLUND, R. E.; MAGDZIAK, D. Development of a Novel Pd-CatalyzedN-Acyl Vinylogous Carbamate Synthesis for the Key Intermediate of ICE Inhibitor VX-765. Org. Lett., v. 10, p. 185-188, **2008**.

[12] XIAO, Z.-P.; MA, T.-W.; LIAO, M.-L.; FENG, Y.-T.; PENG, X.-C.; LI, J.-L.; LI, Z.-P.; WU, Y.; LUO, Q.; DENG, Y.; LIANG, X.; ZHU, H.-L. Tyrosyl-tRNA synthetase inhibitors as antibacterial agents: Synthesis, molecular docking and structure–activity relationship analysis of 3-aryl-4-arylaminofuran-2(5H)-ones. Eur. J. Med. Chem., v. 46, p. 4904-4914, **2011**.

[13] KUMAR, A.; KUMAR, V.; E. ALEGRIA, A.; V. MALHOTRA, S. Synthetic and Application Perspectives of Azapodophyllotoxins: Alternative Scaffolds of Podophyllotoxin. Curr. Med. Chem., v. 18, p. 3853-3870, **2011**.

[14] KAMAL, A.; SRINIVASA REDDY, T.; POLEPALLI, S.; PAIDAKULA, S.; SRINIVASULU, V.; GANGA REDDY, V.; JAIN, N.; SHANKARAIAH, N. Synthesis and biological evaluation of 4-aza-2,3-dihydropyridophenanthrolines as tubulin polymerization inhibitors. Bioorg. Med. Chem. Lett., v. 24, p. 3356-3360, **2014**.

[15] GEORGIADIS, D.; ZOGRAFOS, A. Synthetic Strategies towards Naturally Occurring Tetronic Acids. Synthesis, p. 3157-3188, **2006**.

[16] SCHOBERT, R.; SCHLENK, A. Tetramic and tetronic acids: An update on new derivatives and biological aspects. Bioorg. Med. Chem., v. 16, p. 4203-4221, **2008**.

[17] IINUMA, H.; NAKAMURA, H.; NAGANAWI, H.; MASUDA, T.; TAKANO, S.; TAKEUCHI, T.; UMEZAWA, H.; IITAKA, Y.; OBAYASHI, A. Basidalin,a new antibiotic from basidiomycetes. J. Antibiot. (Tokyo), v. 36, p. 448-450, **1983**.

[18] ACOSTA, J. A. M.; MUDDALA, R.; BARBOSA, L. C. A.; BOUKOUVALAS, J. Total Synthesis of the Antitumor Antibiotic Basidalin. J. Org. Chem., v. 81, p. 6883-6886, **2016**.

[19] JESCHKE, P.; NAUEN, R.; GUTBROD, O.; BECK, M. E.; MATTHIESEN, S.; HAAS, M.; VELTEN, R. Flupyradifurone (Sivanto™) and its novel butenolide pharmacophore: Structural considerations☆. Pest. Biochem. Physiol., v. 121, p. 31-38, **2015**.

[20] NAUEN, R.; JESCHKE, P.; VELTEN, R.; BECK, M. E.; EBBINGHAUS-KINTSCHER, U.; THIELERT, W.; WÖLFEL, K.; HAAS, M.; KUNZ, K.; RAUPACH, G. Flupyradifurone: a brief profile of a new butenolide insecticide. Pest Manag. Sci., v. 71, p. 850-862, **2015**.

[21] SEMENOVA, M. N.; KISELYOV, A. S.; TSYGANOV, D. V.; KONYUSHKIN, L. D.; FIRGANG, S. I.; SEMENOV, R. V.; MALYSHEV, O. R.; RAIHSTAT, M. M.; FUCHS, F.; STIELOW, A.; LANTOW, M.; PHILCHENKOV, A. A.; ZAVELEVICH, M. P.; ZEFIROV, N. S.; KUZNETSOV, S. A.; SEMENOV, V. V. Polyalkoxybenzenes from Plants. 5. Parsley Seed Extract in Synthesis of Azapodophyllotoxins Featuring Strong Tubulin Destabilizing Activity in the Sea Urchin Embryo and Cell Culture Assays. J. Med. Chem., v. 54, p. 7138-7149, **2011**.

[22] LATTMANN, E.; DUNN, S.; NIAMSANIT, S.; SATTAYASAI, N. Synthesis and antibacterial activities of 5-hydroxy-4-amino-2(5H)-furanones. Bioorg. Med. Chem. Lett., v. 15, p. 919-921, **2005**.

[23] LIU, G.; WU, Y.; XU, H.; LIU, H. A Green Route for the Synthesis of Antiepileptic Drug Losigamone and Its Analogues. Chinese J. Org. Chem., v. 33, p. 1527, **2013**.

[24] XIAO, Y.; LUO, M.; WANG, J.; LUO, H.; WANG, J. Losigamone add-on therapy for partial epilepsy. Cochrane Database Syst. Rev. , v. 12, p. CD009324, **2015**.

[25] ŁUSZCZKI, J. J. Third-generation antiepileptic drugs: mechanisms of action, pharmacokinetics and interactions. Pharmacol. Rep., v. 61, p. 197-216, **2009**.

[26] BAUER, J.; DIENEL, A.; ELGER, C. E. Losigamone add-on therapy in partial epilepsy: a placebo-controlled study. Acta Neurol. Scand., v. 103, p. 226-230, **2001**.

[27] BAULAC, M.; KLEMENT, S. Efficacy and safety of Losigamone in partial seizures: a randomized double-blind study. Epilepsy Res., v. 55, p. 177-189, **2003**.

[28] For some of our recent work on the synthesis and biological activities of heterosubstituted butenolides, see [**Ref. 28-30**].BARBOSA, L. C. A.; MALTHA, C. R. A.; LAGE, M. R.; BARCELOS, R. C.; DONÀ, A.; CARNEIRO, J. W. M.; FORLANI, G. Synthesis of Rubrolide Analogues as New Inhibitors of the Photosynthetic Electron Transport Chain. J. Agri. Food Chem., v. 60, p. 10555-10563, **2012**.

[29] PEREIRA, U. A.; BARBOSA, L. C. A.; MALTHA, C. R. A.; DEMUNER, A. J.; MASOOD, M. A.; PIMENTA, A. L. γ-Alkylidene-γ-lactones and isobutylpyrrol-2(5H)-ones analogues to rubrolides as inhibitors of biofilm formation by Gram-positive and Gram-negative bacteria. Bioorg. Med. Chem. Lett., v. 24, p. 1052-1056, **2014**.

[30] PEREIRA, U. A.; BARBOSA, L. C. A.; MALTHA, C. R. A.; DEMUNER, A. J.; MASOOD, M. A.; PIMENTA, A. L. Inhibition of Enterococcus faecalis biofilm formation by highly active lactones and lactams analogues of rubrolides. Eur. J. Med. Chem., v. 82, p. 127-138, **2014**.

[31] Recent Reviews on VA reaction, see [**Ref. 31-34**]. CASIRAGHI, G.; ZANARDI, F.; APPENDINO, G.; RASSU, G. The Vinylogous Aldol Reaction: A Valuable, Yet Understated Carbon−Carbon Bond-Forming Maneuver. Chem. Rev., v. 100, p. 1929-1972, **2000**.

[32] CASIRAGHI, G.; BATTISTINI, L.; CURTI, C.; RASSU, G.; ZANARDI, F. The Vinylogous Aldol and Related Addition Reactions: Ten Years of Progress†. Chem. Rev., v. 111, p. 3076-3154, **2011**.

[33] PANSARE, S. V.; PAUL, E. K. The Organocatalytic Vinylogous Aldol Reaction: Recent Advances. Chem. – Eur. J., v. 17, p. 8770-8779, **2011**.

[34] BISAI, V. Organocatalytic Asymmetric Vinylogous Aldol Reactions. Synthesis, v. 44, p. 1453-1463, **2012**.

[35] BROWN, D. W.; CAMPBELL, M. M.; TAYLOR, A. P.; ZHANG, X.-A. Regio- and diastereoselectivity in aldol reactions of cyclopent-2-enone, 2-(5H)furanone and their derived trimethylsilyloxydienes. Tetrahedron Lett., v. 28, p. 985-988, **1987**.

[36] JEFFORD, C. W.; JAGGI, D.; BOUKOUVALAS, J. Diastereoselectivity in the directed aldol condensation of 2-trimethylsiloxyfuran with aldehydes. A stereodivergent route to threo and erythro δ-hydroxy-γ-lactones. Tetrahedron Lett., v. 28, p. 4037-4040, **1987**.

[37] JEFFORD, C. W.; JAGGI, D.; BERNARDINELLI, G.; BOUKOUVALAS, J. The synthesis of (±)-cavernosine. Tetrahedron Lett., v. 28, p. 4041-4044, **1987**.

[38] BOUKOUVALAS, J.; MALTAIS, F. An efficient total synthesis of neopatulin. Tetrahedron Lett., v. 35, p. 5769-5770, **1994**.

[39] LÓPEZ, C. S.; ÁLVAREZ, R.; VAZ, B.; FAZA, O. N.; DE LERA, Á. R. Simple Diastereoselectivity of the BF3·OEt2-Catalyzed Vinylogous Mukaiyama Aldol Reaction of 2-(Trimethylsiloxy)furans with Aldehydes. J. Org. Chem., v. 70, p. 3654-3659, **2005**.

[40] BOUKOUVALAS, J.; BELTRÁN, P. P.; LACHANCE, N.; CÔTÉ, S.; MALTAIS, F.; POULIOT, M. A New, Highly Stereoselective Synthesis of β-Unsubstituted (Z)-γ-Alkylidenebutenolides Using Bromine as a Removable Stereocontrol Element. Synlett, p. 0219-0222, **2007**.

[41] DAS SARMA, K.; ZHANG, J.; CURRAN, T. T. Novel Synthons from Mucochloric Acid: The First Use of α,β-Dichloro-γ-butenolides and γ-Butyrolactams for Direct Vinylogous Aldol Addition. J. Org. Chem., v. 72, p. 3311-3318, **2007**.

[42] LIU, G.-Y.; GUO, B.-Q.; CHEN, W.-N.; CHENG, C.; ZHANG, Q.-L.; DAI, M.-B.; SUN, J.-R.; SUN, P.-H.; CHEN, W.-M. Synthesis, Molecular Docking, and Biofilm Formation Inhibitory Activity of 5-Substituted 3,4-Dihalo-5H-furan-2-one Derivatives on Pseudomonas aeruginosa. Chem. Biol. Drug. Des., v. 79, p. 628-638, **2012**.

[43] For a related VAR leading to tetramic acid aldolates see: DAVID, J. G.; BAI, W.-J.; WEAVER, M. G.; PETTUS, T. R. R. A General Diastereoselective Catalytic Vinylogous Aldol Reaction Among Tetramic Acid-Derived Pyrroles. Org. Lett., v. 16, p. 4384-4387, **2014**.

[44] KABESHOV, M. A.; KYSILKA, O.; RULÍŠEK, L.; SULEIMANOV, Y. V.; BELLA, M.; MALKOV, A. V.; KOČOVSKÝ, P. Cross-Aldol Reaction of Isatin with Acetone Catalyzed by Leucinol: A Mechanistic Investigation. Chem. – Eur. J., v. 21, p. 12203-12203, **2015**.

[45] FRINGS, M.; ATODIRESEI, I.; WANG, Y.; RUNSINK, J.; RAABE, G.; BOLM, C. C1-Symmetric Aminosulfoximines in Copper-Catalyzed Asymmetric Vinylogous Mukaiyama Aldol Reactions. Chem. – Eur. J., v. 16, p. 4577-4587, **2010**.

[46] YANG, Y.; ZHENG, K.; ZHAO, J.; SHI, J.; LIN, L.; LIU, X.; FENG, X. Asymmetric Direct Vinylogous Aldol Reaction of Unactivated γ-Butenolide to Aldehydes. J. Org. Chem., v. 75, p. 5382-5384, **2010**.

[47] UBE, H.; SHIMADA, N.; TERADA, M. Asymmetric Direct Vinylogous Aldol Reaction of Furanone Derivatives Catalyzed by an Axially Chiral Guanidine Base. Angew. Chem., Int. Ed., v. 49, p. 1858-1861, **2010**.

[48] LUO, J.; WANG, H.; HAN, X.; XU, L.-W.; KWIATKOWSKI, J.; HUANG, K.-W.; LU, Y. The Direct Asymmetric Vinylogous Aldol Reaction of Furanones with α-Ketoesters: Access to Chiral γ-Butenolides and Glycerol Derivatives. Angew. Chem., Int. Ed., v. 50, p. 1861-1864, **2011**.

[49] For VA reactions of tetronic acid dianions, see [**Ref. 49-56**]. KAMETANI, T.; KATOH, T.; TSUBUKI, M.; HONDA, T. One-step stereochemical determination of four contiguous acyclic chiral centers on a steroidal side chain: a novel synthesis of brassinolide. J. Am. Chem. Soc., v. 108, p. 7055-7060, **1986**.

[50] PELTER, A.; AL-BAYATI, R. I. H.; AYOUB, M. T.; LEWIS, W.; PARDASANI, P.; HANSEL, R. Synthetic routes to the piperolides, fadyenolides, epoxypiperolides, and related compounds. J. Chem. Soc., Perkin Trans. 1, p. 717, **1987**.

[51] HONDA, T.; KONDOH, H.; OKUYAMA, A.; HAYAKAWA, T.; TSUBUKI, M.; NAGASE, H. Chelation Controlled Aldol Reaction of Tetronic Acid Dianion with Ketones. Heterocycles, v. 33, p. 67, **1992**.

[52] MALLINGER, A. L.; LE GALL, T.; MIOSKOWSKI, C. 3-Aryltetronic Acids: Efficient Preparation and Use as Precursors for Vulpinic Acids. J. Org. Chem., v. 74, p. 1124-1129, **2009**.

[53] YANG, W.; LIU, J.; ZHANG, H. Total synthesis of pulverolide: revision of its structure. Tetrahedron Lett., v. 51, p. 4874-4876, **2010**.

[54] DUBOIS, S.; RODIER, F.; BLANC, R.; RAHMANI, R.; HÉRAN, V.; THIBONNET, J.; COMMEIRAS, L.; PARRAIN, J.-L. Dramatic influence of the substitution of alkylidene-5H-furan-2-ones in Diels–Alder cycloadditions with o-quinonedimethide as diene partner: en route to the CDEF polycyclic ring system of lactonamycin. Org. Biomol. Chem., v. 10, p. 4712, **2012**.

[55] FRINGS, M.; THOMÉ, I.; SCHIFFERS, I.; PAN, F.; BOLM, C. Catalytic, Asymmetric Synthesis of Phosphonic γ-(Hydroxyalkyl)butenolides with Contiguous Quaternary and Tertiary Stereogenic Centers. Chem. – Eur. J., v. 20, p. 1691-1700, **2014**.

[56] HUANG, P.-Q.; HUANG, S.-Y.; GAO, L.-H.; MAO, Z.-Y.; CHANG, Z.; WANG, A.-E. Enantioselective total synthesis of (+)-methoxystemofoline and (+)-isomethoxystemofoline. Chem. Commun., v. 51, p. 4576-4578, **2015**.

[57] SCHLESSINGER, R. H.; MJALLI, A. M. M.; ADAMS, A. D.; SPRINGER, J. P.; HOOGSTEEN, K. An approach to erythronolide A seco acid via a simple tetronic acid. J. Org. Chem., v. 57, p. 2992-2993, **1992**.

[58] DANKWARDT, J. W.; DANKWARDT, S. M.; SCHLESSINGER, R. H. Synthesis of the C19 through C27 segment of okadaic acid using vinylogous urethane aldol chemistry: Part III. Tetrahedron Lett., v. 39, p. 4979-4982, **1998**.

[59] BRUYÈRE, H.; BALLEREAU, S.; SELKTI, M.; ROYER, J. Asymmetric synthesis of 5-(1-hydroxyalkyl)-5-methyl-5H-furan-2-ones. Tetrahedron, v. 59, p. 5879-5886, **2003**.

[60] ROYER, J.; BRUYÈRE, H.; DOS REIS, C.; SAMARITANI, S.; BALLEREAU, S. Approach to the Eleutherobin Core: Synthesis of a Key Intermediate by Intramolecular Diels-Alder Cycloaddition. Synthesis, v. p. 1673-1681, **2006**.

[61] DECHOUX, L.; EAR, A.; TOUM, V.; THORIMBERT, S. Decarboxylative Knoevenagel-Type Reactions on Tetronamides: Synthesis of 5-Ylidene-4-Amino-2(5H)-Furanones. Synlett, v. 25, p. 1713-1716, **2014**.

[62] CUNHA, S.; OLIVEIRA, C. C.; SABINO, J. R. Synthesis of 3-bromotetronamides via amination of 3,4-dibromofuran-2(5H)-one. J. Braz. Chem. Soc., v. 22, p. 598-603, **2011**.

[63] FARIÑA, F.; MARTÍN, M. V.; SÁNCHEZ, F.; MAESTRO, M. C.; MARTÍN, M. R. Pseudoesters and Derivatives; XVII1. Synthesis of 4-Alkylamino- and 4-Alkylthio-5-methoxyfuran-2(5H)-ones. Synthesis, p. 397-398, **1983**.

[64] BLAZECKA, P. G.; BELMONT, D.; CURRAN, T.; PFLUM, D.; ZHANG, J. Further Utilization of Mucohalic Acids: Palladium-Free, Regioselective Etherification and Amination of α,β-Dihalo γ-Methoxycarbonyloxy and γ-Acetoxy Butenolides. Org. Lett., v. 5, p. 5015-5017, **2003**.

[65] ORITO, Y.; HASHIMOTO, S.; ISHIZUKA, T.; NAKAJIMA, M. Chiral base-catalyzed aldol reaction of trimethoxysilyl enol ethers: effect of water as an additive on stereoselectivities. Tetrahedron, v. 62, p. 390-400, **2006**.

[66] RAMIREDDY, N.; ZHAO, J. C. G. Base-catalyzed reaction between isatins and N-Boc-3-pyrrolin-2-one. Tetrahedron Lett., v. 55, p. 706-709, **2014**.

[67] BUTLER, R. N.; COYNE, A. G. Water: Nature's Reaction Enforcer—Comparative Effects for Organic Synthesis "In-Water" and "On-Water". Chem. Rev., v. 110, p. 6302-6337, **2010**.

[68] KITANOSONO, T.; KOBAYASHI, S. Mukaiyama Aldol Reactions in Aqueous Media. Adv. Synth. Catal., v. 355, p. 3095-3118, **2013**.

[69] YU, J.-S.; LIU, Y.-L.; TANG, J.; WANG, X.; ZHOU, J. Highly Efficient "On Water" Catalyst-Free Nucleophilic Addition Reactions Using Difluoroenoxysilanes: Dramatic Fluorine Effects. Angew. Chem., Int. Ed., v. 53, p. 9512-9516, **2014**.

[70] CURTI, C.; BATTISTINI, L.; ZANARDI, F.; RASSU, G.; ZAMBRANO, V.; PINNA, L.; CASIRAGHI, G. Uncatalyzed, Diastereoselective Vinylogous Mukaiyama Aldol Reactions on Aqueous Media: Pyrrole vs Furan 2-Silyloxy Dienes. J. Org. Chem., v. 75, p. 8681-8684, **2010**.

[71] By-product formation accounts for the low yields of **15** and **23**. In case of compound **23**, two new products **23a** and **23b** were also isolated. Characterization data of these new products and copies of 1H and 13C NMR spectra are available on *Materials and Methods* and *Annex 1*.

[72] Cf. pKa ≈ 12 for rofecoxib (an α,β–diarylbutenolide). REDDY, L. R.; COREY, E. J. Facile air oxidation of the conjugate base of rofecoxib (Vioxx™), a possible contributor to chronic human toxicity. Tetrahedron Lett., v. 46, p. 927-929, **2005**.

[73] FAZIO, F.; SCHNEIDER, M. P. A novel synthesis of 2-deoxy-l-ribose. Tetrahedron: Asymmetry, v. 11, p. 1869-1876, **2000**.

[74] DUFFY, R. J.; MORRIS, K. A.; VALLAKATI, R.; ZHANG, W.; ROMO, D. Asymmetric Synthesis, Structure, and Reactivity of Unexpectedly Stable Spiroepoxy-β-Lactones Including Facile Conversion to Tetronic Acids: Application to (+)-Maculalactone A. J. Org. Chem., v. 74, p. 4772-4781, **2009**.

[75] LUO, S.; ZHOU, P.; LI, J.; CHENG, J.-P. Asymmetric Retro- and Transfer-Aldol Reactions Catalyzed by a Simple Chiral Primary Amine. Chem. – Eur. J., v. 16, p. 4457-4461, **2010**.

[76] FLOCK, A. M.; REUCHER, C. M. M.; BOLM, C. Enantioenrichment by Iterative Retro-Aldol/Aldol Reaction Catalyzed by an Achiral or Racemic Base. Chem. – Eur. J., v. 16, p. 3918-3921, **2010**.

[77] JUNG, M. E.; CHANG, J. J. Total Synthesis of the Proposed Structure of Mycosporulone: Structural Revision and an Unexpected Retro-Aldol/Aldol Reaction. Org. Lett., v. 14, p. 4898-4901, **2012**.

[78] ZHAO, Y.; TRUHLAR, D. G. Density Functionals with Broad Applicability in Chemistry. Acc. Chem. Res., v. 41, p. 157-167, **2008**.

[79] FRISCH, M. J.; TRUCKS, G. W.; SCHLEGEL, H. B.; SCUSERIA, G. E.; ROBB, M. A.; CHEESEMAN, J. R.; SCALMANI, G.; BARONE, V.; MENNUCCI, B.; PETERSSON, G. A.; NAKATSUJI, H.; CARICATO, M.; LI, X.; HRATCHIAN, H. P.; IZMAYLOV, A. F.; BLOINO, J.; ZHENG, G.; SONNENBERG, J. L.; HADA, M.; EHARA, M.; TOYOTA, K.; FUKUDA, R.; HASEGAWA, J.; ISHIDA, M.; NAKAJIMA, T.; HONDA, Y.; KITAO, O.; NAKAI, H.; VREVEN, T.; MONTGOMERY JR., J. A.; PERALTA, J. E.; OGLIARO, F. O.; BEARPARK, M. J.; HEYD, J.; BROTHERS, E. N.; KUDIN, K. N.; STAROVEROV, V. N.; KOBAYASHI, R.; NORMAND, J.; RAGHAVACHARI, K.; RENDELL, A. P.; BURANT, J. C.; IYENGAR, S. S.; TOMASI, J.; COSSI, M.; REGA, N.; MILLAM, N. J.; KLENE, M.; KNOX, J. E.; CROSS, J. B.; BAKKEN, V.; ADAMO, C.; JARAMILLO, J.; GOMPERTS, R.; STRATMANN, R. E.; YAZYEV, O.; AUSTIN, A. J.; CAMMI, R.; POMELLI, C.; OCHTERSKI, J. W.; MARTIN, R. L.; MOROKUMA, K.; ZAKRZEWSKI, V. G.; VOTH, G. A.; SALVADOR, P.; DANNENBERG, J. J.; DAPPRICH, S.; DANIELS, A. D.; FARKAS, Ã. D. N.; FORESMAN, J. B.; ORTIZ, J. V.; CIOSLOWSKI, J.; FOX, D. J. Gaussian 09. Gaussian, Inc., Wallingford CT, v. p. **2009**.

[80] LODEWYK, M. W.; SIEBERT, M. R.; TANTILLO, D. J. Computational Prediction of 1H and 13C Chemical Shifts: A Useful Tool for Natural Product, Mechanistic, and Synthetic Organic Chemistry. Chem. Rev., v. 112, p. 1839-1862, **2012**.

[81] SAROTTI, A. M. Successful combination of computationally inexpensive GIAO 13C NMR calculations and artificial neural network pattern recognition: a new strategy for simple and rapid detection of structural misassignments. Org. Biomol. Chem., v. 11, p. 4847-4859, **2013**.

[82] SAROTTI, A. M.; PELLEGRINET, S. C. A Multi-standard Approach for GIAO 13C NMR Calculations. J. Org. Chem., v. 74, p. 7254-7260, **2009**.

[83] SAROTTI, A. M.; PELLEGRINET, S. C. Application of the Multi-standard Methodology for Calculating 1H NMR Chemical Shifts. J. Org. Chem., v. 77, p. 6059-6065, **2012**.

[84] SMITH, S. G.; GOODMAN, J. M. Assigning the Stereochemistry of Pairs of Diastereoisomers Using GIAO NMR Shift Calculation. J. Org. Chem., v. 74, p. 4597-4607, **2009**.

[85] Hyperchem Professional Release 7.52. Hypercube, Inc., **2005**.

[86] TOMASI, J.; MENNUCCI, B.; CAMMI, R. Quantum Mechanical Continuum Solvation Models. Chem. Rev., v. 105, p. 2999-3094, **2005**.

[87] DITCHFIELD, R. Molecular Orbital Theory of Magnetic Shielding and Magnetic Susceptibility. J. Chem. Phys., v. 56, p. 5688, **1972**.

[88] DITCHFIELD, R. Self-consistent perturbation theory of diamagnetism. Mol. Phys., v. 27, p. 789-807, **1974**.

[89] MCMICHAEL ROHLFING, C.; ALLEN, L. C.; DITCHFIELD, R. Proton and carbon-13 chemical shifts: Comparison between theory and experiment. Chem. Phys., v. 87, p. 9-15, **1984**.

[90] WOLINSKI, K.; HINTON, J. F.; PULAY, P. Efficient implementation of the gauge-independent atomic orbital method for NMR chemical shift calculations. J. Am. Chem. Soc., v. 112, p. 8251-8260, **1990**.

[91] ADAMO, C.; BARONE, V. Exchange functionals with improved long-range behavior and adiabatic connection methods without adjustable parameters: The mPW and mPW1PW models. J. Chem. Phys., v. 108, p. 664, **1998**.

CHAPTER 3

**Substituent-Modulated Conformation
and Supramolecular Assembly of Tetronamides**

1. Introduction

The control of molecular conformation is one of the primary steps in the modulation of supramolecular assembly, which, at ultimate analysis, will be responsible for the properties of designed compounds. For instance, it is well-known that bioactive compounds bind to target macromolecules only in certain shape which is achieved through conformational restriction [1]. Physical properties are also related to conformation and packing. A representative example in this line is the series of thienyl substituted bi-1,3,4-oxadiazoles showing large red shifts in their absorption and emission spectra if they are featured with planar conformation and J-type packing, which occurs only in fluoro-substituted compounds in *ortho* (*o*) and *meta* (*m*) positions of a phenyl ring [2]. Other substitution patterns lead to twisted conformation with different packing slippage and smaller red shift in their corresponding spectra [2]. In addition, there is knowledge of how substitution affects conformation and crystal packing in several compound classes. The role of the substitution degree and the ability to assemble intramolecular classical hydrogen bonds in freezing the conformation of adamantane-type thioureas is well characterized[3], as well as the electron donating or withdrawing propensity and polarity of substituents correlates with *endo* and *exo* conformations of bis(phenyl)acetones [4]. The substitution position is also known to drive conformation and intermolecular interactions, such as in fluoro-*N*-(pyridyl)benzamides [5], polycyclic pyrimidoazepines [6], and 3,3'-dinitro-2,2'-azobipyridines [7].

As described in the Chapter 2, tetronamide-derived aldolates are highly functional molecules possessing NH, OH and C=O groups, which are able to act as both hydrogen donors and/or acceptors. Despite their high potential as supramolecular synthons, the structures of tetronamide aldolates, and their crystals have not been systematically studied. Concerning the structural knowledge in the solid state, there are few crystal structures of tetronamides in the Cambridge Structural Database (CSD version 5.37 of November 2015 with February 2016 update) [8]. A total of eighty one crystal structures are returned from a CSD search for the 4-amino-2(5*H*)-furanone minimal framework of tetronamides [8]. Twelve tetronamides with at least one stereocenter are found in the CSD [9] and only four of them have two chiral carbons making possible the occurrence of *syn*/ *anti* diastereomers [10, 11].

Aiming to better understand the structural features of such compounds to support further structural-biological activities studies, in this Chapter, details of the crystal structure of nine tetronamide-derived aldolates, and one tetronamide-derived bis-aldolate (Figure 3.1, **1-10**) has been described. The structures of all these compounds are characterized by a phenyl ring attached to the nitrogen atom and another aromatic/heteroaromatic moiety

derived from the corresponding aldehydes as shown in Figure 3.1. As described in the Chapter 2 [12], compounds **1-9** are racemic and present with two stereocenters, being seven *syn* (**1**-**6**, **8**) and two *anti* (**7**, **9**) diastereomers (Figure 3.1). Crystal structures of tetronamide-derived bis-aldolate bearing *meta*-nitrophenyl as substituents (**10**) and consolidate the conformational relationship trend found in the other tetronamide-derived aldolates. Based on this considerable number of related crystal structures, it was possible to find a straightforward conformational tendency according to their substitution pattern, which has been understood *via* theoretical calculations for the significantly populated conformers.
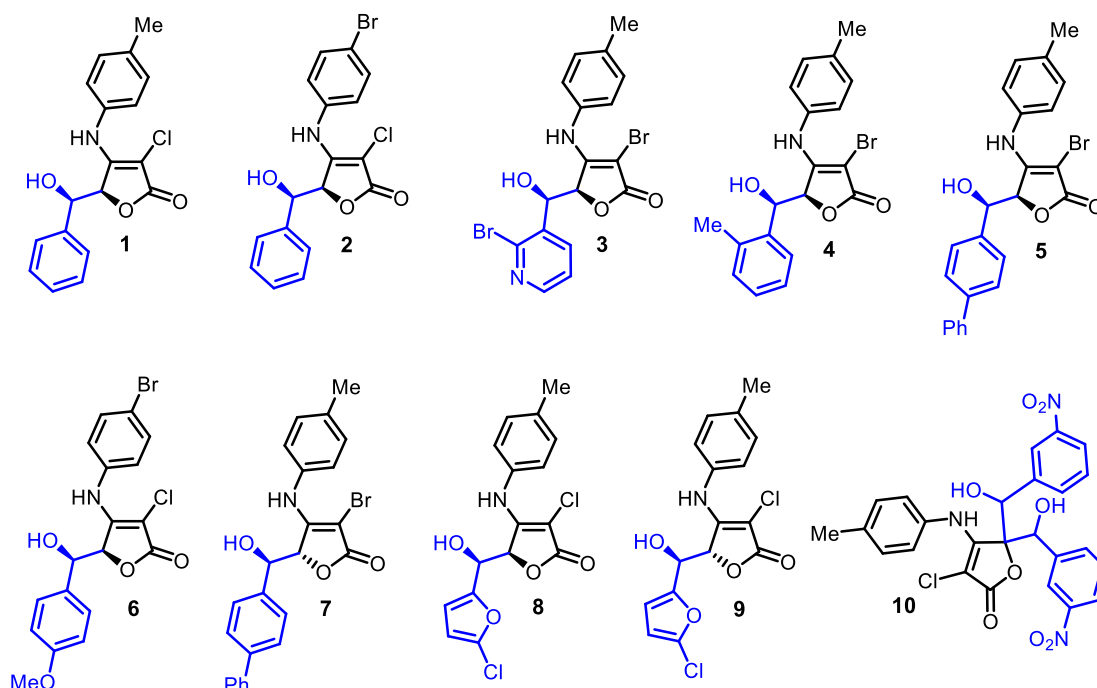
Figure 3.1 Crystallized tetronamide aldol products (compounds **1-10**). Synthetic procedure has already been discussed in **Chapter 2**, with the initial structural characterization by IR, NMR & HRMS.

These disclose of reliable effects of substitution pattern on conformation attracts much interest due to possibility of producing stereochemically defined materials with desirable properties. Previous studies have already demonstrated the electron donating/withdrawing and hydrophilicity effects of substituents in driving the conformation and intermolecular interaction pattern of other classes of compounds [1-7, 13, 14]. The impact of the substitution position on the molecular shape has been also investigated in some sorts of related compounds [1-7, 13, 14]. Herein, the absence of substituents in *meta* and *para* positions of one of the two side rings allowed for a U-shaped conformation stabilized by weak intramolecular contacts. Furthermore, the findings go beyond, since the substitution pattern of the aromatic ring does not affect only the conformation, but also the assembly of supramolecular entities.

2. Results and Discussion

2.1. Crystal Structures (Experimental Conformations)

S*yn* diastereomers **1**–**4** and **6** have crystallized in the centrosymmetric triclinic space group P-1 with the two enantiomers in the unit cell. The enantiomer arbitrarily chosen to be their asymmetric unit was present with C11 and C12 stereocenters at *S* configuration (Figures 3.2 and 3.3). The other enantiomer with these carbons at *R* configuration is generated by inversion symmetry. Both *anti* diastereomers **7** and **9** have also crystallized in centrosymmetric space groups, namely, *P*2₁/*c* and *C*2/*c*, respectively.
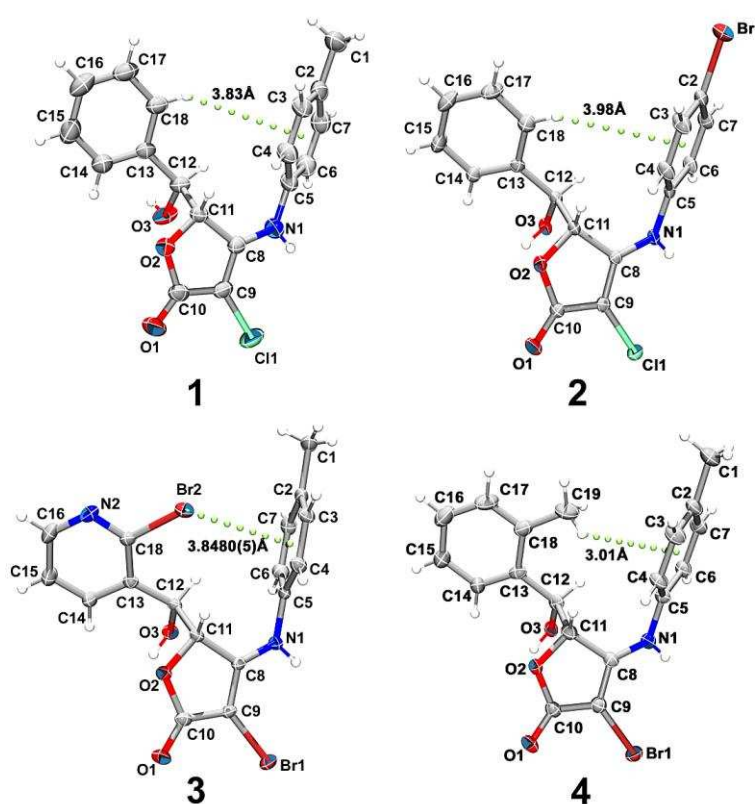
Figure 3.2 50% Ellipsoid plot for the non-hydrogen atoms of the U-shaped tetronamides **1**-**4** present in their asymmetric unit. The dotted green line means the C—H…π (or Br…π) contact and the displayed distance is between H (or Br) and the centroid calculated through C2 to C7 atoms [Cg(A)]. The arbitrary labeling scheme of non-hydrogen atoms are shown.

Their molecule in the chosen asymmetric unit were present with C11 stereocenter at *S* in both compounds and with C12 at either *R* in **7** or *S* in **9** (Figure 3.3), even though their enantiomeric counterpart is also found in the unit cell. The *syn* diastereomer of compound **5** crystallized in the non-centrosymmetric monoclinic space group P2₁, with only one enantiomer in the unit cell instead of two as in the case of compounds **3** and **4**. In the case of

compound **5**, and also in compounds **1** and **6**, one dimethylsulfoxide molecule is present in the asymmetric unit (Figure 3.8). The configuration of C11 and C12 carbons was established for compound **5** as being *R* based on the reliable Flack parameter of 0.013(12).
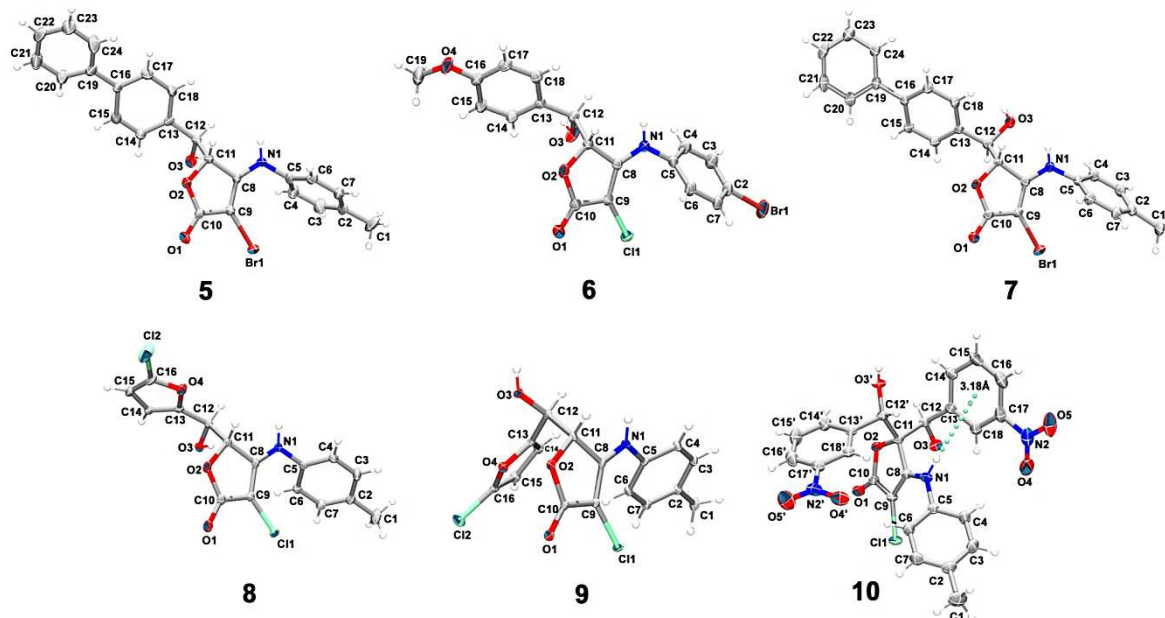
Figure 3.3 50% Ellipsoid plot for the non-hydrogen atoms of the tetronamides **5**-**10** present in their asymmetric units. The dotted green line is the N—H…π interaction and the displayed distance is between H and the centroid calculated through C13 to C18 atoms [Cg(C)]. The arbitrary labeling scheme of non-hydrogen atoms are shown.

However, since the synthetic methodology employed is not enantioselective [12], it was believed that there was chiral resolution upon crystallization and therefore compound **5** is a conglomerate in the form of a mixture of crystals, half of which having only one enantiomer, the other half composed solely by the another one. Although, one crystal of the (*R*)-C11,(*R*)-C12 enantiomer have been selected, but the (*S*)-C11,(*S*)-C12 enantiomer is expected to be found in the crystals collection with the same molecular geometry and crystal packing even though its opposite chirality. Another *syn* diastereomer **8** crystallized in the highest symmetry space group among all tetronamides (orthorhombic *Pccn*), whose C11 and C12 carbons has *S*,*R* configurations and the enantiomer with opposite chirality was also found in the centrosymmetric unit cell.

The molecular backbone of compounds **1**-**4** adopt an U-shape due to the formation of intramolecular contacts involving the C…H moiety or the substituent in the 2-position of ring C (according ring labeling shown in Figure 3.4) and the π-system of ring A. In the known crystal structure of one chiral tetronamide bearing three phenyl rings and one stereocenter,

there was the formation of a line-shaped conformation stabilized through a π…π interaction between two aromatic rings [15]. The intramolecular contacts C18—H18…π (ring A), Br2…π (ring A) and C19—H19b…π (ring A) aid to stabilize the constrained molecular geometry of compounds **1**-**4**, respectively (Figures 3.2 and 3.4).
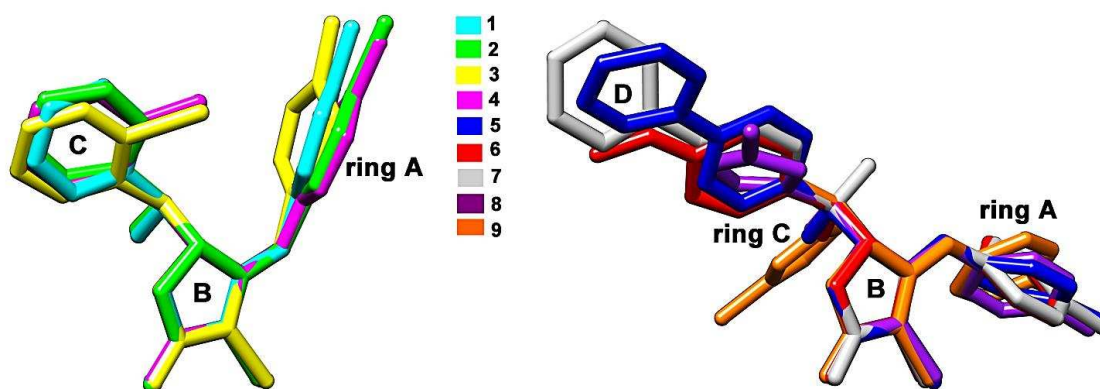
Figure 3.4 Molecular overlay of U-shaped (left) and line-shaped (right) tetronamide aldolates found in their asymmetric units. Only non-hydrogen atoms are shown and the molecules were superimposed through the lactone ring atoms. The labeling scheme for the rings is also shown.

In compounds **1, 2** and **4**, the H18/19b…Cg(A) distance (Table 3.1), where Cg(A) is the centroid calculated through the ring A carbons, is much longer than the shortest corresponding measurements found in literature (around 2.4-2.5 Å) [16-18], but these interactions yet contribute energetically a few to crystal lattice stabilization [19, 20].

In compound **2**, the Br2…Cg(A) distance [3.8480(5) Å] can be also acceptable for occurrence of a halogen…π interaction [21]. This conformational feature is accompanied by similar conformations around the N1—C8 bond axis. In all four compounds, NH hydrogen is on the same side of the halogen bonded lactone ring (Cl in **1** and **2**) or (Br in **3** and **4**), while they are on opposite sides in compounds **5**, **6** and **7** present without such intramolecular contact between rings A and C (Figures 3.3 and 3.4). In fact, these last three compounds are not U-shaped and have a rotation of ca. 180° around the N1—C8 bond axis if compounds **1**-**4** are taken as references. Compared to these last four compounds, the torsions on the N1—C8 bond axis of **5**, **6** and **7** are changed by ca. 180° (Table 3.2).

Table 3.1 Geometric data of the main intramolecular & intermolecular interactions in compounds **1**-**10**

D—H···A[*]	D—H (Å)	H···A (Å)	D···A (Å)	D—H···A (deg)
Compound 1				
N1—H1···O3[i]	0.86	2.48	3.17(4)	138
O3—H3o···O1s[ii]	0.82	1.80	2.59(4)	161
C18—H18···Cg(A)	0.93	3.83	4.6323(30)	146
Compound 2				
N1—H1···O3[iii]	0.86	2.17	3.02(5)	172
O3—H3···O1[iv]	0.82	2.03	2.84(6)	167
C18—H18···Cg(A)	0.93	3.98	4.8137(64)	151
Compound 3				
O3—H3o···O1[v]	0.82	2.05	2.85(4)	166
C1—H1a···N2[iv]	0.96	2.74	3.69(5)	171
N1—H1···Cg(A)[vi]	0.86	3.28	3.8799(32)	129
Compound 4				
O3—H3···O1[v]	0.82	2.05	2.84(1)	161
N1—H1···O3[vii]	0.86	2.14	2.98(2)	166
C19—H19b···Cg(A)	0.96	3.01	3.6201(226)	123
Compound 5				
N1—H1···O1[viii]	0.86	2.13	2.97(6)	168
O3—H3o···O1s[viii]	0.82	1.99	2.75(7)	154
C1s—H1s2···O3	0.96	2.43	3.36(9)	162
C22—H22···O1s[ix]	0.93	2.71	3.44(1)	135
Compound 6				
O3—H3o···O1s[x]	0.82	1.96	2.77(4)	170
N1—H1···O1s[iv]	0.86	2.01	2.86(4)	172
C4—H4···Cg(C)	0.93	2.81	3.6239(37)	147
Compound 7				
N1—H1···O3	0.86	2.17	2.79(3)	129
O3—H3o···O1[xi]	0.82	1.99	2.80(3)	169
Compound 8				
N1—H1···O3[xii]	0.85	2.06	2.82(2)	147
O3—H3o···O1[xii]	0.82	1.86	2.67(1)	176
Compound 9				
N1—H1···O3[xiii]	0.83	2.17	2.95(2)	156
O3—H3o···O1[xii]	0.84	1.91	2.74(1)	170
Compound 10				
N1—H1···Cg(C)	0.86	3.18	3.9398(17)	148
O3—H3o···O1[iv]	0.82	2.09	2.86(3)	156
O3'—H3o'···O1[xiv]	0.82	1.99	2.78(2)	159

[*] In the intermolecular interactions, superscript symmetry operator follows the acceptor atom from a neighboring molecule. Symmetry operators: (i) 1-x, 2-y, 2-z; (ii) x, 1+y, z; (iii) 1-x, -y, 1-z; (iv) 1-x, 1-y, 1-z; (v) 2-x, 2-y, -z; (vi) 1-x, 1-y, -z; (vii) 2-x, 1-y,-z; (viii) x, 1+y, z; (ix) x, 1+y, -1+z; (x) x, y, 1+z; (xi) x, 1/2-y, 1/2+z; (xii) 1.5-x, y, -1/2+z; (xiii) 1.5-x, -1/2+y, 1.5-z; (xiv) -1+x, y, z.

Table 3.2 Selected dihedral angles (^{o}) for compounds **1**-**9** elucidated by single crystal X-ray diffraction

Bond axis	Torsion	1	2	3	4	5[i]	6	7	8	9
C5—N1	C4—C5—N1—C8	44.2(5)	38.6(7)	76.3(5)	45.9(19)	83.4(7)	129.2(4)	134.1(3)	-120.05(15)	-150.92(15)
	C6—C5—N1—C8	-137.5(4)	-142.9(3)	-106.3(4)	-138.3(14)	-99.4(6)	-53.4(5)	-47.0(4)	61.28(19)	33.2(2)
N1—C8	C5—N1—C8—C9	-172.9(3)	-160.1(5)	-176.5(4)	-160.1(14)	-1.2(8)	-4.8(7)	-10.8(5)	5.7(2)	22.5(3)
	C5—N1—C8—C11	10.9(5)	26.0(7)	5.0(5)	26.2(19)	178.2(4)	177.8(3)	168.9(3)	-176.12(12)	-156.16(14)
C11—C12	C8—C11—C12—C13	-174.3(3)	-174.8(4)	174.5(3)	-175.5(11)	-178.6(4)	166.3(3)	171.1(2)	171.43(11)	49.99(16)
	C8—C11—C12—O3	60.4(3)	58.4(5)	47.7(4)	57.9(14)	57.6(5)	43.6(4)	-66.8(3)	53.61(15)	174.02(11)
	O2—C11—C12—C13	69.4(3)	69.9(4)	58.7(3)	68.8(14)	63.0(4)	49.5(4)	54.0(3)	54.21(13)	-66.56(15)
	O2—C11—C12—O3	-55.8(3)	-56.9(4)	-68.1(3)	-57.8(14)	-60.8(4)	-73.2(3)	176.1(2)	-63.61(13)	57.48(14)
C12—C13	C11—C12—C13—C14	-83.8(4)	-106.7(5)	-104.7(3)	-98.3(15)	-94.1(5)	-102.5(4)	-108.0(3)	-131.41(16)	-104.80(19)
	C11—C12—C13—C18[ii]	95.3(4)	74.5(6)	77.6(4)	84.9(15)	81.3(5)	76.1(4)	71.9(4)	45.09(15)	74.85(16)
	O3—C12—C13—C14	37.0(4)	18.9(7)	20.7(4)	26.5(19)	28.3(6)	16.3(5)	135.4(3)	-10.6(2)	133.26(17)
	O3—C12—C13—C18[ii]	-143.9(4)	-159.9(4)	-157.0(3)	-150.3(13)	-156.4(4)	-165.0(3)	-44.6(4)	165.90(11)	-47.10(16)

[i] All torsion signs were inverted to get the same enantiomer of the other tetronamides, it was believed this compound crystallizes as a conglomerate. [ii] In **8** and **9**, the fourth atom is O4 instead of C18.

The two crystal structures of tetronamides with 5-chlorofuran-2-yl moiety have also shown this conformational feature observed in the case of compounds *syn*-**5**, *syn*-**6** and *anti*-**7**. Both isomeric compounds *syn*-**8** and *anti*-**9** were present with NH hydrogen and halogen (chlorine) atom bonded to C9 on opposite sides (Figure 3.3). In these two furan-based crystal structures, no intramolecular contact between ring A π-cloud and the Cl2 chlorine substituent at the furan ring C occurs due to the unfavorable geometry. Similarly, such Cl2 chlorine would be bonded at 3-position of phenyl/pyridine ring in the other tetronamide aldolates reported here. Likewise, in the case of **5**, **6** and **7**, the substituents in the 4-position of ring C are not sterically compatible with the formation of an intramolecular C-H…π interaction as that figured in **1**-**4**. Therefore, tetronamide aldolates should not be substituted at 3- or 4-position of ring C to be U-shaped with NH hydrogen on the same side of lactone oxygens. Such differences in the molecular constraint of tetronamides is only a result from the rotation around the N1—C8 bond axis, as aforementioned, since there is conformational similarity around ring C among U-shaped and line-shaped tetronamides (Figure 3.4). Resembled torsion values on the rotatable C11—C12 and C12—C13 bond axes are found for

compounds **1-7** (Table 3.2; note that torsions of **7** measured through O3, differ from those of **1**-**6** because the C12 opposite stereochemistry).

The conformation of phenyl ring A changes slightly among the tetronamides as a consequence of non-covalent intramolecular (as aforementioned in **1-4**) and intermolecular contacts (see torsion angles around C5—N1). In compound **3**, non-classical hydrogen bonding donation from methyl moiety to pyridyl nitrogen gives rise to one of these intermolecular contacts driving ring A conformation (Figure 3.5).Interestingly, this interaction, together with a Br2…Br2 contact (3.5440(6) Å; normalized contact N_c of 0.96), keeps two centrosymmetry-related molecules in contact, which are further packed into one-dimensional chains through classical hydrogen bonds between hydroxyl and carbonyl groups. Since these molecules interacting via O3—H3o…O1 hydrogen bonds are also related by centrosymmetry, the overall chain is composed by alternate enantiomers of compound **3** in a side-to-side fashion (Figure 3.5). Neighbor chains are tied together to complete the three-dimensional architecture through N1—H1…π (ring A) interactions [16], which are also intermolecular forces dictating the ring A conformation.

α: O3-H3o...O1
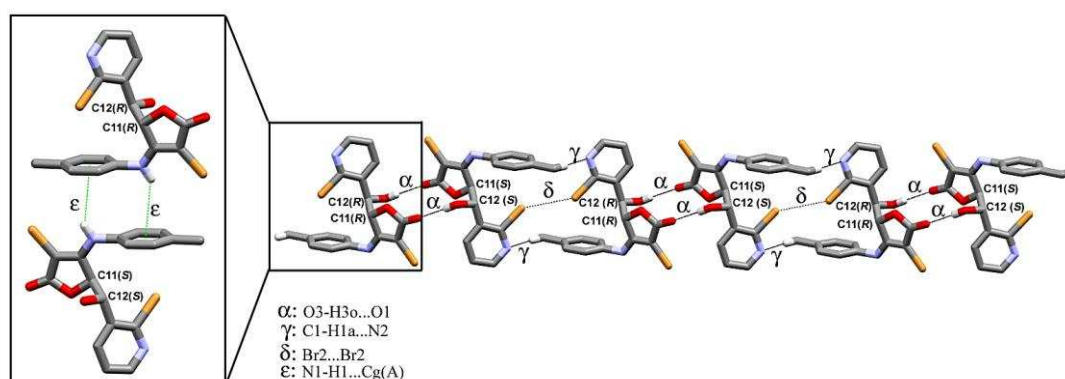γ: C1-H1a...N2
δ: Br2...Br2
ε: N1-H1...Cg(A)

Figure 3.5 The supramolecular chain of compound **3** alternating enantiomers in a side-to-side fashion. Observe the formation of centrosymmetric dimers assembled with two O3-H3o…O1 hydrogen bonds. In the framed box, the N1-H1…Cg(A) (H1…Cg(A) distance is 3.28 Å) interactions are responsible to contact neighboring chains. Cg(A) denotes the centroid calculated through the C2 to C7 atoms.

There are also formation of one-dimensional chains alternating enantiomers in compound **2**, but now in a zigzag fashion (Figure 3.6). Another difference between the chains of compounds **2** and **3** is associated to their hydrogen bonding pattern. While the centrosymmetric dimmer assembled with O3—H3o…O1 hydrogen bonds occurs in both structures, the classical N1—H1…O3 hydrogen bonding is found only in the chains of **2** (Figure 3.6). This same hydrogen bonding pattern assembling the chains of compound **2** is also found in compound **4** (Figure 3.6).
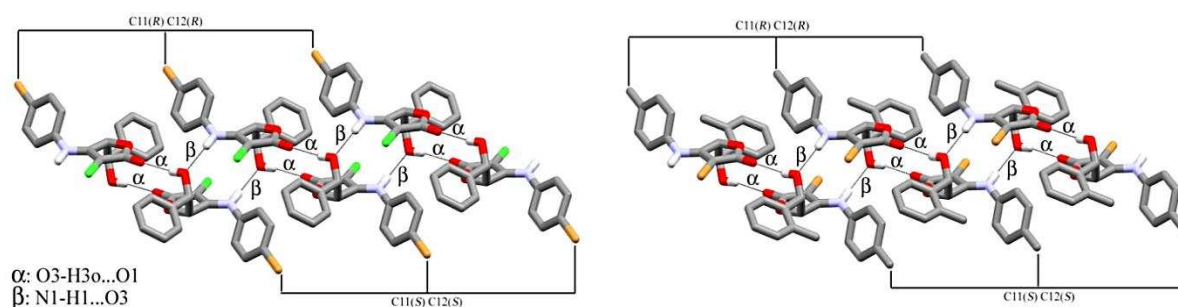
Figure 3.6 Isostructural supramolecular chains in **2** (left) and **4** (right) alternating enantiomers in a zigzag fashion. Observe the formation of centrosymmetric dimers assembled with two O3-H3o…O1 hydrogen bonds.

It is important to note that the formation of such hydrogen-bonded centrosymmetric dimmer is observed only for U-shaped tetronamides. Among these compounds present with constrained molecular backbone, this O3—H3o…O1 dimer is not assembled only in compound **1** due to cocrystallization with DMSO (Figure 3.8). This hydrogen bonding pattern
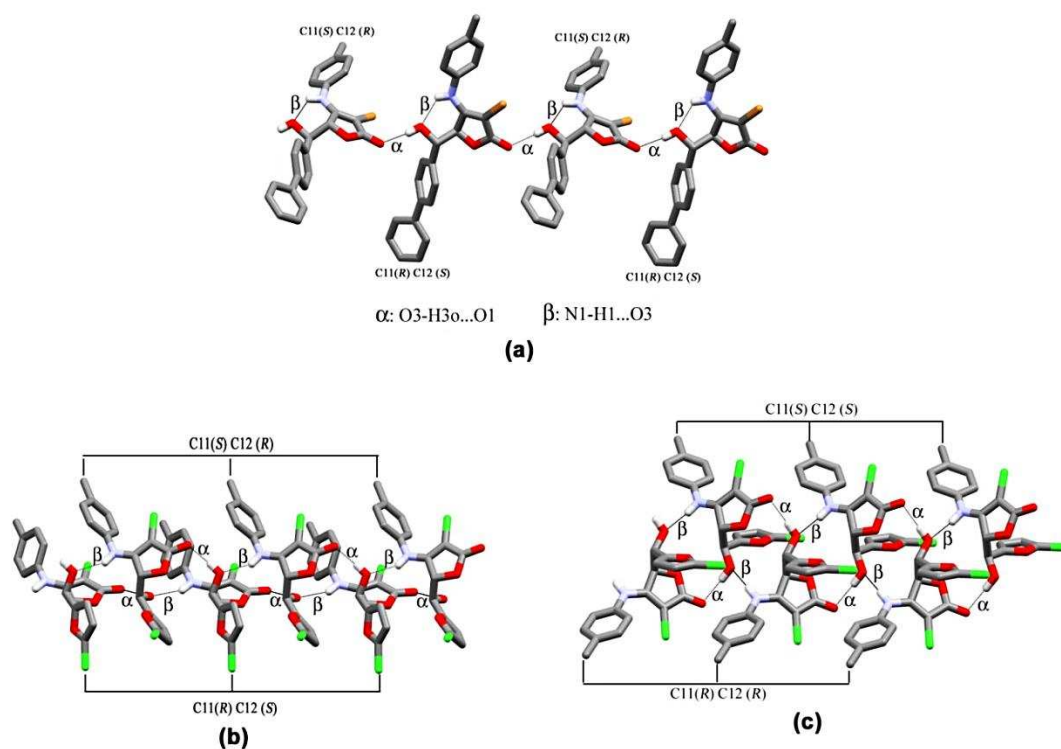

Figure 3.7 The 1D chain alternating enantiomers of compounds **7 (a), 8 (b)** and **9 (c)**

is not observed in the racemic crystal structure of the *anti* diastereomers of compounds **7** and **9** and the *syn* diastereomer of compound **8**. A chain motif made up of O3—H3o…O1 hydrogen bonds occurs there (Figure 3.7). There are also the N1—H1…O3 hydrogen bond

in all three structures. This contact aids the assembly of the chains in compounds **8** and **9**, while it is intramolecular in compound **7** (Figure 3.7).

In compound **5**, enantiopure chains are formed with translation symmetry related molecules through the classical N1—H1…O1 hydrogen bond (Figure 3.8b). The crystallized solvent molecule of DMSO is strongly tied in the crystal structure of compound **5**. It acts as a chain stabilizer through hydrogen bonding acceptor and donor to hydroxyl moiety from neighboring tetronamide molecules into the chain, besides connecting side-to-side neighboring chains through the C22—H22…O1s interaction (Figure 3.8b). The role of DMSO in the crystal packing of compounds **1** and **6** is also evident. It is a hydrogen bonding acceptor from hydroxyl group in both structures (Figure 3.8a and 3.8c). In the last one, it is also an acceptor from NH (Figure 3.8c). The neighboring molecules acting as hydrogen bonding donors to DMSO through their OH and NH moieties are related by centrosymmetry. They are interacting by mean of a C4—H4…π (ring C) contact driving the conformation of these two phenyl rings in **6** (Figure 3.8c). However, in compound **1**, there is occurrence of a centrosymmetric dimer stabilized with the N1-H1…O3 interactions (Figure 3.8a).
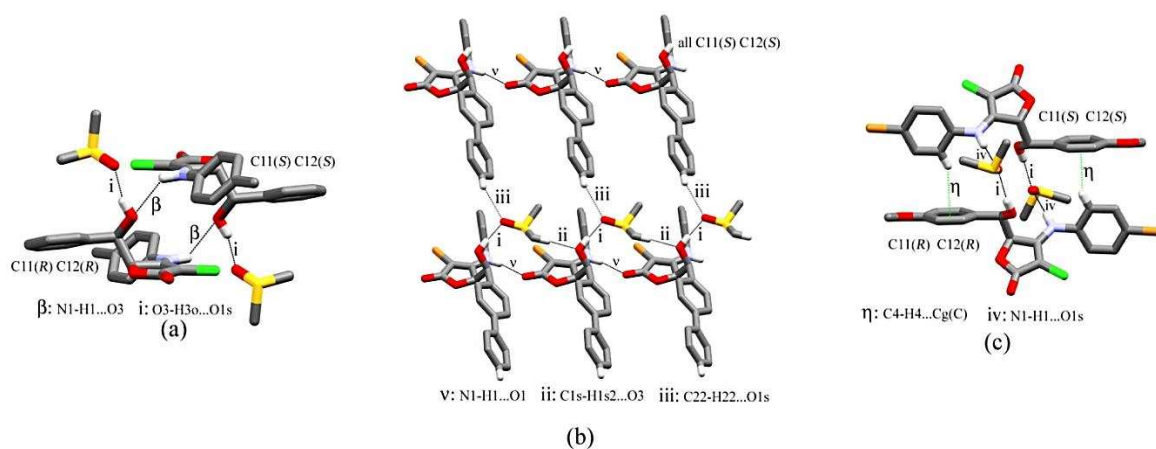
Figure 3.8 Supramolecular architecture of tetronamide aldol products crystallizing together with DMSO. Compounds **1** (a), **5** (b), and **6** (c) [Cg(C) denotes the centroid calculated *via* ring C atoms].

Moreover, compound **10,** a tetronamide bisaldolate (bearing two *m*-nitrophenyl moiety), which reinforced the conclusions drawn from the tetronamide aldolate series (compounds **1**-**9**). As expected from the above findings, the presence of *m*-nitro group in the phenyl ring sterically hinders the formation of the intramolecular contact found in the U-shaped compounds present with either *o*-substituted or non-substituted phenyl/pyridyl ring in the 5-position of the lactone ring. Also in agreement with the absence of a U-shaped conformation, compound **10** is present with the torsions around N1—C8 bond similar to line-

shaped tetronamides with *p*-substitution in this phenyl moiety and those bearing the 5-chlorofuran-2-yl moiety (Table 3.2). Likewise, the NH hydrogen of compound **10** is on the opposite side of the 3-halogen as occurs in compounds **5**-**9** and interacts weakly with π-system of one *m*-nitrophenyl ring through the intramolecular N1—H1…π (ring C) contact [16] (see Figure 3.3 and Table 3.1 for interaction metrics). However, due to the presence of two hydroxy(*m*-nitrophenyl)methyl substituents, its molecular backbone assumes a conformation resembling a scorpion-shape rather than a line-shape, which is compatible with the formation of chains made up of O3—H3o…O1 centrosymmetric dimmers side-to-side cross-linked though O3'—H3o'…O1 hydrogen bonds (Figure 3.9).
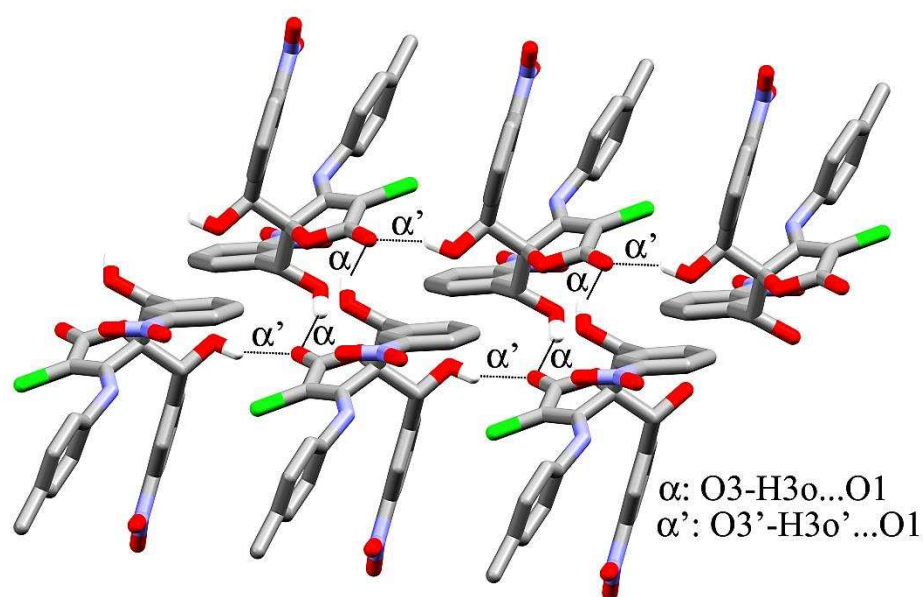

Figure 3.9 Classical hydrogen bonds and weak interactions stabilizing the crystal packing of tetronamide bisaldolate **10**

In summary, tetronamides with the presence of *meta* or *para* substituents in one aromatic ring, regardless of their nature, seems to hinder the U-shaped conformation due to their steric failure to interact with the π-system of the another side ring. According to this point of view, the above studies suggested the role of weak intramolecular contacts in driving tetronamide conformation conditioned to the lack of substituents in *meta* and *para* positions of an either six or five membered peripheral ring.

2.2. Computational Studies (Theoretical Conformations)

In order to get insights into the balance between intra and intermolecular forces driving the U-shaped conformation of tetronamide aldol products, the energy of all significantly populated conformers of the tetronamide aldolates (compounds **1**-**9**) have been calculated at

the B3LYP/6-31G* level of theory. It was found that the energy of each conformer in solution and gas phases have similar values, except for compound **3**, as can be viewed in Table 3.4. All comparisons with crystal conformations made in sequence are relative to solution phase calculations which had even taken into account a chemical environment unable to drive the conformational features found in the solid phase. Table 3.3 shows the relative energies of all significantly populated conformers of compounds **1-9** computed in solution (PCM, solvent=$CHCl_3$), along with the corresponding Boltzmann population (%) computed at room temperature.

Table 3.3 Relative energies (kcal mol^{-1}) of all significantly populated conformers of compounds **1-9** computed at the PCM/B3LYP/6-31G* level (solvent=$CHCl_3$). The Boltzmann population (%) of each conformer is shown in parentheses. The corresponding gas phase energies are given in **Table 3.4**

Conformation	1	2	3	4	5	6	7	8	9
1	0.00 (54)	0.00(64)	0.00 (34)	0.00 (60)	0.00 (34)	0.00 (39)	0.00 (42)	0.00 (37)	0.00 (51)
2	0.48 (24)	0.64 (22)	0.06 (31)	0.62 (21)	0.09 (30)	0.12 (32)	0.06 (38)	0.03 (36)	0.63 (18)
3	1.02 (10)	1.48 (5)	0.24 (23)	1.08 (10)	0.45 (16)	0.66 (13)	1.08 (7)	0.64 (13)	1.01 (10)
4	1.34 (6)	1.78 (3)	0.70 (11)	1.41 (6)	0.60 (13)	0.82 (10)	1.11 (7)	0.75 (11)	1.03 (9)
5		1.82 (3)	1.90 (1)	1.90 (2)	1.37 (4)	1.39 (4)	1.16 (6)	1.45 (3)	1.09 (8)
6		1.92 (3)	2.14 (<1)	2.26 (1)	1.38 (3)	1.93 (2)	2.28 (1)		1.54 (4)
Crystal	conf. 3	conf. 4	conf. 3	conf. 3	3.17 (<1)	4.08 (<1)	conf. 1	4.92 (<1)	5.50 (<1)

Table 3.4 Relative energies and Boltzmann distributions computed in solution (CHCl$_3$) and in gas phase for the tetronamides **1-9** at the B3LYP/6-31G* level of theory. RX inside the parentheses means that conformer has been similar to the corresponding one found in crystal crystal structure.

Compound	Relative Energy (solution)	Contribution (%)	Relative Energy (gas phase)	Contribution (%)
1_c1	0.00	54	0.00	56
1_c2	0.48	24	0.45	26
1_c3 (RX)	1.02	10	1.09	9
1_c4	1.34	6	1.25	7
2_c1	0.00	64	0.00	58
2_c2	0.64	22	0.55	23
2_c3	1.48	5	0.90	13
2_c4 (RX)	1.78	3	1.96	2
2_c5	1.82	3	2.43	1
2_c6	1.92	3	1.88	3
3_c1	0.00	34	0.00	63
3_c2	0.06	31	1.40	6
3_c3 (RX)	0.24	23	0.65	21
3_c4	0.70	11	1.47	5
3_c5	1.90	1	1.71	4
3_c6	2.14	1	2.75	1
4_c1	0.00	60	0.00	56
4_c2	0.62	21	0.61	20
4_c3 (RX)	1.08	10	1.03	10
4_c4	1.41	6	1.06	9
4_c5	1.90	2	1.86	2
4_c6	2.26	1	1.79	3
5_c1	0.00	34	0.00	31
5_c2	0.09	30	0.11	26
5_c3	0.45	16	0.42	15
5_c4	0.60	13	0.63	11
5_c5	1.37	4	0.77	8
5_c6	1.38	3	0.76	9
5_RX	3.17	<1	4.56	<1
6_c1	0.00	39	0.00	39
6_c2	0.12	32	0.21	27
6_c3	0.66	13	0.59	14
6_c4	0.82	10	0.86	9
6_c5	1.39	4	0.90	9
6_c6	1.93	2	1.81	2
6_RX	4.08	<1	5.24	0
7_c1 (RX)	0.00	42	0.00	45
7_c2	0.06	38	0.10	38
7_c3	1.08	7	1.28	5
7_c4	1.11	7	1.31	5
7_c5	1.16	6	1.39	4
7_c6	2.28	1	1.99	2
8_c1	0.00	37	0.41	29
8_c2	0.03	36	0.00	56
8_c3	0.64	13	1.23	7
8_c4	0.75	11	1.34	6
8_c5	1.45	3	2.01	2
8_RX	4.92	<1	6.19	<1
9_c1	0.00	51	0.00	41
9_c2	0.63	18	0.75	12
9_c3	1.01	10	0.83	10
9_c4	1.03	9	1.25	5
9_c5	1.09	8	0.19	30
9_c6	1.54	4	1.80	2
9_RX	5.50	<1	7.26	<1

Both gas phase energies and geometries for all conformations indicated in Table 3.3 are given in the Figures 3.10 to 3.18. In Figures 3.10-3.18, RX inside the parentheses means that conformer has been similar to the corresponding one found in crystal structure.
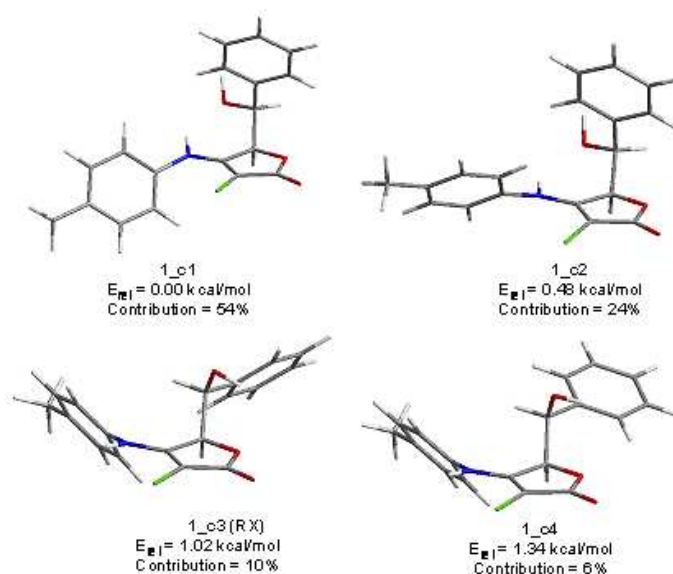

Figure 3.10 B3LYP/6-31G* optimized geometries of all significantly populated conformers of compound **1**, with relative energies computed at the PCM/B3LYP/6-31G* level (solvent=chloroform)
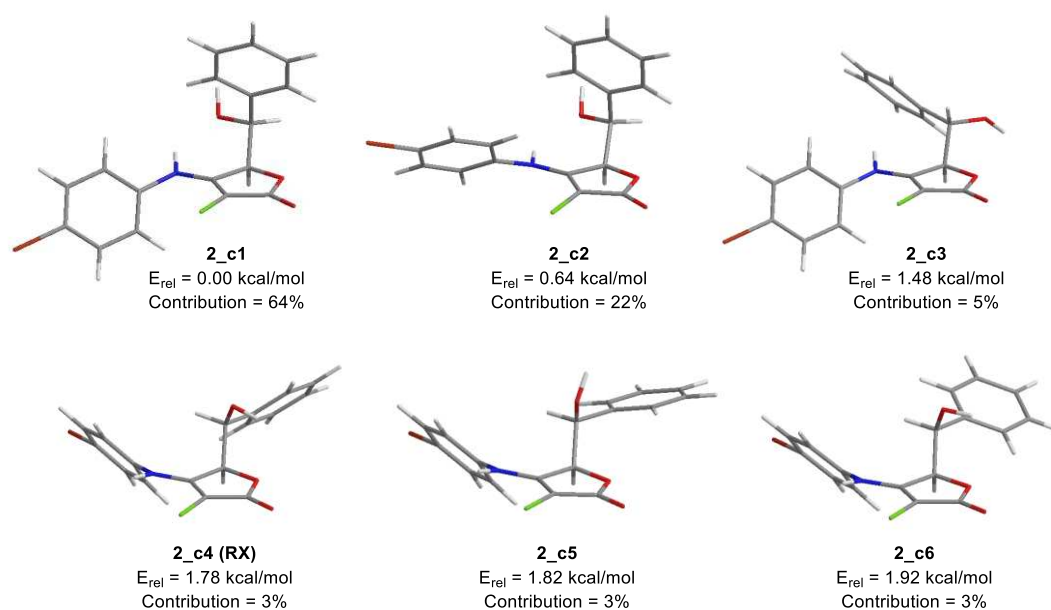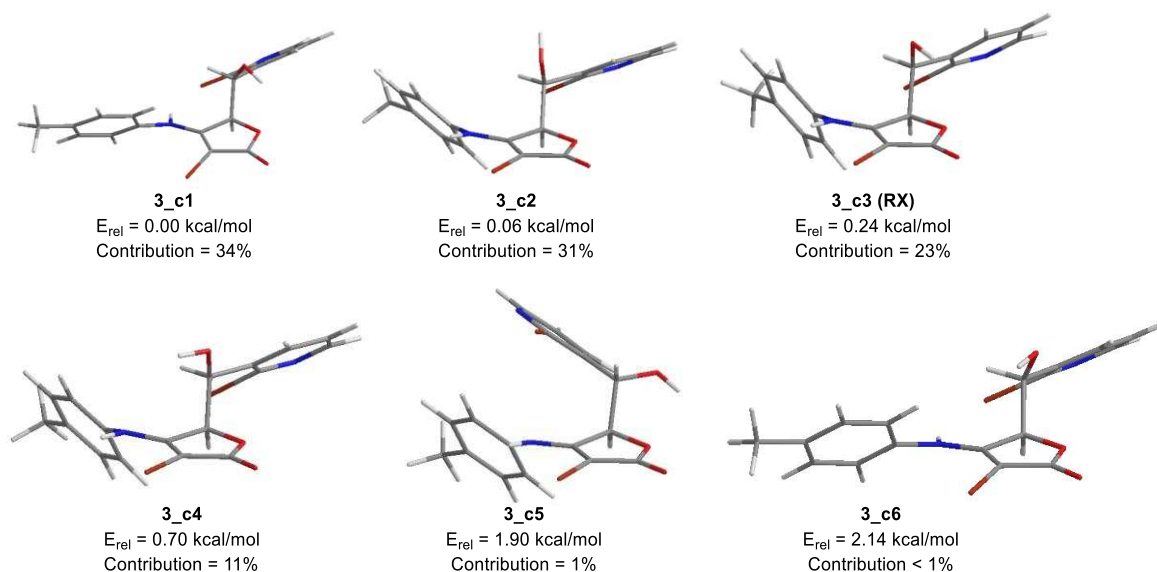

Figure 3.11 B3LYP/6-31G* optimized geometries of all significantly populated conformers of compound **2**, with relative energies computed at the PCM/B3LYP/6-31G* level (solvent=chloroform)
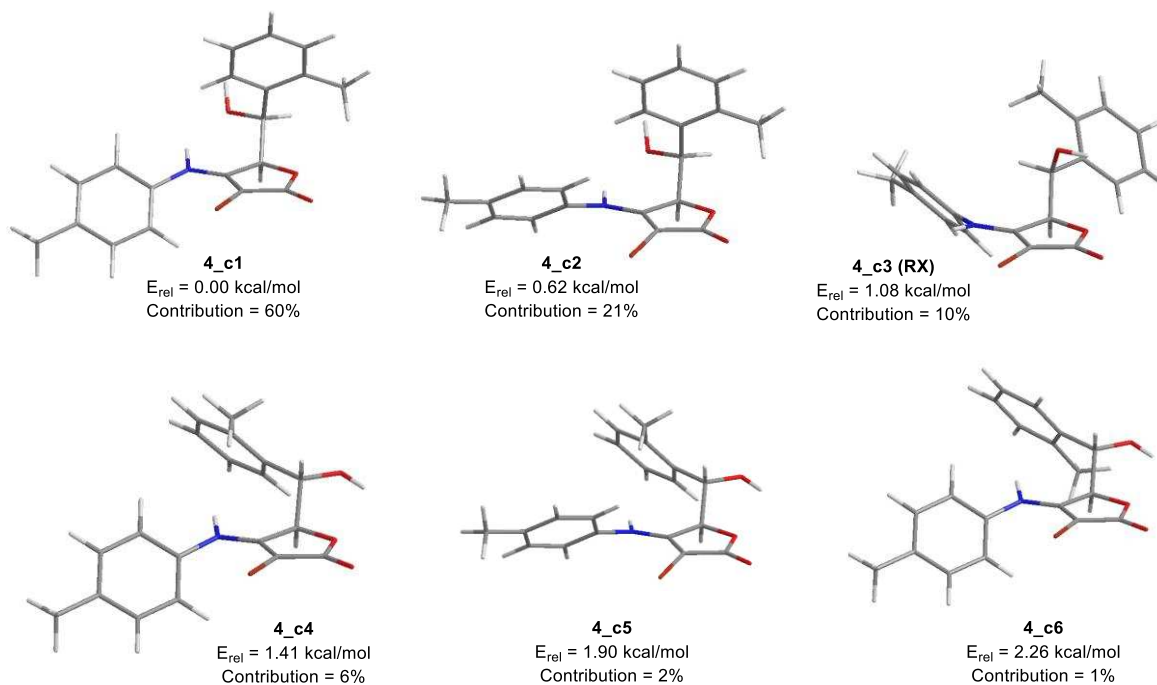
3_c1
E_{rel} = 0.00 kcal/mol
Contribution = 34%

3_c2
E_{rel} = 0.06 kcal/mol
Contribution = 31%

3_c3 (RX)
E_{rel} = 0.24 kcal/mol
Contribution = 23%

3_c4
E_{rel} = 0.70 kcal/mol
Contribution = 11%

3_c5
E_{rel} = 1.90 kcal/mol
Contribution = 1%

3_c6
E_{rel} = 2.14 kcal/mol
Contribution < 1%

Figure 3.12 B3LYP/6-31G* optimized geometries of all significantly populated conformers of compound **3**, with relative energies computed at the PCM/B3LYP/6-31G* level (solvent=chloroform)
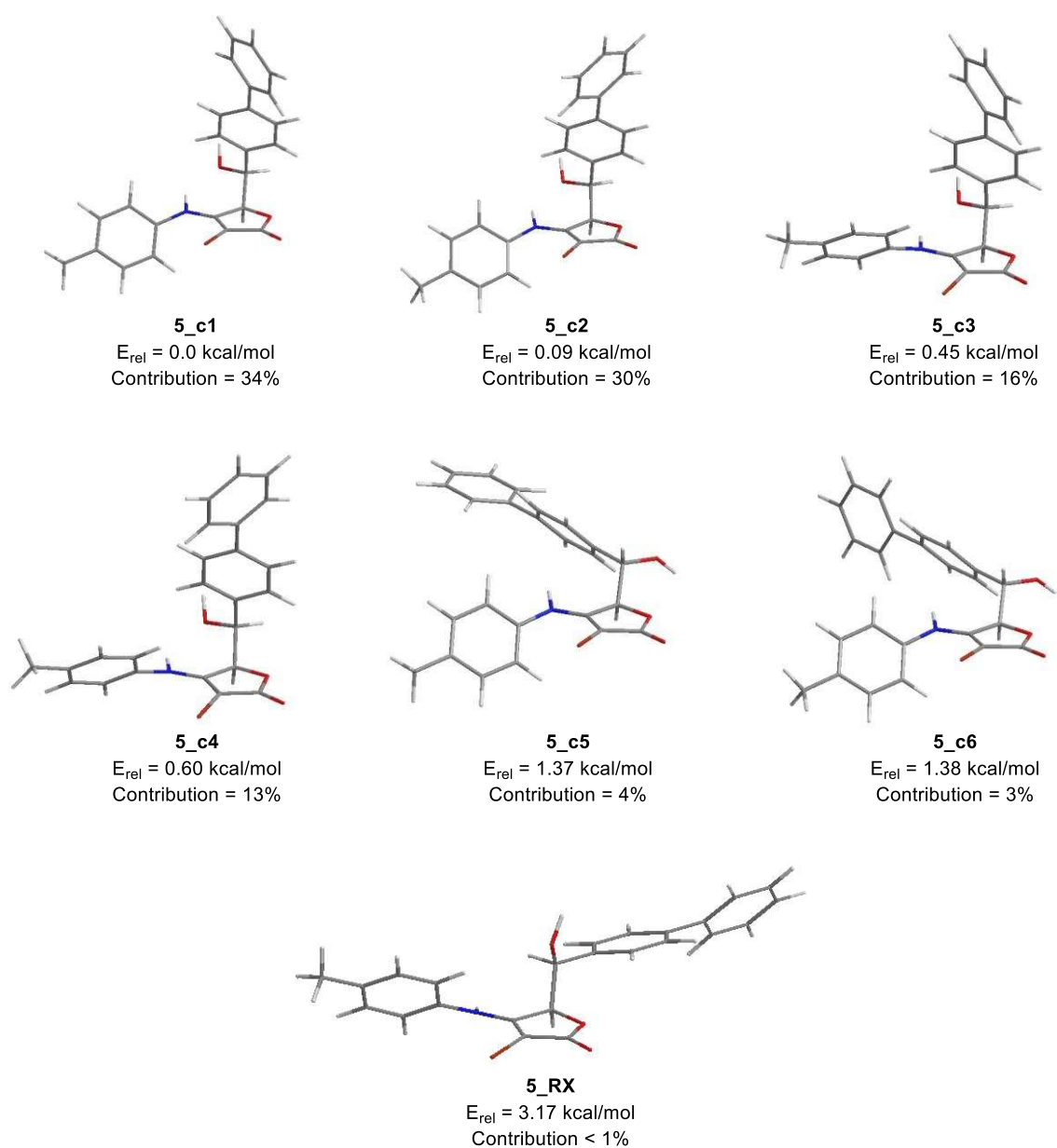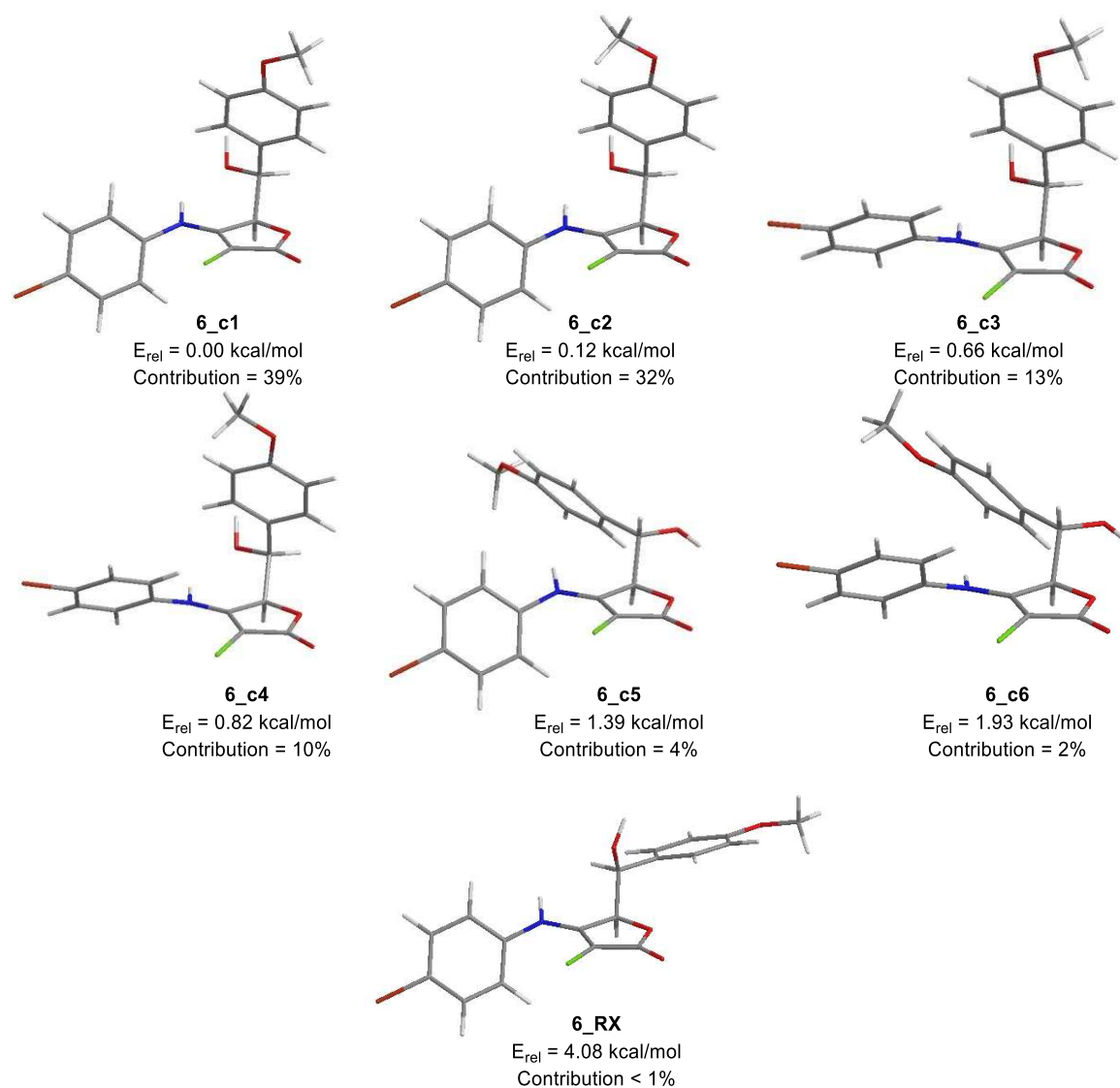

4_c1
E_{rel} = 0.00 kcal/mol
Contribution = 60%

4_c2
E_{rel} = 0.62 kcal/mol
Contribution = 21%

4_c3 (RX)
E_{rel} = 1.08 kcal/mol
Contribution = 10%

4_c4
E_{rel} = 1.41 kcal/mol
Contribution = 6%

4_c5
E_{rel} = 1.90 kcal/mol
Contribution = 2%

4_c6
E_{rel} = 2.26 kcal/mol
Contribution = 1%

Figure 3.13 B3LYP/6-31G* optimized geometries of all significantly populated conformers of compound **4**, with relative energies computed at the PCM/B3LYP/6-31G* level (solvent=chloroform)
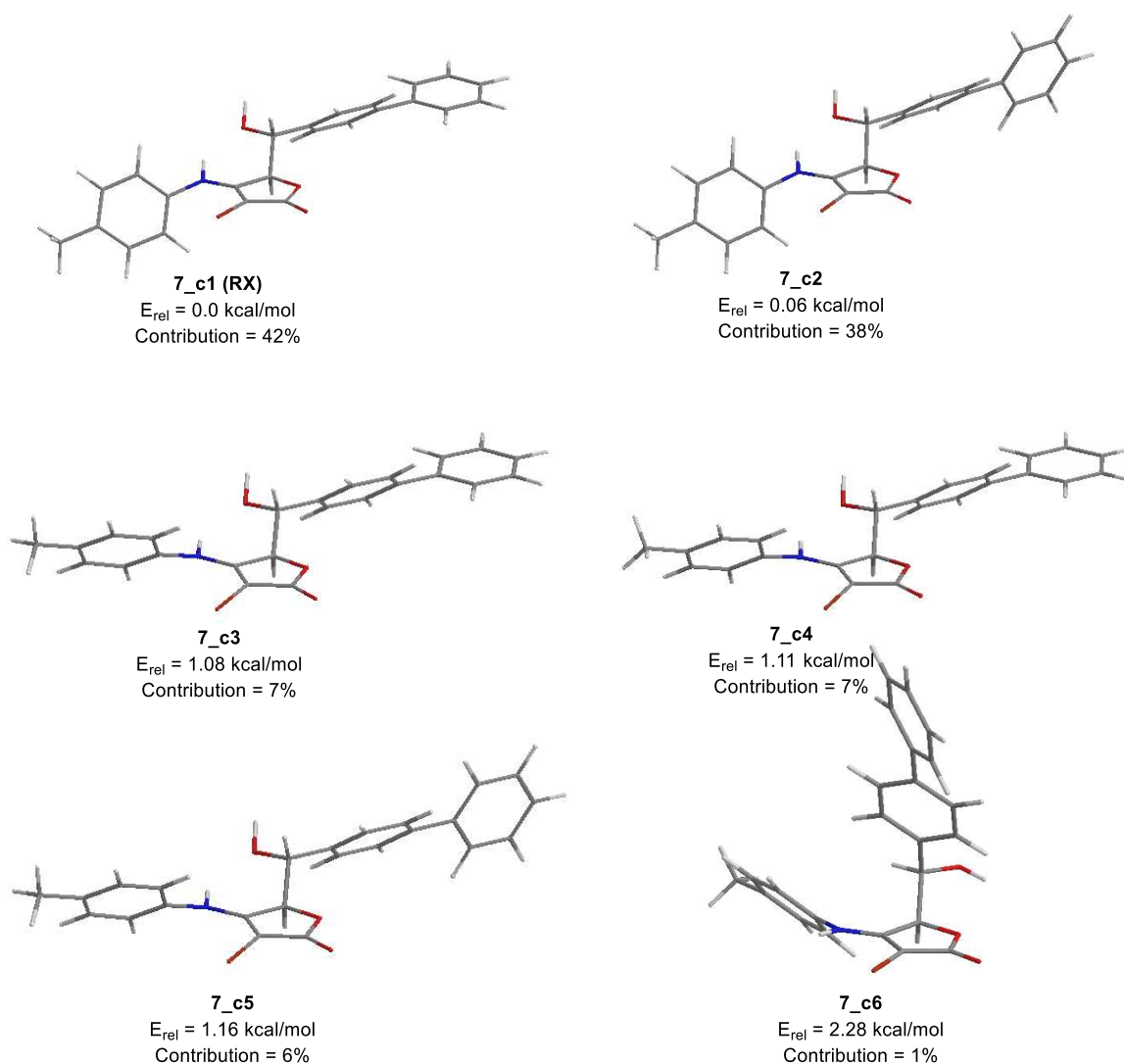
5_c1
E_{rel} = 0.0 kcal/mol
Contribution = 34%

5_c2
E_{rel} = 0.09 kcal/mol
Contribution = 30%

5_c3
E_{rel} = 0.45 kcal/mol
Contribution = 16%

5_c4
E_{rel} = 0.60 kcal/mol
Contribution = 13%

5_c5
E_{rel} = 1.37 kcal/mol
Contribution = 4%

5_c6
E_{rel} = 1.38 kcal/mol
Contribution = 3%

5_RX
E_{rel} = 3.17 kcal/mol
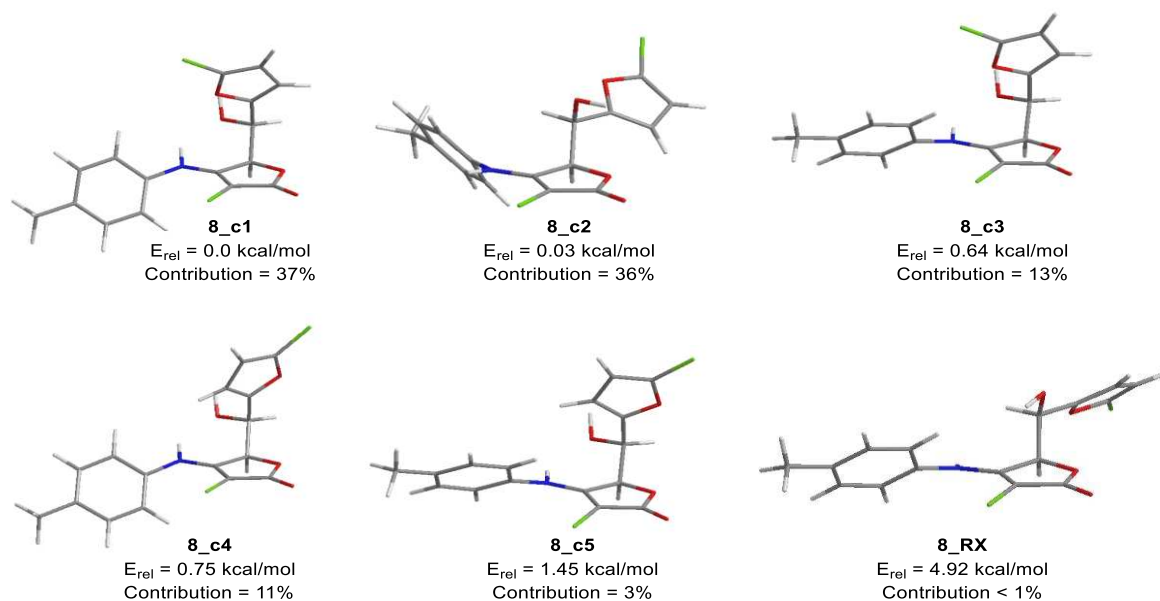Contribution < 1%

Figure 3.14 B3LYP/6-31G* optimized geometries of all significantly populated conformers of compound **5**, with relative energies computed at the PCM/B3LYP/6-31G* level (solvent=chloroform)

6_c1
E_{rel} = 0.00 kcal/mol
Contribution = 39%

6_c2
E_{rel} = 0.12 kcal/mol
Contribution = 32%

6_c3
E_{rel} = 0.66 kcal/mol
Contribution = 13%

6_c4
E_{rel} = 0.82 kcal/mol
Contribution = 10%

6_c5
E_{rel} = 1.39 kcal/mol
Contribution = 4%

6_c6
E_{rel} = 1.93 kcal/mol
Contribution = 2%

6_RX
E_{rel} = 4.08 kcal/mol
Contribution < 1%

Figure 3.15 B3LYP/6-31G* optimized geometries of all significantly populated conformers of compound **6**, with relative energies computed at the PCM/B3LYP/6-31G* level (solvent=chloroform)

7_c1 (RX)
E_{rel} = 0.0 kcal/mol
Contribution = 42%

7_c2
E_{rel} = 0.06 kcal/mol
Contribution = 38%

7_c3
E_{rel} = 1.08 kcal/mol
Contribution = 7%

7_c4
E_{rel} = 1.11 kcal/mol
Contribution = 7%

7_c5
E_{rel} = 1.16 kcal/mol
Contribution = 6%

7_c6
E_{rel} = 2.28 kcal/mol
Contribution = 1%

Figure 3.16 B3LYP/6-31G* optimized geometries of all significantly populated conformers of compound **7**, with relative energies computed at the PCM/B3LYP/6-31G* level (solvent=chloroform)

Figure 3.17 B3LYP/6-31G* optimized geometries of all significantly populated conformers of compound **8**, with relative energies computed at the PCM/B3LYP/6-31G* level (solvent=chloroform)
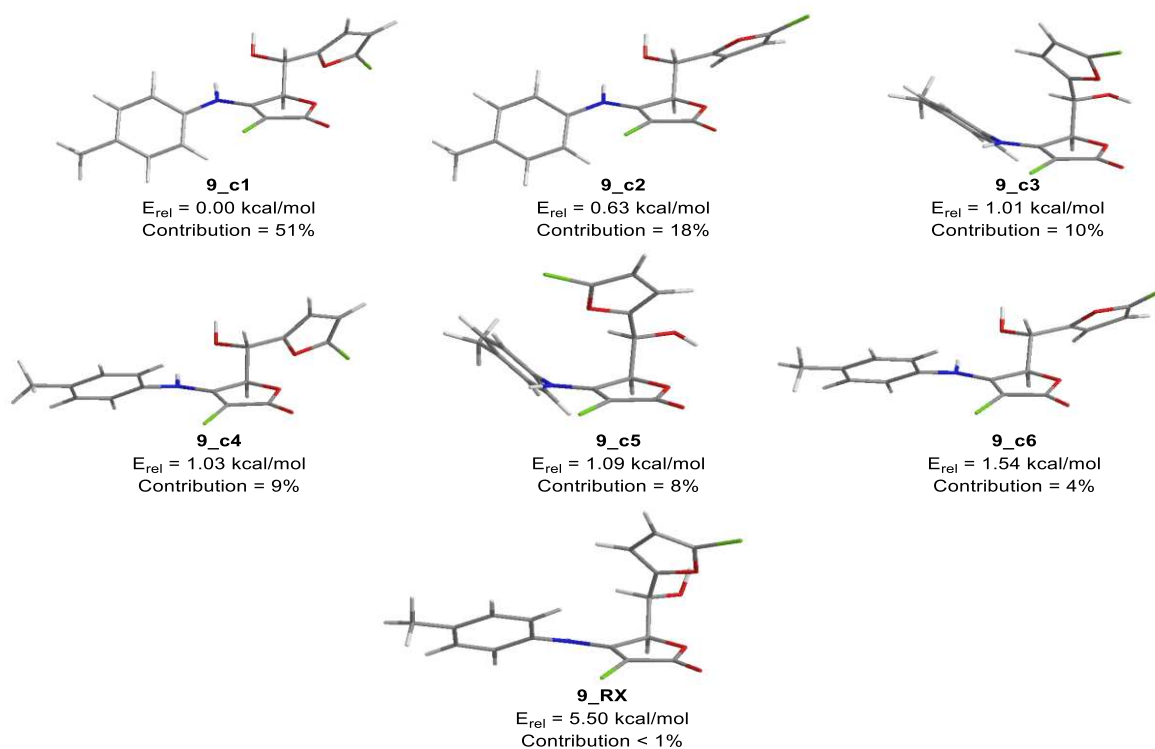
Figure 3.18 B3LYP/6-31G* optimized geometries of all significantly populated conformers of compound **9**, with relative energies computed at the PCM/B3LYP/6-31G* level (solvent=chloroform)

For all tetronamides, the lowest energy conformers were present with the NH hydrogen pointing towards the opposite side of the carbonyl oxygen, as occurs in the crystal

structures of line-shaped tetronamides **5** to **9**. Crystal and theoretical data of **8** and **9** have been briefly presented in the Chapter 2. Except for compound **3**, these theoretical molecular geometries were featured by the intramolecular N1—H1…O3 hydrogen bond found experimentally only in **7**. Indeed, **3** is the only one that have the same lowest energy conformation for gas and crystal structure. A RMSD of 0.3675 Å has been found for the theoretical and experimental coordinates of its non-hydrogen equivalent atoms (Figure 3.19).
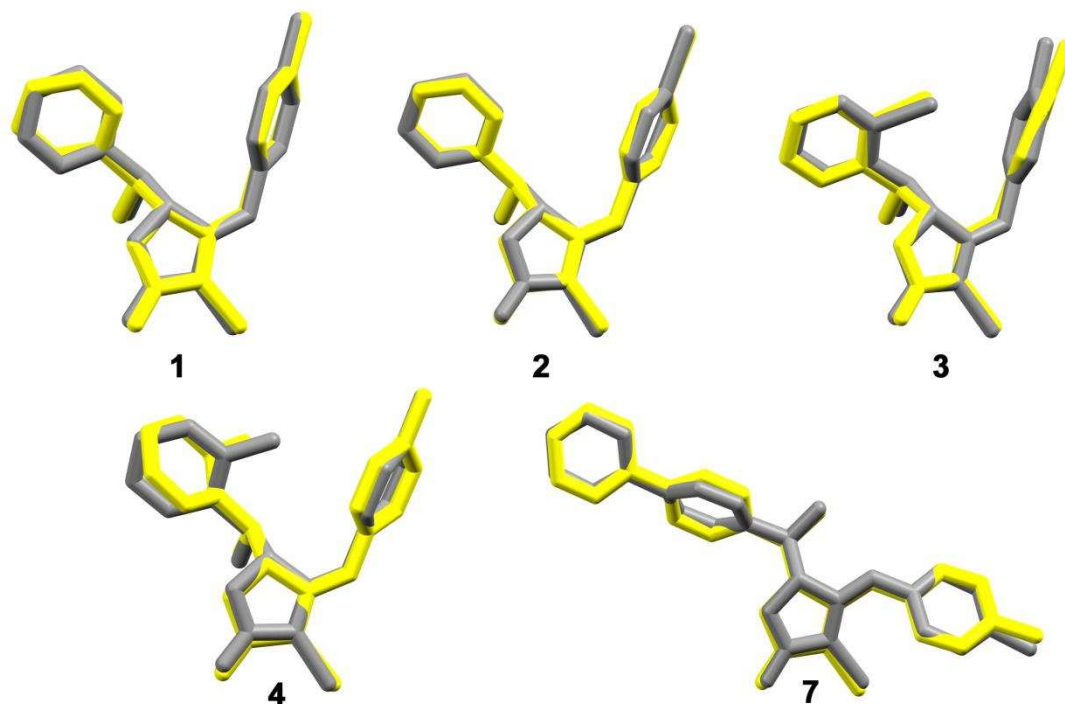
Figure 3.19 Molecular overlay of better-superimposed (RMSD lower than 1 Å) calculated (yellow) and crystal (gray) conformations of the tetronamide aldol products. Calculated conformation (in CHCl$_3$) of compounds **1**, **3** and **4** were ranked third energetically, while that of **2** was ranked fourth (see Table 3.3). Calculated geometry of **7** was that of lowest energy among all its conformers. Only non-hydrogen atoms are shown and the molecules were superimposed through all non-hydrogen atoms.

Herein after, all RMSD values presented refer to the coordinates of equivalent non-hydrogen atoms. In compound **3**, the lowest energy geometry has two intramolecular hydrogen bonds rather than only one in all other analogs. Analogously to N1—H1…O3 contact present in the lowest energy conformers of **1**, **2**, **4** to **9**, there is a classical N1—H1…Br2 hydrogen bonding in **3** meanwhile its hydroxyl group is a donor to lactone endocyclic oxygen in the O3-H3o…O2 interaction. In compounds **1**-**4**, crystal conformation is in good agreement with that of the third (or fourth in case of compound **2**) energetically ranked stable conformer (Table 3.4). The RMSD for these theoretical and crystal geometries is 0.2515 Å, 0.1808 Å, 0.3284 Å and 0.7951 Å, respectively. Their population in gas phase

ranges from 3% (compound **2**) to 23% (compound **3**). Even considering the few populated fourth ranked conformation of compound **2**, its energy is higher only 1.78 kcal mol^{-1} than that of its lowest energy conformer. In compound **3**, the energy difference between the third and first ranked geometries is negligible (0.24 kcal mol^{-1}). Therefore, from a small energetic spent, the lowest energy conformation of **1**-**4** can be promptly converted into a U-shaped one of slightly higher energy. In turn, classical intermolecular hydrogen bonds can be assembled to form a centrosymmetric O3—H3o…O1 dimer (except in compound **1** because of the DMSO co-crystallization), allowing for an intermolecular adjustment even with net energetic gain from this balance between intra and intermolecular driving forces.

Even though the similarity between the third ranked theoretical geometry of **4** and its crystal conformation, there is an noteworthy metric difference between them for the C19—H19b…π (ring A) contact. While the single-crystal X-ray diffraction structure determination supports the occurrence of this contact in the solid state [H19b…Cg(A) distance is 3.01 Å], contributing to stabilize the constrained molecular geometry there, it does not occur in the gas phase [H19b…Cg(A) separation is 4.04 Å, a distance longer than that for any CH…π interaction]. Such finding reinforces the role of contacts of this kind in the crystal structure maintenance. Interestingly, in the case of compounds **5**, **6**, **8** and **9,** the conformations found in the crystal structure were not among the most stable conformers. In fact, the optimized crystal geometries had energy higher than that of the corresponding lowest energy minimum ranging from 3.17 kcal mol^{-1} (compound **5**) to 5.50 kcal mol^{-1} (compound **9**), with negligible gas phase populations lower than 1% in all these cases. For these compounds and also for **7**, U-shaped conformation was not also among the significantly populated ones.

Based on these correlated theoretical and experimental analyses, it can be concluded that the substitution pattern found in **1**-**4** allow for accessible secondary minimum energy conformations which are easily adopted in the crystal structure due to its compatibility with the robust supramolecular synthon observed there (the centrosymmetric OH…O dimer). Such conformational change involves even the loss of the intramolecular N1—H1…O3 hydrogen bonding, which one could say firmly its occurrence in the solid state based simply on a molecular inspection. Therefore, tetronamide aldolates are good examples of how intermolecular motifs can severely deviate a conformation from that of lowest energy through small energetic spent resulted from the substituent pattern of a side aromatic moiety. When the substitution pattern hinders the U-shaped conformation of slightly higher energy, tetronamide aldolates can adopt either the lowest energy geometry or another conformation of higher energy without assembling the centrosymmetric OH…O dimer in both cases.

In order to evaluate the effect of the tetronamide aldolates conformation, the energy for the most stable conformers of related tetronamide aldol products, whose crystal structures are actually unavailable (Figure A3.1; p. 189 and Table A3.1; p. 190) has been computed, at the same theory level used for compounds **1**-**9**. Analogs to the compound **3** substituted either with F (**3F**) or Cl (**3Cl**) in lieu of Br at *o*-position of pyridyl are among those calculated (Figures A3.2 and A3.3; p. 191). From the energetic point of view, the three firstly ranked conformers of **3F** and **3Cl** are U-shaped as its parent tetronamide **3**. Their population sums 96% and 85%, respectively. As in compound **3**, halogen…π interaction stabilizes their conformation, but in F/Cl compounds the contact is localized on C3 and C4 rather than delocalized over the phenyl ring π-cloud as occurs in compound **3**. The analog **6o**, which can be understood as compound **6** with methoxy group in *o*-position instead of *p*-position, was also calculated and its third and fifth energetically ranked conformers, totalizing a population of 26%, are U-shaped with O…π and C-H…π interactions stabilizing this conformation (Figure A3.6; p. 193). This reinforces the role of the substituent position in the side phenyl ring C in modulating the tetronamides conformation, which was further proved in the analog **6m** with methoxy group in *m*-position (Figure A3.7; p. 194). In the former, all most stable conformers are line-shaped without any interaction involving a ring C moiety and the π-system of ring A. Similarly, the C18—H18…π (ring A) interaction is also lost upon changing the methyl moiety in ring C of compound **4** from *o*-position to either *meta* (**4m**) or *para*-position (**4p**). In these compounds (Figures A3.4 and A3.5; p. 192), as well as in the lowest energy conformer of **6o** and **6p**, the most stable molecular geometry is featured by the intramolecular N1—H1…O3 hydrogen bonding. Interestingly, the same intramolecular N1—H1…π (ring C) contact found in the *m*-nitro derivative **10** occurs in the third ranked energetically conformer of **4p**, in the fifth & sixth ones of **4m**, all of them being not U-shaped.

3. Conclusion

The crystal structure of nine related tetronamide aldolates have been reported following conformational and supramolecular trends as substitution pattern of a side aromatic/heteroaromatic ring. Such trend based on the energetic profiles of their main conformers have been rationalized. Even though U-shaped conformations are not the most stable, low energy increases are need to adopt them in compounds **1**-**4** while they do not figure among minimum energy points for compounds **5**-**9**. In this way, substitution pattern of tetronamides plays a decisive role in accessing U-shaped conformations of slightly higher energies which can be assumed upon supramolecular need to assemble the centrosymmetric OH…O dimers. The main contribution of this study concerns therefore in the control of molecular conformation of tetronamides bearing several rotatable bonds and then high conformational freedom through the substitution pattern of a single ring. This control can still be extended to the crystal architecture.

4. Materials and Methods

4.1. Sample Preparation

Crystals of compounds **1**–**2** and **4** were grown from a mixture of $CDCl_3$ and DMSO-d_6 (3:2, v/v) through slow evaporation. Similarly, compounds **3**, **5**–**7** and **10** were grown from a mixture of acetone-d_6 and DMSO-d_6, (9:1, v/v) whereas compounds **8** and **9** were grown from acetone-d_6 as a sole solvent *via* similar procedure. It is noteworthy to mention that, all crystals were grown on clear glass sample vials *via* slow evaporation of solvents.

4.2. Crystallography & Diffraction Techniques

Well-shaped single crystals of tetronamide derivatives were chosen and mounted on a κ-goniostat and exposed to X-ray beam (Mo Kα, λ = 0.71073 Å) using a Bruker-AXS Kappa Duo diffractometer with an APEX II CCD detector. Data collection strategy was calculated by setting φ scans and ω scans with κ offsets using the software APEX2 [22]. Other softwares were used as follows: SAINT [22] (indexing, integration and scaling of raw data), SHELXL-97 [23, 24] (structure solving), SHELXL-97 [23, 24] (structure refinement) and MERCURY [25] (structure analysis and graphical representations). Multi-scan absorption correction was applied to the raw datasets (Table 3.5). Direct methods of phase retrieval were used to solve the crystal structures. All non-hydrogen atoms of asymmetric unit were promptly located from the electronic density Fourier map. The early solved model was refined by full-matrix least squares method based on F^2, adopting isotropic atomic displacement parameters only for hydrogen atoms [U_{iso}(H) = $1.2U_{eq}$ of N and C, except methyl (U_{iso}(H) = $1.5U_{eq}$ of C_{methyl} and O)], which followed a riding model for their coordinates. In compound **1**, the dimethylsulfoxide (DMSO) molecule was disordered over two sets of occupancy sites of 60% and 40%. Its methyl carbon atoms and its oxygen, however, have occupied just one 100% occupancy site, common to both positions. In addition, the X-ray data of compound **4** have outputted not very good statistical parameters from refinement. This was caused by the extremely thin plate shape of the crystals that randomly twinned. In Table 3.5, the main crystal data and information about refinements are shown.

Table 3.5 Summary of crystal data and refinement statistics for compounds **1-10** elucidated in this study using MoKα radiation at 296 K (except compound **8** [CuKα]; compounds **8** and **9** were measured at 100 K and 150 K)

	1	2	3	4	5	6	7	8	9	10
Structural Formula	(C$_{18}$H$_{16}$Cl NO$_3$) (C$_2$H$_6$OS)	C$_{17}$H$_{13}$BrC lNO$_3$	C$_{17}$H$_{14}$Br$_2$ N$_2$O$_3$	C$_{19}$H$_{18}$Br NO$_3$	(C$_{24}$H$_{20}$Br NO$_3$) (C$_2$H$_6$OS)	(C$_{18}$H$_{15}$Br ClNO$_4$) (C$_2$H$_6$OS)	C$_{24}$H$_{20}$Br NO$_3$	C$_{16}$H$_{13}$Cl$_2$ NO$_4$	C$_{16}$H$_{13}$Cl$_2$ NO$_4$	C$_{25}$H$_{20}$Cl N$_3$O$_8$
space group	P-1	P-1	P-1	P-1	P2$_1$	P-1	P2$_1$/c	Pccn	C2/c	P-1
a (Å)	9.9983(3)	6.878(2)	8.0735(3)	6.881(15)	13.468(3)	9.429(2)	7.7938(19)	12.8328(2)	14.7051(13)	7.8058(13)
b (Å)	10.6062(5)	8.991(2)	9.2186(3)	8.912(14)	6.8174(10)	9.491(2)	15.889(4)	26.5383(4)	7.9191(7)	11.603(2)
c (Å)	11.0378(4)	14.710(3)	12.1155(4)	14.71(2)	14.345(2)	12.358(3)	15.984(4)	9.25770(10)	26.746(2)	13.948(3)
α (°)	64.707(2)	105.60(4)	74.499(2)	74.04(5)	90	94.433(8)	90	90	90	76.965(9)
β (°)	84.075(2)	90.17(3)	84.407(2)	85.52(5)	110.150(9)	95.822(8)	96.883(16)	90	93.6625(13)	84.070(8)
γ (°)	74.273(2)	98.71(3)	70.304(2)	80.81(7)	90	91.051(8)	90	90	90	75.174(8)
goodness-of-fit on F^2	1.043	0.996	1.028	1.107	1.040	1.040	1.021	1.067	1.050	1.043
final R1 factor for I >2σ(I)	0.0569	0.0578	0.0346	0.1086	0.0446	0.0447	0.0401	0.0307	0.0334	0.0437
wR2 factor for all data	0.1545	0.1961	0.0967	0.3788	0.1310	0.1281	0.0995	0.0806	0.0816	0.1151
largest $\Delta\rho$ peaks (e/Å^3)	0.333/- 0.271	0.824/- 0.745	0.515/- 0.714	0.893 /- 0.714	1.273/- 0.635	0.773/- 0.589	1.025 /- 0.613	0.411 /- 0.381	0.315 /- 0.359	0.235 /- 0.228

4.3. Computational Methods

All molecular mechanics calculations were performed using Hyperchem with the MM+ force field [26], and the quantum mechanical calculations were performed using Gaussian 09 [27]. Conformational searches were run to locate the minimum energy conformers of all the structures. Initially, the conformational search was done in the gas phase using the MM+ force field, with the number of steps large enough to find all low-energy conformers at least 10 times. All conformers within 5 kcal/mol of the lowest energy conformer were subjected to further optimization at the HF/3-21G level of theory. The most stable conformers (up to 5 kcal/mol of the lowest energy conformer) were then further optimized at the B3LYP/6-31G* level of theory [28-31]. Frequency calculations were used to confirm the nature of the stationary points and to evaluate the thermochemical properties, calculated at 1 atm and 298.15 K. Energies in solution were computed on the structures optimized in the gas phase at the B3LYP/6-31G* level of theory with the Polarizable Continuum Model (PCM) as implemented in Gaussian 09 using chloroform as the solvent [32-34].

5. References and Notes

[1] DE LA FUENTE REVENGA, M.; BALLE, T.; JENSEN, A. A.; FRØLUND, B. Conformationally restrained carbamoylcholine homologues. Synthesis, pharmacology at neuronal nicotinic acetylcholine receptors and biostructural considerations. Eur. J. Med. Chem., v. 102, p. 352-362, **2015**.

[2] CHEN, F.; TIAN, T.; BAI, B.; WANG, J.; WANG, H.; LI, M. Crystal structures, intermolecular interactions and fluorescence properties of a series of symmetrical bi-1,3,4-oxadiazole derivatives. J. Mater. Chem. C, v. 4, p. 4451-4458, **2016**.

[3] SAEED, A.; FLÖRKE, U.; ERBEN, M. F. The role of substituents in the molecular and crystal structure of 1-(adamantane-1-carbonyl)-3-(mono)- and 3,3-(di) substituted thioureas. J. Mol. Struct., v. 1065-1066, p. 150-159, **2014**.

[4] VARUGHESE, S.; DRAPER, S. M. Solid State Conformational Preferences of a Flexible Molecular Backbone Derived from Acetone: Dependence on Electron Donating/Withdrawing Ability of Substitutions. Cryst. Growth Des., v. 10, p. 2298-2305, **2010**.

[5] MOCILAC, P.; DONNELLY, K.; GALLAGHER, J. F. Structural systematics and conformational analyses of a 3 × 3 isomer grid of fluoro-N-(pyridyl)benzamides: physicochemical correlations, polymorphism and isomorphous relationships. Acta Cryst. B, v. 68, p. 189-203, **2012**.

[6] ACOSTA QUINTERO, L. M.; PALMA, A.; COBO, J.; GLIDEWELL, C. Six polycyclic pyrimidoazepine derivatives: syntheses, molecular structures and supramolecular assembly. Acta Cryst. C, v. 72, p. 346-357, **2016**.

[7] KUCHARSKA, E.; HANUZA, J.; LORENC, J. Conformation of azo-bridge in 3,3′ -dinitro-2,2′ -azobipyridine and its 4,4′ (or 5,5′ or 6,6′)-dimethyl-derivatives: Vibrational studies and DFT quantum chemical calculations. Spectrochim. Acta Mol. Biomol. Spectrosc., v. 127, p. 370-380, **2014**.

[8] ALLEN, F. H. The Cambridge Structural Database: a quarter of a million crystal structures and rising. Acta Cryst. B, v. 58, p. 380-388, **2002**.

[9] CSD reference codes ABOTAN, ATOYOX, ATOYUD, ATOZAK, GAMMAI, KUBROO, LOFCOY, QAKYAD, RARKIG, WIFGOI, WIFGUO, and WIFHAV

[10] LI, Y.-J.; LEE, P.-T.; YANG, C.-M.; CHANG, Y.-K.; WENG, Y.-C.; LIU, Y.-H. [2,3]-Wittig rearrangement of methyl β-pyrrolidinyl-γ-allyloxy-(E)-2-butenoate. Expeditious synthesis of 5-alkenyl-4-pyrrolidin-1-yl-5H-furan-2-ones. Tetrahedron Lett., v. 45, p. 1865-1868 (CSD reference codes ATOYOX, ATOYUD, ATOZAK), **2004**.

[11] ROYER, J.; BRUYÈRE, H.; SAMARITANI, S.; BALLEREAU, S.; TOMAS, A. Intramolecular Diels-Alder Strategy in a Synthetic Approach to the -Eleutherobin Core. Synlett, p. 1421-1424, **2005**.

[12] KARAK, M.; BARBOSA, L. C. A.; ACOSTA, J. A. M.; SAROTTI, A. M.; BOUKOUVALAS, J. Thermodynamically driven, syn-selective vinylogous aldol reaction of tetronamides. Org. Biomol. Chem., v. 14, p. 4897-4907, **2016**.

[13] WANG, L.; ZHAO, L.; XU, L.; CHEN, R.; YANG, Y. Interesting organic supramolecular structures constructed by piperazine/N,N′ -dimethylpiperazine with aromatic multicomponent acids: synthon cooperation and structural diversity. CrystEngComm, v. 14, p. 6998, **2012**.

[14] WANG, L.; XUE, R.; LI, Y.; ZHAO, Y.; LIU, F.; HUANG, K. Hydrogen-bonding patterns in a series of multi-component molecular solids formed by 2,3,5,6-tetramethylpyrazine with selected carboxylic acids. CrystEngComm, v. 16, p. 7074, **2014**.

[15] ALIEV, Z. G.; KRASNYKH, O. P.; MASLIVETS, A. N.; ANDREICHIKOV, Y. S.; ATOVMYAN, L. O. Chemistry of acyl(imidoyl)ketenes. RUSS CHEM B+, v. 48, p. 2131-2135, **1999**.

[16] Desiraju, G. R.; Steiner, T. The Weak Hydrogen Bond: In Structural Chemistry and Biology, Oxford University Press, The University of Michigan, 1999,

[17] DAVIDSON, M. G.; GOETA, A. S. E.; HOWARD, J. A. K.; LAMB, S.; MASON, S. A. The shortest C–H···O hydrogen bonds yet determined by single crystal neutron diffraction: a structural study of two phosphonium aryloxides. New J. Chem., v. 24, p. 477-479, **2000**.

[18] SURESHAN, K. M.; GONNADE, R. G. Weak becomes strong: remarkable strength of C–H···π hydrogen bond in the presence of O–H···O hydrogen bonds in the crystal stabilization. CrystEngComm, v. 15, p. 1676, **2013**.

[19] N. LAXMI MADHAVI, N.; R. DESIRAJU, G.; K. KATZ, A.; L. CARRELL, H.; NANGIA, A. Evidence for the characterisation of the C–H···π interaction as a weak hydrogen bond: toluene and chlorobenzene solvates of 2,3,7,8-tetraphenyl-1,9,10-anthyridine. Chem. Comm., v. p. 1953, **1997**.

[20] TSUZUKI, S.; HONDA, K.; UCHIMARU, T.; MIKAMI, M.; TANABE, K. The Magnitude of the CH/π Interaction between Benzene and Some Model Hydrocarbons. J. Am. Chem. Soc., v. 122, p. 3746-3753, **2000**.

[21] MUKHERJEE, A.; TOTHADI, S.; DESIRAJU, G. R. Halogen Bonds in Crystal Engineering: Like Hydrogen Bonds yet Different. Acc. Chem. Res., v. 47, p. 2514-2524, **2014**.

[22] SADABS, APEX2 and SAINT. Bruker AXS Inc., Madison, Wisconsin, USA, 2009.,

[23] SHELDRICK, G. M. Crystal structure refinement withSHELXL. Acta Cryst. C, v. 71, p. 3-8, **2015**.

[24] SHELDRICK, G. M. A short history ofSHELX. Acta Cryst. A, v. 64, p. 112-122, **2007**.

[25] MACRAE, C. F.; BRUNO, I. J.; CHISHOLM, J. A.; EDGINGTON, P. R.; MCCABE, P.; PIDCOCK, E.; RODRIGUEZ-MONGE, L.; TAYLOR, R.; VAN DE STREEK, J.; WOOD, P. A. Mercury CSD 2.0– new features for the visualization and investigation of crystal structures. J. Appl. Crystallogr., v. 41, p. 466-470, **2008**.

[26] Hyperchem Professional Release 7.52, Hypercube, Inc., 2005.

[27] FRISCH, M. J.; TRUCKS, G. W.; SCHLEGEL, H. B.; SCUSERIA, G. E.; ROBB, M. A.; CHEESEMAN, J. R.; SCALMANI, G.; BARONE, V.; MENNUCCI, B.; PETERSSON, G. A.; NAKATSUJI, H.; CARICATO, M.; LI, X.; HRATCHIAN, H. P.; IZMAYLOV, A. F.; BLOINO, J.; ZHENG, G.; SONNENBERG, J. L.; HADA, M.; EHARA, M.; TOYOTA, K.; FUKUDA, R.; HASEGAWA, J.; ISHIDA, M.; NAKAJIMA, T.; HONDA, Y.; KITAO, O.; NAKAI, H.; VREVEN, T.; MONTGOMERY JR., J. A.; PERALTA, J. E.; OGLIARO, F. O.; BEARPARK, M. J.; HEYD, J.; BROTHERS, E. N.; KUDIN, K. N.; STAROVEROV, V. N.; KOBAYASHI, R.; NORMAND, J.; RAGHAVACHARI, K.; RENDELL, A. P.; BURANT, J. C.; IYENGAR, S. S.; TOMASI, J.; COSSI, M.; REGA, N.; MILLAM, N. J.; KLENE, M.; KNOX, J. E.; CROSS, J. B.; BAKKEN, V.; ADAMO, C.; JARAMILLO, J.; GOMPERTS, R.; STRATMANN, R. E.; YAZYEV, O.; AUSTIN, A. J.; CAMMI, R.; POMELLI, C.; OCHTERSKI, J. W.; MARTIN, R. L.; MOROKUMA, K.; ZAKRZEWSKI, V. G.; VOTH, G. A.; SALVADOR, P.; DANNENBERG, J. J.; DAPPRICH, S.; DANIELS, A. D.; FARKAS, Ã. D. N.; FORESMAN, J. B.; ORTIZ, J. V.; CIOSLOWSKI, J.; FOX, D. J. Gaussian 09. Gaussian, Inc., Wallingford CT, **2009**.

[28] BECKE, A. D. Density-functional exchange-energy approximation with correct asymptotic behavior. Phys. Rev. A, v. 38, p. 3098-3100, **1988**.

[29] LEE, C.; YANG, W.; PARR, R. G. Development of the Colle-Salvetti correlation-energy formula into a functional of the electron density. Phys. Rev. B, v. 37, p. 785-789, **1988**.

[30] BECKE, A. D. Density-functional thermochemistry. III. The role of exact exchange. J. Chem. Phys., v. 98, p. 5648, **1993**.

[31] STEPHENS, P. J.; DEVLIN, F. J.; CHABALOWSKI, C. F.; FRISCH, M. J. Ab Initio Calculation of Vibrational Absorption and Circular Dichroism Spectra Using Density Functional Force Fields. J. Phys. Chem., v. 98, p. 11623-11627, **1994**.

[32] TOMASI, J.; MENNUCCI, B.; CAMMI, R. Quantum Mechanical Continuum Solvation Models. Chem. Rev., v. 105, p. 2999-3094, **2005**.

[33] BARONE, V.; IMPROTA, R.; REGA, N. Quantum Mechanical Computations and Spectroscopy: From Small Rigid Molecules in the Gas Phase to Large Flexible Molecules in Solution. Acc. Chem. Res., v. 41, p. 605-616, **2008**.

[34] HELGAKER, T.; CORIANI, S.; JØRGENSEN, P.; KRISTENSEN, K.; OLSEN, J.; RUUD, K. Recent Advances in Wave Function-Based Methods of Molecular-Property Calculations. Chem. Rev., v. 112, p. 543-631, **2012**.

CHAPTER 4

Total Synthesis of Rubrolides I and O and Analogues Thereof

1. Introduction

Butenolide containing marine natural products have been extensively investigated in recent years due to their vast structural diversity and biological activities [1-9], [10-16]. The rubrolides are a family of approximately 20 polysubstituted butenolides isolated mainly from ascidia (tunicates) [17-22], but also from a marine fungus [23] (Figure 4.1). Most rubrolides contain brominated phenol groups, and nearly half of them further possess a chloro substitutent attached directly to the butenolide nucleus (Figure 4.1). Besides densely functionalized structures, several rubrolides display highly sought biological properties including antibacterial [17, 20, 21], anticancer [18], antidiabetic [24], anti-inflammatory [19], and antiviral [23] activities. In addition, some of their synthetic analogues have been shown to possess significant herbicidal and biofilm inhibitory activities [25-28].
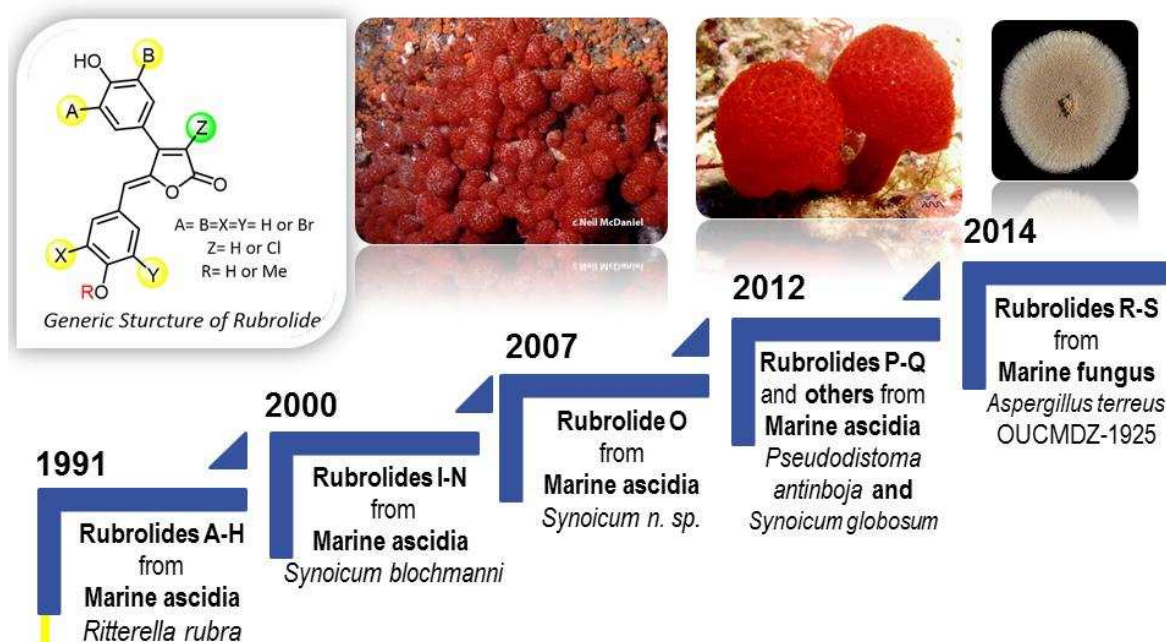
Figure 4.1 Generic structures and isolation timeline of rubrolides from different sources

Unsurprisingly, the synthesis of rubrolides has attracted worldwide attention for nearly two decades. In 1997, Negishi reported the first synthesis of rubrolide C (Scheme 4.1) by using Pd-catalyzed tandem ene-yne coupling/lactonization [29]. Shortly thereafter, Boukouvalas group described a short synthesis of rubrolides C and E by a new strategy based on Suzuki cross-coupling and furanolate chemistry [30]. Subsequent syntheses of rubrolide E have employed Meerwein coupling [31], a Heck-type reaction [32], ring-closing
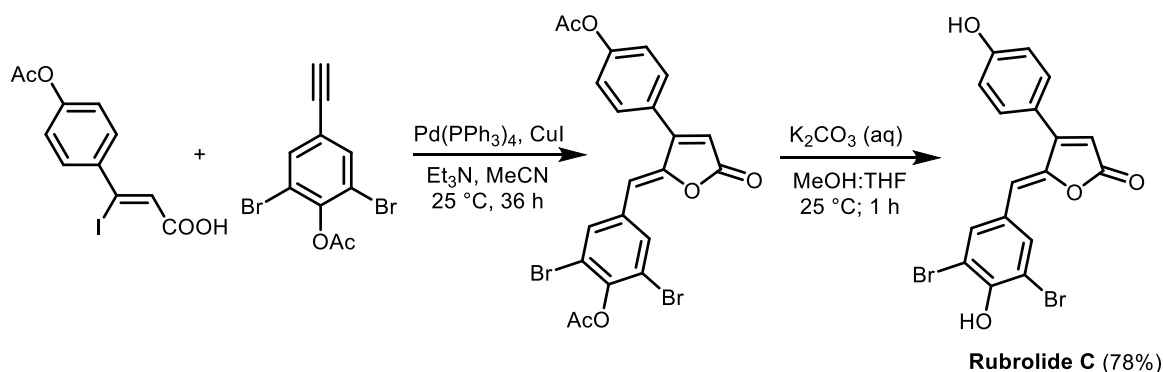
Scheme 4.1 Negishi's first synthesis of rubrolide C [29]

metathesis [33], and an intramolecular Wittig reaction which also enabled the synthesis of rubrolide C [34] (Scheme 4.2).
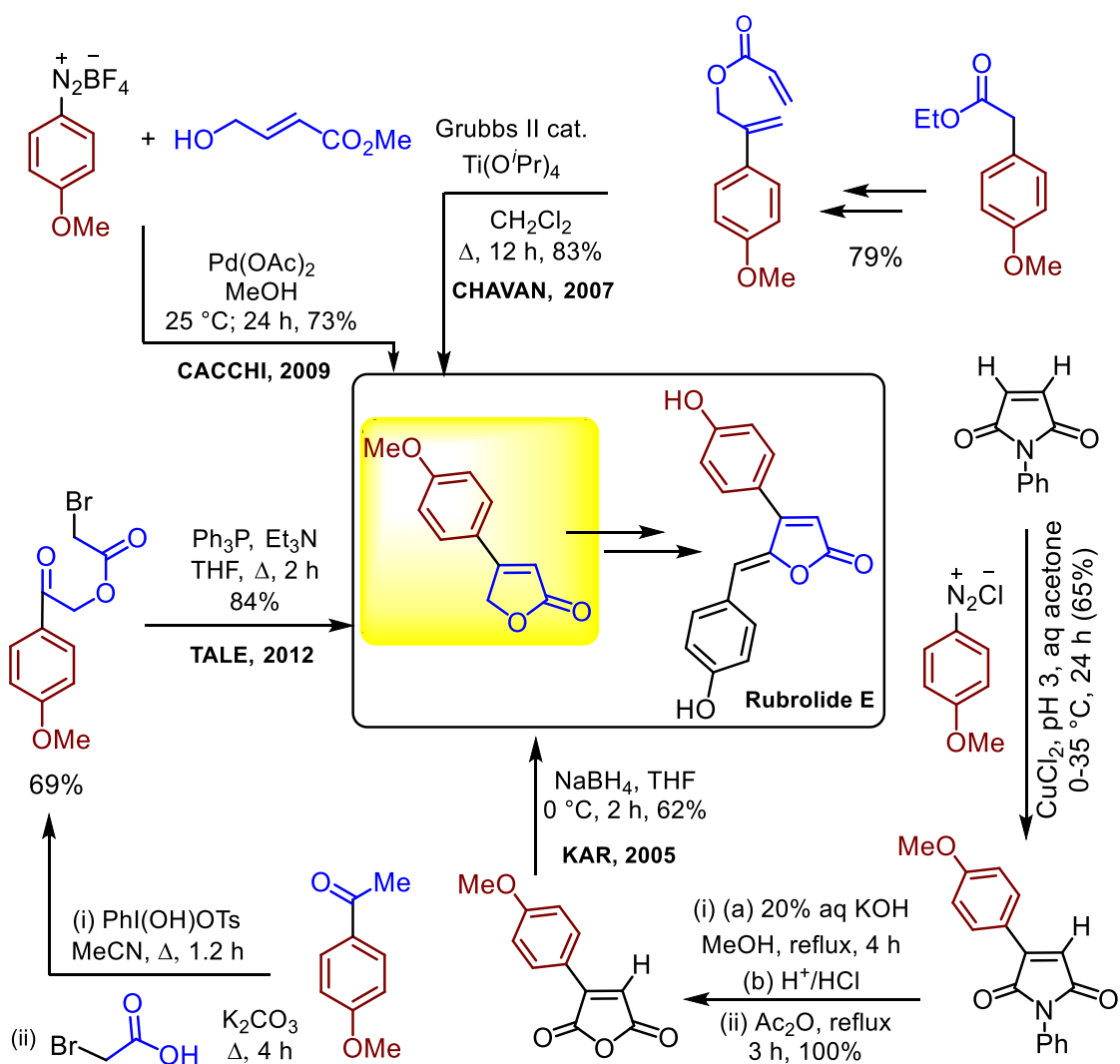
Scheme 4.2 Several recent syntheses of rubrolide E

The first α-chloro substituted rubrolide M was synthesized by Bellina et al. employing site-selective Suzuki cross-coupling (Scheme 4.3) [35].
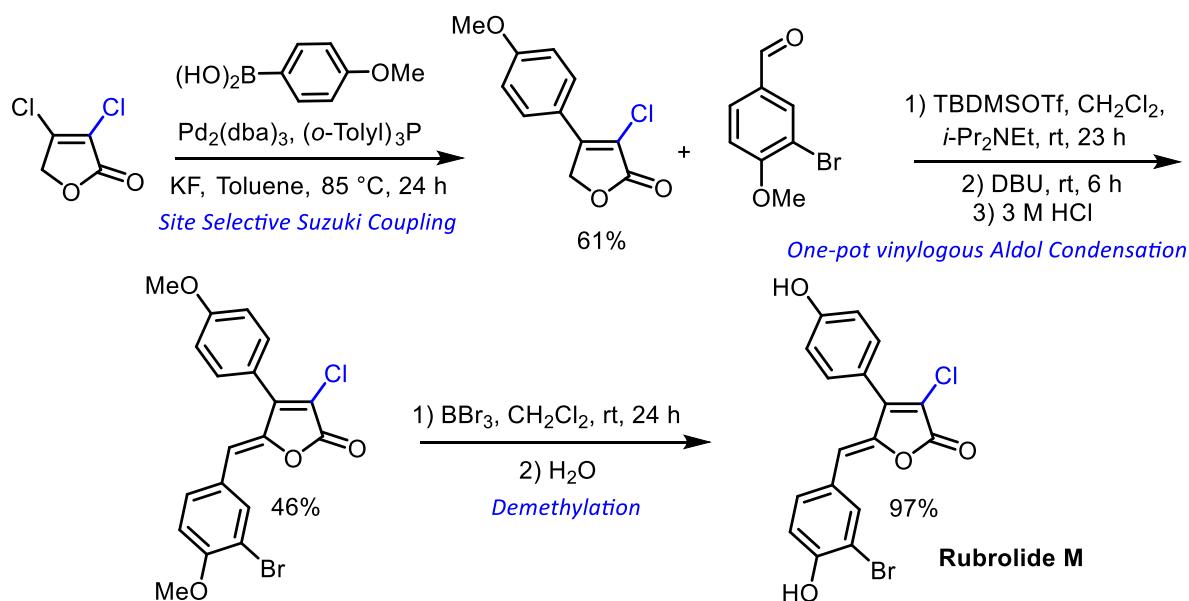
Scheme 4.3 Bellina's first synthesis of Rubrolide M [35]

Lately, Boukouvalas et al. employed a different strategy, starting from 3-chlorotetronic acid, to synthesis the aldose reductase inhibitor rubrolide L [36] (Scheme 4.4).
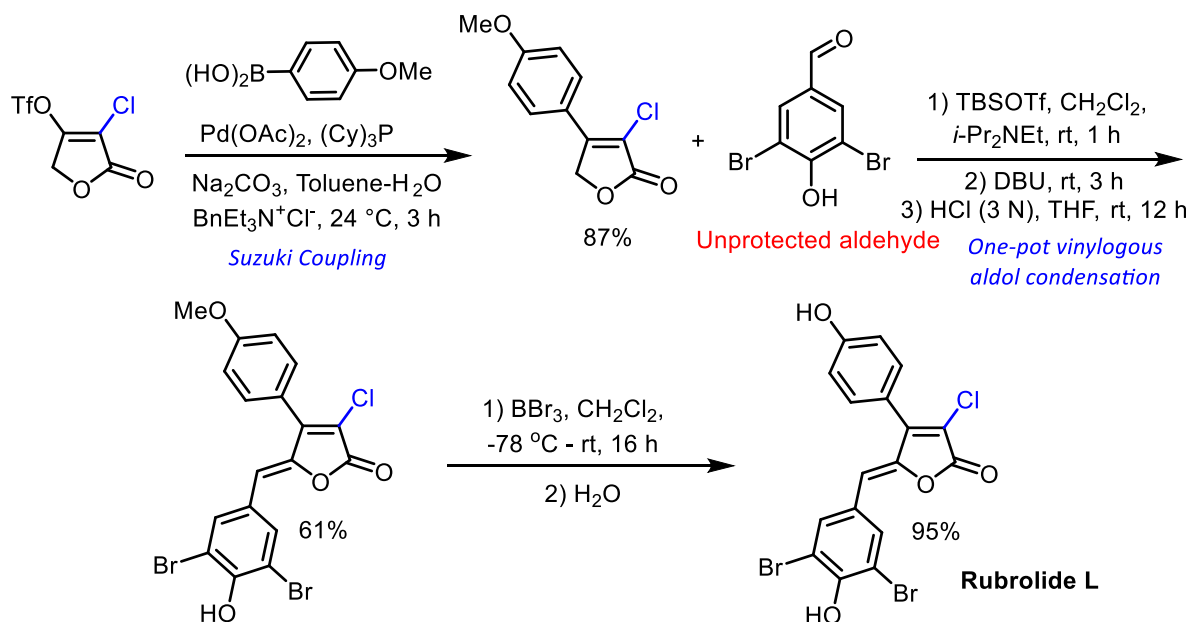
Scheme 4.4 Boukouvalas's first synthesis of Rubrolide L [36]

When compared to simple rubrolides, their α-chloro counterparts are not as easily accessible by existing methodologies, due to the challenges associated with vinylogous aldol condensation of the appropriately halogenated butenolide and benzaldehyde partners [35-37]. In this Chapter, a late-stage bromination tactic was employed to overcome such complications, as illustrated by the first synthesis of rubrolides I and O (Figure 4.2). Moreover, some analogous were also prepared for further biological evaluations.
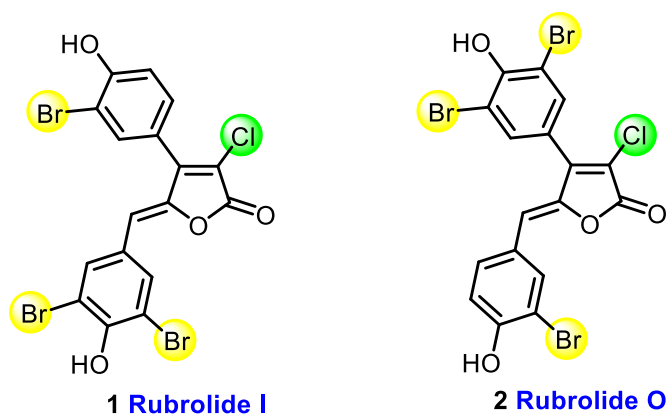
Figure 4.2 Structures of rubrolide I [isolated from ascidian *Synoicum blochmanni*, Spain (**2000**)] and rubrolide O [isolated from *Synoicum* n. sp. ascidian, New Zealand (**2007**)]

Retrosynthetic Analysis

As outlined in Scheme 4.5, the synthetic plan was based on the premise that bromination would occur preferentially at the aromatic ring bearing the *p*-hydroxy substituent, which is a more powerful directing group than the methoxy (Hammett substituent constants, σ_{para} = -0.37 and -0.27, respectively; Figure 4.3) [38, 39].
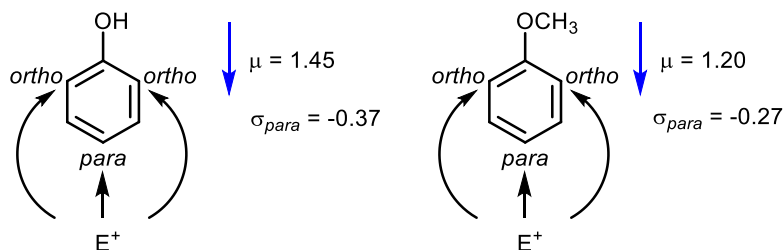
Figure 4.3 Comparative electron donating effect of *p*-hydroxy and *p*-methoxy groups

Moreover, the benzylidene ring (ring **B**) was expected to be inherently more reactive toward electrophilic bromination than ring **A,** as the latter is more strongly deactivated through direct conjugation with the C=C-C=O functionality. Accordingly, the desired

selectivity could be controlled through judicious choice of the appropriate demethylation/bromination sequence.
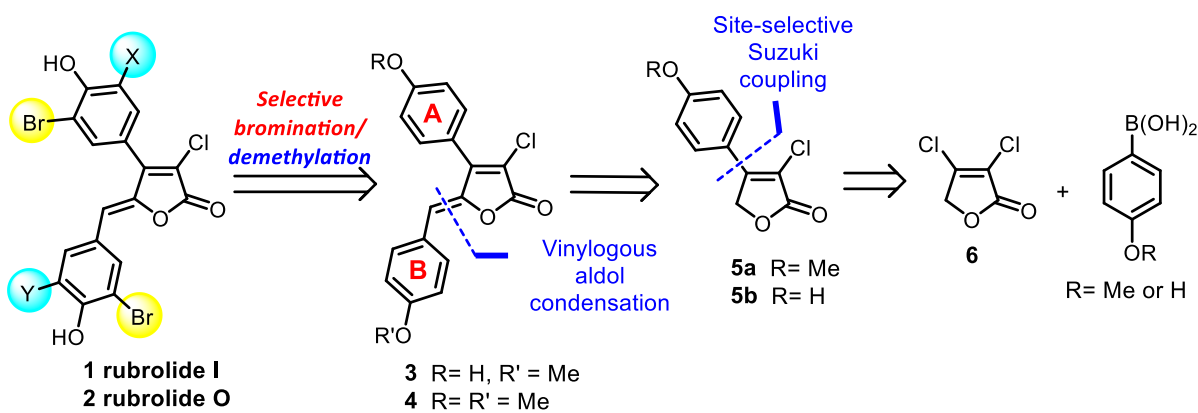
Scheme 4.5 Retrosynthesis of the target rubrolides

Thus, demethylation of **4** will afford the dihydroxylated compound that should, in principle, be amenable to selective bromination to generate rubrolides I. Also, bromination of **3,** followed by demethylation, would lead to rubrolide O. Intermediates **3**, **4** could be obtained directly from alkylidenation of **5a-b** *via* vinylogous aldol condensation. Practical access to **5a-b** was envisioned from commercially available α,β-dichloro-γ-butenolide **6** by site-selective Suzuki-Miyaura cross-coupling reaction.

2. Results and Discussion

2.1. Preparation of α-Chloro-β-Arylsubstituted Butenolides

The starting β-arylsubstituted butenolides of the present work were prepared by utilizing a procedure previously reported [35, 40, 41]. These compounds were accessible from **6** as shown in Scheme 4.6. Palladium catalyzed Suzuki-Miyaura cross-coupling of **6** with the appropriate boronic acids afforded **5a-e** in good yields. Demethylation of **5a** with boron tribromide also gave **5b** in 97% yield.
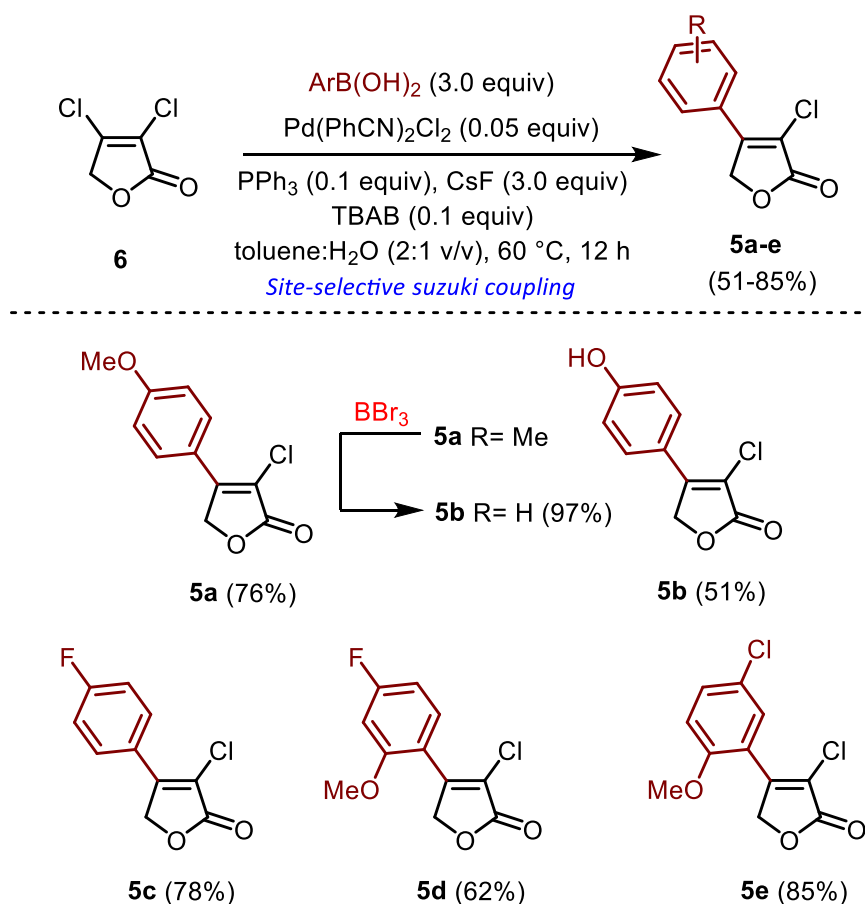
Scheme 4.6 Preparation of α-chloro-β-arylsubstituted butenolides **5a-e** from **6**

2.2. Scope of the Halogenation of Precursors 5a-b Equipped with Ring A

With gram quantities of **5a-b** in hand, the scope of regioselective halogenation reaction was explored (Table 4.1). Initially, reaction of **5a** with 2.0 equiv of bromine led exclusively to the monobrominated product **15a** (56%, entry 1). On the basis of GC-MS analysis of the crude product mixture, no dibrominated compound was detected even upon running the reaction for more than 4 h. Since the dibrominated product would be a logical

Table 4.1 Scope and optimization of halogenation of **5a-b**

5a R= Me
5b R= H

Halogen sources
Additive
Solvent
25 ºC, 2-4 h

7a R= Me, X= Br
7b R= H, X= Br
7c R= Me, X= Cl

Not observed
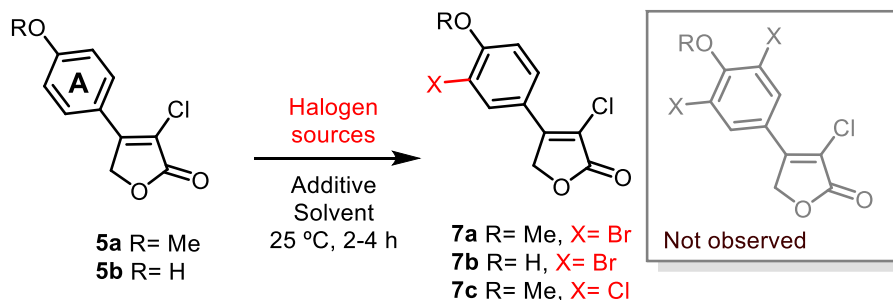
Entry	SM	Halogen Sources (equiv)	Additives (equiv)	Solvent	Product (%)
1	**5a**	Br$_2$ (2.0)	-	CH$_2$Cl$_2$	**7a** (56)
2	**5a**	Br$_2$ (2.0)	KBr (0.1)	CH$_2$Cl$_2$	**7a** (68)
3[a]	**5a**	Br$_2$ (5.0)	KBr (0.1)	CH$_2$Cl$_2$	**7a** (72)
4[b]	**5a**	Br$_2$ (5.0)	AcOH[c]	CH$_2$Cl$_2$	**7a** (59)
5	**5a**	NBS (2.0)	-	CH$_2$Cl$_2$	**7a** (30)
6	**5a**	NBS (2.0)	KBr (0.1)	CH$_2$Cl$_2$	**7a** (41)
7	**5b**	Br$_2$ (2.0)	KBr (0.1)	CH$_2$Cl$_2$	**7b** (72)
8	**5b**	NBS (2.0)	KBr (0.1)	CH$_2$Cl$_2$	**7b** (46)
9	**5b**	Br$_2$ (2.0)	KBr (0.1)	Et$_2$O	NR[d]
10	**5a**	Br$_2$ (2.0)	KBr (0.1)	THF	NR[d]
11	**5a**	Br$_2$ (2.0)	KBr (0.1)	H$_2$O	**7a** (21)
12	**5a**	Br$_2$ (2.0)	KBr (0.1)	MeCN	**7a** (62)
13	**5a**	Br$_2$ (2.0)	KBr (0.1)	DMF	**7a** (67)
14	**5a**	Cl$_2$ (g)	-	CH$_2$Cl$_2$	**7c** (38)
15	**5a**	Cl$_2$ (g)	AcOH	CH$_2$Cl$_2$	**7c** (51)

SM = Starting Materials. [a] Reaction time = 12 h. [b] Reaction run at 60 ºC. [c] CH$_2$Cl$_2$ and AcOH were used in a ratio of 1:1 (v/v). [d] No monobrominated product was detected even after 12 h; only starting material was recovered.

precursor for the synthesis of rubrolide O, the bromination of **5a** was investigated under various conditions. First, when the reaction was carried out in dichloromethane, it was observed that addition of KBr significantly improved the yield of **7a** (68%, entry 2, Table 4.1). A further improvement in the yield of **7a** was observed upon use of excess bromine (72%, entry 3). In this case, even though 5.0 equivalents of bromine were used, no dibrominated compound was formed. Next, using acetic acid as an additive and increasing the reaction temperature to 60 ºC resulted in a lower yield of **7a** (59%, entry 4). Switching to NBS as the bromine source resulted in an even lower yield of **7a** but no dibrominated product was

observed (entries 5-6). Since we were unable to generate the dibrominated derivative from **5a**, the reaction of the more electron-rich lactone **5b** with bromine and NBS was tried. In both cases only the monobrominated product **7b** was obtained (entries 7-8). Next, the effect of the solvent (entries, 9-13) was investigated. The use of THF or diethyl ether resulted in no reaction (entries 9-10), while only 21% of **7a** was obtained using water (entry 11). Better yields were obtained with acetonitrile (62%, entry 12) and DMF (67%, entry 13). Although DMF was as good as CH_2Cl_2, the latter was used in all further experiments (*vide infra*). Finally, more reactive chlorine was introduced to the substrate **5a**, but only the monochlorinated product **7c** was formed (entries 14-15). Based on the results obtained so far, it was concluded that the best yields of the brominated products **7a-b** are obtained when bromine is used together with a small amount of KBr, presumably due to *in situ* generation of KBr_3 [42]. Since unprotected phenols can be easily polybrominated [43-45], it was assumed that the low nucleophilicity of the phenol ring in **5a-b** is due to conjugation, *via* the butenolide C=C bond, with the carbonyl group (Figure 4.4) [46].

5a-b
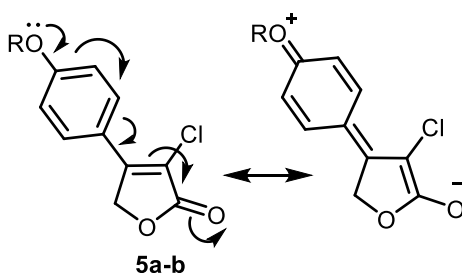
Figure 4.4 Conjugation effect in compound **5a-b** (π-cloud delocalization)

2.3.   Scope of the Bromination of Benzylidene Precursors Equipped with Ring B

At this point, attention was directed to the bromination of the benzylidene moiety. Thus, the vinylogous aldol condensation was employed to prepare model substrates **8a-b** bearing *p*-methoxy and *p*-hydroxyphenyl substituent, respectively (Scheme 4.7) [47-49].
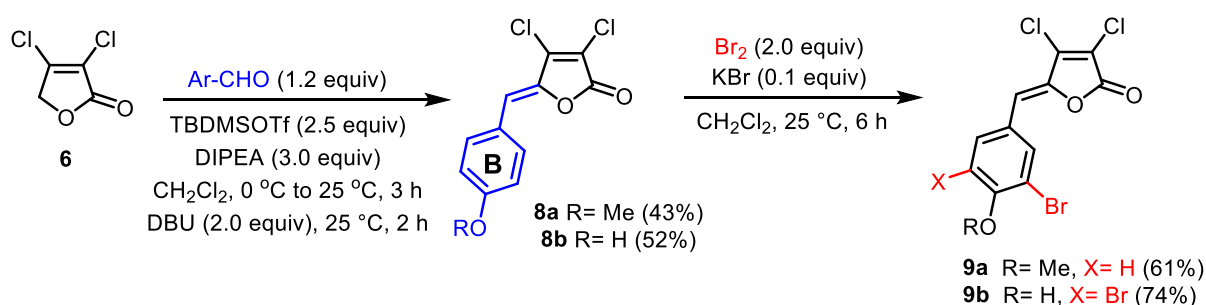
Scheme 4.7 Scope of the bromination of benzylidene precursors **8a-b**

Treatment of **8a** with 2.0 equiv of bromine and a catalytic amount of KBr, afforded the monobromo-derivative **9a** in 61% yield [50]. Under the same conditions, the more electron-rich **8b** delivered dibromophenol **9b** in 74% yield as the sole product. In contrast, only a small amount of dibrominated product (<10% according to GC-MS) could be obtained from **8a** when using a large excess of bromine (5.0 equiv)/KBr combination. However, reacting compound **8b** with 1.0 equiv of bromine, under similar conditions, resulted in a complex mixture of monobrominated product, dibrominated **9b** and starting material **8b**, as judged by GC-MS analysis of the crude mixture. When taken together with the results presented in Table 4.1, these findings lend support to the notion that the γ-benzylidene aromatic ring (ring **B**) is more reactive than the β-aryl (ring **A**) towards bromination.

2.4.   Attempted Synthesis of Rubrolide I and Precursors

Returning to the synthesis of rubrolides, the aldol condensation of **7a-b** with aldehydes **10a-b** was investigated to generate appropriately brominated precursors of rubrolide I in a straightforward way (Scheme 4.8).
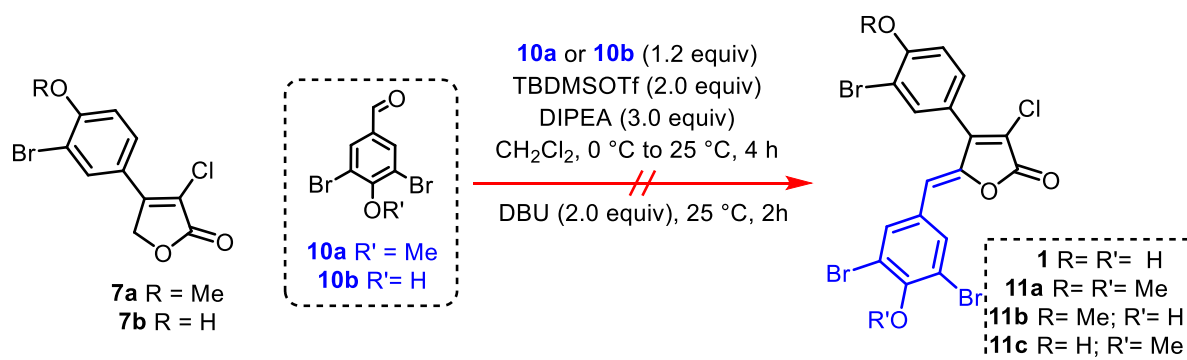
Scheme 4.8 Attempted synthesis of the brominated scaffolds of rubrolide I

However, attempts to prepare **1** and **11a-c** starting from **7a-b** and **10a-b** were unsuccessful. Only trace amounts of **11b**-**c** were observed by GC-MS analysis, while degradation of **7a**-**b** occurred after addition of DBU. These results mirror those previously reported in the literature [35, 36].

2.5.   Preparation of α-Chloro-β-Aryl-γ-Arylidenesubstituted Butenolides

From the above studies it was clear that the selective bromination/demethylation sequence of compounds **3** and **4** is crucial to the success of the synthesis the above mentioned rubrolides, as shown in the retrosynthetic analysis. Access to relay intermediates **3** and **4** was accomplished from β-arylsubstituted butenolides **5a-b** by vinylogous aldol

condensation (Scheme 4.9). Thus, one-pot vinylogous aldol condensation of **5a** with 4-methoxybenzaldehyde delivered relay intermediate **4** in 72% yield [30, 35, 36]. Likewise, another key intermediate **3** was synthesized in 78% yield from unprotected butenolide **5b**
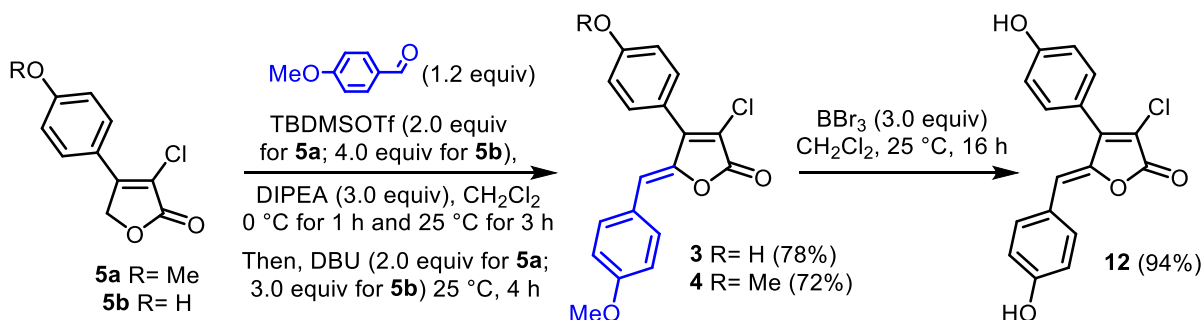
Scheme 4.9 Preparation of compounds **3,4** and **12** from **5a-b**

and 4-methoxybenzaldehyde.Ensuing removal of the methyl groups from compound **4** using boron tribromide, afforded compound **12** in 94% yield.

2.6.   End Game: Completion of the Synthesis of Rubrolide I and O

Finally, late-stage bromination tactics were employed to access the desired rubrolides from **3** and **12**. Thus, bromination of **12** led to a mixture of rubrolide I and rubrolide B in 31 and 25% yields respectively. Given the results of the model studies (Table 4.1, entries 7-8), the dibromination of ring **A** in **12** to give rubrolide B (Figure 4.5) was rather unexpected.

Rubrolide B is favorable due to the extended conjugations in compound **12**

Extended conjugation of the benzylidene moiety (ring **B**) mitigates the electron-withdrawing effect of the lactone carbonyl group (ring **A**)
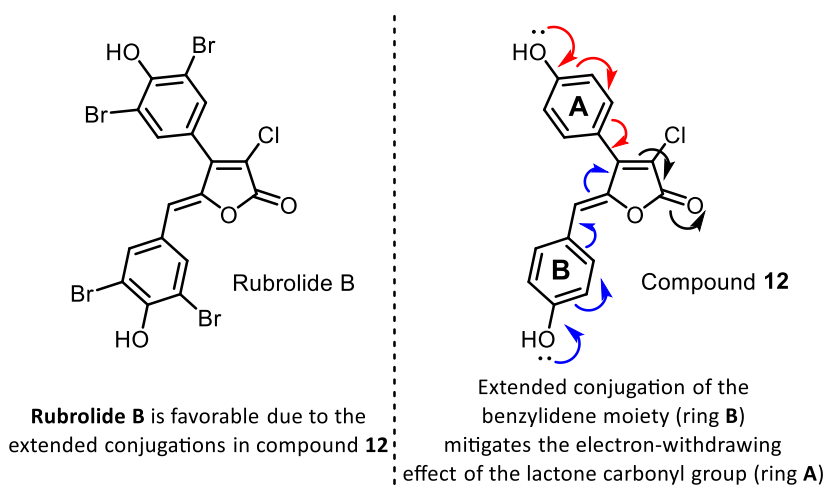
Figure 4.5 Comparative conjugation effects of ring **A** and ring **B** in compound **12**

It was beleived that the higher reactivity of **12** compared to **5b**, is due to the extended conjugation of the benzylidene moiety which mitigates the electron-withdrawing effect of the

lactone carbonyl group on ring **A** (Figure 4.5). In an attempt to improve the selectivity of bromination, the reaction was investigated under various conditions (Table 4.2, entries 1-4). Ultimately, the use of 3.2 equiv of bromine at a lower temperature (0-5 ℃) gave predominantly rubrolide I in 68% yield (35% overall) along with a small amount (9%) of rubrolide B (Table 4.2, entry 3 and Scheme 4.10).

Table 4.2 Optimized bromination conditions for rubolide I and O

Entry	SM	Br$_2$/KBr (equiv)	Time (h)	Temp. (℃)	Product (% of yield)			
					Rubrolide B	Rubrolide I	Rubrolide K	Rubrolide O
1	**12**	3.0/0.1	4	25	25	31	-	-
2[a]	**12**	2.5/0.1	4	25	20	29	-	-
3	**12**	3.2/0.1	4	0-5	09	68	-	-
4	**12**	3.2/3.2	4	0-5	16	64	-	-
5	**12**	4.5/0.1	6	25	79	-	-	-
6[b]	**3**	3.0/0.1	6	25	-	-	60	-
7[b]	**3**	5.0/0.1	6	25	-	-	25[c]	34[c]
8[b]	**3**	10.0/0.1	6	25	04	-	-	63

SM= Starting Material. [a] A complex mixture of rubrolides B, I and starting material **12** was detected by ^{1}H NMR. [b] Natural rubrolides obtained after demethylation of the crude brominated scaffolds by reaction with BBr$_3$. [c] An inseparable mixture of rubrolide K and O detected by ^{1}H NMR after demethylation of the crude product. The percentages were calculated from the ^{1}H NMR.
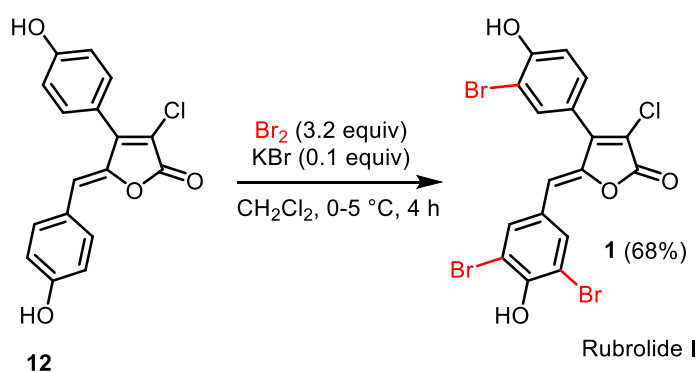
Scheme 4.10 Completion of the synthesis of Rubrolide I

Furthermore, treatment of compound **12** with 4.5 equiv of bromine in the presence of KBr afforded exclusively rubrolide B in 79% yields (Table 4.2, entry 5).

It is therefore clear from the above studies that ring **B** is always more reactive than ring **A** when both rings bear the same *para*-substituent. This makes it difficult, if not impossible, to find suitable conditions for transforming **12** to rubrolide O, since selective dibromination of ring **A** is required. Therefore, compound **3** was used as a precursor**,** in which the **B** ring bears a less electron-donating *para*-substituent (MeO *vs* HO). Reaction of **3** with 3.0 equiv of bromine, followed by demethylation, unexpectedly provided only rubrolide K in 60% yield (Table 4.2, entry 6 and Scheme 4.11).
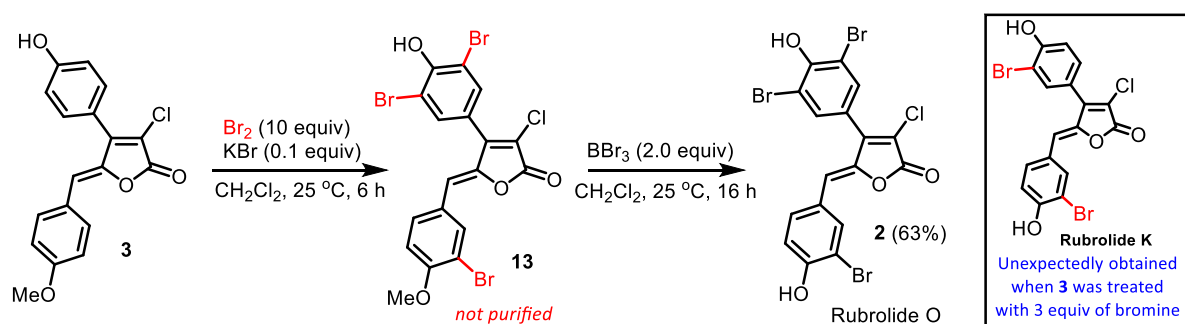
Scheme 4.11 Synthesis of rubrolide O and an unexpected synthesis of rubrolide K

On the other hand, attentive investigations (Table 4.2, entries 7-8) revealed that reaction of **3** with a large excess of bromine (10 equiv), followed by demethylation of the crude product delivered rubrolide O in 63% yield (36% overall, Scheme 4.11). The physical and spectroscopic data of obtained rubrolides were in excellent agreement with those reported in the literature [19].

2.7. Synthesis of Some Unnatural Congeners of Rubrolides

As part of the ongoing research program focused on the discovery of new bioactive compounds using rubrolides as model compounds [25-28], this research was further expanded on preparing new derivatives of rubrolides for biological investigation. Thus, one-pot vinylogous aldol condensation of **5c-e** and **7c** with different aldehydes delivered compounds **14a-d** in good yields (Scheme 4.12).
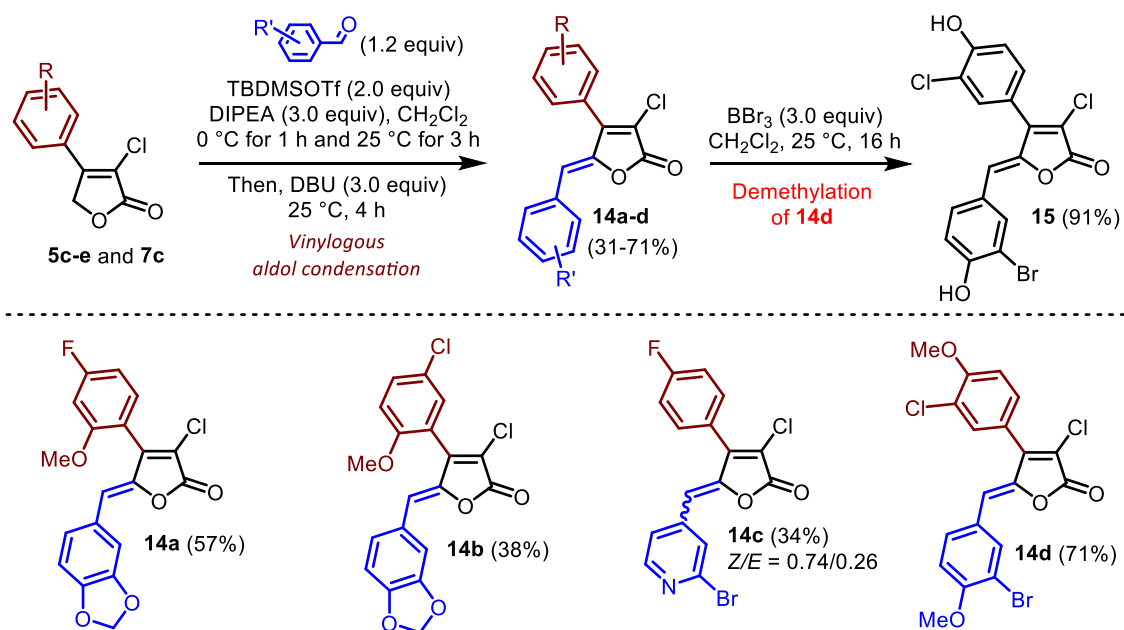
Scheme 4.12 Preparation of rubrolide analogous

Moreover, ensuing removal of the methyl groups from compound **14d** using boron tribromide, provided **15**, a chlorinated analouge of rubrolide K in 91% yields (Scheme 4.12).

3. Conclusion

In conclusion, the first total synthesis of rubrolides I and O has been accomplished by a unified pathway from readily available intermediates **4** and **3** in overall 35 and 36% yields, respectively. The foregoing syntheses demonstrate a versatile late-stage bromination strategy that should be applicable to the preparation of other biologically important rubrolides from easily accessible precursors. Moreover, in this work the preparation of a range of unnatural congeners of rubrolides **14a-d** and **15** also has been described. All the synthesized compounds are currently under evaluation with desirable biological activities.

4. Materials and Methods

4.1. General Experimental

All reactions were performed using analytical grade solvents. Reagents and solvents were purified, when necessary. All reactions were carried out under a protective atmosphere of dry nitrogen. The ^{1}H and ^{13}C NMR spectroscopic data were recorded at 400 and 100 MHz, respectively on a Bruker NMR spectrometer with $CDCl_3$, DMSO-d_6 or Acetone-d_6 as solvent and in some cases tetramethylsilane (TMS) as internal standard (δ = 0). Chemical shifts of ^{1}H and ^{13}C NMR spectra are reported in ppm. All coupling constants (J values) were expressed in Hertz (Hz). Multiplicities are reported as follows: singlet (s), doublet (d), doublet of doublets (dd), triplet (t), multiplet (m) and broad (br). Infrared spectra were recorded on a Varian 660-IR, equipped with GladiATR scanning from 4000 to 500 cm^{-1}. Melting points are uncorrected and were obtained from MQAPF-301 melting point apparatus (Microquimica, Brazil). High resolution mass spectra were recorded on a Bruker MicroTof (resolution = 10,000 FWHM) under electrospray ionization (ESI) and are given to four decimal places. Analytical thin layer chromatography analysis was conducted on aluminum packed precoated silica gel plates. Column chromatography was performed over silica gel (230-400 mesh).

4.2. General Procedure for the Preparation of Compounds 5a-e

3-Chloro-4-(4-methoxyphenyl)furan-2(5*H*)-one (5a)

To a 100 mL two-neck round-bottom flask α,β-dichlorobutenolide **6** (2.0 g, 13.1 mmol) was combined with (4-methoxyphenyl)boronic acid (2.4 g, 39.2 mmol), cesium fluoride (5.96 g, 39.3 mmol), Pd(PhCN)$_2$Cl$_2$ (0.25 g, 5 mol %), PPh$_3$ (0.35 g, 10 mol%), Bu$_4$N$^+$Br$^-$ (0.26 g, 10 mol %), and toluene/water (16/8 mL; v/v). The reaction mixture was then degassed for 10 min under flow of nitrogen. The reaction mixture was stirred at 60 ^{o}C for 12 h before it was filtered through a pad of Celite. The filtrate was extracted with ethyl acetate (3×50 mL). The combined organic layer was dried over anhydrous Na$_2$SO$_4$, and concentrated under reduced pressure. The crude product was purified by column chromatography on silica gel eluted with hexane/ethyl acetate (9:1 v/v) to afford compound **5a** as white solid in 62% yield (2.2 g, 9.3 mmol).
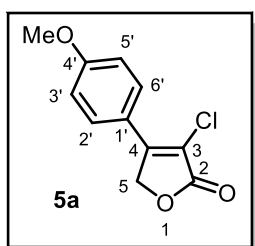
MP: 174.4-175.3 ^{o}C. **FTIR:** $\bar{v}_{max}$ 3033, 2937, 1749, 1603, 1510, 1444, 1254, 1201, 1184, 1022, 751, 734 cm^{-1}. ^{1}**H NMR** (400 MHz, CDCl$_3$) δ: 7.79 (d, J= 8.4 Hz, 2H, H-2′ and H-6′), 7.01 (d, J= 8.4 Hz, 2H, H-3′ and H-5′), 5.19 (s, 2H, H-5) and 3.88 (s, 3H, -OCH$_3$). ^{13}**C NMR** (100 MHz, CDCl$_3$) δ: 169.46 (C-2),

162.23 (C-4′), 151.28 (C-4), 129.05 (2C, C-2′ and C-6′), 121.25 (C-3), 114.82 (C-1′), 114.63 (2C, C-3′ and C-5′), 69.96 (C-5), 55.50 (-OCH$_3$). **HRMS** (ESI) [M+H]$^+$ calculated for C$_{11}$H$_{10}$ClO$_3$, 225.0313; found, 225.0317

3-Chloro-4-(4-hydroxyphenyl)furan-2(5H)-one (5b)

Procedure A: Compound **5b** was synthesized using a method similar to that of **5a** and was isolated as white solid in 51% yield (1.4 g, 6.7 mmol).

Procedure B: To a 50 mL two-neck round-bottom flask with a stirred solution of compound **5a** (500 mg, 2.23 mmol) in anhydrous CH$_2$Cl$_2$ (15 mL) at 0 °C, boron tribromide (0.32 mL, 3.35 mmol) was added dropwise. The resulting mixture was then allowed to warm to room temperature and stirred further for 16 h. The reaction was then quenched with aqueous NH$_4$Cl solution (20 mL) and CH$_2$Cl$_2$ was removed under vacuum. Then the aqueous phase was extracted with EtOAc (3×20 mL) and the organic layer dried over Na$_2$SO$_4$, filtered and evaporated under reduced pressure. The crude was purified by column chromatography on
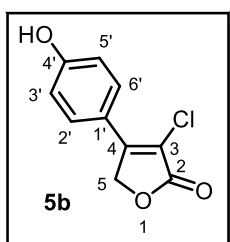
silica gel eluted with hexane/ethyl acetate (8:2 v/v) to afford the **5b** as white solid in 97% yield (456 mg, 2.16 mmol); **MP**: 254.8-255.2 °C. **FTIR**: $\bar{v}_{max}$ 3271, 1725, 1604, 1580, 1510, 1441, 1330, 1274, 1181, 751, 751 cm^{-1}. **^{1}H NMR** (400 MHz, DMSO-d_6) δ: 10.38 (s, 1H, -OH), 7.76 (d, J= 8.0 Hz, 2H, H-2′ and H-6′), 6.93 (d, J= 8.0 Hz, 2H, H-3′ and H-5′) and 5.39 (s, 2H, H-5). **^{13}C NMR** (100 MHz, DMSO-d_6) δ: 169.68 (C-2),

161.21 (C-4′), 153.80 (C-4), 130.11 (2C, C-2′ and C-6′), 119.81 (C-3), 116.43 (2C, C-3′ and C-5′), 111.91 (C-1′) and 70.86 (C-5). **HRMS** (ESI) [M+H]$^+$ calculated for C$_{10}$H$_8$ClO$_3$, 211.0156; found, 211.0167

3-chloro-4-(4-fluorophenyl)furan-2(5H)-one (5c)

Compound **5c** was synthesized using a method similar to that used to prepare **5a** and was
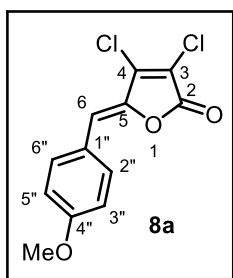

isolated as a light brown solid in 78% yield (325 mg, 1.53 mmol), purified by column chromatography, eluting with hexane/ethyl acetate (8:2, v/v). **MP:** 120.1-121.7 °C. **FTIR:** $\bar{v}_{max}$ 3037, 2916, 1753, 1607, 1506, 1437, 1259, 1188, 998 cm^{-1}. **^{1}H NMR** (400 MHz, CDCl$_3$) δ: 7.93-7.88 (m, 2H, H-2′ and H-6′), 7.23 (t, J= 8.2 Hz, 2H, H-3′ and H-5′), and 5.23 (s, 2H, H-5). **^{13}C NMR** (100 MHz, CDCl$_3$) δ: 168.90 (C-2), 164.40
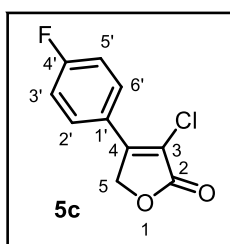
(d, J= 254.65 Hz, C-4′), 150.66 (C-4), 129.57 (d, J= 8.8 Hz, 2C, C-2′ and C-6′), 125.08 (d, J= 3.2 Hz, C-1′), 117.10 (C-3), 116.61 (d, J= 22.0 Hz, 2C, C-3′ and C-5′), 70.03 (C-5). **HRMS** (ESI) [M+H]$^+$ calculated for C$_{10}$H$_7$ClFO$_2$, 213.0119; found, 213.0112

3-chloro-4-(4-fluoro-2-methoxyphenyl)furan-2(5H)-one (5d)

Compound **5c** was synthesized using a method similar to that used to prepare **5a** and was isolated as a white solid in 62% yield, purified by column chromatography, eluting with hexane/ethyl acetate (8:2, v/v). **^{1}H NMR** (400 MHz, CDCl$_3$) δ: 8.05-7.87 (br, 1H, H-6'), 7.42 (m, 6.88-6.68, 2H, H-3' and H-5'), 5.29 (s, 2H, H-5) and 3.89 (s, 3H, -OCH$_3$). **^{13}C NMR** (100 MHz, CDCl$_3$) δ: 168.98 (C-2), 165.28 (d, J= 253.3 Hz, C-4'), 159.34 (C-2'), 151.81 (C-4), 131.70 (C-6'), 117.63 (C-3), 114.24 (C-1'), 108.02 (d, J= 21.9 Hz, C-5'), 99.96 (d, J= 25.9 Hz, C-3'), 72.10 (C-5) and 55.97 (-OCH$_3$). **HRMS** (ESI) [M+H]$^+$ calculated for C$_{11}$H$_9$ClFO$_3$, 243.0224; found, 243.0231
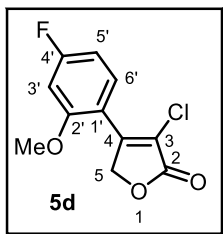
3-chloro-4-(5-chloro-2-methoxyphenyl)furan-2(5H)-one (5e)

Compound **5e** was synthesized using a method similar to that used to prepare **5a** and was isolated as a white solid in 85% yield (376 mg, 1.45 mmol), purified by column chromatography, eluting with hexane/ethyl acetate (8:2, v/v). **MP:** 205.1-206.3 ^{o}C. **FTIR:** $\bar{v}_{max}$ 3028, 2982, 2851, 1750, 1624, 1496, 1339, 1259, 1184, 824, 756, 732 cm^{-1}. **^{1}H NMR** (400 MHz, CDCl$_3$) δ: 7.85 (s, 1H, H-6'), 7.42 (d, J= 8.4 Hz, 1H, H-3'), 6.96 (d, J= 8.4 Hz, 1H, H-4') 5.28 (s, 2H, H-5) and 3.89 (s, 3H, -OCH$_3$). **^{13}C NMR** (100 MHz, CDCl$_3$) δ: 168.67 (C-2), 156.08 (C-2'), 151.33 (C-4), 132.21 (C-4'), 129.60 (C-6'), 126.07 (C-1'), 119.29 (C-5'), 118.99 (C-3), 112.87 (C-3'), 72.03 (C-5) and 56.01 (-OCH$_3$). HRMS (ESI) [M+H]$^+$ calculated for C$_{11}$H$_9$Cl$_2$O$_3$, 258.9929; found, 258.9907
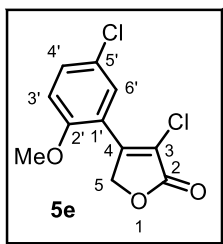
4.3.   General Procedure for the Preparation of Compounds 7a-c

4-(3-Bromo-4-methoxyphenyl)-3-chlorofuran-2(5H)-one (7a)

To a 25 mL two-neck round-bottom flask with a solution of compound **5a** (100 mg, 0.45 mmol) and KBr (5 mg, 0.04 mmol) in CH$_2$Cl$_2$ (5 mL), bromine (0.04 mL, 0.89 mmol) was added slowly at room temperature, and the resulting solution was stirred for 6 h under nitrogen atmosphere. After TLC analysis, the reaction mixture was quenched by saturated Na$_2$S$_2$O$_3$ solution and CH$_2$Cl$_2$ was removed under vacuum. Then the aqueous phase was extracted with ethyl acetate (3×15 mL) and the organic layer dried over Na$_2$SO$_4$, filtered and evaporated under reduced pressure. The crude residue of the white solid showed only pure product **7a** in 68% yield (92 mg, 0.3 mmol).

MP: 152.9-153.4 ºC. **FTIR:** $\bar{v}_{max}$ 3091, 2946, 2858, 1758, 1616, 1594, 1503, 1444, 1326, 1261, 1202, 1034, 1005, 828, 752, 678, 599 cm^{-1}. **^{1}H NMR** (400 MHz, CDCl$_3$) δ: 7.99 (s, 1H, H-2'), 7.81 (d, J= 8.5 Hz, 1H, H-6'), 7.01 (d, J= 8.5 Hz, 1H, H-5'), 5.17 (s, 2H, H-5) and 3.97 (s, 3H, -OCH$_3$). **^{13}C NMR** (100 MHz, CDCl$_3$) δ: 169.00 (C-2), 158.39 (C-4'), 149.89 (C-4), 132.13 (C-2'), 128.09 (C-6'), 122.44 (C-1'), 116.10 (C-3), 112.63 (C-3'), 111.95 (C-5'), 69.84 (C-5) and 56.51 (-OCH$_3$). **HRMS** (ESI) [M+H]$^+$ calculated for C$_{10}$H$_9$BrClO$_3$, 302.9418; found, 302.9425
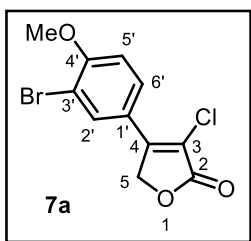
4-(3-Bromo-4-hydroxyphenyl)-3-chlorofuran-2(5*H*)-one (7b)

Compound **7b** was synthesized using a method similar to that of **7a** from compound **5b** and was isolated as white solid in 72% yield (99 mg, 0.34 mmol). **MP:** 213.5-214.4 ºC. **FTIR:** $\bar{v}_{max}$ 3287, 1748, 1595, 1562, 1504, 1445, 1423, 1295, 1199. 1156, 1055, 1013, 814, 741, 627, 591 cm^{-1}. **^{1}H NMR** (400 MHz, DMSO-d_6) δ: 7.99 (s, 1H, H-2'), 7.79 (d, J= 8.6 Hz, 1H, H-6'), 7.10 (d, J= 8.6 Hz, 1H, H-5') and 5.40 (s, 2H, H-5). **^{13}C NMR** (100 MHz, DMSO-d_6) δ: 169.39 (C-2), 157.67 (C-4'), 152.64 (C-4), 132.73 (C-2'), 129.13 (C-6'), 121.33 (C-1'), 117.04 (C-3), 113.26 (C-3'), 110.48 (C-5') and 70.90 (C-5). **HRMS** (ESI) [M+H]$^+$ calculated for C$_{10}$H$_7$BrClO$_3$, 288.9262; found, 288.9263
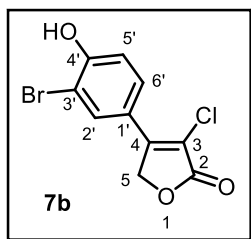
3-chloro-4-(3-chloro-4-methoxyphenyl)furan-2(5*H*)-one (7c)

Chlorination of compound **5a** with Cl$_2$ (g) and AcOH as an additive in anhydrous CH$_2$Cl$_2$ (5 mL), afforded the corresponding chlorinated product **7c** and was isolated as white solid in 51% yield; purified by column chromatography, eluent hexane/ethyl acetate (17:3 v/v). **MP:** 160.8-161.7 ºC. **FTIR:** $\bar{v}_{max}$ 3101, 2950, 1756, 1614, 1598, 1508, 1444, 1329, 1263, 1199, 1075, 1036, 1007, 830, 702 cm^{-1}. **^{1}H NMR** (400 MHz, CDCl$_3$) δ: 7.85 (s, 1H, H-2'), 7.77 (d, J= 7.8 Hz, 1H, H-6'), 7.07 (d, J= 7.8 Hz, 1H, H-5'), 5.19 (s, 2H, H-5) and 4.00 (s, 3H, -OCH$_3$). **^{13}C NMR** (100 MHz, CDCl$_3$) δ: 168.99 (C-2), 157.58 (C-4'), 150.02 (C-4), 129.07 (C-2'), 127.36 (C-6'), 123.67 (C-1'), 122.00 (C-3'), 116.67 (C-3), 112.21 (C-5'), 69.84 (C-5) and 56.41 (-OCH$_3$). **HRMS** (ESI) [M+H]$^+$ calculated for C$_{11}$H$_9$Cl$_2$O$_3$, 258.9923; found, 258.9928
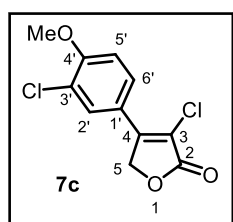
4.4. General Procedure for the Preparation of Compounds 8a-b and 9a-b

(*Z*)-3,4-Dichloro-5-(4-methoxybenzylidene)furan-2(5*H*)-one (8a)

To a 25 mL two-neck round-bottom flask with a solution of **6** (400 mg, 2.61 mmol) in anhydrous CH_2Cl_2 (10 mL) at 0 °C were successively added *i*-Pr₂NEt (1.38 mL, 7.83 mmol) and TBDMSOTf (1.2 mL, 5.22 mmol) under nitrogen atmosphere. The mixture was stirred for 30 min at 0 °C, and then *p*-anisaldehyde (0.36 mL, 3.13 mmol) was added. After stirring at 0 °C for 1 h, the reaction mixture was left for 3 h in room temperature. Then DBU (0.76 mL, 5.22 mmol) was added and the resulting solution was allowed to stir for an additional 4 h before quenching with aqueous solution of HCl (1M, 10 mL). Then CH_2Cl_2 was removed under vacuum and the aqueous phase was extracted with e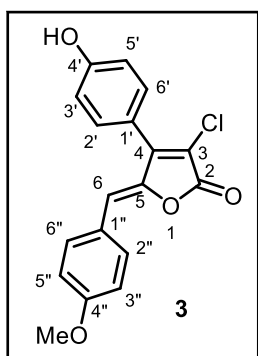thyl acetate (3×20 mL) and the combined organic layers were washed with saturated brine solution, dried over Na_2SO_4 and concentrated under reduced pressure. The crude was purified by column chromatography on silica gel eluted with hexane/ethyl acetate (17:3 v/v) to afford aldol product **8a** as yellow solid in 43% yield (304 mg, 1.12 mmol); purified by column chromatography, eluent hexane/ethyl acetate (9:1 v/v).

MP: 111.3-112.8 °C. **¹H NMR** (400 MHz, CDCl₃) *δ*: 7.72 (d, *J*= 8.5 Hz, 2H, H-2″ and H-6″), 6.92 (d, *J*= 8.5 Hz, 2H, H-3″ and H-5″), 6.32 (s, 1H, H-6), 3.84 (s, 3H, -OCH₃). **¹³C NMR** (100 MHz, CDCl₃) *δ*: 162.46 (C-1), 161.27 (C-4″), 142.62 (C-4), 141.75 (C-5), 132.99 (2C, C-2″ and C-6″), 124.44 (C-1″), 118.02 (C-3), 114.62 (2C, C-3″ and C-5″), 112.77 (C-6) and 55.42 (-OCH₃). **HRMS** (ESI) [M+H]⁺ calculated for $C_{12}H_9Cl_2O_3$, 270.9923; found, 270.9929

(*Z*)-3,4-Dichloro-5-(4-hydroxybenzylidene)furan-2(5*H*)-one (8b)

Compound **8b** was synthesized using a method similar to that of **8a** from compound **6** and 4-hydroxybenzaldehyde and was isolated as yellow solid in 52% yield (348 mg, 1.36 mmol); purified by column chromatography, eluent hexane/ethyl acetate (8:2 v/v). **MP:** 178.1-179.7 °C. **¹H NMR** (400 MHz, Acetone-*d₆*) *δ*: 9.06 (s, 1H, -OH), 7.74 (d, *J*= 7.5 Hz, 2H, H-2″ and H-6″), 6.96 (d, *J*= 7.5 Hz, 2H, H-3″ and H-5″) and 6.52 (s, 1H, H-6). **¹³C NMR** (100 MHz, Acetone-*d₆*) *δ*: 161.85 (C-2), 159.51 (C-4″), 142.34 (C-4), 141.44 (C-5), 133.18 (2C, C-2″ and C-6″), 123.76 (C-1″), 117.37 (C-3), 116.11 (2C, C-3″ and C-5″) and 112.67 (C-6). **HRMS** (ESI) [M+H]⁺ calculated for $C_{11}H_7Cl_2O_3$, 256.9767; found, 256.9756
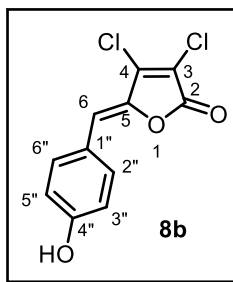
**5-(3-Bromo-4-methoxybenzylidene)-3,4-dichlorofuran-2(5H)-one (9a; Z/E = 92:08)**

Compound **9a** was synthesized using a method similar to that of **7a** from compound **8a** and was isolated as yellow solid in 61% yield (79 mg, 0.22 mmol); purified by column chromatography, eluent hexane/ethyl acetate (50:1 v/v). **MP:** 143.4-144.2 °C. **^{1}H NMR** (400 MHz, CDCl$_3$) δ: 7.81 (s, 0.92H, H-2″), 7.78 (s, 0.08H, H-2″), 7.60 (d, J= 8.6 Hz, 0.92H, H-6″), 7.41 (d, J= 8.7 Hz, 0.08H, H-6″), 6.96 (d, J= 8.6 Hz, 0.92H, H-5″), 6.86 (d, J= 8.7 Hz, 0.08H, H-5″), 6.35 (s, 0.92H, H-6), 6.37 (s, 0.08H, H-6) and 3.98 & 3.93 (s, 3H, -OCH$_3$). **^{13}C NMR** (100 MHz, CDCl$_3$) δ: 161.35 (C-2), 157.04 (C-4″), 153.98 (C-4), 134.79 (C-5), 130.56 (C-2″), 128.21 (C-6″), 123.10 (C-1″), 117.35 (C-3), 111.65 (C-5″), 111.57 (C-3″), 111.12 (C-6) and 56.40 (-OCH$_3$). **HRMS** (ESI) [M+H]$^+$ calculated for C$_{12}$H$_8$BrCl$_2$O$_3$, 348.9034; found, 348.9021
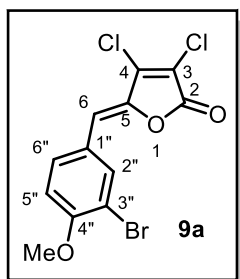
(Z)-3,4-Dichloro-5-(3,5-dibromo-4-hydroxybenzylidene)furan-2(5H)-one (9b)

Compound **9b** was synthesized using a method similar to that of **7a** from compound **8b** and was isolated as yellow solid in 74% yield (119 mg, 0.29 mmol); purified by column chromatography, eluent hexane/ethyl acetate (4:1 v/v). **MP:** 211.5-212.9 °C. **^{1}H NMR** (400 MHz, Acetone-d_6) δ: 8.08 (s, 2H, H-2″ and H-6″) and 6.58 (s, 1H, H-6). **^{13}C NMR** (100 MHz, Acetone-d_6) δ: 161.39 (C-2), 152.17 (C-4″), 143.29 (C-4), 142.22 (C-5), 134.58 (2C, C-2″ and C-6″), 126.71 (C-1″), 119.20 (C-3), 111.01 (C-6) and 109.07 (2C, C-3″ and C-5″). **HRMS** (ESI) [M+H]$^+$ calculated for C$_{11}$H$_5$Br$_2$Cl$_2$O$_3$, 412.7977; found, 412.7963
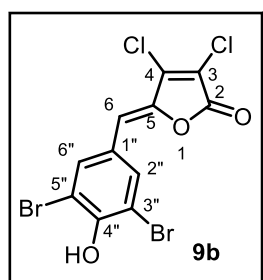
4.5.   General Procedure for the Preparation of Compounds 3, 4 and 12

(Z)-3-Chloro-5-(4-methoxybenzylidene)-4-(4-methoxyphenyl)furan-2(5H)-one (4)

To a 25 mL two-neck round-bottom flask with a solution of **5a** (200 mg, 0.89 mmol) in anhydrous CH$_2$Cl$_2$ (5 mL) at 0 °C were successively added i-Pr$_2$NEt (0.46 mL, 2.67 mmol) and TBDMSOTf (0.4 mL, 1.78 mmol) under nitrogen atmosphere. The mixture was stirred for 30 min at 0 °C, and then p-anisaldehyde (0.12 mL, 1.07 mmol) was added. After stirring at 0 °C for 1 h, the reaction mixture was left for 3 h in room temperature. Then DBU (0.26 mL, 1.78 mmol) was added and the resulting solution was allowed to stir for an additional 4 h before quenching with aqueous solution of HCl (1M, 10 mL). Then CH$_2$Cl$_2$ was removed under vacuum and the aqueous phase was extracted with ethyl acetate (3×15 mL) and the

combined organic layers were washed with saturated brine solution, dried over Na_2SO_4 and concentrated under reduced pressure. The crude was purified by column chromatography on silica gel eluted with hexane/ethyl acetate (17:3 v/v) to afford aldol product **4** as yellow solid in 72% yield (256 mg, 0.64 mmol).
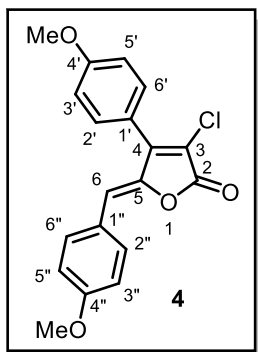
MP: 170.5-171.8 °C. **FTIR:** $\bar{\nu}_{max}$ 3021, 2939, 2842, 1767, 1640, 1602, 1565, 1503, 1429, 1348, 1306, 1256, 1179, 1015, 824, 751 cm^{-1}. **¹H NMR** (400 MHz, CDCl₃) *δ*: 7.75 (d, *J*= 8.8 Hz, 2H, H-2″ and H-6″), 7.51 (d, *J*= 8.7 Hz, 2H, H-2′ and H-6′), 7.09 (d, *J*= 8.8 Hz, 2H, H-3″ and H-5″), 6.92 (d, *J*= 8.7 Hz, 2H, H-3′ and H-5′), 6.13 (s, 1H, H-6), 3.92 (s, 3H, -OCH₃) and 3.86 (s, 3H, -OCH₃). **¹³C NMR** (100 MHz, CDCl₃) *δ*: 165.02 (C-2), 161.36 (C-4′), 160.78 (C-4″), 149.82 (C-4), 145.03 (C-5), 132.74 (2C, C-2″ and C-6″), 130.82 (2C, C-2′ and C-6′), 125.62 (C-1″), 120.47 (C-1′), 116.74 (C-3), 114.68 (C-6), 114.55 (2C, C-3″ and C-5″), 114.51 (2C, C-3′ and C-5′), 55.55 and 55.46 (-OCH₃). **HRMS** (ESI) [M+H]⁺ calculated for $C_{19}H_{16}ClO_4$, 343.0732; found, 343.0726

(*Z*)-3-Chloro-4-(4-hydroxyphenyl)-5-(4-methoxybenzylidene)furan-2(5*H*)-one (3)

Compound **3** was synthesized using a method similar to that of **4** from compound **5b** and was isolated as yellow solid in 78% yield (244 mg, 0.74 mmol); purified by column chromatography, eluent hexane/ethyl acetate (8:2 v/v). **MP:** 201.5-202.2 °C. **FTIR:** $\bar{\nu}_{max}$ 3329, 2840, 1716, 1598, 1562, 1503, 1427, 1356, 1305, 1254, 1221, 1171, 1024, 835, 754, 645, 525 cm⁻¹. **¹H NMR** (400 MHz, DMSO-*d₆*) *δ*: 7.76 (d, *J*= 8.8 Hz, 2H, H-2″ and H-6″), 7.44 (d, *J*= 8.6 Hz, 2H, H-2′ and H-6′), 7.01 (d, *J*= 8.8 Hz, 2H, H-3″ and H-5″), 6.97 (d, *J*= 8.6 Hz, 2H, H-3′ and H-5′), 6.28 (s, 1H, H-6), 3.79 (s, 3H, -OCH₃). **¹³C NMR** (100 MHz, DMSO-*d₆*) *δ*: 164.56 (C-2), 160.72 (C-4′), 160.08 (C-4″), 150.38 (C-4), 144.83 (C-5), 133.00 (2C, C-2″ and C-6″), 131.40 (2C, C-2′ and C-6′), 125.72 (C-1″), 118.42 (C-1′), 116.32 (2C, C-3″ and C-5″), 115.30 (C-3), 114.98 (2C, C-3′ and C-5′), 114.68 (C-6) and 55.78 (-OCH₃). **HRMS** (ESI) [M+H]⁺ calculated for $C_{18}H_{14}ClO_4$, 329.0575; found, 329.0575

(*Z*)-3-Chloro-5-(4-hydroxybenzylidene)-4-(4-hydroxyphenyl)furan-2(5*H*)-one (12)

Treatment of compound **4** (100 mg, 0.29 mmol) with boron tribromide (0.08 mL, 0.88 mmol)
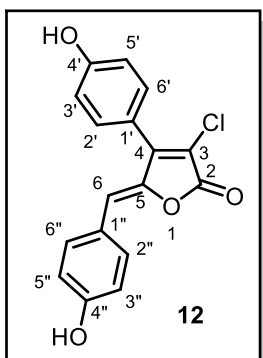
in CH_2Cl_2 accomplished removal of all methyl groups to afford the intermediate **12** as yellow solid in 94% yield (86 mg, 0.27 mmol). **MP:** 234.1-234.8 °C. **^{1}H NMR** (400 MHz, Acetone-d_6) *δ*: 7.73 (d, *J*= 8.8 Hz, 2H, H-2″ and H-6″), 7.51 (d, *J*= 8.7 Hz, 2H, H-2′ and H-6′), 7.07 (d, *J*= 8.8 Hz, 2H, H-3″ and H-5″), 6.93 (d, *J*= 8.7 Hz, 2H, H-3′ and H-5′) and 6.27 (s, 1H, H-6). **^{13}C NMR** (100 MHz, Acetone-d_6) *δ*: 164.21 (C-2), 159.57 (C-4′), 159.00 (C-4″), 150.34 (C-4), 144.69 (C-5), 132.90 (2C, C-2″ and C-6″), 131.09 (2C, C-2′ and C-6′), 124.89 (C-1″), 119.98 (C-1′), 115.99 (2C, C-3″ and C-5″), 115.92 (2C, C-3′ and C-5′), 115.45 (C-3), 114.55 (C-6). **HRMS** (ESI) [M+H]$^+$ calculated for $C_{17}H_{12}ClO_4$, 315.0424; found, 315.0421

4.6. Synthesis of Rubrolide I

Bromination of **12** (40 mg, 0.13 mmol) with Br_2 (0.02 mL, 0.40 mmol) and KBr (2 mg, 0.013 mmol) in CH_2Cl_2 (5 mL) under 0-5 °C temperature, delivered natural product rubrolide I as an amorphous orange-yellow powder in 68% yield (49 mg, 0.09 mmol).

MP: 253.2-254.1 °C. **FTIR:** $\bar{v}_{max}$ 3426, 3241, 1730, 1600, 1596, 1470, 1402, 1321, 1289,
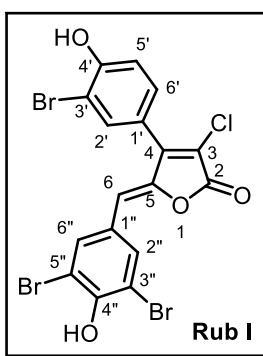
1192, 1137, 1026, 823, 751, 728, 650, 576, 497 cm^{-1}. **^{1}H NMR** (400 MHz, Acetone-d_6) *δ*: 8.06 (s, 2H, H-2″ and H-6″), 7.80 (d, *J*= 2.1 Hz, 1H, H-2′), 7.50 (dd, *J*= 2.1, 8.4 Hz, 1H, H-6′), 7.24 (d, *J*= 8.4 Hz, H-5′) and 6.32 (s, 1H, H-6). **^{13}C NMR** (100 MHz, Acetone-d_6) *δ*: 164.29 (C-2), 156.89 (C-4′), 152.58 (C-4″), 149.41 (C-4), 147.02 (C-5), 135.29 (2C, C-2″ and C-6″), 134.75 (C-2′), 131.00 (C-6′), 128.50 (C-1″), 121.31 (C-1′), 118.69 (C-3), 117.53 (C-5′), 111.92 (C-6), 111.74 (2C, C-3″ and C-5″) and 110.80 (C-3′). **HRMS** (ESI) [M+H]$^+$ calculated for $C_{17}H_9Br_3ClO_4$, 548.7734; found, 548.7719

4.7. Synthesis of Rubrolide O

Bromination of intermediate **3** (90 mg, 0.27 mmol) with Br_2 (0.14 mL, 2.7 mmol) and KBr (3 mg, 0.027 mmol) in CH_2Cl_2 (5 mL) afforded the fully brominated scaffold of rubrolide O. After workup the crude scaffold (without purification) was demethylated by boron tribromide (0.05 mL, 0.54 mmol) to deliver the corresponding natural product rubrolide O as amorphous yellow solid in 63% yield (94 mg, 0.17 mmol).

MP: 262.3-264.2 °C. **FTIR:** $\bar{v}_{max}$ 3429, 3230, 1741, 1680, 1594, 1474, 1403, 1208, 1135, 1028, 824, 749, 724, 653, 578 cm⁻¹. **¹H NMR** (400 MHz, Acetone-d_6) δ: 8.05 (d, J= 2.0, 1H, H-2″), 7.80 (s, 2H, H-2′ and H-6′), 7.74 (dd, J= 2.0, 8.5 Hz, 1H, H-6″), 7.12 (d, J= 8.5 Hz, H-5″) and 6.35 (s, 1H, H-6). **¹H NMR** (400 MHz, DMSO-d_6) δ: 7.99 (d, J= 2.1, 1H, H-2″), 7.72 (s, 2H, H-2′ and H-6′), 7.67 (dd, J= 2.1, 8.6 Hz, 1H, H-6″), 7.00 (d, J= 8.6 Hz, H-5″) and 6.26 (s, 1H, H-6). **¹³C NMR** (100 MHz, DMSO-d_6) δ: 164.13 (C-2), 155.97 (C-4″), 153.32 (C-4′), 147.92 (C-4), 144.73 (C-5), 135.84 (C-2″), 133.31 (2C, C-2′ and C-6′), 132.16 (C-6″), 125.80 (C-1″), 121.56 (C-1′), 117.53 (C-3), 117.11 (C-5″), 113.65 (C-6), 112.55 (2C, C-3′ and C-5′) and 110.27 (C-3″). **HRMS** (ESI) [M+H]⁺ calculated for $C_{17}H_9Br_3ClO_4$, 548.7734; found, 548.7715
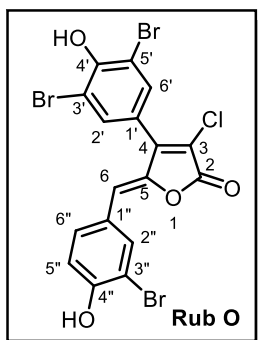
4.8. Synthesis of rubrolides analogous 14a-d and 15

5-(benzo[*d*][1,3]dioxol-5-ylmethylene)-3-chloro-4-(4-fluoro-2-methoxyphenyl)furan-2,5*H*-one (14a)

Compound **14a** was synthesized using a method similar to that of **4** from compound **5d** and was isolated as yellow solid in 57% yields; purified by column chromatography, eluent hexane/ethyl acetate (8:2 v/v). **¹H NMR** (400 MHz, CDCl₃) δ: 7.45 (s, 1H, H-6′), 7.31-7.21 (m, 1H, H-3′), 7.15-7.05 (m, 1H, H-5′), 6.91-6.72 (m, 3H, H-2″, H-5″ and H-6″), 6.01 (s, 2H, H-7″), 5.84 (s, 1H, H-6) and 3.86 (s, 3H, -OCH₃). **¹³C NMR** (100 MHz, CDCl₃) δ: 166.97 (d, J= 243.1 Hz, C-4′), 164.53 (C-2), 158.51 (d, J= 10.0 Hz, C-2′), 148.90 (C-3″), 148.35 (C-4″), 147.35 (C-5), 145.09 (C-4), 131.61 (d, J= 10.6 Hz, C-6′), 127.02 (C-6″), 126.48 (C-1″), 120.02 (C-3), 113.75 (C-6), 112.90 (d, J= 3.1 Hz, C-1′), 110.05 (C-2″), 108.58 (C-5″), 107.59 (d, J= 22.0 Hz, C-5′), 101.59 (C-7″), 100.20 (d, J= 26.0 Hz, C-3′), and 55.96 (-OCH₃). **HRMS** (ESI) [M+H]⁺ calculated for $C_{19}H_{13}ClFO_5$, 375.0436; found, 375.0432
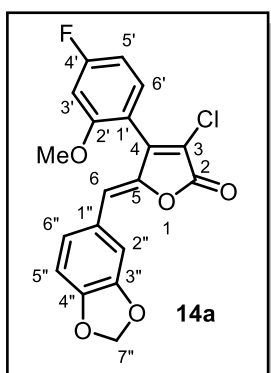
5-(benzo[*d*][1,3]dioxol-5-ylmethylene)-3-chloro-4-(5-chloro-2-methoxyphenyl)furan-2,5*H*-one (14b)

Compound **14b** was synthesized using a method similar to that of **4** from compound **5e** and was isolated as yellow solid in 38% yields; purified by column chromatography, eluent hexane/ethyl acetate (8:2 v/v). **¹H NMR** (400 MHz, CDCl₃) δ: 7.47 (s, 2H, H-6′ and H-2″), 7.26 (br s, 1H, H-4′), 7.13 (d, J= 7.6 Hz, 1H, H-3′), 7.02 (d, J= 8.8 Hz, 1H, H-6″), 6.82 (d, J=

14b
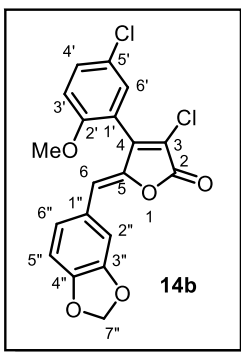
8.8 Hz, 1H, H-5″), 6.02 (s, 2H, H-7″), 5.85 (s, 1H, H-6) and 3.86 (s, 3H, -OCH$_3$). **^{13}C NMR** (100 MHz, CDCl$_3$) δ: 164.35 (C-2), 156.62 (C-2′), 148.99 (C-3″), 148.38 (C-4″), 146.74 (C-5), 144.72 (C-4), 131.57 (C-6′), 130.03 (C-4′), 126.94 (C-1″), 126.62 (C-6″), 125.71 (C-1′), 120.36 (C-5′), 118.44 (C-3), 113.92 (C-3′), 112.97 (C-6), 110.11 (C-5″), 108.61 (C-2″), 101.61 (C-7″), 56.05 (-OCH$_3$). **HRMS** (ESI) [M+H]$^+$ calculated for C$_{19}$H$_{13}$Cl$_2$O$_5$, 391.0140; found, 391.0225

(*Z*)-5-((2-bromopyridin-4-yl)methylene)-3-chloro-4-(4-fluorophenyl)furan-2(5*H*)-one (14c)

Compound **14c** was synthesized using a method similar to that of **4** from compound **5c** and was isolated as yellow solid in 34% yield; purified by column chromatography, eluent hexane/ethyl acetate (6.5:3.5 v/v). The compound **14c** is the mixture of ***Z/E* (0.74/0.26)**

14c
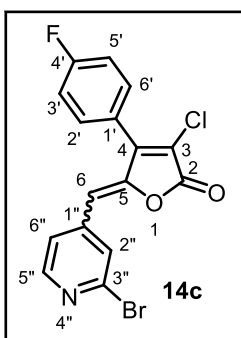
isomers. **^{1}H NMR** (400 MHz, CDCl$_3$) δ: 8.47 (br s, 0.74H/0.26H, H-5″), 8.25 (d, *J*= 7.8 Hz, 0.26H, H-6″), 8.22 (d, *J*= 8.2 Hz, 0.74H, H-6″), 7.65-7.47 (m, 0.74H, H-2″, H-2′ and H-6′; 0.26H, H-2″), 7.46-7.39 (m, 0.26H, H-2′ and H-6′), 7.38-7.16 (m, 0.74H, H-3′ and H-5′), 7.08-6.92 (m, 0.26H, H-3′ and H-5′), 6.05 (s, 0.74H, H-6), 5.89 (s, 0.26H, H-6). **^{13}C NMR** (100 MHz, CDCl$_3$) δ: 167.60 (0.74C, C-2), 167.44 (0.26C, C-2), 164.33 (d, *J*= 231.9 Hz, 0.74C, C-4′), 164.16 (d, *J*= 234.7 Hz, 0.26C, C-4′), 151.48 (0.74C, C-5″), 151.30 (0.26C, C-5″), 148.45 (0.74C, C-3″), 148.27 (0.74C, C-5), 142.72 (0.74C, C-4), 142.17 (0.26C, C-4), 138.97 (0.74C, C-1″), 138.87 (0.26C, C-1″), 131.18 (d, *J*= 8.6 Hz, 0.74C, C-2′ and C-6′), 131.14 (d, *J*= 8.1 Hz, 0.26C, C-2′ and C-6′), 128.61 (0.26C, C-6″), 128.49 (0.74C, C-2″), 128.39 (0.26C, C-2″),127.99 (0.74C, C-6″), 123.45 (d, *J*= 3.2 Hz, C-1″), 120.62 (C-3), 116.66 (d, *J*= 22.1 Hz, 0.74C, C-3′ and C-5′), 115.80 (d, *J*= 21.8 Hz, 0.26C, C-3′ and C-5′), 108.94 (0.74C, C-6), and 107.66 (0.26C, C-6). **HRMS** (ESI) [M+H]$^+$ calculated for C$_{16}$H$_9$BrClFNO$_2$, 379.9489; found, 379.9457

14d
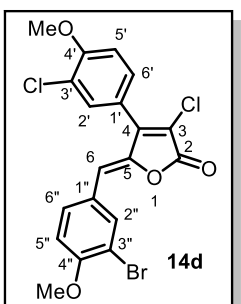
5-(3-bromo-4-methoxybenzylidene)-3-chloro-4-(3-chloro-4-methoxyphenyl)furan-2(5*H*)-one (14d)

Compound **14d** was synthesized using a method similar to that of **4** from compound **7c** and was isolated as yellow solid in 71% yield; purified by column chromatography, eluent hexane/ethyl acetate (8:2 v/v). **^{1}H NMR** (400 MHz, CDCl$_3$) δ: 7.95 (d, *J*= 1.9 Hz, 1H, H-2′), 7.80 (dd, *J*= 1.9 and 8.7 Hz, 1H, H-6′), 7.58 (d, *J*= 2.0 Hz, 1H, H-2″), 7.45 (dd, *J*= 2.0 and 8.5 Hz,

1H, H-6″), 7.13 (d, J= 8.5 Hz, 1H, H-5″), 6.94 (d, J= 8.7 Hz, 1H, H-5′), 6.03 (s, 1H, H-6), 4.03 (s, 3H, -OCH$_3$) and 3.96 (s, 3H, -OCH$_3$). ^{13}C NMR (100 MHz, CDCl$_3$) δ: 164.17 (C-2), 156.88 (C-4″), 156.78 (C-4′), 148.23 (C-4), 145.37 (C-5), 135.56 (C-2″), 131.49 (C-2′), 130.77 (C-6′), 128.98 (C-6″), 126.61 (C-1′), 123.45 (C-1″), 120.87 (C-3′), 118.15 (C-3), 112.89 (C-6), 112.30 (C-5″), 112.22 (C-3″), 111.96 (C-5′), 56.38 (2C, -OCH$_3$). **HRMS** (ESI) [M+H]$^+$ calculated for C$_{19}$H$_{14}$BrCl$_2$O$_4$, 454.9453; found, 454.9432

5-(3-bromo-4-hydroxybenzylidene)-3-chloro-4-(3-chloro-4-hydroxyphenyl)furan-2(5*H*)-one (15)

Compound **14d** was demethylated by boron tribromide to deliver the compound **15** and was isolated as yellow solid in 92% yield; purified by column chromatography, eluent hexane/ethyl acetate (7:3 v/v). ^{1}**H NMR** (400 MHz, Acetone-d$_6$) δ: 9.52 (br, 2H, -OH), 8.03 (d, J= 1.6 Hz, 1H, H-2′), 7.72 (dd, J= 1.6 and 8.5 Hz, 1H, H-6′), 7.63 (d, J= 1.9 Hz, 1H, H-2″), 7.45 (dd, J= 1.9 and 8.4 Hz, 1H, H-6″), 7.23 (d, J= 8.4 Hz, 1H, H-5″), 7.07 (d, J= 8.5 Hz, 1H, H-5′), and 6.29 (s, 1H, H-6). ^{13}**C NMR** (100 MHz, Acetone-d$_6$) δ: 164.53 (C-2), 156.06 (C-4″), 155.81 (C-4′), 149.64 (C-4), 146.08 (C-5), 136.37 (C-2″), 132.51 (C-2′), 131.69 (C-6′), 130.34 (C-6″), 127.34 (C-1′), 121.77 (C-1″), 121.15 (C-3′), 118.00 (C-5″), 117.96 (C-3), 117.57 (C-5′), 113.64 (C-6), 110.85 (C-3″). **HRMS** (ESI) [M+H]$^+$ calculated for C$_{17}$H$_{10}$BrCl$_2$O$_4$, 426.9140; found, 426.9132.
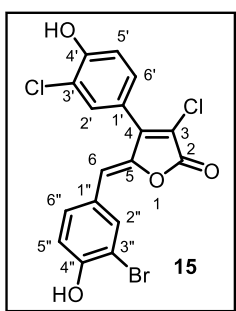
5. References and Notes

[1] For total synthesis of selected marine butenolides, see: [**Ref. 1-9**] BOUKOUVALAS, J.; MALTAIS, F.; LACHANCE, N. Furanolate-based strategy for sequential 2,3,4-trisubstitution of butenolide: Total synthesis of nostoclides I and II. Tetrahedron Lett., v. 35, p. 7897-7900, **1994**.

[2] BELLINA, F.; ROSSI, R. Synthetic Applications of 3,4-Dihalo-2(5H)-furanones: A Formal Total Synthesis of Nostoclides I and II. Synthesis, v. 18, p. 2729-2732, **2002**.

[3] BOUKOUVALAS, J.; POULIOT, M. Short and Efficient Synthesis of Cadiolide B. Synlett, v. 2, p. 343-345, **2005**.

[4] KAR, A.; GOGOI, S.; ARGADE, N. P. Synthesis of naturally occurring bioactive butyrolactones: maculalactones A–C and nostoclide I. Tetrahedron, v. 61, p. 5297-5302, **2005**.

[5] BOUKOUVALAS, J.; ROBICHAUD, J.; MALTAIS, F. A Unified Strategy for the Regiospecific Assembly of Homoallyl-Substituted Butenolides and γ-Hydroxybutenolides: First Synthesis of Luffariellolide. Synlett, v. 2006, p. 2480-2482, **2006**.

[6] PEIXOTO, P. A.; BOULANGÉ, A.; LELEU, S.; FRANCK, X. Versatile Synthesis of Acylfuranones by Reaction of Acylketenes with α-Hydroxy Ketones: Application to the One-Step Multicomponent Synthesis of Cadiolide B and Its Analogues. Eur. J. Org. Chem., v. 2013, p. 3316-3327, **2013**.

[7] NGI, S. I.; PETRIGNET, J.; DUWALD, R.; EL HILALI, E. M.; ABARBRI, M.; DUCHÊNE, A.; THIBONNET, J. Copper-Catalyzed Domino Route to Natural Nostoclides and Analogues: A Total Synthesis of Nostoclides I and II. Adv. Synth. Catal., v. 355, p. 2936-2941, **2013**.

[8] BOULANGÉ, A.; PARRAGA, J.; GALÁN, A.; CABEDO, N.; LELEU, S.; SANZ, M. J.; CORTES, D.; FRANCK, X. Synthesis and antibacterial activities of cadiolides A, B and C and analogues. Bioorg. Med. Chem., v. 23, p. 3618-3628, **2015**.

[9] BOUKOUVALAS, J.; THIBAULT, C. Step-Economical Synthesis of the Marine Ascidian Antibiotics Cadiolide A, B, and D. J. Org. Chem., v. 80, p. 681-684, **2015**.

[10] For reviews on butenolides, see: [**Ref. 10-16**]. CARTER, N. B.; NADANY, A. E.; SWEENEY, J. B. Recent developments in the synthesis of furan-2(5H)-ones. J. Chem. Soc., Perkin Trans. 1, v. 21, p. 2324-2342, **2002**.

[11] BELLINA, F.; ROSSI, R. Mucochloric and Mucobromic Acids: Inexpensive, Highly Functionalised Starting Materials for the Selective Synthesis of Variously Substituted 2(5H)-Furanone Derivatives, Sulfur- or Nitrogen-Containing Heterocycles and Stereodefined Acyclic Unsaturated Dihalogenated Compounds. Curr. Org. Chem., v. 8, p. 1089-1103, **2004**.

[12] DE SOUZA, M. V. N. The Furan-2(5H)-ones: Recent Synthetic Methodologies and its Application in Total Synthesis of Natural Products. Mini Rev. Org. Chem., v. 2, p. 139-145, **2005**.

[13] CUNHA, S.; OLIVEIRA, C. C. Aplicações sintéticas do ácido mucobrômico e da 3,4-dibromofuran-2(5H)-ona. Quim. Nova, v. 34, p. 1425-1438, **2011**.

[14] ZHANG, J.; SARMA, K. D.; CURRAN, T. T. Recent Progress in the Chemistry of Mucohalic Acids: Versatile Building Blocks in Organic Synthesis. Synlett, v. 24, p. 550-569, **2013**.

[15] ZHANG, J.; ZHANG, Y. Reinvestigation of Mucohalic Acids: Recent Development and Application in Drug Discovery. Chinese J. Org. Chem., v. 33, p. 409, **2013**.

[16] BARBOSA, L C. A.; TEIXEIRA, R. R.; AMARANTE, G. W. Synthetic Strategies for the Preparation of Butenolides and Their Transformation into Other Derivatives. Curr. Org. Synth., v. 12, p. 746-771, **2015**.

[17] MIAO, S.; ANDERSEN, R. J. Rubrolides A-H, metabolites of the colonial tunicate Ritterella rubra. J. Org. Chem., v. 56, p. 6275-6280, **1991**.

[18] ORTEGA, M. A. J.; ZUBíA, E.; OCAÑA, J. M.; NARANJO, S.; SALVÁ, J. New Rubrolides from the Ascidian Synoicum blochmanni. Tetrahedron, v. 56, p. 3963-3967, **2000**.

[19] PEARCE, A. N.; CHIA, E. W.; BERRIDGE, M. V.; MAAS, E. W.; PAGE, M. J.; WEBB, V. L.; HARPER, J. L.; COPP, B. R. E/Z-Rubrolide O, an Anti-inflammatory Halogenated Furanone from the New Zealand Ascidian Synoicum n. sp. J. Nat. Prod., v. 70, p. 111-113, **2007**.

[20] SIKORSKA, J.; PARKER-NANCE, S.; DAVIES-COLEMAN, M. T.; VINING, O. B.; SIKORA, A. E.; MCPHAIL, K. L. Antimicrobial Rubrolides from a South African Species of Synoicum Tunicate. J. Nat. Prod., v. 75, p. 1824-1827, **2012**.

[21] WANG, W.; KIM, H.; NAM, S.-J.; RHO, B. J.; KANG, H. Antibacterial Butenolides from the Korean Tunicate Pseudodistoma antinboja. J. Nat. Prod., v. 75, p. 2049-2054, **2012**.

[22] SMITHA, D.; KUMAR, M. M. K.; RAMANA, H.; RAO, D. V. Rubrolide R: a new furanone metabolite from the ascidian Synoicum of the Indian Ocean. Nat. Prod. Res., v. 28, p. 12-17, **2013**.

[23] ZHU, T.; CHEN, Z.; LIU, P.; WANG, Y.; XIN, Z.; ZHU, W. New rubrolides from the marine-derived fungus Aspergillus terreus OUCMDZ-1925. J. Antibiot., v. 67, p. 315-318, **2014**.

[24] MANZANARO, S.; SALVÁ, J.; DE LA FUENTE, J. Á. Phenolic Marine Natural Products as Aldose Reductase Inhibitors§. J. Nat. Prod., v. 69, p. 1485-1487, **2006**.

[25] Biologically active rubrolide analogues from our group, see [**Ref 25-28**]. BARBOSA, L. C. A.; MALTHA, C. R. A.; LAGE, M. R.; BARCELOS, R. C.; DONÀ, A.; CARNEIRO, J. W. M.; FORLANI, G. Synthesis of Rubrolide Analogues as New Inhibitors of the Photosynthetic Electron Transport Chain. J. Agri. Food Chem., v. 60, p. 10555-10563, **2012**.

[26] PEREIRA, U. A.; BARBOSA, L. C. A.; MALTHA, C. R. A.; DEMUNER, A. J.; MASOOD, M. A.; PIMENTA, A. L. Inhibition of Enterococcus faecalis biofilm formation by highly active lactones and lactams analogues of rubrolides. Eur. J. Med. Chem., v. 82, p. 127-138, **2014**.

[27] PEREIRA, U. A.; BARBOSA, L. C. A.; MALTHA, C. R. A.; DEMUNER, A. J.; MASOOD, M. A.; PIMENTA, A. L. γ-Alkylidene-γ-lactones and isobutylpyrrol-2(5H)-ones analogues to rubrolides as inhibitors of biofilm formation by Gram-positive and Gram-negative bacteria. Bioorg. Med. Chem. Lett., v. 24, p. 1052-1056, **2014**.

[28] VAREJÃO, J. O. S.; BARBOSA, L. C. A.; RAMOS, G. Á.; VAREJÃO, E. V. V.; KING-DÍAZ, B.; LOTINA-HENNSEN, B. New rubrolide analogues as inhibitors of photosynthesis light reactions. J. Photochem. Photobiol. B, v. 145, p. 11-18, **2015**.

[29] KOTORA, M.; NEGISHI, E.-I. Highly Efficient and Selective Procedures for the Synthesis of γ-Alkylidenebutenolides via Palladium-Catalyzed Ene-Yne Coupling and Palladium- or Silver Catalyzed Lactonization of (Z)-2-En-4-ynoic Acids. Synthesis of Rubrolides A, C, D, and E. Synthesis, v. 01, p. 121-128, **1997**.

[30] BOUKOUVALAS, J.; LACHANCE, N.; OUELLET, M.; TRUDEAU, M. Facile access to 4-aryl-2(5H)-furanones by Suzuki cross coupling: Efficient synthesis of rubrolides C and E. Tetrahedron Lett., v. 39, p. 7665-7668, **1998**.

[31] KAR, A.; ARGADE, N. P. A Facile Synthesis of Rubrolide E. Synthesis, v. 14, p. 2284-2286, **2005**.

[32] CACCHI, S.; FABRIZI, G.; GOGGIAMANI, A.; SFERRAZZA, A. Palladium-Catalyzed Reaction of Arenediazonium Tetrafluoroborates with Methyl 4-Hydroxy-2-butenoate: An Approach to 4-Aryl Butenolides and an Expeditious Synthesis of Rubrolide E. Synlett, v. 08, p. 1277-1280, **2009**.

[33] CHAVAN, S. P.; PATHAK, A. B.; PANDEY, A.; KALKOTE, U. R. Short and Efficient Synthesis of Rubrolide E. Synth. Commun., v. 37, p. 4253-4263, **2007**.

[34] TALE, N. P.; SHELKE, A. V.; TIWARI, G. B.; THORAT, P. B.; KARADE, N. N. New Concise and Efficient Synthesis of Rubrolides C and E via Intramolecular Wittig Reaction. Helv. Chim. Acta, v. 95, p. 852-857, **2012**.

[35] BELLINA, F.; ANSELMI, C.; ROSSI, R. Total synthesis of rubrolide M and some of its unnatural congeners. Tetrahedron Lett., v. 43, p. 2023-2027, **2002**.

[36] BOUKOUVALAS, J.; MCCANN, L. C. Synthesis of the human aldose reductase inhibitor rubrolide L. Tetrahedron Lett., v. 51, p. 4636-4639, **2010**.

[37] BELLINA, F.; ANSELMI, C.; MARTINA, F.; ROSSI, R. Mucochloric Acid: A Useful Synthon for the Selective Synthesis of 4-Aryl-3-chloro-2(5H)-furanones, (Z)-4-Aryl-5-[1-(aryl)methylidene]-3-chloro-2(5H)-furanones and 3,4-Diaryl-2(5H)-furanones. Eur. J. Org. Chem., v. 2003, p. 2290-2302, **2003**.

[38] MCDANIEL, D. H.; BROWN, H. C. An Extended Table of Hammett Substitutent Constants Based on the Ionization of Substituted Benzoic Acids. J. Org. Chem., v. 23, p. 420-427, **1958**.

[39] HANSCH, C.; LEO, A.; TAFT, R. W. A survey of Hammett substituent constants and resonance and field parameters. Chem. Rev., v. 91, p. 165-195, **1991**.

[40] ZHANG, J.; BLAZECKA, P. G.; BELMONT, D.; DAVIDSON, J. G. Reinvestigation of Mucohalic Acids, Versatile and Useful Building Blocks for Highly Functionalized α,β-Unsaturated γ-Butyrolactones. Org. Lett., v. 4, p. 4559-4561, **2002**.

[41] BISWAS, K.; GHOLAP, R.; SRINIVAS, P.; KANYAL, S.; SARMA, K. D. [small beta]-Substituted [gamma]-butyrolactams from mucochloric acid: synthesis of (+/-)-baclofen and other [gamma]-aminobutyric acids and useful building blocks. RSC Adv., v. 4, p. 2538-2545, **2014**.

[42] KUMAR, L.; SHARMA, V.; MAHAJAN, T.; AGARWAL, D. D. Instantaneous, Facile and Selective Synthesis of Tetrabromobisphenol A using Potassium Tribromide: An Efficient and Renewable Brominating Agent. Org. Process Res. Dev., v. 14, p. 174-179, **2010**.

[43] BOEHLOW, T. R.; HARBURN, J. J.; SPILLING, C. D. Approaches to the Synthesis of Some Tyrosine-Derived Marine Sponge Metabolites: Synthesis of Verongamine and Purealidin N. J. Org. Chem., v. 66, p. 3111-3118, **2001**.

[44] AITKEN, H. R. M.; FURKERT, D. P.; HUBERT, J. G.; WOOD, J. M.; BRIMBLE, M. A. Enantioselective access to benzannulated spiroketals using a chiral sulfoxide auxiliary. Org. Biomol. Chem., v. 11, p. 5147, **2013**.

[45] MISHRA, A. K.; NAGARAJAIAH, H.; MOORTHY, J. N. Trihaloisocyanuric Acids as Atom-Economic Reagents for Halogenation of Aromatics and Carbonyl Compounds in the Solid State by Ball Milling. Eur. J. Org. Chem., v. 2015, p. 2733-2738, **2015**.

[46] HOU, J.; LI, Z.; JIA, X.-D.; LIU, Z.-Q. Bromination of Arenes Using I2O5-KBr in Water. Synth. Commun., v. 44, p. 181-187, **2013**.

[47] BARBOSA, L. C. A.; MALTHA, C. R. A.; DEMUNER, A. J.; PINHEIRO, P. F.; VAREJÃO, J. O. S.; MONTANARI, R. M.; ANDRADE, N. J. Síntese e avaliação da atividade antimicrobiana de furanonas halogenadas e de compostos análogos aos nostoclídeos. Quim. Nova, v. 33, p. 2020-2026, **2010**.

[48] LIU, G.-Y.; GUO, B.-Q.; CHEN, W.-N.; CHENG, C.; ZHANG, Q.-L.; DAI, M.-B.; SUN, J.-R.; SUN, P.-H.; CHEN, W.-M. Synthesis, molecular docking, and biofilm formation inhibitory activity of 5-substituted 3,4-dihalo-5h-furan-2-one derivatives on Pseudomonas aeruginosa. Chem. Biol. Drug Des., v. 79, p. 628-638, **2012**.

[49] WANG, F.; SUN, J.-R.; HUANG, M.-Y.; WANG, H.-Y.; SUN, P.-H.; LIN, J.; CHEN, W.-M. Design, synthesis and anti-inflammatory evaluation of novel 5-benzylidene-3,4-dihalo-furan-2-one derivatives. Eur. J. Med. Chem., v. 72, p. 35-45, **2014**.

[50] Exposure of **9a** to silica gel for prolonged periods of time resulted in some isomerization; for *(E)/(Z)* isomerization of related compounds by silica gel, see: KRAFFT, G. A.; KATZENELLENBOGEN, J. A. J. Am. Chem. Soc. v. 103, p. 5459–5466, **1981**.

CHAPTER 5

An Efficient Method for the α-Dehalogenation of Butenolides: Application to the Synthesis of Marine Natural Products Rubrolides

1. Introduction

The β-substituted butenolides are found in many natural [1-5] and unnatural products [6-11] with diverse biological activities. Among them, benfurodil hemisuccinate (Eucilat®; **1**), a synthetic drug, used for the chronic treatment of congestive heart failure [6], flupyradifurone (Sivanto®; **2**), a synthetic β-aminosubstituted butenolide insecticide, recently commercialized by *Bayer CropScience* for sucking pest control [10, 11], β-(2,5-dihydroxyphenyl) butenolide (**3**), a synthetic compound has two hydroxyl groups *para* to each other, is as potent as the anti-cancer chemotherapy drug Adriamycin® [8]. Moreover, amisnolide (**4**), a β-benzenoid substituted butenolide natural product, recently has been isolated from the *Amischotolype hispida* plant [5]. The biological activity of amisnolide has yet to be uncovered.
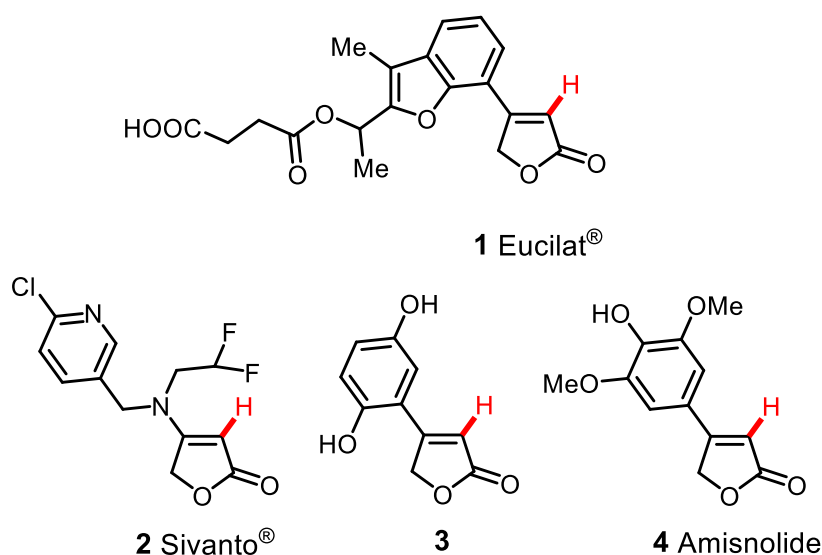
Figure 5.1 Examples of some natural and unnatural β-substituted butenolides

Mucohalic acids, such as the mucochloric acid **5a** and mucobromic acid **5b** are commercially available and are also synthesized from furfural [12-15] which can be obtained by heating of xylose containing biomass with sulfuric acid (Scheme 5.1) [16]. Mucohalic acids **5a-b** can be easily reduced by using sodium borohydride and sulfuric acid to afford α,β-dihalo butenolides **6a-b** in high yields (Scheme 5.1) [17].

The α,β-dihalo butenolides **6a-b** [15, 18, 19] are highly functionalized compounds, fairly stable, inexpensive, and also commercially available that have been frequently used in the site-selective synthesis to prepare α-halo-β-substituted butenolides as potential chemical intermediates [20-33]. Although the most frequent methods used for synthesizing β-substituted butenolides are based on the transition metal catalyzed coupling reactions of

tetronic acid derivatives, α-dehalogenation could be a useful method to prepare β-substituted butenolides, as a chemical application of furfural presents an important example of using a renewable resource from biomass.
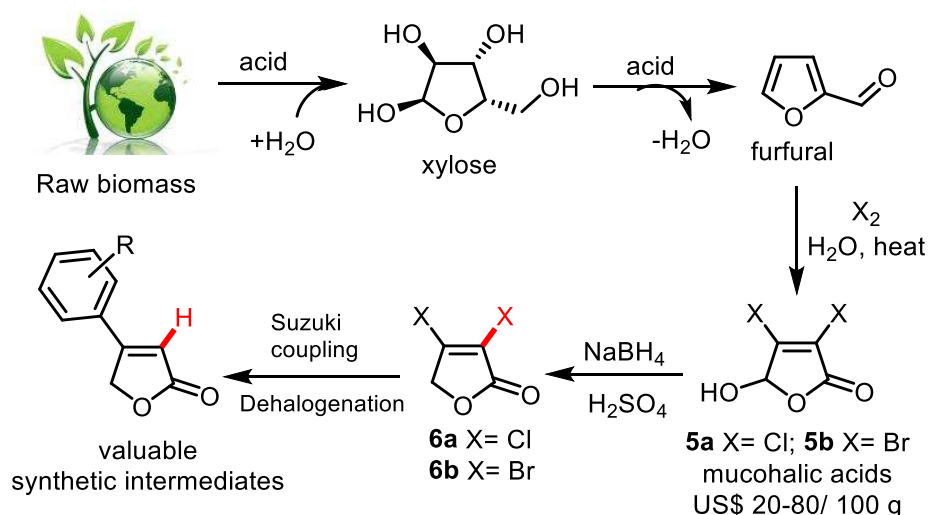
Scheme 5.1 Schematic diagram of preparation of β-arylsubstituted butenolides from biomass

Conventional methods for reducing C–X (X= Cl, Br, I, etc.) bonds are performed through transition-metal catalysts with molecular hydrogen, metal hydrides, or other hydrogen sources such as formic acid and its salts, hydrazine, etc [34-39]. Some of these procedures are often problematic to practically-conduct in the laboratory since the molecular hydrogen and metal hydrides ignite easily. More recently, a visible light photoredox-mediated radical reductive dehalogenation protocol was also developed (Scheme 5.2) [40, 41].
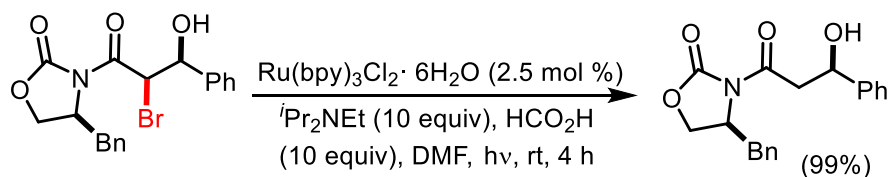
Scheme 5.2 Reductive dehalogenation *via* electron-transfer photoredox catalysis [40]

Although several aromatic including heteroaromatic halides have been used as substrates in the dehalogenation reactions [42, 43], surprisingly little is known concerning the availability of butenolides. The few relevant examples that employ only *N*-monosubstituted tetronamides in combination with palladium catalyst leading to the α-dehalogenated products (Scheme 5.3) [44, 45]. Furthermore, Rossi and co-workers reported the dehalogenation reaction of α-bromo-β-aryl-2(5*H*)-furanones affording only two examples; one was obtained

by using a palladium catalyst and another one was achieved by employing activated zinc catalyst with the yields of 41% and 74% respectively [20, 25].
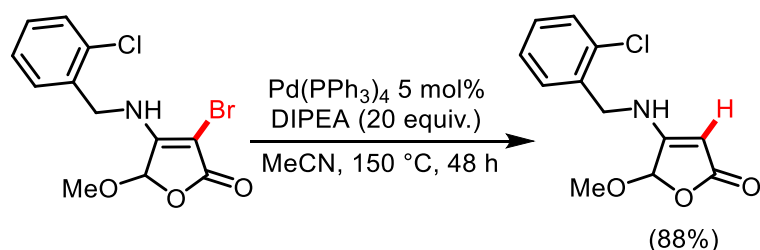
Scheme 5.3 Palladium catalyzed reductive dehalogenation of tetronamides [45]

Reported in this Chapter, is the hitherto less explored reductive dehalogenation of α-halo-β-substituted butenolides under mild conditions with high yields and regioselectivity. In addition, a new synthesis of marine natural products rubrolide E and F [1, 2] and the compound with the structure corresponding to that reported for naturally occurring 3"-bromorubrolide F [2] has been reported by employing this protocol.

2. Results and Discussion

2.1. Preparation of α-Halo-β-Substituted Butenolides

The starting α-halo-β-substituted butenolides of the present work were prepared by utilizing the procedures discussed in Chapter 2 and 3 [33, 46]. Thus, palladium catalyzed Suzuki-Miyaura reaction of **6a-b** with the appropriate boronic acids afforded **7a-i** in high yields (Scheme 5.4). On other hand, treatment of α,β-dichlorobutenolide **6a** with amines in the presence of $NaHCO_3$ at room temperature readily accomplished an aza-Michael addition/elimination to deliver the α-halotetronamides **7k-l** in good yields (Scheme 5.4).
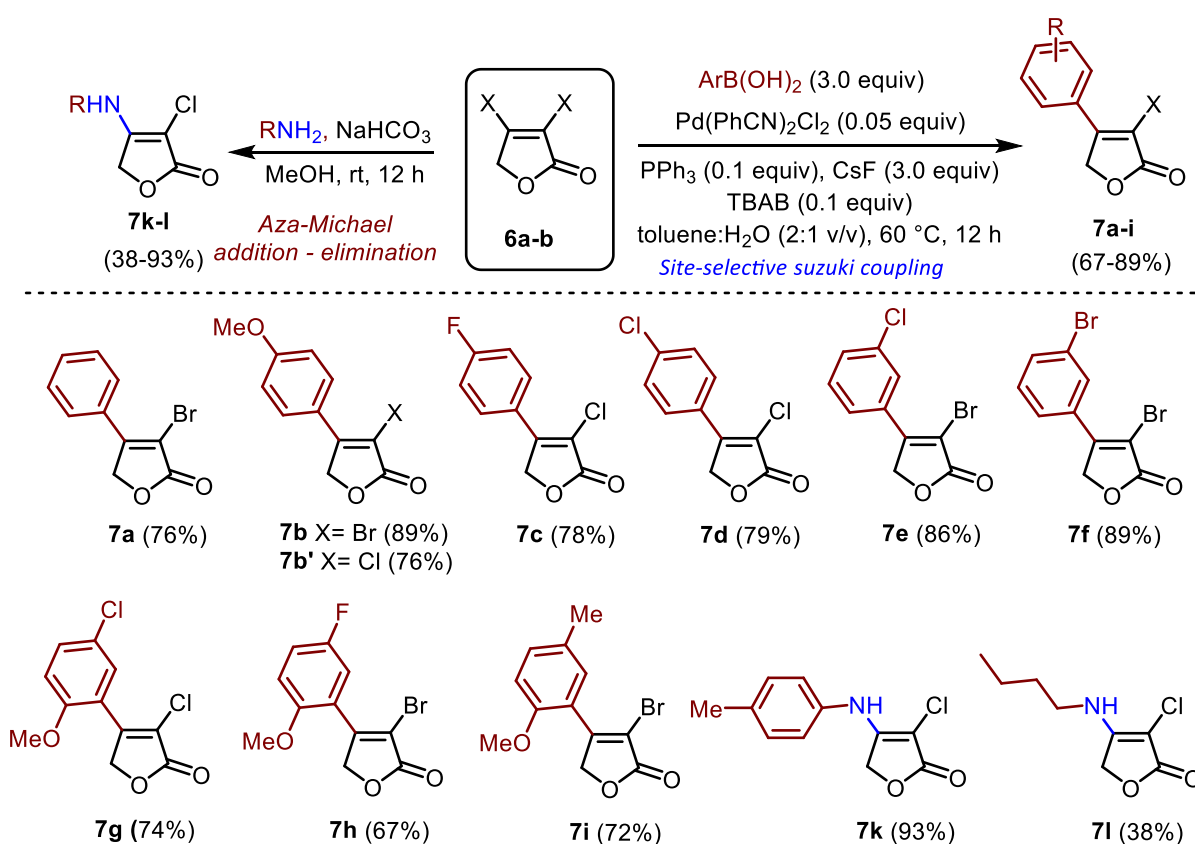
Scheme 5.4 Preparation of α-halo-β-substituted butenolides (all yields are isolated)

However, compound **7j** was prepared by a procedure that previously reported by Barbosa et al. few years back [47]. The isopropyl group insertion at the β–position of compound **6b** was performed by using isopropylmagnesium bromide with $CuBr.Me_2S$ and $BF_3.Et_2O$ (Scheme 5.5). A Grignard reaction was performed to prepare isopropylmagnesium bromide by using magnesium metal with isopropyl bromide in THF as a solvent.
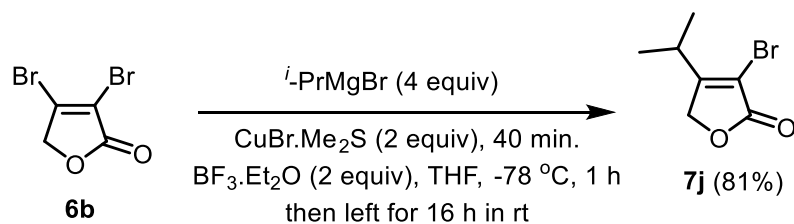
Scheme 5.5 Preparation of 3-bromo-4-isopropylfuran-2(5H)-one (**7j**)

2.2. Optimization of the Dehalogenation Reaction

To assess the improvement in yields of the α-dehalogenation reaction, compound **7a** was subjected to a range of catalysts, ligands, hydrogen sources/bases and solvent combinations as outlined in Table 5.1.

Table 5.1 Optimization of the reductive dehalogenation of **7a**

Entry	Catalysts[a]	Ligand[b]	Hydrogen Sources[c]	Solvent	Yield[f] (%)
1	Pd(OAc)$_2$	PPh$_3$	Et$_3$N[d]	DMF	29
2	Pd(PPh$_3$)$_4$	-	Et$_3$N[d]	DMF	21
3	PdCl$_2$(PPh$_3$)$_2$	-	Et$_3$N	DMF	26
4	Pd(PhCN)$_2$Cl$_2$	PPh$_3$	Et$_3$N[d]	DMF	58
5	Pd(MeCN)$_2$Cl$_2$	PPh$_3$	Et$_3$N[d]	DMF	59
6	Pd(MeCN)$_2$Cl$_2$	PPh$_3$	Et$_3$N	DMF	47
7	Pd(MeCN)$_2$Cl$_2$	AsPh$_3$	Et$_3$N[d]	DMF	31
8	Pd(MeCN)$_2$Cl$_2$	dppf	Et$_3$N	DMF	22
9	Pd(MeCN)$_2$Cl$_2$	PPh$_3$	DIPEA[d]	DMF	61
10	Pd(MeCN)$_2$Cl$_2$	PPh$_3$	DIPEA[d]	MeCN	64
11	Pd(MeCN)$_2$Cl$_2$	PPh$_3$	DIPEA[d]	Toluene	56
12	Pd(MeCN)$_2$Cl$_2$	PPh$_3$	DIPEA[d]	DCM	33
13	Pd(MeCN)$_2$Cl$_2$	PPh$_3$	DIPEA[d]	DMSO	58
14	Pd(MeCN)$_2$Cl$_2$	PPh$_3$	DIPEA[d]	Dioxane	47
15[e]	Pd(OAC)$_2$/ Pd(MeCN)$_2$Cl$_2$	PPh$_3$	DIPEA[d]	MeCN	81

[a] catalysts (5.0 mol%); [b] ligands (10.0 mol%); [c] hydrogen sources/base (5.0 equiv.); [d] equimolar HCOOH was used with the bases together (5.0 equiv. each); [e] each catalysts were used 2.5 mol%; [f] Isolated yield after purification.

Adaptation of the conditions of Rossi et al. [20], were reasonably effective in providing the desired dehalogenation product **8a** (29% yield, Table 5.1, entry 1). Next, the impacts of different catalysts were evaluated (entry 2–5). It was found that $Pd(PhCN)_2Cl_2$ (entry 4) and $Pd(MeCN)_2Cl_2$ (entry 5) worked better than the others. These conditions provided the reduced product in 58 and 59% yields, respectively. Interestingly, addition of equimolar formic acid with triethylamine improves the yield significantly (entry 5 *vs* 6). Replacing the ligand triphenylphosphine with triphenylarsine or dppf did not improve the yields, anyway (entries 7–8). Between two organic bases (entries 5 *vs* 9), DIPEA gives a little better results over triethylamine, and the yield of **8a** is 61% (entry 9). Subsequent optimization revealed that acetonitrile is the best choice of the solvent (entry 9–14). It was found that less polar solvent like dichloromethane, toluene, dioxane etc. was detrimental to product yields (entries 11–12 and 14 *vs* entries 9–10). Ultimately, it was found that equimolar $Pd(OAC)_2/Pd(MeCN)_2Cl_2$ catalytic system under the above mentioned condition improved the product yield significantly (entry 15; 81% yields).

2.3.   Substrates Scope of the Dehalogenation Reaction

Having established a simple and efficient method to access **8a** in high yields, the next task was to investigate the substrate scope.
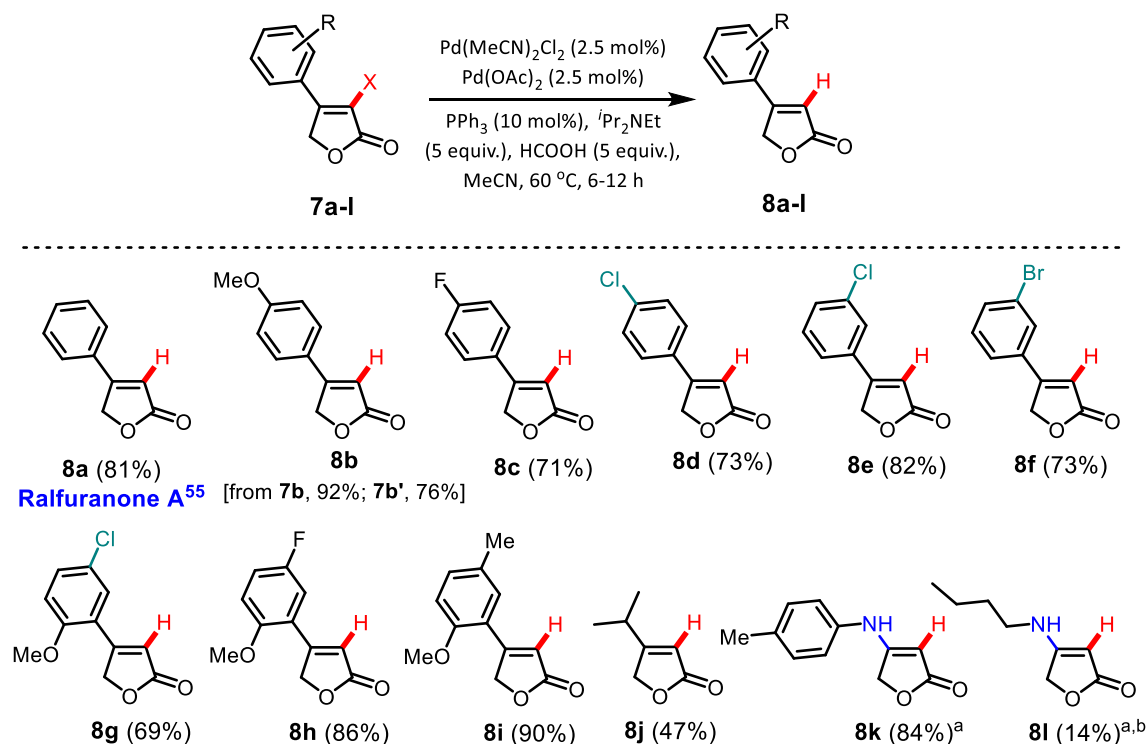
Scheme 5.6 Substrates scope of the dehalogenation reactions (all yields are isolated). [a] Reaction was performed at 120 °C for 16 h. [b] 80% of the starting material (**8l**) was recovered.

The scope of this process is illustrated by the examples detailed in Scheme 5.6. The optimized reaction conditions successfully allowed the reduction of both C_{sp2}–Br and C_{sp2}–Cl bonds at the α–position selectively in the presence of different β-substituted groups. The results show that product yields are generally good to excellent (69–93%). When β-aromatic ring was substituted by strong EDGs such as methoxy and methyl groups, excellent product yields were obtained (compounds **8b** and **8i**). Interestingly, β-aromatic group substituted by both EDGs and EWGs such as methoxy, chloro and fluoro (compounds **8g**-**h**) or solely substituted by EWGs such as fluoro (compound **8c**) the product yields are still very good. Furthermore, excellent selectivity was found for the reductive dehalogenation of α–substituted bromides and chlorides over β-substituted aryl halides (compounds **8d**-**g**). Importantly, good results were obtained with a β-alkylsubstituted butenolide tried, providing the dehalogenated product in moderate yield (compound **8j**). Apart from the β-aryl substituents, β-amino substituents also provided the moderate to very good yield under optimized conditions (compounds **8k**-**I**).

2.4. Plausible Pd-catalyzed Dehalogenation Mechanism

According to previous studies [40, 45], this Pd-catalyzed dehalogenation mechanism
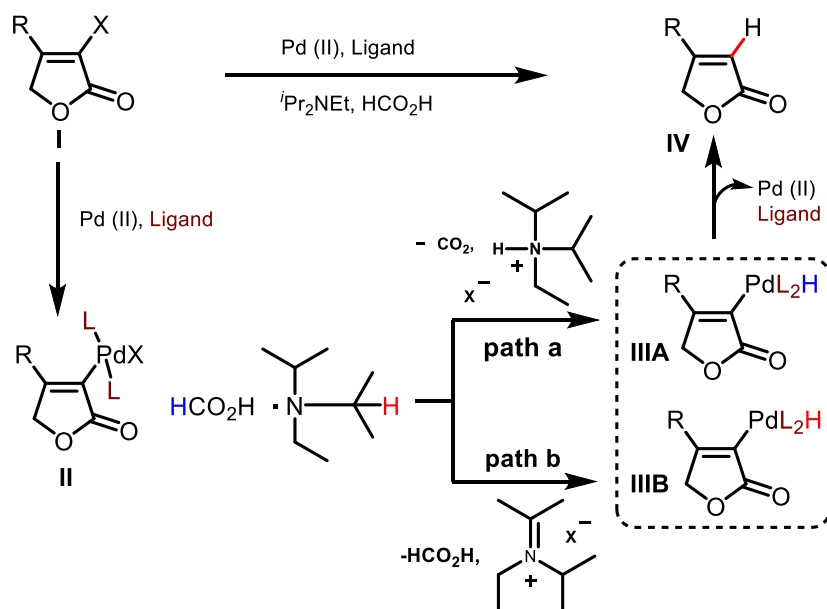
Figure 5.2 Plausible Pd-catalyzed Dehalogenation Mechanism [40, 45]

involves the initial reaction of substrates **I** with Pd(II) to form the desired intermediate **II** (Figure 5.2). Then, the halogen anion (X⁻) is replaced by the palladium-hydride complex either *via* **IIIA** or **IIIB**, which can be accomplished by the abstraction of a hydrogen atom from the methine carbons of the cationic of ${}^{i}Pr_2NEt$ (**path b**) or from formic acid (**path a**).

However, it was reported that ^{i}Pr$_2$NEt likely to be the major hydrogen atom source in the reduction step [40]. Finally, the intermediates **IIIA** and **IIIB** affords the reduced product **IV** and regenerates the Pd(II) catalyst.

2.5.   One-pot Sequential Suzuki Coupling and Reductive Dehalogenation

The developed methodology has also been extended to one-pot sequential dehalogenation reactions for the preparation of β-arylsubstituted butenolides. Thus, after completion of the Suzuki–Miyaura cross-coupling of **6b** with the appropriate boronic acids under the standard conditions, Pd(OAc)$_2$, DIPEA and formic acid were subsequently added to the reaction mixture and heated at the same temperature for another 6h. The dehalogenation products **8b-c** could be obtained in 57 and 39%, respectively (Scheme 5.7).
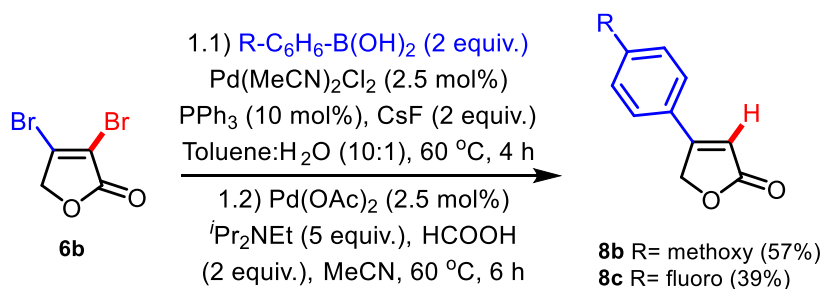
Scheme 5.7 One-pot sequential Suzuki coupling and reductive dehalogenation

Although the one-pot Suzuki coupling and reductive dehalogenation reactions works well, the percentage of yields are relatively lower than the previous methods (Scheme 5.6 *vs* Scheme 5.7). Another problem associated to this one-pot method is the complex mixture of byproducts (e.g. triphenyl phosphine oxide, low amount of α,β-diaryl butenolides) along with the desired products make it difficult to separate due to similar chromatographic mobility.

2.6.   Synthesis of Rubrolides E, F and 3''-Bromorubrolide F

The utility of α-dehalogenation reaction has been demonstrated by the application to the synthesis of marine natural products rubrolides E, F and 3"-bromorubrolide F [1, 2]. Rubrolides E and F were first isolated from a marine tunicate *Ritterella rubra* and possessed antibacterial as well as protein phosphatases 1 and 2A inhibition activity [1]. Lately, 3''-bromorubrolide F was isolated from *Synoicum globosum* ascidian along with rubrolide E and F and showed moderate antibacterial activity [2]. More recently, rubrolides E, F and 3''-bromorubrolide F were shown to inhibit NO (nitric oxide) production at a concentration of 10.53, 8.53 and 11.91 µmol/L, respectively [48].

The simple molecular architecture in conjunction with diverse biological activities of rubrolides have attracted the attention from synthetic community for nearly two decades [22, 26, 33, 49-54]. Among them, rubrolide E was synthesized by several research groups, to date [50-54]. More recently, Jun et al. reported a new synthesis of rubrolide E and the first syntheses of rubrolides F, R, S and 3''-bromorubrolide F using Wittig-Horner reaction, and SeO$_2$-induced tandem allylic hydroxylation/intramolecular cyclization as key steps [48].

Notwithstanding the individual merits of Jun's strategy [48], as yet, none have been shown the protecting group free approach to the preparation of rubrolide F and 3''-bromorubrolide F. Herein, therefore, a concise, protecting group free and step-economical approach to these target rubrolides has been reported from an unprotected lactone moiety **8m** as illustrated in Scheme 5.8.
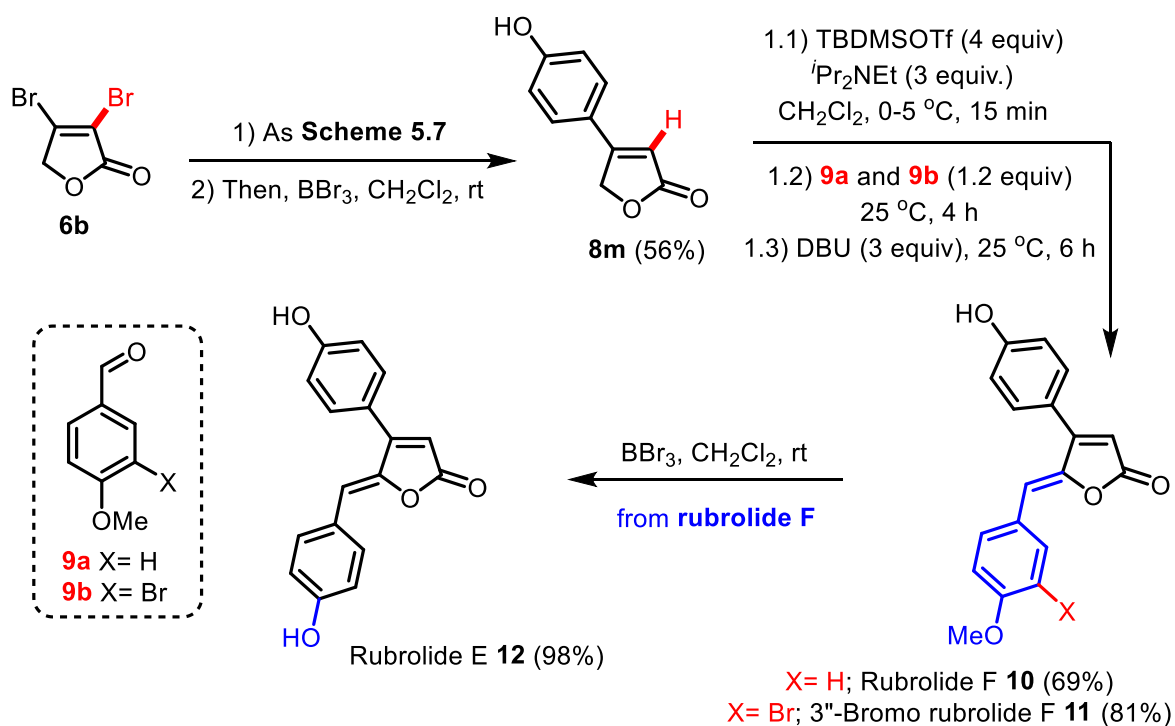
Scheme 5.8 Total synthesis of rubrolides E (**12**), F (**10**) and 3''-bromo rubrolide F (**11**)

Thus, one-pot sequential Suzuki coupling and reductive dehalogenation reaction of **6b** provided **8b** which was further treated with boron tribromide to afford **8m** in 56% overall yield. Subsequently, one-pot vinylogous aldol condensation of unprotected lactone **8m** with 4-methoxybenzaldehyde (**9a**) and 3-bromo-4-methoxybenzaldehyde (**9b**) readily delivered rubrolide F (**10**) and proposed structure of 3''-bromorubrolide F (**11**) in 69 and 81% yields, respectively (Scheme 5.8). Furthermore, exposure of rubrolide F to boron tribromide

accomplished removal of benzylidene methyl group to furnish natural product rubrolide E (**12**) in 98% yield (Scheme 5.8).

Physical and spectroscopic data for the synthetic rubrolides E and F are in excellent agreement with that reported in the literature[1, 2]. However, from HMBC correlations, it was observed that C-1" and C-3" peaks in ^{13}C NMR of synthetic rubrolide **11** were significantly different from those reported in the literature for 3"-bromo rubrolide F [2], even though, our spectroscopic data for rubrolide **11** clearly resembles to the data provided by Jun et al. [48].

3. Conclusion

In conclusion, a catalytic, non-toxic method for reductive dehalogenation of butenolides by employing a binary palladium catalytic system has been developed. The reaction conditions are mild, efficient and tolerate various functional groups, allowing highly regioselective reactions in high yields. Moreover, a new protecting group free, step-economical synthesis of marine metabolites rubrolides E, F and proposed structure of 3"-bromorubrolide F has been accomplished by utilizing the developed protocol in high yields.

4. Materials and Methods

4.1. General Experimental

All reactions were performed using analytical grade solvents. Reagents and solvents were purified, when necessary. All reactions were carried out under a protective atmosphere of dry nitrogen. The ^{1}H and ^{13}C NMR spectroscopic data were recorded at 400 and 100 MHz, respectively on a Bruker NMR spectrometer with CDCl$_3$, DMSO-d$_6$ or Acetone-d$_6$ as solvent and in some cases tetramethylsilane (TMS) as internal standard (δ = 0). Chemical shifts of ^{1}H and ^{13}C NMR spectra are reported in ppm. All coupling constants (J values) were expressed in Hertz (Hz). Multiplicities are reported as follows: singlet (s), doublet (d), doublet of doublets (dd), triplet (t), multiplet (m) and broad (br). Infrared spectra were recorded on a Varian 660-IR, equipped with GladiATR scanning from 4000 to 500 cm^{-1}. Melting points are uncorrected and were obtained from MQAPF-301 melting point apparatus (Microquimica, Brazil). High resolution mass spectra were recorded on a Bruker MicroTof (resolution = 10,000 FWHM) under electrospray ionization (ESI) and are given to four decimal places. Analytical thin layer chromatography analysis was conducted on aluminum packed precoated silica gel plates. Column chromatography was performed over silica gel (230-400 mesh).

4.2. General Procedure for the Preparation of Compounds 7a-i

3-bromo-4-phenylfuran-2(5*H*)-one (7a)

To a 50 mL two-neck round-bottom flask α,β-dibromobutenolide **6b** (300 mg, 1.24 mmol) was combined with phenyl boronic acid (302 mg, 2.48 mmol), cesium fluoride (565 mg, 3.72 mmol), Pd(PhCN)$_2$Cl$_2$ (24 mg, 5 mol %), PPh$_3$ (33 mg, 10 mol%), Bu$_4$N$^+$Br$^-$ (40 mg, 10 mol %), and toluene/water (6/3 mL; v/v). The reaction mixture was then degassed for 10 min under flow of nitrogen. The reaction mixture was stirred at 60 °C for 10 h before it was filtered through a pad of Celite. The filtrate was extracted with ethyl acetate (3×15 mL). The combined organic layer was dried over anhydrous Na$_2$SO$_4$, and concentrated under reduced pressure. The crude product was purified by column chromatography on silica gel eluted with hexane/ethyl acetate (9:1 v/v) to afford compound **7a** as white solid in 83% yield (246 mg, 1.03 mmol).
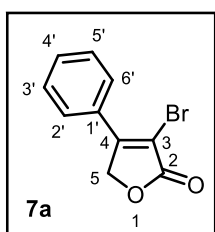
MP: 116.4-117.3 °C. **FTIR:** $\bar{v}_{max}$ 1753, 1608, 1339, 1060, 1039, 987 cm^{-1}. **^{1}H NMR** (400 MHz, CDCl$_3$) δ: 7.83 (d, *J*= 6.9 Hz, 2H, H-2′ and H-6′), 7.60-7.45 (m, 3H, H-3′, H-4′ and H-5′), 5.16 (s, 2H, H-5). **^{13}C NMR** (100 MHz, CDCl$_3$) δ: 169.47 (C-2), 156.18 (C-4), 131.84 (C-1′), 129.21 (C-4′), 129.19 (2C, C-2′ and C-

6'), 127.23 (2C, C-3' and C-5'), 106.41 (C-3), 71.86 (C-5). **HRMS** (ESI) [M+H]$^+$ calculated for C$_{10}$H$_8$BrO$_2$, 238.9708; found, 238.9753

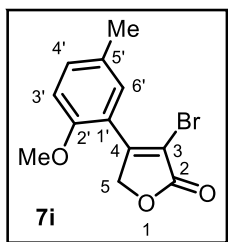**3-bromo-4-(4-methoxyphenyl)furan-2(5*H*)-one (7b)**

Compound **7b** was synthesized using a method similar to that used to prepare **7a** and was isolated as a white solid in 89% yield (297 mg, 1.10 mmol), purified by column chromatography, eluting with hexane/ethyl acetate (8:2, v/v). **MP:** 180.4-181.7 ^{o}C. **FTIR:** $\bar{v}_{max}$ 1775, 1608, 1341, 1054, 1037, 981, 821, 739 cm^{-1}. **^{1}H NMR** (400 MHz, CDCl$_3$) *δ*: 7.84 (d, *J*= 8.6 Hz, 2H, H-2' and H-6'), 7.01 (d, *J*= 8.6 Hz, 2H, H-3' and H-5'), 5.16 (s, 2H, H-5) and 3.88 (s, 3H, -OCH$_3$). **^{13}C NMR** (100 MHz, CDCl$_3$) *δ*: 170.10 (C-2), 162.31 (C-4), 155.19 (C-4'), 126.79 (2C, C-2' and C-6'), 126.22 (C-1'), 114.50 (2C, C-3' and C-5'), 108.31 (C-3), 72.83 (C-5). **HRMS** (ESI) [M+H]$^+$ calculated for C$_{11}$H$_{10}$BrO$_3$, 268.9813; found, 268.9822
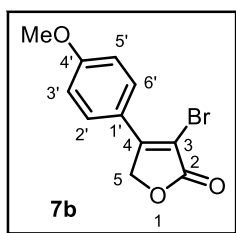
3-chloro-4-(4-methoxyphenyl)furan-2(5*H*)-one (7b')

The detailed synthetic procedure to prepare compound **7b'** has already been discussed in **Chapter 4**, along with the structural characterization by IR, NMR and HRMS.

3-chloro-4-(4-fluorophenyl)furan-2(5*H*)-one (7c)

The detailed synthetic procedure to prepare compound **7c** has already been discussed in **Chapter 4**, along with the structural characterization by IR, NMR and HRMS.

3-chloro-4-(4-chlorophenyl)furan-2(5*H*)-one (7d)

Compound **7d** was synthesized using a method similar to that used to prepare **7a** and was isolated as a white solid in 79% yield (355 mg, 1.55 mmol), purified by column chromatography, eluting with hexane/ethyl acetate (8:2, v/v). **MP:** 170.4-171.3 ^{o}C. **FTIR:** $\bar{v}_{max}$ 3036, 2915, 1746, 1619, 1496, 1318, 1198, 1041, 824 cm^{-1}. **^{1}H NMR** (400 MHz, CDCl$_3$) *δ*: 7.75 (d, *J*= 8.2 Hz, 2H, H-2' and H-6'), 7.50 (d, *J*= 8.2 Hz, 2H, H-3' and H-5'), and 5.20 (s, 2H, H-5). **^{13}C NMR** (100 MHz, CDCl$_3$) *δ*: 168.75 (C-2), 150.55 (C-4), 137.98 (C-4'), 130.60 (C-1'), 129.61 (2C, C-2' and C-6'), 128.51 (2C, C-3' and C-5'), 117.86 (C-3), 69.97 (C-5). **HRMS** (ESI) [M+H]$^+$ calculated for C$_{10}$H$_7$Cl$_2$O$_2$, 228.9823; found, 228.9831
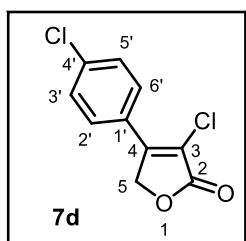
3-bromo-4-(3-chlorophenyl)furan-2(5*H*)-one (7e)

Compound **7e** was synthesized using a method similar to that used to prepare **7a** and was
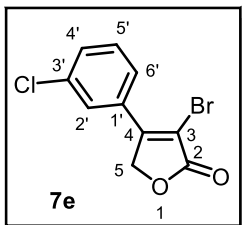
isolated as a light yellow solid in 86% yield (292 mg, 1.07 mmol), purified by column chromatography, eluting with hexane/ethyl acetate (8:2, v/v). **MP**: 190.6-190.9 $^{\circ}$C. **FTIR:** $\bar{v}_{max}$ 3033, 2912, 1749, 1623, 1499, 1315, 1201, 1038, 828 cm^{-1}. **^{1}H NMR** (400 MHz, CDCl$_3$) *δ*: 7.81 (br s, 1H, H-2'), 7.71 (d, *J*= 7.4 Hz, 1H, H-6'), 7.57-7.41 (m, 2H, H-4' and H-5'), 5.17 (s, 2H, H-5). **^{13}C NMR** (100 MHz, CDCl$_3$) *δ*: 169.34 (C-2), 154.71 (C-4), 135.27 (C-1'), 131.70 (C-5'), 130.89 (C-3'), 130.55 (C-4'), 127.14 (C-2'), 125.39 (C-4'), 107.92 (C-3), 71.76 (C-5). **HRMS** (ESI) [M+H]$^+$ calculated for C$_{10}$H$_7$BrClO$_2$, 272.9318; found, 272.9344

3-bromo-4-(3-bromophenyl)furan-2(5*H*)-one (7f)

Compound **7f** was synthesized using a method similar to that used to prepare **7a** and was
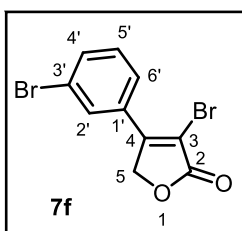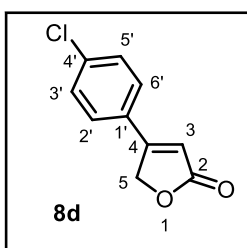

isolated as a light yellow solid in 89% yield (351 mg, 1.10 mmol), purified by column chromatography, eluting with hexane/ethyl acetate (8:2, v/v). **MP:** 198.7-199.4 $^{\circ}$C. **FTIR:** $\bar{v}_{max}$ 3030, 2857, 1751, 1629, 1489, 1314, 1203, 1037, 824, 728, 662, cm^{-1}. **^{1}H NMR** (400 MHz, CDCl$_3$) *δ*: 7.97 (s, 1H, H-2'), 7.78 (d, *J*= 7.5 Hz, 1H, H-6'), 7.69 (d, *J*= 7.5 Hz, 1H, H-4') 7.42 (t, *J*= 7.8 Hz, 1H, H-5'), 5.17 (s, 2H, H-5). **^{13}C NMR** (100 MHz, CDCl$_3$) *δ*: 169.21 (C-2), 154.41 (C-4), 134.62 (C-1'), 131.20 (C-4'), 130.71 (C-5'), 130.01 (C-2'), 125.74 (C-6'), 123.34 (C-3'), 108.14 (C-3), 71.65 (C-5). **HRMS** (ESI) [M+H]$^+$ calculated for C$_{10}$H$_7$Br$_2$O$_2$, 316.8813; found, 316.8842

3-chloro-4-(5-chloro-2-methoxyphenyl)furan-2(5*H*)-one (7g)

The detailed synthetic procedure to prepare compound **7g** has already been discussed in **Chapter 4**, along with the structural characterization by IR, NMR and HRMS.

3-bromo-4-(5-fluoro-2-methoxyphenyl)furan-2(5*H*)-one (7h)
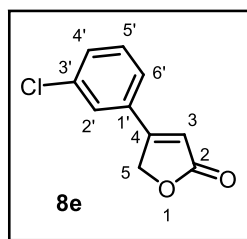
Compound **7h** was synthesized using a method similar to that used to prepare **7a** and was isolated as a white solid in 67% yield (238 mg, 0.83 mmol), purified by column chromatography, eluting with hexane/ethyl acetate (8:2, v/v). **MP:** 202.6-203.9 $^{\circ}$C. **FTIR:** $\bar{v}_{max}$ 3028, 2992, 2908, 2857, 1744, 1608, 1571, 1491, 1350, 1261, 1189, 977, 823, 755, 729 cm^{-1}. **^{1}H NMR** (400 MHz, CDCl$_3$) *δ*: 7.59 (br s, 1H, H-6'), 7.17 (br s, 1H, H-4'), 6.96 (br s,
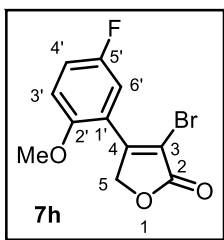
1H, H-3′) 5.25 (s, 2H, H-5) and 3.87 (s, 3H, -OCH₃). ^{13}**C NMR** (100 MHz, CDCl₃) *δ*: 169.39 (C-2), 156.44 (d, *J*= 239.0 Hz, C-5′), 156.04 (C-4), 153.63 (C-2′), 119.44 (d, *J*= 8.7 Hz, C-1′), 118.87 (d, *J*= 23.0 Hz, C-4′), 116.48 (d, *J*= 24.9 Hz, C-6′), 112.67 (d, *J*= 7.8 Hz, C-3′), 108.79 (C-3), 73.45 (C-5) and 56.16 (-OCH₃). **HRMS** (ESI) [M+H]⁺ calculated for C₁₁H₉BrFO₃, 286.9719; found, 286.9759

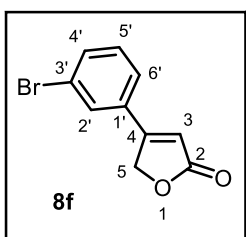### 3-bromo-4-(2-methoxy-5-methylphenyl)furan-2(5*H*)-one (7i)

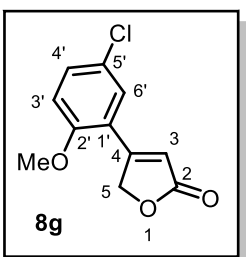Compound **7i** was synthesized using a method similar to that used to prepare **7a** and was isolated as a light orange solid in 72% yield (253 mg, 0.89 mmol), purified by column chromatography, eluting with hexane/ethyl acetate (8:2, v/v). **MP:** 97.9-99.5 °C. **FTIR:** $\bar{v}_{max}$ 3026, 2989, 2955, 2910, 2854, 1749, 1610, 1575, 1494, 1444, 1346, 1260, 1190, 989, 822, 752, 726, 660, 560 cm⁻¹. ^{1}**H NMR** (400 MHz, CDCl₃) *δ*: 7.59 (s, 1H, H-6′), 7.25 (d, *J*= 8.5 Hz, 1H, H-4′), 6.89 (d, *J*= 8.5 Hz, 1H, H-3′) 5.21 (s, 2H, H-5), 3.83 (s, 3H, -OCH₃) and 2.33 (s, 3H, -CH₃). ^{13}**C NMR** (100 MHz, CDCl₃) *δ*: 169.81 (C-2), 157.71 (C-2′), 156.22 (C-4), 133.17 (C-6′), 130.18 (C-4′), 130.11 (C-5′), 118.19 (C-1′), 111.50 (C-3′), 107.42 (C-3), 73.61 (C-5), 55.65 (-OCH₃) and 20.36 (-CH₃). **HRMS** (ESI) [M+H]⁺ calculated for C₁₂H₁₂BrO₃, 282.9970; found, 282.9979

4.3. Procedure for the Preparation of Compounds 7k-l

The detailed synthetic procedure to prepare such tetronamides has already been discussed in **Chapter 2**, along with the structural characterization by IR, NMR and HRMS.

4.4. Preparation of 3-bromo-4-isopropylfuran-2(5*H*)-one (7j)

To a two-neck round bottom flask under nitrogen atmosphere was added magnesium metal (124 mg, 5.1 mmol), anhydrous THF (5 mL), Iodine (catalytic amount) and the solution isopropyl bromide in anhydrous THF (418 mg, 3.4 mmol, 5 mL anhydrous THF). The reaction mixture was kept under magnetic stirring for 40 min. In another two-neck round bottom flask CuBr.Me₂S (175 mg, 0.8 mmol) and THF (5 mL) was added under nitrogen atmosphere at -78 °C. After 5 min under vigorous stirring, this mixture was slowly added to the flask containing Grignard reagent with the aid of syringe. Then a solution of 3,4-dibromofuran- 2 (5*H*) -one (**6b**) (205 mg, 0.85 mmol) and BF₃.Et₂O (241 mg, 1.7 mmol) in 10 mL of anhydrous THF was added to the flask, keeping the temperature at -78 °C for 1 h and room temperature for 16 h. Saturated solution of ammonium chloride (30 mL) was added to the mixture.

Aqueous phase extracted with diethyl ether (3×20 mL) and the organic phase concentrated in a rotary evaporator, dried over anhydrous Na_2SO_4, filtered and concentrated in a rotary evaporator. The lactone **7j** was obtained as yellowish oil in 81% yield (141 mg, 0.69 mmol). **FTIR:** $\bar{v}_{max}$ 1770, 1632, 1348, 1172, 1016, 988, 759 cm^{-1}. **^{1}H NMR** (400 MHz, CDCl$_3$): 4.82 (d, J= 0.7 Hz, 2H, H-5), 3.09 (hept, J= 7.0 Hz, 1H, H-1′), 1.23 (d, J= 7.0 Hz, 6H, -CH$_3$). **^{13}C NMR** (100 MHz, CDCl$_3$): 169.45 (C-2), 169.12 (C-4), 106.83 (C-3), 70.50 (C-5), 28.95 (C-1′), 19.84 (2C, -CH$_3$). **HRMS** (ESI) [M+H]$^+$ calculated for C$_7$H$_{10}$BrO$_2$, 204.9864; found, 204.9833

4.5. General Procedure for the Preparation of Compound 8a-l

4-phenylfuran-2(5H)-one (8a)

To a 25 mL two-neck round-bottom flask compound **7a** (200 mg, 0.82 mmol) was combined with Pd(MeCN)$_2$Cl$_2$ (6 mg, 2.5 mol %), Pd(OAc)$_2$ (5 mg, 2.5 mol %), PPh$_3$ (21 mg, 10 mol%), DIPEA (0.7 ml, 4.1 mmol), formic acid (0.15 ml, 4.1 mmol) and acetonitrile (without further purification, 6 mL). The reaction mixture was then degassed for 10 min under flow of nitrogen. Then the mixture was stirred at 60 °C for 6 h before it was filtered through a pad of Celite. The filtrate was extracted with ethyl acetate (3×15 mL). The combined organic layer was dried over anhydrous Na$_2$SO$_4$, and concentrated under reduced pressure. The crude product was purified by column chromatography on silica gel eluted with hexane/ethyl

acetate (9:1 v/v) to afford compound **8a** as an off-white solid in 81% yield (109 mg, 0.68 mmol).
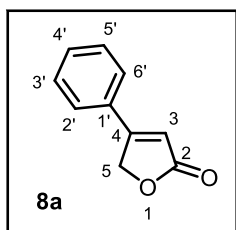
MP: 95.1-96.4 °C. **FTIR:** $\bar{v}_{max}$ 3030, 2910, 1790, 1750, 1710, 1610, 1575, 1348, 1258, 1189, 981, 824, 756, 728 cm^{-1}. **^{1}H NMR** (400 MHz, CDCl3) δ: 7.50 (br s, 5H, H-2′ to H-6′), 6.38 (s, 1H, H-3), 5.23 (s, 2H, H-5). **^{13}C NMR** (100 MHz, CDCl$_3$) δ: 173.86 (C-2), 163.99 (C-4), 131.80 (C-1′), 129.69 (C-4′), 129.32 (2C, C-2′ and C-6′), 126.67 (2C, C-3′ and C-5′), 113.04 (C-3), 71.04 (C-5). **HRMS** (ESI) [M+H]$^+$ calculated for C$_{10}$H$_9$O$_2$, 161.0603; found, 161.0612

4-(4-methoxyphenyl)furan-2(5H)-one (8b)
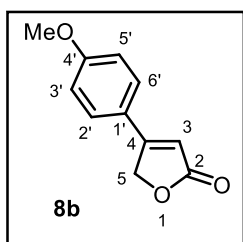
Compound **8b** was synthesized using a method similar to that used to prepare **8a** and was isolated as a white solid in 92 and 76% yields from **7b** and **7b′**, respectively, purified by column chromatography, eluting with hexane/ethyl acetate (7.5:2.5, v/v). **MP:** 120.4-121.3 °C. FTIR: $\bar{v}_{max}$ 3035, 2913, 1785, 1722, 1619, 1572, 1350, 1198, 977 cm^{-1}. **^{1}H**

NMR (400 MHz, CDCl$_3$) δ: 7.67 (d, J= 8.8 Hz, 2H, H-2′ and H-6′), 7.05 (d, J= 8.8 Hz, 2H, H-3′ and H-5′), 6.57 (s, 1H, H-3), 5.33 (d, J= 1.1 Hz, 2H, H-5) and 3.83 (s, 3H, -OCH$_3$). **^{13}C NMR** (100 MHz, CDCl$_3$) δ: 174.52 (C-2), 165.09 (C-4), 162.30 (C-4′), 129.34 (2C, C-2′ and C-6′), 122.67 (C-1′), 114.92 (2C, C-3′ and C-5′), 110.31 (C-3), 71.42 (C-5) and 55.93 (OCH$_3$). **HRMS** (ESI) [M+H]$^+$ calculated for C$_{11}$H$_{11}$O$_3$, 191.0708; found, 191.0717

4-(4-fluorophenyl)furan-2(5*H*)-one (8c)

Compound **8c** was synthesized using a method similar to that used to prepare **8a** and was
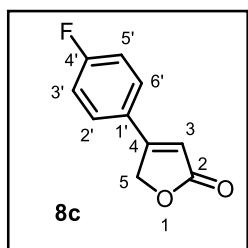
isolated as a light brown solid in 71% yield (119 mg, 0.67 mmol), purified by column chromatography, eluting with hexane/ethyl acetate (7:3, v/v). **MP:** 143.2-144.7 °C. **FTIR:** $\bar{v}_{max}$ 3116, 3068, 1789, 1737, 1628, 1229, 1159, 989 cm^{-1}. **^{1}H NMR** (400 MHz, CDCl$_3$) δ: 7.62-7.45 (m, 2H, H-2′ and H-6′), 7.18 (t, J= 8.1 Hz, 2H, H-3′ and H-5′), 6.34 (s, 1H, H-3), and 5.21 (s, 2H, H-5). **^{13}C NMR** (100 MHz, CDCl$_3$) δ: 173.63

(C-2), 164.64 (d, J= 254.2 Hz, C-4′), 162.67 (C-4), 128.65 (d, J= 8.9 Hz, 2C, C-2′ and C-6′), 126.06 (d, J= 3.3 Hz, C-1′), 116.62 (d, J= 22.2 Hz, 2C, C-3′ and C-5′), 112.87 (C-3), 70.90 (C-5). **HRMS** (ESI) [M+H]$^+$ calculated for C$_{10}$H$_8$FO$_2$, 179.0508; found, 179.0530

4-(4-chlorophenyl)furan-2(5*H*)-one (8d)

Compound **8d** was synthesized using a method similar to that used to prepare **8a** and was

isolated as an off-white in 73% yield (124 mg, 0.64 mmol), purified by column chromatography, eluting with hexane/ethyl acetate (7:3, v/v). **MP:** 174.5-175.2 °C. **FTIR:** $\bar{v}_{max}$ 3024, 2910, 1780, 1749, 1720, 1610, 1579, 1497, 1189, 823, 729 cm^{-1}. **^{1}H NMR** (400 MHz, CDCl$_3$) δ: 7.45 (apparent singlet, 4H, H-2′ to H-6′), 6.37 (s, 1H, H-3), and 5.20 (s, 2H, H-5). **^{13}C NMR** (100 MHz, CDCl$_3$) δ: 173.53 (C-2), 162.51 (C-4),

137.91 (C-4′), 129.65 (2C, C-2′ and C-6′), 128.07 (C-1′), 127.69 (2C, C-3′ and C-5′), 113.54 (C-3), 70.85 (C-5). **HRMS** (ESI) [M+H]$^+$ calculated for C$_{10}$H$_8$ClO$_2$, 195.0231; found, 195.0220

4-(3-chlorophenyl)furan-2(5*H*)-one (8e)

Compound **8e** was synthesized using a method similar to that used to prepare **8a** and was isolated as a light yellow solid in 82% yield (117 mg, 0.6 mmol), purified by column chromatography, eluting with hexane/ethyl acetate (7:3, v/v). **MP:** 175.6-176.2 °C. **FTIR:** $\bar{v}_{max}$ 3028, 2916, 1784, 1754, 1718, 1604, 1574, 1502, 1148, 831, 727 cm^{-1}. **^{1}H**

NMR (400 MHz, CDCl$_3$) δ: 7.51-7.35 (m, 4H, H-2', H-4' to H-6'), 6.39 (s, 1H, H-3) and 5.20 (s, 2H, H-5). **^{13}C NMR** (100 MHz, CDCl$_3$) δ: 173.31 (C-2), 162.37 (C-4), 135.42 (C-1'), 131.65 (C-5'), 131.31 (C-3'), 130.62 (C-4'), 126.49 (C-2'), 124.57 (C-4'), 114.37 (C-3), 70.85 (C-5). **HRMS** (ESI) [M+H]$^+$ calculated for C$_{10}$H$_8$ClO$_2$, 195.0231; found, 195.0201

4-(3-bromophenyl)furan-2(5*H*)-one (8f)

Compound **8f** was synthesized using a method similar to that used to prepare **8a** and was isolated as a white solid in 73% yield (110 mg, 0.46 mmol), purified by column c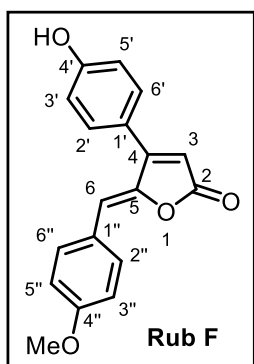hromatography, eluting with hexane/ethyl acetate (7:3, v/v). **MP:** 188.5-189.1 ^{o}C. **FTIR:** $\bar{v}_{max}$ 3034, 2956, 1782, 1756, 1710, 1609, 1578, 1496, 1144, 828, 725 cm^{-1}. **^{1}H NMR** (400 MHz, CDCl$_3$) δ: 7.65 (apparent singlet, 2H, H-2' and H-5'), 7.46 (d, *J*= 7.2 Hz, 1H, H-6'), 7.38 (d, *J*= 7.2 Hz, 1H, H-4') 6.40 (s, 1H, H-3), 5.21 (s, 2H, H-5). **^{13}C NMR** (100 MHz, CDCl$_3$) δ: 173.20 (C-2), 162.25 (C-4), 134.57 (C-1'), 131.67 (C-4'), 130.84 (C-5'), 129.42 (C-2'), 125.01 (C-6'), 123.47 (C-3'), 114.47 (C-3), 70.82 (C-5). **HRMS** (ESI) [M+H]$^+$ calculated for C$_{10}$H$_8$BrO$_2$, 238.9708; found, 238.9721

4-(5-chloro-2-methoxyphenyl)furan-2(5*H*)-one (8g)

Compound **8g** was synthesized using a method similar to that used to prepare **8a** and was isolated as a pink solid in 69% yield (120 mg, 0.53 mmol), purified by column chromatography, eluting with hexane/ethyl acetate (8:2, v/v). **MP:** 201.2-202.7 ^{o}C. **FTIR:** $\bar{v}_{max}$ 3031, 2915, 1780, 1751, 1720, 1608, 1578, 1500, 1151, 823, 724 cm^{-1}. **^{1}H NMR** (400 MHz, CDCl$_3$) δ: 7.40 (dd, *J*= 2.1 and 8.9 Hz, 1H, H-4'), 7.35 (d, *J*= 2.1 Hz, 1H, H-6'), 6.95 (d, *J*= 8.9 Hz, 1H, H-3') 6.56 (s, 1H, H-3), 5.23 (s, 2H, H-5) and 3.92 (s, 3H, -OCH$_3$). **^{13}C NMR** (100 MHz, CDCl$_3$) δ: 174.14 (C-2), 159.41 (C-2'), 156.91 (C-4), 132.25 (C-4'), 127.93 (C-6'), 126.07 (C-1'), 120.08 (C-5'), 116.15 (C-3'), 113.01 (C-3), 72.47 (C-5) and 55.95 (-OCH$_3$). **HRMS** (ESI) [M+H]$^+$ calculated for C$_{11}$H$_{10}$ClO$_3$, 225.0318; found, 225.0324

4-(5-fluoro-2-methoxyphenyl)furan-2(5*H*)-one (8h)

Compound **8h** was synthesized using a method similar to that used to prepare **8a** and was isolated as a white solid in 86% yield (125 mg, 0.6 mmol), purified by column chromatography, eluting with hexane/ethyl acetate (7:3, v/v). **MP:** 199.6-200.2 ^{o}C. **FTIR:** $\bar{v}_{max}$ 3119, 3067, 1790, 1734, 1632, 1227, 1154, 992 cm^{-1}. **^{1}H NMR** (400 MHz, CDCl$_3$) δ:
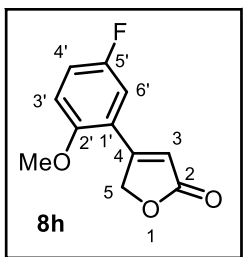
7.22-7.07 (m, 2H, H-3′ and H-4′), 6.99-6.90 (m, 1H, H-6′), 6.55 (s, 1H, H-3) 5.23 (s, 2H, H-5) and 3.91 (s, 3H, -OCH$_3$). **^{13}C NMR** (100 MHz, CDCl$_3$) δ: 174.19 (C-2), 158.23 (C-4), 157.21 (d, J= 239.5 Hz, C-5′), 155.05 (C-2′), 119.53 (d, J= 7.4 Hz, C-1′), 119.05 (d, J= 23.1 Hz, C-4′), 116.01 (C-3), 114.59 (d, J= 24.0 Hz, C-6′), 112.77 (d, J= 8.2 Hz, C-3′), 72.54 (C-5) and 56.05 (-OCH$_3$). **HRMS** (ESI) [M+H]$^+$ calculated for C$_{11}$H$_{10}$FO$_3$, 209.0614; found, 209.0589

4-(2-methoxy-5-methylphenyl)furan-2(5*H*)-one (8i)

Compound **8i** was synthesized using a method similar to that used to prepare **8a** and was isolated as a white solid in 90% yield (130 mg, 0.64 mmol), purified by column chromatography, eluting with hexane/ethyl acetate (7:3, v/v). **MP:** 102.7-103.5 °C. **FTIR:** $\bar{v}_{max}$ 3028, 2991, 2952, 2911, 2859, 1743, 1614, 1576, 1489, 1190, 977, 824, 752 cm^{-1}. **^{1}H NMR** (400 MHz, CDCl$_3$) δ: 7.24 (dd, J= 1.8 and 8.4 Hz, 1H, H-4′), 7.19 (d, J= 1.8 Hz, 1H, H-6′), 6.89 (d, J= 8.4 Hz, 1H, H-3′), 6.52 (s, 1H, H-3), 5.24 (s, 2H, H-5), 3.88 (s, 3H, -OCH$_3$) and 2.32 (s, 3H, -CH$_3$). **^{13}C NMR** (100 MHz, CDCl$_3$) δ: 174.81 (C-2), 161.14 (C-2′), 156.43 (C-4), 133.43 (C-6′), 130.19 (C-4′), 128.66 (C-5′), 118.33 (C-1′), 114.57 (C-3), 111.60 (C-3′), 72.80 (C-5), 55.54 (-OCH$_3$) and 20.34 (-CH$_3$). **HRMS** (ESI) [M+H]$^+$ calculated for C$_{12}$H$_{13}$O$_3$, 205.0865; found, 205.0846
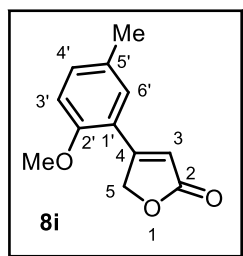
4-isopropylfuran-2(5*H*)-one (8j)

Compound **8j** was synthesized using a method similar to that used to prepare **8a** and was isolated as a light yellow oil in 47% yield (130 mg, 0.64 mmol), purified by column chromatography, eluting with hexane/ethyl acetate (7:3, v/v). **FTIR:** $\bar{v}_{max}$ 1777, 1742, 1629 1341, 1165, 980, 766 cm^{-1}. **^{1}H NMR** (400 MHz, CDCl$_3$): 5.87 (s, 1H, H-3), 4.86 (d, J= 1.8 Hz, 2H, H-5), 2.79 (m, 1H, H-1′), 1.22 (d, J= 7.1 Hz, 6H, -CH$_3$). **HRMS** (ESI) [M+H]$^+$ calculated for C$_7$H$_{11}$O$_2$, 127.0759; found, 127.0756
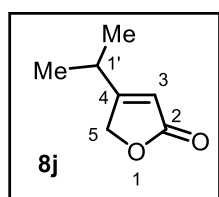
4-(*p*-tolylamino)furan-2(5*H*)-one (8k)

Compound **8k** was synthesized using a method similar to that used to prepare **8a** and was isolated as a white solid in 84% yield, purified by column chromatography, eluting with hexane/ethyl acetate (6:4, v/v). **MP:** 219.3-220.1 °C. **FTIR:** $\bar{v}_{max}$ 3230, 3060, 1744, 1632, 1047, 981, 904, 744, 544 cm^{-1}. **^{1}H NMR** (400 MHz, DMSO-d$_6$) δ 9.62 (s, 1H, -NH), 7.15 (d, J=
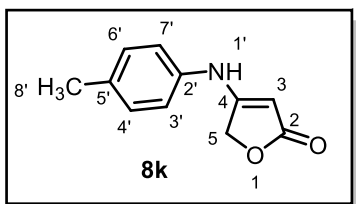
8.3 Hz, 2H, H-4' and H-6'), 7.06 (d, *J*= 8.3 Hz, 2H, H-3' and H-7'), 5.19 (s, 1H, H-3), 4.82 (s, 2H, H-5), 2.24 (s, 3H, H-8'). **^{13}C NMR** (100 MHz, DMSO-d$_6$) *δ*: 175.51 (C-2), 163.45 (C-4), 138.03 (C-2'), 132.71 (C-5'), 130.31 (2C, C-4' and C-6'), 119.13 (2C, C-3' and C-7'), 83.39 (C-3), 68.38 (C-5), 20.78 (C-8'). **HRMS (ESI) [M+H]$^+$** calculated for C$_{11}$H$_{12}$NO$_2$, 190.0868; found, 190.0863

4-(butylamino)furan-2(5*H*)-one (8l)

Compound **8l** was synthesized using a method similar to that used to prepare **8a** and isolated as a light yellow liqiud in 14% yield; purified by column chromatography, eluent hexane/ethyl acetate (6:4 v/v). **^{1}H NMR** (400 MHz, CDCl$_3$) *δ* 5.91 (br s, 1H, -NH), 4.66 (s, 2H, H-5), 4.63 (s, 1H, H-3), 3.14 (quartet, *J* = 6.9 Hz, 2H, H-2'), 1.59 (quintet, *J* = 7.4 Hz, 2H, H-3'), 1.39 (sextet, *J* = 7.4 Hz, 2H, H-4'), and 0.94 (t, *J* = 7.4 Hz, 3H, H-5'). **^{13}C NMR** (100 MHz, CDCl$_3$) *δ* 176.34 (C-2), 168.42 (C-4), 80.29 (C-3), 67.64 (C-5), 44.83 (C-2'), 30.69 (C-3'), 19.99 (C-4') and 13.64 (C-5'). **HRMS (ESI)** calculated for C$_8$H$_{14}$NO$_2$ **[M+H]$^+$,** 156.1025; found, 156.0987
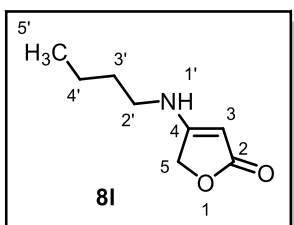
4.6.   One-Pot Procedure for the Preparation of 8b-c & Subsequent Preparation of 8m

4-(4-methoxyphenyl)furan-2(5*H*)-one (8b)

To a 50 mL two-neck round-bottom flask α,β-dibromobutenolide **6b** (300 mg, 1.24 mmol) was combined with (4-methoxyphenyl)boronic acid (302 mg, 2.48 mmol), cesium fluoride (376 mg, 2.48 mmol), Pd(MeCN)$_2$Cl$_2$ (8 mg, 2.5 mol %), PPh$_3$ (33 mg, 10 mol%), and toluene/water (5/0.5 mL; v/v). The reaction mixture was then degassed for 10 min under flow of nitrogen. The reaction mixture was stirred at 60 °C for 6 h. Then, Pd(OAc)$_2$ (7 mg, 2.5 mol %), DIPEA (1.1 ml, 6.2 mmol), formic acid (0.24 ml, 6.2 mmol) and acetonitrile (without further purification, 5 mL). The reaction mixture was stirred at same temperature for another 6 h before it was filtered through a pad of Celite. The filtrate was extracted with ethyl acetate (3×15 mL). The combined organic layer was dried over anhydrous Na$_2$SO$_4$, and concentrated under reduced pressure. The crude product was purified by column chromatography on silica gel eluted with hexane/EtOAc (8:2 v/v) to afford compound **8b** as white solid in 57% yield.

Compound **8c** was also synthesized using this method from (4-fluorophenyl)boronic acid and was isolated as a light brown solid in 39% yield.

Compound **8m** was synthesized through demethylation of compound **8b** (200 mg, 1.05 mmol), using boron tribromide (3 equiv) and was isolated as a white solid in 98% yield (182 mg, 1.03 mmol); purified by column chromatography, eluent hexane/ethyl acetate (7:3 v/v).
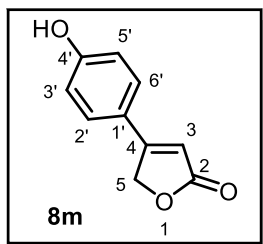
MP: 256.2-257.4 °C. **FTIR**: $\bar{v}_{max}$ 3264, 1729, 1609, 1583, 1511, 1444, 1339, 1267, 1180, 750 cm^{-1}. **^{1}H NMR** (400 MHz, Acetone-d_6) δ: 9.07 (br, 1H, -OH), 7.61 (d, J= 6.9 Hz, 2H, H-2′ and H-6′), 6.97 (d, J= 6.9 Hz, 2H, H-3′ and H-5′) 6.34 (d, J= 1.4 Hz, 1H, H-3), and 5.29 (s, 2H, H-5). **^{13}C NMR** (100 MHz, Acetone-d_6) δ: 164.35 (C-2), 160.52 (C-4′), 156.02 (C-4), 128.71 (2C, C-2′ and C-6′), 121.71 (C-3), 115.94 (2C, C-3′ and C-5′), 109.47 (C-1′) and 70.66 (C-5). **HRMS** (ESI) [M+H]$^+$ calculated for C$_{10}$H$_9$O$_3$, 177.0552; found, 177.0543

4.7. Synthesis of Rubrolide F(10), E (12) and 3″-Bromorubrolide F (11)

(Z)-4-(4-hydroxyphenyl)-5-(4-methoxybenzylidene)furan-2(5H)-one (10)

To a 25 mL two-neck round-bottom flask with a solution of **8m** (100 mg, 0.57 mmol) in anhydrous CH$_2$Cl$_2$ (5 mL) at 0 °C were successively added i-Pr$_2$NEt (0.3 mL, 1.70 mmol) and TBDMSOTf (0.5 mL, 2.28 mmol) under nitrogen atmosphere. The mixture was stirred for 15 min at 0 °C, and then 4-methoxybenzaldehyde **9a** (0.08 mL, 0.68 mmol) was added. After stirring at 0 °C for 1 h, the reaction mixture was left for 3 h in room temperature. Then DBU (0.25 mL, 1.71 mmol) was added and the resulting solution was allowed to stir for an additional 6 h before quenching with aqueous solution of HCl (1M, 5 mL). Then CH$_2$Cl$_2$ was removed under vacuum and the aqueous phase was extracted with ethyl acetate (3×10 mL) and the combined organic layers were washed with saturated brine solution, dried over Na$_2$SO$_4$ and concentrated under reduced pressure. The crude was purified by column chromatography on silica gel eluted with hexane/ethyl acetate (8:2 v/v) to afford the natural rubrolide F **10** as a yellow solid in 69% yield (116 mg, 0.39 mmol); purified by column chromatography, eluent hexane/ethyl acetate (8:2 v/v).

FTIR: $\bar{v}_{max}$ 2929, 2859, 1746, 1604, 1509, 1421, 1170, 1089, 1032 cm^{-1}. **^{1}H NMR** (CD$_3$OD, 400 MHz) δ: 7.79 (d, J = 8.4 Hz, 2H, H-2″ and H-6″), 7.46 (d, J = 8.0 Hz, 2H, H-2′ and H-6′), 6.98 (d, J = 8.4 Hz, 2H, H-3″ and H-5″), 6.96 (d, J = 8.0 Hz, 2H, H-3′ and H-5′), 6.30 (s, 1H, H-6), 6.18 (s, 1H, H-3) and 3.85 (s, 3H, -OCH$_3$). **^{13}C NMR** (CD$_3$OD, 100 MHz) δ: 171.39 (C-

2), 162.13 (C-4″), 161.28 (C-4′), 160.67 (C-4), 147.98 (C-5), 134.64 (2C, C-2″ and C-6″), 131.39 (2C, C-2′ and C-6′), 127.35 (C-1″), 122.79 (C-1′), 117.01 (2C, C-3′ and C-5′), 115.37 (2C, C-3″ and C-5″), 115.13 (C-3), 112.22 (C-6). **HRMS** (ESI) [M+H]$^+$ calculated for C$_{18}$H$_{15}$O$_4$, 295.0970; found, 295.0979

(*Z*)-5-(4-hydroxybenzylidene)-4-(4-hydroxyphenyl)furan-2(5*H*)-one (12)

Ensuing removal of the methyl groups from compound **10** (50 mg, 0.17 mmol) using boron
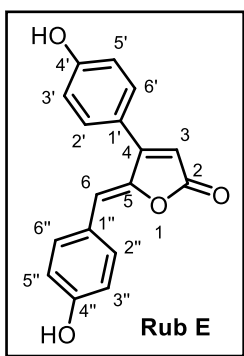
tribromide (3 equiv), provided rubrolide E **12** as a yellow solid in 98% yields (46 mg, 0.16 mmol); purified by column chromatography, eluent hexane/ethyl acetate (7:3 v/v). **MP:** 282–283 °C. **FTIR:** $\bar{v}_{max}$ 3270, 1746, 1674, 1597 cm^{-1}. **^{1}H NMR** (DMSO-d_6, 400 MHz) δ: 10.05 (br, 2H, -OH), 7.70 (d, *J* = 8.0 Hz, 2H, H-2″ and H-6″), 7.50 (d, *J* = 7.9 Hz, 2H, H-2′ and H-6′), 6.94 (d, *J* = 7.9 Hz, 2H, H-3′ and H-5′), 6.85 (d, *J* = 8.0 Hz, 2H, H-3″ and H-5″), 6.37 (s, 1H, H-6), 6.32 (s, 1H, H-3). **^{13}C NMR** (DMSO-d_6, 100 MHz) δ: 170.13 (C-2), 161.22 (C-4), 160.20 (C-4′), 159.57 (C-4″), 146.80 (C-5), 134.05 (2C, C-2″ and C-6″), 131.87 (2C, C-2′, C-6′), 125.71 (C-1″), 122.17 (C-1′), 117.39 (2C, C-3″ and C-5″), 117.37 (2C, C-3′ and C-5′), 114.89 (C-6), 112.35 (C-3). **HRMS** (ESI) [M+H]$^+$ calculated for C$_{17}$H$_{13}$O$_4$, 281.0814; found, 281.0806

(*Z*)-5-(3-bromo-4-methoxybenzylidene)-4-(4-hydroxyphenyl)furan-2(5*H*)-one (11)

Compound **11** was synthesized using a method similar to that used to prepare **10** and
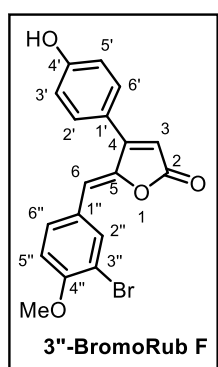
isolated as a yellow solid in 81% yield (172 mg, 0.46 mmol); purified by column chromatography, eluent hexane/ethyl acetate (75:25 v/v). **MP:** 221-223°C **FTIR:** $\bar{v}_{max}$ 3240, 1752, 1610, 1416, 1289, 1154, 831 cm^{-1}. **^{1}H NMR** (CD$_3$OD, 400 MHz) δ: 8.10 (d, *J* = 1.8 Hz, 1H, H-2″), 7.79 (dd, *J* = 1.8 and 8.7 Hz, 1H, H-6″), 7.48 (d, *J* = 8.6 Hz, 2H, H-2′ and H-6′), 7.10 (d, *J* = 8.7, 1H, H-5″), 6.97 (d, *J* = 8.6 Hz, 2H, H-3′ and H-5′), 6.28 (s, 1H, H-3), 6.24 (s, 1H, H-6) and 3.94 (s, 3H, -OCH$_3$). **^{1}H NMR** (DMSO-d_6, 400 MHz) δ: 8.08 (d, *J* = 1.5 Hz, 1H, H-2″), 7.81 (dd, *J* = 1.5 and 8.7 Hz, 1H, H-6″), 7.49 (d, *J* = 8.4 Hz, 2H, H-2′ and H-6′), 7.18 (d, *J* = 8.7, 1H, H-5″), 6.91 (d, *J* = 8.4 Hz, 2H, H-3′ and H-5′), 6.43 (s, 1H, H-3), 6.38 (s, 1H, H-6) and 3.87 (s, 3H, -OCH$_3$). **^{13}C NMR** (DMSO-d_6, 100 MHz) δ: 168.82 (C-2), 160.29 (C-4′), 158.34 (C-4), 156.26 (C-4″), 147.03 (C-5), 135.04 (C-2″), 132.12 (C-6″), 130.96 (2C, C-2′ and C-6′), 127.65 (C-1″), 120.81 (C-1′), 116.36 (2C, C-3′ and C-5′), 113.25 (C-3), 112.17 (C-5″), 111.70 (C-6) 111.38 (C-3″) and 56.86 (-OCH$_3$). **HRMS** (ESI) [M+H]$^+$ calculated for C$_{18}$H$_{14}$BrO$_4$, 373.0075; found, 373.0084.

5. References and Notes

[1] MIAO, S.; ANDERSEN, R. J. Rubrolides A-H, metabolites of the colonial tunicate Ritterella rubra. J. Org. Chem., v. 56, p. 6275-6280, **1991**.

[2] SIKORSKA, J.; PARKER-NANCE, S.; DAVIES-COLEMAN, M. T.; VINING, O. B.; SIKORA, A. E.; MCPHAIL, K. L. Antimicrobial Rubrolides from a South African Species of Synoicum Tunicate. J. Nat. Prod., v. 75, p. 1824-1827, **2012**.

[3] WANG, W.; KIM, H.; NAM, S.-J.; RHO, B. J.; KANG, H. Antibacterial Butenolides from the Korean Tunicate Pseudodistoma antinboja. J. Nat. Prod., v. 75, p. 2049-2054, **2012**.

[4] ZHU, T.; CHEN, Z.; LIU, P.; WANG, Y.; XIN, Z.; ZHU, W. New rubrolides from the marine-derived fungus Aspergillus terreus OUCMDZ-1925. J. Antibiot., v. 67, p. 315-318, **2014**.

[5] CHANG, C.-W.; CHANG, H.-S.; CHENG, M.-J.; PENG, C.-F.; CHEN, I.-S. Identification of Five New Minor Constituents from the Whole Plant ofAmischotolype hispida. Helv. Chim. Acta, v. 98, p. 347-358, **2015**.

[6] SCHMITT, J.; SUGNET, M.; SALLE, J.; COMOY, P.; CALLET, G.; LEMEUR, J. Chim. Ther., v. 5-6, p. 305, **1966**.

[7] EVERS, B.; JESUDASON, C. D.; KARANJAWALA, R. E.; REMICK, D. M.; RUEHTER, G.; SALL, D. J.; SCHOTTEN, T.; SIEGEL, M. G.; STENZEL, W.; STUCKY, R. D., Beta3 adrenergic agonists, WO2002006276, **2002**.

[8] NAM, N.-H.; KIM, Y.; YOU, Y.-J.; HONG, D.-H.; KIM, H.-M.; ANN, B.-Z. Synthesis and cytotoxicity of some rigid derivatives of methyl 2,5-Dihydroxycinnamate. Arch. Pharm. Res., v. 25, p. 590-599, **2002**.

[9] KUMAR, N.; ISKANDER, G., Furanone compounds and lactam analogues thereof, WO2008040097, **2008**.

[10] JESCHKE, P.; NAUEN, R.; GUTBROD, O.; BECK, M. E.; MATTHIESEN, S.; HAAS, M.; VELTEN, R. Flupyradifurone (Sivanto™) and its novel butenolide pharmacophore: Structural considerations☆. Pest. Biochem. Physiol., v. 121, p. 31-38, **2015**.

[11] NAUEN, R.; JESCHKE, P.; VELTEN, R.; BECK, M. E.; EBBINGHAUS-KINTSCHER, U.; THIELERT, W.; WÖLFEL, K.; HAAS, M.; KUNZ, K.; RAUPACH, G. Flupyradifurone: a brief profile of a new butenolide insecticide. Pest Manag. Sci., v. 71, p. 850-862, **2015**.

[12] SIMONIS, H. Ber. Dtsch. Chem. Ges., v. 32, p. 2085, **1899**.

[13] SIMONIS, H. Ber. Dtsch. Chem. Ges., v. 34, p. 509, **1901**.

[14] MOWRY, D. T. Mucochloric Acid. I. Reactions of the Pseudo Acid Group. J. Am.Chem. Soc., v. 72, p. 2535-2537, **1950**.

[15] ZHANG, J.; ZHANG, Y. Reinvestigation of Mucohalic Acids: Recent Development and Application in Drug Discovery. Chinese J. Org. Chem., v. 33, p. 409, **2013**.

[16] WANG, J.; LIU, X.; HU, B.; LU, G.; WANG, Y. Efficient catalytic conversion of lignocellulosic biomass into renewable liquid biofuels via furan derivatives. RSC Adv., v. 4, p. 31101, **2014**.

[17] ROSSI, R.; BELLINA, F. An Efficient and Inexpensive Multigram Synthesis of 3,4-Dibromo- and 3,4-Dichlorofuran-2(5H)-one. Synthesis, v. 2007, p. 1887-1889, **2007**.

[18] BELLINA, F.; ROSSI, R. Mucochloric and Mucobromic Acids: Inexpensive, Highly Functionalised Starting Materials for the Selective Synthesis of Variously Substituted 2(5H)-Furanone Derivatives, Sulfur- or Nitrogen-Containing Heterocycles and Stereodefined Acyclic Unsaturated Dihalogenated Compounds. Curr. Org. Chem., v. 8, p. 1089-1103, **2004**.

[19] CUNHA, S.; OLIVEIRA, C. C. Aplicações sintéticas do ácido mucobrômico e da 3,4-dibromofuran-2(5H)-ona. Quim. Nova, v. 34, p. 1425-1438, **2011**.

[20] ROSSI, R.; BELLINA, F.; RAUGEI, E. Selective Synthesis of Unsymmetrical 3,4-Disubstituted and 4-Substituted 2(5H)-Furanones. Synlett, v. 2000, p. 1749-1752, **2000**.

[21] BELLINA, F.; ANSELMI, C.; ROSSI, R. Synthesis of 4-alkyl-3-bromo-2(5H)-furanones and unsymmetrically disubstituted 3,4-dialkyl-2(5H)-furanones by palladium-catalyzed cross-coupling reactions. Tetrahedron Lett., v. 42, p. 3851-3854, **2001**.

[22] BELLINA, F.; ANSELMI, C.; ROSSI, R. Total synthesis of rubrolide M and some of its unnatural congeners. Tetrahedron Lett., v. 43, p. 2023-2027, **2002**.

[23] BLAZECKA, P. G.; BELMONT, D.; CURRAN, T.; PFLUM, D.; ZHANG, J. Further Utilization of Mucohalic Acids: Palladium-Free, Regioselective Etherification and Amination of α,β-Dihalo γ-Methoxycarbonyloxy and γ-Acetoxy Butenolides. Org. Lett., v. 5, p. 5015-5017, **2003**.

[24] BELLINA, F.; ANSELMI, C.; MARTINA, F.; ROSSI, R. Mucochloric Acid: A Useful Synthon for the Selective Synthesis of 4-Aryl-3-chloro-2(5H)-furanones, (Z)-4-Aryl-5-[1-(aryl)methylidene]-3-chloro-2(5H)-furanones and 3,4-Diaryl-2(5H)-furanones. Eur. J. Org. Chem., v. 2003, p. 2290-2302, **2003**.

[25] BELLINA, F.; FALCHI, E.; ROSSI, R. Regioselective synthesis of cytotoxic 4-(1-alkynyl)-substituted 2-(5H)-furanones. Tetrahedron, v. 59, p. 9091-9100, **2003**.

[26] BOUKOUVALAS, J.; MCCANN, L. C. Synthesis of the human aldose reductase inhibitor rubrolide L. Tetrahedron Lett., v. 51, p. 4636-4639, **2010**.

[27] BARBOSA, L. C. A.; MALTHA, C. R. A.; LAGE, M. R.; BARCELOS, R. C.; DONÀ, A.; CARNEIRO, J. W. M.; FORLANI, G. Synthesis of Rubrolide Analogues as New Inhibitors of the Photosynthetic Electron Transport Chain. J. Agric. Food Chem., v. 60, p. 10555-10563, **2012**.

[28] BISWAS, K.; GHOLAP, R.; SRINIVAS, P.; KANYAL, S.; SARMA, K. D. [small beta]-Substituted [gamma]-butyrolactams from mucochloric acid: synthesis of (+/-)-baclofen and other [gamma]-aminobutyric acids and useful building blocks. RSC Adv., v. 4, p. 2538-2545, **2014**.

[29] PEREIRA, U. A.; BARBOSA, L. C. A.; MALTHA, C. R. A.; DEMUNER, A. J.; MASOOD, M. A.; PIMENTA, A. L. Inhibition of Enterococcus faecalis biofilm formation by highly active lactones and lactams analogues of rubrolides. Eur. J. Med. Chem., v. 82, p. 127-138, **2014**.

[30] PEREIRA, U. A.; BARBOSA, L. C. A.; MALTHA, C. R. A.; DEMUNER, A. J.; MASOOD, M. A.; PIMENTA, A. L. γ-Alkylidene-γ-lactones and isobutylpyrrol-2(5H)-ones analogues to rubrolides as inhibitors of biofilm formation by Gram-positive and Gram-negative bacteria. Bioorg. Med. Chem., v. 24, p. 1052-1056, **2014**.

[31] VAREJAO, J. O. S.; BARBOSA, L. C. A.; MALTHA, C. R. A.; LAGE, M. R.; LANZNASTER, M.; CARNEIRO, J. W. M.; FORLANI, G. Voltammetric and Theoretical Study of the Redox Properties of Rubrolide Analogues. Electrochim. Acta, v. 120, p. 334-343, **2014**.

[32] VAREJÃO, J. O. S.; BARBOSA, L. C. A.; RAMOS, G. Á.; VAREJÃO, E. V. V.; KING-DÍAZ, B.; LOTINA-HENNSEN, B. New rubrolide analogues as inhibitors of photosynthesis light reactions. J. Photochem. Photobiol. B, v. 145, p. 11-18, **2015**.

[33] KARAK, M.; ACOSTA, J. A. M.; BARBOSA, L. C. A.; BOUKOUVALAS, J. Late-Stage Bromination Enables the Synthesis of Rubrolides B, I, K, and O. Eur. J. Org. Chem., v. 2016, p. 3780-3787, **2016**.

[34] VICIU, M. S.; GRASA, G. A.; NOLAN, S. P. Catalytic Dehalogenation of Aryl Halides Mediated by a Palladium/Imidazolium Salt System. Organometallics, v. 20, p. 3607-3612, **2001**.

[35] DESMARETS, C.; KUHL, S.; SCHNEIDER, R.; FORT, Y. Nickel(0)/Imidazolium Chloride Catalyzed Reduction of Aryl Halides. Organometallics, v. 21, p. 1554-1559, **2002**.

[36] ALONSO, F.; BELETSKAYA, I. P.; YUS, M. Metal-Mediated Reductive Hydrodehalogenation of Organic Halides. Chem. Rev., v. 102, p. 4009-4092, **2002**.

[37] XIA, C. Pd/C-catalyzed hydrodehalogenation of aromatic halides in aqueous solutions at room temperature under normal pressure. Catal. Commun., v. 5, p. 383-386, **2004**.

[38] CHEN, J.; ZHANG, Y.; YANG, L.; ZHANG, X.; LIU, J.; LI, L.; ZHANG, H. A practical palladium catalyzed dehalogenation of aryl halides and α-haloketones. Tetrahedron, v. 63, p. 4266-4270, **2007**.

[39] JIMENEZ, L.; RAMANATHAN, A. Reductive Dehalogenation of Aryl Bromides and Chlorides and Their Use as Aryl Blocking Groups. Synthesis, v. 2010, p. 217-220, **2009**.

[40] NARAYANAM, J. M. R.; TUCKER, J. W.; STEPHENSON, C. R. J. Electron-Transfer Photoredox Catalysis: Development of a Tin-Free Reductive Dehalogenation Reaction. J. Am. Chem. Soc., v. 131, p. 8756-8757, **2009**.

[41] NGUYEN, J. D.; D'AMATO, E. M.; NARAYANAM, J. M. R.; STEPHENSON, C. R. J. Engaging unactivated alkyl, alkenyl and aryl iodides in visible-light-mediated free radical reactions. Nat. Chem., v. 4, p. 854-859, **2012**.

[42] CZAPLIK, W. M.; GRUPE, S.; MAYER, M.; WANGELIN, A. J. V. Practical iron-catalyzed dehalogenation of aryl halides. Chem. Commun., v. 46, p. 6350, **2010**.

[43] CHELUCCI, G.; BALDINO, S.; RUIU, A. Room-Temperature Hydrodehalogenation of Halogenated Heteropentalenes with One or Two Heteroatoms. J. Org. Chem., v. 77, p. 9921-9925, **2012**.

[44] CUNHA, S.; OLIVEIRA, C. C.; SABINO, J. R. Synthesis of 3-bromotetronamides via amination of 3,4-dibromofuran-2(5H)-one. J. Braz. Chem. Soc., v. 22, p. 598-603, **2011**.

[45] XUE, F.-L.; QI, J.; PENG, P.; MO, G.-Z.; WANG, Z.-Y. An Efficient and Selective Pd-catalyzed Dehalogenation Reaction. Lett. Org. Chem., v. 11, p. 64-79, **2014**.

[46] KARAK, M.; BARBOSA, L. C. A.; ACOSTA, J. A. M.; SAROTTI, A. M.; BOUKOUVALAS, J. Thermodynamically driven, syn-selective vinylogous aldol reaction of tetronamides. Org. Biomol. Chem., v. 14, p. 4897-4907, **2016**.

[47] BARBOSA, L. C.; MALTHA, C. R.; DEMUNER, A. J.; PINHEIRO, P. F.; VAREJÃO, J. O.; MONTANARI, R. M.; ANDRADE, N. J. Synthesis and evaluation of antimicrobial activity of halogenated furanones and compounds analogues to nostoclides. Quím. Nova, v. 33, p. 2020-2026, **2010**.

[48] DAMODAR, K.; KIM J-K.; JUN J-G. Efficient, collective synthesis and nitric oxide inhibitory activity of rubrolides E, F, R, S and their derivatives. Tetrahedron Lett., v. xx, p. xxxx–xxxx, **2016**.

[49] KOTORA, M.; NEGISHI, E.-I. Highly Efficient and Selective Procedures for the Synthesis of γ-Alkylidenebutenolides via Palladium-Catalyzed Ene-Yne Coupling and Palladium- or Silver Catalyzed Lactonization of (Z)-2-En-4-ynoic Acids. Synthesis of Rubrolides A, C, D, and E. Synthesis, v. 01, p. 121-128, **1997**.

[50] BOUKOUVALAS, J.; LACHANCE, N.; OUELLET, M.; TRUDEAU, M. Facile access to 4-aryl-2(5H)-furanones by Suzuki cross coupling: Efficient synthesis of rubrolides C and E. Tetrahedron Lett., v. 39, p. 7665-7668, **1998**.

[51] KAR, A.; ARGADE, N. P. A Facile Synthesis of Rubrolide E. Synthesis, v. 14, p. 2284-2286, **2005**.

[52] CACCHI, S.; FABRIZI, G.; GOGGIAMANI, A.; SFERRAZZA, A. Palladium-Catalyzed Reaction of Arenediazonium Tetrafluoroborates with Methyl 4-Hydroxy-2-butenoate: An Approach to 4-Aryl Butenolides and an Expeditious Synthesis of Rubrolide E. Synlett, v. 08, p. 1277-1280, **2009**.

[53] CHAVAN, S. P.; PATHAK, A. B.; PANDEY, A.; KALKOTE, U. R. Short and Efficient Synthesis of Rubrolide E. Synth. Commun., v. 37, p. 4253-4263, **2007**.

[54] TALE, N. P.; SHELKE, A. V.; TIWARI, G. B.; THORAT, P. B.; KARADE, N. N. New Concise and Efficient Synthesis of Rubrolides C and E via Intramolecular Wittig Reaction. Helv. Chim. Acta, v. 95, p. 852-857, **2012**.

[55] Compound **8a** itself a secondary metabolite, namely ralfuranone A. The β-aryl-substituted γ-lactone ralfuranone A was isolated after feeding $_L$-[1-^{13}C]-phenylalanine to a liquid culture of the plant pathogenic bacterium *Ralstonia solanacearum*. For more details about this natural product please see: (A) SCHNEIDER, P.; JACOBS, J. M.; NERES, J.; ALDRICH, C. C.; ALLEN, C.; NETT, M.; HOFFMEISTER, D. ChemBioChem v. 10, p. 2730−2732, **2009**. (B) WACKLER, B.; SCHNEIDER, P.; JACOBS, J. M.; PAULY, J.; ALLEN, C.; NETT, M.; HOFFMEISTER, D. Chem. Biol. v. 18, p. 354−360, **2011**. (C) PAULY, J.; SPITELLER, D.; LINZ, J.; JACOBS, J.; ALLEN, C.; NETT, M.; HOFFMEISTER, D. ChemBioChem v. 14, p. 2169−2178, **2013**. (D) PAULY, J.; NETT, M.; HOFFMEISTER, D. J. Nat. Prod., v. 77, p. 1967−1971, **2014**.

GENERAL CONCLUSION

In this part, the major findings are summarized and general conclusions based on the findings of the works presented in this thesis are described. Furthermore, the strengths and limitations of this thesis are considered and suggestions for further research.

The research work developed in the present thesis explores the development of a highly diastereoselective vinylogous aldol reaction of unprotected tetronamides with various aldehydes. Strong bases NaOH and LiOH represent the most powerful catalysts for this aldol reaction. The procedure is simple and scalable, works well with both aromatic and aliphatic aldehydes, and affords mainly the corresponding *syn*-aldol adducts. Several lines of evidence (both experimental and computational) suggest that the observed diastereoselectivity arises from *anti*-to-*syn* isomer interconversion *via* an iterative retro-aldol/aldol reaction sequence. Although the excellent diastereoselective vinylogous aldol reaction of tetronamides is reported here, the asymmetric vinylogous aldol reaction of tetronamides has yet to be developed. Moreover, the substrates scope of aliphatic tetronamides with aldehydes and ketones need to be developed as well.

In addition, to better understand the structural features for further structural-biological activities studies, details of the crystal structure of several tetronamide aldol products has been demonstrated in this thesis. The major contribution of this studies concerns in the control of molecular conformation of tetronamide aldolates bearing several rotatable bonds and then high conformational freedom through the substitution pattern of a single ring.

The thesis also contributes to the first total synthesis of marine natural products, rubrolides I and O and their synthetic analogous. These rubrolides are not as easily accessible by existing methodologies, due to the challenges associated with vinylogous aldol condensation of the appropriately brominated butenolide and benzaldehyde partners. To overcome such problems, an advanced late-stage bromination strategy has been employed which allowed functionalization of the aromatic rings in a highly regioselective fashion. The procedure was further applied to prepare some synthetic analogous of rubrolides.

Finally, a robust palladium catalyzed reductive dehalogenation of α-halo-β-substituted butenolides with high yields and regioselectivity has been reported. Besides, a new synthesis of rubrolide E, F and 3"-bromorubrolide F has been reported by employing this protocol.

Investigation of the possible biological activities of tetronamides and their aldol derivatives, rubrolides and their synthetic analogous and other β-substituted butenolides are currently underway in our collaborator's laboratories.

APPENDIX

1. Appendix 1 (Publications Relevant to the Thesis)

Natural Product Synthesis

Late-Stage Bromination Enables the Synthesis of Rubrolides B, I, K, and O

Milandip Karak,[a,b] Jaime A. M. Acosta,[a] Luiz C. A. Barbosa*[a,b] and John Boukouvalas[a,c]

Abstract: A concise and efficient synthesis of the marine natural products rubrolides B, I, K, and O was accomplished in 3–4 steps from commercially available 3,4-dichloro-2(5H)-furanone. Key steps include: (i) a site-selective Suzuki cross-coupling, (ii) a vinylogous aldol condensation, and (iii) a late-stage bromination. The latter reaction allowed functionalization of the aromatic rings in a highly regioselective fashion, enabling rapid access to the target rubrolides from common precursors.

Introduction

Butenolide-containing marine natural products have been extensively investigated in recent years due to their vast structural diversity and biological activities.[1,2] The rubrolides are a family of approximately 20 polysubstituted butenolides isolated mainly from ascidia (tunicates),[3] but also from a marine fungus.[4] Most rubrolides contain brominated phenol groups, and nearly half of them also contain a chloro substituent attached directly to the butenolide nucleus, as illustrated by rubrolides B, I, K, L, M and O (Figure 1, **1–4**, **7** and **8**). In addition to their densely functionalized structures, several rubrolides display highly sought-after biological properties including antibacterial,[3a,3d,3e] anticancer,[3b] antidiabetic,[5] anti-inflammatory,[3c] and antiviral[4] activities. Moreover, some of their synthetic analogues have been shown to possess significant herbicidal and biofilm inhibitory activities.[6]

Unsurprisingly, the synthesis of rubrolides has attracted worldwide attention for nearly two decades. In 1997, Negishi reported the first synthesis of rubrolide C (Figure 1, **5**) using a Pd-catalyzed tandem ene-yne coupling/lactonization.[7] Shortly thereafter, we described a short synthesis of rubrolides C and E (Figure 1, **5** and **6**) using a new strategy based on Suzuki cross-coupling and furanolate chemistry.[8] Subsequent syntheses of rubrolide E have employed Meerwein coupling,[9] a Heck-type reaction,[10] ring-closing metathesis,[11] and an intramolecular Wittig reaction, which also enabled the synthesis of rubrolide C.[12] The first α-chloro-substituted congener (rubrolide M,
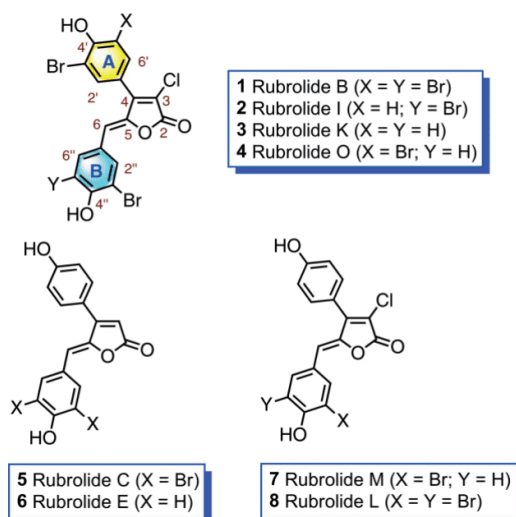
Figure 1. Structures of some selected rubrolides.

Figure 1, **7**) was synthesized by Bellina et al. by application of a site-selective Suzuki cross-coupling.[13] More recently, we employed a different strategy, starting from 3-chlorotetronic acid, to synthesize the potent aldose reductase inhibitor rubrolide L (Figure 1, **8**).[14]

Relative to the simple rubrolides, their α-chloro counterparts are not as easily accessible by existing methodologies, in part due to the challenges associated with the vinylogous aldol condensation of the appropriately halogenated butenolide and benzaldehyde partners.[13–15] Herein, we describe late-stage bromination tactics that overcome such complications, as illustrated by the first synthesis of rubrolides B, I, K, and O.

As outlined in Scheme 1, our synthesis plan was based on the premise that bromination would occur preferentially at the aromatic ring bearing the p-hydroxy substituent, which is a more powerful directing group than the methoxy group (Hammett substituent constants: σ_{para} = –0.37 and –0.27, respec-

[a] Department of Chemistry, Universidade Federal de Minas Gerais
Av. Pres. Antônio Carlos, 6627, Campus Pampulha, CEP 31270-901, Belo Horizonte, MG, Brazil
E-mail: lcab@ufmg.br
http://www.luizclaudiobarbosa.com.br
[b] Department of Chemistry, Universidade Federal de Viçosa
Av. Peter Henry Rolfs, s/n Campus Universitário, CEP 36570-900, Viçosa, MG, Brazil
[c] Department of Chemistry, Université Laval
Pavillon Alexandre-Vachon, 1045 Avenue de la Médecine, Quebec City, Quebec G1V 0A6, Canada
Supporting information and ORCID(s) from the author(s) for this article are available on the WWW under http://dx.doi.org/10.1002/ejoc.201600473.

171

Substituent-Modulated Conformation and Supramolecular Assembly of Tetronamides

Milandip Karak,[†,‡] Jaime A. M. Acosta,[†] Luiz C. A. Barbosa,*[,†,‡] Ariel M. Sarotti,[§] Cameron C. da Silva,[∥] John Boukouvalas,[⊥] and Felipe T. Martins*[,∥]

[†]Department of Chemistry, Instituto de Ciências Exatas, Universidade Federal de Minas Gerais, Av. Pres. Antônio Carlos 6627, Campus Pampulha, 31270-901 Belo Horizonte-MG, Brazil

[‡]Department of Chemistry, Universidade Federal de Viçosa, 36570-900 Viçosa-MG, Brazil

[§]Instituto de Química Rosario (IQUIR), Universidad Nacional de Rosario−CONICET, Suipacha 531, S2002LRK Rosario, Argentina

[∥]Instituto de Química, Universidade Federal de Goiás, Campus Samambaia, CP 131, 74001-970 Goiânia-GO, Brazil

[⊥]Département de Chimie, Pavillon Alexandre-Vachon, Université Laval, 1045 Avenue de la Médecine, Quebec City, Quebec G1V 0A6, Canada

S *Supporting Information*

ABSTRACT: The crystal structures of nine compounds (**1**−**9**) bearing the 4-aminofuran-2(5*H*)-one scaffold (commonly known as tetronamide, $C_4H_5NO_2$) and two decorating aromatic/heteroaromatic moieties with two stereocenters have been determined. Tetronamides bearing at the 5-position a phenyl moiety (**1** and **2**, 3-chloro derivatives with either a 4-*p*-tolylamino or 4-*p*-bromophenylamino substituent), an *o*-bromopyridyl moiety (**3**, a 3-bromo-4-*p*-tolylamino derivative), or an *o*-tolyl moiety (**4**, a 3-bromo-4-*p*-tolylamino derivative) adopt a U-shaped conformation. This conformation is stabilized by an intramolecular contact involving either the phenyl *o*-CH moiety (**1** and **2**) or the substituent at the ortho position (**3** and **4**) and the π system of the *N*-phenyl ring. The other five tetronamides (**5**−**9**) are not present with such an intramolecular contact. In fact, these last five compounds are not U-shaped and feature the presence at the 5-position of a *p*-biphenyl moiety (**5** and **7**, 3-bromo-4-*p*-tolylamino diastereomers differing as 5*R* and 5*S*), a *p*-methoxyphenyl moiety (**6**, a 3-chloro-4-*p*-bromophenylamino derivative), or a 5-chlorofuran-2-yl moiety (**8** and **9**, 3-chloro-4-*p*-tolylamino diastereomers differing as 5*R* and 5*S*). Crystal structures of a 5,5-disubstituted tetronamide bearing *m*-nitrophenyl moieties (**10**) and a parent tetronamide without a substituent at the 5-position (**11d**) reinforce the conformational trend found in **1**−**9**. Furthermore, OH···O centrosymmetric dimers are formed only in the crystal structures of the U-shaped tetronamides. Chain motifs assembled through OH···O and NH···O hydrogen bonds are preferred in the line-shaped tetronamides. Furthermore, the conformer energies were calculated in both the gas and solution phases (B3LYP/6-31G*). The lowest-energy conformations feature an intramolecular N−H···O hydrogen bond as in the crystal structure of **7**. In the U-shaped tetronamides, the crystal structure conformations are similar to the third or fourth energetically ranked stable calculated conformer. Therefore, it is concluded that the substitution pattern in the U-shaped tetronamides allows for accessible secondary minimum-energy conformations that are easily adopted in the crystal structure as a result of their compatibility with the robust centrosymmetric O−H···O dimer formation.
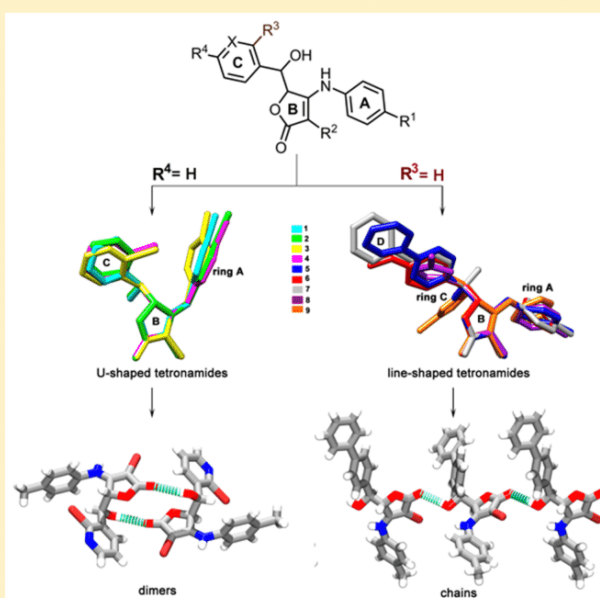
■ INTRODUCTION

Compounds containing the 4-aminofuran-2(5*H*)-one scaffold, commonly known as tetronamides (Figure 1, **I**), include the natural product basidalin (**III**)[1−3] and various synthetic molecules[4−12] (e.g., **II** and **IV**), which are considered important templates for the development of agrochemicals[6,7] and pharmaceuticals[8−12] Because of the diverse biological properties of

tetronamides, extensive studies of the synthesis of both chiral and achiral derivatives of such compounds have been conducted in recent years.[10−27]

PAPER

Thermodynamically driven, *syn*-selective vinylogous aldol reaction of tetronamides†

Milandip Karak,[a,b] Luiz C. A. Barbosa,*[a,b] Jaime A. M. Acosta,[a] Ariel M. Sarotti[c] and John Boukouvalas[d]

A stereoselective vinylogous aldol reaction of *N*-monosubstituted tetronamides with aldehydes is described. The procedure is simple and scalable, works well with both aromatic and aliphatic aldehydes, and affords mainly the corresponding *syn*-aldol adducts. In many cases, the latter are obtained essentially free of their *anti*-isomers (dr > 99 : 1) in high yields (70–90%). Experimental and computational studies suggest that the observed diastereoselectivity arises through *anti*–*syn* isomer interconversion, enabled by an iterative retro-aldol/aldol reaction.

Introduction

Tetronamides are an important class of β-heterosubstituted butenolides that have attracted growing attention from synthetic and medicinal chemists alike.[1,2] Although not nearly as common as their tetronate counterparts,[3] several tetronamides have been shown to display significant biological activities, as represented by the fungal antitumor antibiotic basidalin 1,[4] the newly marketed systemic insecticide flupyradifurone (Sivanto®, 2),[5] some potent antimitotic aza-lignans, *e.g.* 3,[6] and broad-acting antibacterials[7] (4–5, Fig. 1). Inspired by the structure of the tetronate *syn*-aldol adduct losigamone 6, an experimental drug advanced to phase III clinical trials for the treatment of epilepsy,[3b,8] we sought to prepare a library of new analogues in which the alkoxy group is replaced by an aromatic amine (*cf.* tetronamides A).[9]

The vinylogous aldol reaction (VAR), carried our either directly from butenolides or, *via* conversion to the corresponding 2-silyloxyfurans (Mukaiyama variant; VMAR), represents one of the most widely explored avenues for installing a γ-carbon substituent (Scheme 1).[10] Much effort has been devoted in recent years in controlling the relative and absolute
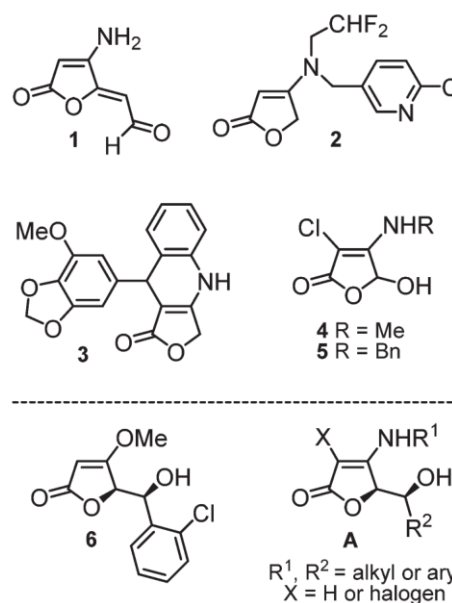
Fig. 1 Bioactive tetronamides 1–5, tetronate 6 and analogues A.

configuration of the newly formed stereogenic centers.[11,12] Although several heterosubstituted butenolides,[11e–h,12c,d] including tetronates, have been utilized as substrates in VA reactions, surprisingly little is known concerning the serviceability of tetronamides.[8b,13] The few pertinent examples invariably employ *N*,*N*-disubstituted tetronamides in conjuction with a strong base (*t*-BuLi, −78 °C), leading mainly to *anti*-aldolate adducts.[14] To date, only two *N*-monosubstituted tetronamide-derived aldolates have been described in the literature; both were obtained as mixtures of diastereoisomers (dr ≈ 1 : 1 to 2 : 1) using a decarboxylative Knoevenagel-type reaction of γ-carboxymethyl tetronamides with aldehydes.[15]

[a]*Department of Chemistry, Instituto de Ciências Exatas, Universidade Federal de Minas Gerais, Av. Pres. Antônio Carlos, 6627, Campus Pampulha, Belo Horizonte, 31270-901 MG, Brazil. E-mail: lcab@ufmg.br*
[b]*Department of Chemistry, Universidade Federal de Viçosa, Viçosa, 36570-900 MG, Brazil*
[c]*Instituto de Química Rosario (IQUIR), Universidad Nacional de Rosario–CONICET, Suipacha 531, S2002LRK Rosario, Argentina*
[d]*Département de Chimie, Pavillon Alexandre-Vachon, Université Laval, 1045 Avenue de la Médecine, Quebec City, Quebec G1V 0A6, Canada*
†Electronic supplementary information (ESI) available. CCDC 1469893 and 1450009. For ESI and crystallographic data in CIF or other electronic format see DOI: 10.1039/c6ob00895j

This journal is © The Royal Society of Chemistry 2016

Org. Biomol. Chem., 2016, **14**, 4897–4907 | **4897**

Recent mechanistic developments and next generation catalysts for the Sonogashira coupling reaction

Milandip Karak,[a] Luiz C. A. Barbosa*[ab] and Gráinne C. Hargaden[c]

The Pd-catalyzed Sonogashira reaction is a powerful method for the formation of C_{sp2}–C_{sp} bonds and has found application in a wide variety of areas including medicinal chemistry, agrochemistry, materials and electronics. Development of competent catalysts for the Sonogashira reaction is a particular scientific challenge since it is traditionally a di-metallic-mediated homogeneous catalytic process including some major drawbacks. This review provides a concise overview of the mechanistic aspects of the Cu co-catalyzed, Cu-free and Au-catalyzed Sonogashira coupling processes. More recent developments and next generation catalysts for the Sonogashira reaction are also presented. These include non transition-metal catalysts, metal free couplings and photo-induced protocols. Finally, the application of metal nanoparticles in Sonogashira reactions is presented. These include Pd nanoparticles, Pd bi- and tri-metallic nanoparticles, magnetically separable Pd/Fe_3O_4 nanoparticles, Ru nanoparticles and Au nanoparticles.

aDepartamento de Química, Universidade Federal de Viçosa, Av. Peter Henry Rolfs, s/n Campus Universitário, CEP 36570-900, Viçosa, MG, Brazil. E-mail: lcab@ufmg.br
bDepartamento de Química, Universidade Federal de Minas Gerais, Av. Pres. Antônio Carlos, 6627, Campus Pampulha, CEP 31270-901, Belo Horizonte, MG, Brazil
cSchool of Chemical and Pharmaceutical Sciences, Dublin Institute of Technology, Kevin Street, Dublin 8, Ireland

1. Introduction

Over the past 15 years, there has been a growing interest in the Sonogashira coupling reaction[1] which is one of the most powerful methods for the formation of C_{sp2}–C_{sp} bonds. The Pd catalyzed C_{sp2}–C_{sp} coupling reaction between aryl halides and terminal alkynes (Scheme 1) has become the most important method for preparing aryl alkynes and conjugated alkynes, which are often intermediates or precursors in the synthesis of

Mr Karak graduated with Honours in Chemistry in 2009 from Vidyasagar University, India, and received the MSc degree in Chemistry from Nagpur University, India in 2011. Shortly after completion of his Masters, he joined Chemgen Pharma International, India as a Research Chemist in October 2011 and spent more than one year there. In April 2013 he joined the Universidade Federal de Viçosa (UFV) in Brazil as a doctoral student under the supervision of Professor Luiz C. A. Barbosa. His research is directed towards the design of new synthetic routes and their application to the synthesis of novel organic molecules that can lead to current pharmaceuticals, agrochemicals or new materials.

Professor Luiz C. A. Barbosa, received a BSc (1981) and MSc (1986) from Federal University of Viçosa (UFV–Brazil). In 1991 completed his PhD in Organic Synthesis at the University of Reading (UK) and spent a sabbatical year (2008–2009) in the group of Professor Timothy J. Donohoe at the University of Oxford. He started his academic career as an auxiliary professor at UFV (1983) raising to Professor in 1997. Since 2012 he is a Full Professor at Federal University of Minas Gerais. His research interest includes the synthesis of biologically active compounds analogues of natural products. More details at http://www.luizclaudiobarbosa.com.br

2. Appendix 2 (NMR Spectra Relevant to Chapter 2)

2.1. ^{1}H and ^{13}C NMR Spectra of Selected Tetronamides
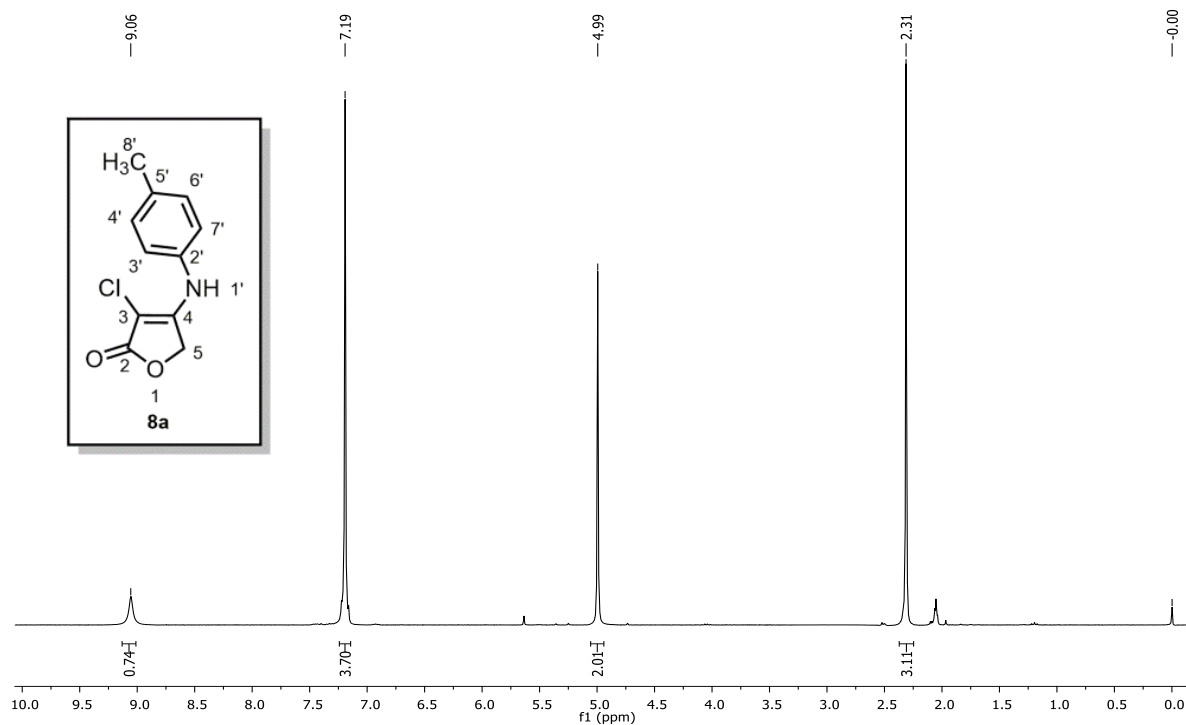
Figure A2.1 ^{1}H NMR spectrum (300 MHz, Acetone-d$_6$:DMSO-d$_6$; 9:1) of compound **8a**
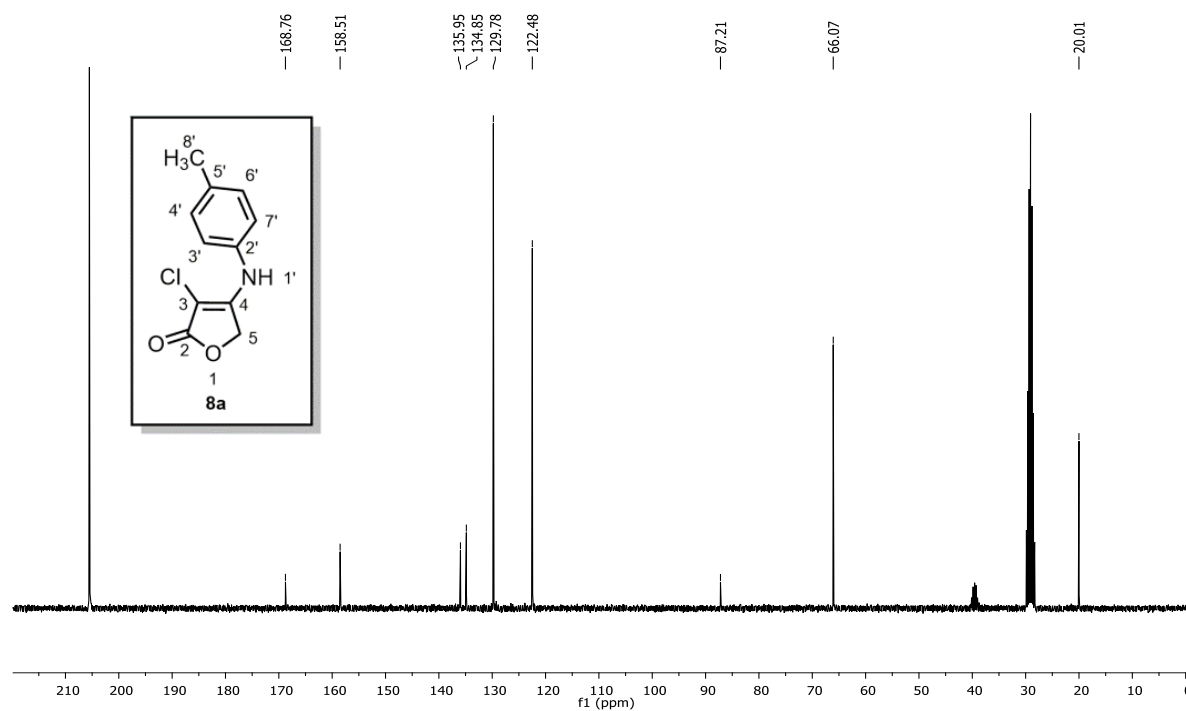
Figure A2.2 ^{13}C NMR spectrum (75 MHz, Acetone-d$_6$:DMSO-d$_6$; 9:1) of compound **8a**

Figure A2.3 ^{1}H NMR spectrum (400 MHz, CDCl$_3$) of compound **8e**

Figure A2.4 ^{13}C NMR spectrum (100 MHz, CDCl$_3$) of compound **8e**

176
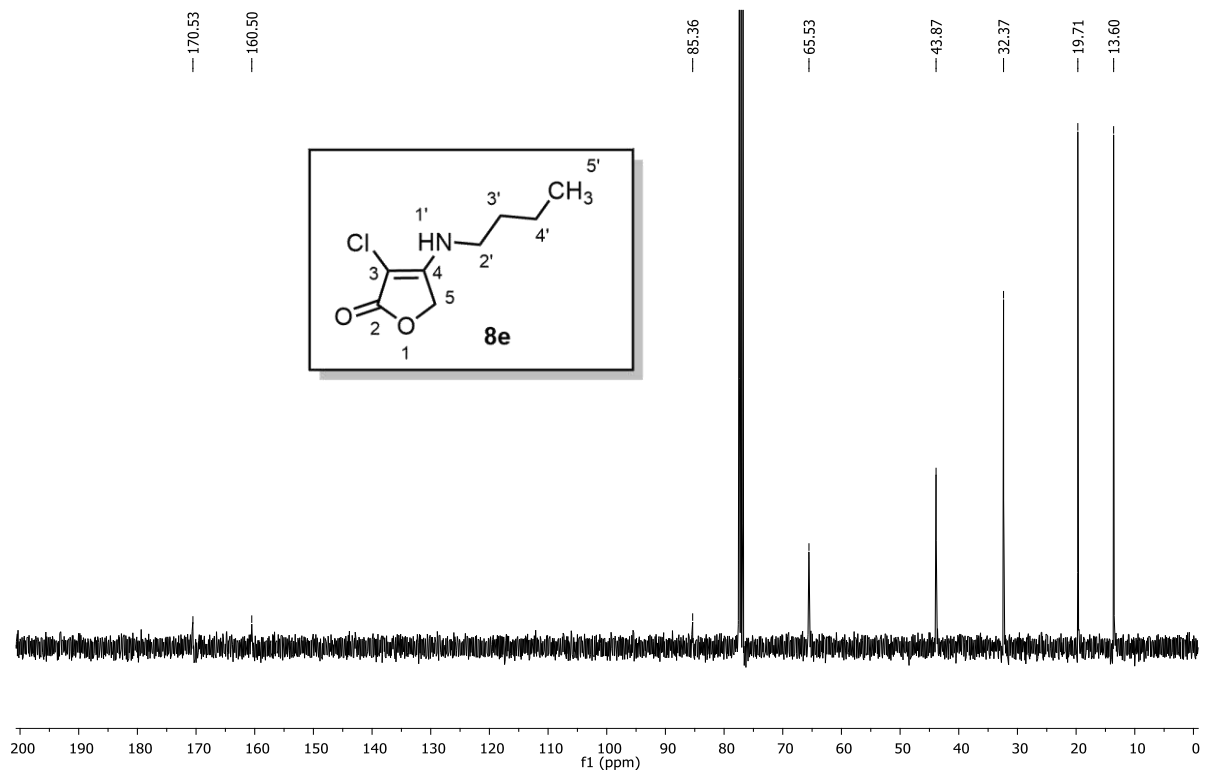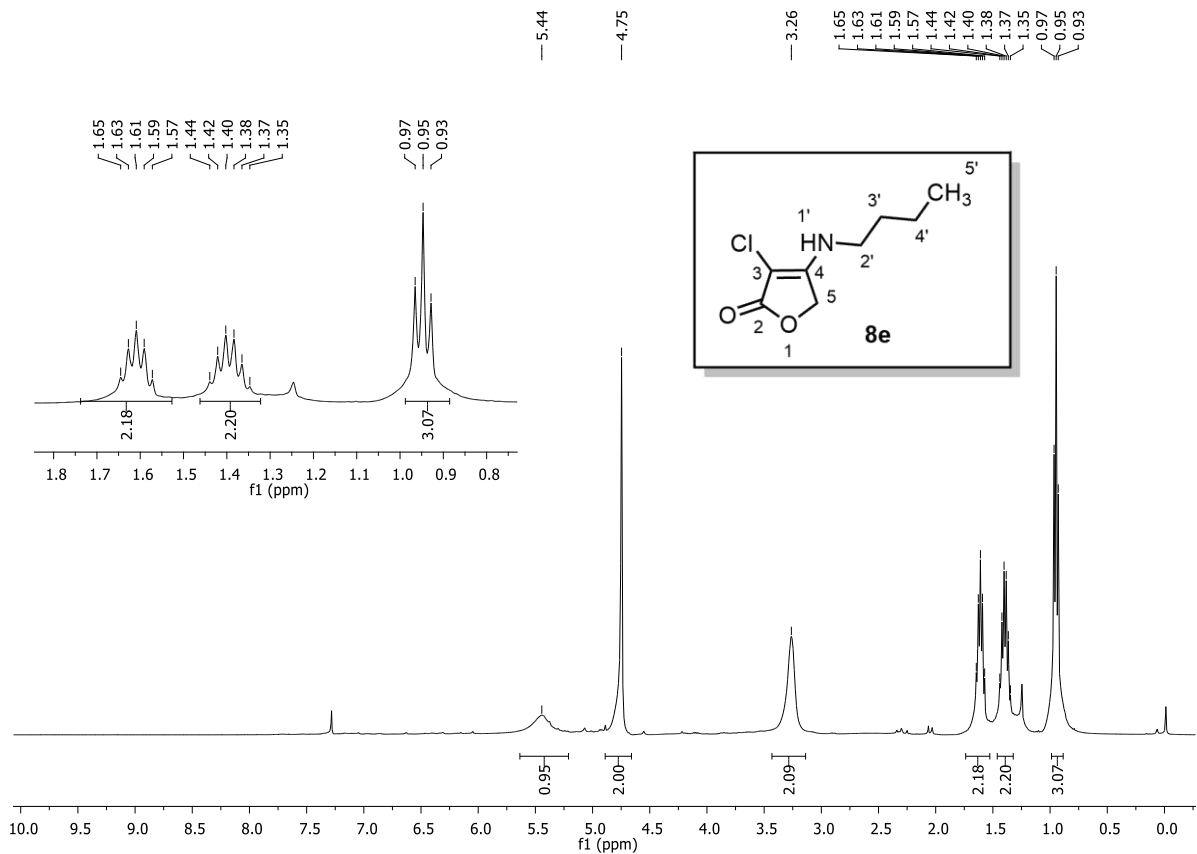
2.2. ^{1}H and ^{13}C NMR Spectra of Selected Aldol Products
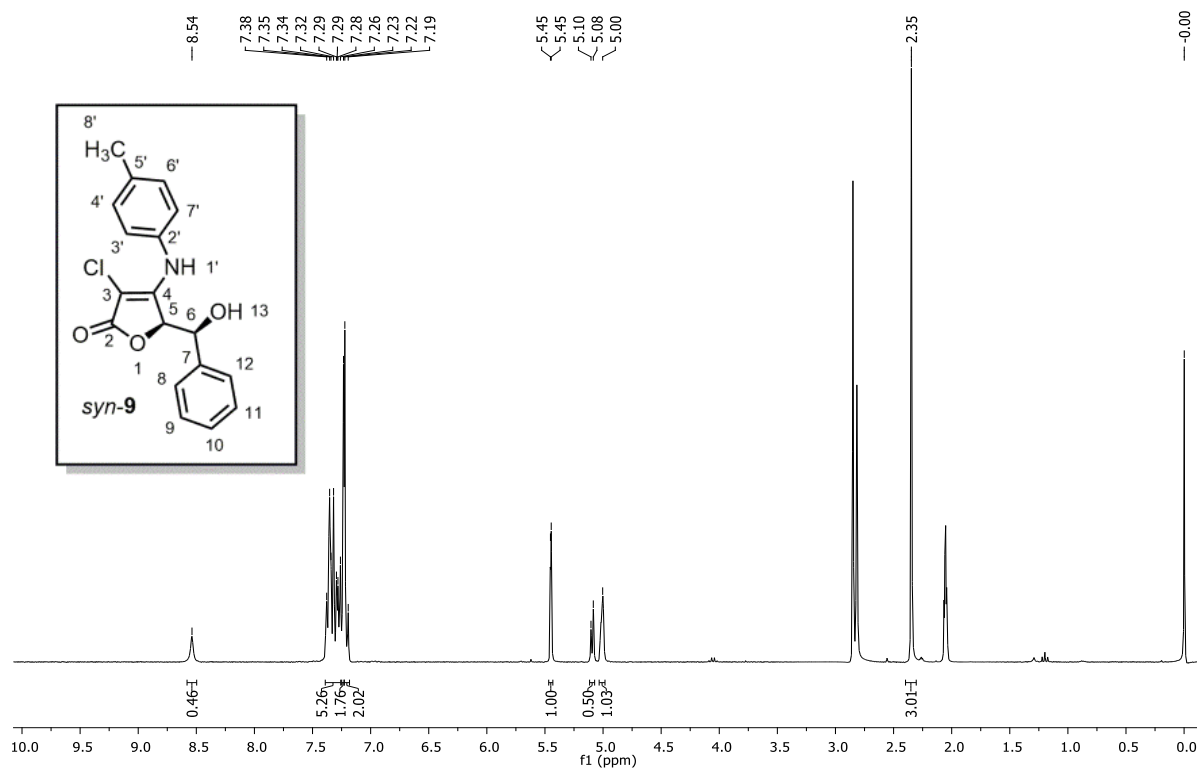
Figure A2.5 ^{1}H NMR spectrum (300 MHz, Acetone-d$_6$) of compound ***syn*-9**
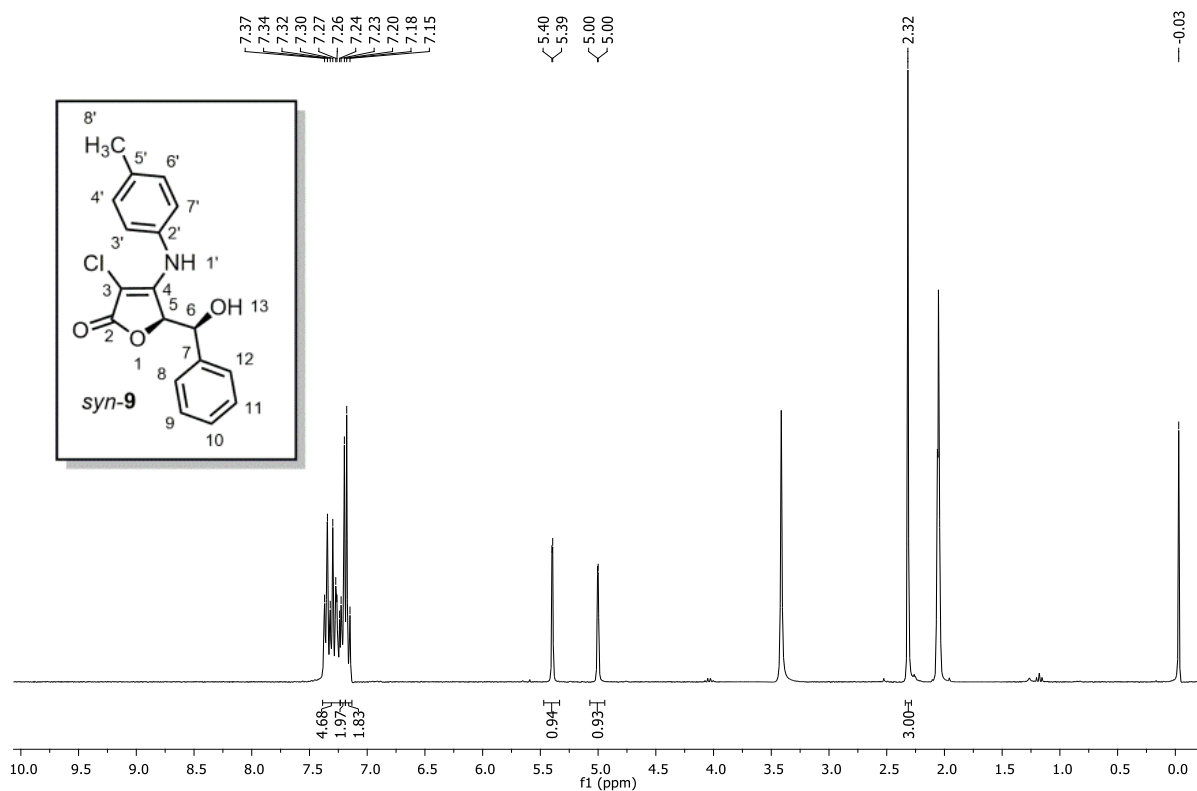
Figure A2.6 ^{1}H NMR spectrum (300 MHz, Acetone-d$_6$ + D$_2$O) of compound ***syn*-9**

Figure A2.7 ^{1}H NMR spectrum (300 MHz, CDCl$_3$:DMSO-d$_6$; 9:1) of compound *syn*-9

Figure A2.8 ^{13}C NMR spectrum (75 MHz, CDCl$_3$:DMSO-d$_6$; 9:1) of compound *syn*-9
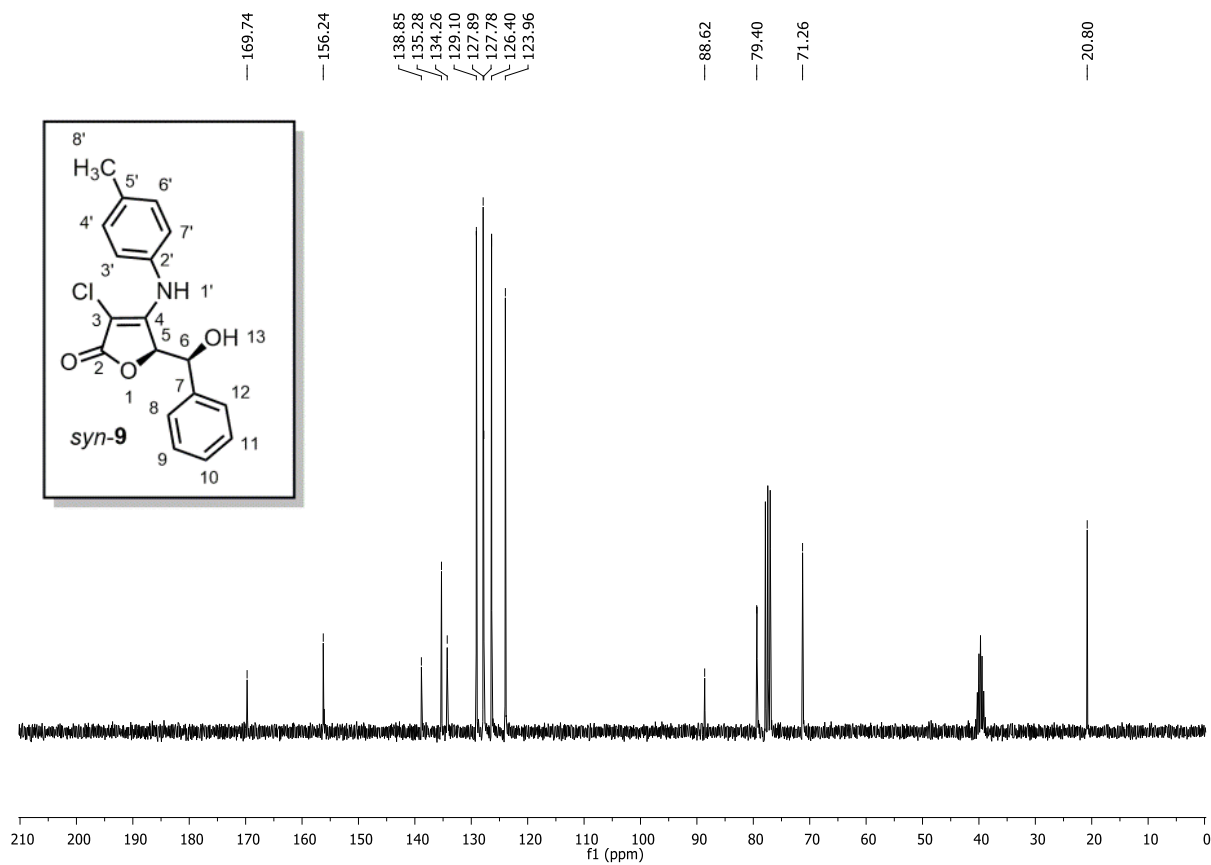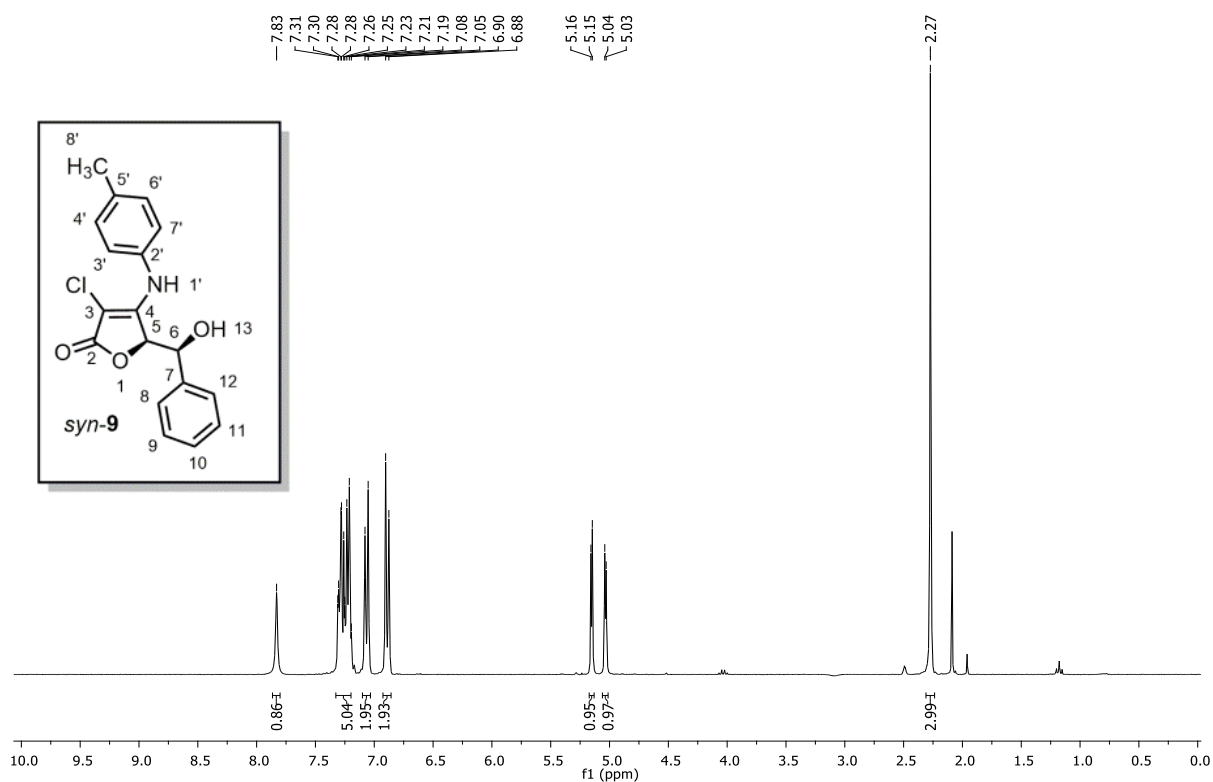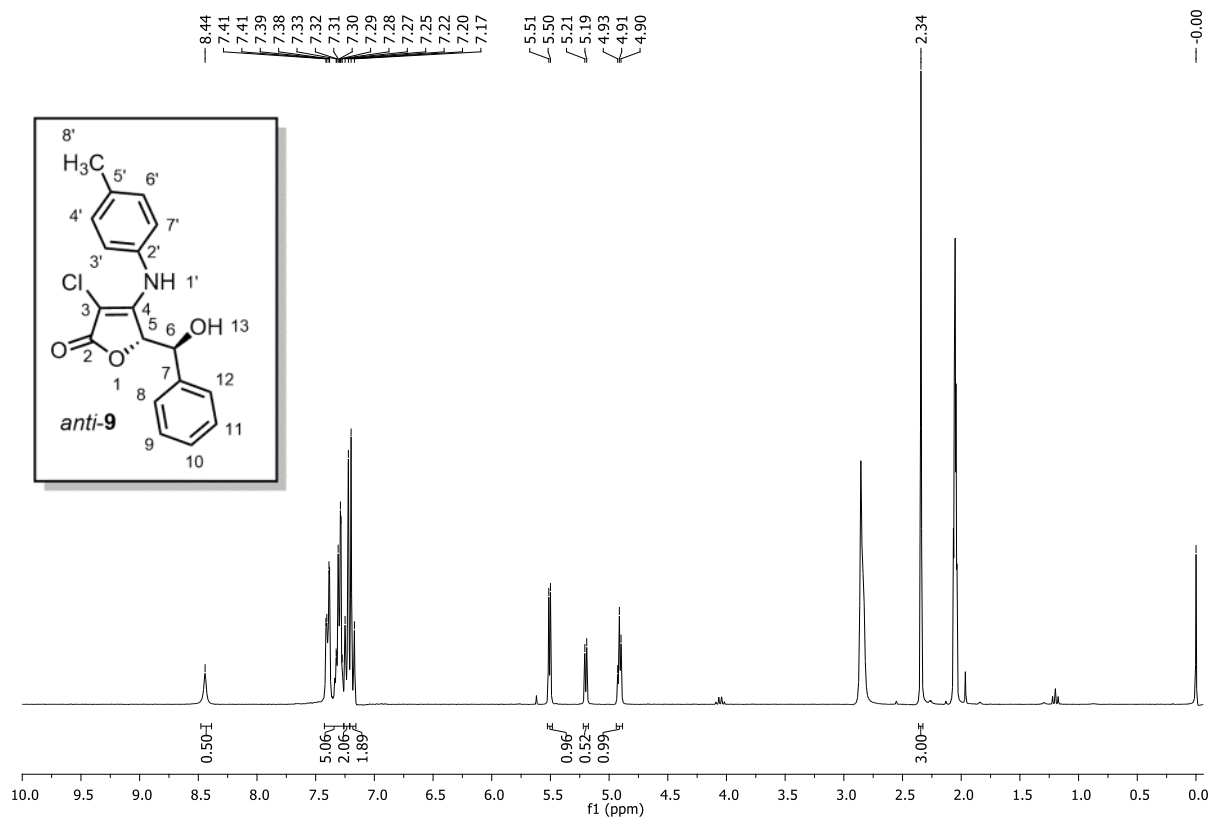
Figure A2.9 ^{1}H NMR spectrum (300 MHz, Acetone-d$_6$) of compound *anti*-9
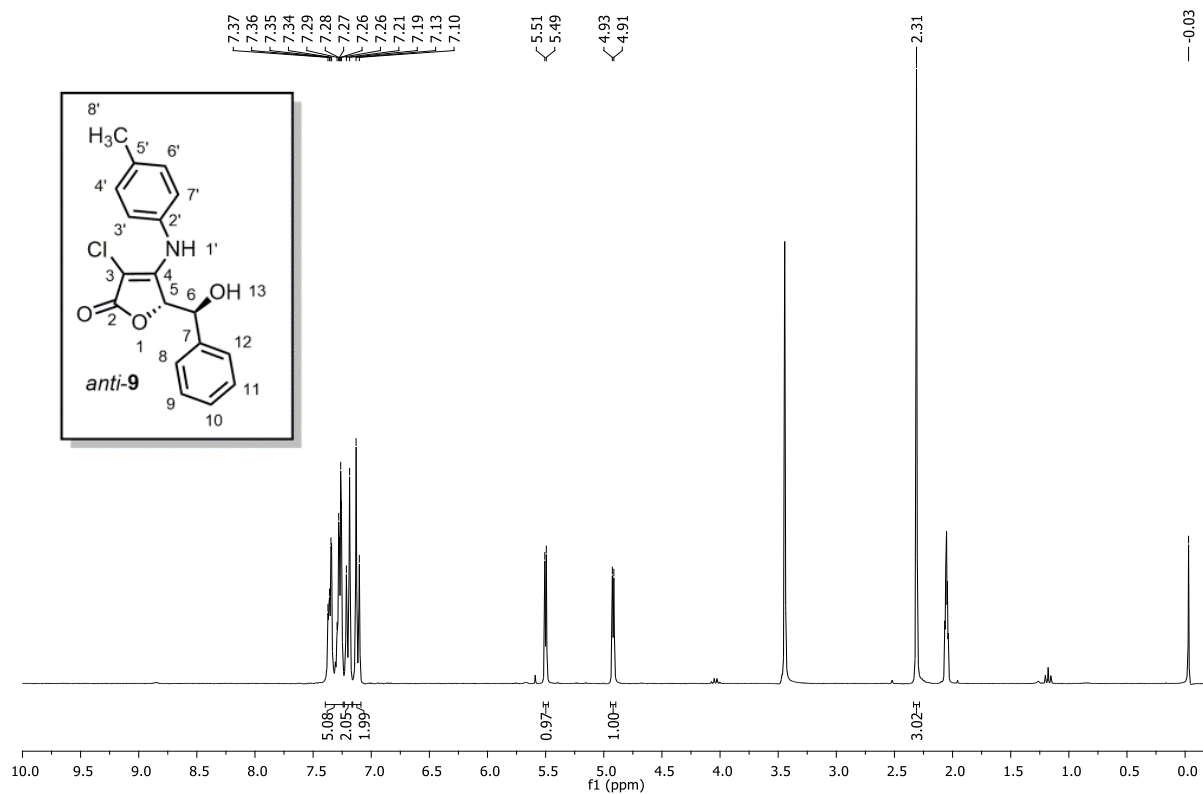
Figure A2.10 ^{1}H NMR spectrum (300 MHz, Acetone-d$_6$ + D$_2$O) of compound *anti*-9

179
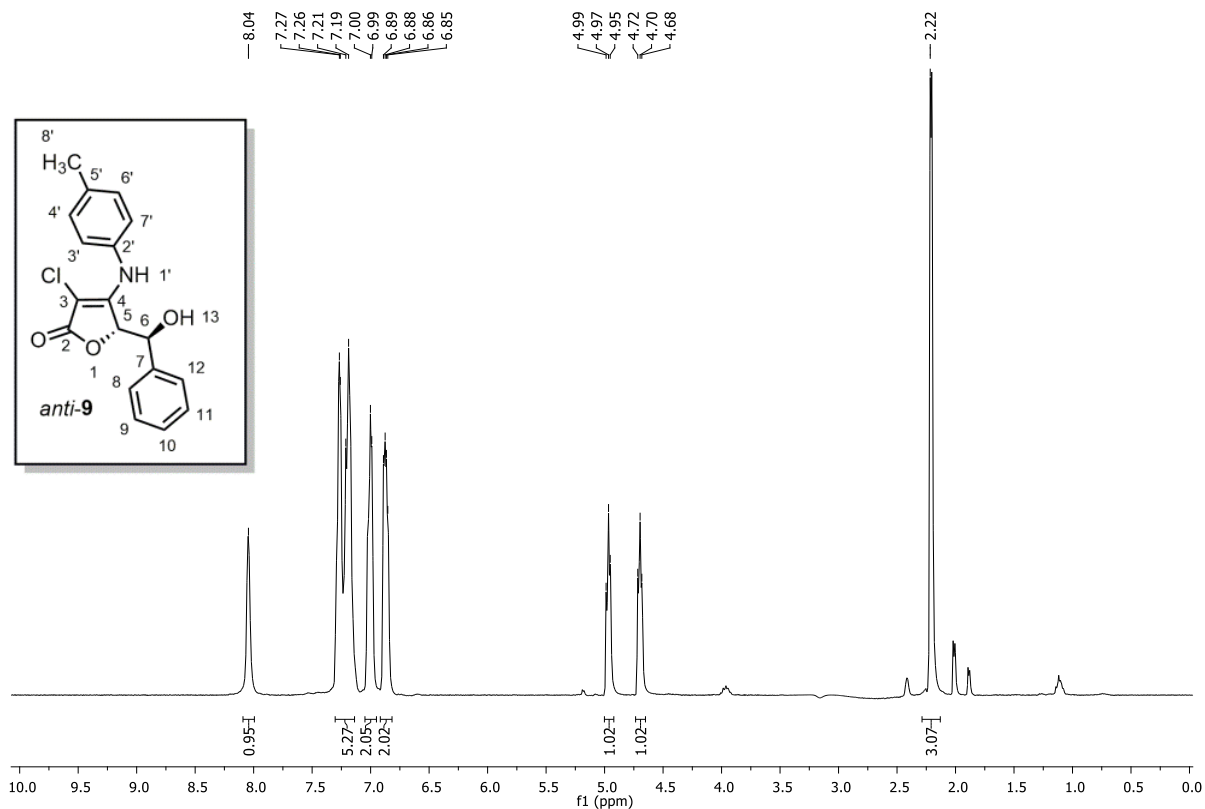
Figure A2.11 ^{1}H NMR spectrum (300 MHz, CDCl$_3$:DMSO-d$_6$; 9:1) of compound ***anti*-9**
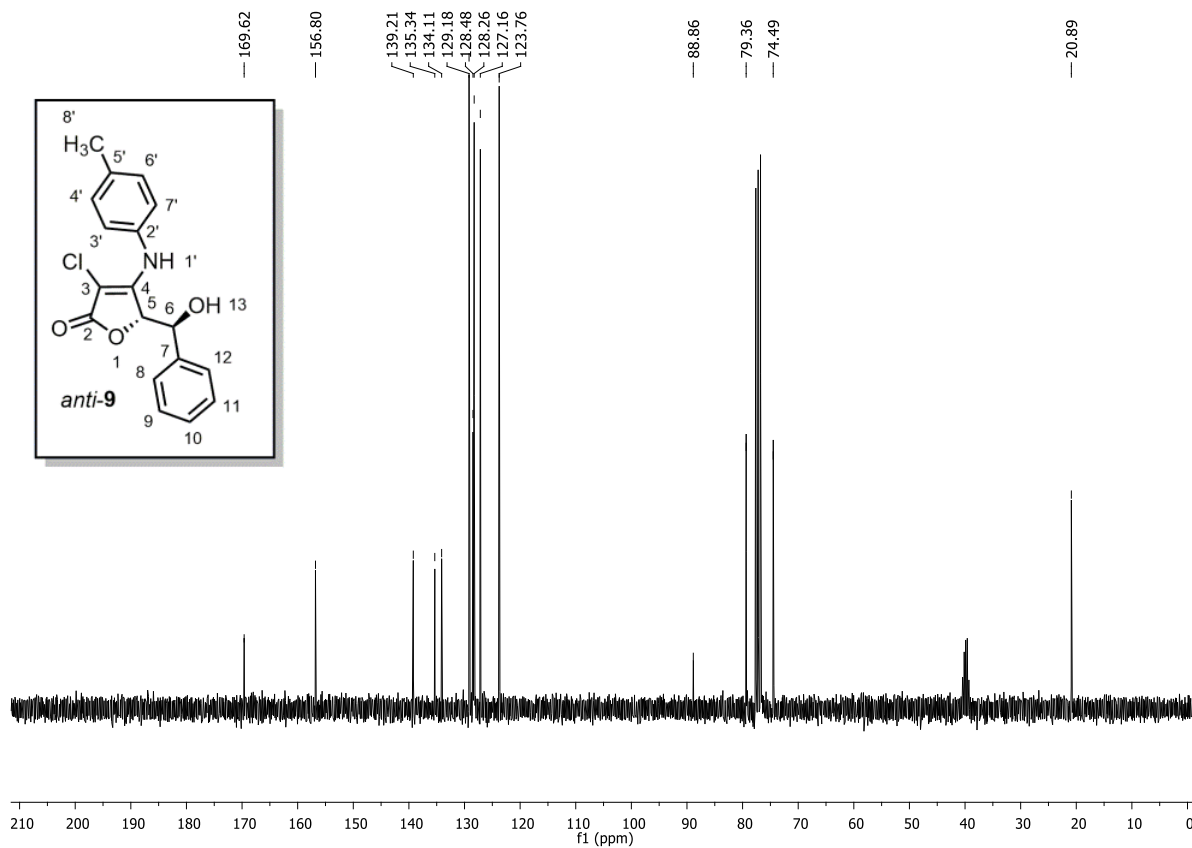
Figure A2.12 ^{13}C NMR spectrum (75 MHz, CDCl$_3$:DMSO-d$_6$; 9:1) of compound ***anti*-9**
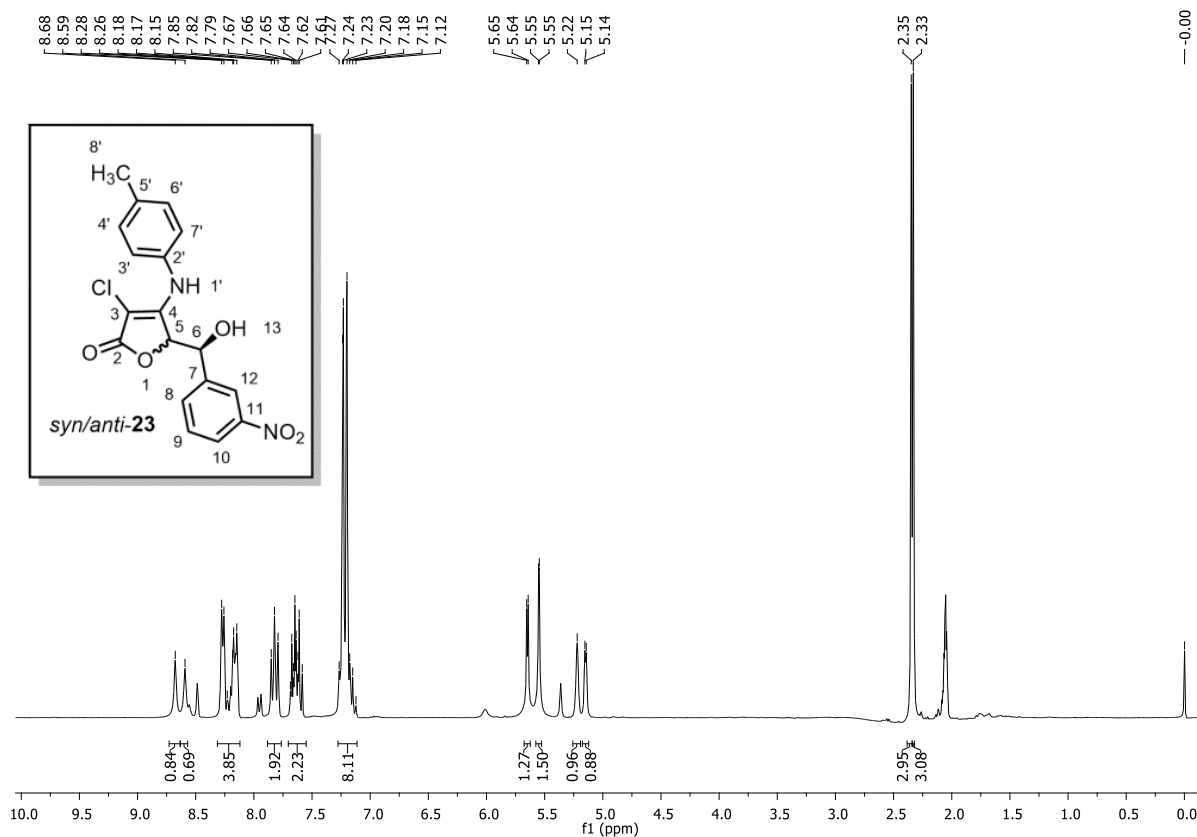
Figure A1.13 ^{1}H NMR (300 MHz, Acetone-d$_6$) of compound *syn/anti*-23
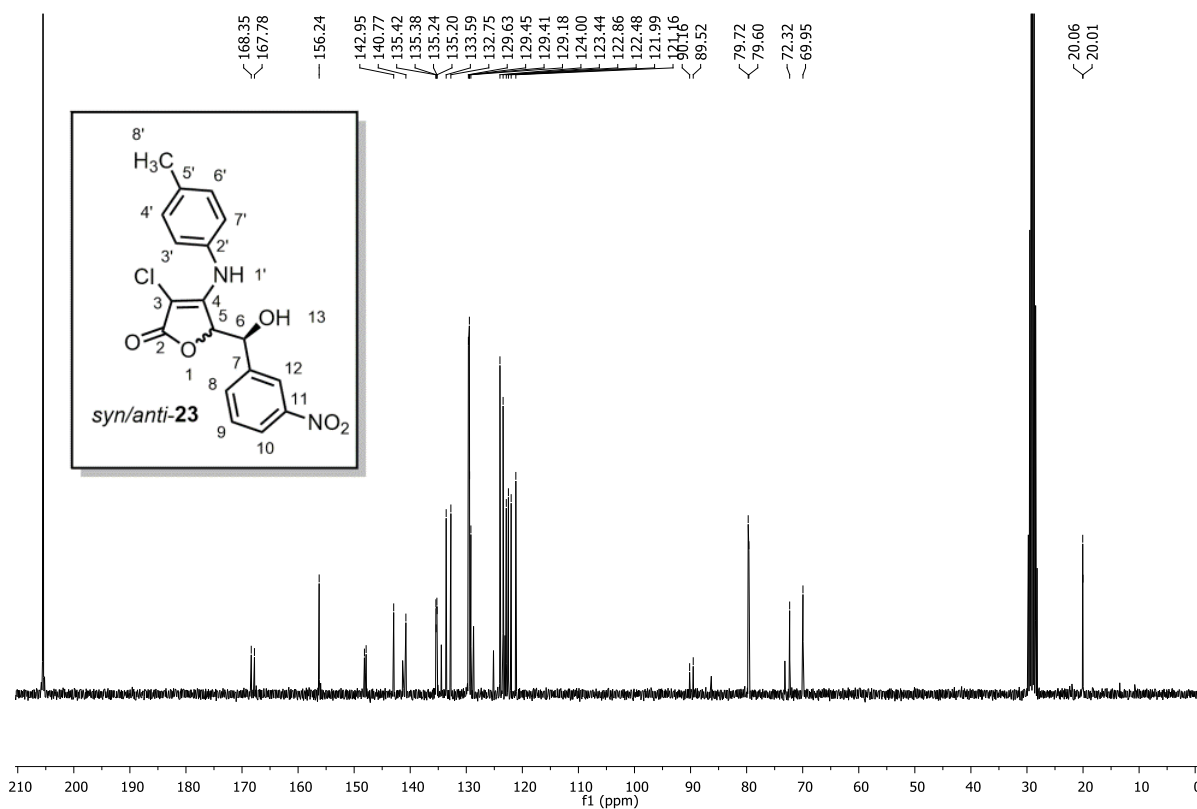
Figure A2.14 ^{13}C NMR (75 MHz, Acetone-d$_6$) of compound *syn/anti*-23

Figure A2.15 ^{1}H NMR (300 MHz, Acetone-d$_6$) of compound **23a**

Figure A2.16 ^{13}C NMR (75 MHz, Acetone-d$_6$) of compound **23a**
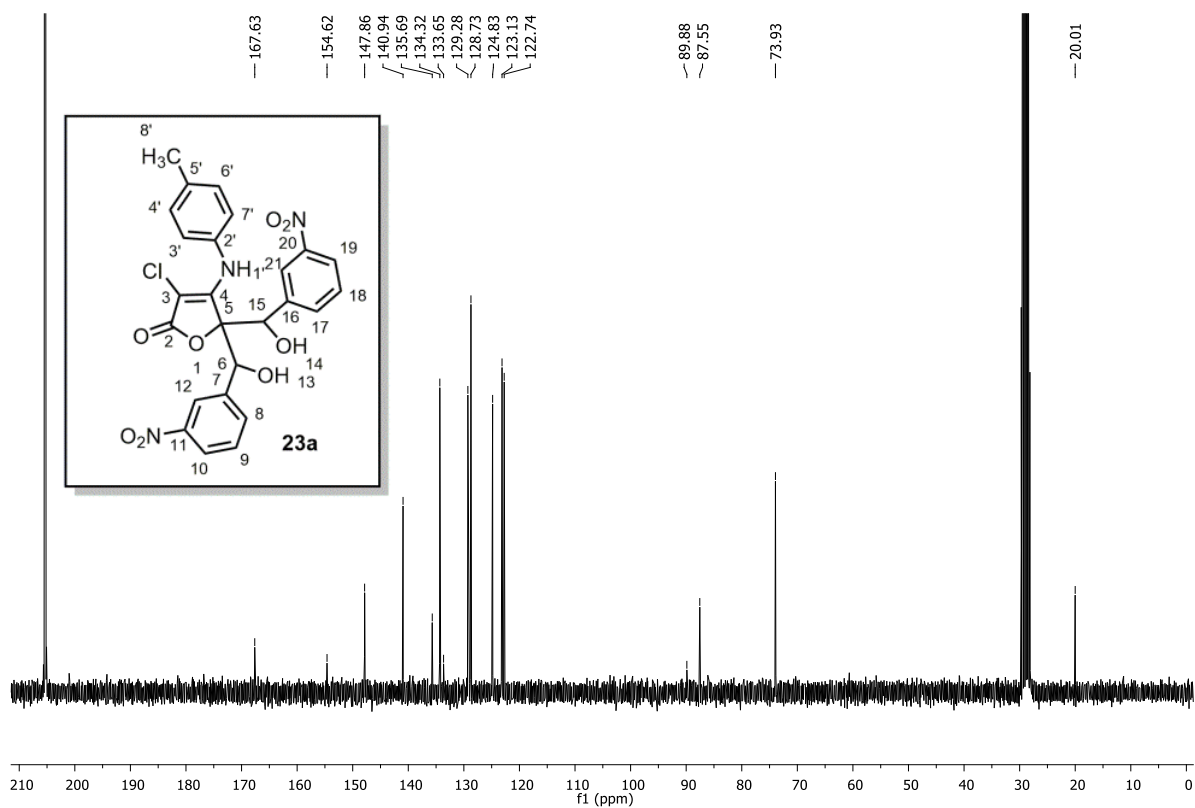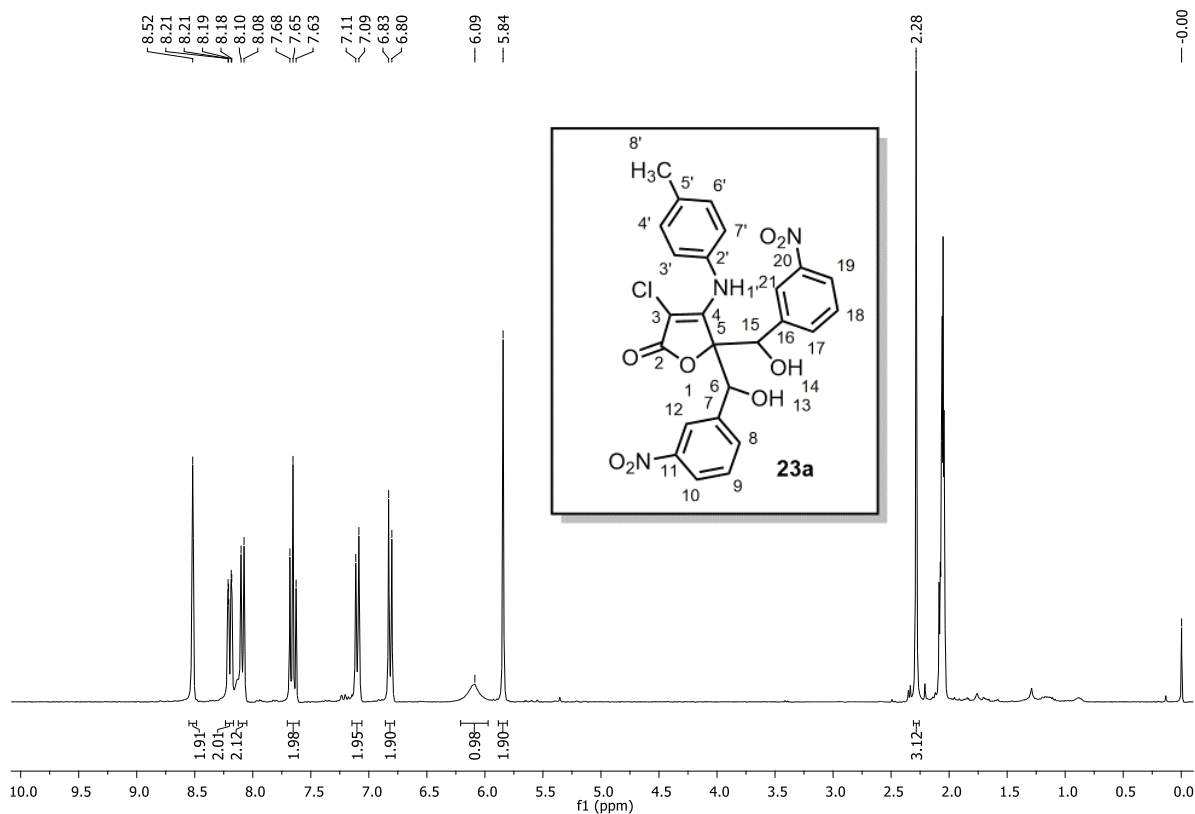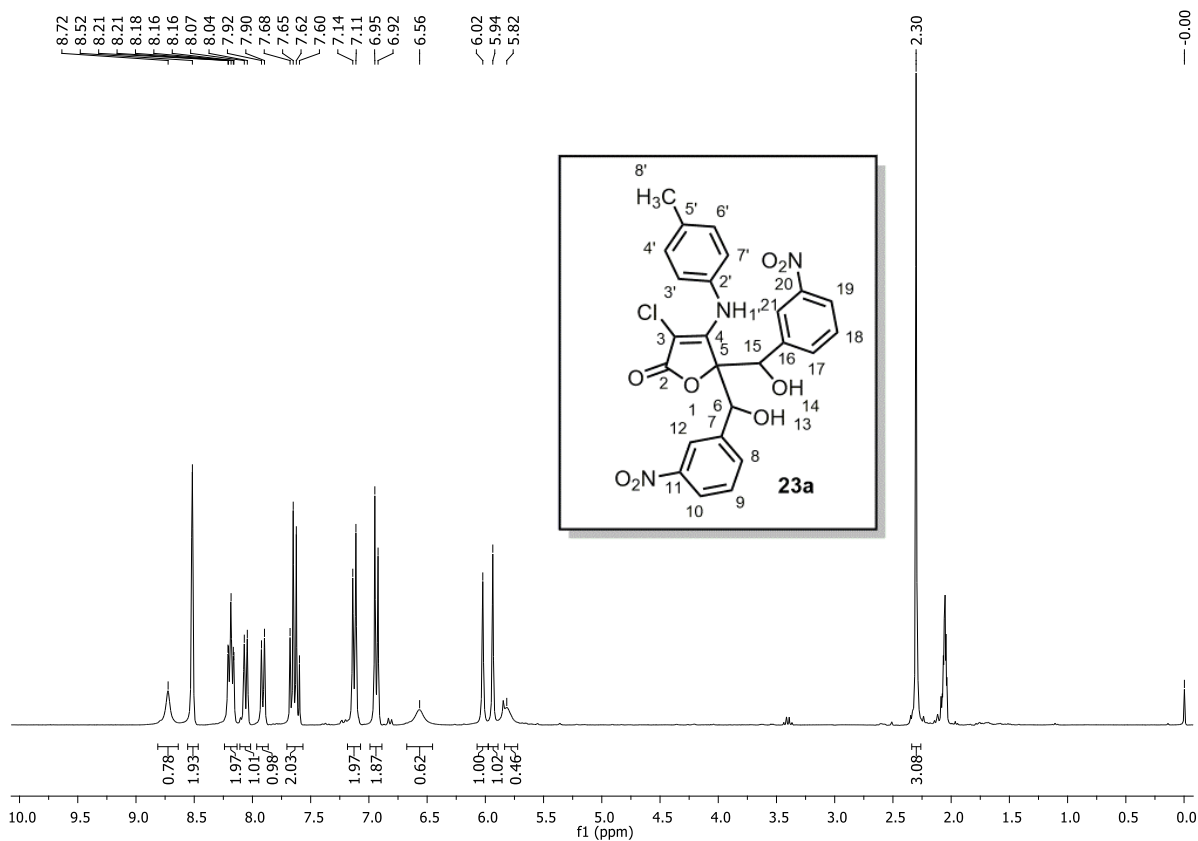
Figure A2.17 ^{1}H NMR (300 MHz, Acetone-d$_6$) of compound **23b**
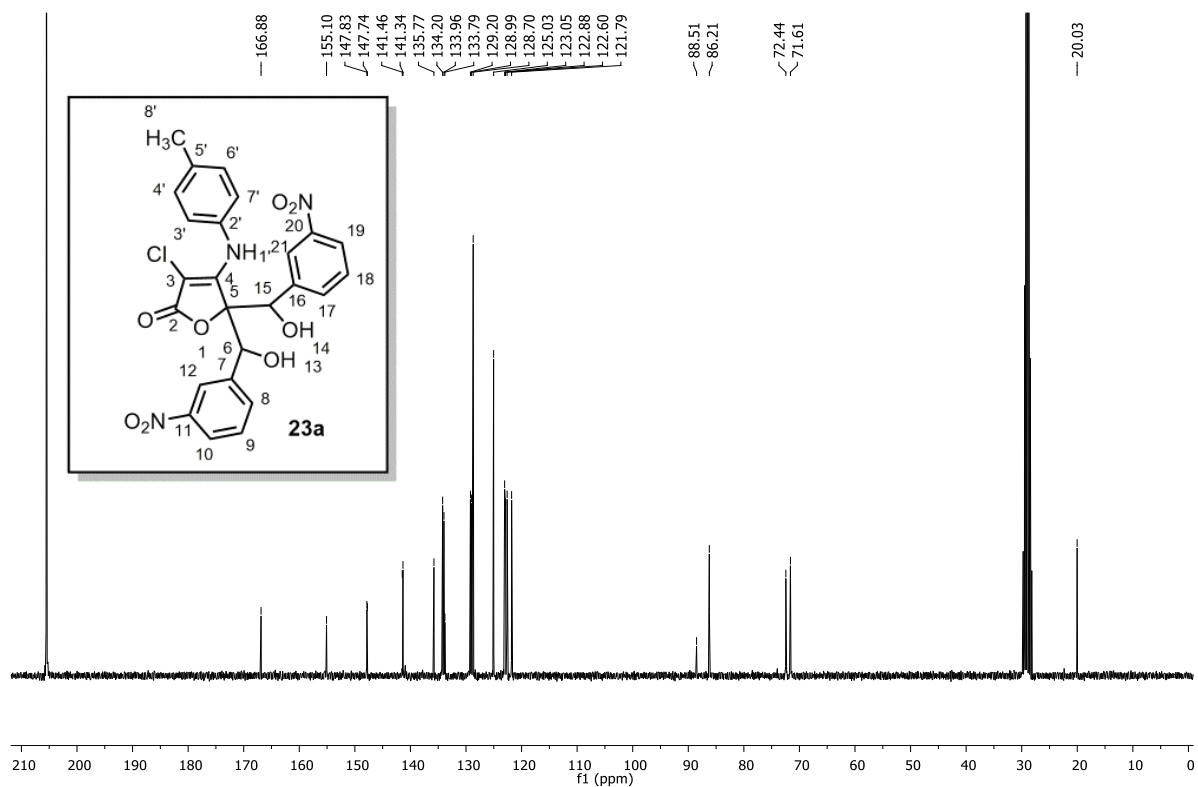
Figure A2.18 ^{13}C NMR (75 MHz, Acetone-d$_6$) of compound **23b**
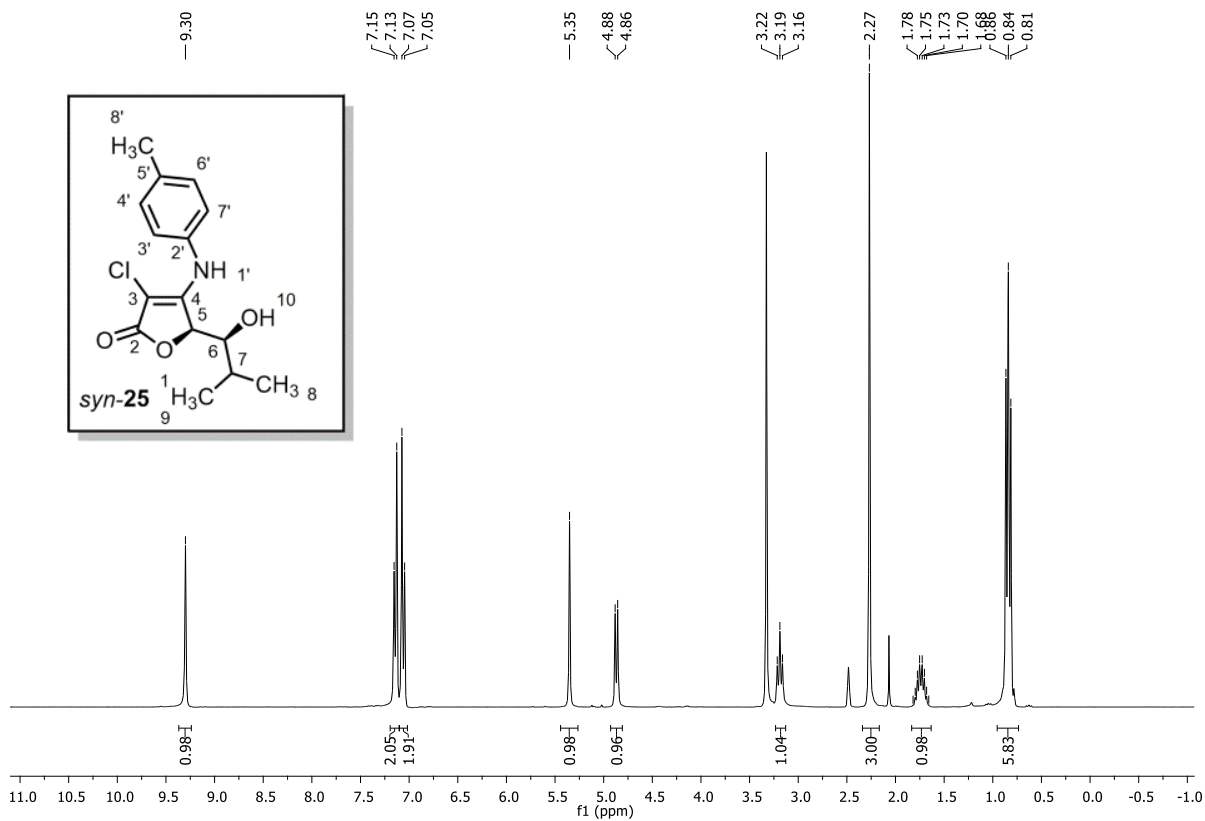
Figure A2.19 ^{1}H NMR (300 MHz, DMSO-d$_6$) of compound *syn*-25
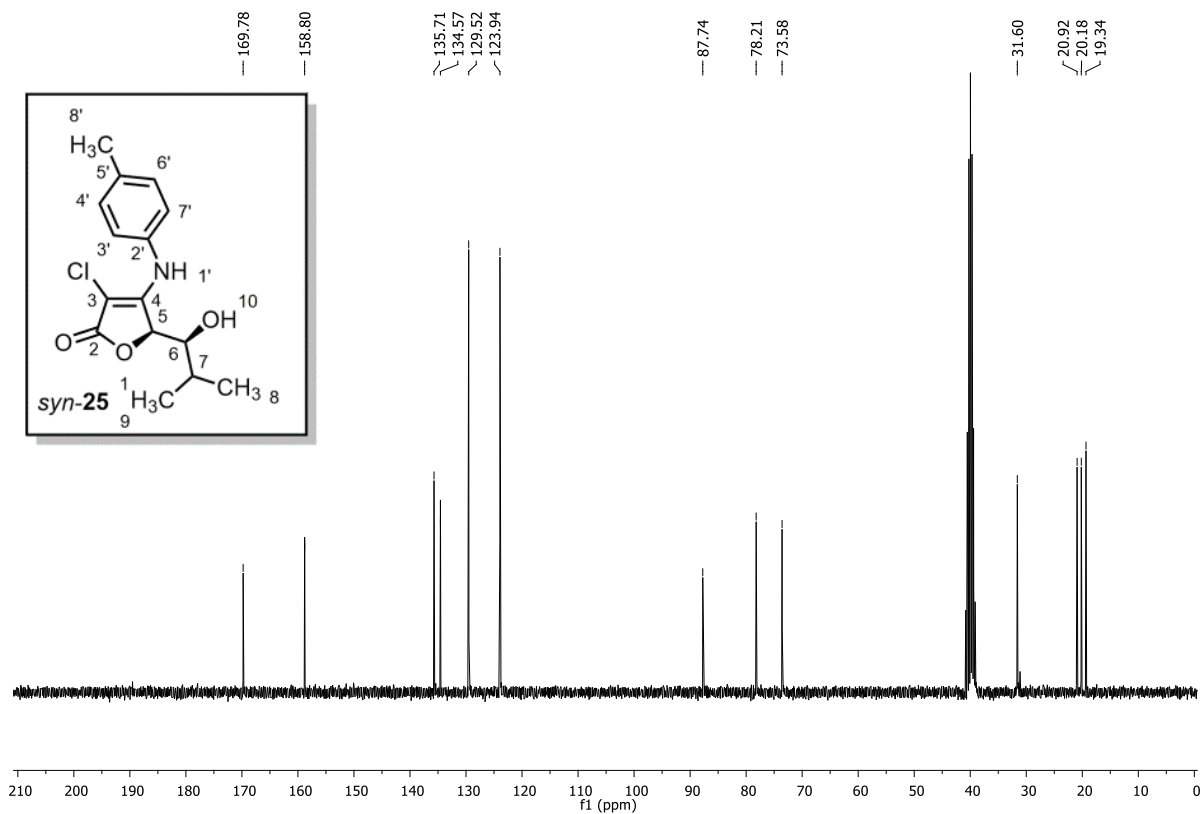
Figure A2.20 ^{13}C NMR (75 MHz, DMSO-d$_6$) of compound *syn*-25

184

2.3. ^{1}H NMR Spectra of Retro-Aldol Products
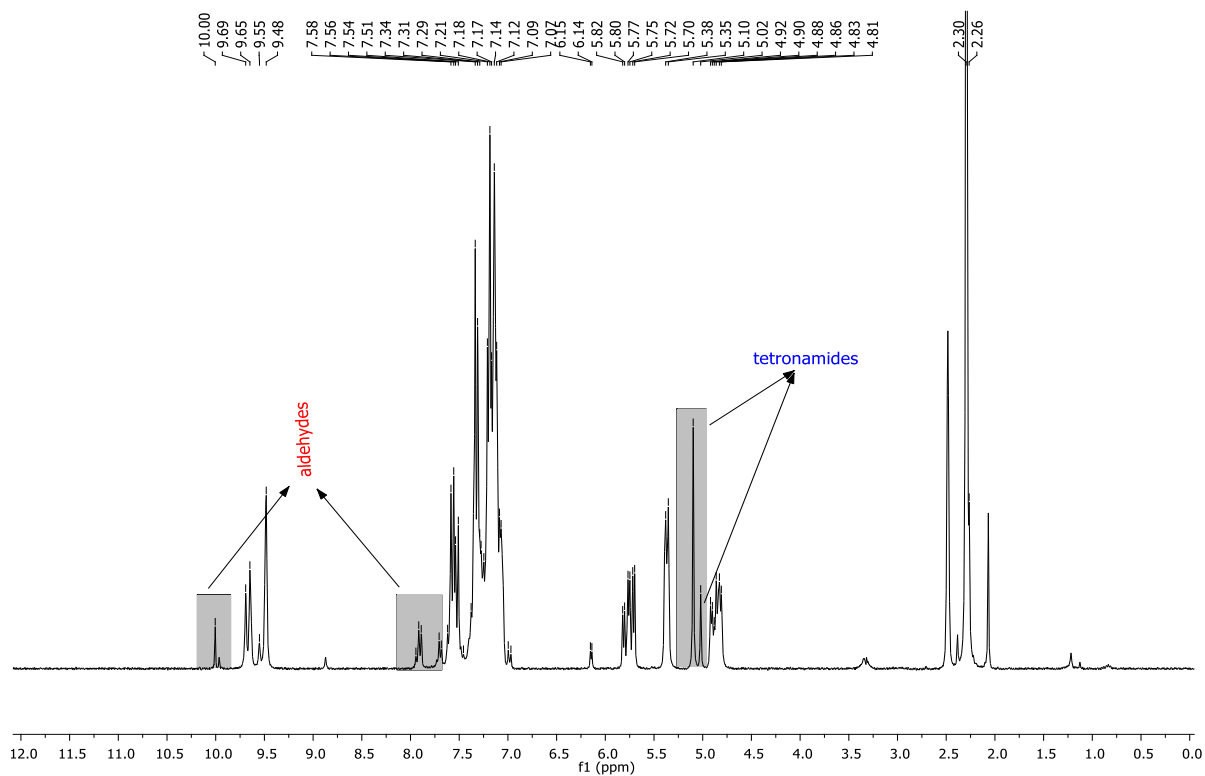
Figure A2.21 ^{1}H NMR (300 MHz, DMSO-d$_6$) of the crude (retro-aldol products)

2.4. ^{1}H NMR Spectra of *Anti*-9 for the 'D' Incorporation vs. Isomerization
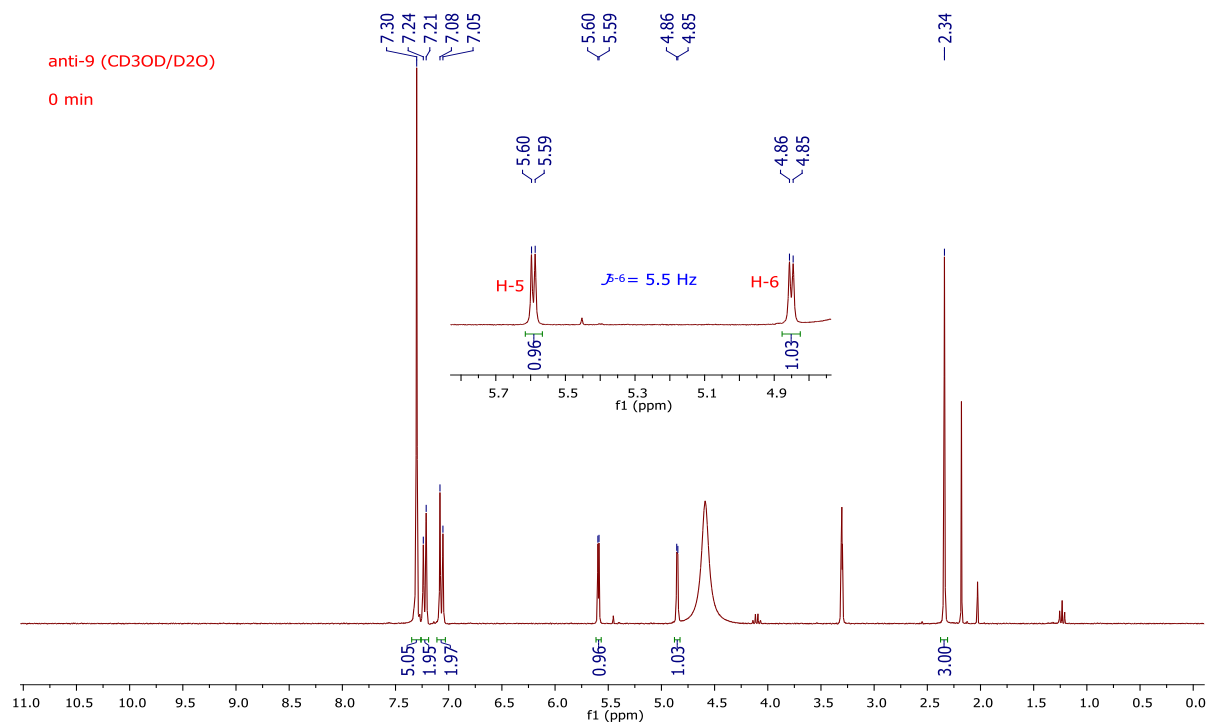
Figure A2.22 ^{1}H NMR (300 MHz, CD$_3$OD/D$_2$O; 2:1) recorded before addition of NaOH
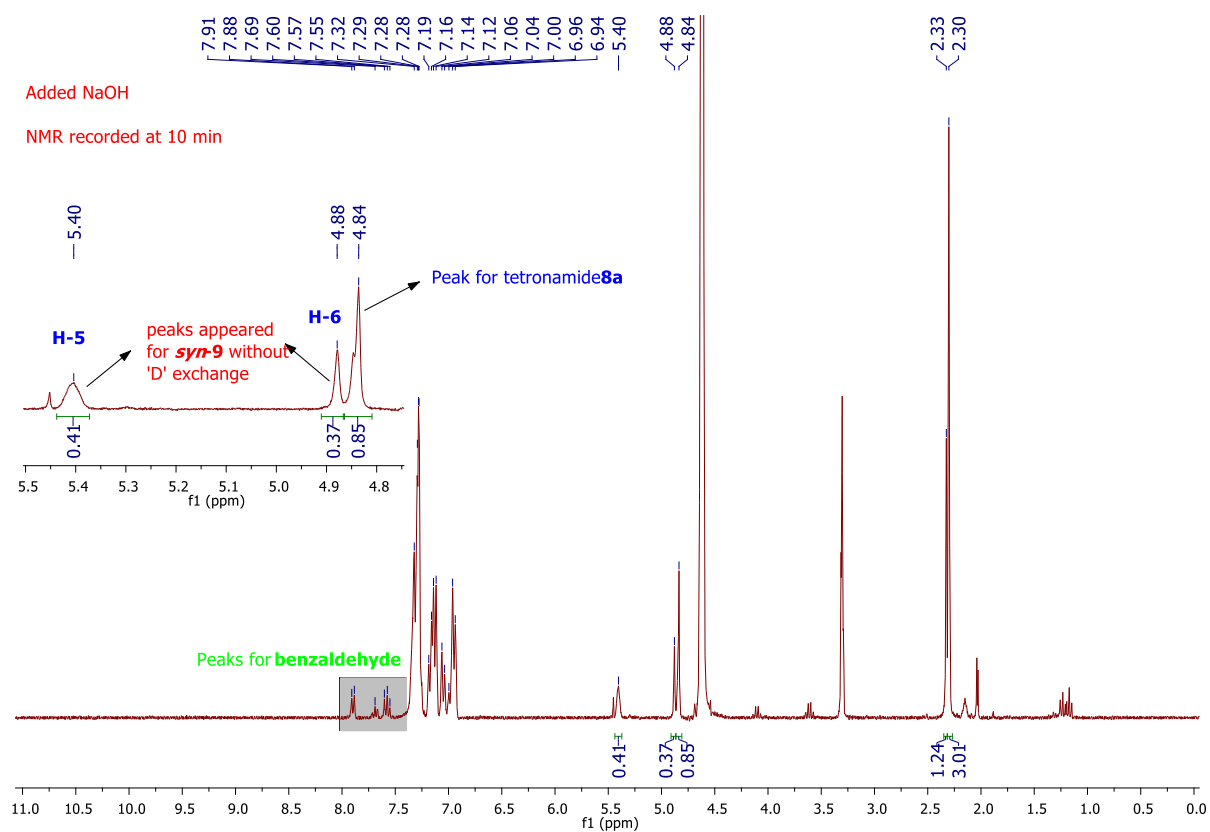
Figure A2.23 ^{1}H NMR (300 MHz, CD$_3$OD/D$_2$O; 2:1) recorded at 10 min after addition of NaOH
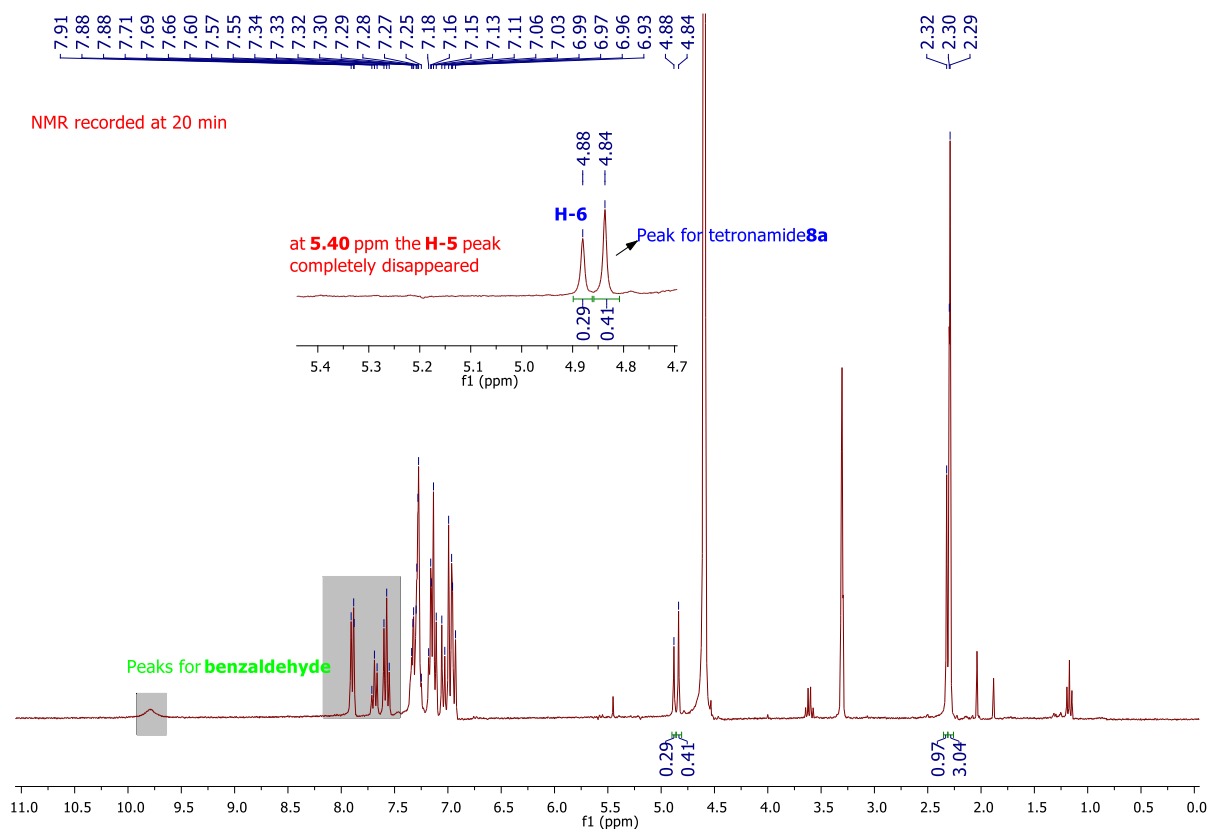
Figure A2.24 ^{1}H NMR (300 MHz, CD$_3$OD/D$_2$O; 2:1) recorded at 20 min after addition of NaOH
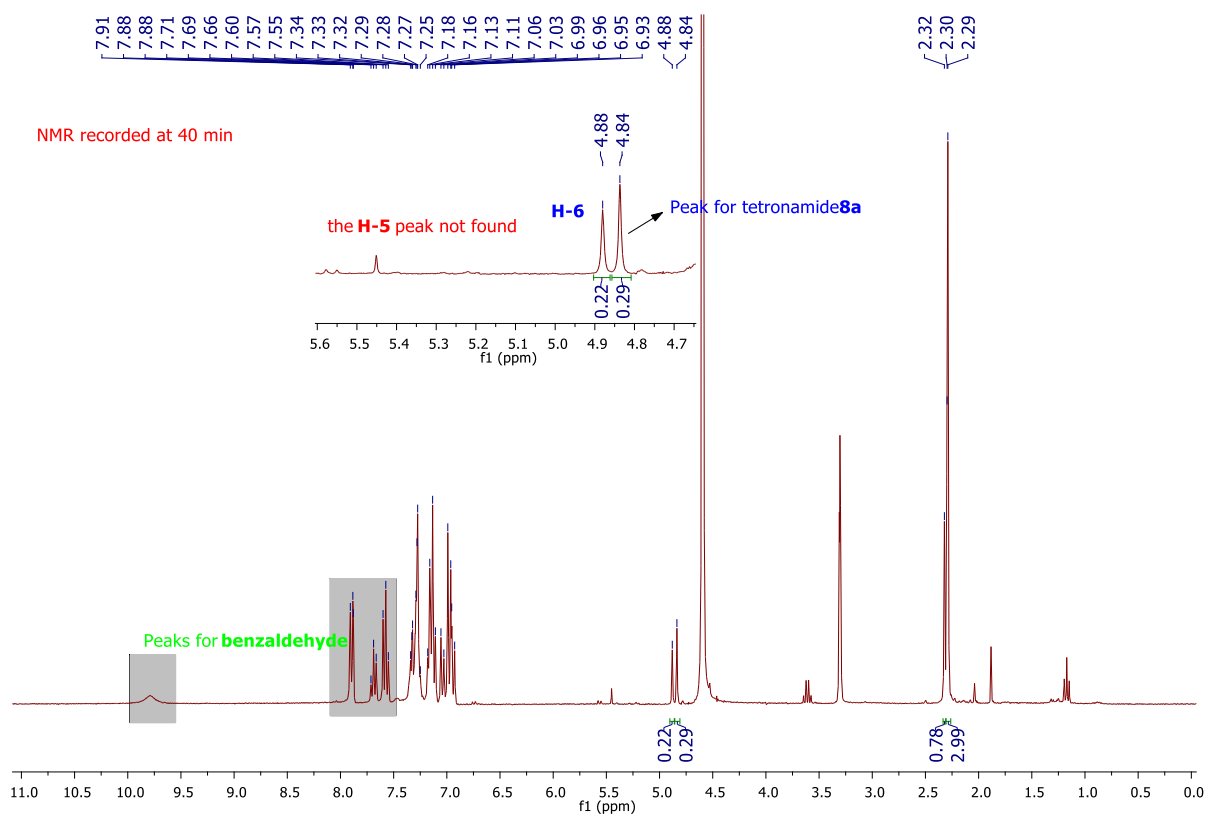
Figure A2.25 ^{1}H NMR (300 MHz, CD$_3$OD/D$_2$O; 2:1) recorded at 40 min after addition of NaOH
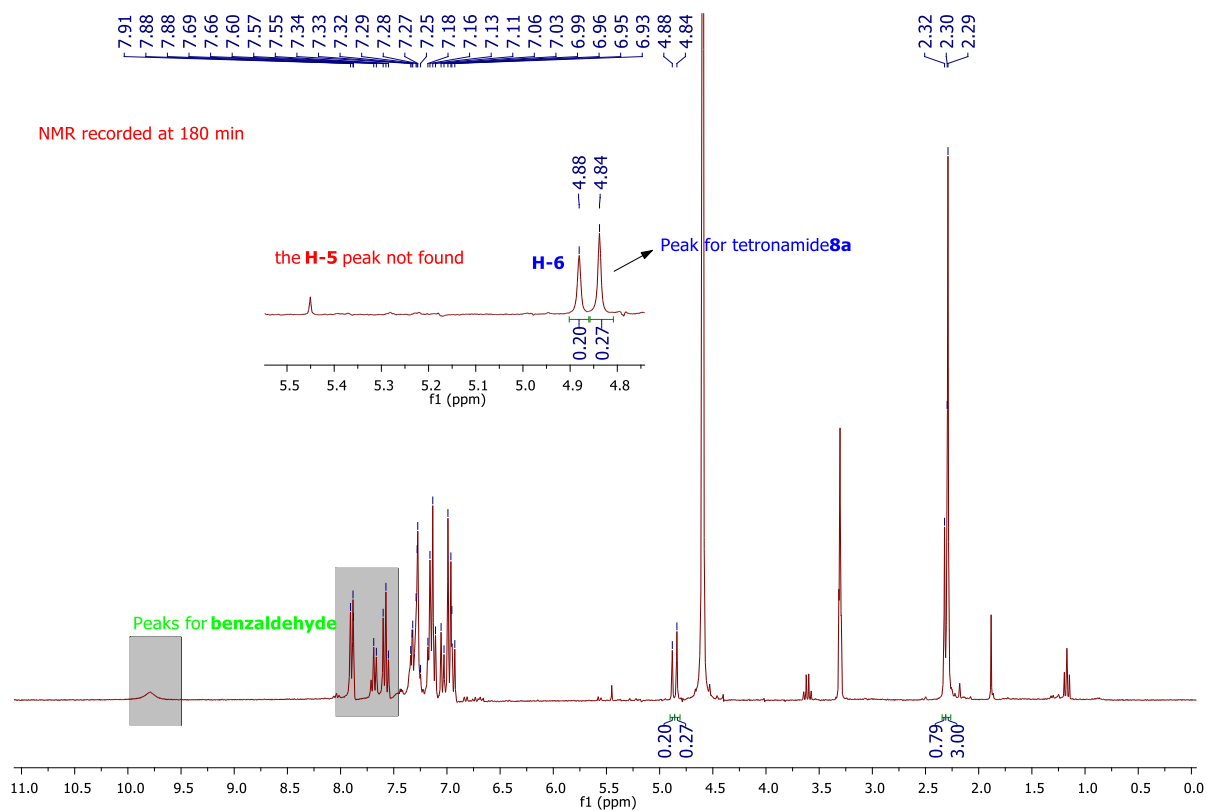
Figure A2.26 ^{1}H NMR (300 MHz, CD$_3$OD/D$_2$O; 2:1) recorded at 180 min after addition of NaOH

188

3. Appendix 3 (Further Computational Studies Relevant to Chapter 3)
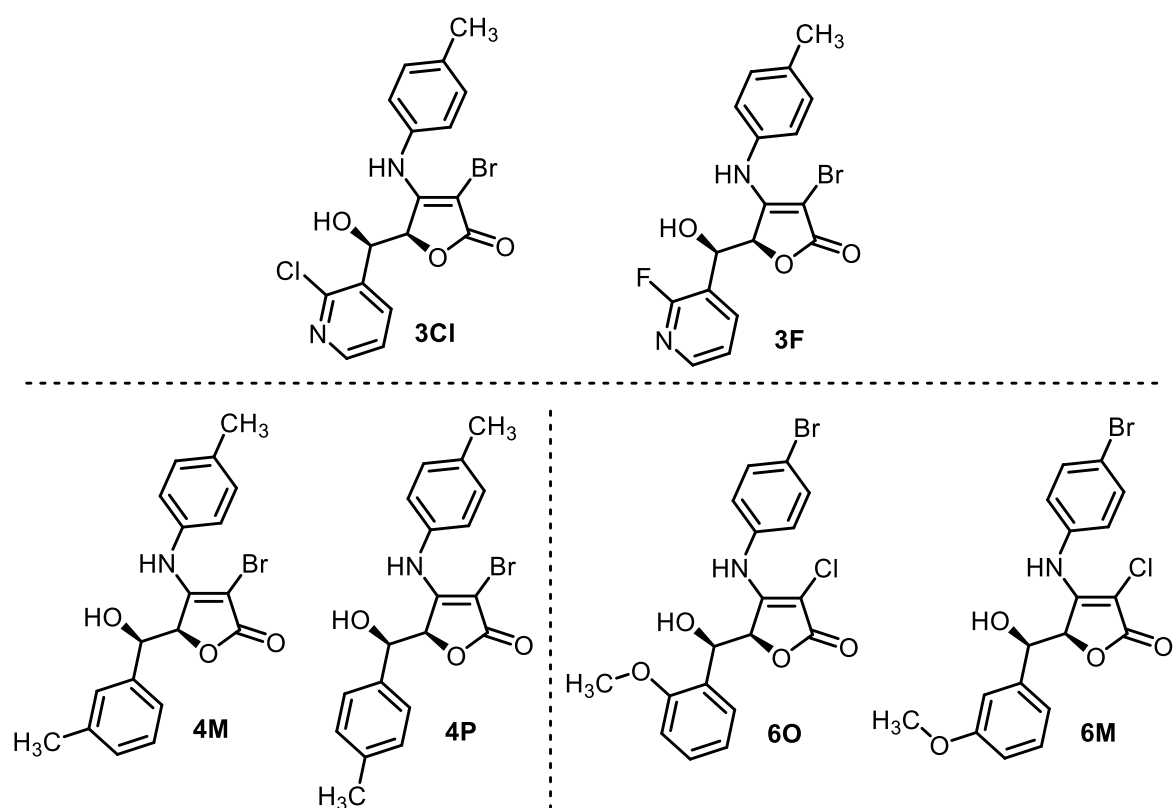
Figure A3.1 Comparative tetronamides whose crystal structures are not available up to now, were optimized (B3LYP/6-31G*) and their relative energies were computed at the PCM/B3LYP/6-31G* level (solvent=chloroform).

Table A3.1 Relative energies and Boltzmann distributions computed in solution ($CHCl_3$) and in gas phase for the tetronamides whose crystal structure is not available up to now (**Figure A3.1**) at the B3LYP/6-31G* level of theory.

Compound	RelativeEnergy (solution)	Contribution (%)	RelativeEnergy (gas phase)	Contribution (%)
3F_c1	0.00	75	0.00	88
3F_c2	0.98	15	2.20	2
3F_c3	1.55	6	2.21	2
3F_c4	1.99	3	1.83	4
3F_c5	2.35	1	1.96	3
3F_c6	3.44	0	4.60	0
3Cl_c1	0.00	47	0.00	17
3Cl_c2	0.39	24	-0.50	38
3Cl_c3	0.72	14	0.23	11
3Cl_c4	0.86	11	-0.24	25
3Cl_c5	1.74	3	0.44	8
3Cl_c6	2.19	1	1.98	1
4p_c1	0.00	62	0.00	52
4p_c2	0.51	26	0.47	24
4p_c3	1.18	9	0.61	19
4p_c4	1.75	3	1.45	5
4m_c1	0.00	33	0.00	31
4m_c2	0.08	29	0.17	23
4m_c3	0.47	15	0.48	14
4m_c4	0.47	15	0.45	15
4m_c5	1.23	4	0.71	9
4m_c6	1.29	4	0.85	7
6o_c1	0.00	23	0.00	21
6o_c2	0.26	15	-0.11	25
6o_c3	0.27	15	1.03	4
6o_c4	0.32	14	0.23	14
6o_c5	0.42	11	0.55	8
6o_c6	0.59	9	0.31	12
6o_c7	0.86	6	0.80	5
6o_c8	1.07	4	0.81	5
6o_c9	1.09	4	0.84	5
6m_c1	0.00	25	0.00	16
6m_c2	0.10	22	-0.57	41
6m_c3	0.33	15	0.49	7
6m_c4	0.49	11	0.59	6
6m_c5	0.66	8	-0.07	18
6m_c6	0.69	8	0.74	5
6m_c7	0.87	6	0.81	4
6m_c8	0.96	5	1.06	3

3F_c1
E_rel = 0.00 kcal/mol
Contribution = 75%

3F_c2
E_rel = 0.98 kcal/mol
Contribution = 15%

3F_c3
E_rel = 1.55 kcal/mol
Contribution = 6%

3F_c4
E_rel = 1.99 kcal/mol
Contribution = 3%

3F_c5
E_rel = 2.35 kcal/mol
Contribution = 1%

3F_c6
E_rel = 3.44 kcal/mol
Contribution < 1%
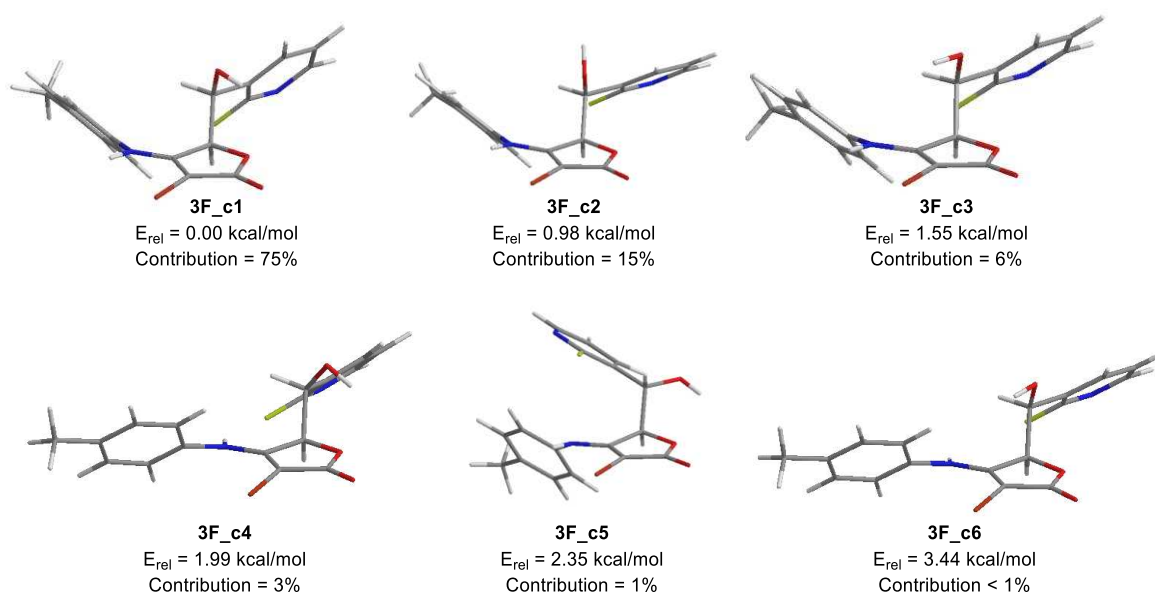
Figure A3.2 B3LYP/6-31G* optimized geometries of all significantly populated conformers of compound **3F**, with relative energies computed at the PCM/B3LYP/6-31G* level (solvent=chloroform).

3Cl_c1
E_rel = 0.00 kcal/mol
Contribution = 47%

3Cl_c2
E_rel = 0.39 kcal/mol
Contribution = 24%

3Cl_c3
E_rel = 0.72 kcal/mol
Contribution = 14%

3Cl_c4
E_rel = 0.86 kcal/mol
Contribution = 11%

3Cl_c5
E_rel = 1.74 kcal/mol
Contribution = 3%

3Cl_c6
E_rel = 2.19 kcal/mol
Contribution < 1%
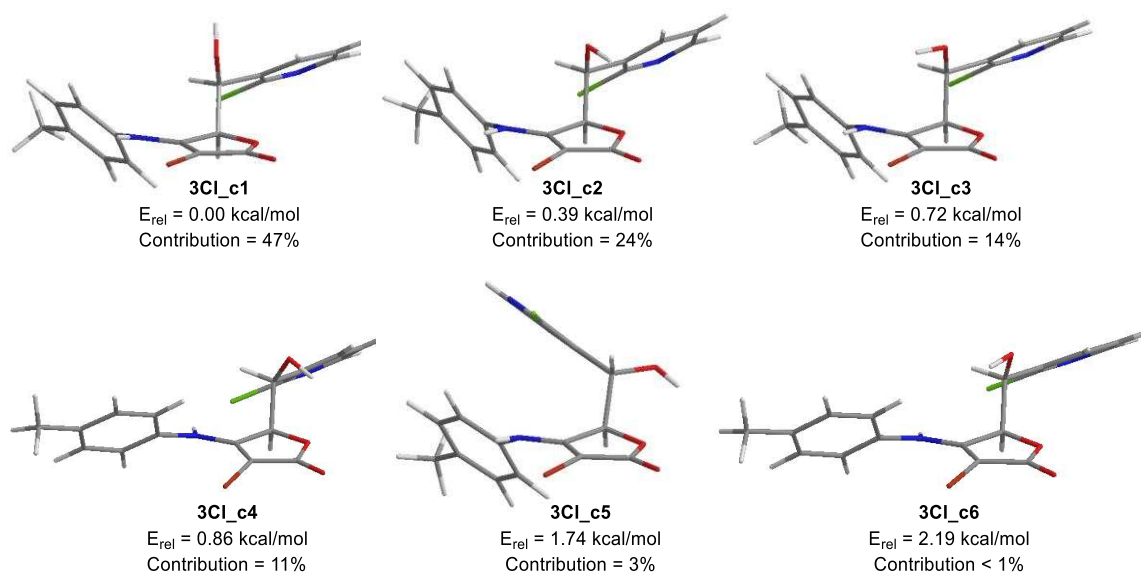
Figure A3.3 B3LYP/6-31G* optimized geometries of all significantly populated conformers of compound **3Cl**, with relative energies computed at the PCM/B3LYP/6-31G* level (solvent=chloroform).
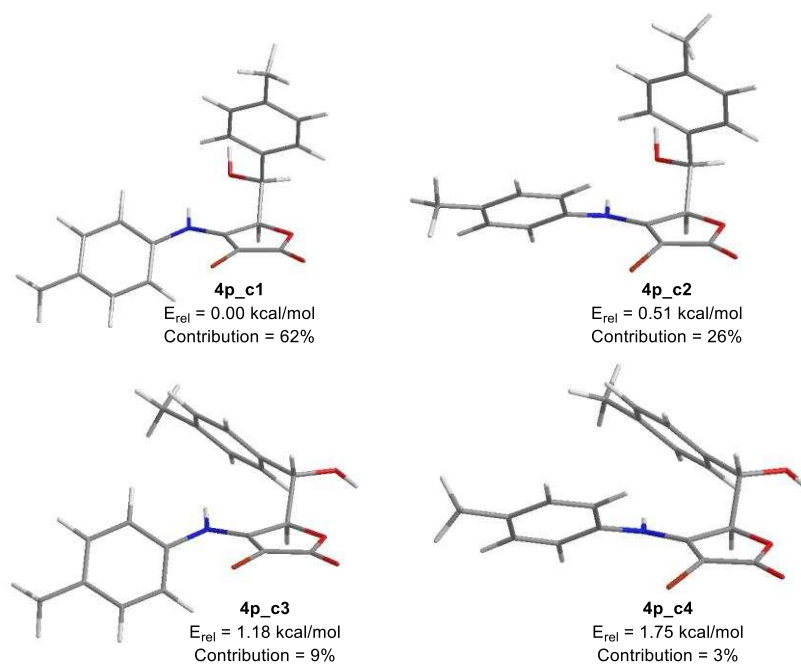
Figure A3.4 B3LYP/6-31G* optimized geometries of all significantly populated conformers of compound **4p**, with relative energies computed at the PCM/B3LYP/6-31G* level (solvent=chloroform).
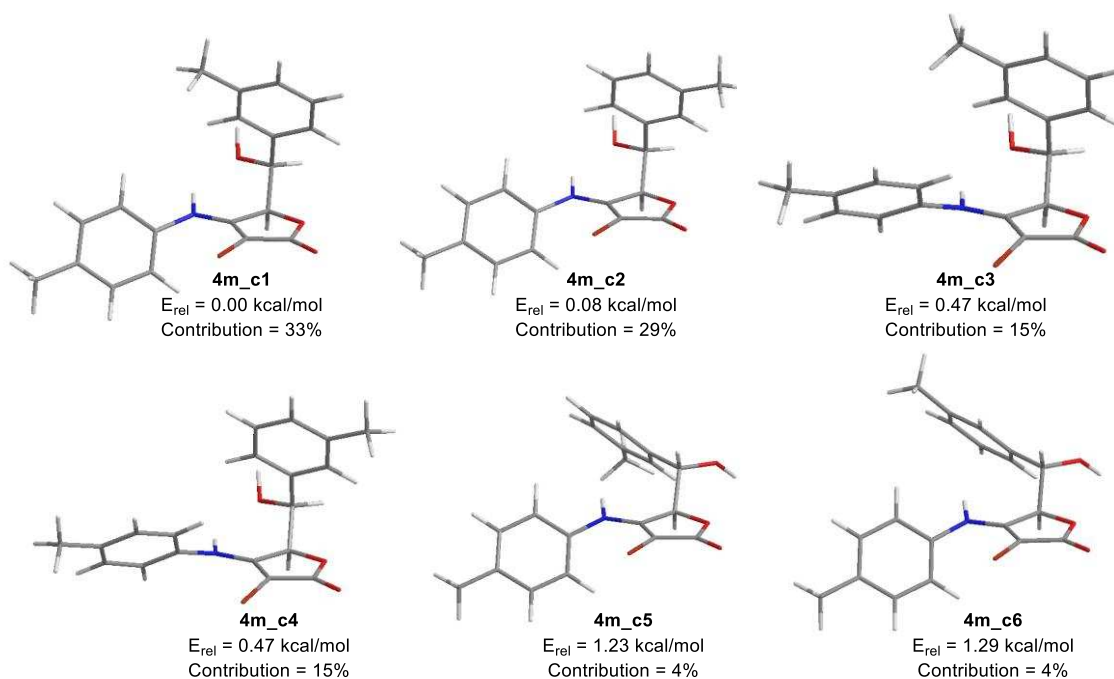
Figure A3.5 B3LYP/6-31G* optimized geometries of all significantly populated conformers of compound **4m**, with relative energies computed at the PCM/B3LYP/6-31G* level (solvent=chloroform).

6o_c1
E_{rel} = 0.00 kcal/mol
Contribution = 23%

6o_c2
E_{rel} = 0.26 kcal/mol
Contribution = 15%

6o_c3
E_{rel} = 0.27 kcal/mol
Contribution = 15%

6o_c4
E_{rel} = 0.32 kcal/mol
Contribution = 14%

6o_c5
E_{rel} = 0.42 kcal/mol
Contribution = 11%

6o_c6
E_{rel} = 0.59 kcal/mol
Contribution = 9%

6o_c7
E_{rel} = 0.86 kcal/mol
Contribution = 6%

6o_c8
E_{rel} = 1.07 kcal/mol
Contribution = 4%

6o_c9
E_{rel} = 1.09 kcal/mol
Contribution = 4%
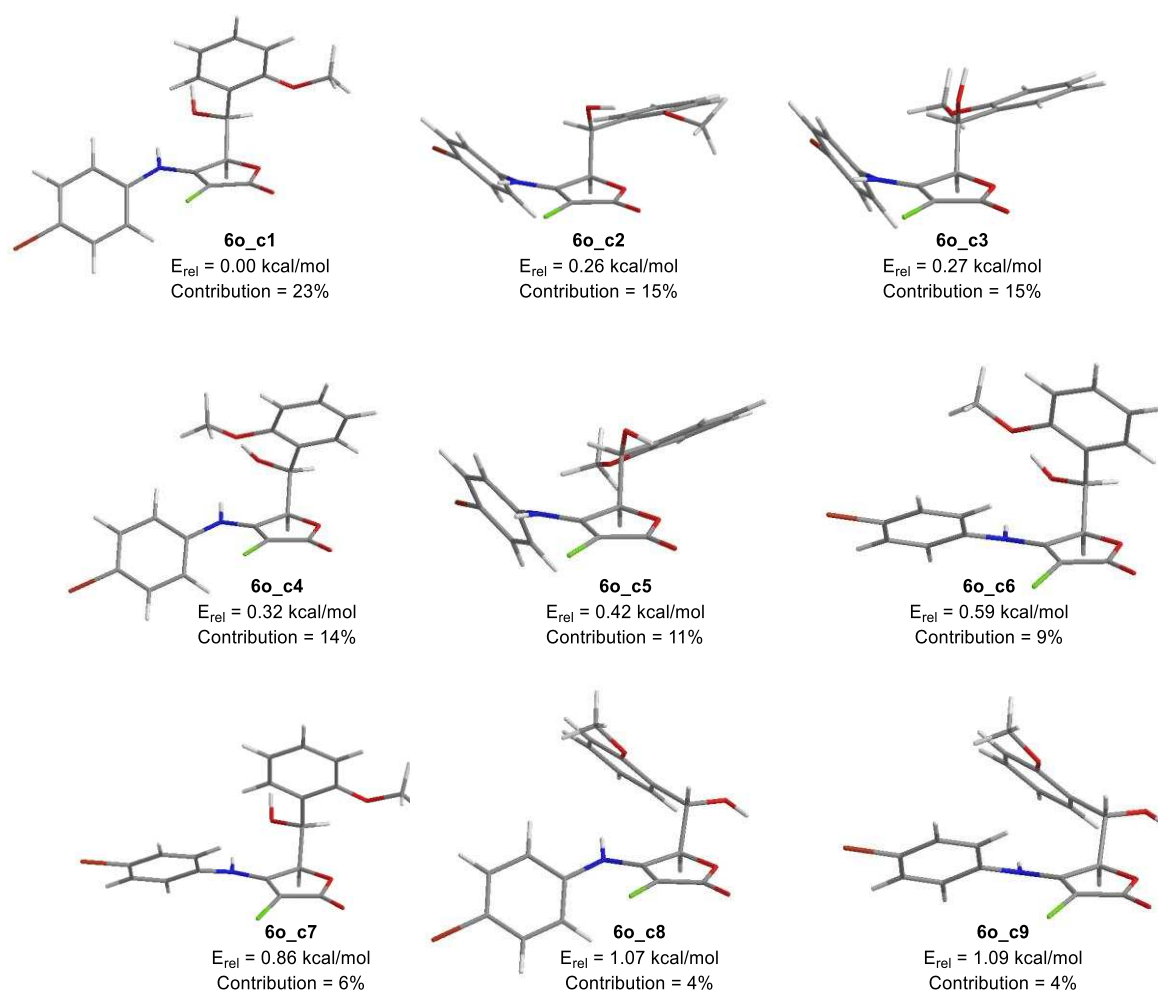
Figure A3.6 B3LYP/6-31G* optimized geometries of all significantly populated conformers of compound **6o**, with relative energies computed at the PCM/B3LYP/6-31G* level (solvent=chloroform).

6m_c1
E_{rel} = 0.00 kcal/mol
Contribution = 25%

6m_c2
E_{rel} = 0.10 kcal/mol
Contribution = 22%

6m_c3
E_{rel} = 0.33 kcal/mol
Contribution = 15%

6m_c4
E_{rel} = 0.49 kcal/mol
Contribution = 11%

6m_c5
E_{rel} = 0.66 kcal/mol
Contribution = 8%

6m_c6
E_{rel} = 0.69 kcal/mol
Contribution = 8%

6m_c7
E_{rel} = 0.87 kcal/mol
Contribution = 6%

6m_c8
E_{rel} = 0.96 kcal/mol
Contribution = 5%
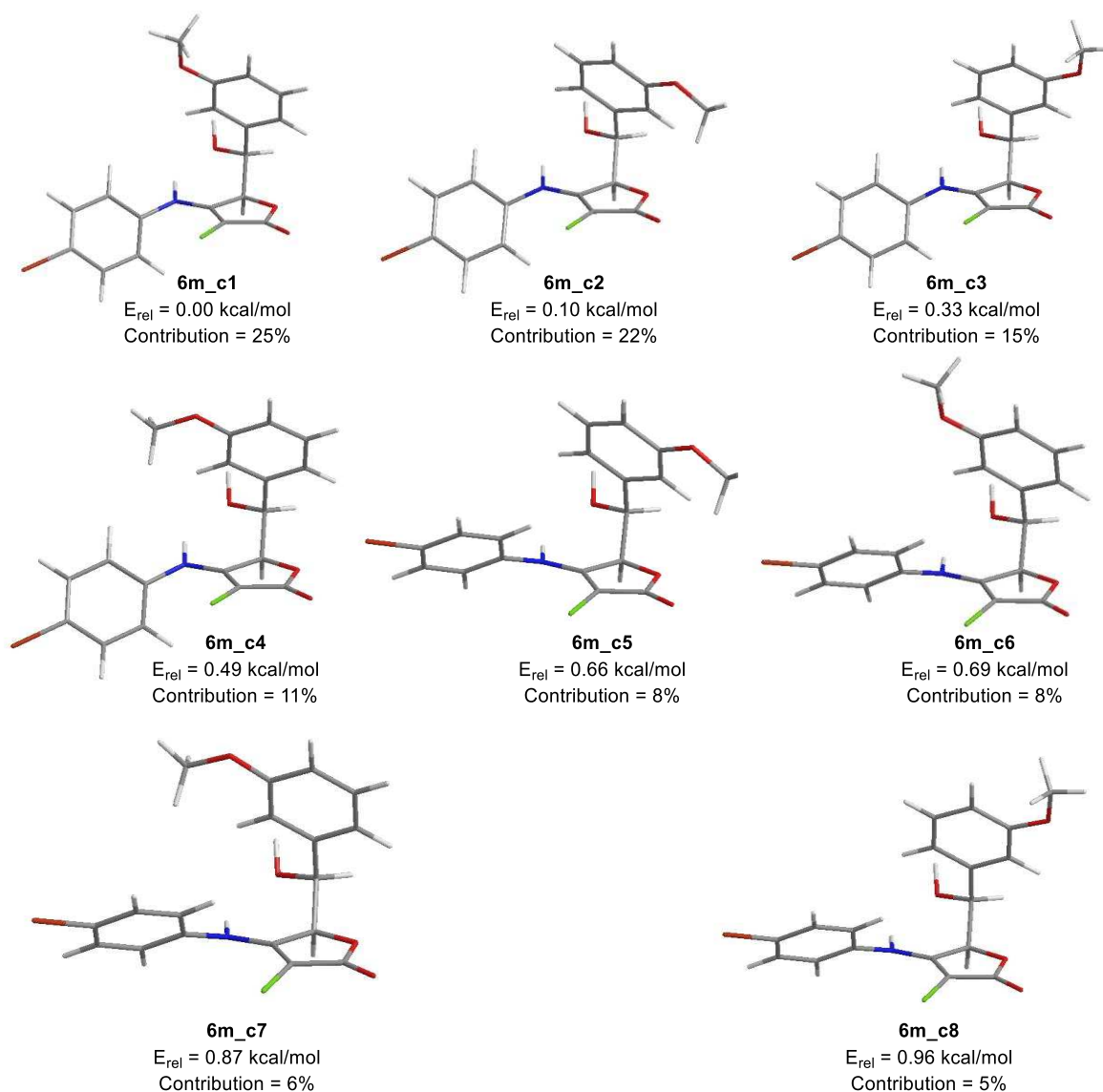
Figure A3.7 B3LYP/6-31G* optimized geometries of all significantly populated conformers of compound **6m**, with relative energies computed at the PCM/B3LYP/6-31G* level (solvent=chloroform).

4. Appendix 4 (NMR Spectra Relevant to Chapter 4)

4.1. NMR Spectra of Suzuki Coupling Products 5a-e
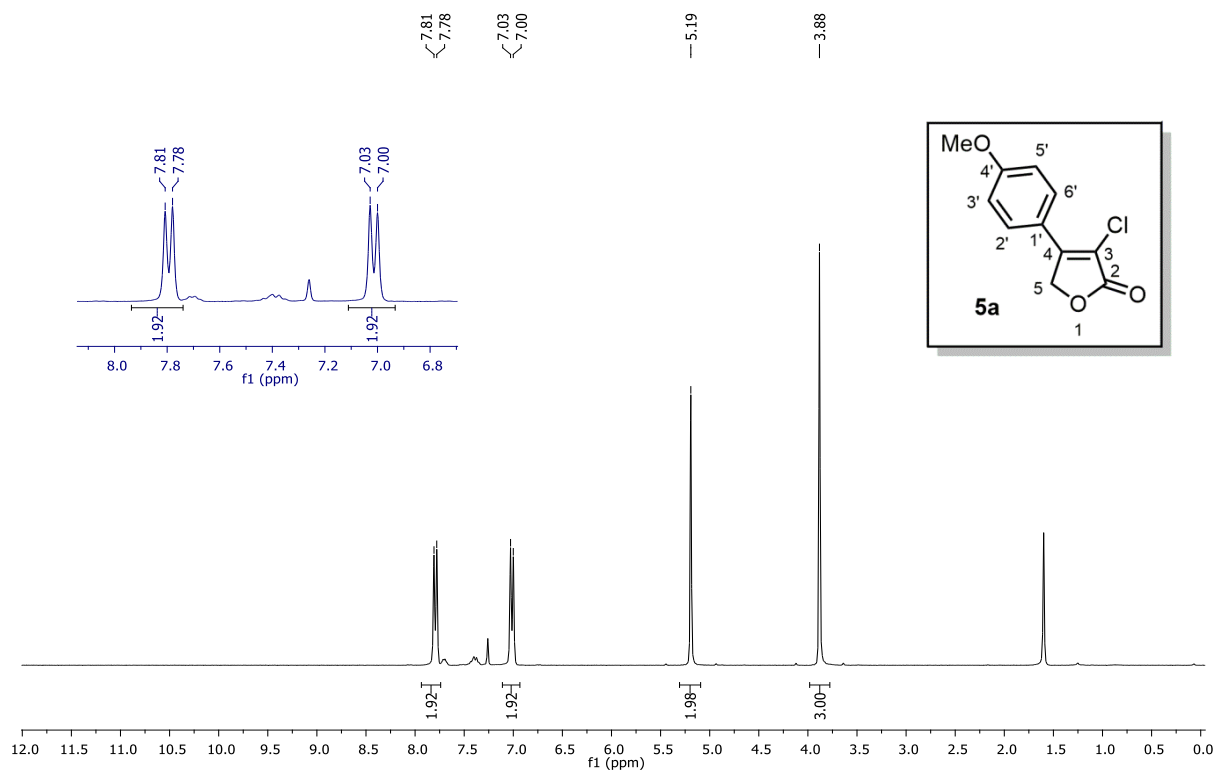
Figure A4.1 ^{1}H NMR (400 MHz, CDCl$_3$) of compound **5a**
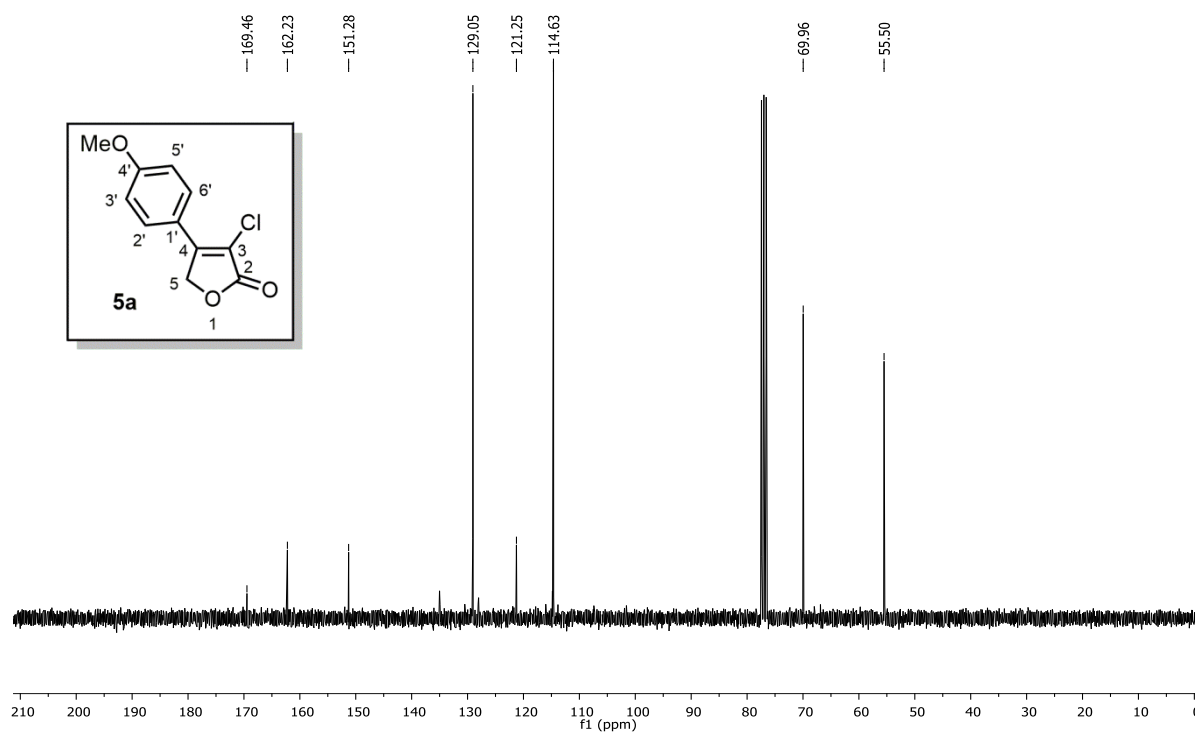
Figure A4.2 ^{13}C NMR (100 MHz, CDCl$_3$) of compound **5a**

Figure A4.3 ^{1}H NMR (400 MHz, DMSO-d$_6$) of compound **5b**

Figure A4.4 ^{13}C NMR (100 MHz, DMSO-d$_6$) of compound **5b**

196
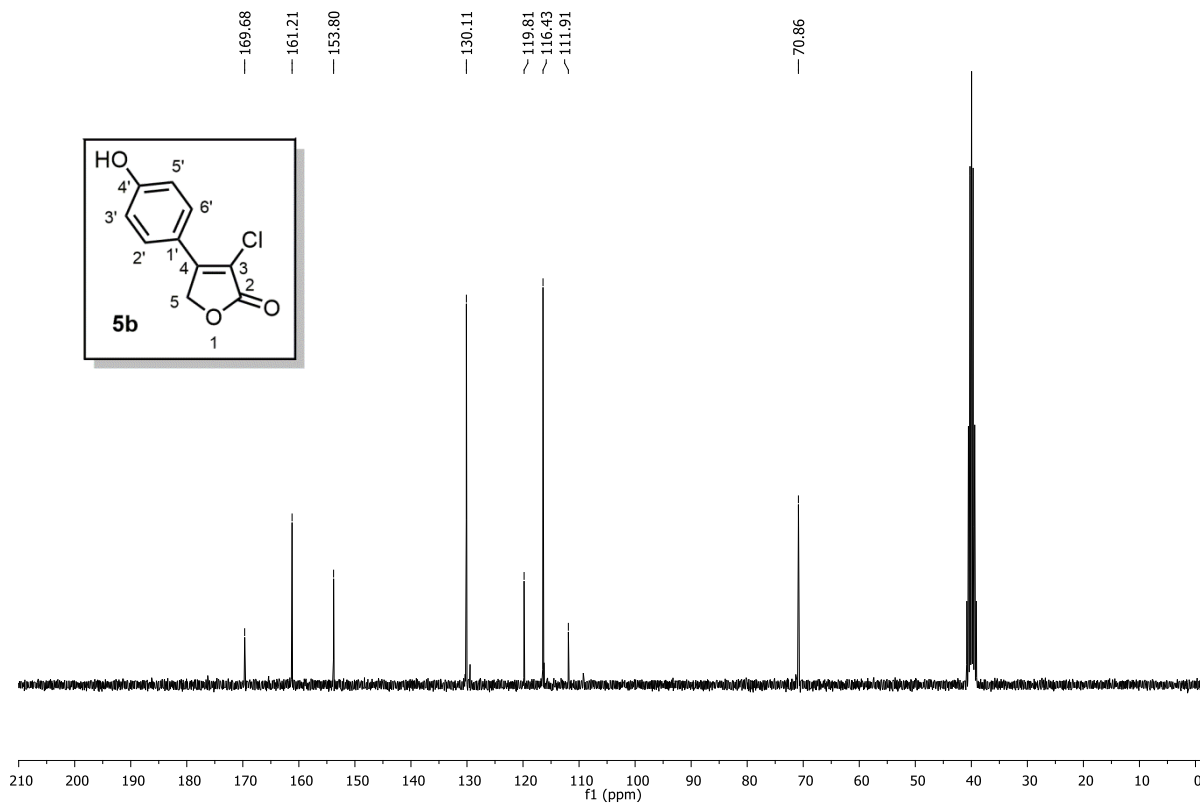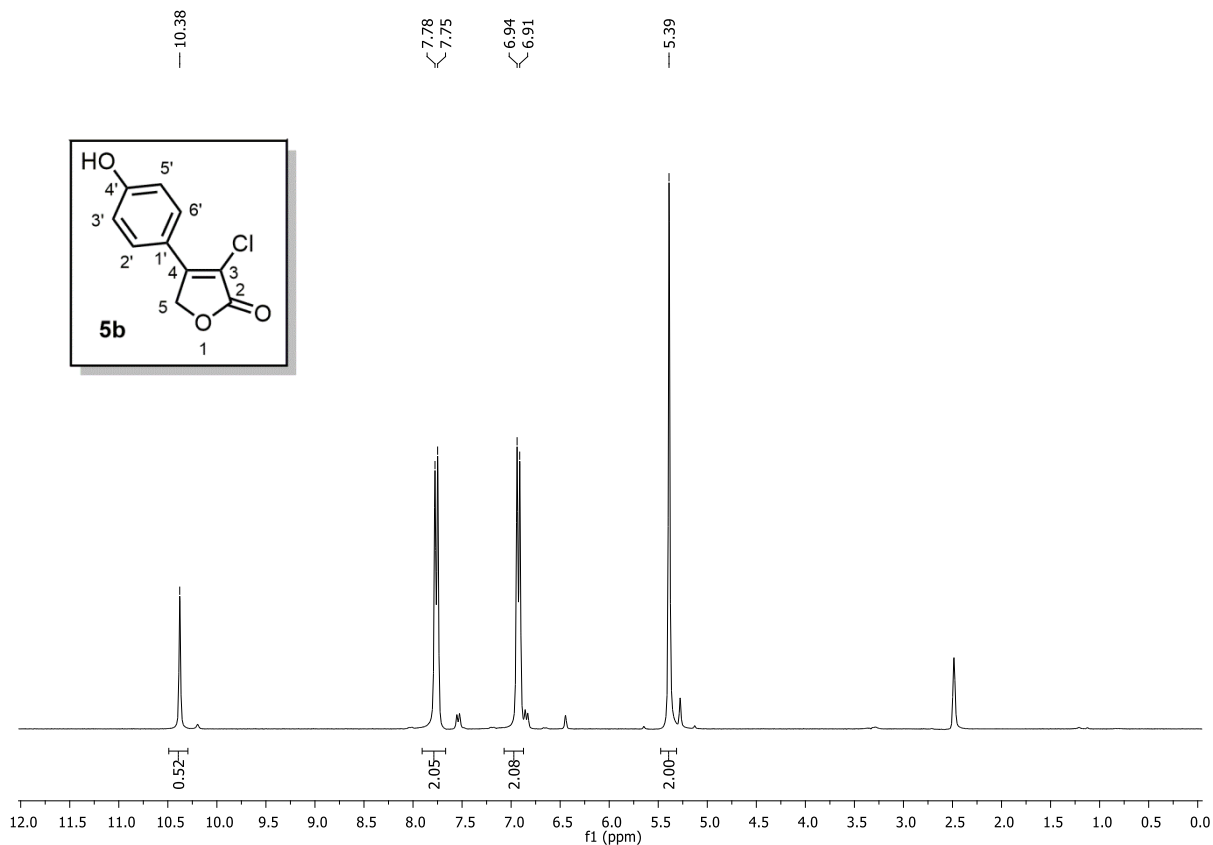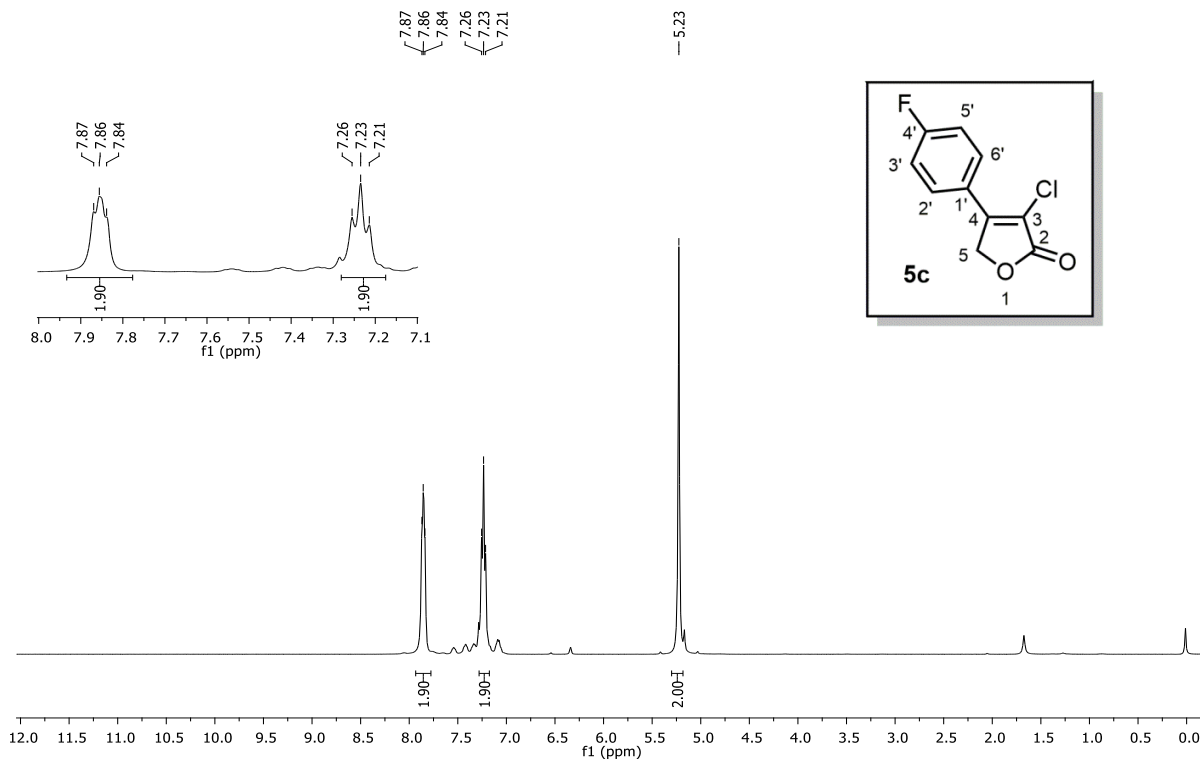
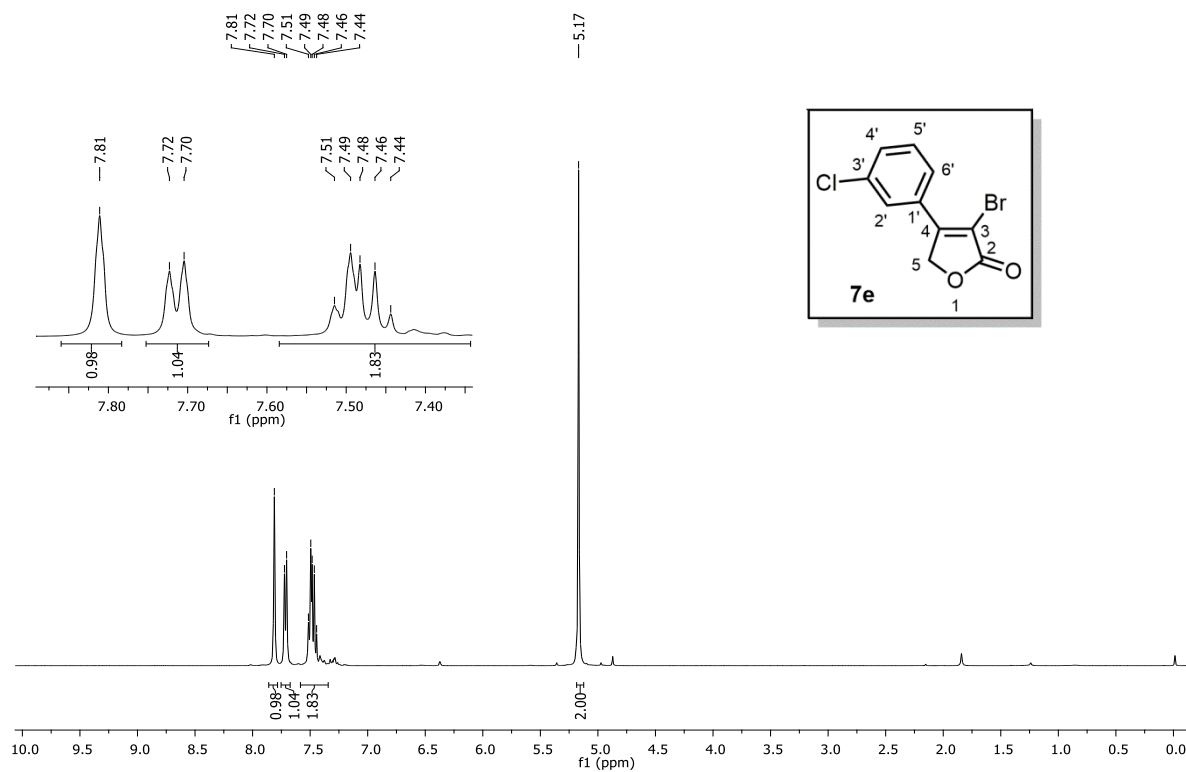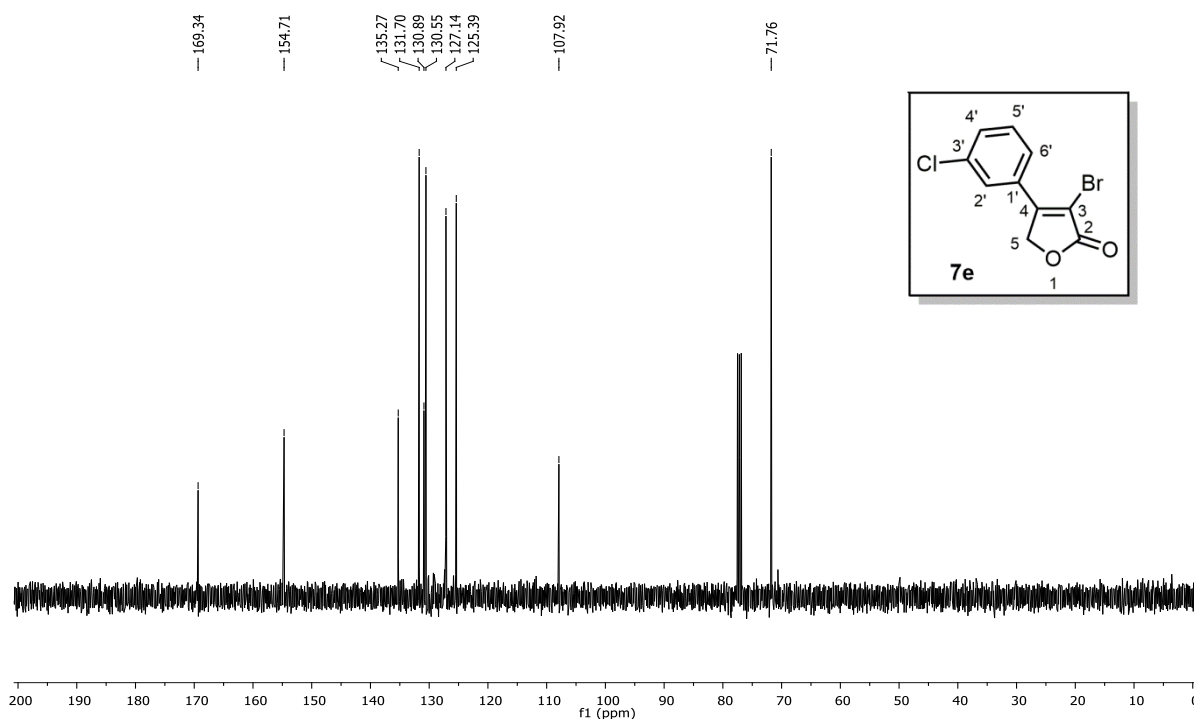**Figure A4.5** ^{1}H NMR (400 MHz, CDCl$_3$) of compound **5c**
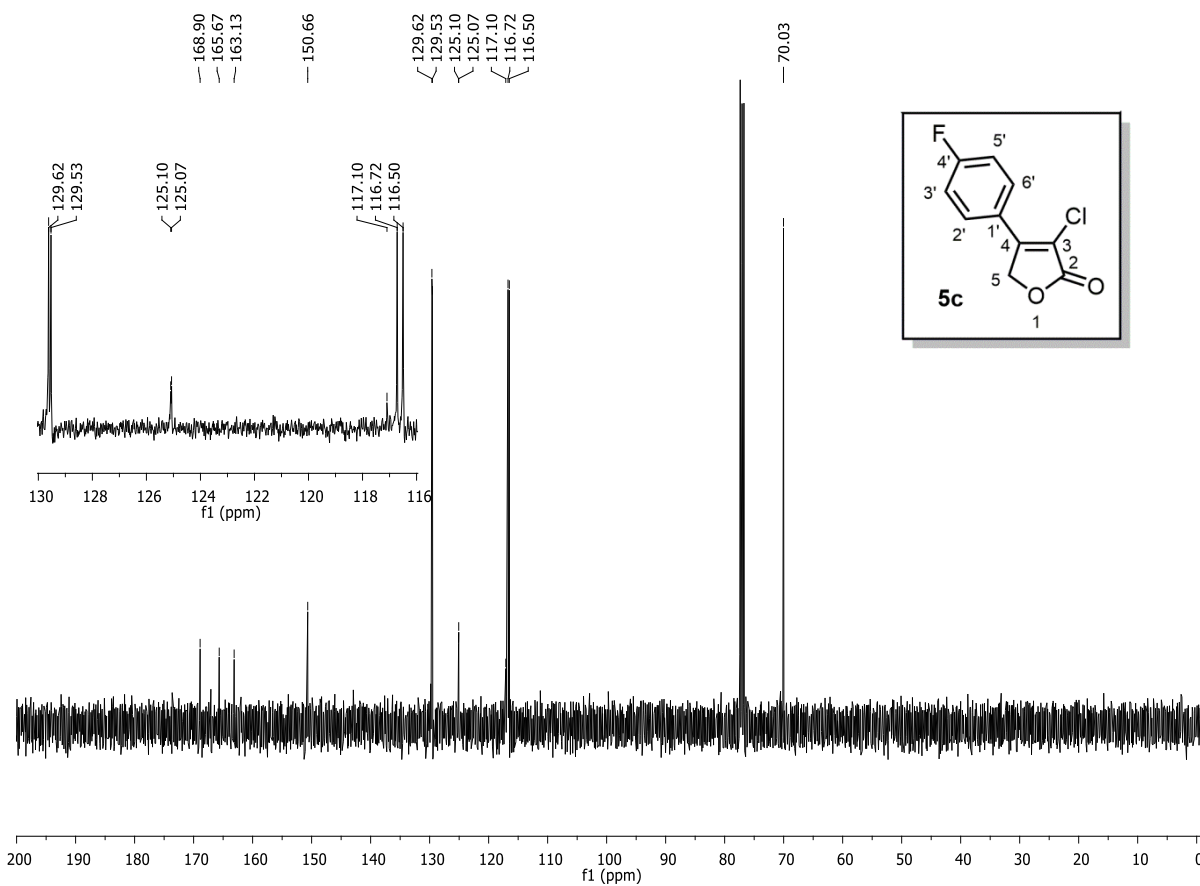
Figure A4.6 ^{13}C NMR (100 MHz, CDCl$_3$) of compound **5c**
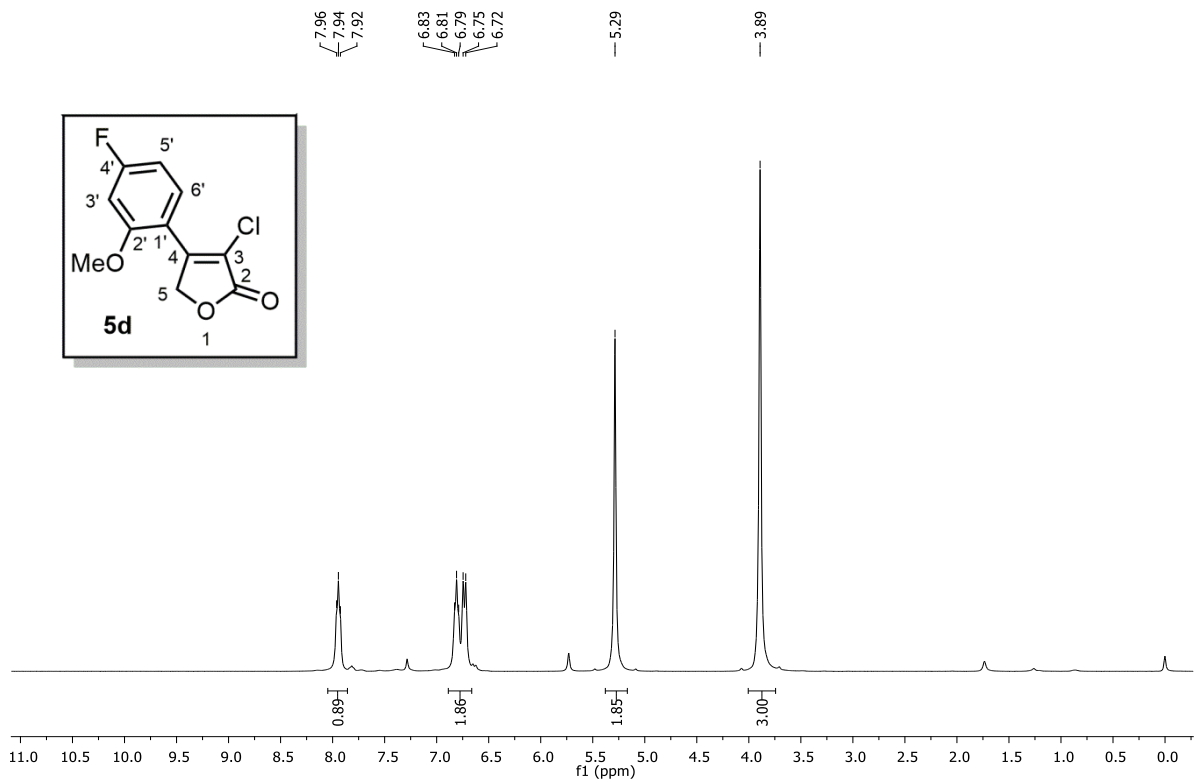
Figure A4.7 ^{1}H NMR (400 MHz, CDCl$_3$) of compound **5d**
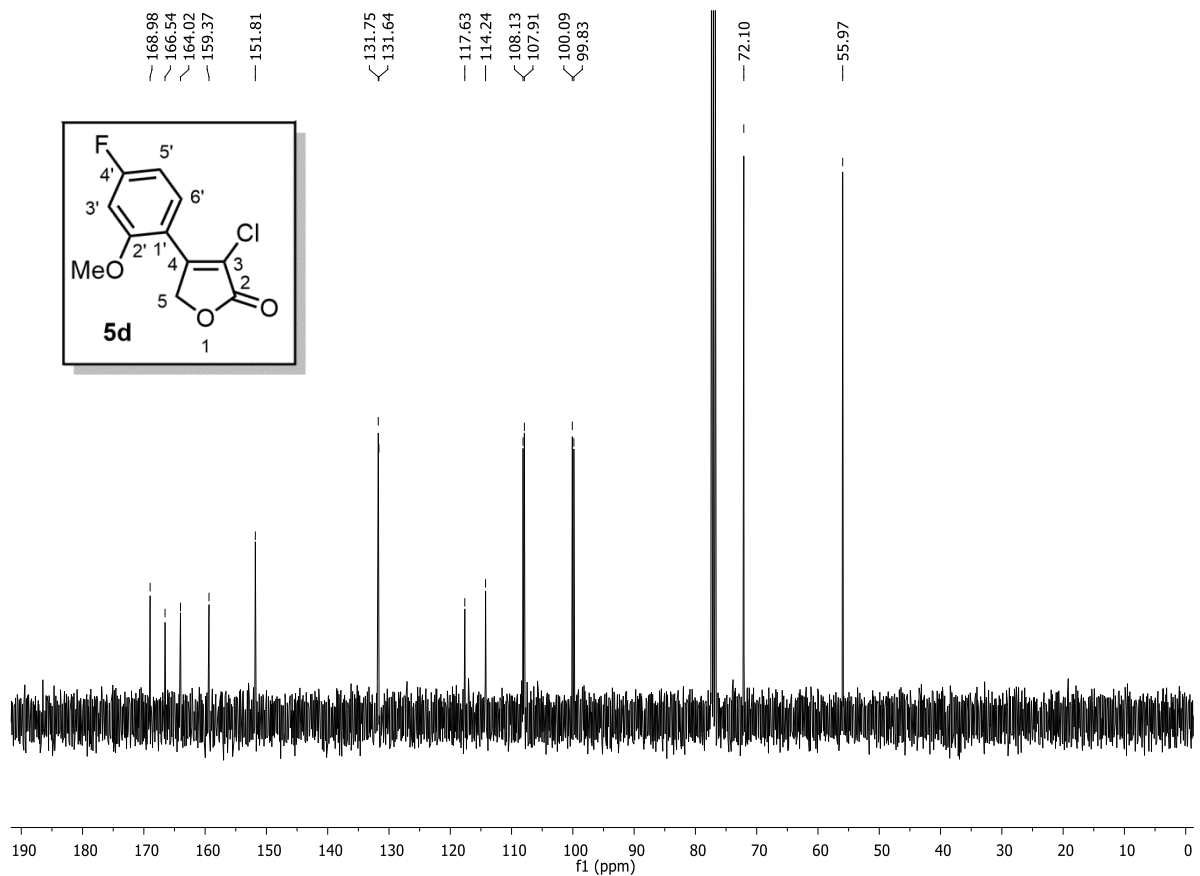
Figure A4.8 ^{13}C NMR (100 MHz, CDCl$_3$) of compound **5d**

198
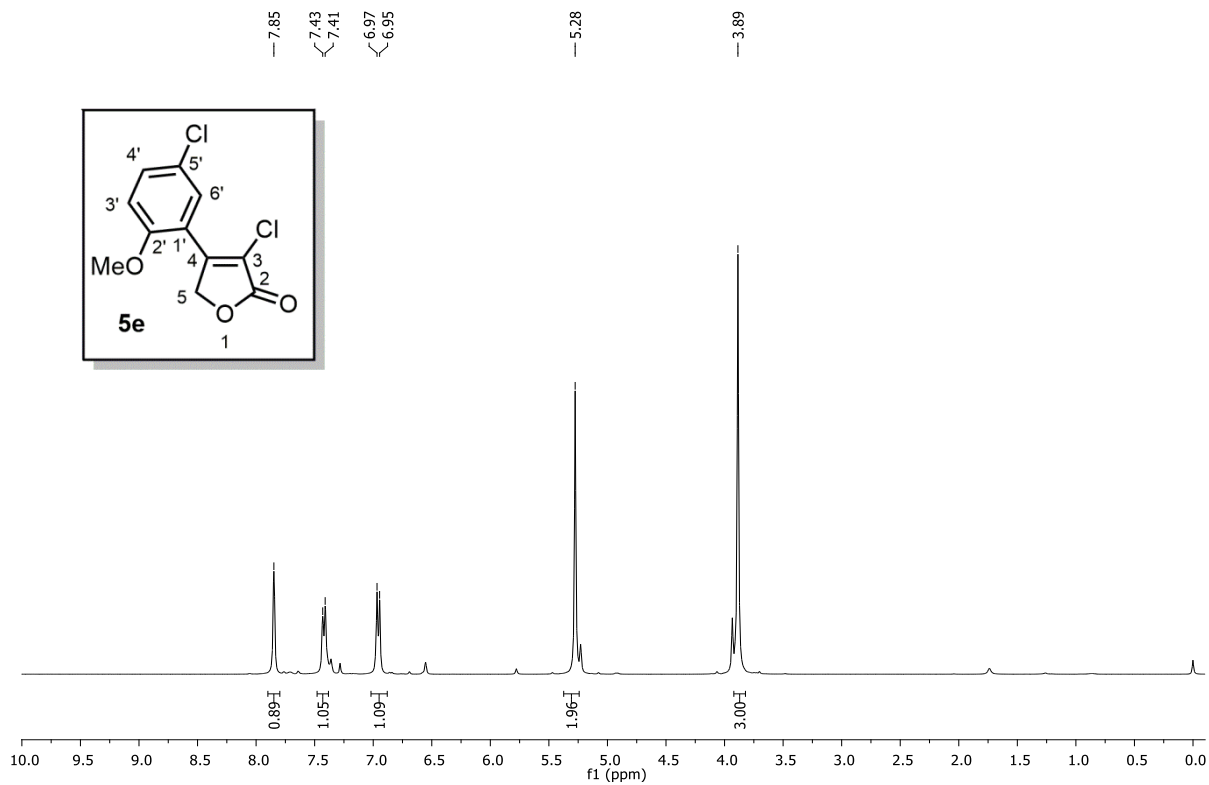
Figure A4.9 ^{1}H NMR (400 MHz, CDCl$_3$) of compound **5e**
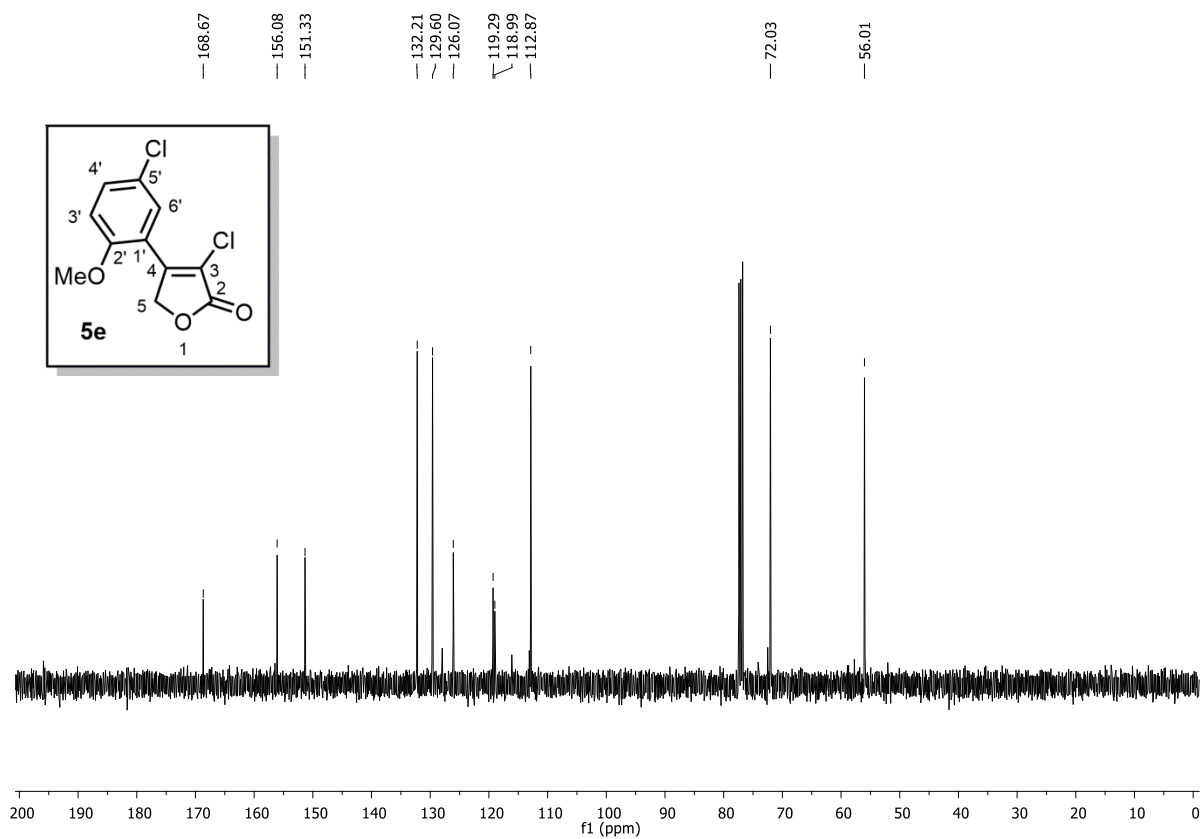
Figure A4.10 ^{13}C NMR (100 MHz, CDCl$_3$) of compound **5e**

4.2. NMR Spectra of Halogenation Products 7a-c
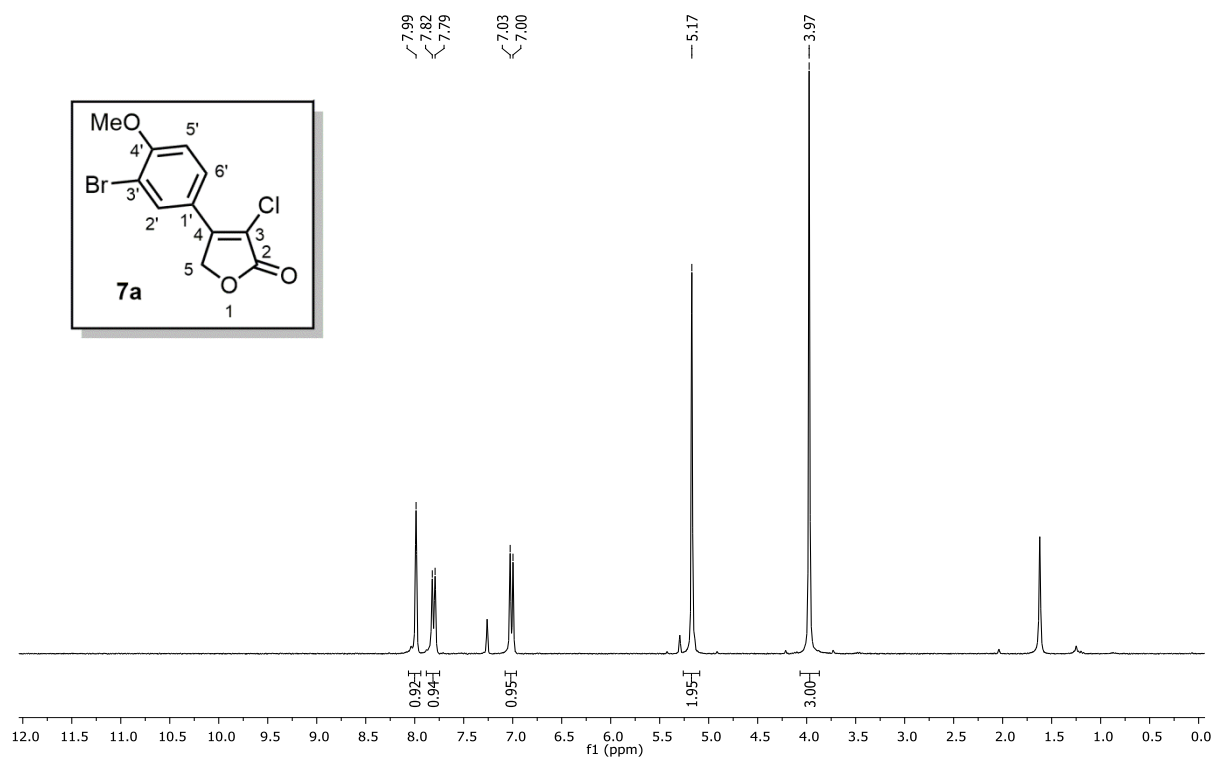
Figure A4.11 ^{1}H NMR (400 MHz, CDCl$_3$) of compound **7a**
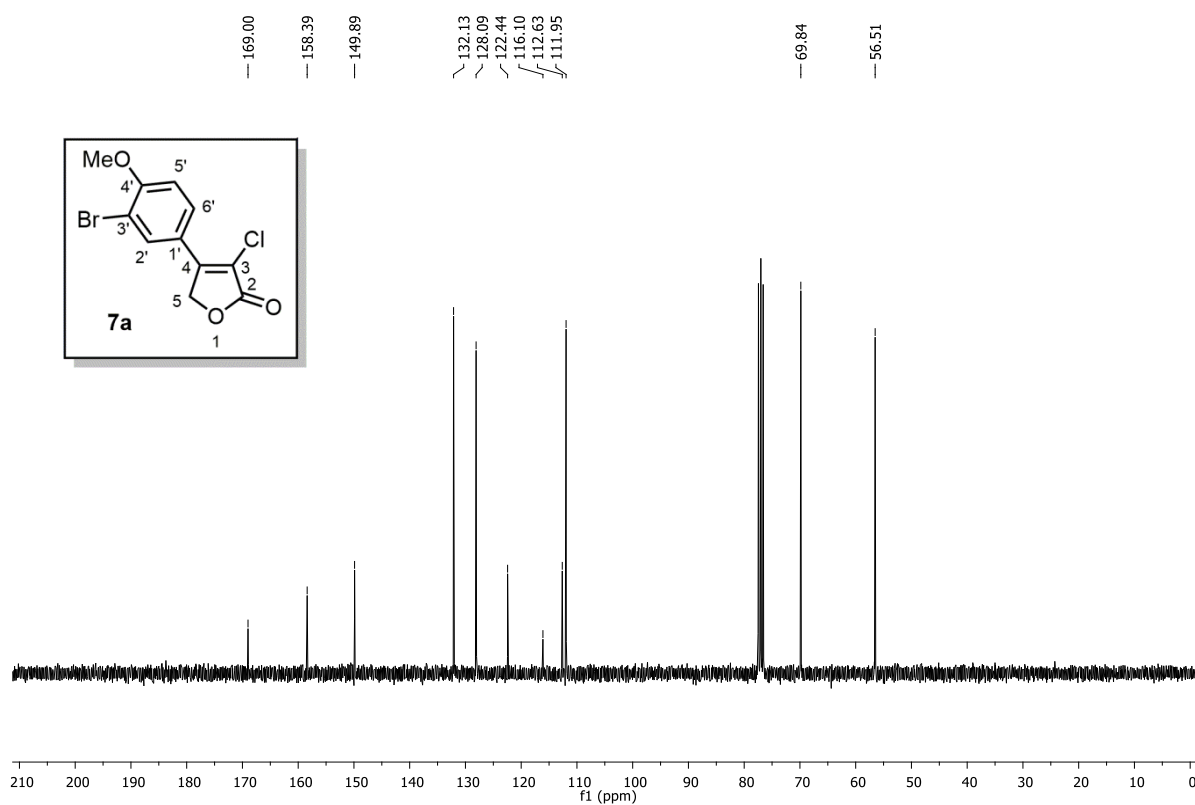
Figure A4.12 ^{13}C NMR (100 MHz, CDCl$_3$) of compound **7a**

Figure A4.13 ^{1}H NMR (400 MHz, DMSO-d$_6$) of compound **7b**

Figure A4.14 ^{13}C NMR (100 MHz, DMSO-d$_6$) of compound **7b**

201

Figure A4.15 ^{1}H NMR (400 MHz, CDCl$_3$) of compound **7c**

Figure A4.16 ^{13}C NMR (100 MHz, CDCl$_3$) of compound **7c**
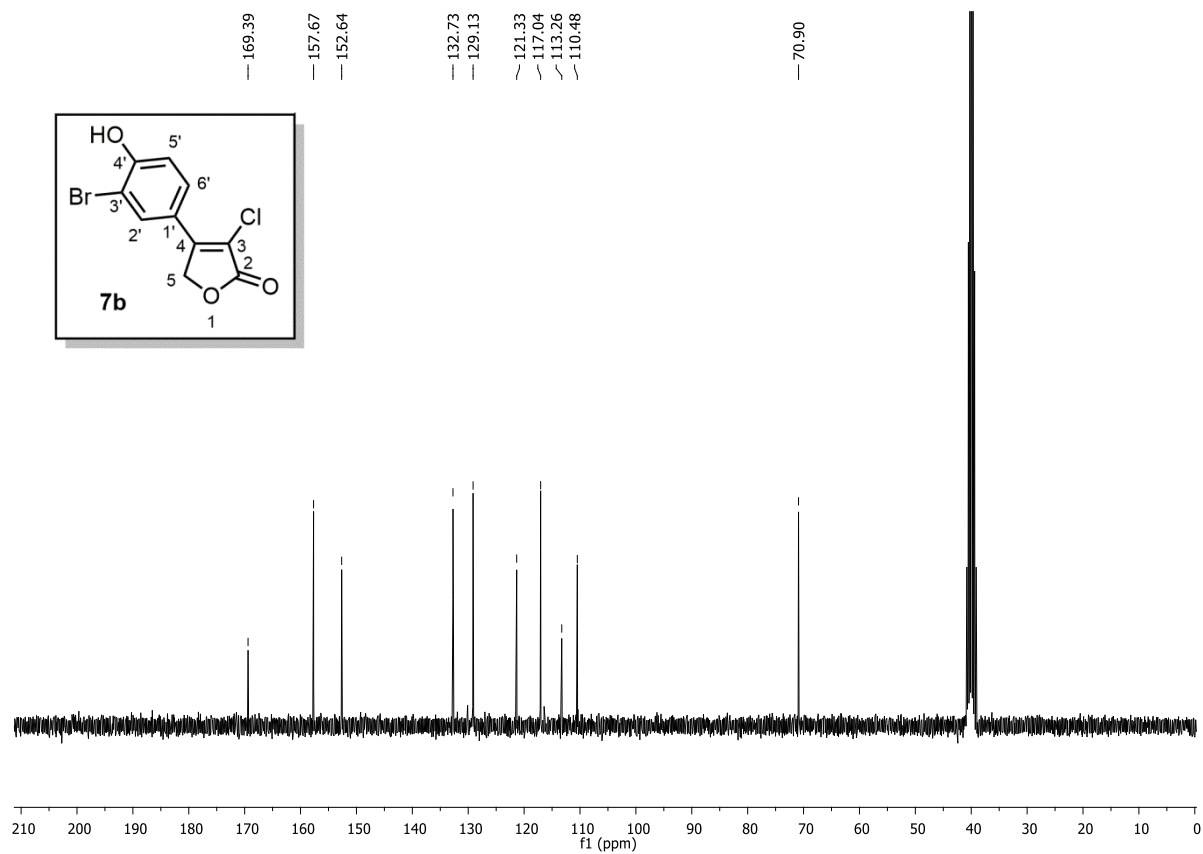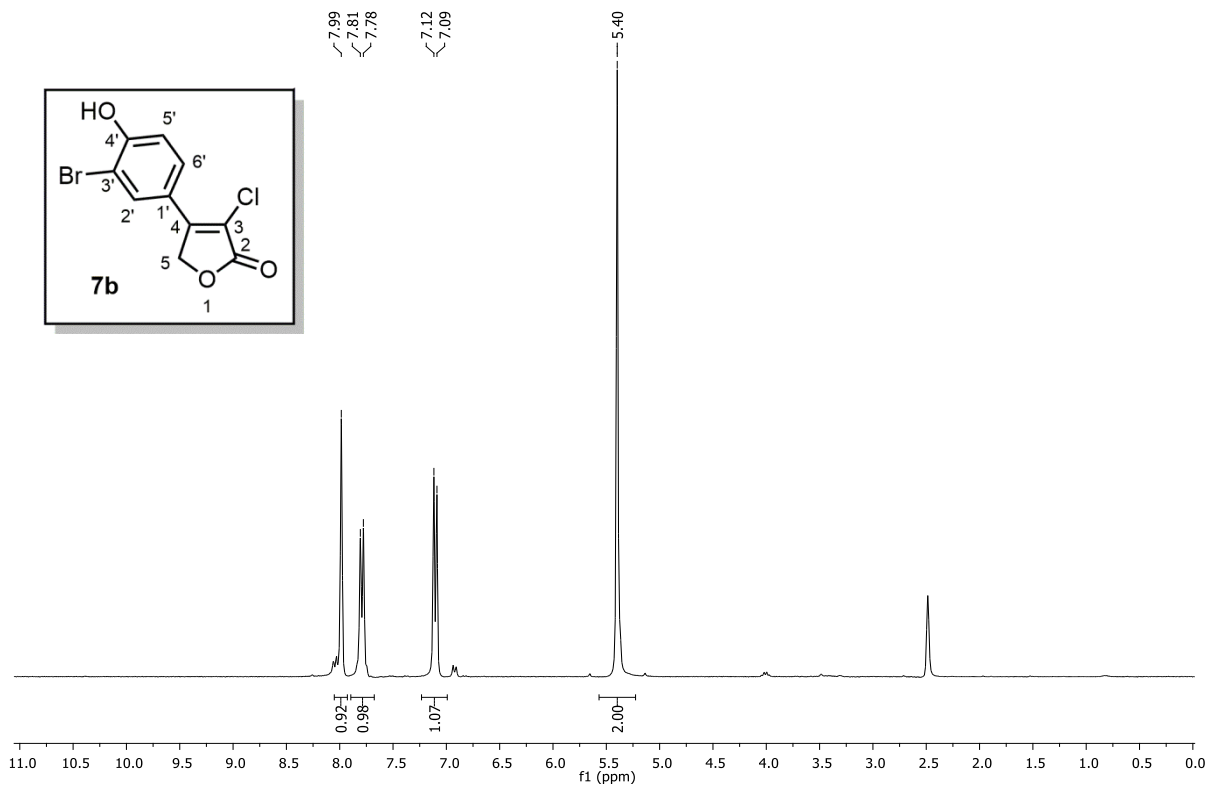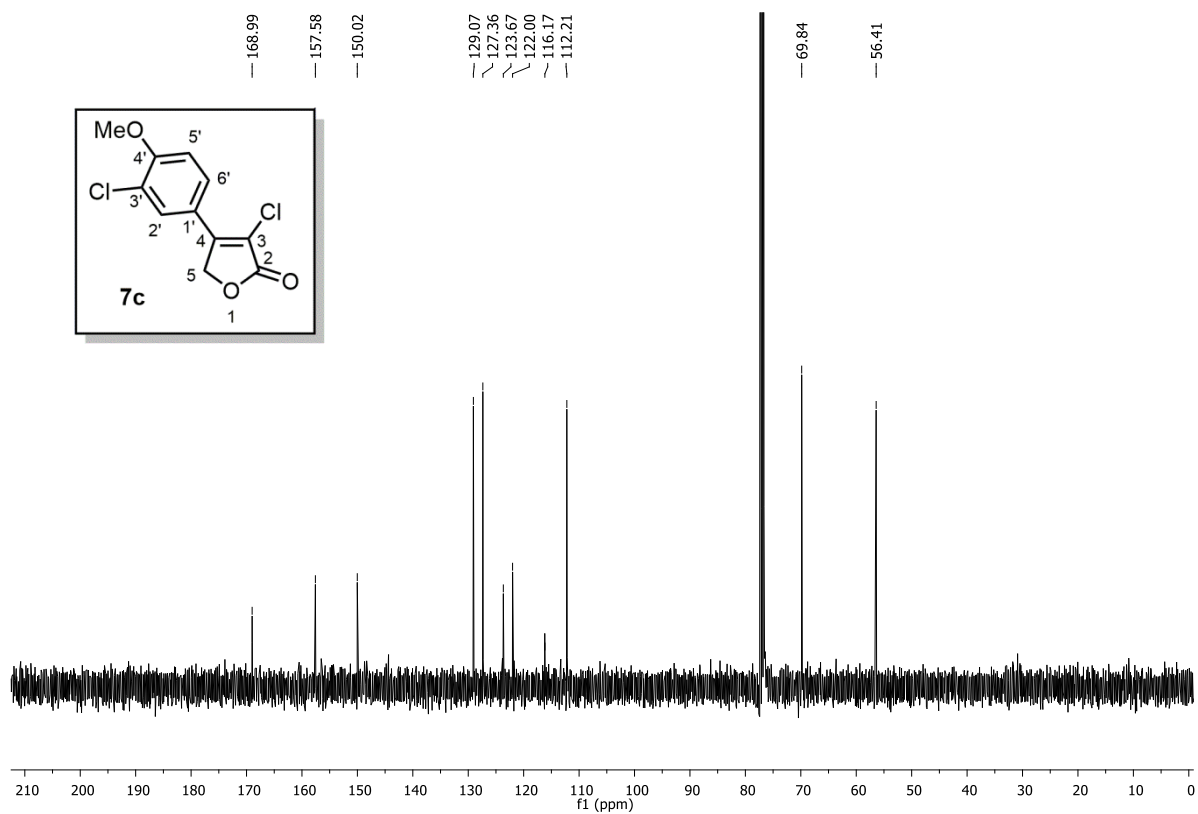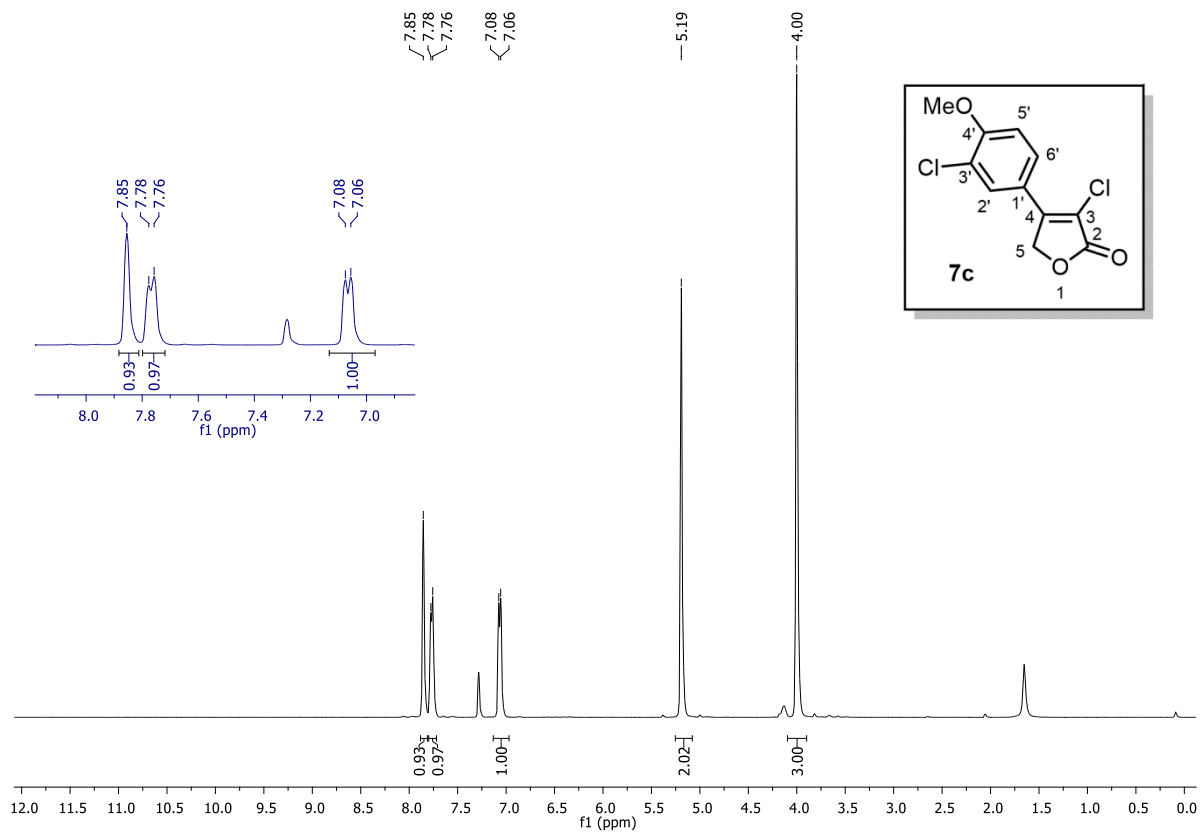
4.3.   NMR Spectra of Compounds 8a-b and 9a-b
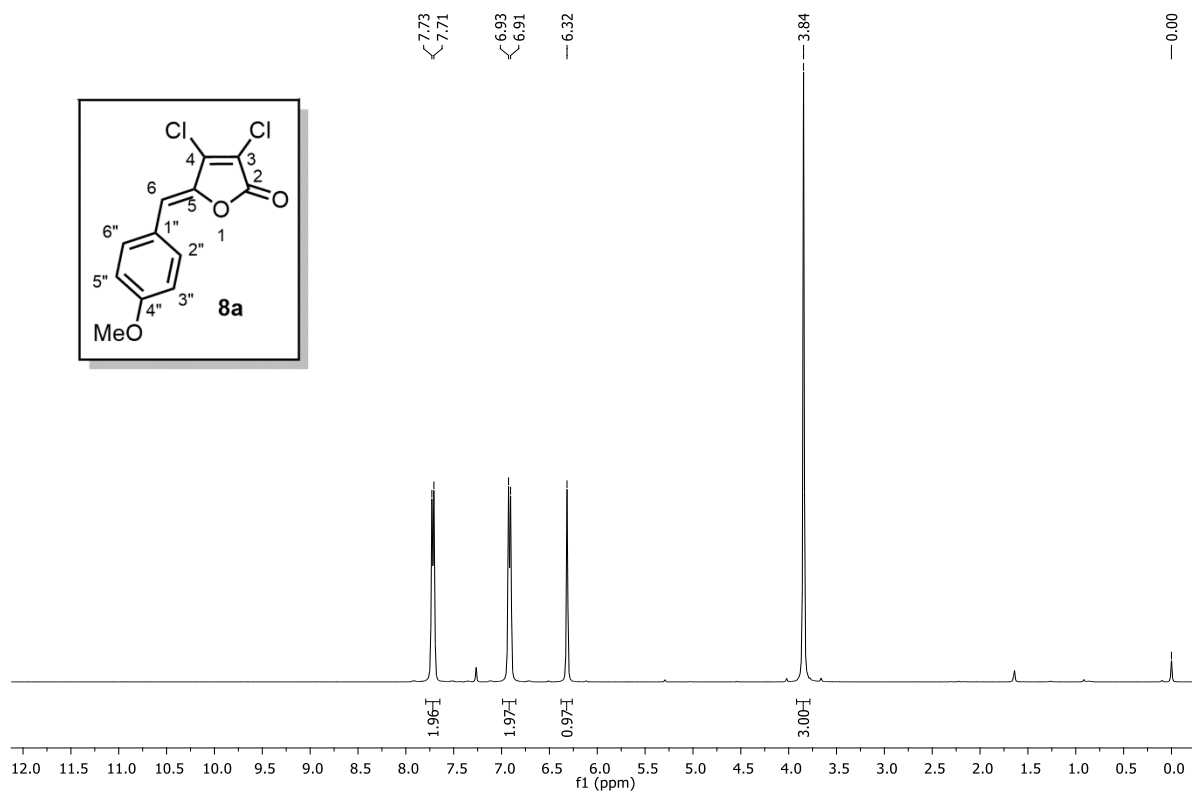
Figure A4.17 ^{1}H NMR (400 MHz, CDCl$_3$) of compound **8a**
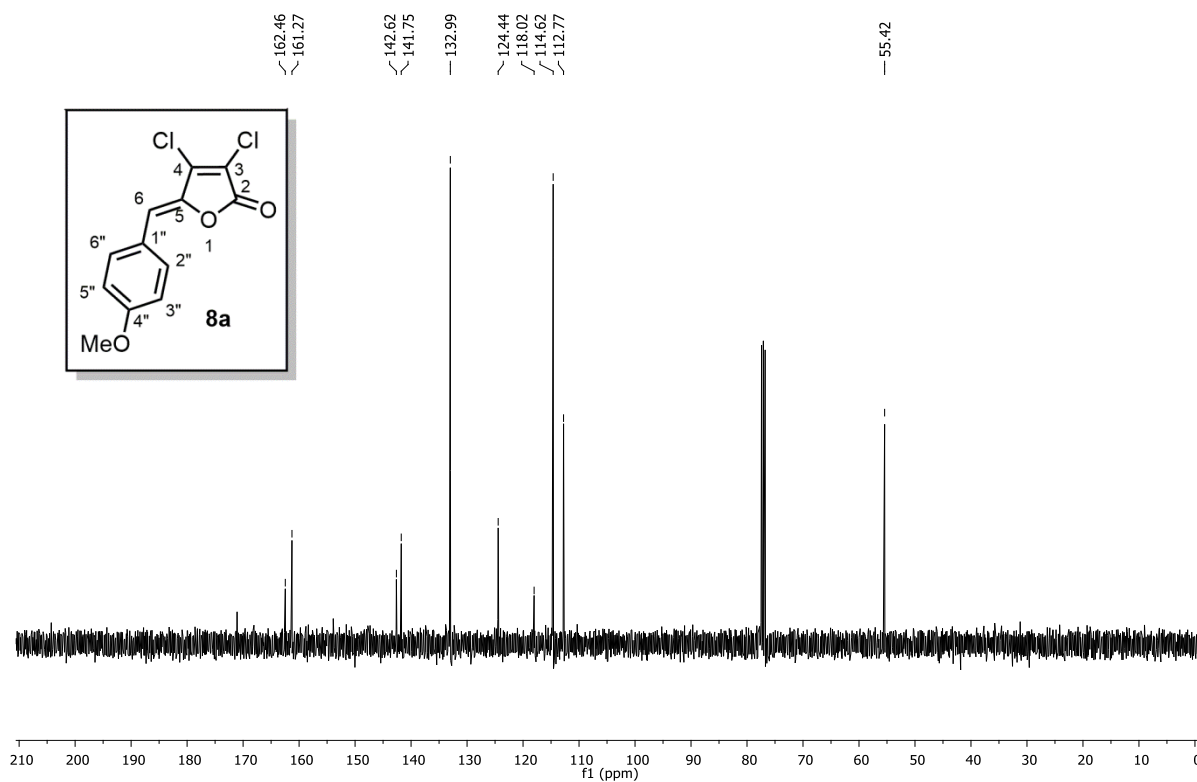
Figure A4.18 ^{13}C NMR (100 MHz, CDCl$_3$) of compound **8a**

Figure A4.19 ^{1}H NMR (400 MHz, Acetone-d$_6$) of compound **8b**

Figure A4.20 ^{13}C NMR (100 MHz, Acetone-d$_6$) of compound **8b**

Figure A4.21 ^{1}H NMR (400 MHz, CDCl$_3$) of compound **9a**

Figure A4.22 ^{13}C NMR (100 MHz, CDCl$_3$) of compound **9a**

Figure A4.23 ^{1}H NMR (400 MHz, Acetone-d$_6$) of compound **9b**

Figure A4.24 ^{13}C NMR (100 MHz, Acetone-d$_6$) of compound **9b**
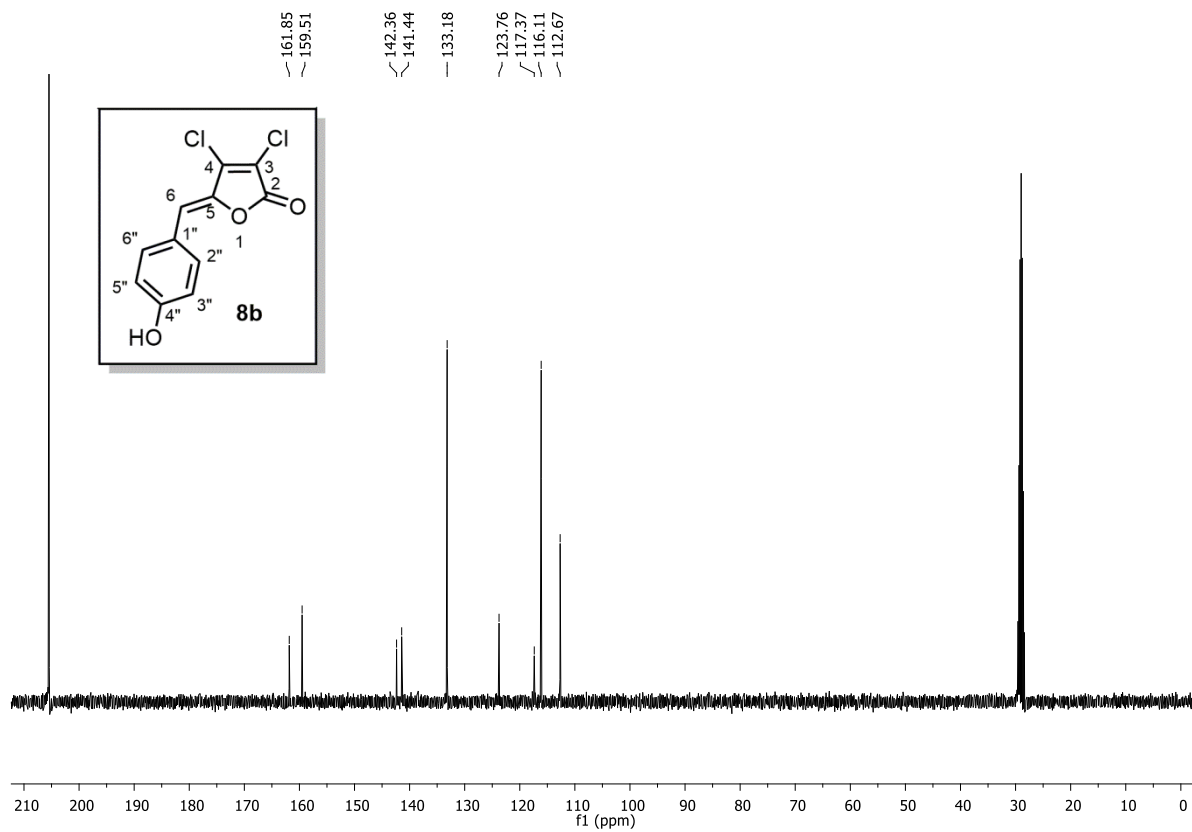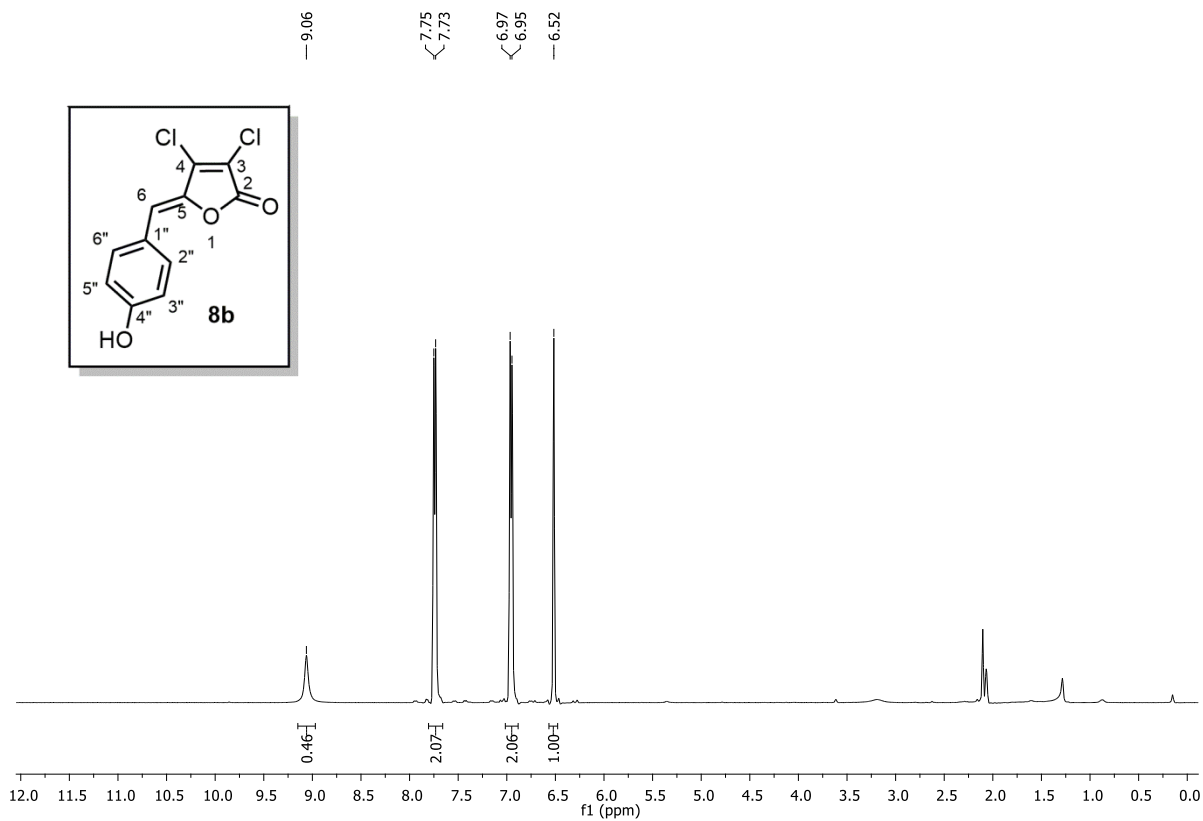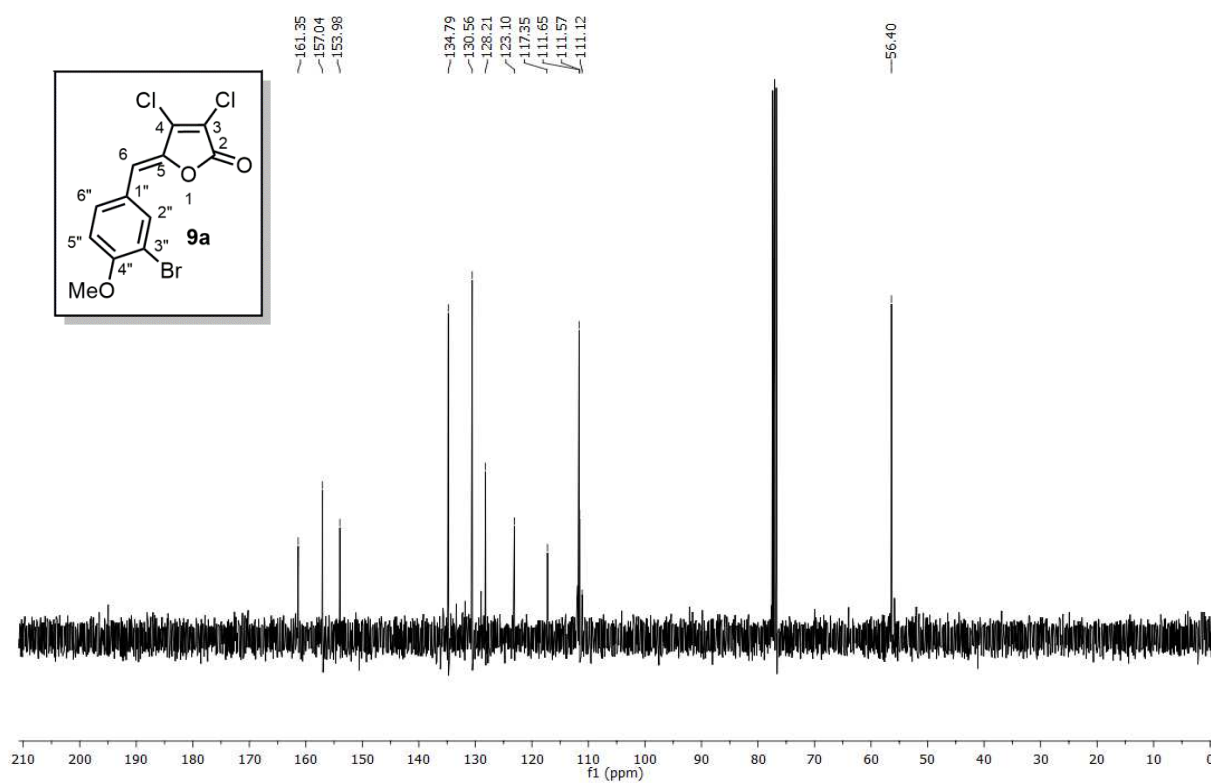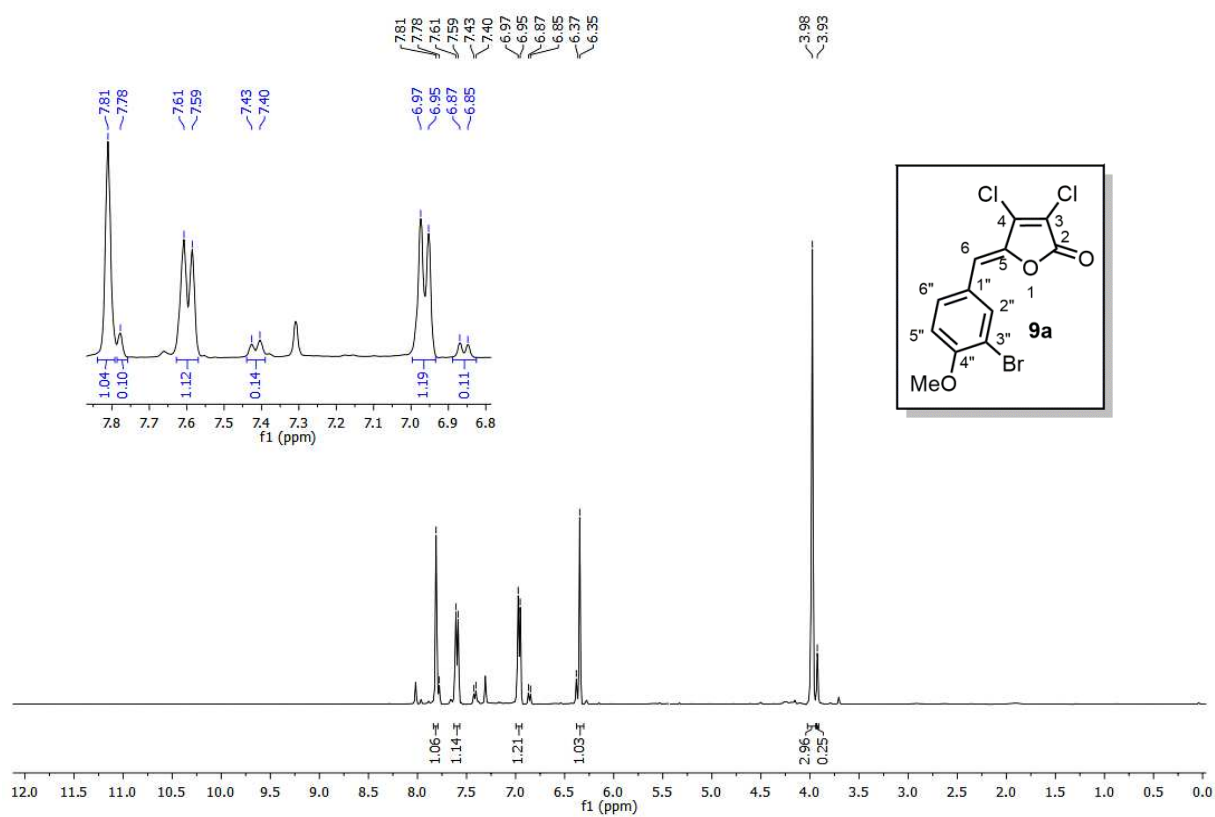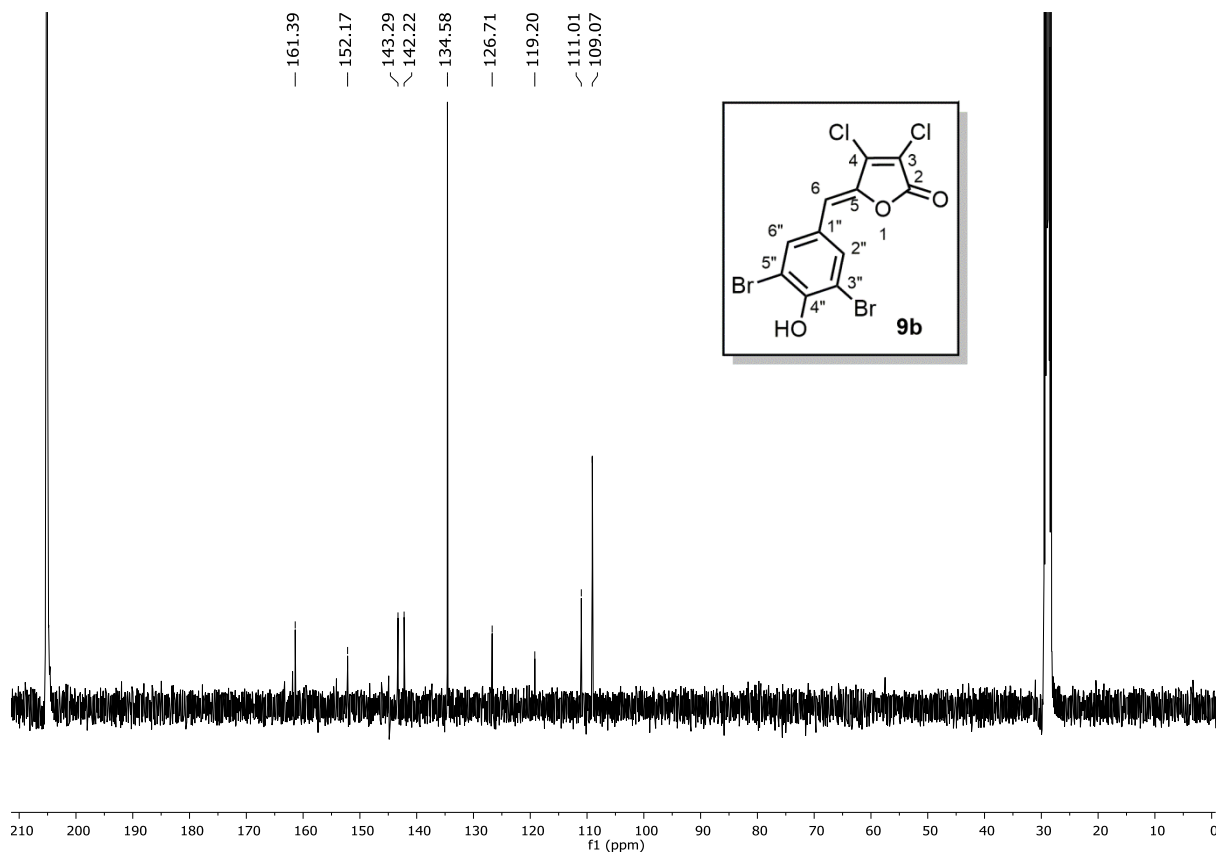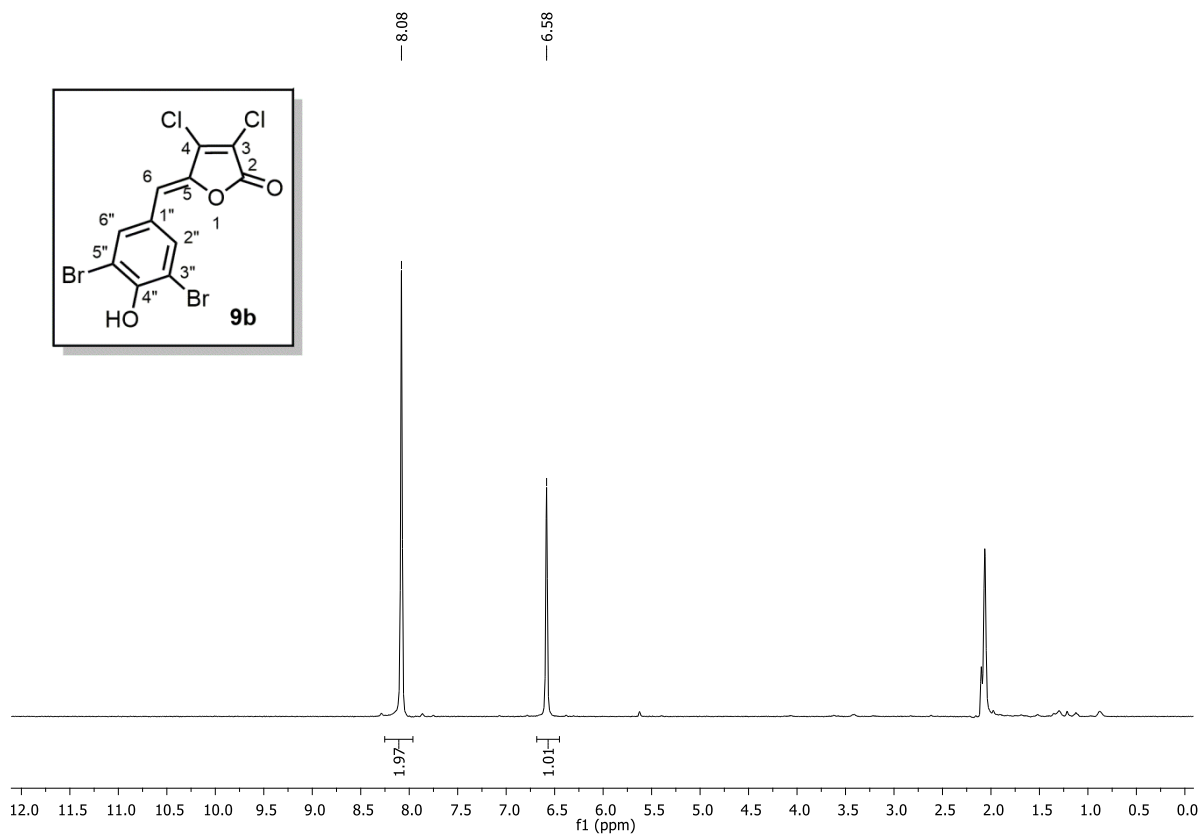
4.4. NMR Spectra of Compounds 3, 4 and 12
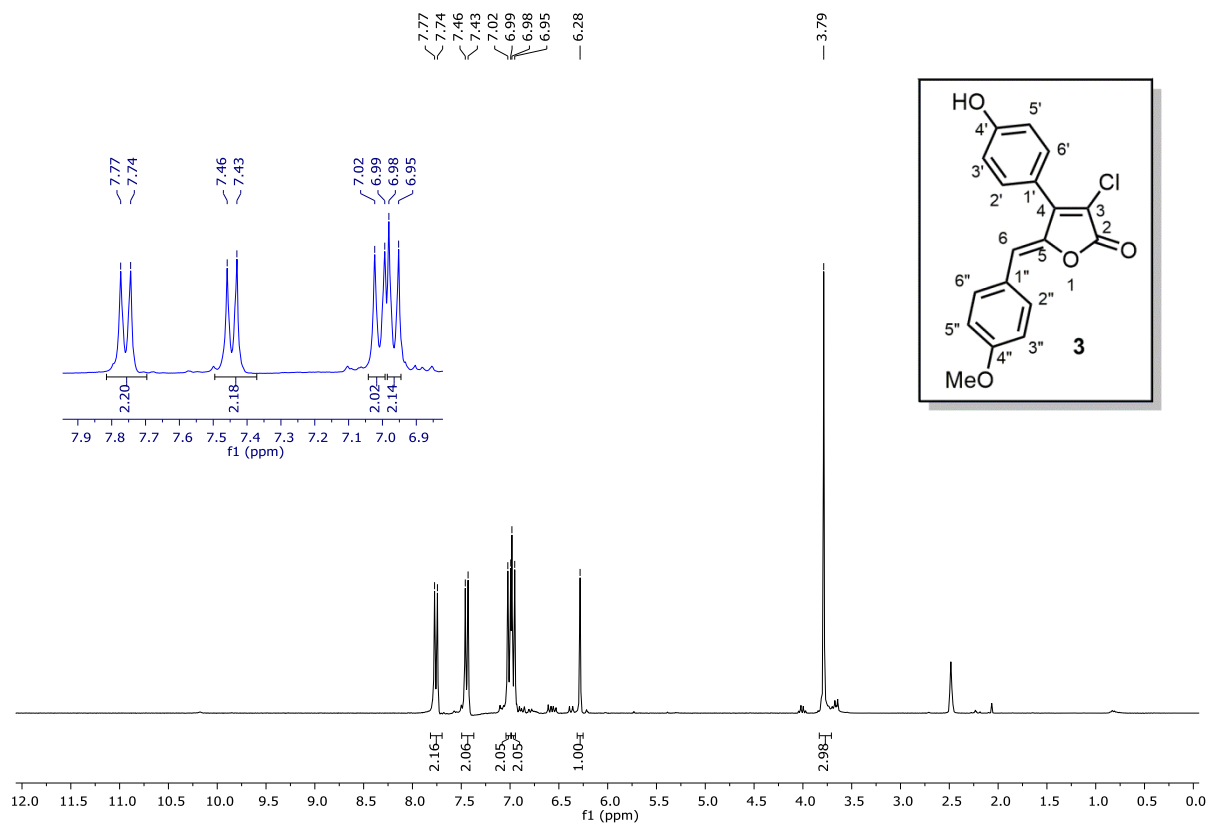
Figure A4.25 ^{1}H NMR (400 MHz, DMSO-d$_6$) of compound **3**
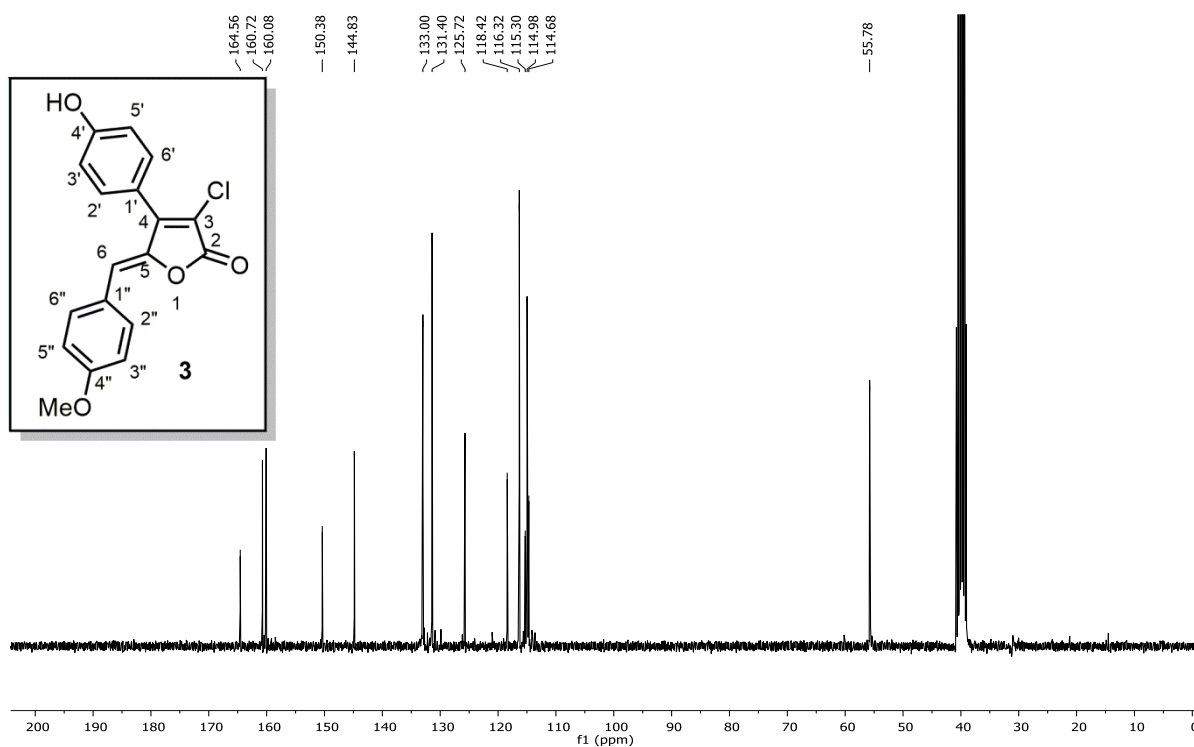
Figure A4.26 ^{13}C NMR (100 MHz, DMSO-d$_6$) of compound **3**
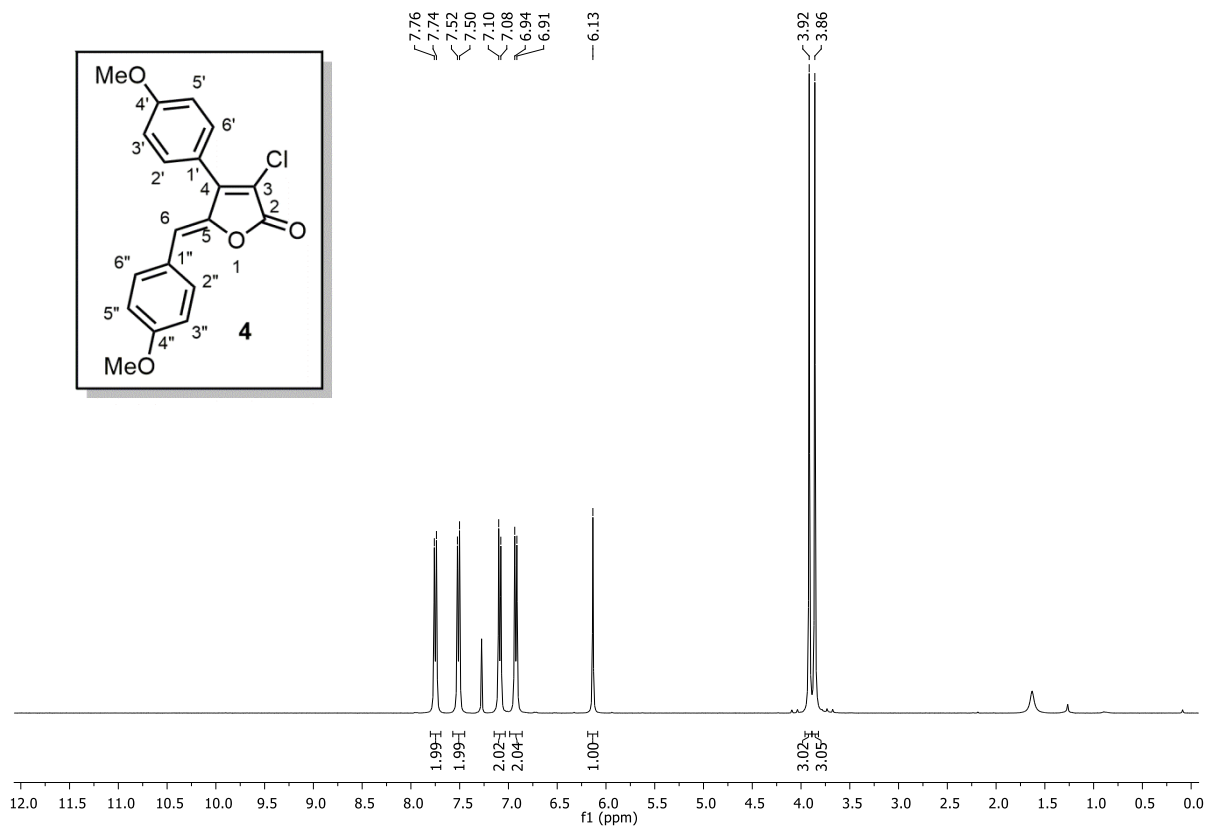
Figure A4.27 ^{1}H NMR (400 MHz, CDCl$_3$) of compound **4**
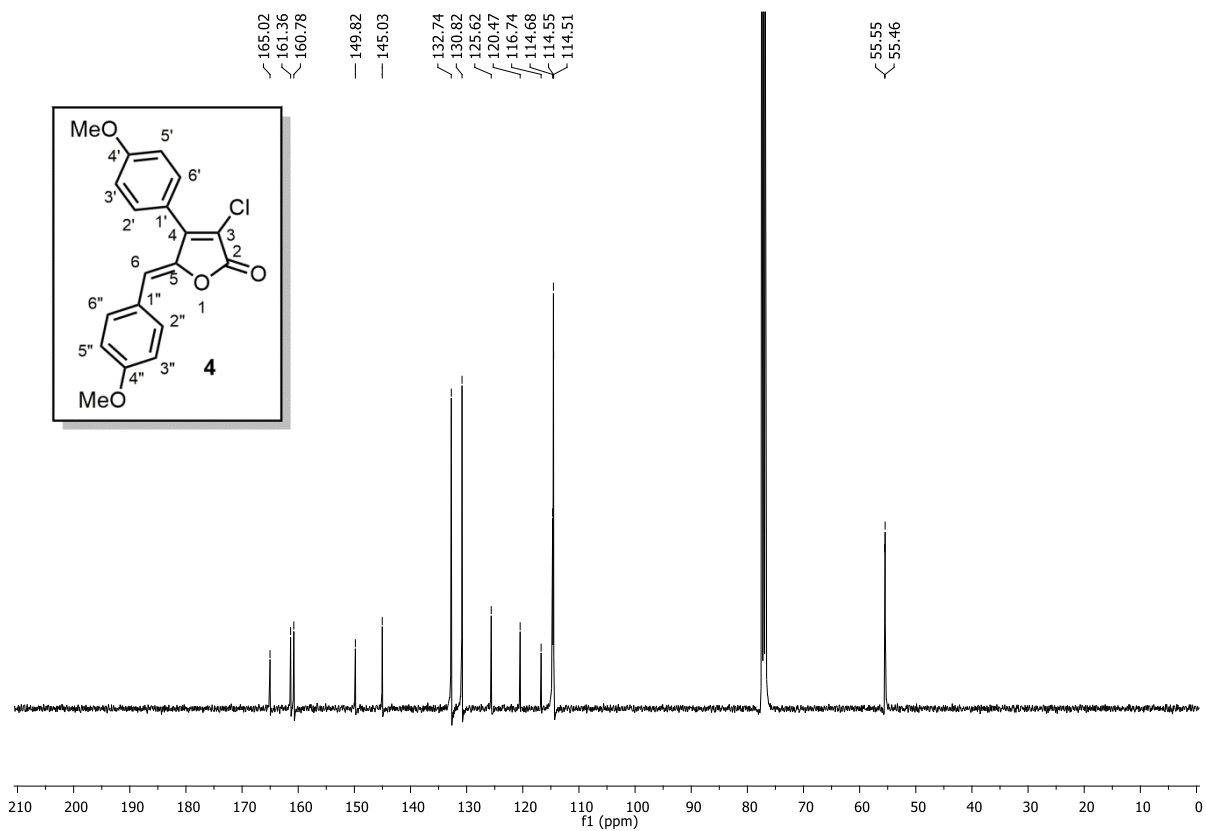
Figure A4.28 ^{13}C NMR (100 MHz, CDCl$_3$) of compound **4**
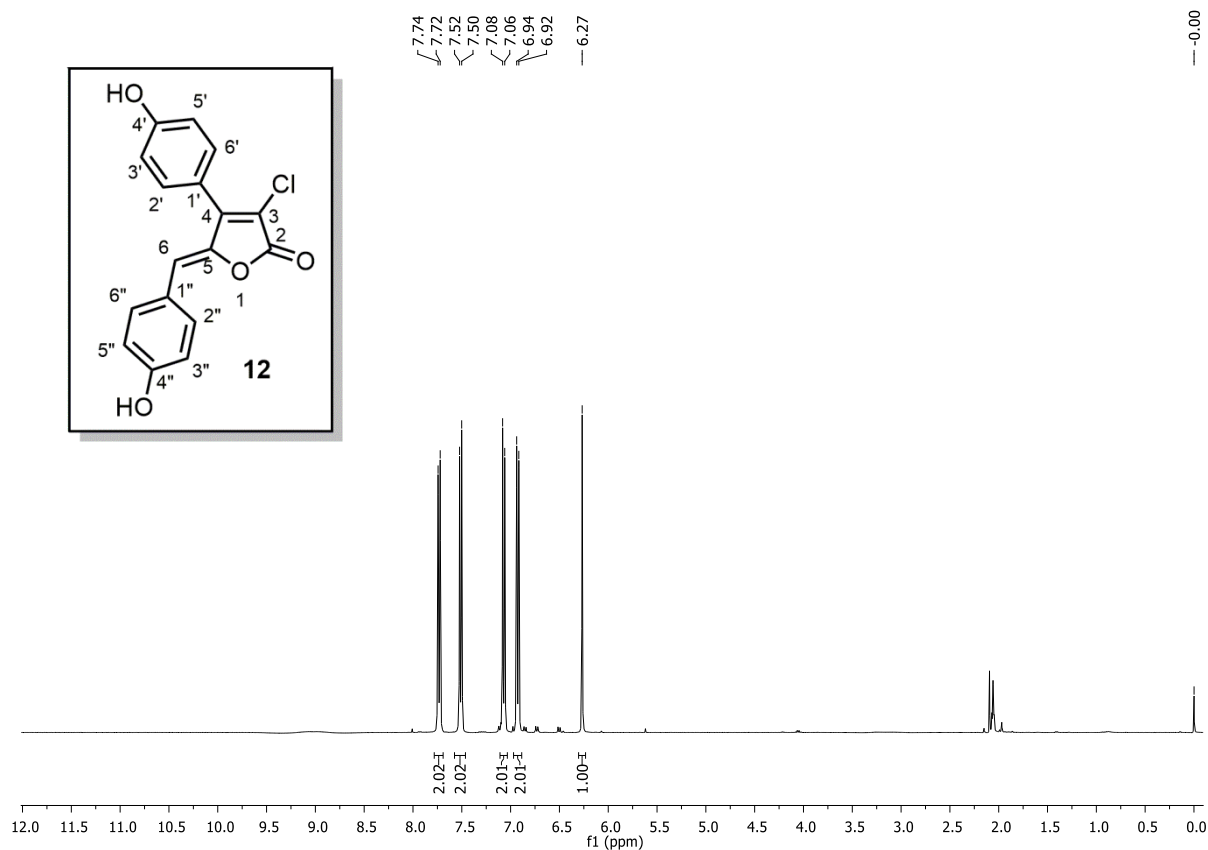
Figure A4.29 ^{1}H NMR (400 MHz, Acetone-d$_6$) of compound **12**
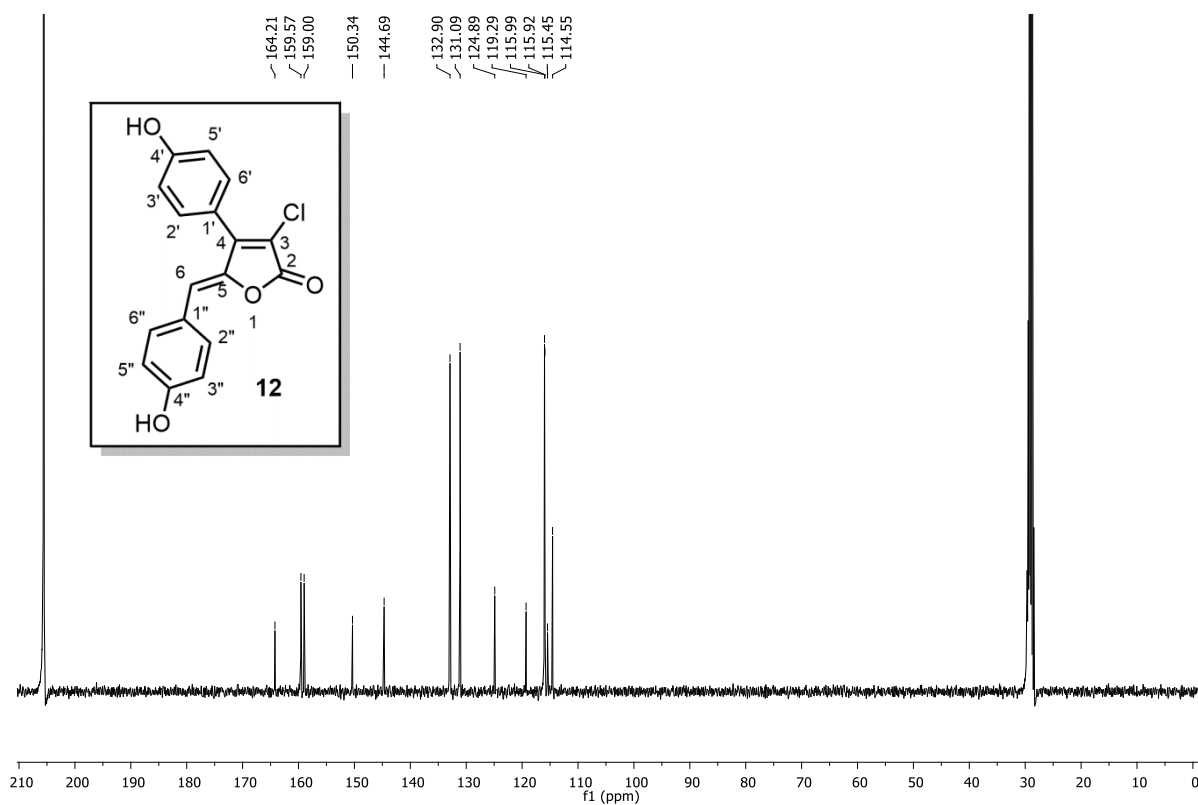
Figure A4.30 ^{13}C NMR (100 MHz, Acetone-d$_6$) of compound **12**

209

4.5.   NMR Spectra of Synthesized Rubrolide I and O
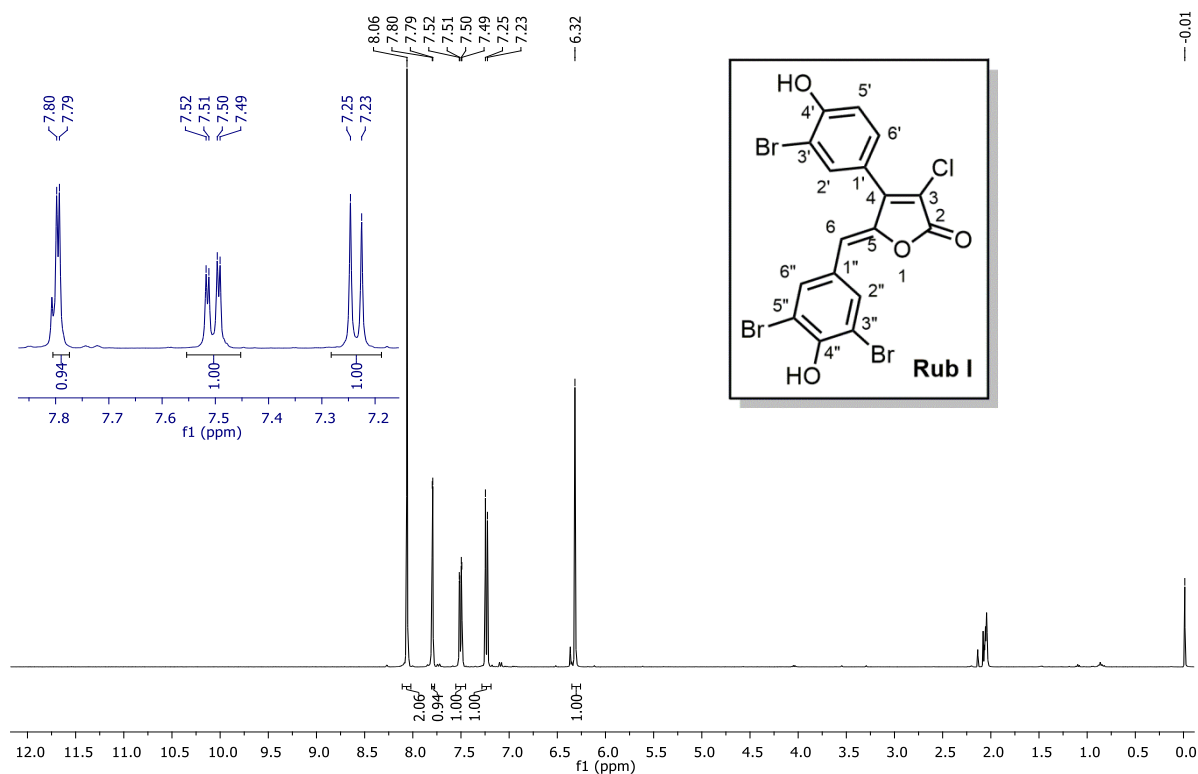
Figure A4.31 ^{1}H NMR (400 MHz, Acetone-d$_6$) of rubrolide I
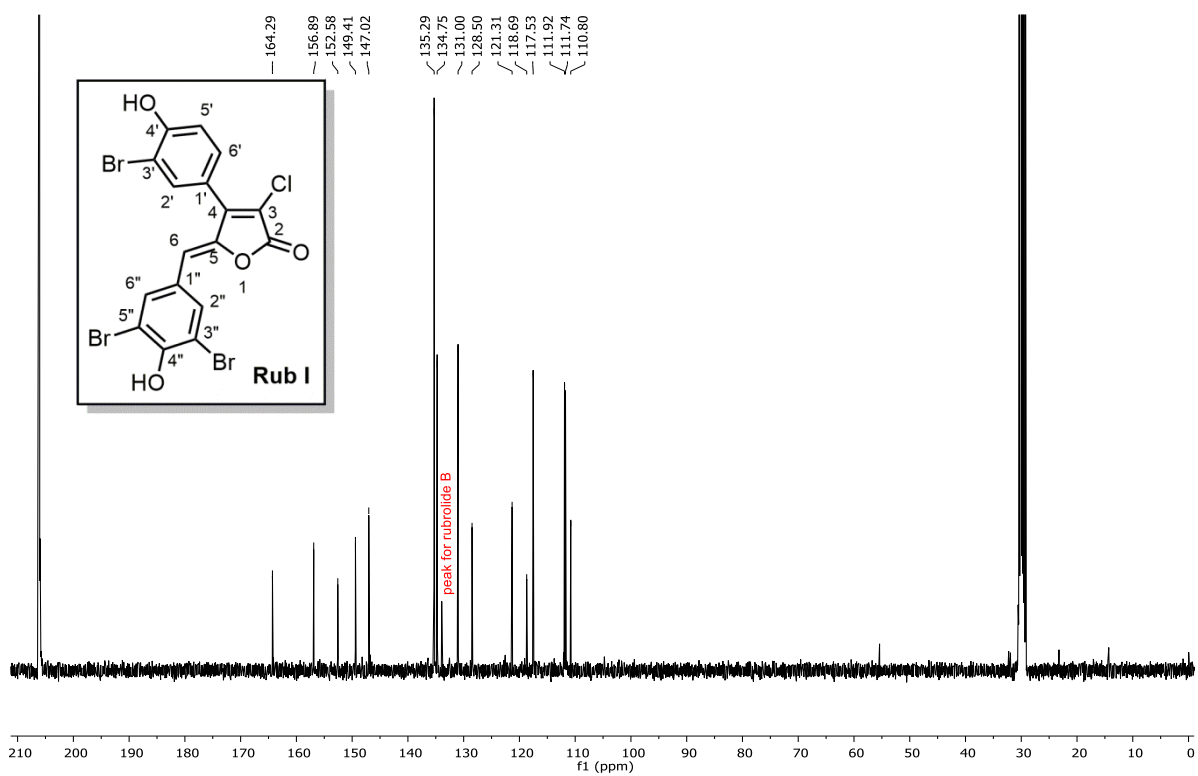
Figure A4.32 ^{13}C NMR (100 MHz, Acetone-d$_6$) of rubrolide I
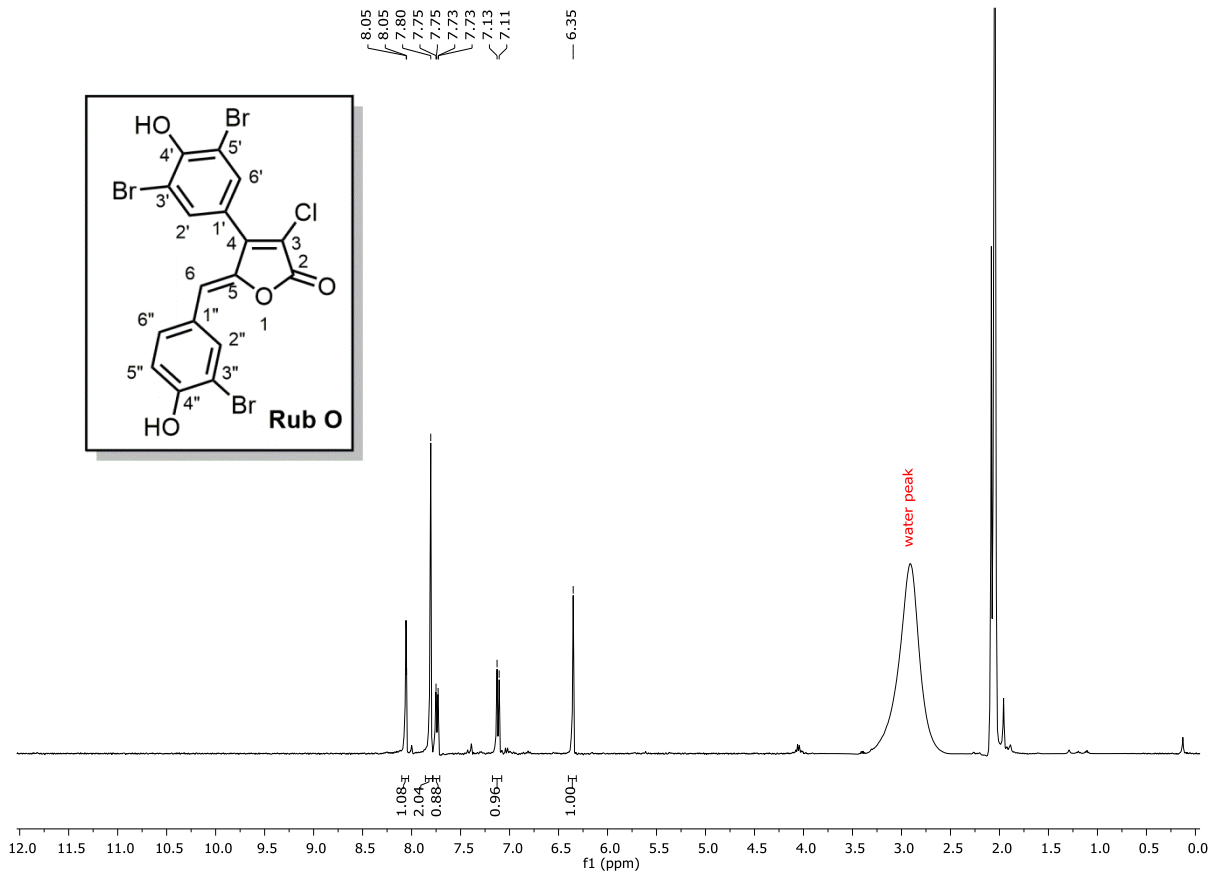
Figure A4.33 ^{1}H NMR (400 MHz, Acetone-d$_6$) of rubrolide O
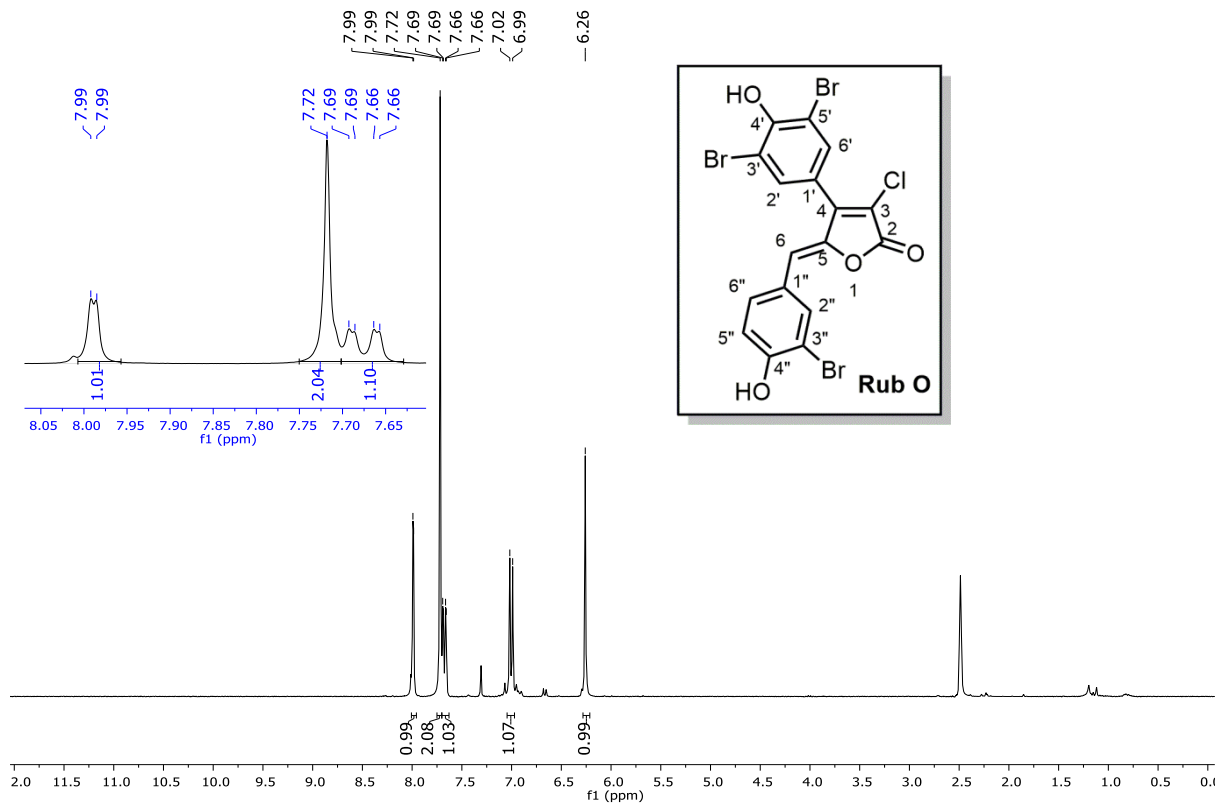
Figure A4.34 ^{1}H NMR (300 MHz, DMSO-d$_6$) of rubrolide O

211

Figure A4.35 ^{13}C NMR (75 MHz, DMSO-d$_6$) of rubrolide O

Figure A4.36 COSY (300 MHz, DMSO-d$_6$) of rubrolide O
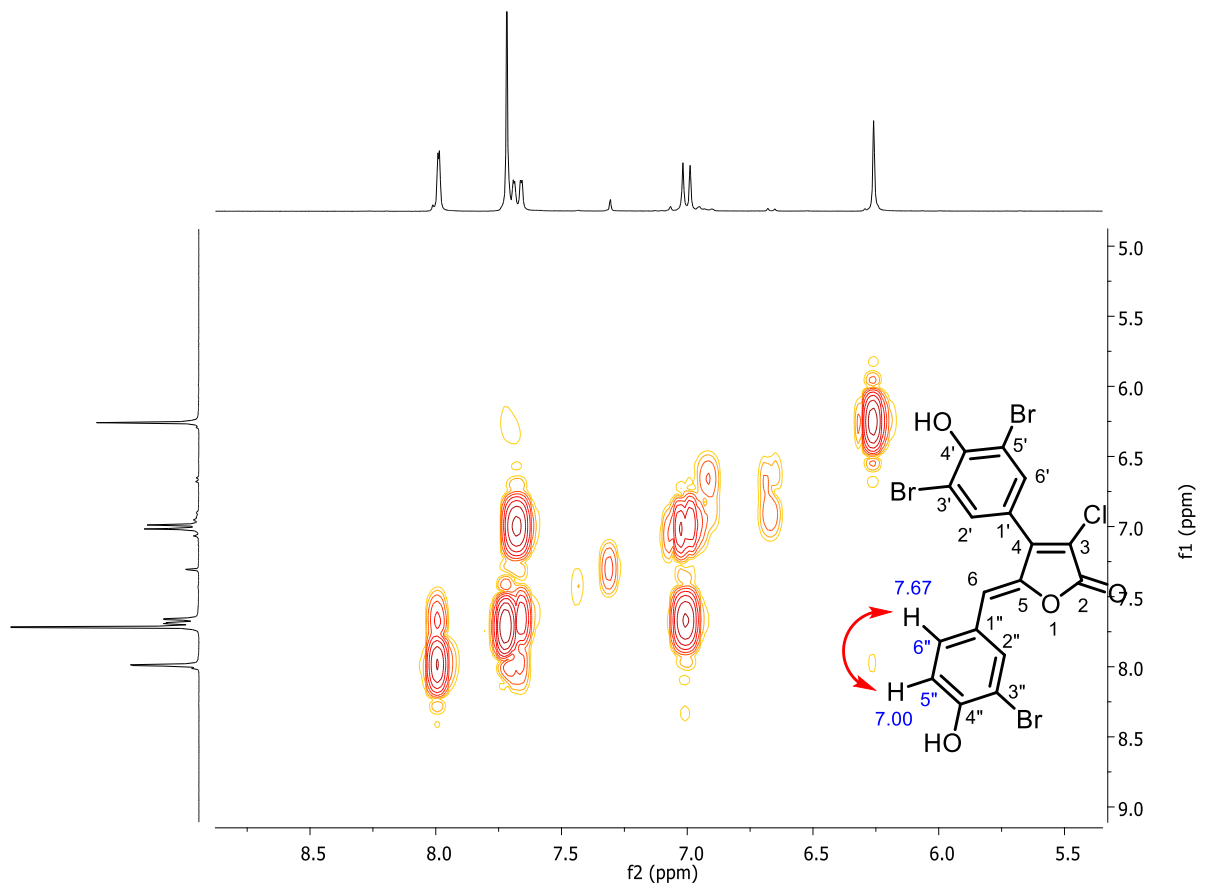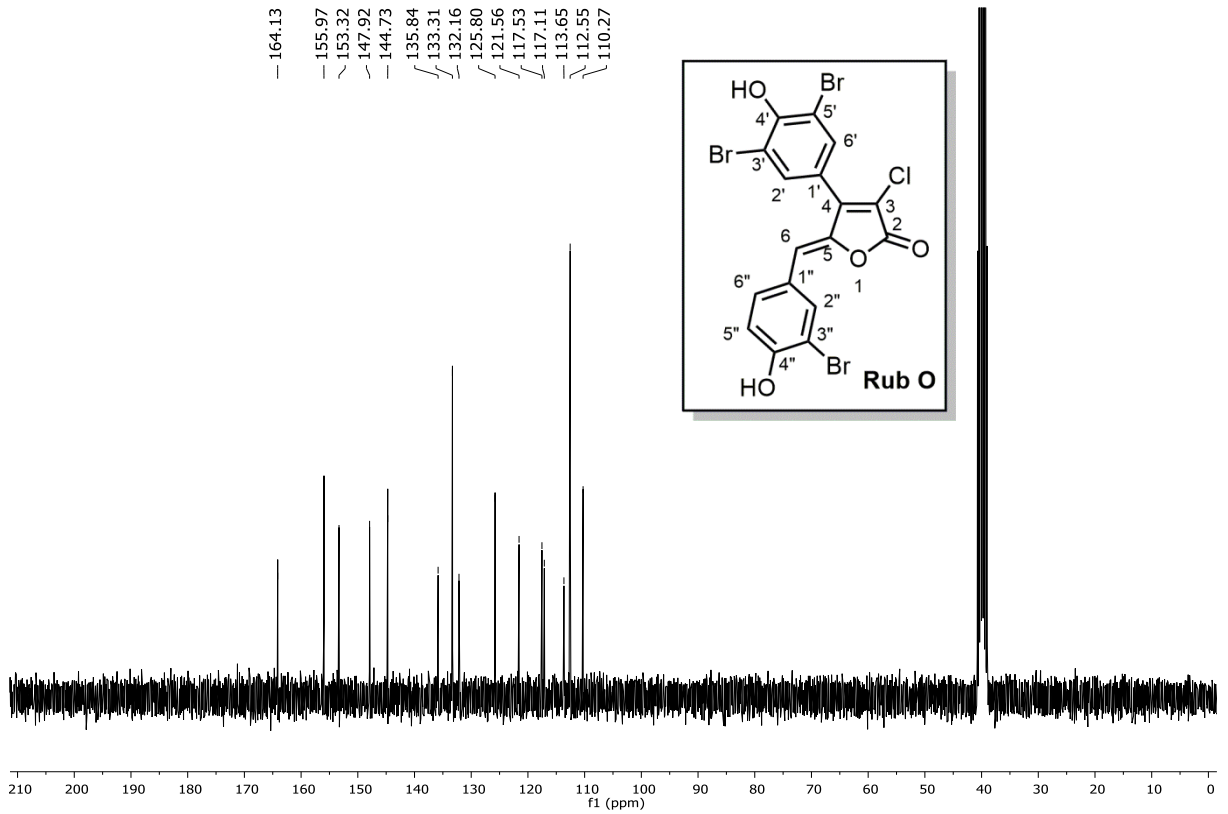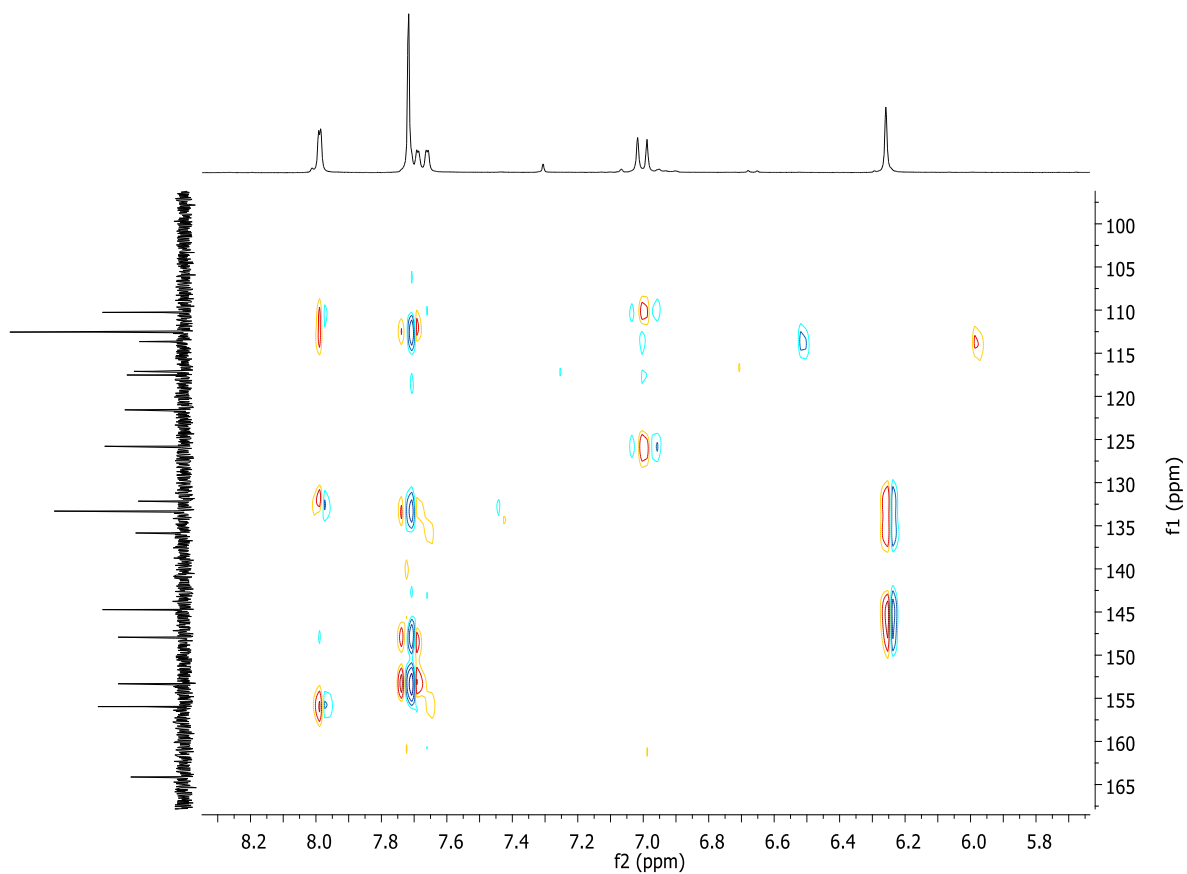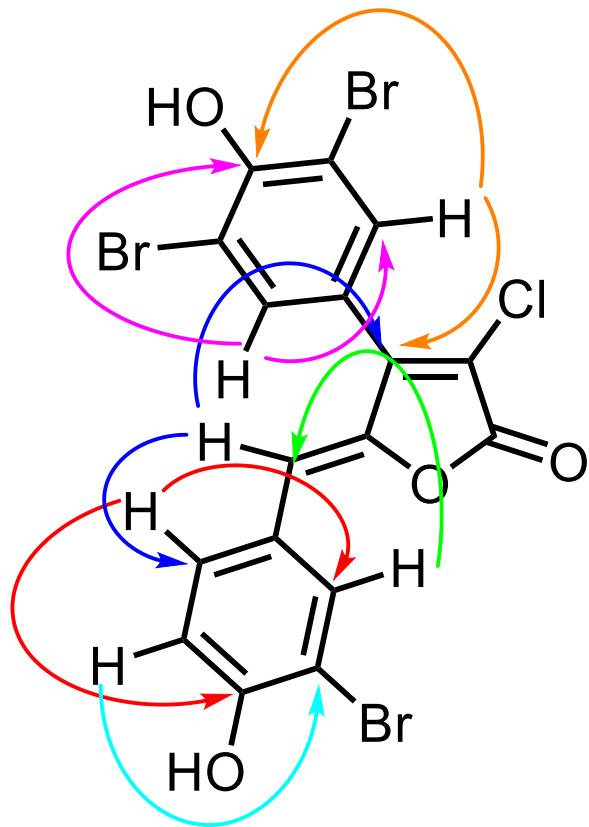
Figure A4.37 HMBC (300 MHz, DMSO-d$_6$) of rubrolide O

4.6. NMR Spectra of Synthesized Rubrolide Analogous 14a-d and 15
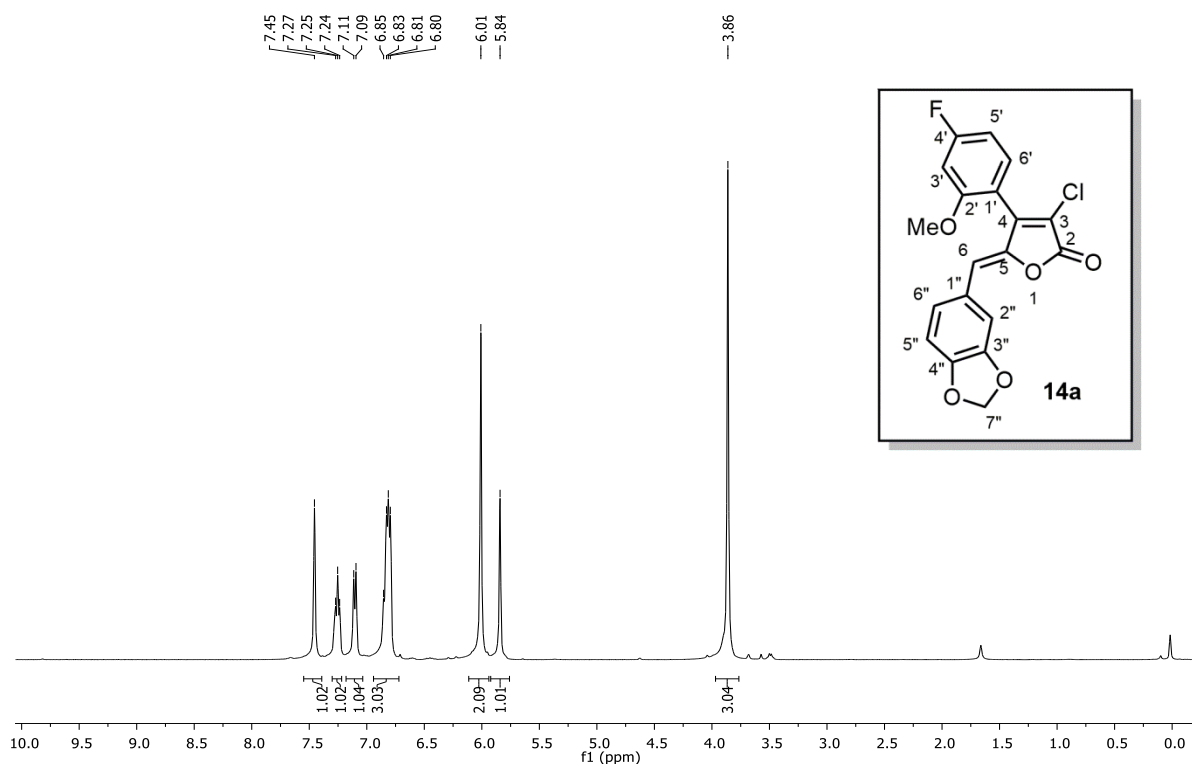
Figure A4.38 ^{1}H NMR (400 MHz, CDCl$_3$) of compound **14a**
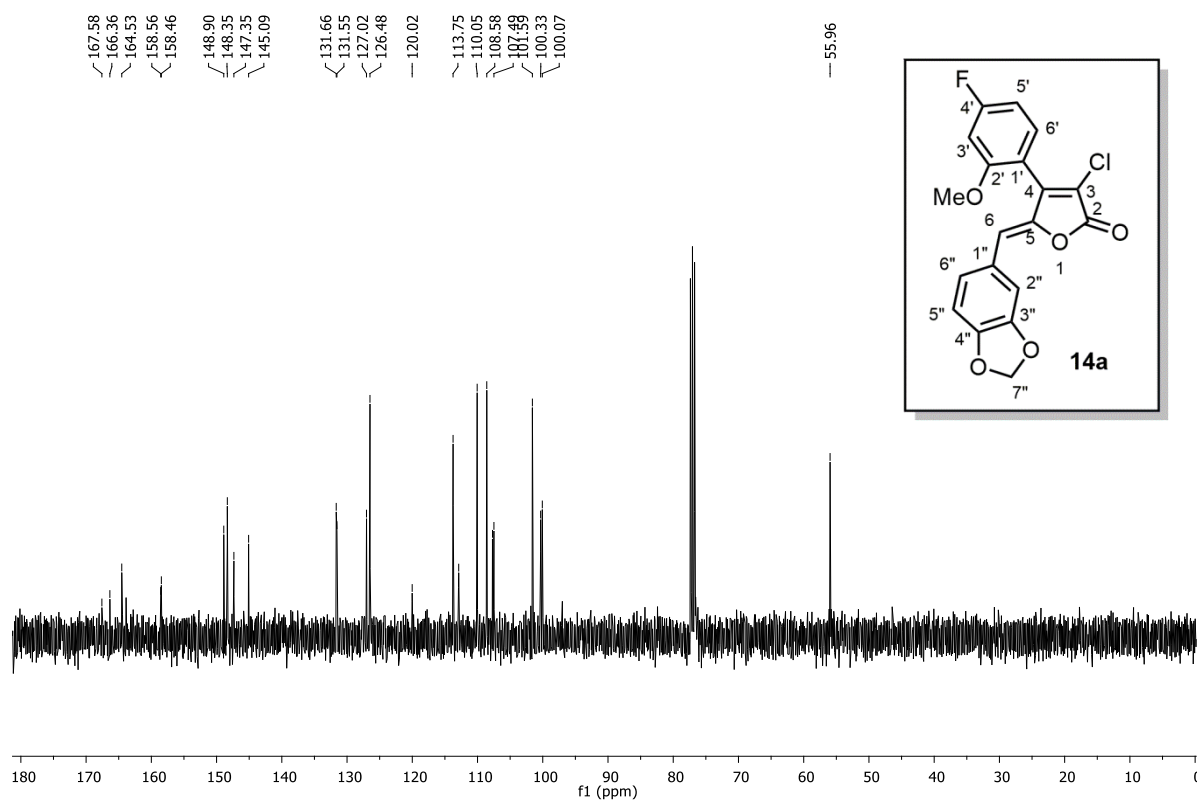
Figure A4.39 ^{13}C NMR (100 MHz, CDCl$_3$) of compound **14a**
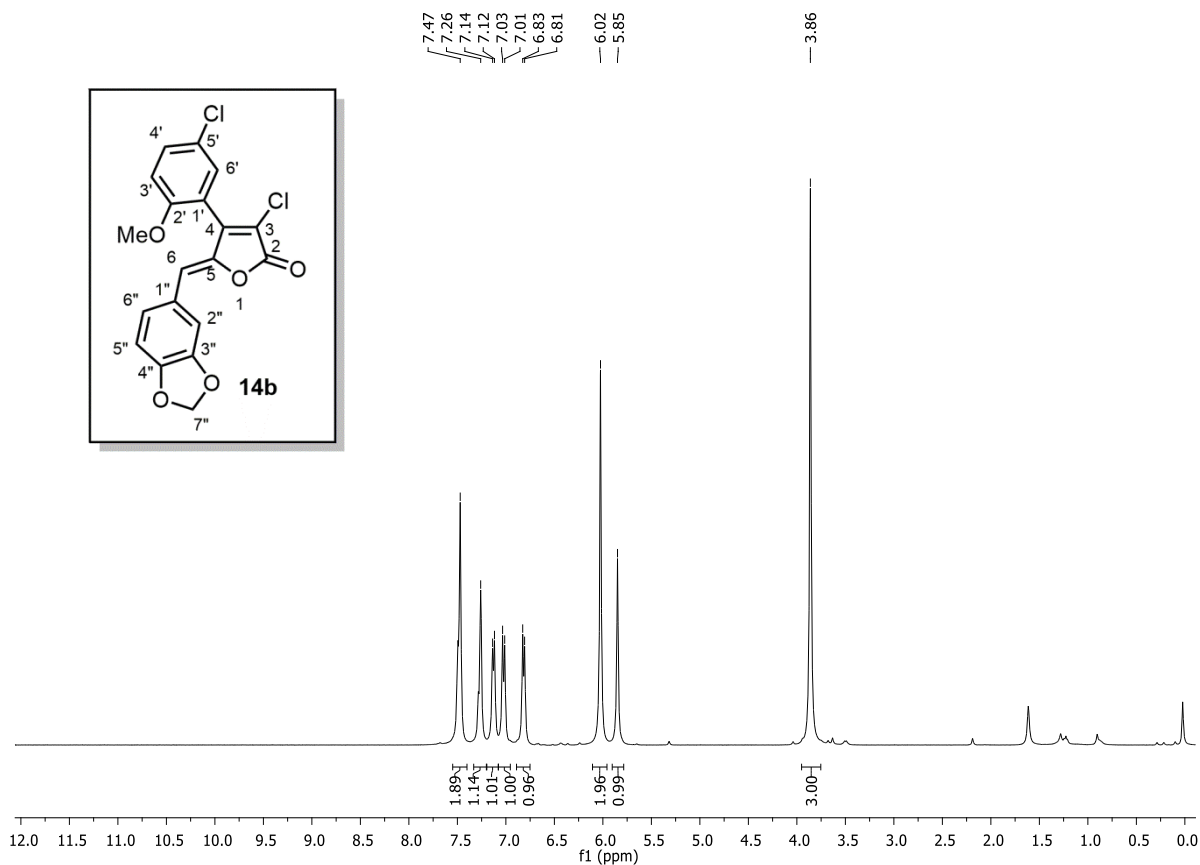
Figure A4.40 ^{1}H NMR (400 MHz, CDCl$_3$) of compound **14b**
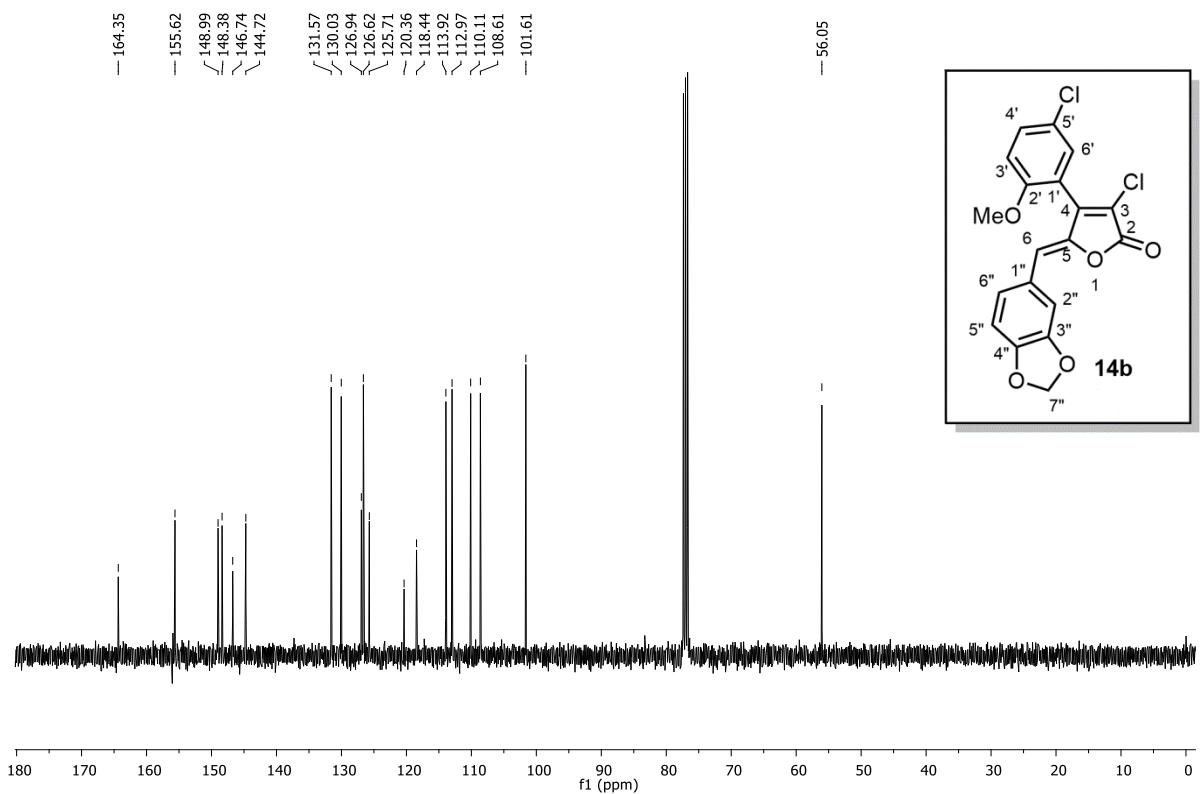
Figure A4.41 ^{13}C NMR (100 MHz, CDCl$_3$) of compound **14b**

215
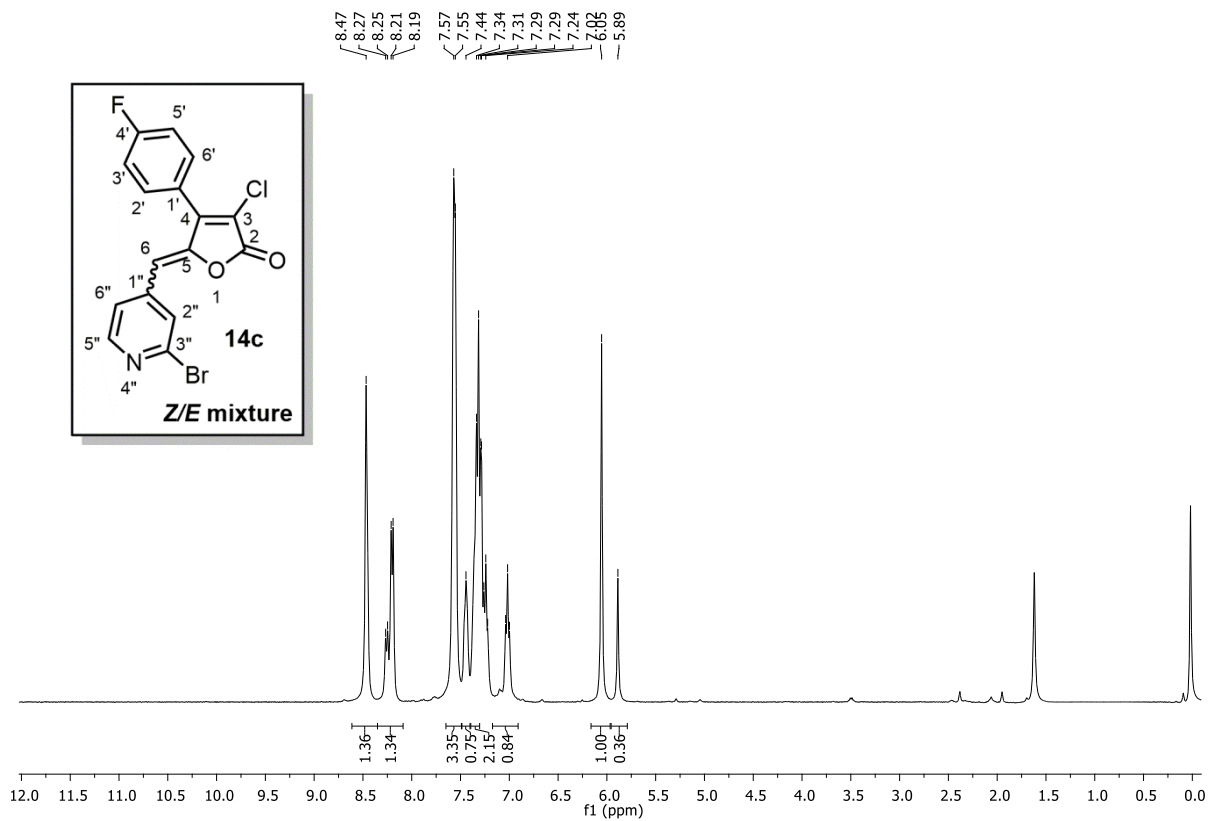
Figure A4.42 ^{1}H NMR (400 MHz, CDCl$_3$) of compound **14c**
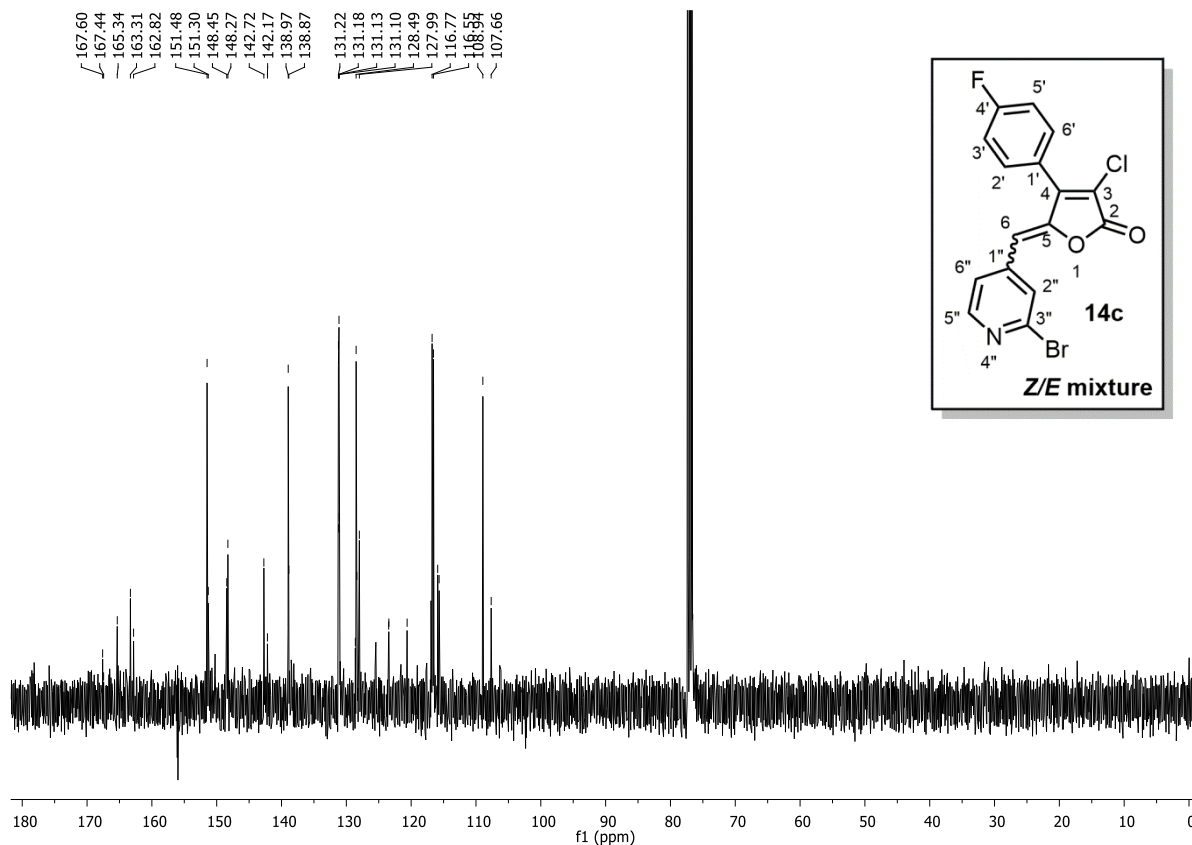
Figure A4.43 ^{13}C NMR (100 MHz, CDCl$_3$) of compound **14c**
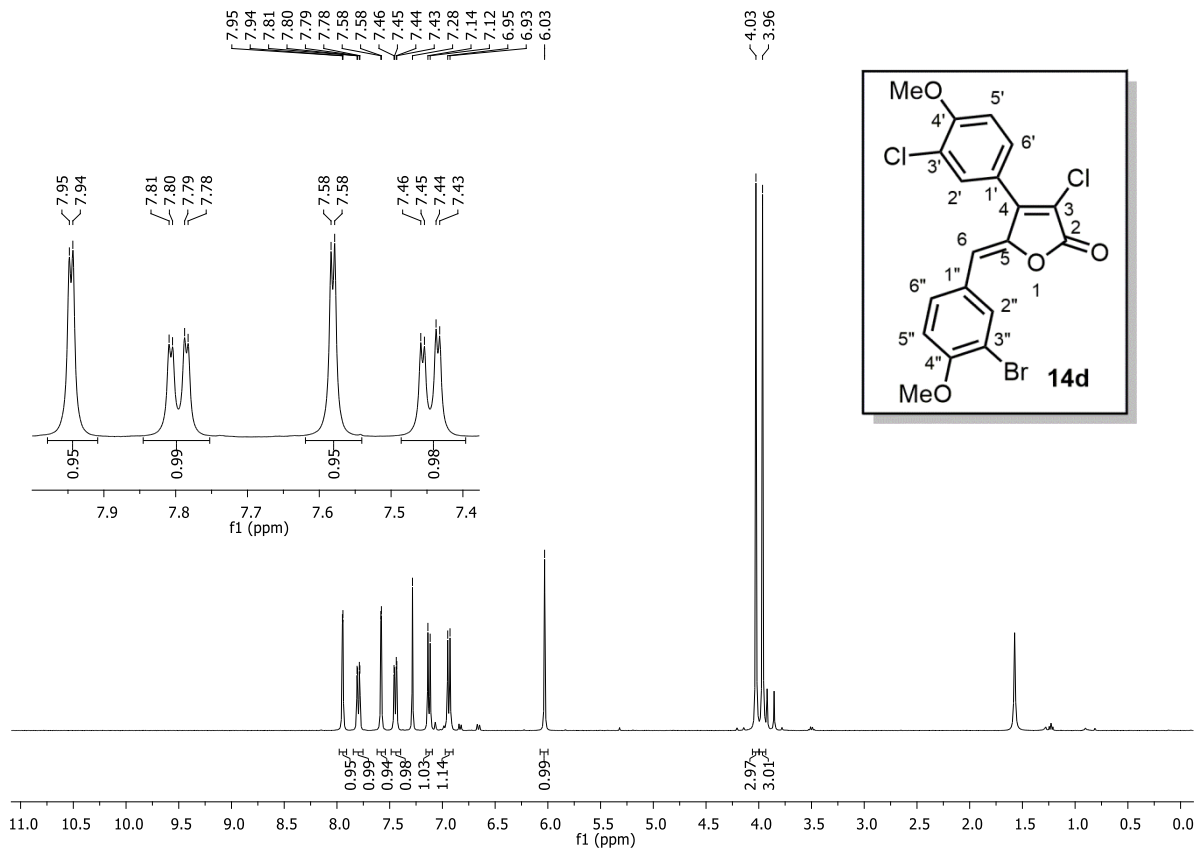
Figure A4.44 ^{1}H NMR (400 MHz, CDCl$_3$) of compound **14d**
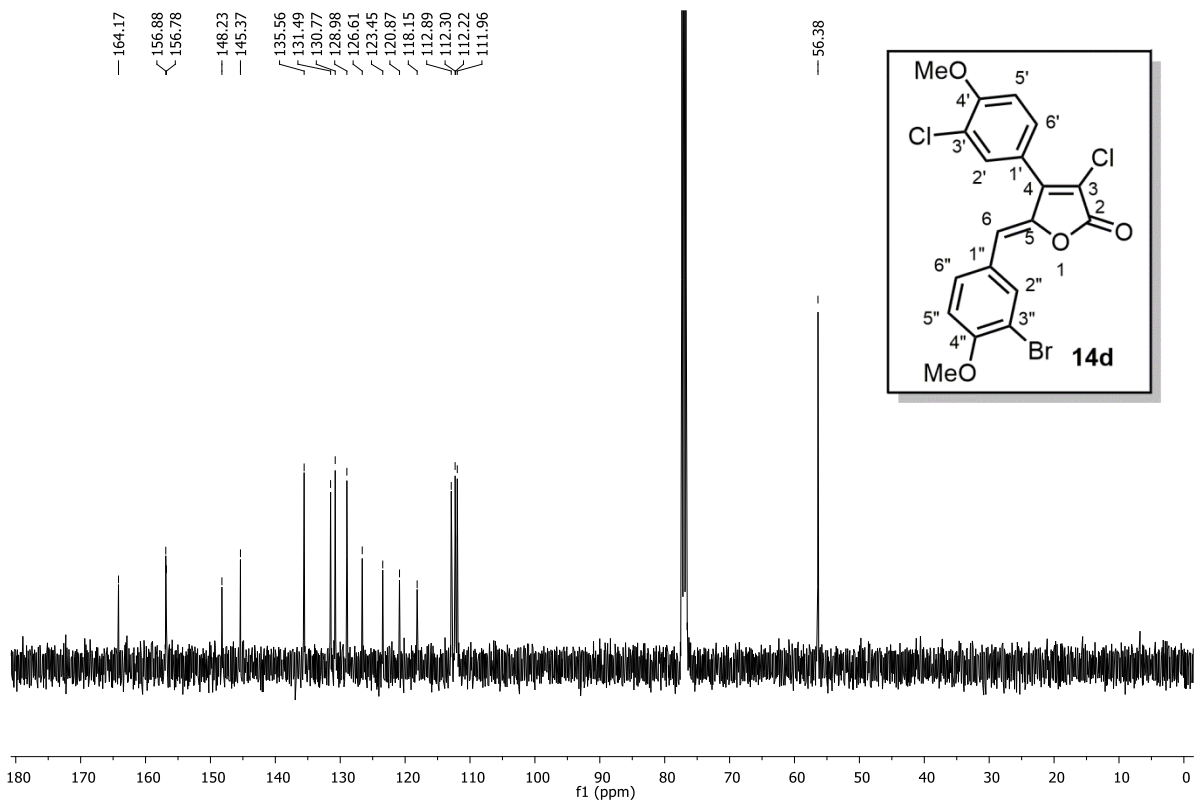
Figure A4.45 ^{13}C NMR (100 MHz, CDCl$_3$) of compound **14d**

217

Figure A4.46 ^{1}H NMR (400 MHz, Acetone-d$_6$) of compound **15**

Figure A4.47 ^{13}C NMR (100 MHz, Acetone-d$_6$) of compound **15**
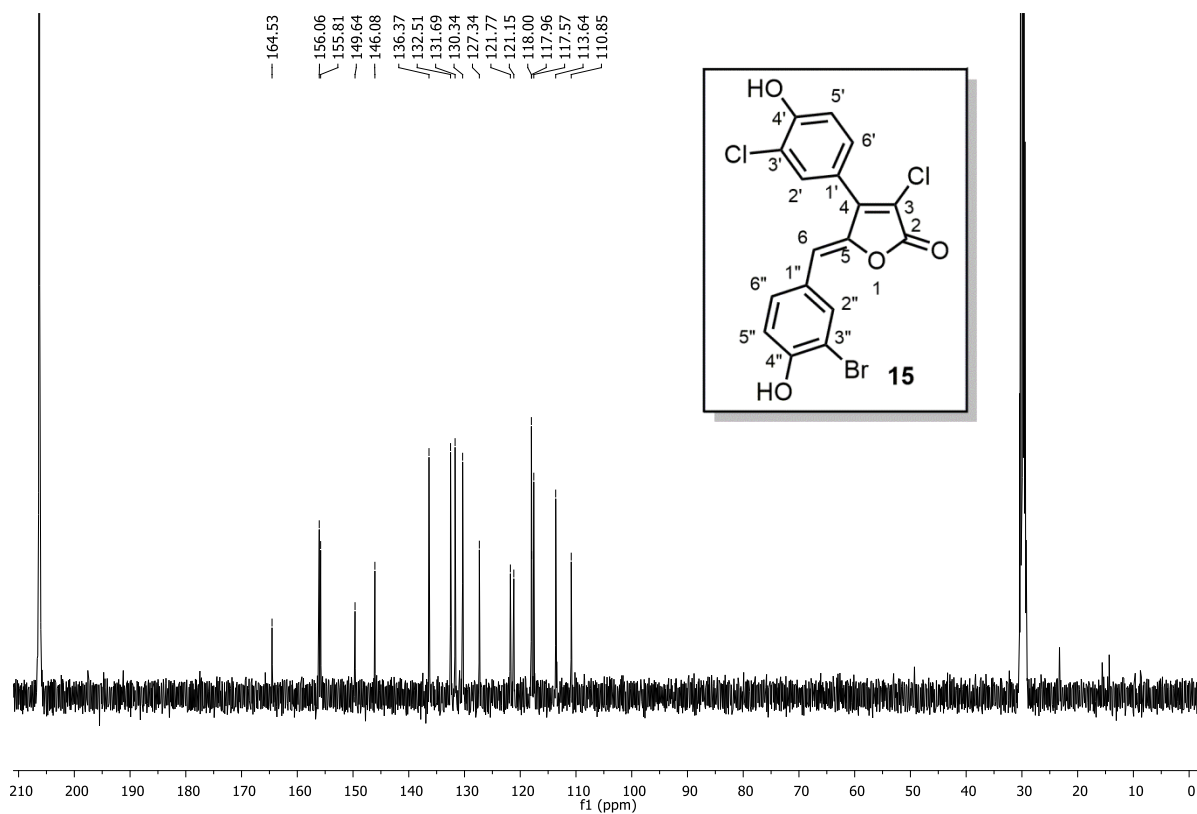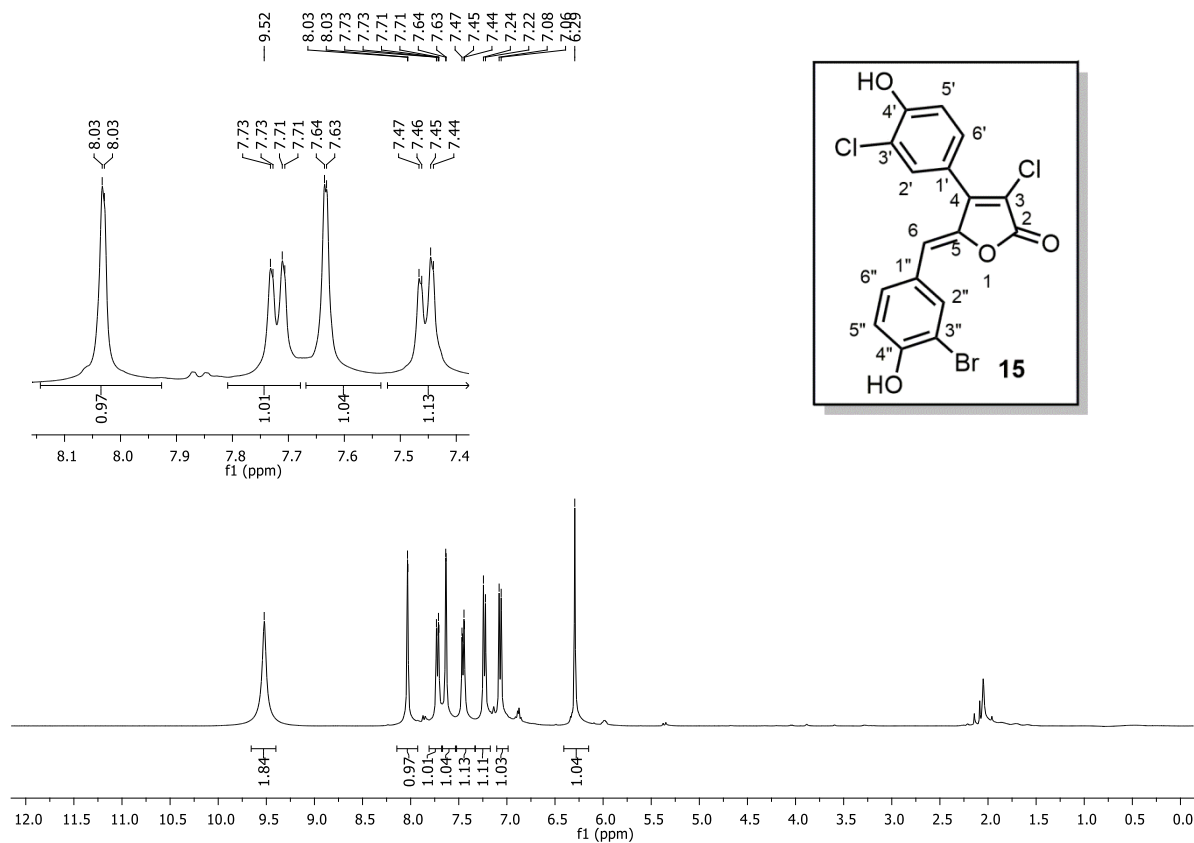
5. Appendix 5 (NMR Spectra Relevant to Chapter 5)

5.1. NMR Spectra of Selected Suzuki Coupling Products

Figure A5.1 ^{1}H NMR (400 MHz, CDCl$_3$) of compound **7e**

Figure A5.2 ^{13}C NMR (100 MHz, CDCl$_3$) of compound **7e**
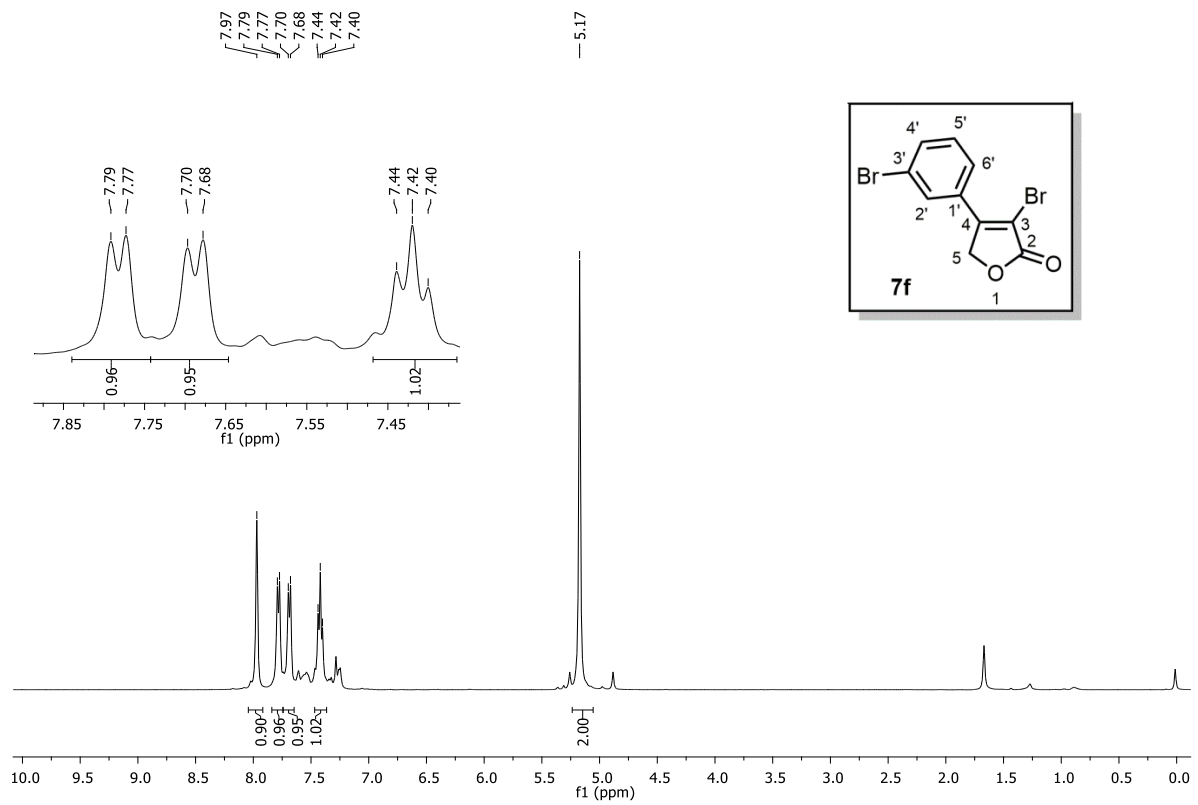
Figure A5.3 ^{1}H NMR (400 MHz, CDCl$_3$) of compound **7f**
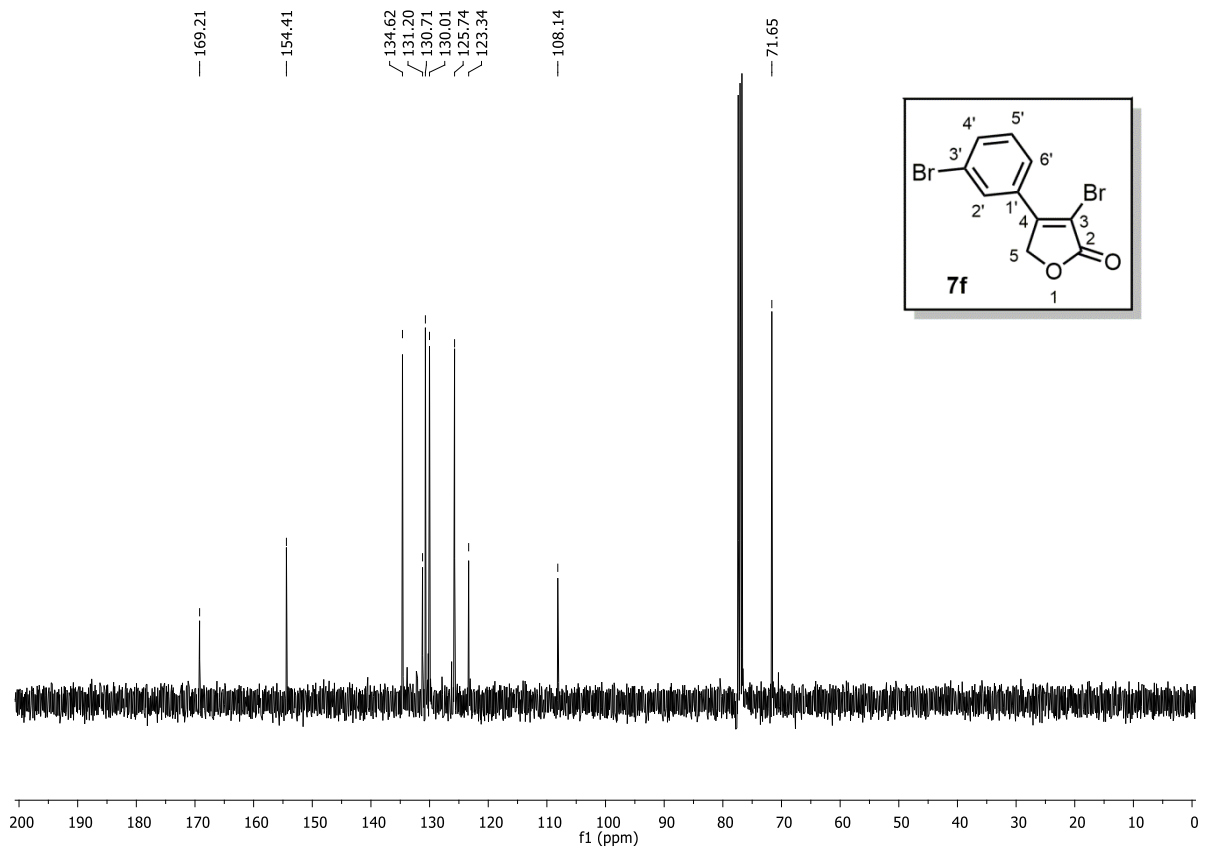
Figure A5.4 ^{13}C NMR (100 MHz, CDCl$_3$) of compound **7f**

220
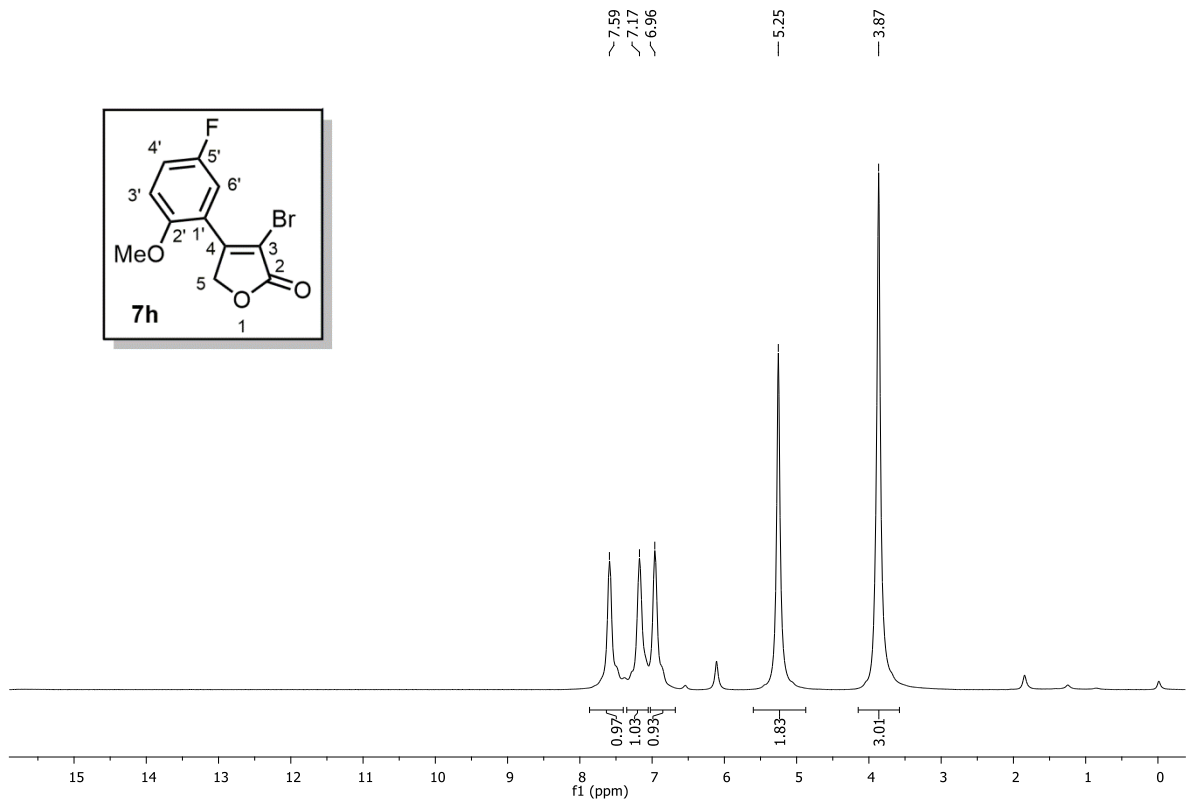
Figure A5.5 ^{1}H NMR (400 MHz, CDCl$_3$) of compound **7h**
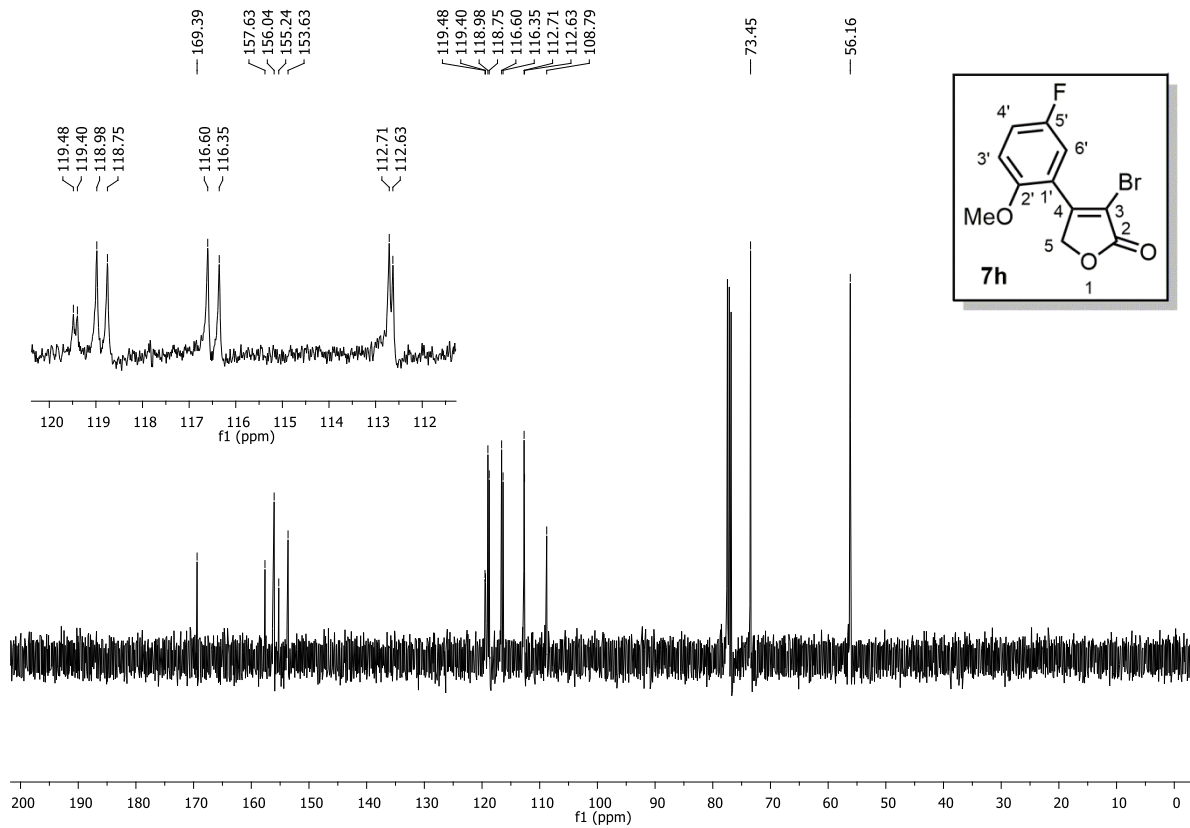
Figure A5.6 ^{13}C NMR (100 MHz, CDCl$_3$) of compound **7h**

5.2. NMR Spectra of Selected Dehalogenation Products
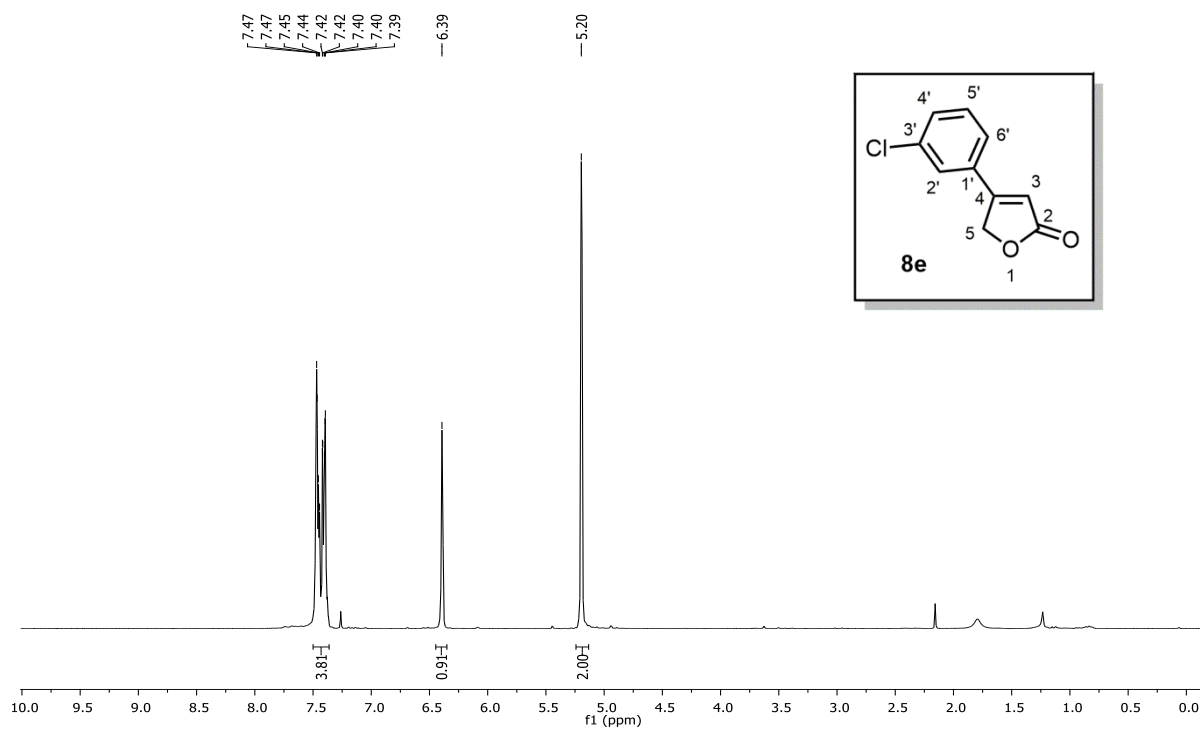
Figure A5.7 ^{1}H NMR (400 MHz, CDCl$_3$) of compound **8e**
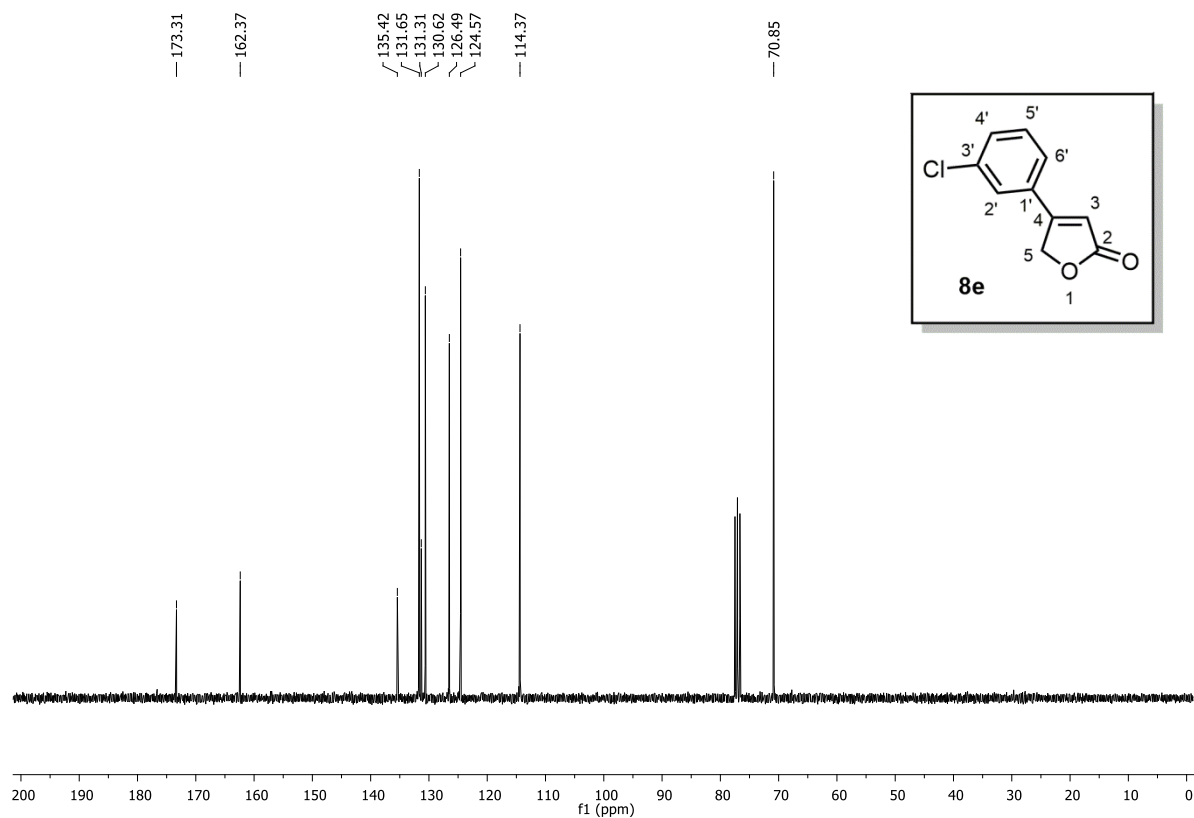
Figure A5.8 ^{13}C NMR (100 MHz, CDCl$_3$) of compound **8e**
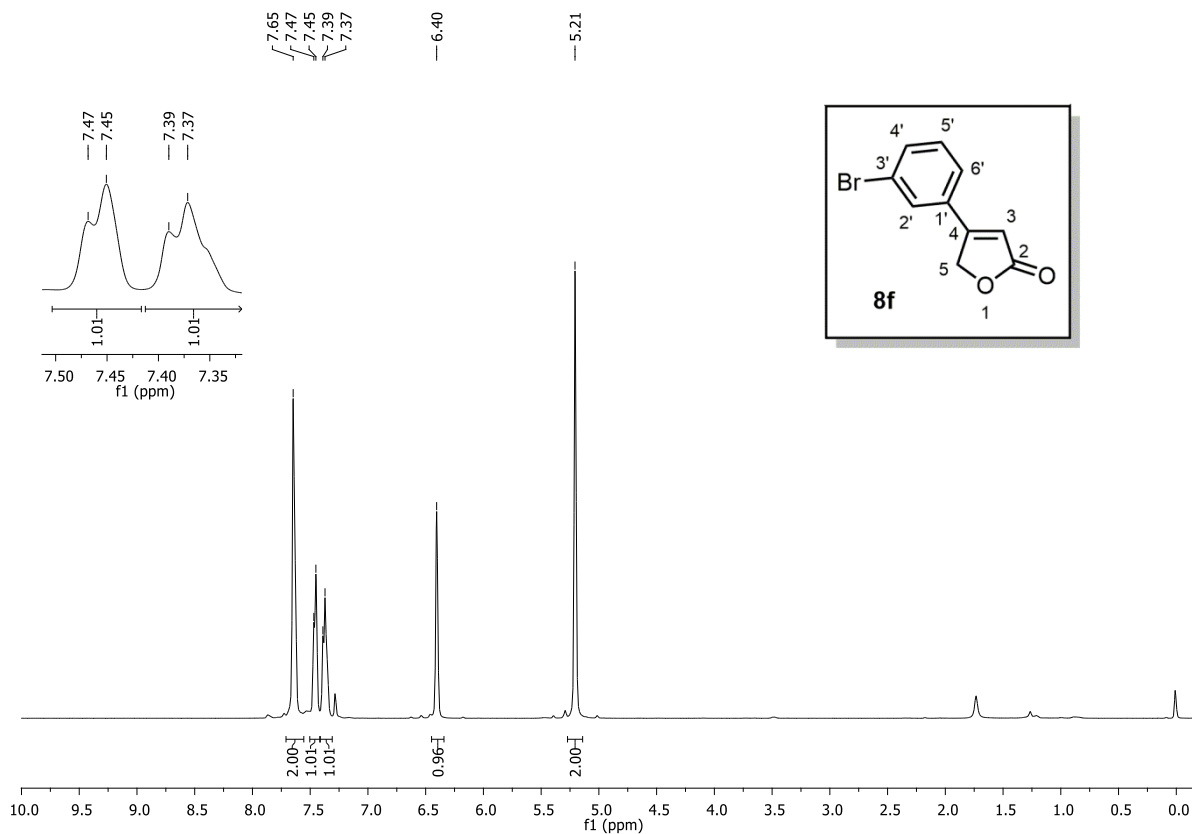
Figure A5.9 ^{1}H NMR (400 MHz, CDCl$_3$) of compound **8f**
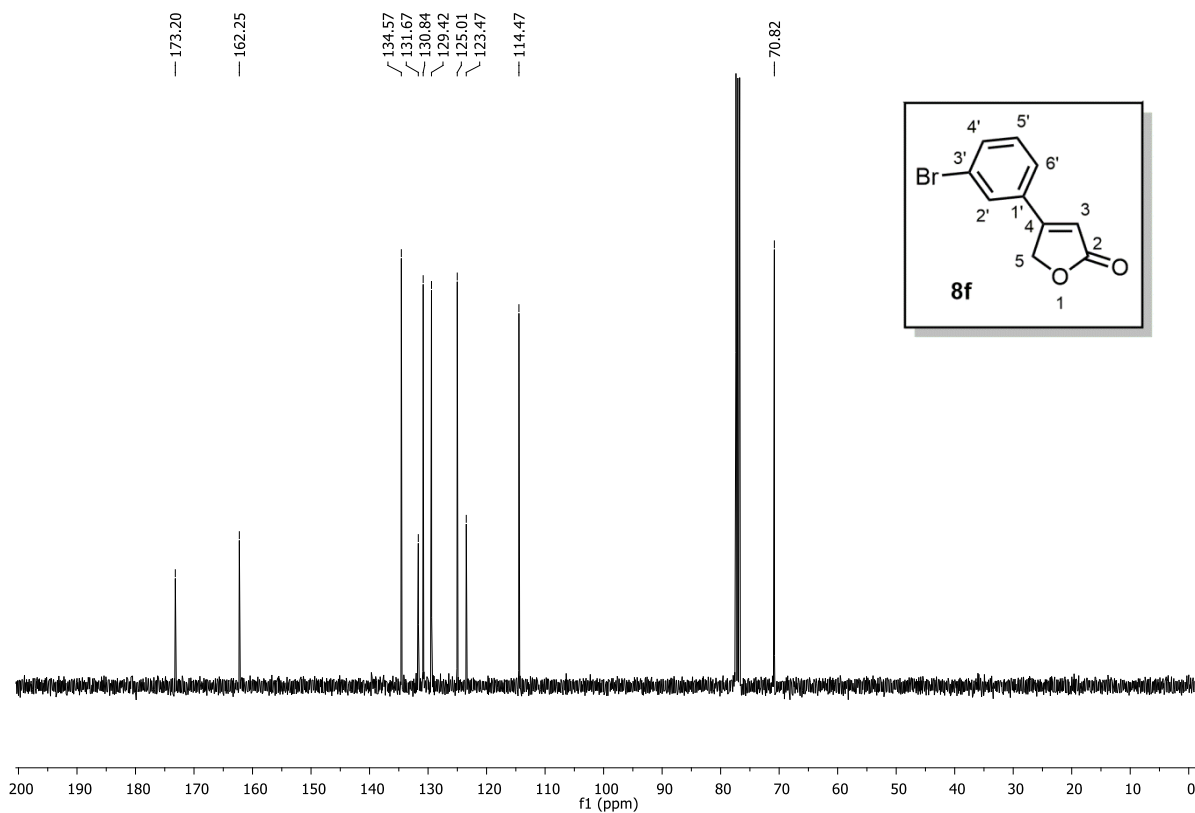
Figure A5.10 ^{13}C NMR (100 MHz, CDCl$_3$) of compound **8f**

Figure A5.11 ^{1}H NMR (400 MHz, CDCl$_3$) of compound **8g**

Figure A5.12 ^{13}C NMR (100 MHz, CDCl$_3$) of compound **8g**

Figure A5.13 ^{1}H NMR (400 MHz, CDCl$_3$) of compound **8h**

Figure A5.14 ^{13}C NMR (100 MHz, CDCl$_3$) of compound **8h**
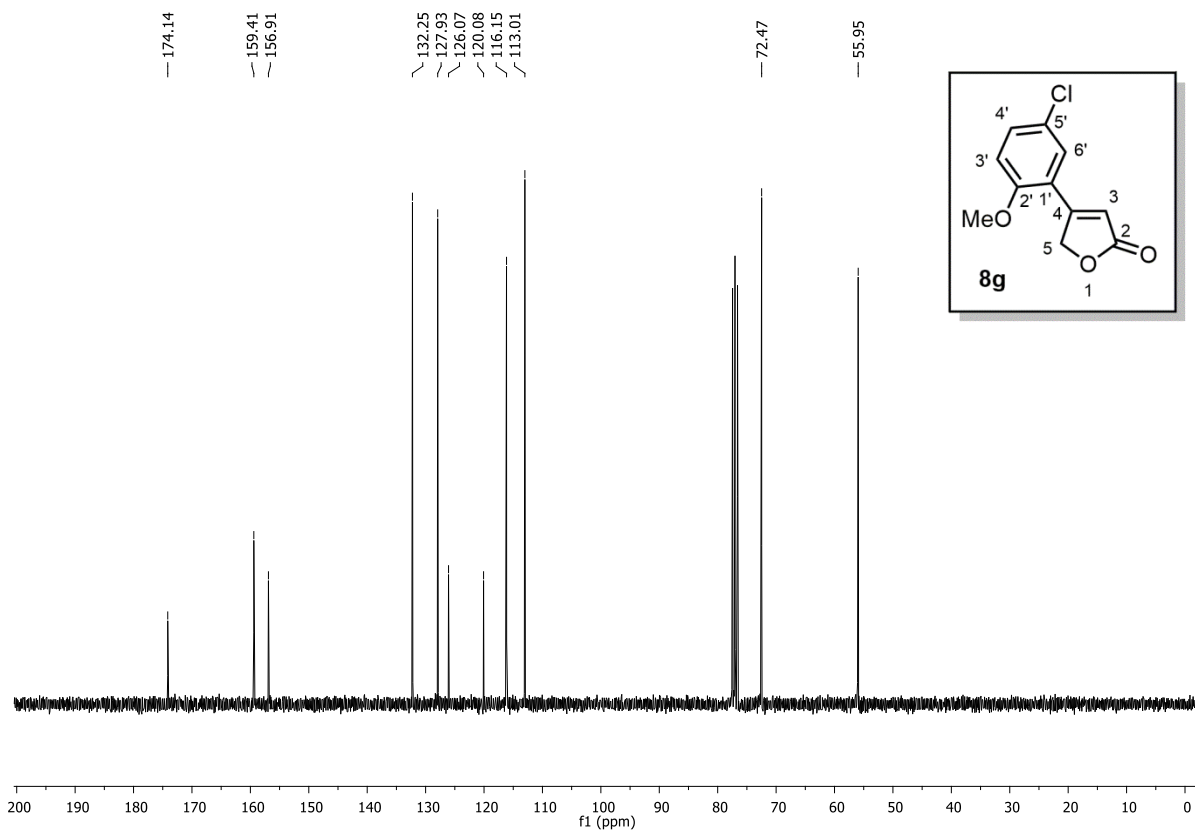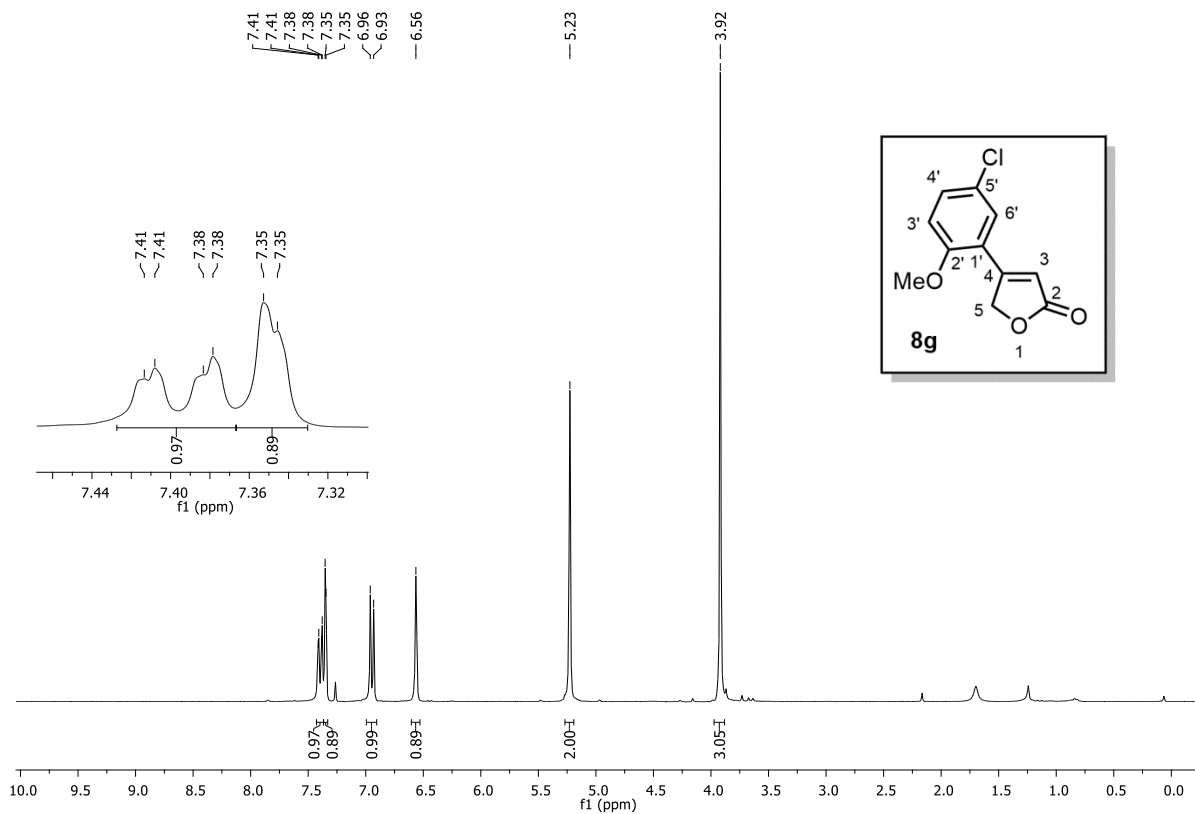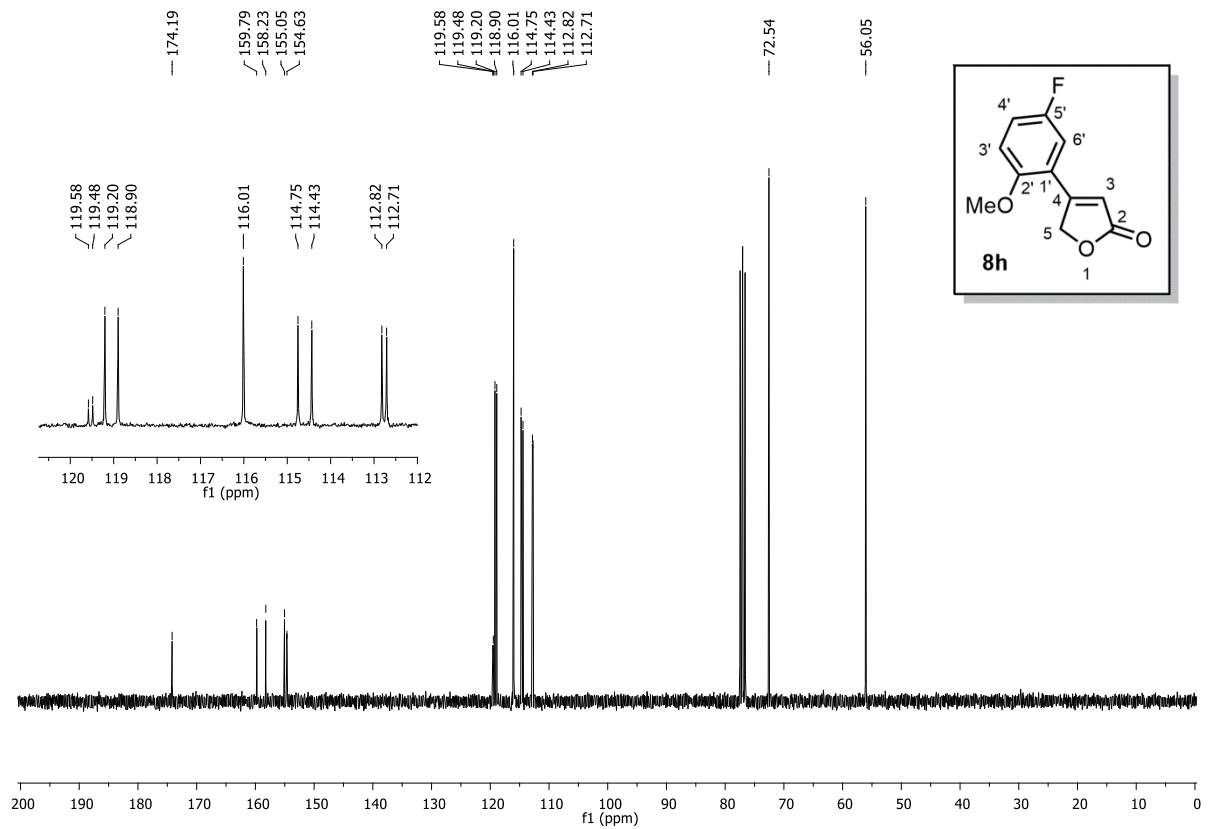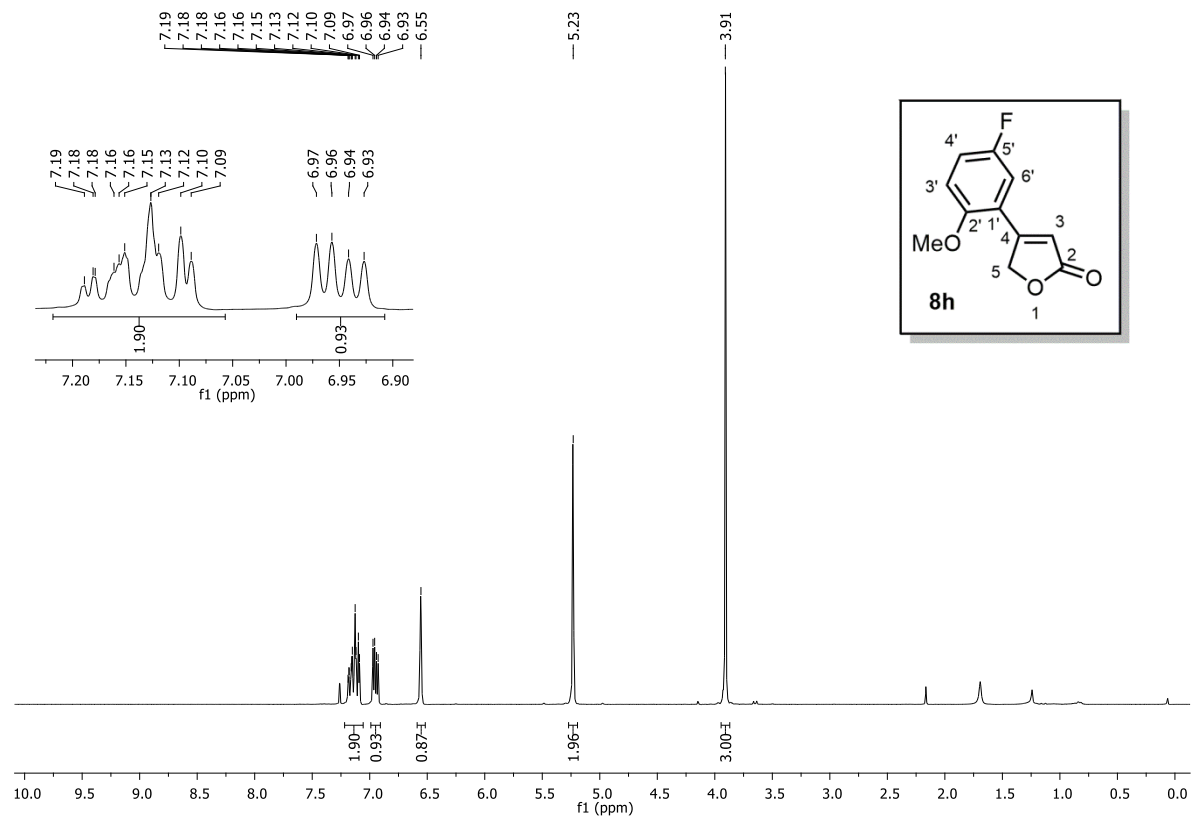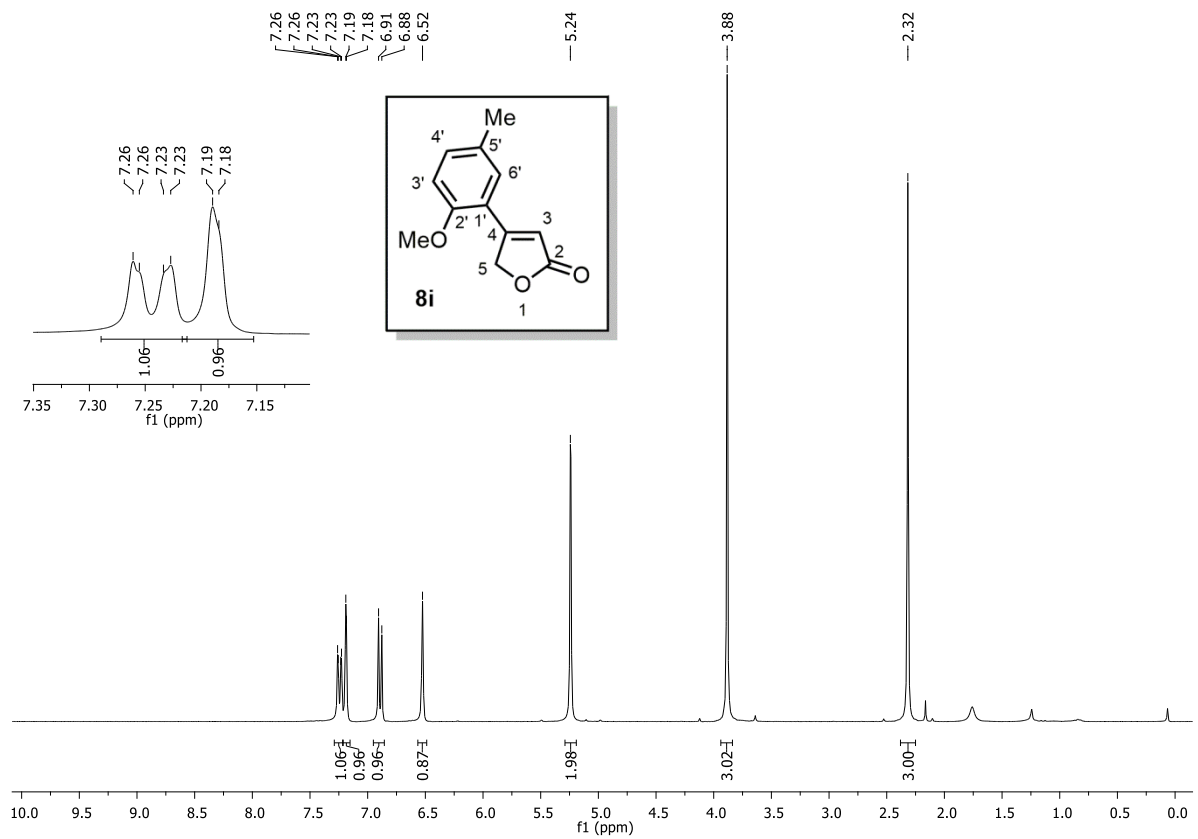
Figure A5.15 ^{1}H NMR (400 MHz, CDCl$_3$) of compound **8i**
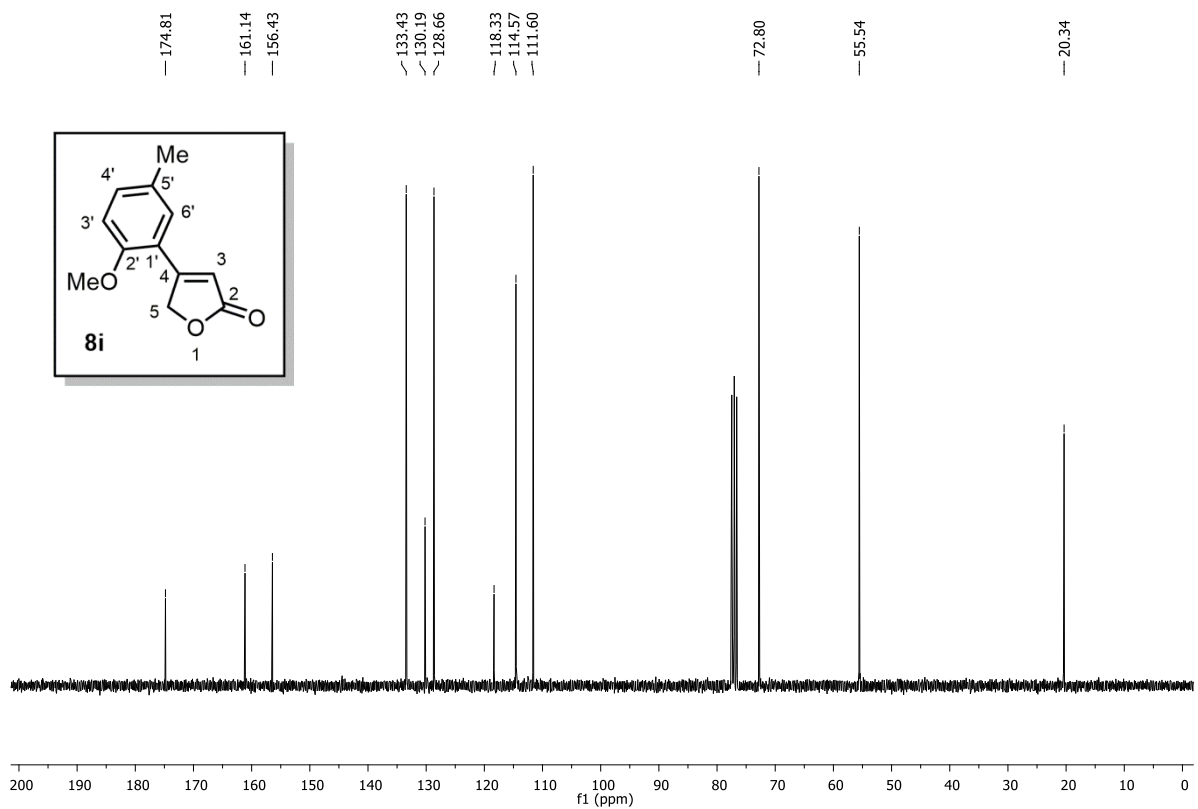
Figure A5.16 ^{13}C NMR (100 MHz, CDCl$_3$) of compound **8i**

226

Figure A5.17 ^{1}H NMR (400 MHz, DMSO-d$_6$) of compound **8k**

Figure A5.18 ^{13}C NMR (100 MHz, DMSO-d$_6$) of compound **8k**

227

Figure A5.19 ^{1}H NMR (400 MHz, CDCl$_3$) of compound **8l**

Figure A5.20 ^{13}C NMR (100 MHz, CDCl$_3$) of compound **8l**

228
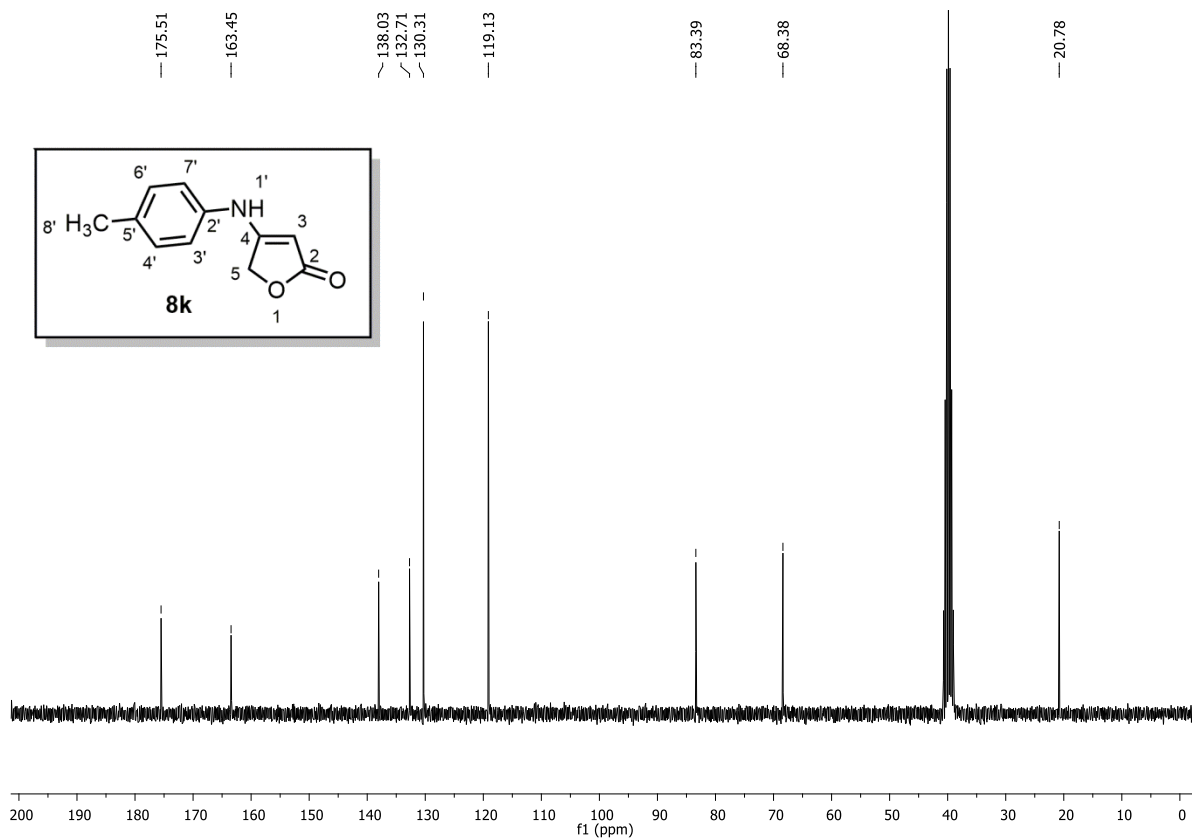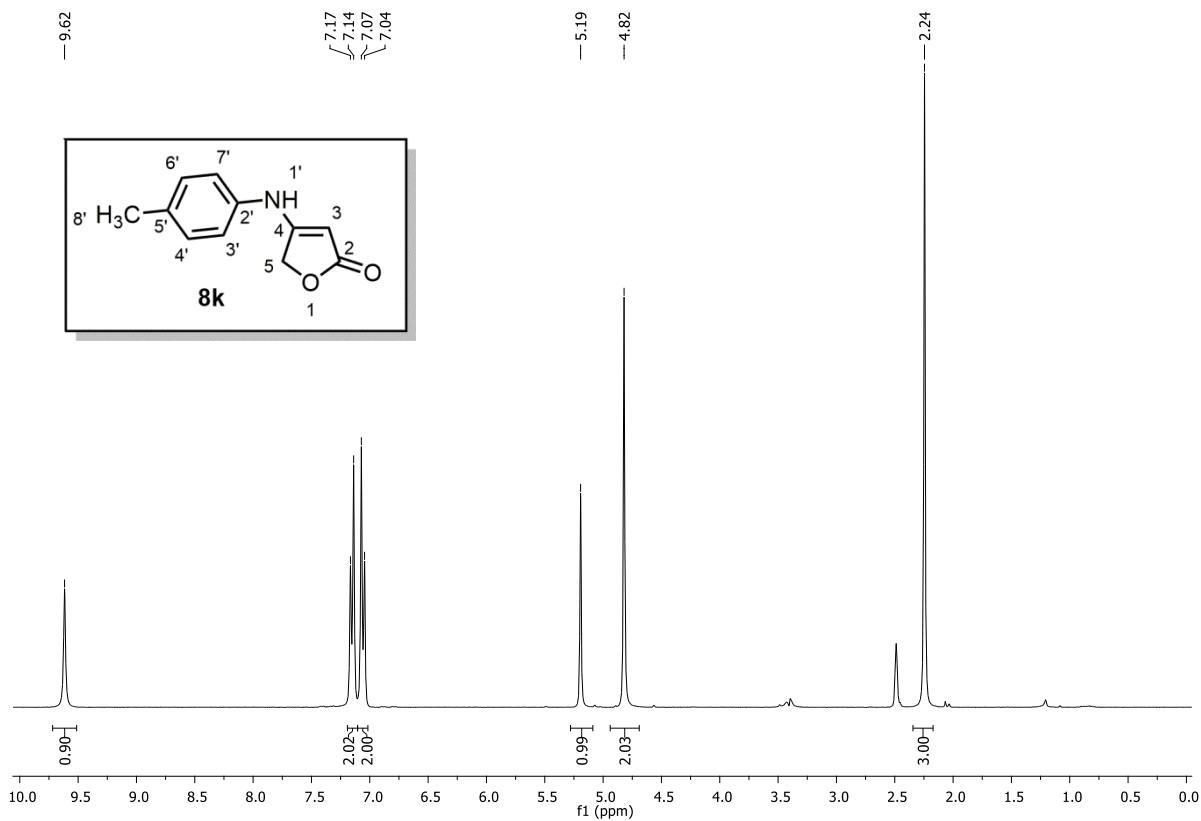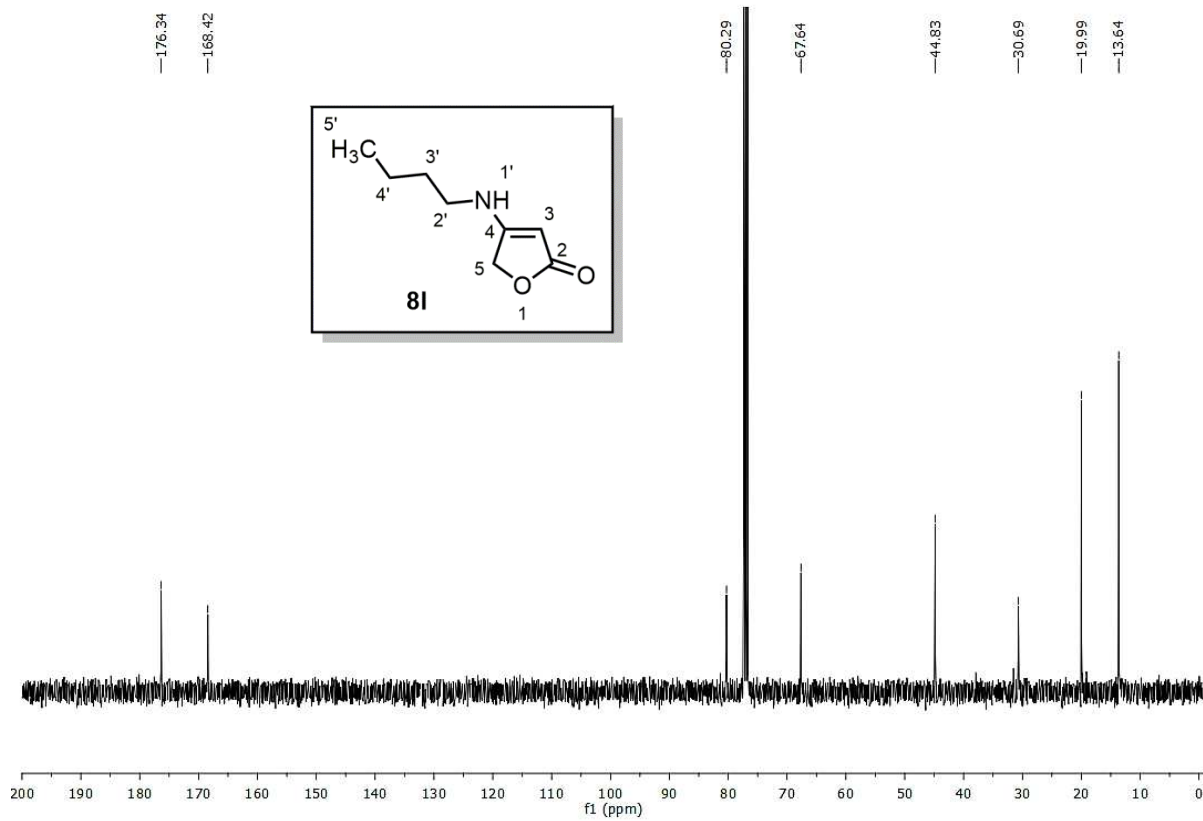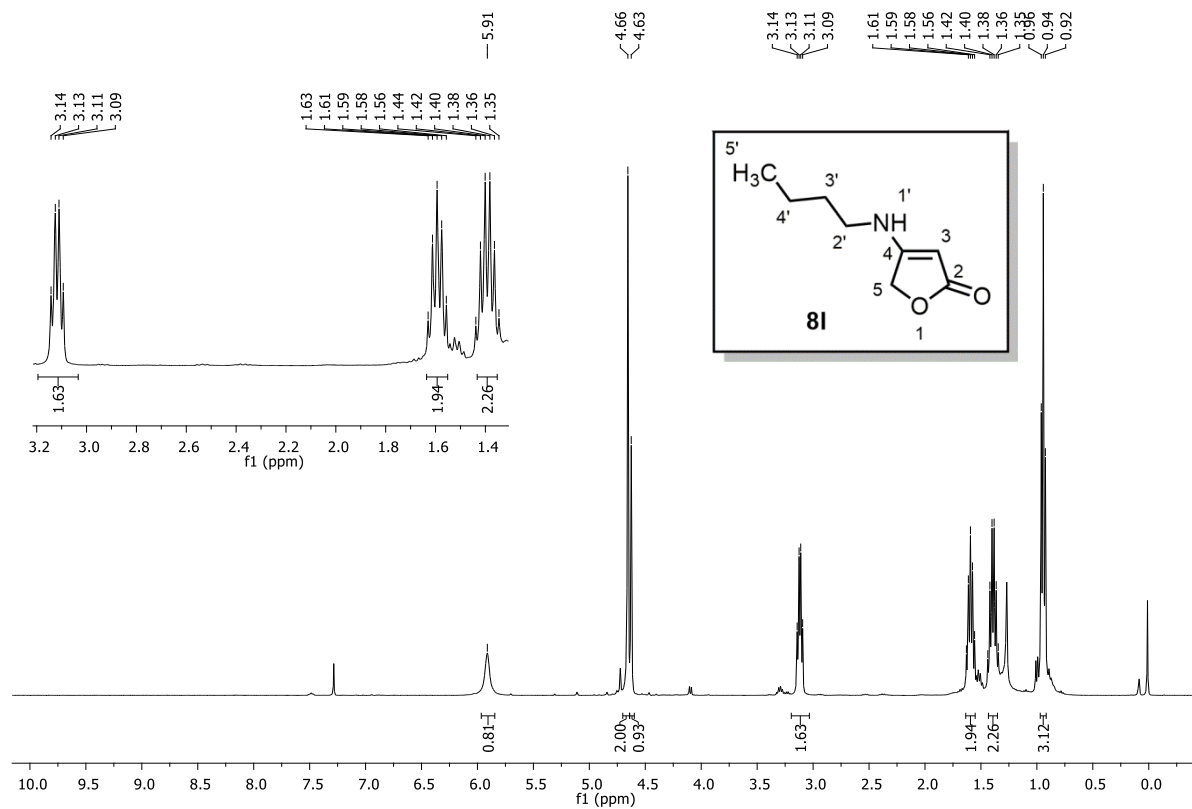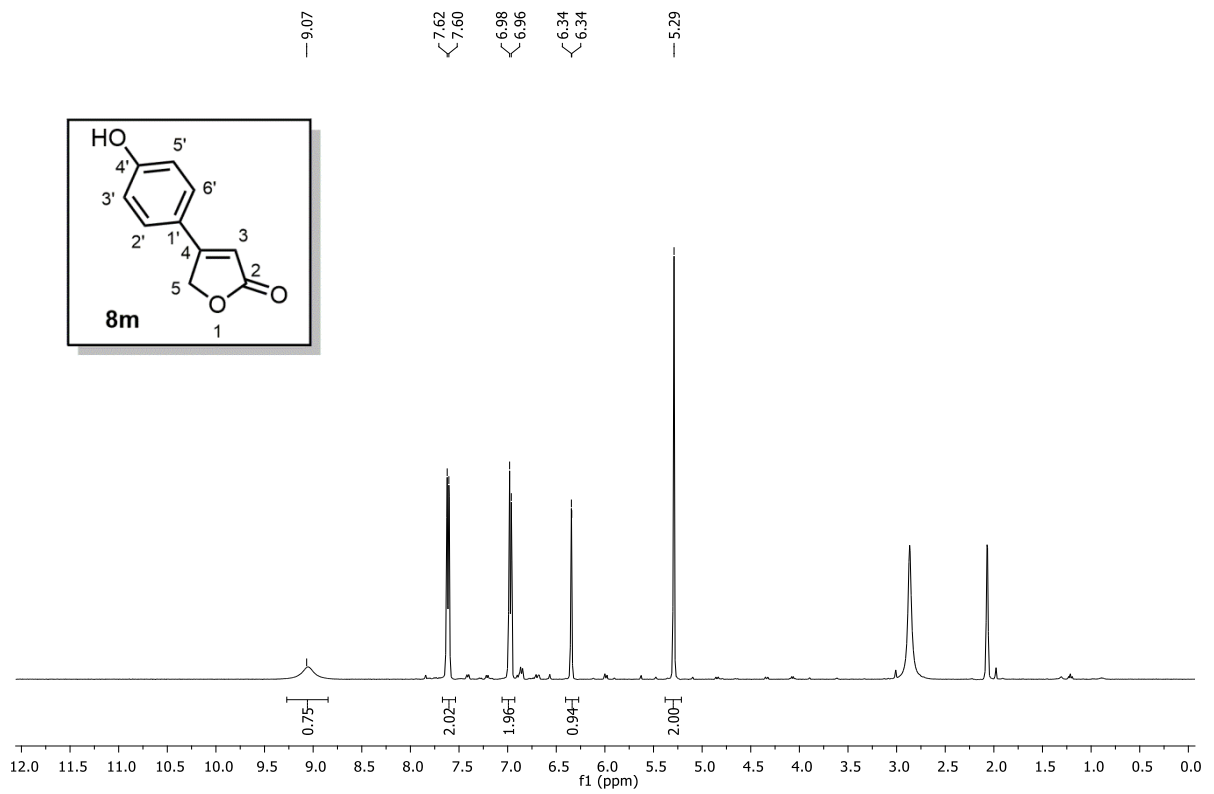
Figure A5.21 ^{1}H NMR (400 MHz, Acetone-d$_{6}$) of compound **8m**
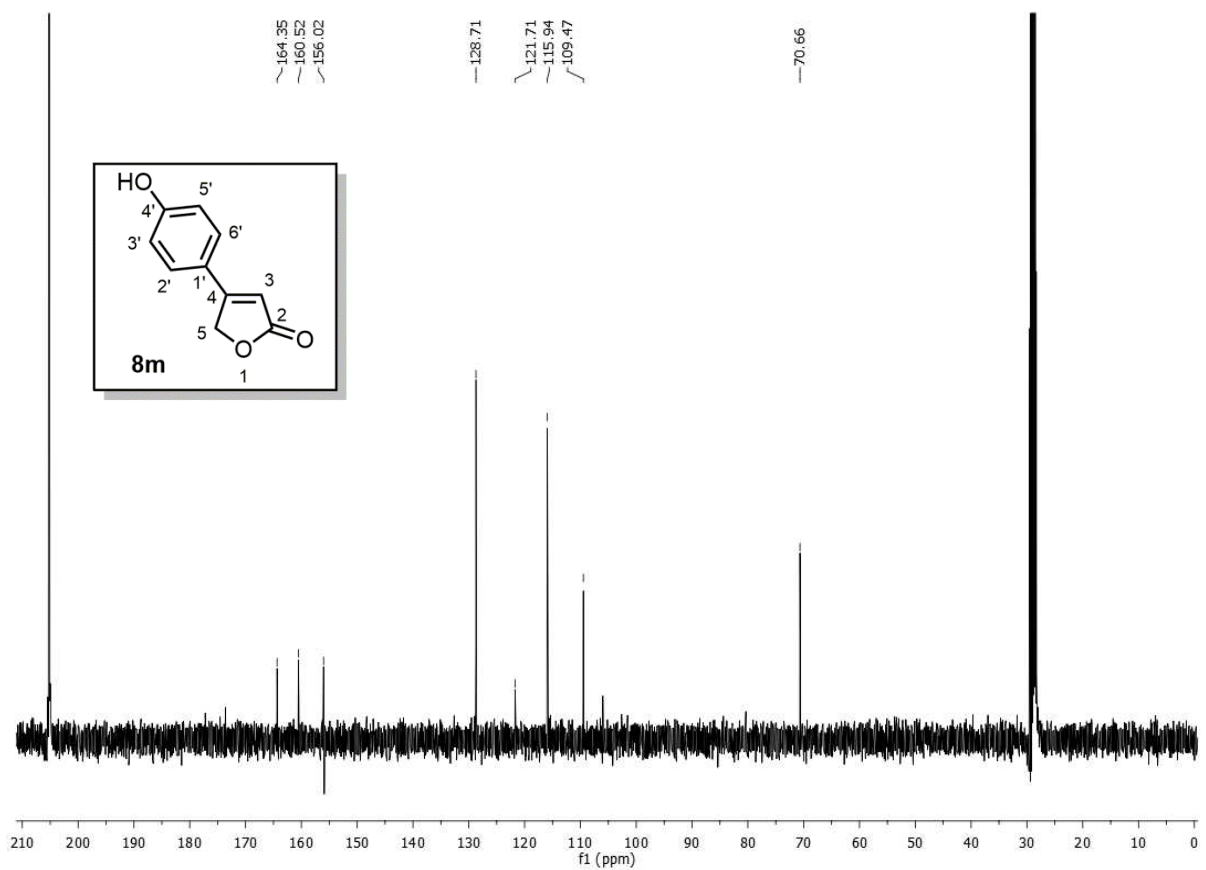
Figure A5.22 ^{13}C NMR (100 MHz, Acetone-d$_{6}$) of compound **8m**

5.3. NMR Spectra of Rubrolide E, F, and 3"-Bromorubrolide F
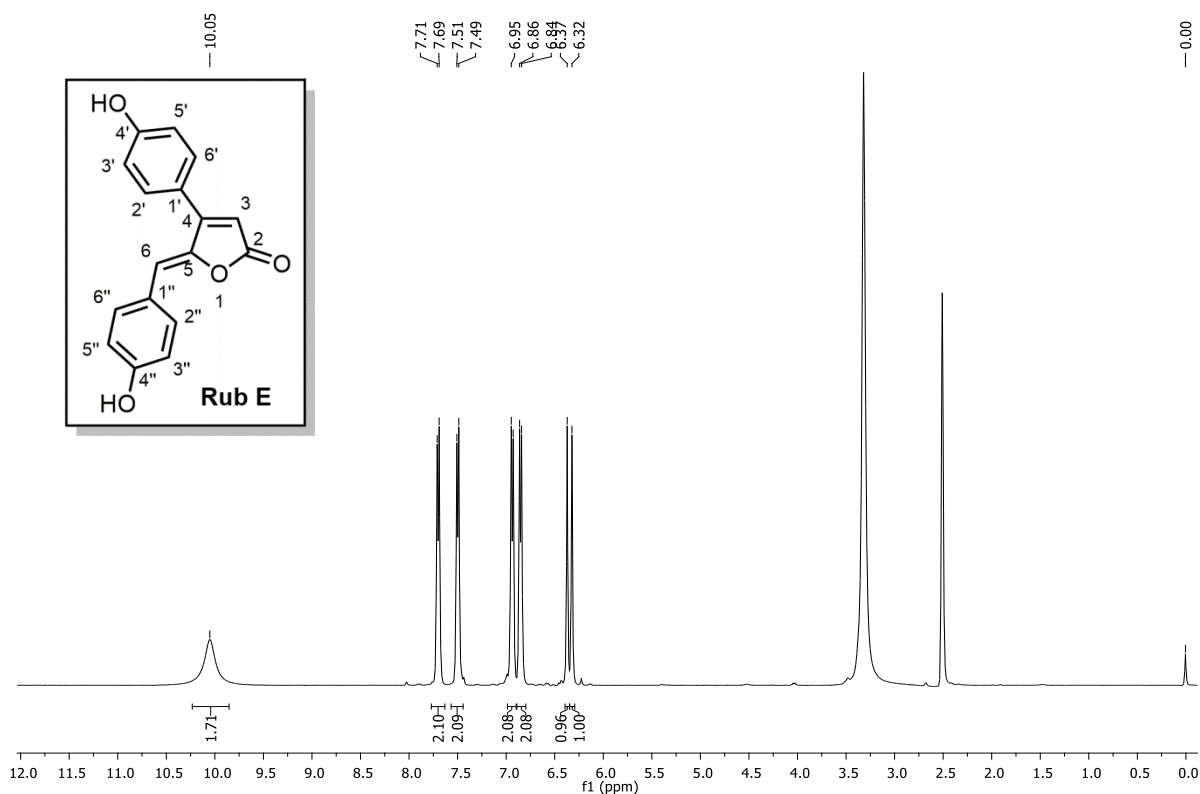
Figure A5.23 ^{1}H NMR (400 MHz, DMSO-d$_6$) of rubrolide E
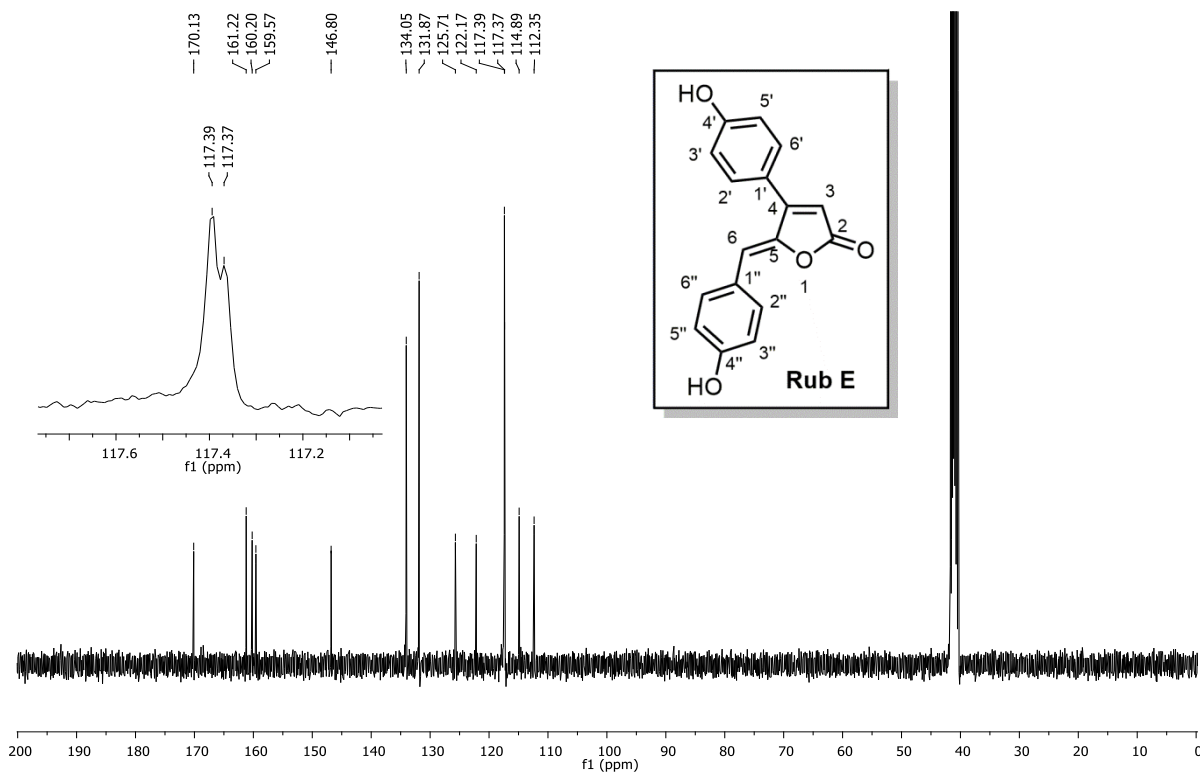
Figure A5.24 ^{13}C NMR (100 MHz, DMSO-d$_6$) of rubrolide E
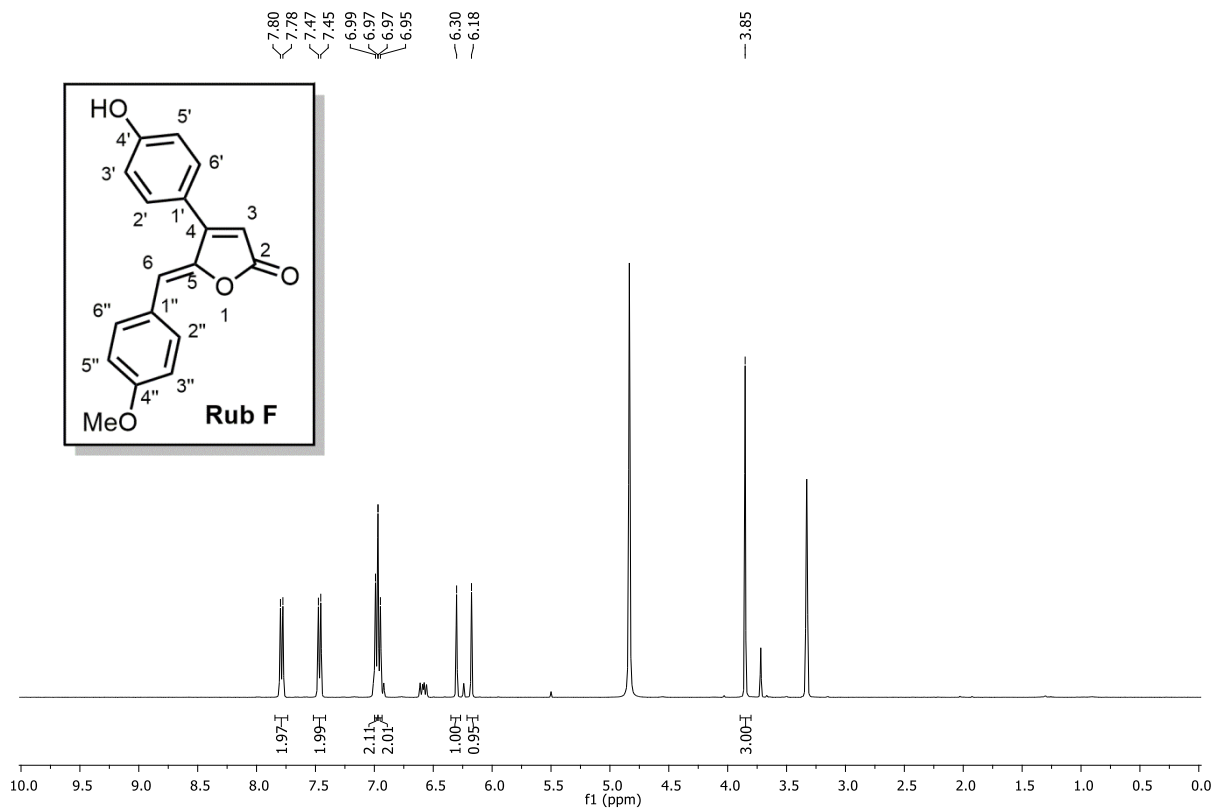
Figure A5.25 ^{1}H NMR (400 MHz, CD$_3$OD) of rubrolide F
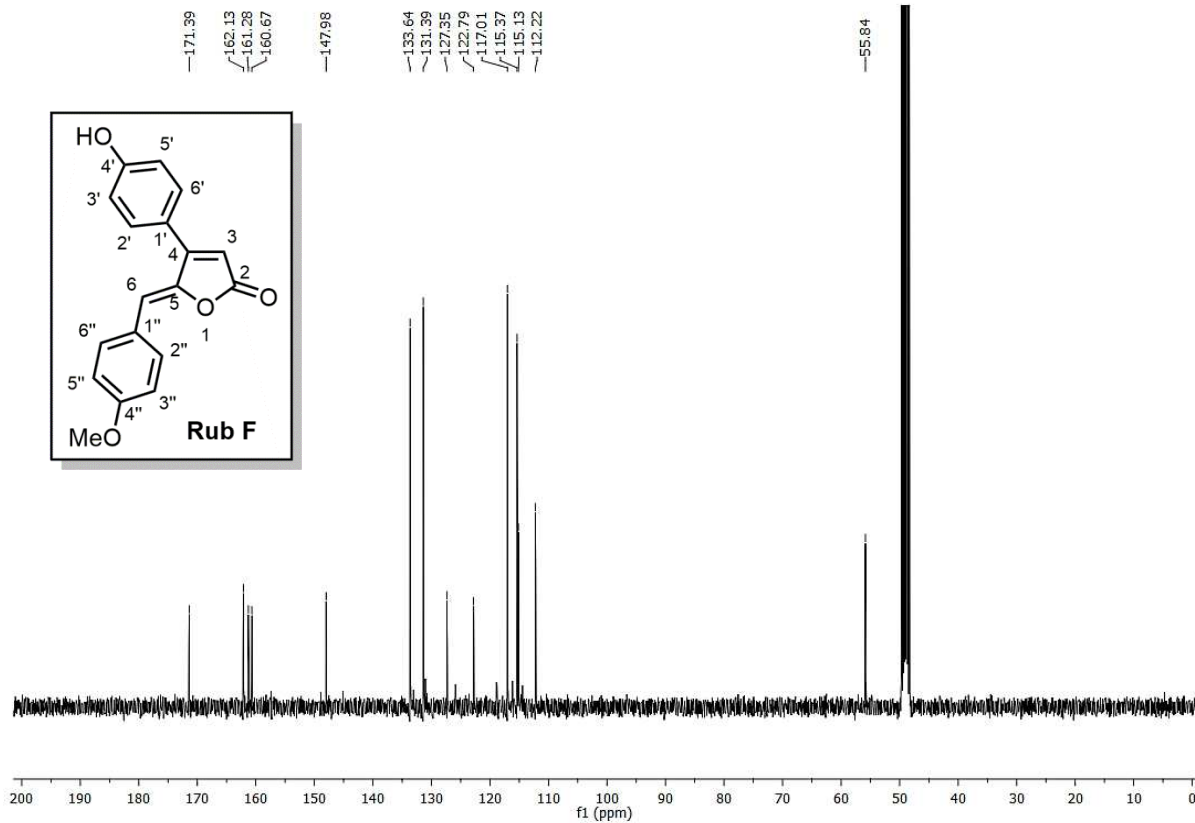
Figure A5.26 ^{13}C NMR (100 MHz, CD$_3$OD) of rubrolide F
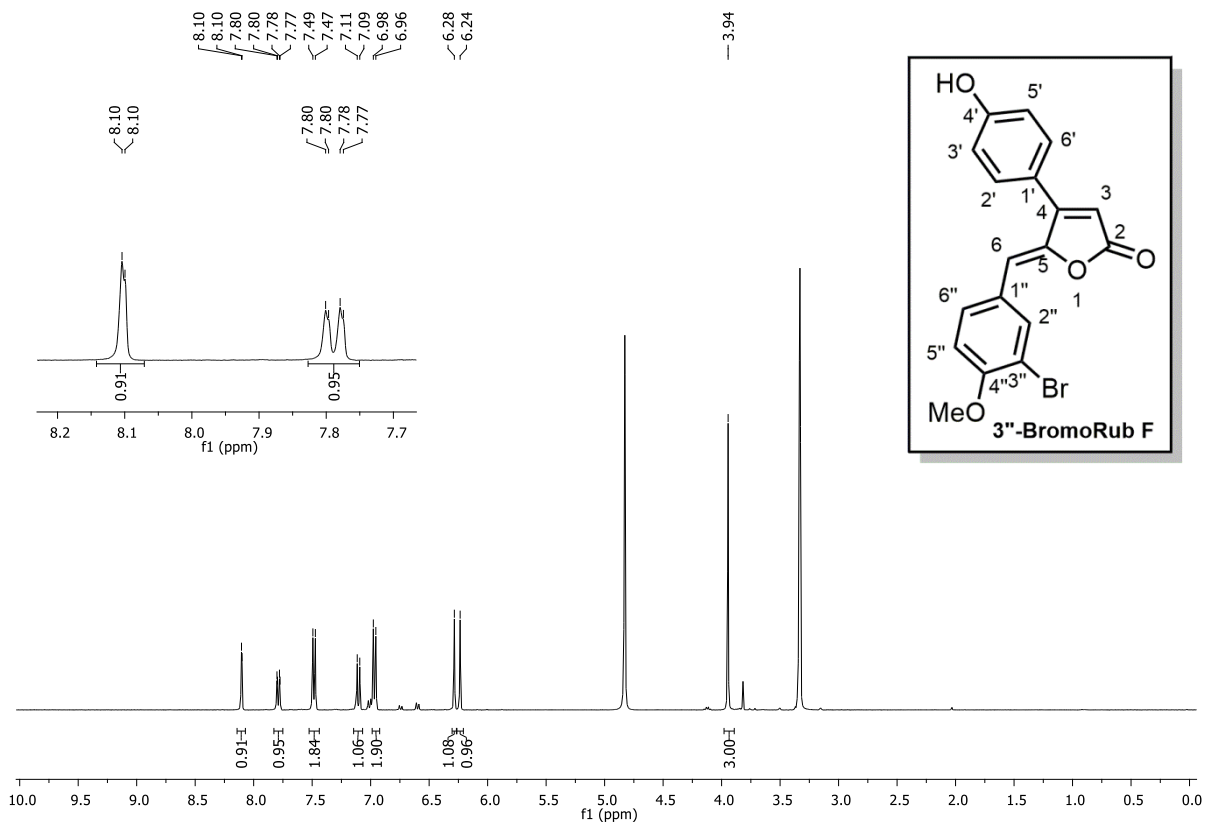
Figure A5.27 ^{1}H NMR (400 MHz, CD$_3$OD) of 3''-bromorubrolide F
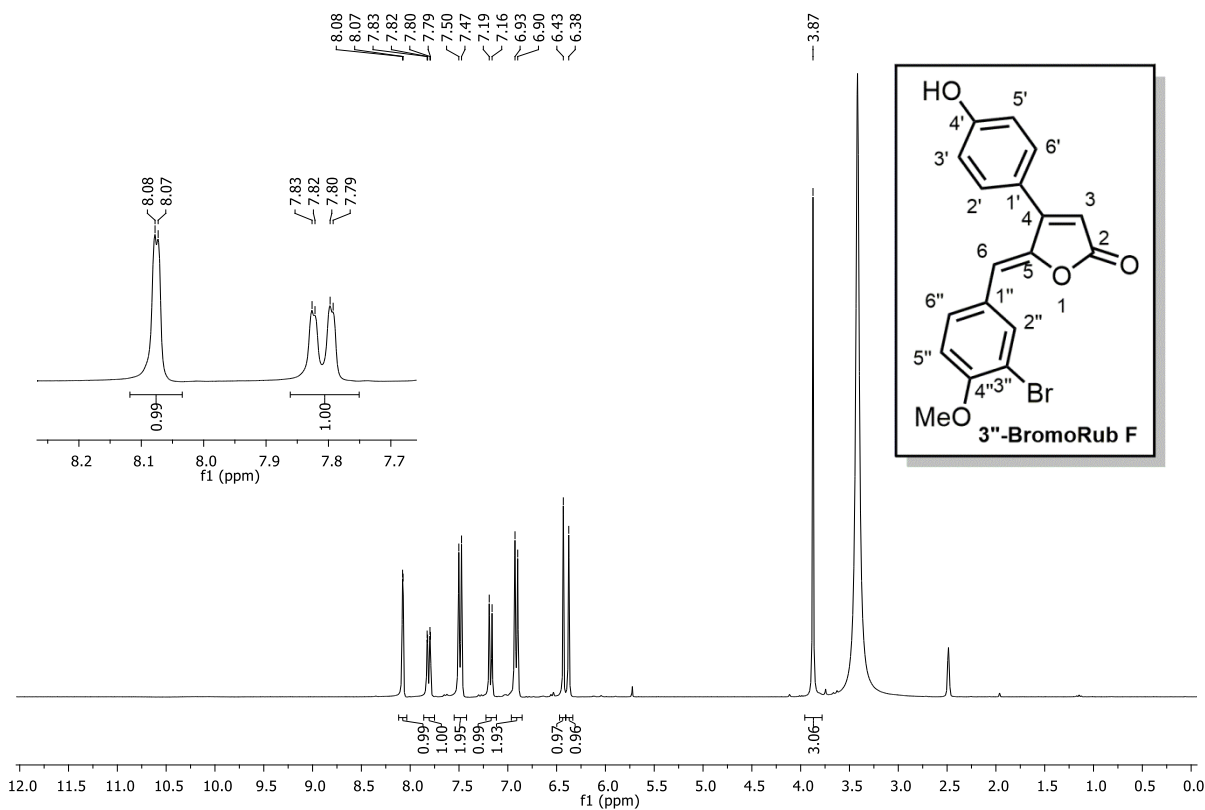
Figure A5.28 ^{1}H NMR (300 MHz, DMSO-d_6) of 3''-bromorubrolide F
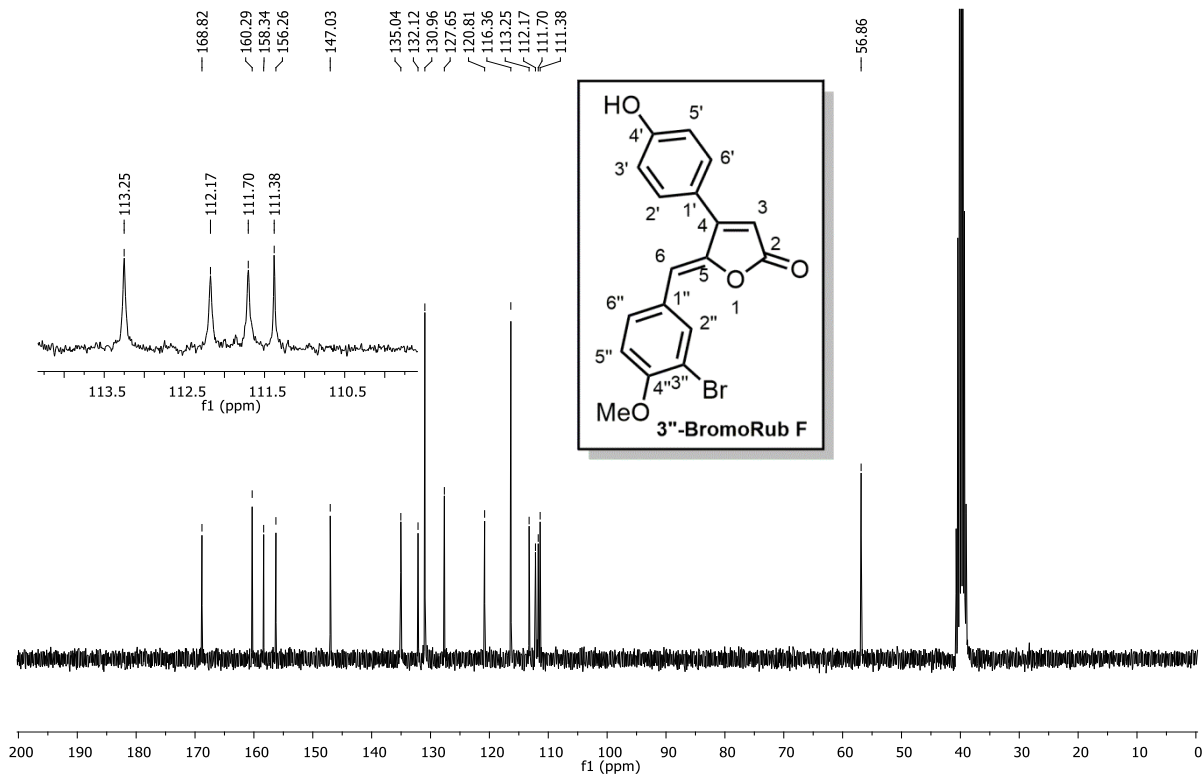
Figure A5.29 ^{13}C NMR (75 MHz, DMSO-d_6) of 3''-bromorubrolide F

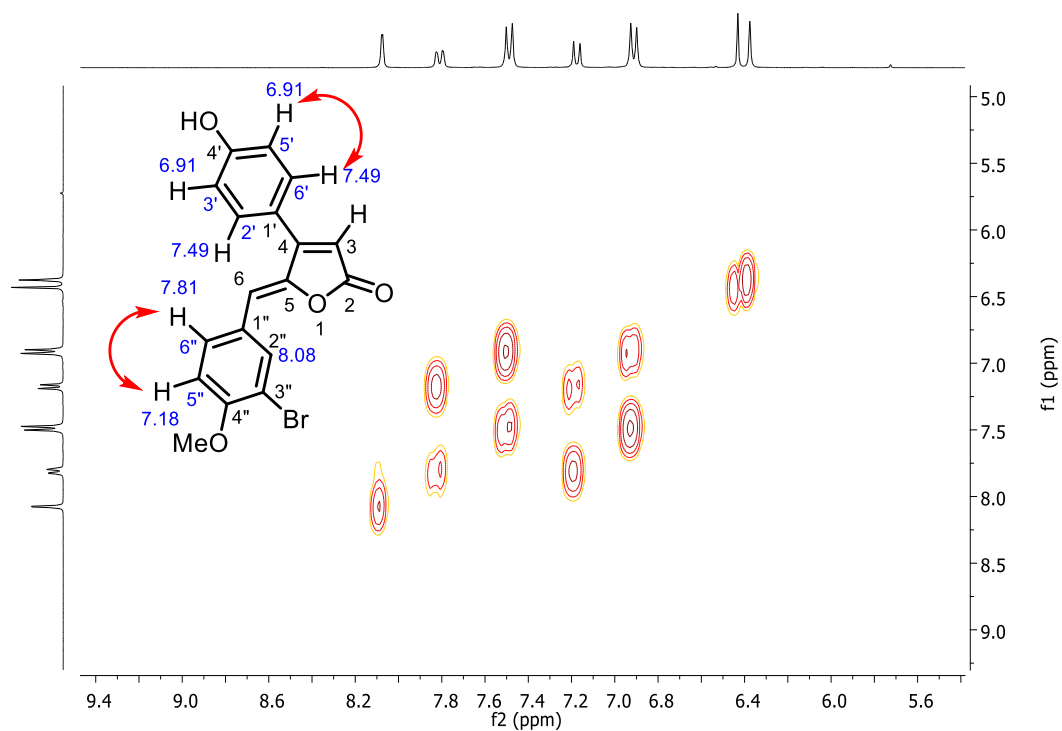**Figure A5.31** COSY (300 MHz, DMSO-d_6) of 3''-bromorubrolide F
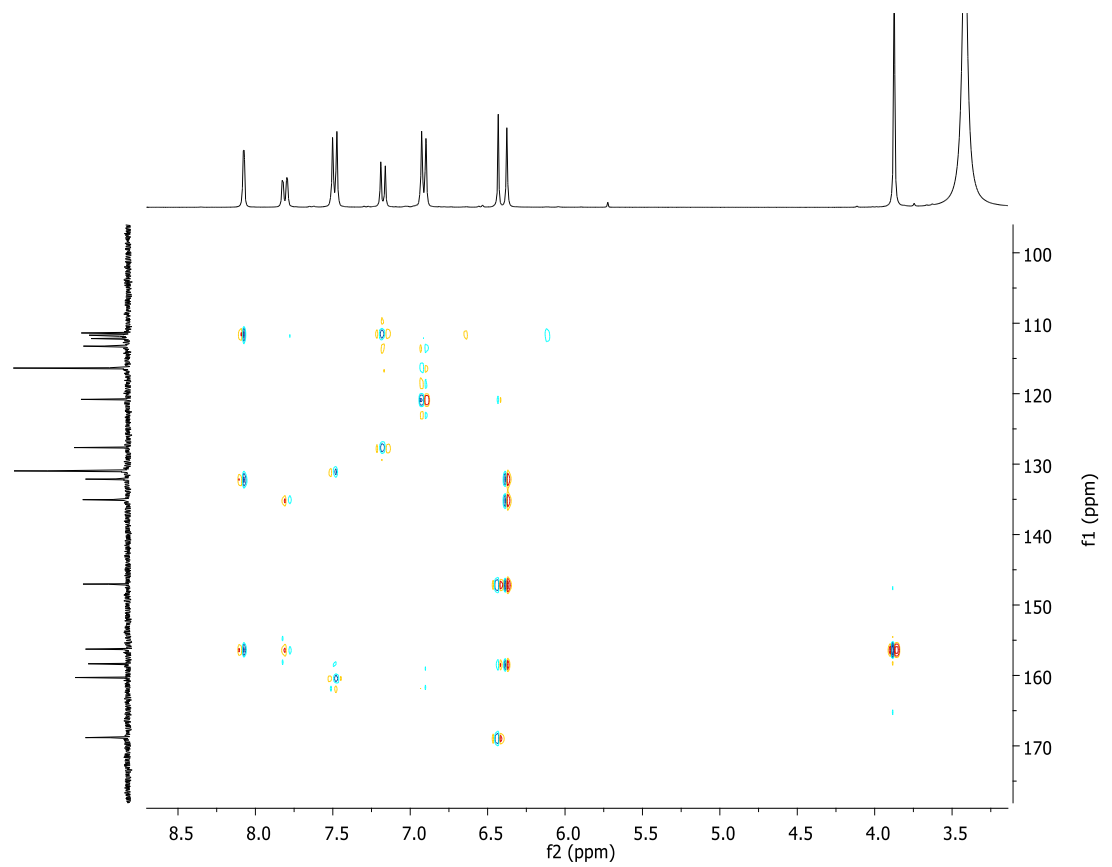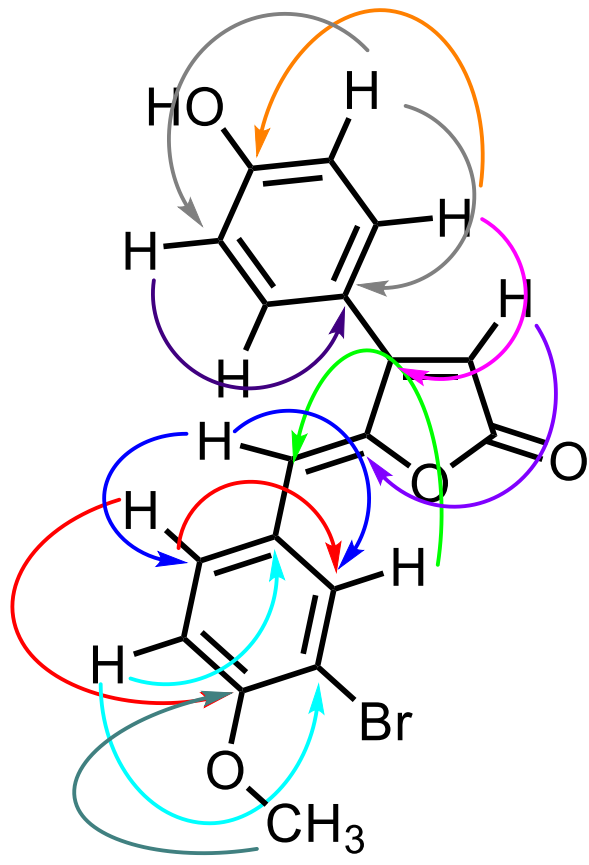
233

Figure A5.31 HMBC (300 MHz, DMSO-d_6) of 3''-bromorubrolide F